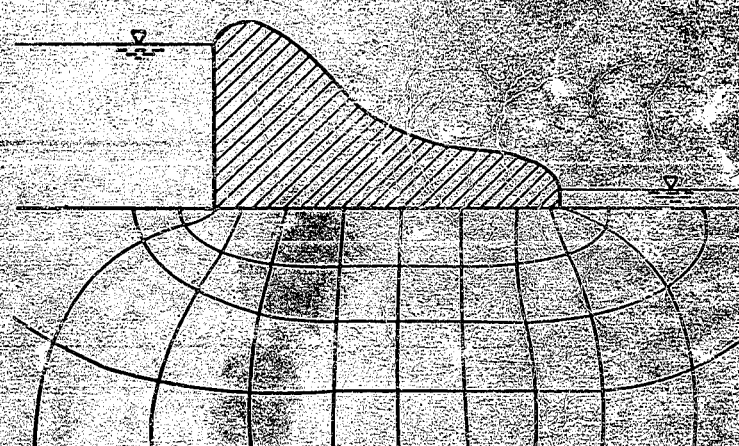
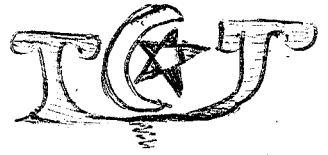


SOIL MECHANICS



ALEMAYEHU TEFERRA
MESFIN LEIKUN



SOIL MECHANICS

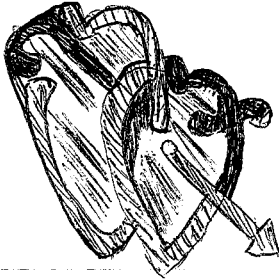


ALEMAYEHU TEFERRA
Professor of Civil Engineering
Addis Ababa University

*Gashaw
Legas
Amha*

and

MESFIN LEIKUN
Associate Professor of Civil Engineering
Addis Ababa University



000323

Faculty of Technology
Addis Ababa University
1999

CONTENTS

	PAGE
	x
Preface	
1. INTRODUCTION	1
1.1 General	1
1.2 Soil Formation	3
1.2.1 Weathering of Rocks	
1.3 Common soil Types	
2. INDEX PROPERTIES AND CLASSIFICATION OF SOILS.	5
2.1 General	5
2.2 Volume Relationships	6
2.2.1 Void Ratio and Porosity	7
2.2.2 Degree of Saturation	8
2.3 Weight Relationships	8
2.3.1 Moisture Content	9
2.3.2 Unit Weight of Solids	9
2.3.3 Specific Gravity	9
2.3.4 Unit Weight of soil	12
2.3.5 Relative Density	16
2.4 Size and Shape of soil Particles	16
2.5 Grain size Distribution	16
2.5.1 Sieve Analysis	17
2.5.2 Hydrometer Analysis	17
2.5.3 Grain Size Distribution Curve	18
2.5.4 Brief Outline of Experimental Procedure for Hydrometer Analysis	20
2.6 Soil Consistency	24
2.6.1 Atterberg Limits	24
2.6.2 Engineering Definition of Atterberg Limits	26
2.6.3 Determination of Atterberg Limits	27
2.7 Properties of Clay Particles	30
2.7.1 Surface Activity and Adsorbed Layer	30
2.7.2 Colloids	31
2.7.3 Clay Minerals	32

2.8.1	Grain size classification	33
2.8.2	U.S. Bureau of Soils Textural Classification	34
2.8.3	Casagrande Classification System.	35
2.9	Examples	37
2.10	Exercises.	46
3.	SOIL WATER AND SEEPAGE	50
3.1	Soil Water	50
3.1.2	Classification of Soil Moisture	50
3.2	Permeability	63
3.2.1	General	63
3.2.2	Laboratory Measurement of Permeability	64
3.2.3	Sources of Errors in the Determination of Permeability Coefficient	68
3.2.4	Factors Affecting Permeability	68
3.2.5	Coefficient of Permeability Value	69
3.2.6	Field Measurement of Permeability	69
3.2.7	Permeability of Natural Deposits	73
3.3	Seepage Through Soils	77
3.3.1	Differential Equation for Seepage	77
3.3.2	Flow Nets	81
3.3.3	Construction of Flow Nets	83
3.3.4	Determination of Discharge from Flow Net	84
3.4	Seepage Through Homogeneous Earth Embankments	86
3.4.1	General Consideration	86
3.4.2	Analytical Procedure of Determination of Discharge and Seepage	87
3.5	Seepage Through Stratified Soils	97
3.6	Effect of Core-Wall on Seepage	98
3.7	Filters	101
3.8	Effective and Total Stresses in Soils	102
3.8.1	General	102
3.8.2	Derivation of Formulas	104
3.9	Critical Hydraulic Gradient	106
3.10	Seepage Forces	107
3.11	Uplift Pressure	109
3.12	Examples	110
3.13	Exercises	119

4.	STRESS DISTRIBUTION IN SOILS	122
4.1	Stress due to Soil Weight	122
4.2	Stress due to Concentrated Surface Loading	122
4.3	Stress due to Uniform Line Loading	126
4.4	Stress due to Uniformly Distributed Surface Load	126
4.5	Stress due to Non-Uniformly Distributed Surface Load	130
4.6	Stress due to Uniformly Distributed Load by Approximate Method	137
4.7	Examples	139
4.8	Exercises	152
5.	COMPRESSIBILITY AND CONSOLIDATION OF SOILS	154
5.1	Compressibility of Soils	154
5.1.1	General	154
5.1.2	Measurement of Compressibility	155
5.1.3	Void ratio-Pressure Diagram	157
5.1.4	Coefficient of Compressibility	158
5.1.5	Compression Index	
5.1.6	Swelling Index	163
5.1.7	Modulus of Compressibility	163
5.2	Influence of Time on the Development of Strain	167
5.3	Consolidation	168
5.3.1	General	168
5.3.2	Mechanics of Consolidation	169
5.3.3.	General Outline of Terzaghi - Froelich 's Theory of Consolidation	172
5.3.4	Mathematical formulation of Terzaghi - Frohlich 's Theory of Consolidation	176
5.3.5	General Description of Consolidation Test and Determination of Time Settlement Parameters	176
5.4	Settlement of Structures	186
5.4.1	General	186
5.4.2	Settlement Analysis	187
5.4.3	Correction of Settlement	199
5.5	Examples	204
5.6	Exercises	213

6.	SHEARING STRENGTH OF SOILS	217
6.1	General	217
6.2	General Consideration of Friction between Solid	218
6.3	Shearing Strength of Granular Soils	219
6.4	Shearing Strength of Cohesive soils	
6.5	Shearing Strength of soils with both Cohesion and Friction	221
6.6	Shear Tests	221
6.6.1	Direct Shear Test	222
6.6.2	Triaxial Compression Test	223
6.6.3	Unconfined Compression Test	226
6.7	Shear Characteristics of Granular soils	227
6.7.1	Angle of Internal Friction	227
6.7.2	Saturated Granular Soil	234
6.8	Shear Characteristics of Clays	234
6.8.1	Normally Loaded Clays	230
6.8.2	Precompressed Clays	230
6.9	Stress at a Point	230
6.9.1	General	230
6.9.2	Derivation	231
6.9.3	Mohr Circle	233
6.9.4	Mohr Strength Theory	235
6.9.5	Relationships Derived from Mohr Strength Theory	236
6.10	Application of Mohr Diagram to Conventional Shear Tests	238
6.10.1	Triaxial Compression Test	238
6.10.2	Direct Shear Test	239
6.10.3	Unconfined Compression Test	240
6.10.4	Drainage During Shear	240
6.11	Examples	245
6.12	Exercises	253
7.	EARTH PRESSURES	256
7.1	General	256
7.2	Earth Pressure Theories	260
7.2.1	Rankine ' s Earth Pressure Theory	260
7.2.2	Influence of Wall Friction on Rankine Theory	275
7.2.3	Coulomb ' s Earth Pressure Theory	275

7.2.4	Culmann 's Graphical Construction	279
7.2.5	Semi-Graphical Methods for Determining the Passive Resistance in Soils	282
7.2.6	Tables for Active and Passive Pressure	290
7.2.7	Earth Pressure at Rest	292
7.3	Sheet Piles	292
7.3.1	General	292
7.3.2	Types of sheet Piles	293
7.3.3	Graphical Methods of Analysis	301
7.3.4	Comparison Between Free Earth and Fixed Earth Support Methods	301
7.4	Arching Effect	303
7.5	Examples	309
7.6	Exercises	333
8	STABILITY OF SLOPES	337
8.1	General	337
8.2	Slope Movements	337
8.2.1	Soil-Creep	337
8.2.1	Mass Slides	338
8.2.3	Flow Slides	338
8.3	Factor of Safety	338
8.4	Methods of Analysis	339
8.4.1	Infinite Slope	340
8.4.2	Simple Slope	346
8.5	Examples	365
8.6	Exercises	375
9	BEARING CAPACITY OF SOILS	377
9.1	General	377
9.1.1	Ultimate Bearing Capacity	377
9.1.2	Allowable Bearing Capacity	377
9.2	Bearing Capacity of shallow Foundation	380
9.2.	General	380
9.2.2	Failure Zones Below Smooth Base: Footing Loaded at Ground Level	381
9.2.3	Failure Zones Below Rough Base: Footing Loaded at Ground Level	381
9.2.4	Ultimate Bearing Capacity of Shallow Foundation	382

9.3	Examples	415
9.4	Exercises	433
10	EXPANSIVE SOILS	436
10.1	General	436
10.2	Origin of Expansive Soils	436
10.3	Distribution of Expansive Soils	438
10.4	Mineralogy of Expansive Clay Soils	438
10.4.1	Kaolinite	438
10.4.2	Illite	438
10.4.3	Montmorillonite	440
10.5	Identification and Classification of Expansive Soils	440
10.5.1	Identification of Expansive Soils	442
10.5.2	Classification Methods of Expansive Clays	442
10.6	Swelling Potential and Swelling Pressure	447
10.6.1	General	447
10.6.2	Factors Affecting Swelling Potential	449
10.6.3	Laboratory Testing Methods for Determining Swelling Potential	452
11	IMPROVING SOIL CONDITIONS AND PROPERTIES	458
11.1	Soil Stabilization	458
11.1.1	General	458
11.1.2	Compaction	459
11.1.3	Excavation and Replacement	465
11.1.4	Mixing of Different Soils	466
11.1.5	Lime Stabilization	467
11.1.6	Cement Stabilization	467
11.1.7	Asphalt Stabilization	468
11.2	Injection and Grouting	468
11.3	Dynamic Stabilization	468
11.3.1	Vibroflotation	469
11.3.2	Blasting	469
11.3.3	Compaction Piles	469

viii CONTENT

11.4	Precompression	469
11.5	Drainage	470
11.6	Example	471
11.7	Exercises	472
11.8	REFERENCES	473
	SUBJECT INDEX	480

PREFACE

This text-book evolved from teaching materials originally prepared by the authors for the use of civil engineering students at the Faculty of Technology. After having used the teaching materials for several years, the authors found it necessary to upgrade them to a text-book. Hence, the preparation of this book came into being.

The text-book tries to present the fundamentals of soil mechanics as clearly as possible so as to enable the student to grasp the basic concepts. Subject matters are logically arranged and developed for the benefit of the students of civil engineering and practicing engineers. Some topics have been treated in great depth so as to be also of use to graduate students in the geotechnical area. Topics falling in these categories are those found in chapter 3, 7, 8 and 9.

Chapter 10 has been devoted to expansive soils which are rarely treated in other soil mechanics text-book. It is hoped that the inclusion of this chapter will serve as an introduction into special geotechnical problems that have drawn a lot of attention here and in other countries as well.

At the end of each chapter ample examples have been worked out and additional exercise have been assigned.

ACKNOWLEDGEMENTS

The authors wish to express their gratitude to Research and Publication Office of Addis Ababa University for granting financial assistance for the preparation of the book. Sincere thanks are due also to W/ro Almaz Abera and W/ro Emeyu Yoseph for word processing the manuscript and Ato Daniel Ababayehu for the preparation of the diagrams. Last but not least the authors wish to express their sincere gratitude to their families for their understanding and encouragement throughout the arduous task of preparation of this text-book.

Alemayehu Teferra
Mesfin Leikun

September 1995

1. INTRODUCTION

1.1 GENERAL

In engineering, soils are considered to include all organic and inorganic earth materials occurring in the zone overlying the rock crust. They are usually non-homogeneous porous material whose engineering behaviour is greatly affected by changes in moisture content and density. The engineering definition of soil is quite different from the agronomist definition of the same. According to this discipline, soil is considered as the earth mold capable of supporting plant life. In geology-soil has different connotations and may simply be stated as a material found in the relatively thin surface zone.

Soil Mechanics is the science which deals with the engineering properties and behaviour of soils under stress. By applying the laws of mechanics and hydraulics, it attempts to give solutions to Civil Engineering problems such as

- (a) the determination of allowable soil pressure under buildings or bridge piers etc. (Fig. 1.1 a,b,c)
- (b) evaluation of the magnitude and distribution of earth pressures against various structures (Fig. 1.1 d,e)
- (c) prediction of water movement through soil.
- (d) evaluation of stability of dams and embankments. (Fig. 1.1 f,g)
- (e) analysis and design of dams.
- (f) improvement of soil properties by chemical or mechanical methods.

1.2. SOIL FORMATION

1.2.1. Weathering of Rocks

Soils are formed from igneous or metamorphic rocks by many processes of nature, both physical and chemical. Mechanical weathering is the fragmentation of rock by physical

forces, in which the crystal structure of the material remains unchanged. Among the many physical forces responsible for the degradation of rock (or mechanical splitting) the following may be cited.

(a) *Temperature changes*

Temperature fluctuations cause unequal expansion and contraction within the rock mass resulting in the spalling of the layers of rock and disintegration.

(b) *Freezing action of water*

Water that enters the pores and small cracks freezes during cold periods. As the water freezes it increases in volume thereby exerting pressure against the sides of the cracks. This enlarges the cracks and loosens particles of rock.

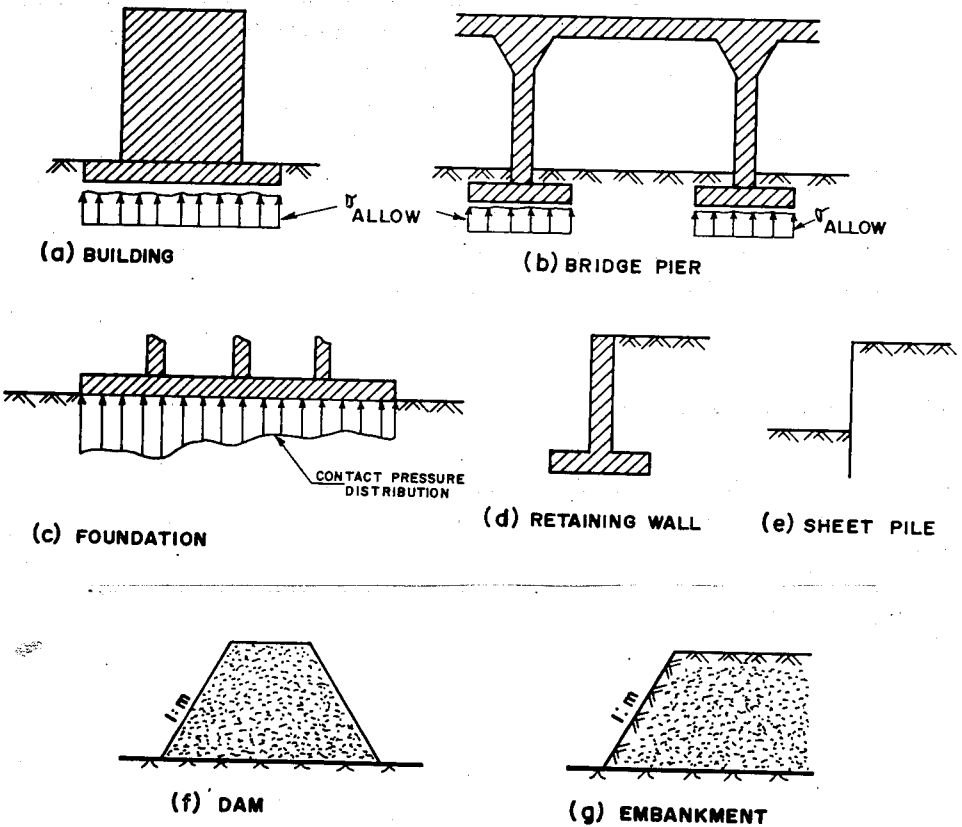


Fig 1.1 Some fundamental problems in Soil Mechanics

(c) *Wedging action of plant roots*

Small rootlets of trees and shrubs may grow into cracks in rocks in search of moisture and plant food. As these rootlets grow, they act as wedges which gradually force the rock segments apart.

(d) *Impact action*

The impact action of flowing water, ice, and of wind-borne sand particles serve to scour and erode rock strata and rock fragments.

Chemical weathering is the result of attack on rock minerals by water or oxygen or by alkaline or acid materials dissolved in the soil water. Carbon dioxide from the air and organic matter in the top soil are common sources of such dissolved acids. The most common processes of decomposition in this regard are oxidation (in which oxygen unites with rock minerals), carbonation (in which rock minerals are attacked by carbonic acid) and solution. Chemical decomposition (weathering) of rocks go hand in hand with the physical weathering and the two process mutually accelerate each other.

1.2.2 Transportation and Deposition of Soils

The soils resulting from the weathering of rocks stay in their place of formation, in which case they are referred to as *residual soils*. If they are carried away by such transporting agencies as wind, water, and ice and deposited at another location, they are known as *transported soils* or *sediments*.

Transported soils are mixed with soils of different origin in the course of transportation. They also disintegrate and alter still further. With the decreasing velocity of the water, or wind transporting them, the coarser particles are deposited first followed by fine particles. Thus transported soils are sorted out according to grain sizes.


1.3. COMMON SOIL TYPES

- (1) Sand, gravel, and boulders are coarse-grained cohesion-less soils. Grain size ranges are used to distinguish between them. Boulder refers to sizes greater than 20-30 cm. Particles larger than 2mm are generally classified as gravel.

- (2) Organic silt is a fine grained soil somewhat plastic, highly compressible, relatively impervious. It is a very poor foundation material because of compressibility.
- (3) Inorganic silts (rock flour) contain only mineral grains and are free from organic material. They are mostly coarser than 0.002mm. They may be incompressible depending upon whether they contain bulky or flat grains.
- (4) Clay is composed of microscopic particles of weathered rock. Within a wide range of water content, clay exhibits plasticity. Organic clay contains some finely divided organic particles. Organic clays are highly compressible when saturated and their dry strength is very high.
- (5) Black Cotton Soils are clay soils which are highly expansive. They contain a large percentage of montmorillonite. Because of their expansive nature when in contact with moisture, they present foundation problem.
- (6) Hardpan is a term often used to describe any hard cemented layer which does not soften when wet.
- (7) Peat is composed of fibrous particles of decayed vegetable matter. It is so compressible that it is entirely unsuitable to support any type of foundation.

2. INDEX PROPERTIES AND CLASSIFICATION OF SOILS

2.1 General

 *Index properties* are bases for distinguishing soils. Index properties may be divided into two main categories namely, soil grain properties and soil aggregate properties. The *soil grain properties* are the properties of the individual grains as expressed by size, shape and mineralogical characteristics. The *soil aggregate properties* are the properties of the soil mass as a whole. The soil mass is commonly considered to consist of solids and voids. The void spaces, often called pores or pore spaces may be partially or wholly filled with water or air. Although the solids and voids in a soil sample do not occupy separate spaces, they are represented in a block diagram as having separate weights and occupying separate volumes (Fig. 2.1).

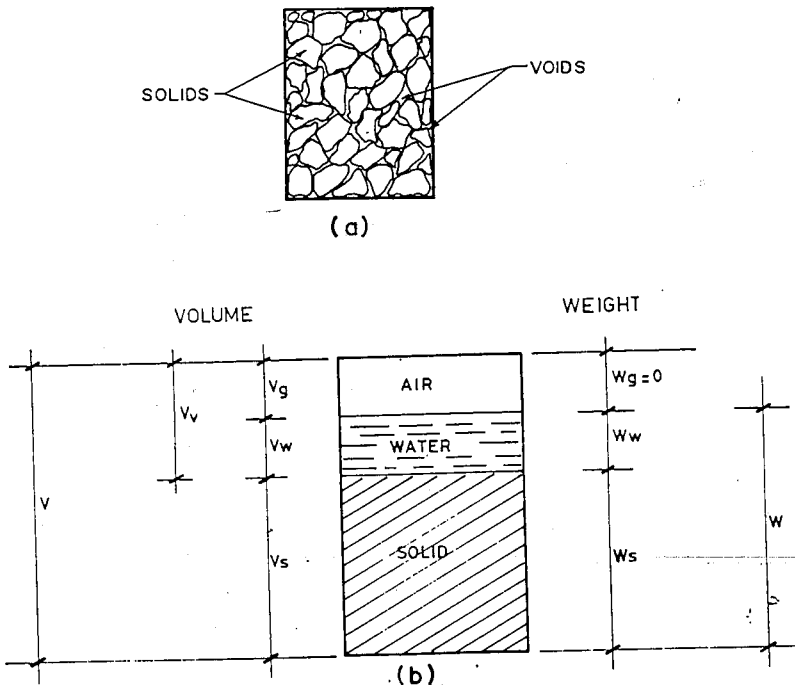


Fig. 2.1 Block diagram

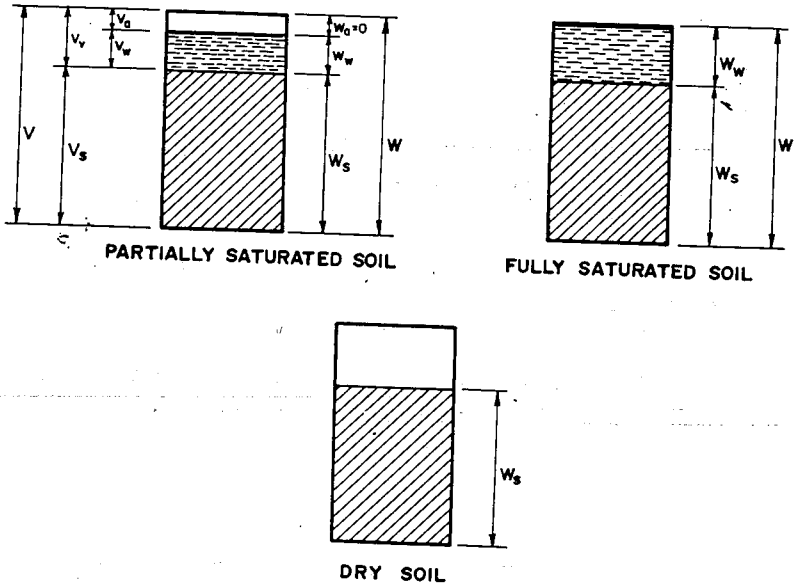


Fig 2.2 Phase diagram

A given volume of soil system may be considered as a system consisting of three fundamental phases (Fig. 2.2) which are:

- a. The *solid phase* or skeleton which may be mineral, organic or both.
- b. The *liquid phase* filling part or all of the voids between the soil particles.
- c. The *gaseous or vapour phase* which occupies that part of the voids which is not occupied by liquid.

Basically, there is no real means of separating the soil phase as shown in the sketch. The separation of solids from the voids can only be imagined. Such theoretical phase separation is very convenient for the visualization of the phase relationships and for the solution of problems.

2.2 VOLUME RELATIONSHIPS

The total volume of a given soil mass is designated by V . (Fig. 2.1b).

$$V = V_s + V_v$$

where V_s = volume of solids

(2.1)

V_v = total volume of voids

$V_v = V_a + V_w$

V_a = volume of air or gas in the voids

V_w = volume of water in the voids

$V = V_s + V_a + V_w$

2.2.1. Void Ratio and Porosity

★ The void ratio of the soil mass is defined as the ratio of the volume of voids to the volume of solids. It is usually designated by e and expressed as a ratio

$$e = \frac{V_v}{V_s} \quad (2.2)$$

★ The porosity of the soil mass is defined as the ratio of the volume of the voids to the total volume of the soil mass. It is designated by n and is expressed as a percentage.

$$n = \frac{V_v}{V} (100) \quad (2.3)$$

Substitution of equations (2.2) and (2.3) in equation (2.1) yields the following relationships.

$$V = V_s + V_v$$

$$e = \frac{V_v}{V_s}$$

$$n = \frac{V_v}{V}$$

$$V = \frac{V_v}{n}$$

$$\frac{V_v}{n} = V_s + V_v$$

$$V_v = nV_s + nV_v$$

$$V_v (1 - n) = nV_s$$

$$n = \frac{V_v}{V_s} (1-n) = e(1-n)$$

$$e = \frac{n}{1-n} \quad (2.4)$$

$$V = V_s + V_v$$

$$V = V_s + eV_s = V_s(1+e)$$

$$n = \frac{V_v}{V} = \frac{eV_s}{V_s(1+e)} = \frac{e}{1+e} \quad (2.5)$$

2.2.2 Degree of Saturation

The moisture content of soil may vary from zero if the soil is perfectly dry to a maximum value when the soil is saturated.

The degree of saturation is the actual amount of moisture in soil expressed as a percentage of maximum amount which it would contain if saturated. The degree of saturation is designated by S .

$$S = \frac{V_w}{V_v} (100) \quad (2.6)$$

2.3 WEIGHT RELATIONSHIPS

The total weight of the soil mass, W , consists of the following (Fig. 2.1b).

$$W = W_w + W_s \quad (2.7)$$

where W_w = weight of water
 W_s = weight of solids

$$S = \frac{W_w}{W_s} \times 100$$

2.3.1. Moisture Content

The moisture content of soil refers to the total amount of water contained in the soil either as free water or capillary water. It is always expressed as a percentage of the weight of solids in the soil.

$$\omega = \frac{W_w}{W_s} (100) \quad (2.8)$$

In the laboratory the moisture content is determined first by weighing a representative sample of soil in its natural or wet state. The sample is then dried for 24 hrs in an oven at a temperature of 105° C and then weighed. The difference between the weights of the sample before and after drying represents the amount of water in the sample. This weight, computed as a percentage of the dried sample, is the moisture content of the soil.

2.3.2 Unit Weight of Solids

This is defined as weight per unit volume of solids. The expression for the unit weight of solids may be written as

$$\gamma_s = \frac{W_s}{V_s} \quad (2.9)$$

where γ_s = unit of weight of solid matter
 W_s = weight of solid matter
 V_s = volume of solid matter

2.3.3. Specific Gravity

2.3.3.1. True or Absolute Specific Gravity

The specific gravity of solid matter in a soil particle may be defined as the ratio of the unit weight of solid matter to the unit weight of water. The specific gravity of the solid particles without the void spaces is called the *true* or *absolute* or *real* specific gravity and is usually designated by a letter G_s .

An expression for specific gravity for solid matter may be written as follows:-

$$G_s = \frac{\gamma_s}{\gamma_w}$$

$$G_s = \frac{W_s}{V_s \gamma_w} \quad (2.10)$$

where G_s = specific gravity of solid matter
 γ_w = unit weight of water

The ordinary range in value of G_s is from about 2.5 to 2.8. For many approximate calculations it is adequate to assume G_s as 2.65 or 2.7.

2.3.3.2. The Bulk Specific Gravity (Apparent Specific Gravity)

This is defined as the ratio of the dry weight of a unit volume of soil (volume of solids plus volume of voids) to the unit weight of water. It is designated by a letter G_b and expressed as follows.

$$G_b = \frac{W_s}{(V_s + V_v)\gamma_w} = \frac{W_s}{\gamma_w V} \quad (2.11)$$

Where G_b = bulk specific gravity
 W_s = weight of solids (or dry weight of soil)
 V = total volume of soil

2.3.3.3 Determination of Specific Gravity

The specific gravity determination of a sample of soil is made by displacement in water using pycnometer (volumetric bottle). The specific gravity we get by this method is the absolute specific gravity. In this test a known weight of oven dried soil sample is carefully put in a pycnometer which is then half filled with distilled water. The air entrapped in the soil sample is removed by heating or by means of vacuum pumps. The bottle is then topped up with distilled water upto a calibration mark and brought up to a constant temperature. The calculation proceeds as follows:

$$\text{Weight of pycnometer bottle + water} = W_2$$

$$\text{Weight of pycnometer bottle + water + soil} = W_1$$

$$\text{Weight of dry soil} = W_s$$

Let the weight of displaced water be equal to W_{wD}

$$W_2 + W_s = W_1 + W_{wD}$$

$$W_{wD} = W_s + W_2 - W_1$$

$$\text{Volume of displaced water} = \frac{W_s + W_2 - W_1}{\gamma_{wT}}$$

$$\text{Since, } G_T = \frac{\gamma_T}{\gamma_w}$$

$$\gamma_{wT} = G_T \gamma_w$$

where

G_T = specific gravity of water at temperature T

γ_T = unit weight of water at temperature T

$$\text{Volume of displaced water} = \frac{W_s + W_2 - W_1}{G_T \gamma_w}$$

This is equal to the volume of solids V_s . Hence, $V_s = \frac{W_s + W_2 - W_1}{G_T \gamma_w}$

$$\text{Since } G_s = \frac{\gamma_s}{\gamma_w} = \frac{W_s/V_s}{\gamma_w}, \text{ then}$$

$$G_s = \left[\frac{W_s G_T \gamma_w}{W_s + W_2 - W_1} \right] \left[\frac{1}{\gamma_w} \right] = \frac{W_s \cdot G_T}{W_s + W_2 - W_1} \quad (2.12)$$

2.3.4 Unit Weight of Soil

This is generally defined as the weight per unit volume of soil mass. Under varying circumstances, the weight may be weight of solids only, or weight of solids plus weight of pore water or submerged weight of solids. The volume, however, is always the volume of soil plus volume of voids. The unit weight of soil is designated by γ . The general expression of unit weight of soil is written in the following manner.

$$\gamma = \frac{W}{V} \quad (2.13)$$

where

γ = unit weight of soil

W = weight of soil

V = total volume of soil (or volume of solids plus volume of voids)

The general equation may be taken as unit wet weight, unit dry weight, or unit submerged weight depending upon the condition prevailing.

2.3.4.1. Unit Dry Weight

This is defined as weight of solids (or dry soil) per unit volume of soil.

$$\gamma_{dry} = \frac{W_s}{V} \quad (2.14)$$

$$= \frac{W_s}{V_s + V_v}$$

$$= \frac{W_s}{V_s \left(1 + \frac{V_v}{V_s}\right)} = \frac{W_s}{V_s} \cdot \frac{1}{\left(1 + \frac{V_v}{V_s}\right)}$$

$$\gamma_{dry} = \gamma_s \cdot \frac{1}{(1 + e)}$$

From equation (2.9) $\gamma_s = G_s \cdot \gamma_w$. Hence,

$$\gamma_{dry} = \frac{G_s \gamma_w}{1+e} \quad (2.15)$$

2.3.4.2. Unit Wet Weight

The unit wet weight of soil is defined as total weight per unit volume of moist or wet soil.

$$\gamma_{wet} = \frac{W}{V} \quad (2.16)$$

$$= \frac{W_s + W_w}{V_s + V_v}$$

$$= \frac{W_s \left(1 + \frac{W_w}{W_s}\right)}{V_s \left(1 + \frac{V_v}{V_s}\right)}$$

Using equations (2.8) and (2.9) $\gamma_{wet} = \frac{W_s(1+\omega)}{V_s(1+e)}$

$$\gamma_{wet} = \frac{\gamma_s(1+\omega)}{(1+e)} = G_s \gamma_w \frac{(1+\omega)}{(1+e)} \quad (2.17)$$

Another expression of unit wet weight can be developed using volume relationships.

$$\gamma_{wet} = \frac{W_s + W_w}{V_s + V_v}$$

Since $W_s = G_s \gamma_w V_s$, $W_w = V_w \gamma_w$ or $W_w = SV_v \gamma_w$

$$\begin{aligned} \text{then } \gamma_{wet} &= \frac{G_s \gamma_w V_s + SV_v \gamma_w}{V_s + V_v} \\ &= \frac{\gamma_w (G_s + e.S)}{1 + e} \end{aligned} \quad (218)$$

2.3.4.3. Saturated Unit Weight

This is the unit weight of the soil sample when the voids are completely filled with water.

$$\gamma_{sat} = \frac{\text{Saturated Weight}}{\text{Total Volume}}$$

Equation (2.18) which is given for γ_{wet} , may be used to determine γ_{sat} for the condition that $S=1$

$$\gamma_{sat} = \frac{\gamma_w (G_s + e)}{(1 + e)} \quad (219)$$

One may express γ_{sat} in terms of ω by deriving a relationship between S , e , ω and G_s

$$\gamma_{sat} = \frac{\gamma_w (G_s + \omega.G_s)}{1 + e}$$

$$\omega = \frac{W_w}{W_s}$$

$$W_w = V_v \gamma_w S$$

$$W_s = V_s \gamma_w G_s$$

$$\omega = \frac{V_v \gamma_w S}{V_s \gamma_w G_s} = \frac{eS}{G_s}$$

$$\omega G_s = eS \quad (2.20)$$

For fully saturated soil $S = 1$

$$\therefore e = \omega G_s$$

2.3.4.4 Submerged Unit Weight

This is defined as the unit weight of saturated soil mass minus the unit weight of water. It is designated by γ_b .

$$\begin{aligned} \gamma_b &= \gamma_{sat} - \gamma_w \\ &= \frac{(G_s + e)\gamma_w}{(1 + e)} - \gamma_w \\ &= \frac{\gamma_w(G_s - 1)}{(1 + e)} \end{aligned} \quad (2.21)$$

2.3.5. Relative Density

To judge whether a soil at a given void ratio, e , is to be described as dense or loose, it is essential to compare its existing void ratio with the range of possible void ratios for that particular soil. Such a comparison is made by means of relative density which is expressed by the following relationship. Relative density mostly applies to granular soil.

$$I_D = \frac{e_{max} - e}{e_{max} - e_{min}} \quad (2.22)$$

Where

- I_D = relative density (expressed in percent)
- e_{max} = void ratio of the soil in the loosest possible state
- e_{min} = void ratio of the soil in the densest possible state
- e = void ratio of the soil in the natural state

A soil in its loosest possible condition would have a relative density of zero and in its densest condition 100%.

Soils are normally classified on the basis of their relative density as indicated below

Classification	Relative Density, I_D in %
Loose	0 - 50
Firm	50 - 70
Dense	70 - 90
Very Dense	90 - 100

2.4 SIZE AND SHAPE OF SOIL PARTICLES

The sizes of soil particles vary in general from boulders to that of a large molecule. Sizes larger than 0.06 mm are termed coarse fractions and sizes ranging from 0.06 mm to .001mm are termed fine fractions. These fractions may be separated by mechanical analysis. The shape of soil particles ranges from spherical to needle like or thin plate like structure.

2.5 GRAIN SIZE DISTRIBUTION

The sizes of soil particles and their distribution throughout the soil mass are important factors which influence soil properties and performance. Particle size is expressed in terms of single diameter. For the larger particles this is taken as being equal to the size of the smallest square hole of a sieve through which the particle will pass.

There are two methods commonly used for the determination of grain size distribution of soil. They are sieve and hydrometer analyses.

A sieve analysis is often used for the determination of grain size distribution of coarse-grained materials while a hydrometer analysis is usually employed for determining the grain size distribution of the fine grained soils.

The determination of grain size distribution by these methods is known as mechanical analysis.

2.5.1 Sieve Analysis

For determining the grain size distribution of soil, a known weight of dry soil specimen is placed on a set of sieves arranged according to their size and shaken for about ten minutes on a sieve shaker. The soil retained on each sieve is weighed. Percentage retained on any sieve is expressed as

$$\text{Per cent retained} = \frac{\text{Wt. of soil retained}}{\text{Total weight}} (100)$$

The finest sieve used in mechanical analysis is usually the one corresponding to 0.074mm (100 mesh) according to ASTM.

2.5.2 Hydrometer Analysis

If the soil contains a large portion of grains below 0.074 mm diameter, the grain size distribution of this fine fraction is determined by means of hydrometer analysis or wet analysis. The hydrometer analysis is based on Stokes law which states that spherical grains of different sizes fall through a liquid at different velocities. According to this theory, spherical soil particle falling through a liquid will have first a velocity increasing rapidly under the influence of gravity, but within few seconds assume a constant terminal velocity which is maintained indefinitely. The terminal velocity of spherical soil particle settling in water is expressed by Stoke's law as:

$$v = \frac{\gamma_s - \gamma_w}{18\mu} D^2 \quad (2.23)$$

where

γ_s = unit weight of soil grains

γ_w = unit weight of water

μ = viscosity of water

D = diameter of the spherical particle

v = velocity of the spherical particle

In practice soil particles are never truly spherical. To overcome this, particle size is defined in terms of equivalent diameter. Any particle which sinks in water with the same velocity as an imaginary sphere of the same unit weight and of diameter D, will be said to have an equivalent diameter D.

2.5.3 Grain Size Distribution Curve

The results of grain size analysis are usually presented in the form of grain size distribution curve, known as gradation curve, on a semilogarithmic plot. The ordinate of this curve represents the percentage finer than any given diameter D, while the abscissa represents the size, D (usually expressed in mm) in a logarithmic scale.

The shape and slope of gradation curve indicate the type of gradation. A steep or broken slope indicates poor gradation for most engineering purposes. A gentle or even slope indicates good gradation. A soil is said to be *well graded* if all particles are represented fairly well while a soil is *poorly graded* if there is a deficiency or excess of certain sizes. Typical forms of gradation curve are as shown on Fig.2.3.

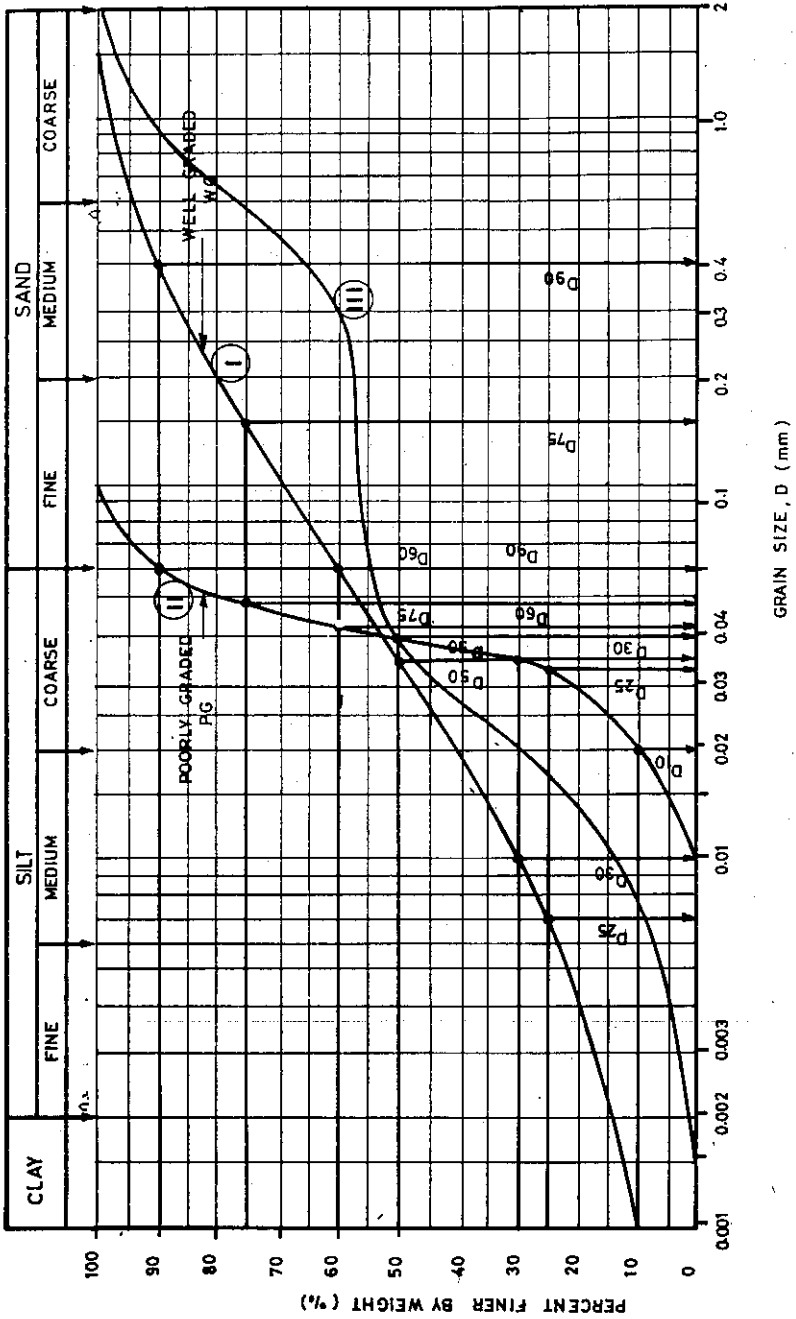


Fig. 2.3 Grain-size distribution curve

Curve I represents good gradation. Such material is relatively stable and resistant to scour or erosion. It can readily be compacted to a very dense condition and will develop high shearing resistance and bearing capacity. Curve II represents poor gradation. Such specimen is primarily composed of particles of single size (uniform soil). It will easily be displaced under load and has less supporting power.

Curve III shows skip-graded material. This is also a form of poor or uneven gradation because the specimen is lacking in particles of certain sizes.

To quantify the grain size distribution the following parameters are used.

Uniformity Coefficient

In order to determine if a material is well graded or poorly graded, its coefficient of uniformity is determined. Uniformity coefficient, C_u , is defined as the ratio of the diameter at the 60% finer point to that at 10% finer point on the gradation curve (Fig.2.3).

$$C_u = \frac{D_{60}}{D_{10}} \tag{2.24}$$

Where C_u = uniformity coefficient

D_{10} = diameter corresponding to 10% finer by weight which is also known as effective size.

D_{60} = diameter corresponding to 60% finer by weight

$C_u = 1$, usually indicates a soil in which the grains are practically of the same size (uniform soil). A large coefficient represents a well graded soil.

Concavity Coefficient

$$U_1 = \frac{D_{75}}{D_{25}} \tag{2.25}$$

Other measures of uniformity are:

$$U_2 = \frac{D_{30}}{D_{60} \cdot D_{10}} \tag{2.26}$$

$$\text{and } U_3 = \frac{D_{50}}{\sqrt{D_{10} \cdot D_{90}}} \tag{2.27}$$

Heaven 27/11/00
 2L 27/11/00
 27/11/00

2.5.4. Brief Outline of Experimental Procedure for Hydrometer Analysis

According to Lambe [17] 50 grams of soil passing sieve No.200 are agitated with water and dispersing agent in 1000 c.c. jar. The specific gravity of the suspension is then measured with a stream lined hydrometer at given intervals of time. The hydrometer reading, r , is observed at the surface of the fluid on a scale on the stem and this indicates the specific gravity of the suspension. Readings are usually taken at intervals of $\frac{1}{4}$, $\frac{1}{2}$, 1 and 2 minutes with the hydrometer remaining in the suspension all the time. For longer intervals, that is 5, 10, 20 etc. minutes the hydrometer is put in the suspension just before each reading and removed after each reading.

If a soil particle of size D , falls through a distance z in time, t , its velocity will be given as: Using Stokes' Law,

$$v = \frac{\gamma_s - \gamma_w}{18\mu} D^2 \tag{2.28}$$

$$v = \frac{z_r}{t}$$

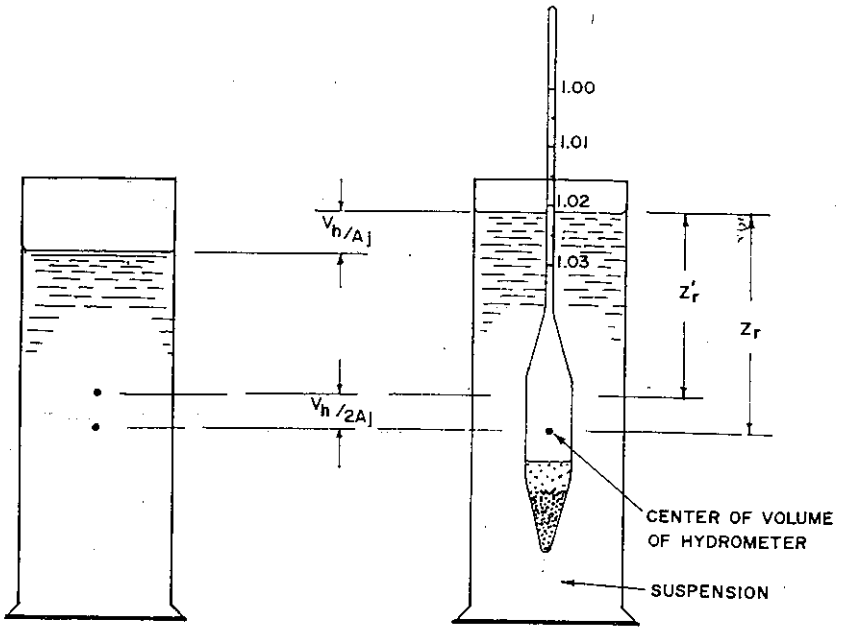
$$D = \sqrt{\frac{v 18\mu}{\gamma_s - \gamma_w}} = \sqrt{\frac{18\mu}{\gamma_s - \gamma_w} \cdot \frac{z_r}{t}} \tag{2.29}$$

After a time, t , all particles of diameter equal to and larger than D have settled through a depth z_r . All the remaining particles finer than D are still in suspension and their concentration need to be determined.

Equation (2.29) applies to early readings taken between $\frac{1}{4}$ and 2 minutes intervals. For the readings taken at intervals of 5, 10, 20, etc. minutes, emersion correction is applied to equation (2.29).

When the hydrometer is placed in the jar, it displaces its own volume as shown in Fig. 2.4. As a result, the surface of the suspension rises. If the hydrometer has a Volume = V_h and the jar a cross-sectional area A_j , then the surface of the suspension as indicated on the above

figure will rise by $\frac{V_h}{A_j}$. We realize that the hydrometer measures the specific gravity at



$$Z_r = H + \frac{1}{2}(h)$$

$$Z'_r = Z_r - \frac{V_h}{2A_j} = H + \frac{1}{2} \left(h - \frac{V_h}{A_j} \right)$$

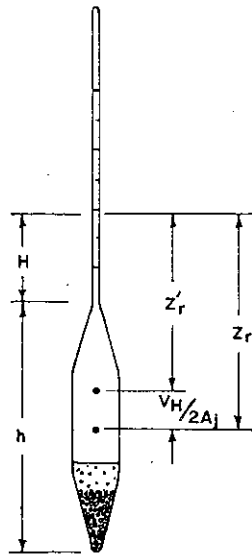


Fig. 2.4 Hydrometer method of grain-size analysis

the center of its bulb. The liquid now at the center of the bulb was previously at a lower level (i.e. before the insertion of the hydrometer). Since the displacement below the center of the

bulb is due to half of its volume, the liquid now at the center must be lower by $\frac{V_h}{2A_j}$

Therefore, actual distance of settlement is:

$$z'_r = z_r - \frac{V_h}{2A_j} \tag{2.30}$$

$$D = \sqrt{\left(\frac{18\mu}{\gamma_s - \gamma_w}\right) \left(\frac{z_r - \frac{V_h}{2A_j}}{t}\right)} \tag{2.31}$$

z'_r can be obtained from the calibration curve which is a plot of z' against hydrometer readings. The corrections that need to be applied to hydrometer readings are meniscus and temperature corrections.

Having known the limiting diameter D after t minutes, the concentration can be determined as follows:

Mass of solid in suspension = W (gm)

Mass of solids per unit volume of suspension = $\frac{W}{V}$ (gm/cm³)

Volume of solid per unit volume of suspension

$$= \frac{W/V}{\gamma_s} = \frac{W}{G_s V \gamma_w} \quad (\text{cm}^3)$$

Volume of water per unit volume of suspension = $1 - \frac{W}{G_s V \gamma_w}$ (cm³)

Mass of water per unit volume of suspension,

$$= \gamma_w \left(1 - \frac{W}{G_s V \gamma_w}\right) \quad (\text{gm/cm}^3)$$

$$= \gamma_w - \frac{W}{G_s V}$$

Density of suspension, $\gamma_i = \frac{W}{V} + \left(\gamma_w - \frac{W}{G_s V}\right)$ (gm/cm³)

The percentages of particles N smaller than D

$$= \frac{\text{weight of solids per cm}^3 \text{ at depth } z, \text{ after time } t}{\text{weight of solids per cm}^3 \text{ in the original suspension}} \quad (100)$$

Weight of solid finer than D per unit volume of suspension after

$$\text{time } t = \frac{NW}{V}$$

Weight of water per unit volume $= \gamma_w - \frac{NW}{G_s V}$

Unit weight, $\gamma = \frac{NW}{V} + \gamma_w - \frac{NW}{G_s V}$

$$\frac{NW}{V} - \frac{NW}{G_s V} = \gamma - \gamma_w$$

$$G_s NW - NW = G_s V (\gamma - \gamma_w)$$

$$NW (G_s - 1) = G_s V (\gamma - \gamma_w)$$

Percent finer than D, or $N = \frac{V}{W} \frac{G_s}{(G_s - 1)} (\gamma - \gamma_w)$

$$= \frac{G_s V \gamma_c}{W(G_s - 1)} (r - r_w)$$

where

γ_c = unit weight of water at temperature of hydrometer calibration (usually 20° C).

r = hydrometer reading in suspension

r_w = hydrometer reading in water at the same temperature as suspension

For combined analysis (i.e. sieve analysis + hydrometer analysis)

$$N' = \frac{NW}{W_s}$$

W = total weight of dry soil passing sieve No.200

W_s = total weight of dry soil used in the sieve analysis.

2.6 SOIL CONSISTENCY

Soil Consistency is a term often used to describe the degree of firmness of soil and is expressed by such terms as soft, firm or hard. It usually applies to fine grained soils whose condition is affected by changes in moisture content. As the consistency of soil changes, its engineering properties also change. Such soil properties as shearing strength and bearing capacity vary significantly with consistency.

2.6.1. Atterberg Limits

The Swedish scientist, Atterberg, developed a method of describing quantitatively the effect of varying water content on the consistency of fine grained soils. He established the four states of soil consistency (Fig 2.5) which are called the *liquid*, the *plastic*, the *semi-solid*, and the *solid* states. He also proposed a series of tests for determining the boundaries known as Atterberg limits between the physical states of soil. Each boundary or limit is defined by the water content that produces a specified consistency.

The liquid state is produced when a fine grained soil is mixed with a large quantity of water. In such state, the soil behaves like a liquid. That is, it flows freely like a liquid and has no resistance to deformation. If, however, its water content is gradually reduced, it will begin to show a small shearing strength. The limit at which soil suspension passes from no strength to a very small strength is the *liquid limit*. This limit is defined by moisture content of the soil at the point and is designated by ω_L .

At a moisture content lower than its liquid limit, the soil is in a *plastic state*. If the sample is subjected to a further decrease in moisture content, it will eventually lose its plasticity. The moisture content at which the sample, when it is rolled into a thread, starts to crumble rather than distort plastically, is called its *plastic limit* and is designated by ω_P .

After the plastic limit, the soil displays the properties of *semi-solid*. With a further decrease in moisture content, the soil sample will finally reach a point where it can no longer change in volume. At this point, the soil is said to have reached its *shrinkage limit* designated by ω_s .

The limits described above are all expressed by their percentage water contents.

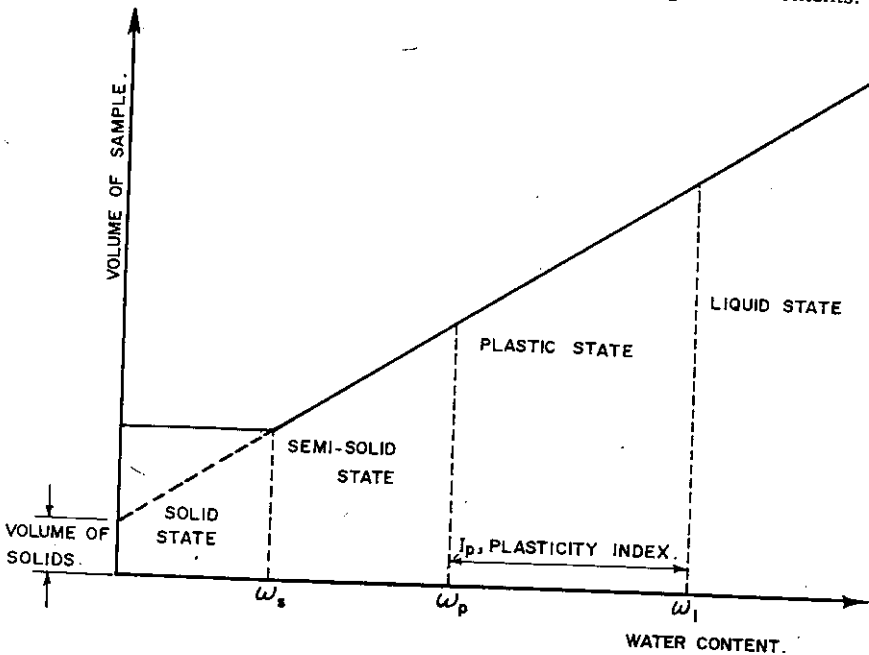


Fig. 2.5 Consistency limits

2.6.2. Engineering Definitions of Atterberg Limits

The *Liquid Limit* is defined as the water content at which a moist soil in a special cup cut by a standard groove closes after 25 taps on hard rubber plate.

The *Plastic Limit* is the water content at which the soil begins to break apart when rolled into a thread approximately 3mm (1/8 in) in diameter.

The *Shrinkage Limit* is the water content at which further loss of moisture does not cause a decrease in volume.

The *Plasticity Index* is the range of water content over which the soil exhibits plasticity. i.e the difference between the liquid limit and plastic limit.

$$I_p = \omega_L - \omega_p \quad (2.32)$$

The most important use of the Atterberg limits is in classifying fine grained soils. In addition, a number of relationships involving the Atterberg limits are useful in correlating soil behaviour with simple test data.

Liquidity Index relates the natural water content of the soil to the plastic limit and plastic index.

$$I_L = \frac{\omega - \omega_p}{I_p} \quad (2.33)$$

Where ω = natural water content

Relative Consistency is the ratio of liquid limit minus the natural water content of the soil over its plasticity index.

$$C_r = \frac{\omega_L - \omega}{I_p} \quad (2.34)$$

2.6.3. Determination of Atterberg Limits

2.6.3.1. Determination of Liquid Limit

A schematic diagram of a liquid limit device is shown in Fig. 2.6. To perform the liquid limit test, a moist soil is placed in the cup. A groove is cut at the center of the soil pat by means of standard grooving tool shown in Fig. 2.6. By turning the crank, the cup is lifted and dropped. The moisture content required to close the groove a distance of 1/2 in (1.27 cm) after 25 blows (drops) is designated as the liquid limit. Since it is difficult to adjust the moisture content in the soil to meet the required 1.27 cm closure of the groove in the soil pat at 25 blows, a minimum of three test trials for the same soil at varying moisture content are made and the required number of blows to close the groove a distance 1.27 cm are noted. The moisture contents of the soil in percent and the corresponding number of blows are plotted on a semi-logarithmic graph paper giving an approximate straight line called the flow curve. The moisture content corresponding to 25 blows ($N=25$) read from the flow curve gives the liquid limit of the soil (Fig. 2.6.).

Liquid limit can also be estimated from the following empirical equation [17]

$$\bar{\omega}_L = \omega_N (N/25)^n \quad (2.35)$$

Where

- N = number of blows in a liquid limit device for 1.27cm groove closure
- ω_N = corresponding moisture content
- n = 0.121

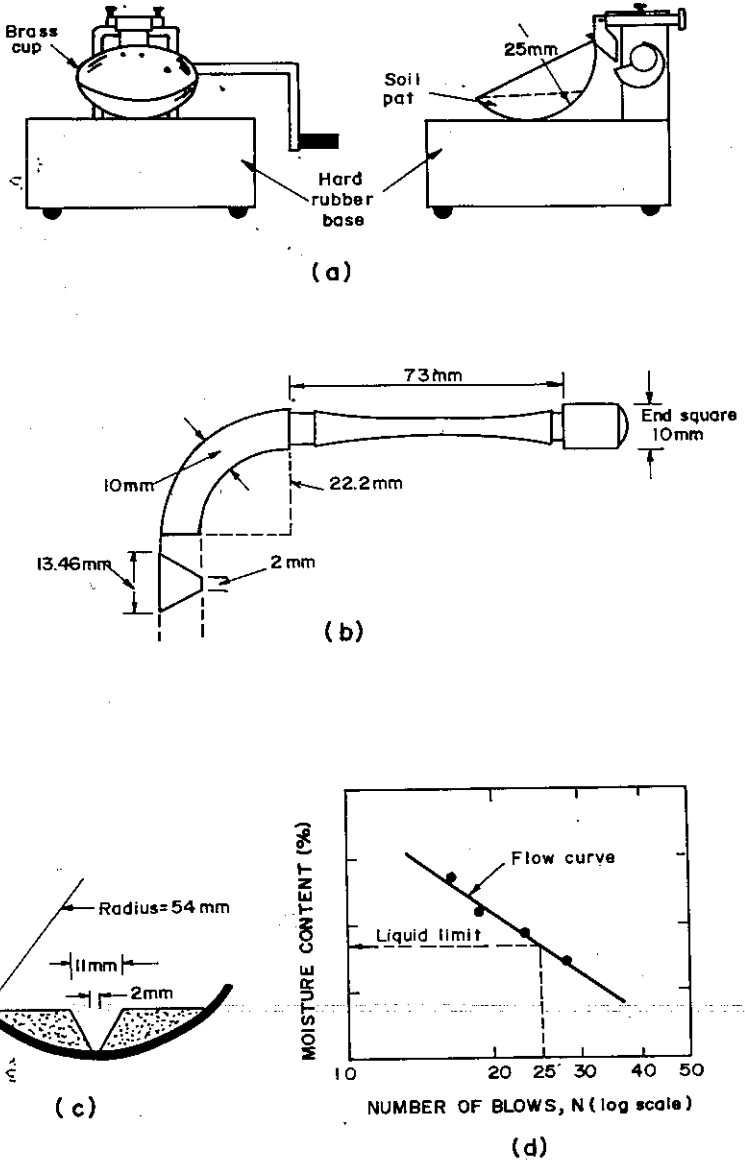


Fig. 2.6 Determination of liquid limit

2.6.3.2. Determination of Plastic Limit

A paste of soil is rolled into a thread on a smooth glass plate until the diameter is $1/8$ in (0.32cm) in diameter. As soon as the thread shows signs of cracking, the operation is stopped and the moisture content of the cracked portion of the thread is determined. A minimum of three trials are made with the same soil and an average of the resulting moisture contents is determined to give the plastic limit of the soil.

2.6.3.3. Determination of Shrinkage Limit

A container of volume V_1 (Fig. 2.7) is filled with a soil paste in a saturated state. The weight of the saturated soil is determined. The specimen is dried gradually, first in air and then in an oven kept at a temperature of 105°C .

Fig. 2.7a represents the saturated soil in a container of volume V_1 , Fig. 2.7b represents the air dried soil at shrinkage limit and Fig. 2.7c represents the dry soil after oven drying. Reduction in moisture content beyond the shrinkage limit does not cause any reduction in the total volume of the soil mass. Hence, the volume in Fig. 2.7b and Fig. 2.7c are the same.

The total volume of the dry soil is determined by immersing the pat of the dried soil in mercury and determining the volume of mercury displaced. The weight of the pat is also determined.

The shrinkage limit, ω_s , in per cent is given as,

$$\omega_s = \frac{W_w}{W_s} = \frac{(W_1 - W_s) - \gamma_w(V_1 - V_2)}{W_s} \quad (100) \quad (2.36)$$

W_1 = weight of saturated soil

V_1 = volume of saturated soil

W_s = weight of dry soil

V_2 = volume of dry soil

W_w = weight of water in the soil mass at the shrinkage limit

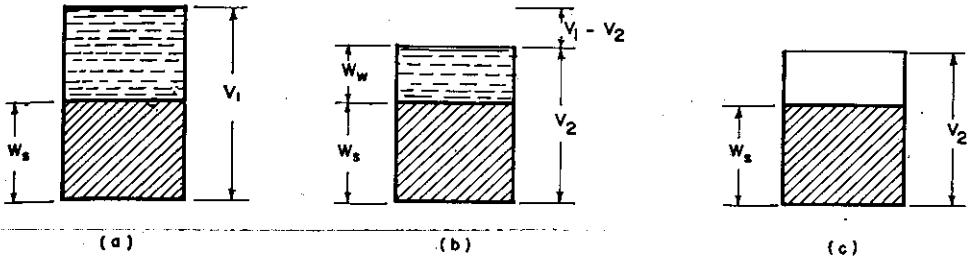


Fig 2.7 Determination of shrinkage limit

2.7 PROPERTIES OF CLAY PARTICLES

2.7.1 Surface Activity and Adsorbed Layer

The surface of fine fraction of soil carries negative electric charge whose intensity depends on the mineralogical character of the particle. The physical and chemical manifestation of the surface charge is called *surface activity*.

In nature, soil particles are normally surrounded with water. In the immediate vicinity of the soil particle, the negative charges attract the positive H^+ of the water. As a result water molecules in the neighbourhood are arranged in a definite pattern defining a certain zone of influence. The water located within the zone is called the *adsorbed layer*. In this layer the properties of the water are different from normal water.

In every clay particle the adsorbed layer contains ions (positive charges) which come from the water molecules since water also dissociates to a certain degree from H_2O to $H^+ + OH^-$. Since the clay particles are negatively charged, the positive charges i.e., H^+ go to the clay particles and base exchange takes place to form the *adsorption complex* (Fig. 2.8)

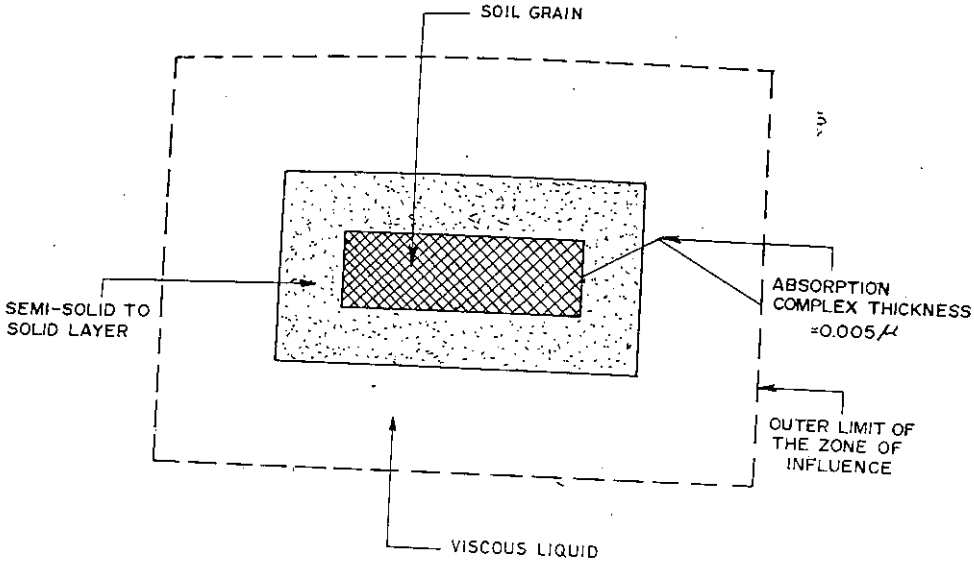


Fig 2.8 Schematic diagram of the adsorbed layer

Due to the property of the adsorption complex, the very fine soil fractions possess *cohesion* which contributes resistance to the soil during shearing deformation. The magnitude of this resistance may be reduced to a considerable degree by disturbing the adsorption complex, say by kneading the soil. However, the soil regains its strength back if allowed to stay for some time at the same moisture content. This phenomenon is called *Thixotropy*

2.7.2 Colloids

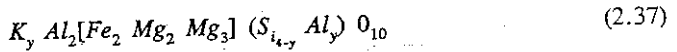
If the particles of any substance are so small that the surface activity has an appreciable influence on the properties of the aggregates, the substance is said to be in a *colloidal state* and the particles are called *colloidal particles*. The properties that are due exclusively to the influence of surface activity are known as *colloidal properties*. Because of the variations of the intensity of the surface activity for different particles, the upper limit for a colloidal size ranges between 2μ and 0.1μ . At 0.1μ every solid substance is in colloidal state.

2.7.3 Clay Minerals

With the help of X-ray techniques three main groups of clay minerals are identified. These are Illite, Kaolinite and Montmorillonite.

2.7.3.1 Illite

Illite is medium active mica like clay mineral and is a predominant constituent of many shells. The composition of the complex illite group may be written as follows [14]



Note: The y subscript varies between 1 and 1.5.

2.7.3.2 Kaolinite

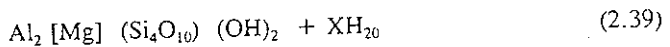
Kaolinite is least active of the three and occurs in soils in high temperature and humid tropical regions. Its general chemical formula is [14]



2.7.3.3 Montmorillonite

Montmorillonite is more colloidal than kaolinite and is an active clay mineral. By taking water molecules into its space lattice it swells considerably.

It has the following general chemical formula [14]:



Montmorillonite is the dominant clay mineral in bentonite. For example, calcium-bentonite absorbs water from 200% - 300% while sodium-bentonite absorbs from 600% - 700%.

2.8 CLASSIFICATION OF SOILS

A soil classification system is an arrangement of different soils into groups having similar properties. The purpose of soil classification is to make possible the estimation of soil properties by association with soils of the same class whose properties are known and to provide the engineer with accurate method of soils description. There are several methods of classifying soils. The most widely used classification systems by engineers are described hereunder.

2.8.1 Grain Size Classifications

The grain-size classification system is based on grain size of the soils and is essentially useful for classifying soils in which single properties are of importance. The classifications that are in common use are the following:

M.I.T. classification

Gravel	Sand			Silt			Clay
	Coarse	Medium	Fine	Coarse	Medium	Fine	
	2	0.6	0.2	0.06	0.02	0.006	0.002 (mm)

International Society of Soil Science Classification

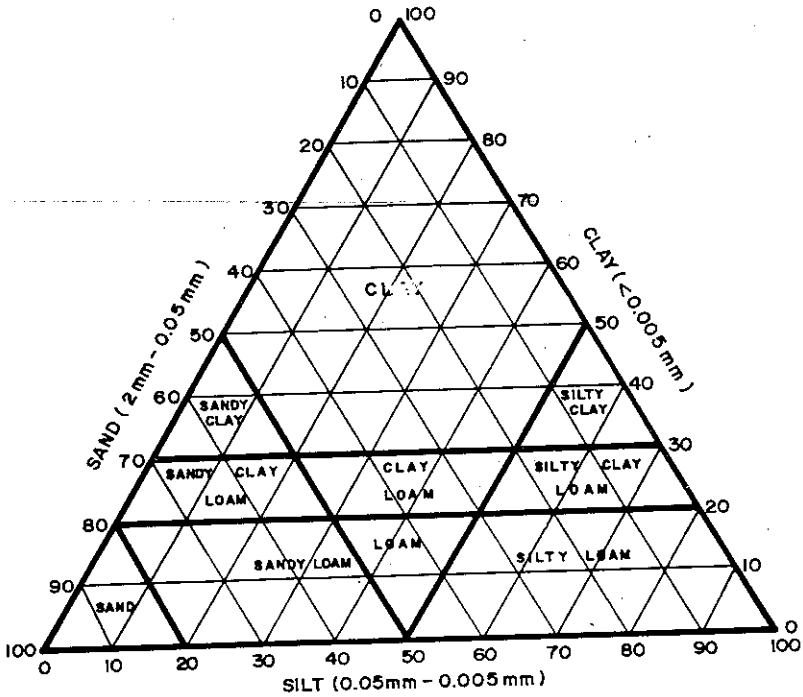
Gravel	Sand		Silt		Clay
	Coarse	Fine			
	2	0.2	0.02		0.002 (mm)

AASHO Classification

Gravel	Sand		Silt		Clay
	2		0.05		0.002 (mm)

2.8.2. U.S. Bureau of Soils Textural Classification

This classification is based on a triangular chart shown in Fig. 2.9. A soil with known percentage of sand, silt, and clay sizes is represented by a given point on a triangular chart of this type.



CLASS	%SAND	%SILT	%CLAY
1 SAND	80 - 100	0 - 20	0 - 20
2 SANDY LOAM	50 - 80	0 - 50	0 - 20
3 LOAM	30 - 50	30 - 50	0 - 20
4 SILTY LOAM	0 - 50	50 - 100	0 - 20
5 SANDY CLAY LOAM	50 - 80	0 - 30	20 - 30
6 CLAY LOAM	20 - 50	20 - 50	20 - 30
7 SILTY CLAY LOAM	0 - 30	50 - 80	20 - 30
8 SANDY CLAY	50 - 70	0 - 20	30 - 50
9 CLAY	0 - 50	0 - 50	30 - 100
10 SILTY CLAY	0 - 20	50 - 70	30 - 50

Fig. 2.9 The triangular soil classification chart

2.8.3 Casagrande Classification System (Unified System of soil Classification)

This system employs visual inspection, grain-size analysis and Atterberg limit tests in classifying soils. The coarse soils are classified by their grain size and fine grained soils are classified with the aid of plasticity chart. The names and symbols used to distinguish between the typical and boundary soil groups are as follows:

<u>Main Soil Types</u>	<u>Symbols</u>
Coarse grained soils	Gravel---G
	Sand----- S
Fine grained soils	Silt ----- M
	Clay ----- C
	Organic silt & clay---O
	Peat --- Pt

<u>Gradation</u>	<u>Liquid limit</u>
Well graded -W	High liquid limit - H
Poorly graded -P	Low liquid limit - L

The symbols indicated above are combined to form the group symbol. The plasticity chart (Fig. 2.10) is a plot of plasticity index versus liquid limit. Fine-grained soils are sub-divided into soils of low, medium and high plasticity following the criteria outlined below.

- Low plasticity $\omega_L < 35\%$
- Intermediate plasticity $\omega_L = 35\% - 50\%$
- High plasticity $\omega_L > 50\%$

The division between inorganic clays and inorganic silts is by an empirical line (A-line) having the following equation:

$$I_p = 0.73 (\omega_L - 20)$$

Clays fall above the A-line and silts below it.

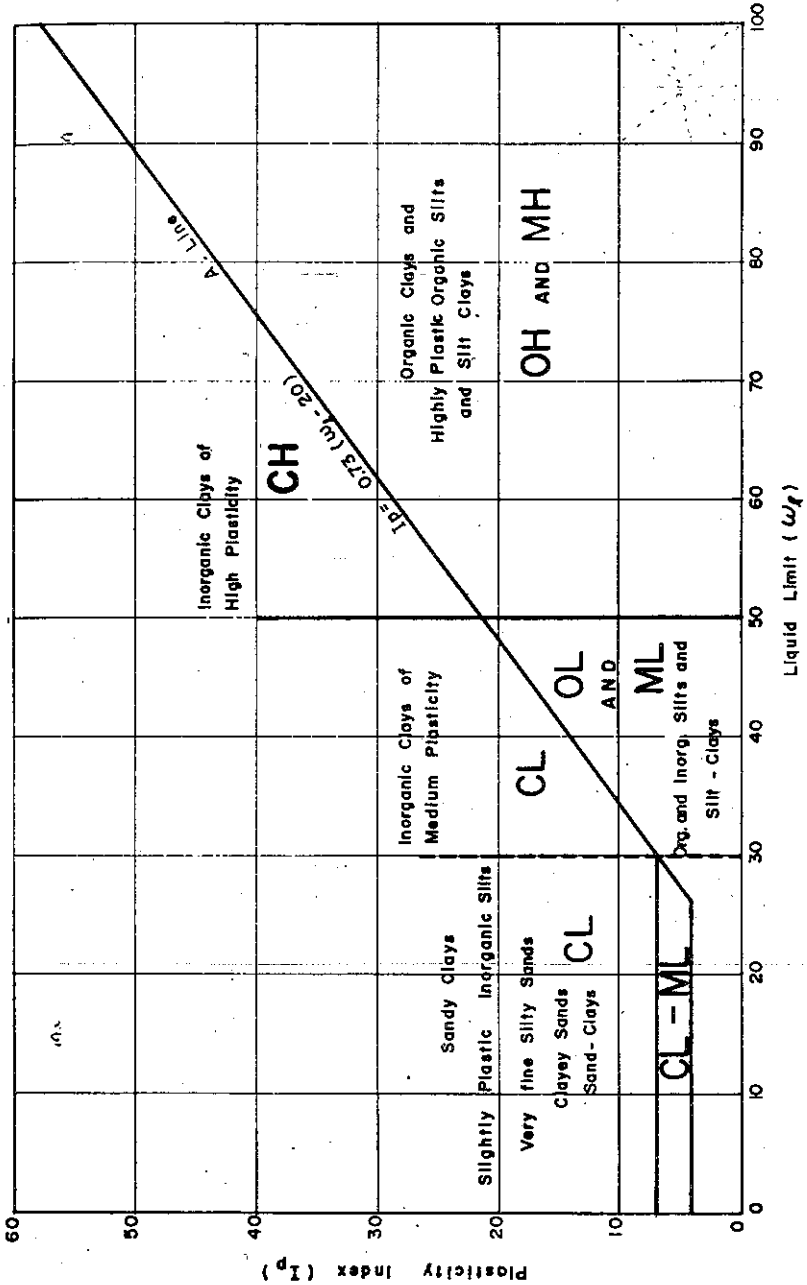


Fig. 2.10 Plasticity chart

2.9 EXAMPLES

E.2.1 A moist sand sample has a volume of 644 cm^3 in natural state and a mass of 793 gm . The dry mass is 735 gm and the specific gravity of soil grains is 2.68 . Determine the void ratio, the porosity, the water content and the degree of saturation.

SOLUTION

$$e = \frac{V_v}{V_s}$$

$$G_s = \frac{\gamma_s}{\gamma_w} = \frac{W_s}{V_s \cdot \gamma_w} = \frac{735}{V_s(1.0)}$$

$$2.68 = \frac{735}{V_s}$$

$$V_s = \frac{735}{2.68} = 274 \text{ cm}^3$$

$$V_v = 644 - 274 = 370 \text{ cm}^3$$

$$e = \frac{370}{274} = 1.35$$

$$n = \frac{V_v}{V} = \frac{370}{644}(100) = 57.5\%$$

$$\omega = \frac{W_w}{W_s}$$

$$W_w = 793 - 735 = 58 \text{ gm}$$

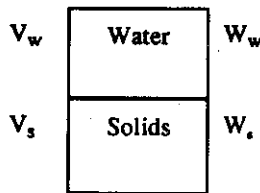
$$\omega = \frac{58}{735}(100) = 7.9\%$$

$$S = \frac{V_w}{V_v} = \frac{58}{370}(100) = 15.7\%$$

E.2.2^c A soil sample with a degree of saturation 100%, has a moisture content of ω and specific gravity of solid particle G_s is given. Express the void ratio and the dry unit weight in terms of the given quantities.

SOLUTION

METHOD I



$$V_w = \frac{W_w}{\gamma_w}$$

$$W_w = \omega \cdot W_s \quad (\text{since } \omega = W_w/W_s)$$

$$V_w = \frac{\omega \cdot W_s}{\gamma_w}$$

$$V_s = \frac{W_s}{G_s \cdot \gamma_w}$$

$$e = \frac{V_v}{V_s} = \frac{V_w}{V_s} = \frac{\frac{\omega \cdot W_s}{\gamma_w}}{\frac{W_s}{G_s \cdot \gamma_w}} = \omega \cdot G_s$$

$$e = G_s \cdot \omega$$

$$\gamma_d = \frac{W_s}{V_w + V_s} = \frac{W_s}{\frac{\omega \cdot W_s}{\gamma_w} + \frac{W_s}{G_s \cdot \gamma_w}} = \frac{1}{\frac{\omega}{\gamma_w} + \frac{1}{G_s \cdot \gamma_w}}$$

For $\gamma_w = 1$.

$$\gamma_d = \frac{1}{\omega + 1/G_s}$$

METHOD II

$$V_w = \omega \quad \begin{array}{|c|} \hline \text{Water} \\ \hline \text{Solids} \\ \hline \end{array} \quad \begin{array}{l} \omega = W_w \\ W_s = 1 \end{array}$$

$$V_s = 1/G_s$$

$$e = \frac{V_v}{V_s} = \frac{\omega}{1/G_s} = \omega G_s$$

$$\gamma_d = \frac{W_s}{V} = \frac{1}{\omega + 1/G_s} = \frac{G_s}{\omega G_s + 1}$$

METHOD III

$$V_w = e \quad \begin{array}{|c|} \hline \text{Water} \\ \hline \text{Solids} \\ \hline \end{array} \quad \begin{array}{l} \omega \\ G_s \end{array}$$

$$V_s = 1$$

$$e = \omega \cdot G_s$$

E.2.3 A sand sample has porosity of 30% and the specific gravity of solid of 2.7.

Compute:

- Dry unit weight of sand
- Unit weight of sand if $S = 56\%$
- Unit weight of saturated sand
- Effective unit weight of submerged sand

SOLUTION

$$n = \frac{V_v}{V}$$

Assume $V = 1 \text{ cm}^3$; $0.30 = \frac{V_v}{1}$

$$V_v = 0.30 \text{ cm}^3$$

$$\gamma_{dry} = \frac{W_s}{V}$$

$$V_s = 1 - 0.3 = 0.7 \text{ cm}^3$$

$$W_s = V_s G_s \gamma_w = (0.7)(2.7)(1) = 1.89 \text{ gm}$$

$$(a) \gamma_{dry} = \frac{1.89}{1} = 1.89 \text{ gm/cm}^3 = 18.9 \text{ kN/m}^3$$

$$\gamma_{wet} = \frac{W_s + W_w}{V}$$

$$S = \frac{V_w}{V_v}$$

$$\frac{56}{100} = \frac{V_w}{0.30}$$

$$V_w = (0.56)(.3) = 0.168 \text{ cm}^3$$

$$W_w = V_w \gamma_w = (0.168)(1) = 0.168 \text{ gm}$$

$$(b) \quad \gamma_{wet} = \frac{1.89 + 0.168}{1} = 2.058 = 2.06 \text{ gm/cm}^3 = 20.6 \text{ kN/m}^3$$

When fully saturated $V_w = V_v$

$$W_w = 0.3 (1) = 0.3 \text{ gm}$$

$$(c) \quad \gamma_{sat} = \frac{1.89 + 0.3}{1} = 2.19 \text{ gm/cm}^3 = 21.9 \text{ kN/m}^3$$

$$\begin{aligned} \gamma_b &= \gamma_{sat} - \gamma_w \\ &= 21.9 - 1 = 1.19 \text{ gm/cm}^3 = 11.9 \text{ kN/m}^3 \end{aligned}$$

E.2.4 A soil sample has a water content of 30% and specific gravity of solids of 2.7. Its unit weight is 15 kN/m^3 . Determine its

- void ratio
- porosity
- degree of saturation

SOLUTION

$$\text{Consider } V = 1 \text{ m}^3$$

$$W = 15 \text{ kN}$$

$$\omega = \frac{W_w}{W_s}$$

$$W_w = \omega W_s = 0.3W_s$$

$$W = W_s + W_w$$

$$1.5 = W_s + 0.3W_s$$

$$W_s = \frac{1.5}{1.3} = 1.15 \text{ kN}$$

$$W_w = (0.3)(1.15) = 0.345 \text{ kN}$$

$$e = \frac{V_v}{V_s}$$

$$G_s = \frac{W_s}{V_s \gamma_w}$$

$$V_s = \frac{W_s}{G_s \gamma_w} = \frac{1.15}{(2.7)(10)} = 0.43 \text{ m}^3$$

$$V_v = 1.15 - 0.43 = 0.72 \text{ m}^3$$

$$\text{a) } e = \frac{0.72}{0.43} = 1.67$$

$$\text{b) } n = \frac{V_v}{V} (100) = \frac{0.72}{1} (100) = 72\%$$

$$\text{c) } S = \frac{\sum V_w}{V_v} (100) = \frac{W_w}{V_v} (100)$$

$$= \frac{0.345}{0.72} (100) = 47.9\%$$

- E.2.5 An undisturbed sample of sandy silt is found to have a weight of 45.4N, a total volume of 2830 cm³ and a specific gravity of solids of 2.7. It is found in the laboratory that the void ratio of the material in its loosest condition is 0.8 and in its densest condition is 0.3. Compute the relative density and classify the material in nature as loose, medium or dense.

SOLUTION

$$I_D = \frac{e_{\max} - e}{e_{\max} - e_{\min}}$$

$$W_s = 45.4\text{N}$$

$$V = 2830\text{cm}^3$$

$$V_s = \frac{W_s}{G_s \gamma_w} = \frac{45.4}{2.7(0.01)} = 1681.5\text{cm}^3$$

$$V_v = 2830 - 1681.5 = 1148.5\text{cm}^3$$

$$e = \frac{1148.5}{1681.5} = 0.68$$

$$I_D = \frac{0.8 - 0.68}{0.8 - 0.3} (100) = 23.4\%$$

The material can be classified as loose.

- E.2.6 A 200 gm (cN) of soil and a series of sieves corresponding to the DIN-Standard are given. It is required to plot the the grain size distribution of the soil in question . The result of the sieve analysis is presented in the following table.

DIN-Standard mesh opening	Retained on sieve		Cumulative retained		Cumulative passing (finer)	
	W_R	$W_{R/W}$	W_{CR}	$W_{CR/W}$	W_{CP}	$W_{CP/W}$
mm	gm(cN)	%	gm (cN)	%	gm(cN)	%
5	0.00	0.00	0.00	0.00	200.00	100.00
2	2.84	1.42	2.84	1.42	197.16	98.58
1	5.66	2.83	8.50	4.25	191.50	95.75
0.5	46.04	23.02	54.54	27.27	145.46	72.72
0.2	44.00	22.00	98.54	49.72	101.46	50.73
0.1	34.90	17.45	133.44	66.27	66.56	33.28
0.064	63.16	31.58	196.60	98.30	3.40	1.70
pan	3.40	1.70	200.00	100.00	0.00	0.00

SOLUTION

The result of the sieve analysis is plotted in Fig. E2.1. The degree of uniformity is calculated using the following Parameters :

$$C_u = \frac{D_{60}}{D_{10}} = \frac{0.30}{0.07} = 4.3 \quad U_2 = \frac{D_{30}^2}{D_{60} \cdot D_{10}} = \frac{(0.092)^2}{(0.30)(0.07)} = 0.4$$

$$U_1 = \frac{D_{75}}{D_{25}} = \frac{0.55}{0.088} = 6.2$$

$$U_3 = \frac{D_{50}}{\sqrt{D_{10} \cdot D_{10}}} = \frac{0.19}{\sqrt{(0.07)(0.82)}} = 0.8$$

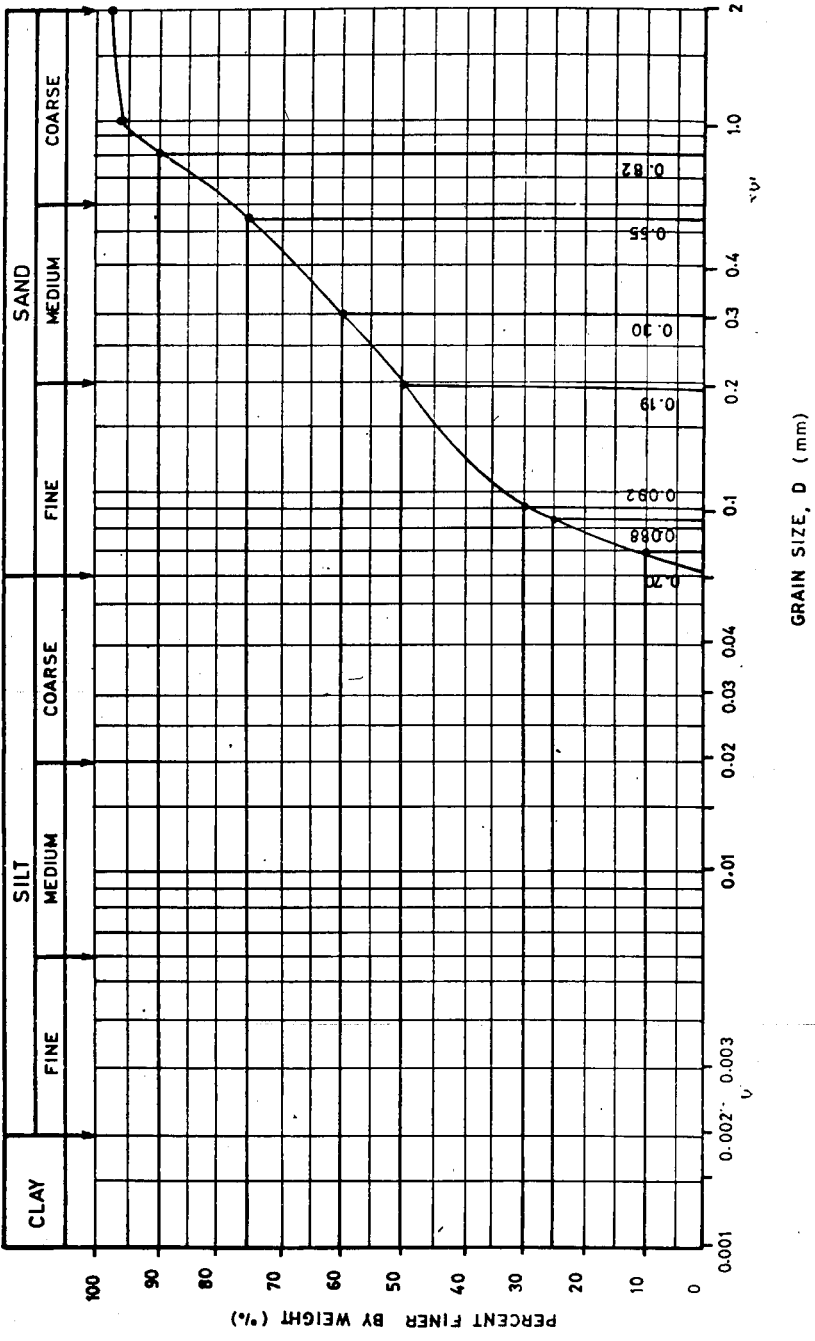


Fig. E 2.1 Result of sieve analysis

2.10 EXERCISES

1 Derive the following expressions

$$(a) V_s = \left(\frac{1}{e+1} \right) V$$

$$(b) V_v = \left(\frac{e}{1+e} \right) V$$

2 If the oven dry weight of $28,000\text{cm}^3$ of soil is 500N , calculate

(a) the volume of solids

(b) the volume of voids

(c) the porosity and void ratio

Assume $G_s = 2.7$

3 A moist sample of soil weighs 0.24N on a tin lid, which itself weighs 0.15N . After drying in an oven for 24 hrs. at 105°C , the tin and the sample weigh 0.20N . Determine the moisture content.

4 A moist sand sample has a volume of 644cm^3 in natural state and a weight of 7.93N . The dry weight is 7.35N and the specific gravity of solids is 2.68 . Determine the void ratio, the porosity, the water content, and the degree of saturation.

5 Given $\gamma_{\text{wet}} = 21.6\text{kN/m}^3$

$$\omega = 10\%$$

$$G_s = 2.7$$

Find the unit weight, the degree of saturation, and the void ratio.

6 A sample of sandy soil was found to have a moisture content of 25% and a unit weight of 19kN/m^3 . Laboratory tests on the same material indicated that the void ratios in the loosest and densest possible states were 0.90 and 0.50 respectively. Compute the relative density and degree of saturation of the sample.

Take $G_s = 2.7$.

- 7 In a hydrometer analysis, the following observations were taken:-
 $t = 4$ minutes, $r = 1.015$. The weight of solids used in suspension of 1000 cm^3 was 0.5N . Assume $G_s = 2.6$
 Calculate the coordinates of the point on the grain size plot. Other particulars of the hydrometer and the jar are as follows.
 $V_b = 50 \text{ cm}^3$, $\mu = 10 \times 10^{-8} \text{ N sec/cm}^2$, $h = 20 \text{ cm}$, $H = 2 \text{ cm}$
 $A_j = 50 \text{ cm}^2$
- 8 A soil, in which the water content is 38% , has $\omega_L = 45\%$ and $\omega_p = 34\%$. In what state of consistency does this soil exist?
- 9 The shrinkage limit of a clay soil is 25% . Its shrinkage and plasticity indexes are 15% and 20% respectively. Calculate the liquid and plastic limits of the soil. If the natural moisture content of the soil is 34% in what state of consistency does it exist?
- 10 The Atterberg limits of a particular soil are reported as $\omega_L = 60\%$, $\omega_s = 40\%$, and $\omega_S = 35\%$. Are these values reasonable?. Explain.
- 11 Derive an expression for the bulk unit weight of partially saturated soil in terms of specific gravity of the particles G_s , the void ratio e , the degree of saturation S and the unit weight of water γ_w . A sample of clay has a void ratio of 0.73 and a specific gravity of solid particles of 2.71 . If the voids are 92% saturated, find the bulk unit weight and the water content. What would be the water content for complete saturation, if the void ratio is kept the same?
- 12 A sample of soil having a volume of 1000 cm^3 weighs in its natural state 17.3N , the degree of saturation being 61.6% . After drying in the oven at 105°C , the sample weighed 14.4N .
 Find (a) the specific gravity of the solids
 (b) the natural water content
 (c) the void ratio
 (d) the wet unit weight, the dry unit weight, the saturated unit weight and the submerged unit weight.

Cassaw

Lagos

Amthor

- 13 A fully saturated clay sample weighs 1.52N and is 86cm³ in volume. Determine the void ratio, porosity, water content, dry unit weight and bulk unit weight of the soil, if the specific gravity of the clay particles is 2.72.
- 14 A clayey soil has a natural moisture content of 15.8%. The specific gravity of solid grains is 2.72. Its degree of saturation is 70.8%. The soil is allowed to soak up in water increasing its degree of saturation to 90.8%. Determine the water content of the soil in the latter case.
-
- 15 How many cubic meters of fill can be constructed at a void ratio of 0.7 from 191,000m³ of borrow material that has a void ratio of 1.2?
- 16 The volume change of a soil mass at the liquid limit is 80% and at its plastic limit 28%. Plastic limit determination gave the plastic limit of the soil as 24%. If the plasticity index of the soil is 35%, determine the liquid and shrinkage limits of the soil.
- 17 A soil specimen has an effective size, D_{10} , of 0.1mm. and a uniformity coefficient of 2.5. Determine the probable classification of the material using the MIT Classification System.
- 18 A sample contains 15% gravel, 32% sand, 33% silt and 20% clay. Classify the material by means of Triangular Classification System.
- 19 A sample of soil has 98% of the particles by weight finer than 1mm, 59% finer than 0.1mm, 24% finer 0.01mm and 11% finer than 0.001mm. Draw the grain size distribution curve and determine the approximate percentage of the total weight in each of the various size ranges according to MIT size classification. Determine the effective size and the uniformity coefficient for this soil. Classify the soil using the triangular chart.
- 20 A moist soil with a total volume of 50 cm³ weight 95 cN. It is dried out and found to weight 75 cN. The specific gravity of the solids is 2.67. Find e, n, ω, S and γ .

- 21 A soil sample taken from a depth that is located below the ground water table has a volume of 75 cm^3 and weighs 120 cN . It is dried out and found to weigh 75 cN . Compute its weight, ω , e , n and G_s .
- 22 A sample of silty clay was found to have a volume of 15.8 cm^3 . Its weight at the natural water content was 30.85 cN and after oven drying was 26.54 cN . The unit weight of the solid constituents was 2.70 cN/cm^3 . Calculate the void ratio and the degree of saturation.
- 23 A saturated soil has a water content of 50 per cent and a unit weight of 18.5 kN/m^3 . Find e , n and G_s .
- 24 A soil has a unit weight of 20.5 kN/m^3 and a water content of 15 per cent. What will be the water content if the soil dries out to a unit weight of 19.5 kN/m^3 and the void ratio remains unchanged.
- 25 A sand sample has a porosity of 40 per cent and a specific gravity of solids of 2.67.
- Calculate the void ratio of the sample.
 - Calculate the unit weight if the sand sample is dry.
 - Calculate the unit weight if the sand sample is 30 per cent saturated.
 - Calculate the unit weight if the sand sample is saturated.
- 26 A soil has a unit weight of 17.5 kN/m^3 and a water content of 5 per cent. How much water in liters should be added to each metre cube of soil to raise the water content to 15 per cent? Assume that the void ratio remains constant.
- 27 A sand sample with a minimum void ratio of 0.45 and a maximum of 1.00 has a relative density of 40 per cent. The specific gravity of solids is 2.68.
- Find the unit weight
 - if the sample is dry.
 - if the sample is wet.
 - How much will a 2 m. stratum of this sand settle if the sand is densified to a relative density of 65 per cent?
 - What will be the new dry and saturated unit weights?

3. SOIL-WATER AND SEEPAGE

3.1 SOIL-WATER

3.1.1 General

Soil engineers are interested in ground water because of its effect on *soil behaviour* and construction operations. Ground water affects many engineering structures adversely by reducing the bearing capacity of the soil. Deep excavation can be difficult because of large inflow of ground water. The presence of water in the soil above and below the *ground water table* may be a controlling factor in many engineering studies and foundation design.

Before taking up the types of soil moisture, it is important to briefly review the *hydrologic cycle*. Moisture vapour in the clouds condenses under the influence of temperature changes and falls to the earth as rain, snow, hail etc. A part of this precipitation may not reach land surface but evaporates in the air while falling or may evaporate from leaves or roofs etc. Most of the precipitation, however, falls on the land. This water is disposed of in three ways. It is evaporated directly from the soil, runs off the surface (runoff) or soaks into the soil. Of interest to soil engineers is the portion of precipitation that soaks into the soil to form ground water.

Ground Water is the continuous body of sub-surface water that fills the soil voids and fissures and is free to move under the influence of gravity. The upper surface of this water is called the *water table* or *phreatic surface*.

3.1.2 Classification of soil Moisture

Soil moisture is classified as adsorbed, capillary, or gravitational water. A brief discussion under each of these headings is given below.

3.1.2.1 Adsorbed Water

This is water held on the surface of soil particles by forces of adsorption. Soil particles under natural conditions normally have a net electrical charge at their surface. Water molecule as a single unit may be considered electrically neutral.

However, its construction is such that the centers of the positive and negative charges of its individual components do not exactly coincide. In consequence, it has in effect two poles, like a small bar magnet (Fig. 3.1a). Water molecules close to electrically charged surfaces of soil particle are strongly attracted to and held by the soil particle (Fig. 3.1b. & c)

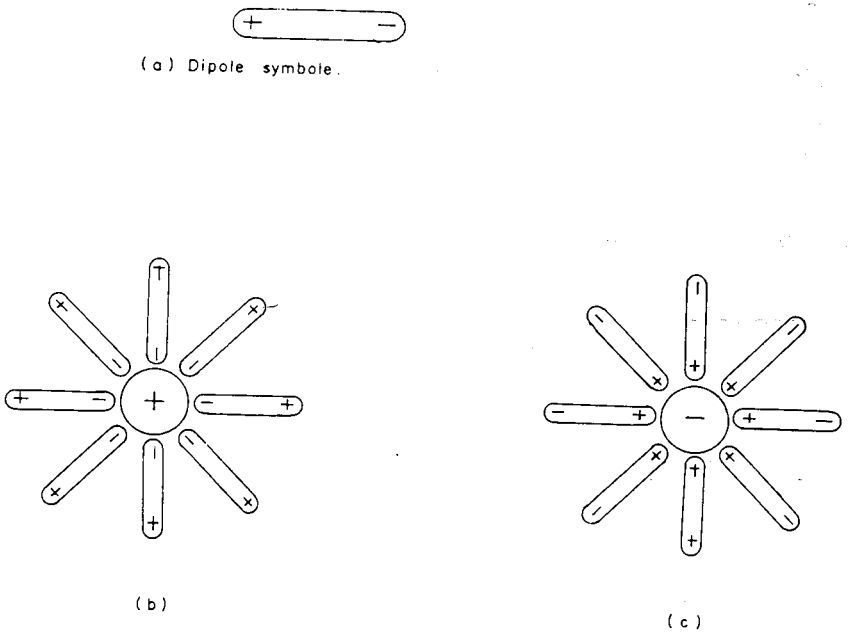


Fig. 3.1 Orientation of water molecules about charged soil particles

Water adsorbed on the surfaces of soil particles is referred to as adsorbed water or because of its immobility, as *bound water*. The amount of water held by adsorption depends on specific surfaces which in turn depend on particle size, shape, and gradation. A relatively fine well graded material will normally have much greater adsorption power.

Adsorbed water reduces the area available for free flow. In fine grained soils the pore passages may be small and the thickness of immobilized water films constitutes a significant part of the pore diameter. Adsorbed water may be removed by evaporation (oven drying of soil).

3.1.2.2 Capillary Water

Capillary phenomenon is one which enables a dry soil to draw water to elevation above the water table. It also enables a draining soil to retain water above the atmospheric line. The movement and retention of water above the ground water table is similar in many respects to the rise and retention of water in capillary tubes as demonstrated in Fig. 3.2(a).

Water pressure varies linearly both below and above the water table as shown in Fig. 3.2(b).

At level BB the water pressure is $\gamma_w h_1$

Total pressure at level BB is $\gamma_w h_1 + P_a$

Where P_a = the atmospheric pressure. The negative water pressure at level CC is $-h_2\gamma_w$. Hence the total pressure at level CC would be $P_a - h_2\gamma_w$. Like adsorbed water, capillary water may be removed by oven drying.

3.1.2.2.1 Capillary Forces and Surface Tension

In fine grained soils or in capillary tubes, water can rise to a certain height and remains there indefinitely. This forces which support the column of water is called *capillary force*.

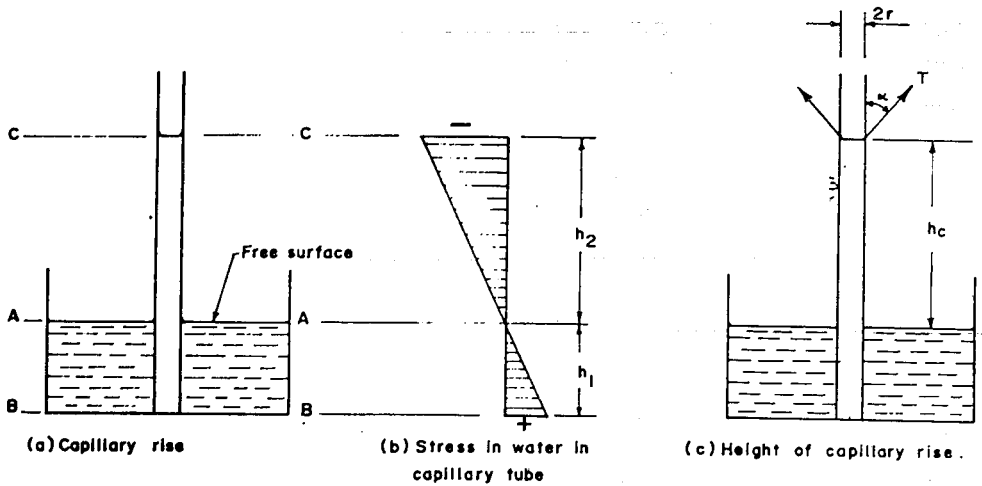


Fig. 3.2 Capillary rise of water in a tube of uniform bore

In order to visualize the mechanics of capillary force, consider the rise of water in a capillary tube as shown in Fig. 3.3.a. At the base of the column of water having a capillary rise of h_c , which has the same elevation as the free, water level outside, the hydrostatic pressure is zero. The shearing stress around the cylindrical surface is also zero and yet the water is in equilibrium. This could only happen if the mechanical properties of the upper most layer of the column of water are different from those of ordinary water. This upper layer called *surface film or meniscus* keeps the element from sinking and be visualized as a membrane from which water is hanging (Fig. 3.3.b). The meniscus joins the wall of the tube at an angle α called the contact angle.

The surface film is in a state of two dimensional tension parallel to its surface. This is the surface tension, T_s , the magnitude of which is 0.075cN/cm at 20°C for water [30]. The tensile stress in the miniscus may be calculated by referring to Fig. 3.4.

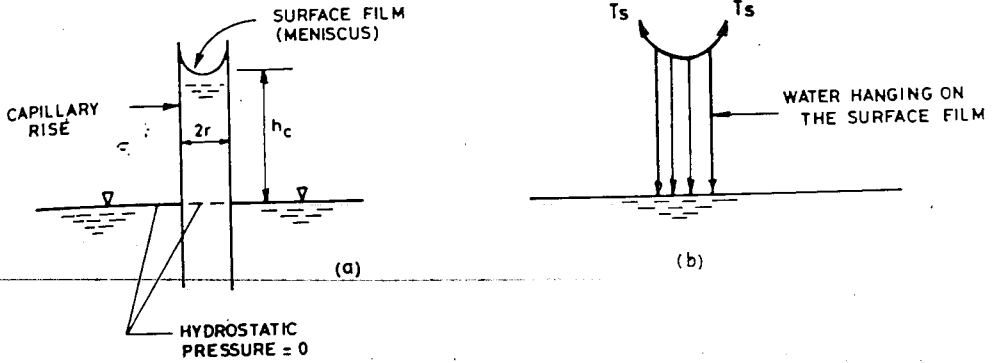


Fig 3.3 Mechanics of capillary force

The total force developed along the perimeter is

$$F = 2\pi r T_s \cos\alpha \tag{3.1}$$

The capillary stress U would then be

$$U = \frac{F}{A} = \frac{2\pi r T_s \cos\alpha}{\pi r^2} = \frac{2T_s \cos\alpha}{r} \tag{3.2}$$

The maximum capillary stress occurs when $\alpha = 0$.

$$\text{Hence } U_{\max} = \frac{2T_s}{r} \tag{3.3}$$

From Fig. 3.4 (c), $r = r_m \cos \alpha$

$$\tag{3.4}$$

To establish a relation between the capillary stress and the radius of the meniscus, the value of r is substituted into Eq.(3.2).

$$U = \frac{2T_s \cos \alpha}{r_m \cos \alpha} = \frac{2T_s}{r_m} \quad (3.5)$$

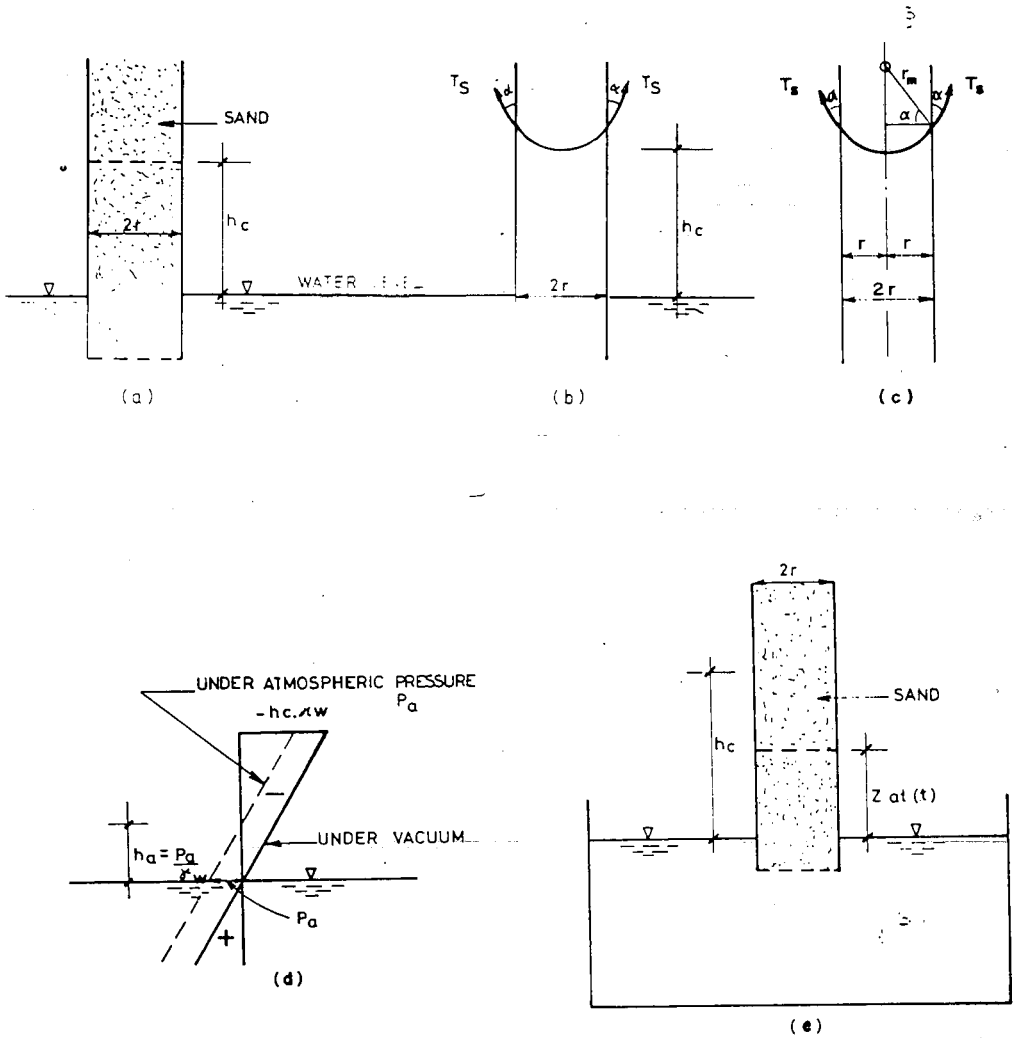


Fig 3.4 Rise of water in capillary tube

3.1.2.2.2 Rise of Water in Capillary Tube of Uniform Internal Diameter

When a thin glass tube open at both ends is dipped into water, the water will rise in the tube to a certain height as shown in Fig. 3.3(c). The capillary rise can easily be related to the surface tension by considering the equilibrium of capillary column.

Let the surface tension per unit perimeter = T_s , and contact angle α

$$\text{Force acting upward} = 2\pi r T_s \cos\alpha$$

$$\text{Force acting downward} = h_c \gamma_w \pi r^2$$

For equilibrium condition

$$h_c \gamma_w \pi r^2 = 2\pi r T_s \cos\alpha$$

$$h_c = \frac{2T_s \cos\alpha}{r \cdot \gamma_w} \quad (3.6)$$

For chemically clean water and clean tube, $\alpha = 0$. Hence

$$h_c = \frac{2T_s}{r \gamma_w} \quad (3.7)$$

Where

h_c = height of capillary rise

As is evident from the above equation, the height of capillary rise increases as the diameter of tube decreases. It can be deduced from this that capillary is more pronounced in fine grained soils than in coarse grained soil.

3.1.2.2.3 Capillary Movement of Water in a Column of Dry Sand

If the lower end of a column of dry sand contained in a vessel perforated at the bottom is immersed in water, the water rise in the same manner as in a capillary tube (Fig 3.4c). The capillary rise in time, t , is given by the following equation:

$$h_c = \frac{t.k}{\left[\ln \frac{h_c}{h_c - z} - \frac{z}{h_c} \right]} \quad (3.8)$$

Where k = coefficient of permeability

As the capillary water rises, air becomes entrapped in the pores and hence variations are included in both h_c and k . From laboratory tests, Taylor found that for $z/h_c < 20\%$, the degree of saturation is relatively higher and the above equation is considered valid.

Approximate formula for determining h_c is also available [30]

$$h_c = \frac{C}{e.D_{10}} \quad (3.9)$$

C = empirical constant varying between 0.1 and 0.5 (cm^2)

e = void ratio

D_{10} = effective diameter (cm)

Typical values of capillary rise h_c for different soil types are given in Table 3.1

Table 3.1 Typical Values of Height of Capillary Rise [11]

Soil type	Height of Capillary Rise, h_c
	cm
Coarse sand	2 - 5
Sand	12 - 35
Fine sand	35 - 70
Silt	70 - 150
Clay	> 150

3.1.2.2.4 Effect of Surface Tension on a Soil Mass

At all points where moisture menisci touch soil particles, surface tension forces act, causing a grain-to-grain pressure within the soil and contribute to the shear and stability of the soil mass. However, this induced strength is only temporary in character and may be destroyed entirely upon full saturation of soil. Since complete saturation eliminates interface menisci, contact pressure reduces to zero.

3.1.2.2.5 Factors Affecting Capillary Rise in Soils

a) Positions of the Ground Water Table

As the position of the ground water table fluctuates so does the capillary rise. This causes saturation of surface soils or subgrades at certain periods. It is for this reason that it is necessary to install drainage systems to hold the water table to a certain minimum level.

b) Evaporation Opportunity

There is a certain amount of vaporization of the water at the upper level of the capillary zone. Water removed by evaporation is replaced by upward flow. For given conditions the degree of saturation at certain level remains fairly constant. If evaporation is prevented (e.g. by sealing) saturation in the ground will gradually increase above the normal upper limit. Thus certain gravel roads which had given satisfactory service for years, start giving trouble when paved, because of weakening of the subgrade by saturation.

c) Grain Size of the Soil

Capillary is more pronounced in fine grained soils than in coarse grained soils.

3.1.2.3. Gravitational Water

This differs from adsorbed and capillary water in that it is completely free to move through or drain from soil under the influence of gravity. That is, the flow of gravitational water in soil is caused by the action of gravity which tends to pull the water downward to a lower elevation. In many respects it is similar to free flow of water in an open channel or conduit.

The gravitational pull acts to overcome resistance to movement or flow of the water. In soil such resistance is due to viscous drag along the side walls of the pore spaces.

In soils the nature of ground water flow may be either *laminar* or *turbulent*. For practical purposes, however, only laminar type of flow is usually considered. Laminar flow is to exist when all particles of water move in parallel paths and the lines of flows are not inter-twined as the water moves forward.

3.1.2.3.1. Discharge Velocity and Seepage Velocity

The discharge velocity is defined as the quantity of fluid that percolates through a unit of total area of the porous medium in a unit time.

As flow can occur only through the pores, the velocity across any section must be thought in a statistical sense (Fig. 3.5)

If m is designated as the effective ratio of the area of pores A_p to the total area A , then

$$m = \frac{A_p}{A} \quad (3.10)$$

The flow quantity becomes:

$$Q = mA\bar{v} \quad (3.11)$$

where $m\bar{v}$ is the discharge velocity and \bar{v} is the seepage velocity. If $A_p(z)$ is designated as the area of pores at any elevation z (Fig.3.5), then

$$m(z) = \frac{A_p(z)}{A} \quad (3.12)$$

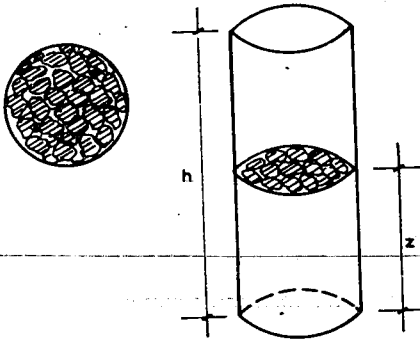


Fig. 3.5 Section through porous medium

The average value of m in the entire cylinder would be,

$$m = 1/h \int_0^h m(z) dz \tag{3.13}$$

Multiplying the right hand side of the equation by A/A

$$m = 1/Ah \int_0^h Am(z) dz \tag{3.14}$$

$$= 1/V \int_0^h A_p(z) dz = \frac{V_v}{V} = n \tag{3.15}$$

where V = the total volume.

The expression within the integral is the volume of voids. Hence the average value of m is the volume porosity n .

i.e., $v_s = n \cdot v$ (3.16)

Hence, discharge velocity is equal to the porosity multiplied by seepage velocity. In Engineering work, we shall be mainly dealing with discharge velocity.

3.1.2.3.2. Darcy's Law

For laminar flow condition, Darcy's law states that the rate of flow of ground water is proportional to gradient.

$$Q = kiA \quad (3.17)$$

where

Q = the discharge passing through the total cross-sectional area of the soil, A , per unit time

i = the hydraulic gradient

k = Darcy's Coefficient of permeability which is usually called coefficient of permeability

The driving force which causes water to flow may be represented by a quantity known as *hydraulic gradient*, i . This is defined as the drop in head divided by the distance in which

the drop occurs (Fig. 3.6). $i = \frac{h_1 - h_2}{L}$. The drop in head or difference in head at two

points, generally referred to as lost head, represents energy lost through viscous friction as the water flows around the soil particles and through the irregular void passages.

3.1.2.3.3 Range of Validity of Darcy's Law

The proportionality in Darcy's law is valid for laminar flow up to a certain critical gradient, i_c , at which the discharge velocity is critical, v_c , (Fig. 3.7).

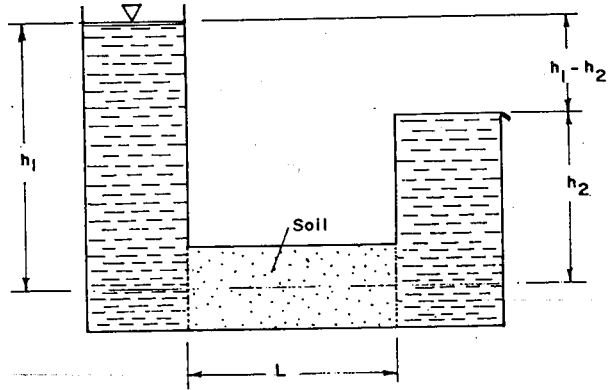


Fig 3.6 Hypothetical flow through soil

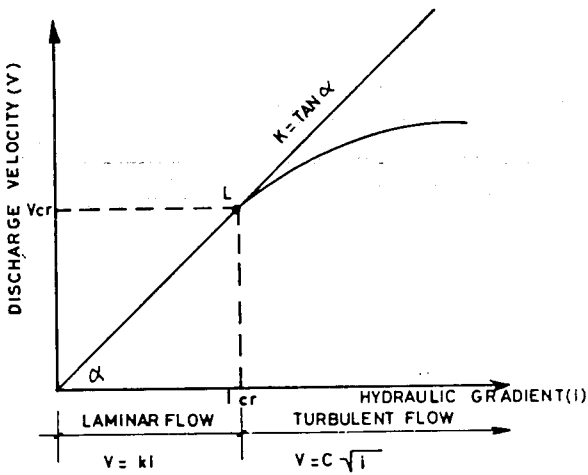


Fig 3.7 Validity of Darcy's Law

Beyond point L , where $i > i_{cr}$, the flow is turbulent. In the turbulent region the discharge velocity can be approximated by,

$$v = C \sqrt{i} \tag{3.18}$$

where C = coefficient

To determine the laminar range of flow one uses the Reynolds number, R , which is defined as:

$$R = \frac{vD\rho}{\mu_T} \quad (3.19)$$

where

v = discharge velocity, cm/sec

D = average of diameters of soil particles, cm

ρ = density of fluid, g/cm³,

μ_T = coefficient of viscosity, g-sec/cm³

The critical value of Reynolds number at which the flow in the soil changes from laminar to turbulent flow has been found by various investigators to range between 1 and 12. However, it is sufficient to accept the validity of Darcy's law when Reynolds number is taken as equal or less than unity.

$$\frac{vD\rho}{\mu_T} \leq 1 \quad (3.20)$$

Substituting the known value of ρ and μ for water into Eq. (3.19) and assuming a conservative velocity of 0.25cm/sec, one gets $D = 0.4$ mm which is representative of the average particle size of coarse sand. It can thus be concluded that in natural flow the equation of Darcy is valid.

3.2 PERMEABILITY

3.2.1 General

Permeability is a soil property which indicates the ease with which water will flow through the soil (i.e. through the voids, or spaces between the soil grains). It denotes the capacity of soil to conduct or discharge water under a given hydraulic gradient.

The permeabilities of soils vary greatly. Coarse sands and gravels are highly pervious and have correspondingly high permeability coefficients. Such high permeability creates difficulties in deep excavation in sands because of the large inflow of water. Clays on the other hand are relatively impervious and hence have low permeability coefficient.

A building founded on clay soils results in slow consolidation settlement, because clays are relatively impermeable and hence a very long time is needed for the water between soil pores to be squeezed out.

Permeability characteristics of soils are used in:

- a) the computation of seepage through earth dams and irrigation ditches.
- b) estimating of pumpage capacity requirements for dewatering excavation below a water table.
- c) the determination of the rate of settlement of a structure resting on a soil foundation.

3.2.2 Laboratory Measurement of Permeability

The various types of equipment used for determining coefficient of permeability of soils in the laboratories are called *permeameters*. The two main types commonly used are the *constant head* type and the *variable head* type.

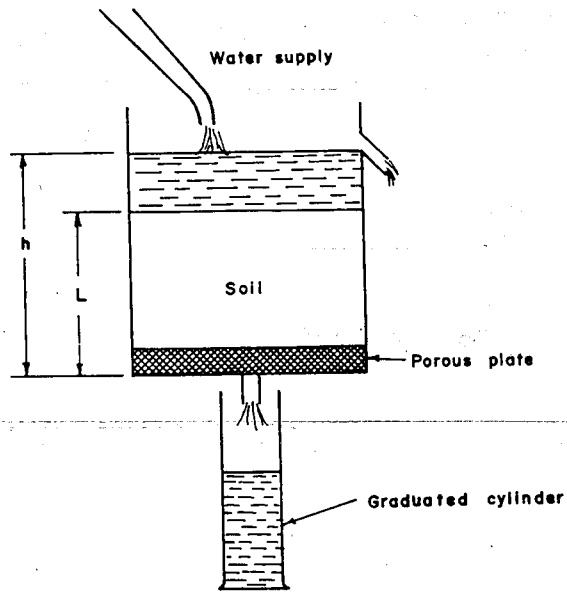


Fig. 3.8 Constant head permeameter

3.2.2.1 Constant Head Permeameter

The set up for constant head permeameter is shown in Fig. 3.8. A constant head permeameter consists of a vertical cylinder containing the soil sample (disturbed or undisturbed) having length, L , and cross-section area, A , whose coefficient of permeability is to be determined (Fig.3.8). Before the test is started, the sample should be completely saturated. During the test the head, h , is kept constant. The amount of water flowing during a specified time is collected in a graduated cylinder and its temperature is recorded. The discharge, Q , is obtained by dividing the volume of water by the time in which it is collected.

The coefficient of permeability is then determined using Darcy's Law,

$$Q = kiA \quad (3.21)$$

$$k = \frac{Q}{iA} = \frac{Q}{\frac{h}{L}A} = \frac{LQ}{Ah} \quad (3.22)$$

The coefficient of permeability, k , is conventionally reported at a standard temperature of 20°C . Tests carried out at different temperature should be corrected as follows [17]:

$$k_{20} = k \frac{\mu_T}{\mu_{20}} \quad (3.23)$$

where

k = coefficient of permeability at test temperature

μ_T = coefficient of viscosity at test temperature T

μ_{20} = coefficient of viscosity at 20°C

The constant head permeability test is more suited for coarse soils such as gravelly sand and coarse and medium sand where the time required for permeability is relatively short.

3.2.2.2 The Variable Head (Falling Head) Permeameter

The arrangement of the apparatus is shown in Fig. 3.9. In the conduct of the test, the water passing through the soil sample causes water in the standpipe to drop from h_0 to h_1 in a measured period of time. h is the head at any intermediate time, t . In any increment of time

dt there is a decrease in head equal to dh.

Let t_1 be the time required for the water level to fall from h_0 to h_1 . For a very small interval of time, the rate of fall is dh/dt .

The rate of flow = $-a dh/dt$ (the negative sign indicates the fall of head with time). Where a is the cross sectional area of the stand pipe.

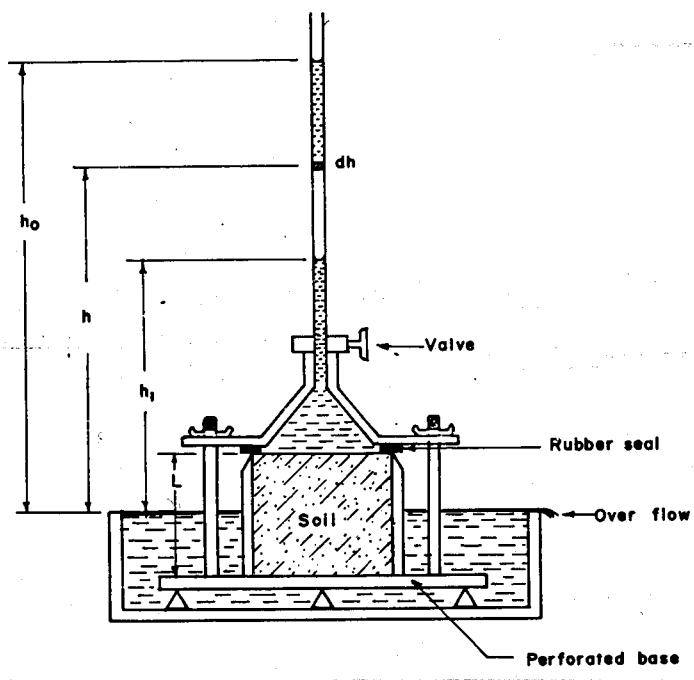


Fig 3.9 Falling head permeameter

Applying Darcy's Law,

$$-a \frac{dh}{dt} = kiA = k \frac{h}{L} A \tag{3.24}$$

Integrating between limits h_0 to h_1 , and t_0 to t_1

$$-a \int_{h_0}^{h_1} \frac{dh}{h} = \frac{kA}{L} \int_{t_0}^{t_1} dt \quad (3.25)$$

One finally sets

$$k = \frac{aL}{At_1} \log_e \frac{h_0}{h_1} \quad (3.26)$$

Changing to common logarithm

$$k = \frac{2.3aL}{At_1} \log_{10} \frac{h_0}{h_1} \quad (3.27)$$

If the test is carried out at a different temperature from 20°C , a correction should be made according to Eq. (3.23). The above method is more suited for fine sands, silts and clays where the time required for permeability is relatively long.

3.2.2.3 Horizontal Permeability Test

A basic sketch of a horizontal permeameter is presented in Fig. (3.10). The discharge, Q , head loss, h , temperature, T , the filtration length, L , and the cross-sectional area perpendicular to the horizontal direction of flow are determined.

The coefficient of permeability, k , is then calculated as:

$$k = \frac{V}{i} = \frac{Q}{A \cdot i} = \frac{Q}{A(h/L)} \quad (3.28)$$

If the test is carried out at a different temperature from 20°C , a correction should be made according to Eq. (3.23). The horizontal permeability is well suited for sandy soils.

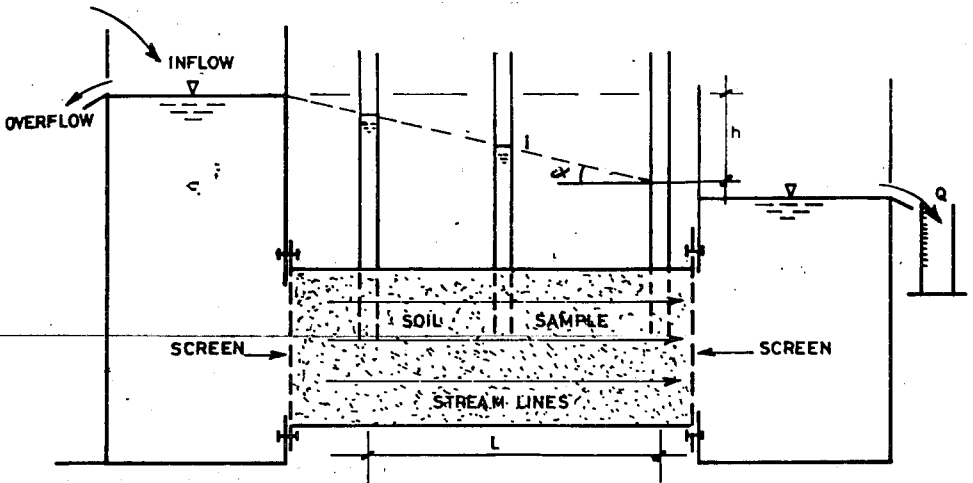


Fig 3.10 Horizontal permeameter

3.2.3 Sources of Errors in the Determination of Permeability Coefficients

The main sources of error are:

- a) the formation of filter skin of fine material on the surface of the sample.
- b) the formation of air bubbles in the soil.

The error in (a) may be reduced by measuring the loss of head between two points in the sample. The error in (b) may be removed by saturating the test sample completely.

3.2.4 Factors Affecting Permeability

It can be shown that the coefficient of permeability may be expressed in a general form according to the following empirical equation [27].

$$k = D_s^2 \frac{\gamma_w}{\eta} \frac{e^3}{1+e} \cdot C \quad (3.29)$$

where

D_s^2 = average grain size

$\frac{\gamma_w}{\eta}$ = properties of pore fluid

C = shape factor of the soil grains

$\frac{e^3}{1+e}$ = void ratio effect

Examining the above relationship, the influence of each parameter on the coefficient of permeability may be assessed.

3.2.5 Value of Coefficient of Permeability

A very useful table has been compiled by Casagrande and Fadum [4] which is given in Table 3.2

3.2.6 Field Measurement of Permeability

For soil condition where stratification is erratic, the laboratory methods of determining the coefficient of permeability do not give reliable results. A more appropriate test for such a case is the field permeability test. Field measurement of permeability is carried out by means of pumping test. In this test the water is pumped out from a test well. The pumping of water causes a drawdown (sinking) of the water table. The change in water table is measured and from that the permeability can be calculated. The detailed outline of this operation is as indicated below.

		COEFFICIENT OF PERMEABILITY k IN CM PER SEC. (LOG SCALE)												
		10 ²	10 ¹	1.0	10 ⁻¹	10 ⁻²	10 ⁻³	10 ⁻⁴	10 ⁻⁵	10 ⁻⁶	10 ⁻⁷	10 ⁻⁸	10 ⁻⁹	
DRAINAGE		GOOD					POOR			PRACTICALLY IMPERVIOUS				
SOIL TYPES	CLEAN GRAVEL	CLEAN SANDS, CLEAN SAND AND GRAVEL					VERY FINE SANDS, ORGANIC AND INORGANIC SILTS, MIXTURES OF SAND SILT AND CLAY GLACIAL TILL, STRATIFIED CLAY DEPOSITS etc.			"IMPERVIOUS" SOILS, e.g. HOMOGENEOUS CLAYS BELOW ZONE OF WEATHERING				
							"IMPERVIOUS" SOILS MODIFIED BY EFFECTS OF VEGETATION AND WEATHERING							
DIRECT DETERMINATION OF k		DIRECT TESTING OF SOIL IN ITS ORIGINAL POSITION-PUMPING TESTS. RELIABLE IF PROPERLY CONDUCTED. CONSIDERABLE EXPERIENCE REQUIRED.												
INDIRECT DETERMINATION OF k		CONSTANT-HEAD PERMEAMETER. LITTLE EXPERIENCE REQUIRED												
			FALLING-HEAD PERMEAMETER. RELIABLE. LITTLE EXPERIENCE REQUIRED.					FALLING-HEAD PERMEAMETER UNRELIABLE. MUCH EXPERIENCE REQUIRED			FALLING-HEAD PERMEAMETER. FAIRLY RELIABLE. CONSIDERABLE EXPERIENCE NECESSARY			
		COMPUTATION FROM GRAIN SIZE DISTRIBUTION. APPLICABLE ONLY TO CLEAN COHESIONLESS SANDS AND GRAVELS												
		COMPUTATION BASED ON RESULTS OF CONSOLIDATION TESTS. RELIABLE. CONSIDERABLE EXPERIENCE REQUIRED.												

After A. Casagrande and R.E. Fadum [9]

Table 3.2 Values of coefficient of permeabilities.

- a) A test well having a perforated casing is sunk through the water bearing soil to an underlying impervious stratum as shown in Fig. 3.11
- b) Observation wells are bored at various radial distance from the test well.
- c) Initial elevations of the ground water table are recorded.
- d) Pumping is started at the test well at a known uniform rate and continued until a steady state of flow into the well is achieved and the water table at the observation wells become constant.
- e) The drop in elevation of the water table at the observation wells, and the rate of discharge from the test well provide the necessary data for computing the coefficient of permeability of the soil within the zone of influence of the test well.

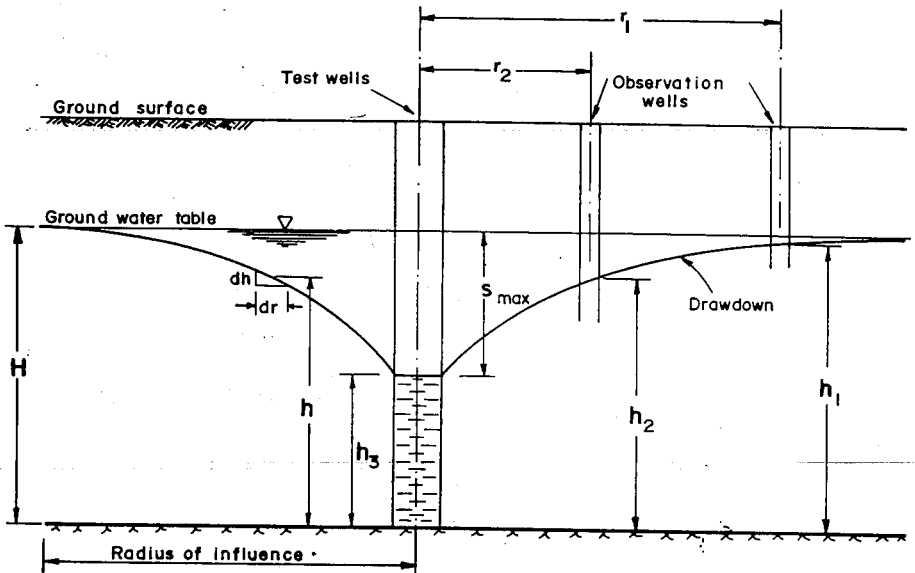


Fig. 3.11 Field permeability test

The flow towards the test well is considered to be radial. Area of soil through which water flows towards the test well = $2\pi rh$. Using Darcy's Law, $Q = kiA$

$$Q = k \frac{dh}{dr} 2\pi rh \quad (3.30)$$

Referring to Fig. 3.11,

$$\int_{r_2}^{r_1} \frac{dr}{r} = \frac{2\pi k}{Q} \int_{h_2}^{h_1} h \cdot dh \quad (3.31)$$

The above integration gives;

$$k = \frac{Q \log_e \frac{r_1}{r_2}}{\pi(h_1^2 - h_2^2)} \quad (3.32)$$

k can also be expressed in terms of influence radius and the radius of the test well

$$k = \frac{Q \log_e \frac{R}{r_0}}{\pi(H^2 - h_3^2)} \quad (3.33)$$

If the maximum drawdown S_{\max} is known, the coefficient of permeability may be expressed as a function S_{\max} .

$$S_{\max} = H - h_3 \quad (3.34)$$

$$\text{But } H^2 - h_3^2 = (H + h_3)(H - h_3) = (H + h_3) S_{\max} \quad (3.35)$$

Noting that $h_3 = H - S_{\max}$

$$(H^2 - h_3^2) = (2H - S_{\max}) S_{\max} \quad (3.36)$$

Finally,

$$k = \frac{Q}{\pi} \log_e \frac{\frac{R}{r_0}}{(2H - S_{\max})S_{\max}} \quad (3.37)$$

Approximate values of the radius of influence is given in Table 3.3.

Table 3.3 Radius of Influence in Various Soils [14]

Soil		Radius of Influence R
Description	Particle Size D	
	mm	m
Coarse gravel	10	1500
Medium gravel	2 - 10	500 - 1500
Fine gravel	1 - 2	400 - 500
Coarse sand	0.5 - 1.0	200 - 400
Medium sand	0.25 - 0.5	100 - 200
Fine sand	0.10 - 0.25	50 - 100
Very fine sand	0.050 - 0.10	10 - 50
Silty sand	0.025 - 0.05	5 - 10

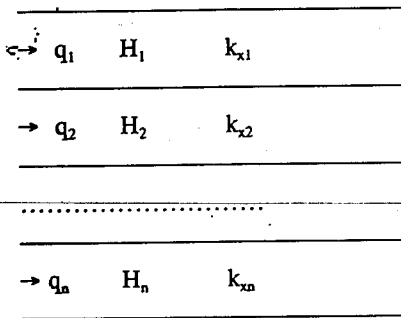
3.2.7 Permeability of Natural Deposits

Natural deposits generally show stratification. In themselves different layers may be homogeneous. The coefficient of permeability to be used for flow through such a deposit depends on the direction of flow.

Derivation of permeability coefficient in stratified soil for horizontal and vertical flow is as shown below.

3.2.7.1. Flow Parallel to Bedding Plane

Consider a stratified soil layer with thicknesses of H_1, H_2, \dots, H_n and the corresponding permeability coefficient parallel to the bedding plane (x- direction) $k_{x1}, k_{x2}, \dots, k_{xn}$. The flow through each layer is designated by q_1, q_2, \dots, q_n .



The hydraulic gradient, i , is the same for all layers.

$$Q = q_1 + q_2 + \dots + q_n \tag{3.38}$$

$$q_i = k_{xi}iA_i = k_{xi}i(H_i \cdot 1) = k_{xi} \cdot H_i \cdot i \tag{3.39}$$

Let k_x be the average permeability in the horizontal direction

$$Q = k_x i A = k_x i H = k_x i (H_1 + H_2 + \dots + H_n) \tag{3.40}$$

The general relationship can be written as:

$$Q = k_x i \sum H_n \tag{3.41}$$

$$k_x i (H_1 + H_2 + \dots + H_n) = k_{x1}iH_1 + k_{x2}iH_2 + \dots + k_{xn}iH_n \tag{3.42}$$

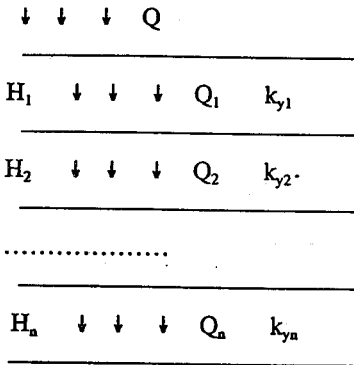
$$k_x = \frac{k_{x1}H_1 + k_{x2}H_2 + k_{x3}H_3 + \dots + k_{xn}H_n}{H_1 + H_2 + H_3 + \dots + H_n} \tag{3.43}$$

The general equation may be written as;

$$k_x = \frac{\sum (k_x H)_n}{\sum H_n} \tag{3.44}$$

3.2.7.2 Flow Normal to Bedding Plane

Taking the same cross section as before but changing the direction of flow to be normal to the bedding plane (v-direction), and using the principle of continuity of flow, the average coefficient of permeability k_y , may be derived as follows.



$$Q = Q_1 = Q_2 = Q_3 = Q_n \tag{3.45}$$

$$Q_1 = k_{y1} \frac{h_{L1}}{H_1} A \tag{3.46}$$

$$Q_2 = k_{y2} \frac{h_{L2}}{H_2} A \tag{3.47}$$

$$Q_3 = k_{y3} \frac{h_{L3}}{H_3} A \tag{3.48}$$

$$Q_n = k_{yn} \frac{h_{Ln}}{H_n} A \tag{3.49}$$

Let the total head loss be h_L . Then,

$$h_L = h_{L1} + h_{L2} + h_{L3} + h_{Ln} \tag{3.50}$$

From Eq. 3.46, 3.47, 3.48 and 3.49

$$Q = k_y \frac{h_L}{H_1 + H_2 + H_3 \dots + H_n} A \quad (3.51)$$

$$h_L = \frac{Q(H_1 + H_2 + H_3 \dots + H_n)}{k_y A} \quad (3.52)$$

$$h_{L1} = \frac{QH_1}{k_{y1} A} \quad (3.53)$$

$$h_{L2} = \frac{QH_2}{k_{y2} A} \quad (3.54)$$

$$h_{L3} = \frac{QH_3}{k_{y3} A} \quad (3.55)$$

$$h_{Ln} = \frac{QH_n}{k_{yn} A} \quad (3.56)$$

One may write,
$$h_L = \frac{QH}{k_y A} \quad (3.57)$$

where

H = total thickness

k_y = average coefficient of permeability

Then,
$$h_L = \frac{Q(H_1 + H_2 + H_3 \dots + H_n)}{k_y A} = \left[\frac{H_1}{k_{y1}} + \frac{H_2}{k_{y2}} + \frac{H_3}{k_{y3}} \dots + \frac{H_n}{k_{yn}} \right] \frac{Q}{A} \quad (3.58)$$

$$\frac{H_1 + H_2 + H_3 \dots + H_n}{k_y} = \frac{H_1}{k_{y1}} + \frac{H_2}{k_{y2}} + \frac{H_3}{k_{y3}} \dots + \frac{H_n}{k_{yn}} \quad (3.59)$$

$$k_y = \frac{H_1 + H_2 + H_3 \dots + H_n}{\frac{H_1}{k_{y1}} + \frac{H_2}{k_{y2}} + \frac{H_3}{k_{y3}} \dots + \frac{H_n}{k_{yn}}} \quad (3.60)$$

The general equation is expressed as,

$$k_y = \frac{\sum H_n}{\sum \left[\frac{H}{k_y} \right]_n} \quad (3.61)$$

3.3 SEEPAGE THROUGH SOILS

3.3.1 Differential Equation for Seepage

All methods of estimating seepage are based on Darcy's Law and assume that the soil consists of relatively incompressible material. In order to compute the rate of flow of water through such soils, it is necessary to determine the intensity and distribution of the neutral stress. Suppose it is desired to compute the quantity of water that percolates from position (1) to position (2) for condition given in Fig. 3.12a. Consider cubic element from the soil mass where seepage occurs. Since the flow system extends in three dimensions the actual velocities should be presented as indicated in Fig. 3.12b. However, in many problems of ground water, the movement of the water is considered to be planar and for the problem at hand one considers two dimensional flow (Fig. 3.13a).

Noting v_x = component of discharge velocity in the x direction

$$i_x = \frac{\partial h}{\partial x} \quad (\text{hydraulic gradient in the x-direction})$$

v_z = component of discharge velocity in the z direction

$$i_z = \frac{\partial h}{\partial z} \quad (\text{hydraulic gradient in the z-direction})$$

h = hydraulic head at place occupied by the element under consideration.

The quantity of water that enters the element per unit of time is:

$$v_x \cdot dz \cdot dy + v_z \cdot dx \cdot dy \quad (3.62)$$

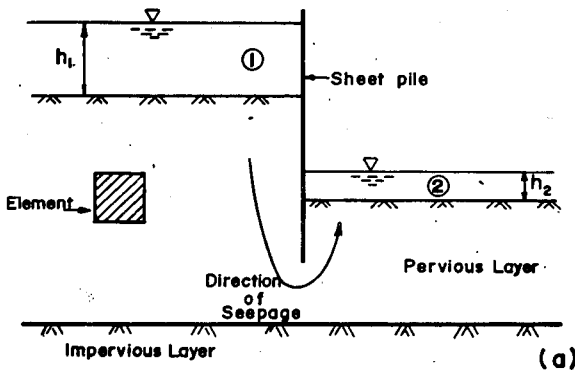
The quantity that leaves is

$$v_x dz.dy + \frac{\partial v_x}{\partial x} .dx.dz.dy + v_z dx.dy + \frac{\partial v_z}{\partial z} .dz.dx.dy \quad (3.63)$$

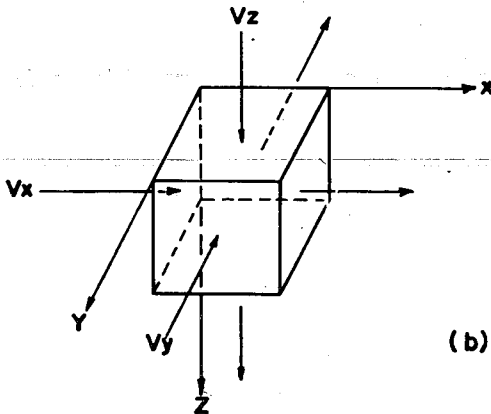
If the liquid is perfectly incompressible and volume of voids occupied by water is constant, the quantity of water that enters the element should be equal to the quantity that leaves.

$$(v_x dz.dy + \frac{\partial v_x}{\partial x} .dx.dz.dy + v_z dx.dy + \frac{\partial v_z}{\partial z} .dz.dx.dy) \quad (3.64)$$

$$-(v_x dz.dy + v_z .dx.dy) = 0$$



(a)



(b)

Fig. 3.12 General consideration of seepage

From here

$$\frac{\partial v_x}{\partial x} + \frac{\partial v_z}{\partial z} = 0 \quad (3.65)$$

From earlier discussions:

$$v_x = k_x i_x = k_x \frac{\partial h}{\partial x} \quad (3.66)$$

$$v_z = k_z i_z = k_z \frac{\partial h}{\partial z} \quad (3.67)$$

If Eq. (3.66) and Eq. (3.67) are differentiated with respect to x and z , respectively, they attain the following;

$$\frac{\partial v_x}{\partial x} = k_x \frac{\partial^2 h}{\partial x^2} \quad (3.68)$$

$$\frac{\partial v_z}{\partial z} = k_z \frac{\partial^2 h}{\partial z^2} \quad (3.69)$$

Then Eq. (3.65) becomes:

$$k_x \frac{\partial^2 h}{\partial x^2} + k_z \frac{\partial^2 h}{\partial z^2} = 0 \quad (3.70)$$

If a homogeneous material is assumed, the coefficients of permeability in the x and z direction will then be the same. i.e. $k_x = k_z = k$. Then Eq. (3.70) will be:

$$k \left[\frac{\partial^2 h}{\partial x^2} + \frac{\partial^2 h}{\partial z^2} \right] = 0 \quad (3.71)$$

Eq. (3.71) may be formulated in a form that is familiar to engineers by letting $\phi = k.h$

$$\frac{\partial^2 \phi}{\partial x^2} = k \frac{\partial^2 h}{\partial x^2} = \frac{\partial v_x}{\partial x} \quad (3.72)$$

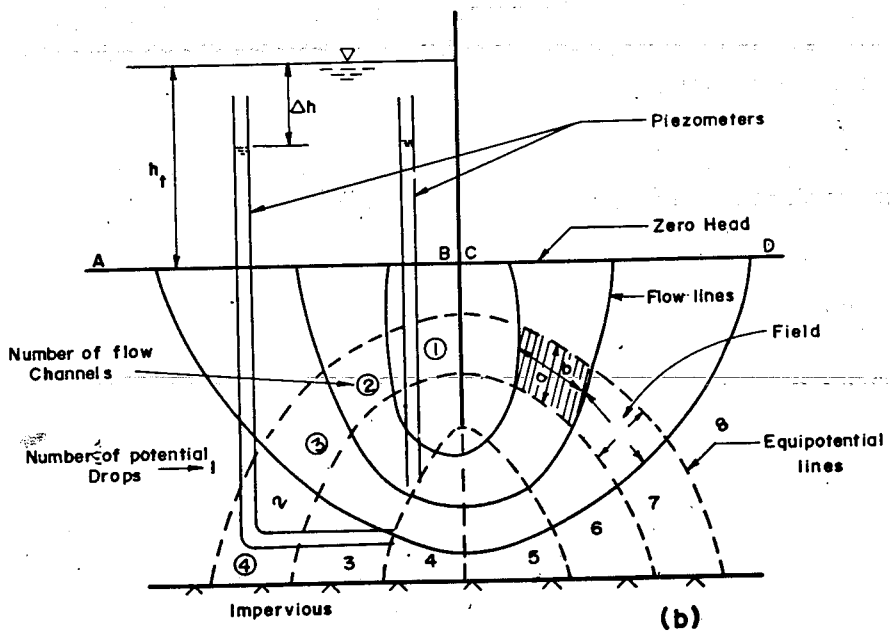
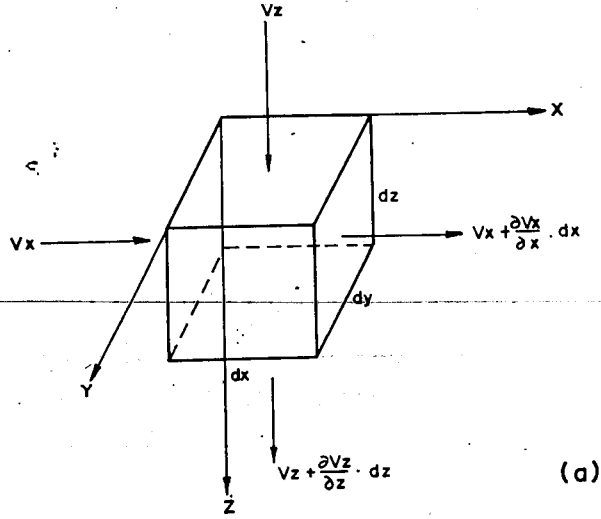


Fig. 3.13 Mathematical representation of seepage

$$\frac{\partial^2 \phi}{\partial z^2} = k \frac{\partial^2 h}{\partial z^2} = \frac{\partial v_z}{\partial z} \quad (3.73)$$

From Eq. (3.65),

$$\frac{\partial^2 \phi}{\partial x^2} + \frac{\partial^2 \phi}{\partial z^2} = 0 \quad (3.74)$$

Eq. (3.74) is Laplacian equation and governs the flow of incompressible fluid through porous material for two dimensional flow condition. Graphically the equation can be represented by two sets of curves that intersect at right angles known as flow net. The curves of one set are called *flow lines*, whereas the curves of the other set are known as *equipotential lines*.

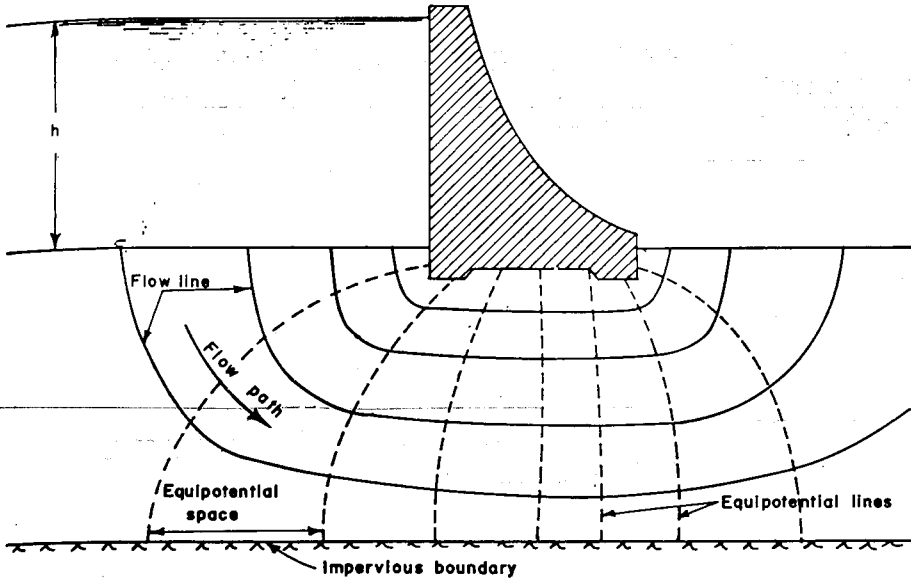
The flow line is the path which a particle of water follows in its course of seepage through a saturated soil mass. Along each flow line there is a point where the water has dissipated a certain portion of its potential. A line connecting all such points of equal head is the *equipotential line*.

At all points along an equipotential line, water would rise in a piezometric tube to a certain elevation obeying the general rule of Bernoulli (Fig.3.13b).

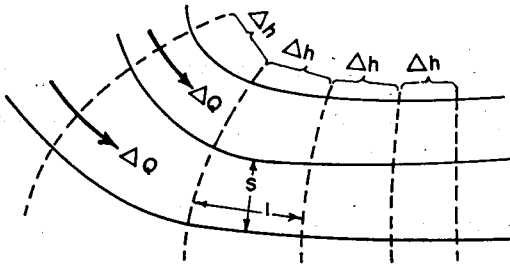
3.3.2 Flow Nets

3.3.2.1 General

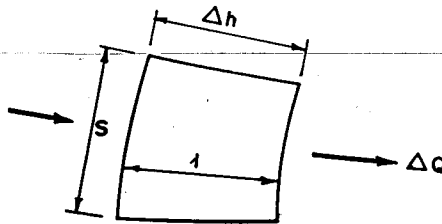
A flow net is a pictorial representation of the paths taken by water in passing through the ground, dams etc. It greatly facilitates the study of gravitational flow and the computation of seepage quantities through ground, dams and levees. A flow net consists of flow lines and equipotential lines, which intersect each other at 90 degrees. (Fig.3.14).



(a) Flow lines and equipotential lines



(b) Flow channels and equipotential drops



(c) Flow in an element of soil

Fig. 3.14 Flow net of seepage beneath a concrete dam.

A *flow line* represents the path which a particle of water follows as it travels from point to point in a soil mass (Fig. 3.14a). Through a soil mass a large number of flow lines and equipotential lines may be drawn (Fig 3.14a). The space between two adjacent flow lines is called the flow path. The space between two adjacent equipotential line is known as an equipotential space and represents a definite increment or drop in head.

3.3.2.2. Methods for Constructing Flow Nets

There are several methods for constructing the flow nets. The common methods are:

- i) Principal stress analogy. Curves are obtained analytically or by means of photo-elastic observation on models.
- ii) Electrical analogy (using electrical models). The equation is of the same form as that for the flow of an electric current through a conducting sheet of uniform thickness. The solution of this equation is represented by a set of orthogonal lines, one set being equipotential and the other flow lines.
- iii) Graphical and computation method. This could be either
 - a) by relaxation method by using the principle of finite difference, or
 - b) by sketching i.e., trial and error.

Of the above listed methods, sketching, being short and uncomplicated, is the most common method used for constructing flow nets.

3.3.3. Construction of flow nets

Before a flow net can be drawn, the boundary lines of both the flow lines and equipotential lines must be established. Having done this, the following points should be noted in the actual drawing of the flow nets.

- a) Flow lines must be drawn parallel to each other. They must be spaced in such a way that the quantity of water flowing in each flow path will be the same. It is advisable to keep the number of flow lines drawn to a minimum.

- b) Equipotential lines are drawn such that they cross the flow lines at right-angles. It is a requirement of true flow net that the geometrical figures formed by the two family of curves must be essentially squares. In practical cases the figures cannot be true squares. However, they must have right angles at the corners and the two median dimensions of each figure must be equal. Each equipotential space must represent an equal drop in head. Typical sketches of flow nets through homogeneous soils are given in Figs. 3.15 a,b,c.

3.3.4 Determination of Discharge from Flow Net

The total quantity of water Q flowing through a unit width of a soil mass is equal to the sum of the quantities in all the flow paths of the flow net. But it is a basic requirement of a flow net that every flow path must transmit the same quantity of water (Fig. 3.14).

Therefore, the quantity in each flow path, $\Delta Q = Q/n_f$. Where n_f = number of flow paths. Likewise, the total head, h , is the sum of the drops in head in all equipotential spaces of the flow net (Fig. 3.14b). The drop in head in each space, $\Delta h = h/n_d$, where n_d = number of equipotential spaces.

$$\Delta Q = k \frac{\Delta h}{l} s \quad (3.75)$$

Consider the flow through any single square as indicated in Fig. 3.14c. The quantity of flow in the square is ΔQ and the drop in head is Δh

Since the figures are squares, $s/l = 1$. Hence Eq. (3.75) becomes $\Delta Q = k \Delta h$. It then follows:

$$Q = kh \frac{n_f}{n_d} \quad (3.76)$$

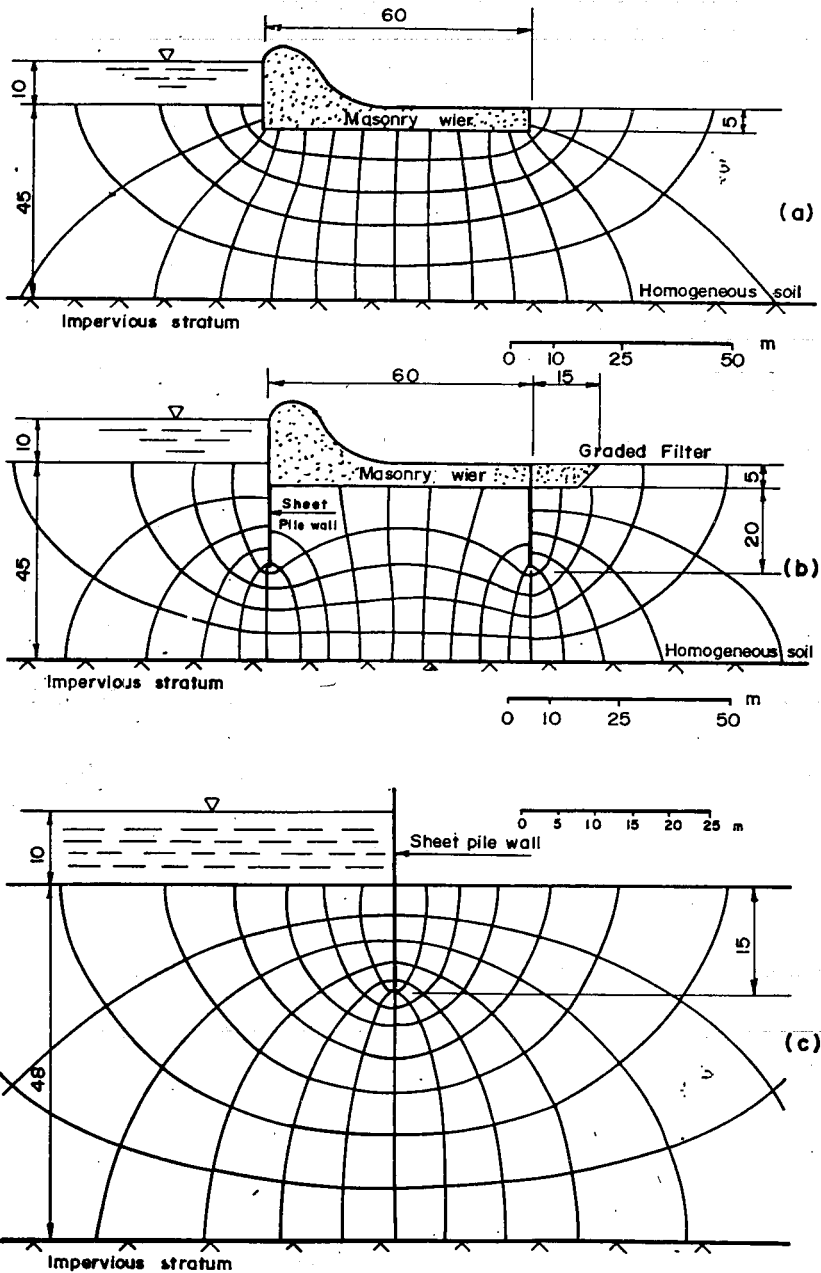


Fig. 3.15 Flow net for different boundary conditions

3.4 SEEPAGE THROUGH HOMOGENEOUS EARTH EMBANKMENTS

Darcy's law can also be applied to calculate discharge of gravity flow through earth dams. In designing and constructing earth dams, the engineer is interested in their general stability, particularly, in the loss of water through earth dams by seepage, as well as in the height of the out crop point of the upper most flow or seepage line. This upper most flow line is also called the saturation line, or the phreatic line (Fig. 3.16)

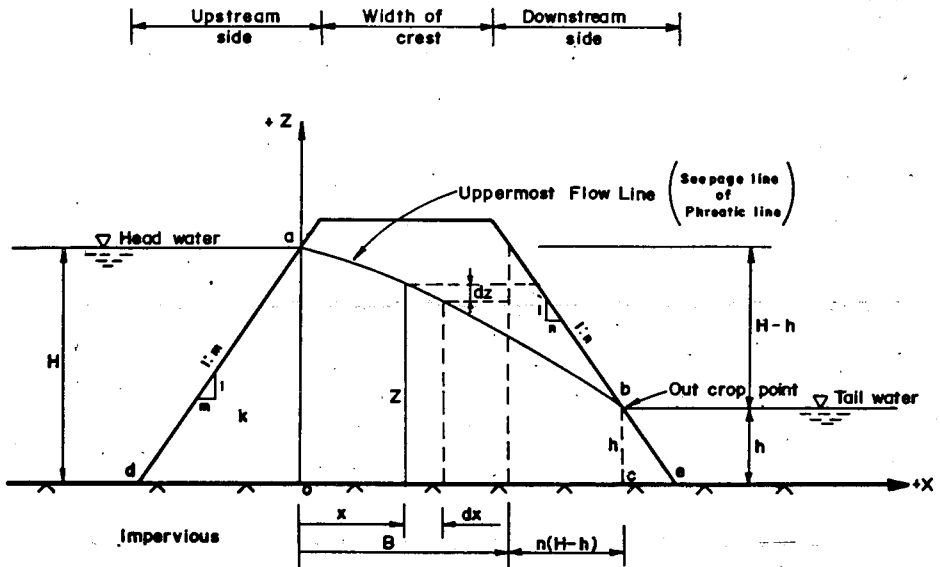


Fig 3.16 Seepage through a homogeneous dam

3.4.1 General Consideration

The upper most flow line is a free water surface forming the upper boundary of flow by seepage. Above the saturation line exists atmospheric pressure and below this line hydraulic pressure prevails.

Below the outcrop point the downstream slope of the earth dam must be protected from being washed out. The curved line a-b is the seepage line and at point b, on the downstream side, the seepage line crops out of the dam. The height b-c (h) is the height of the outcrop point of the seepage line above the impervious stratum and determines the level of the tail water.

3.4.2 Analytical Procedure for Determination of Discharge and Seepage

3.4.2.1 Discharge Equation

The slope of the seepage is

$$i = -\frac{dz}{dx} \quad (3.77)$$

The rate of filtration, v , according to Darcy's Law is

$$v = ki = k\left(-\frac{dz}{dx}\right) \quad (3.78)$$

The discharge through the dam per unit length along the shore line is

$$Q = vA = vz(1) = -kz \frac{dz}{dx} \quad (3.79)$$

Where $A = z(1)$ = area perpendicular to flow.

Separation of variables and integration of Eq. (3.79) yields

$$Q \int dx = -k \int z dz \quad (3.80)$$

$$Qx = -\frac{k}{2}z^2 + C \quad (3.81)$$

The constant of integration may be determined using Fig. 3.16, where at $x=0$, $z = H$. Substituting these values in Eq. (3.81)

$$O = -\frac{k}{2}H^2 + C \quad (3.82)$$

$$\text{Hence, } C = \frac{k}{2}H^2$$

Substituting Eq. (3.82) in Eq. (3.81)

$$Q = \frac{k}{2x}(H^2 - z^2) \quad (3.83)$$

This is the discharge equation per unit length of shore line. In this derivation, one has considered the vertical lines *ao* and *bc* instead of the actual boundaries *ad* and *be* (Fig. 3.16). These two neglected triangular parts of the dam consume a certain magnitude of the pressure head to overcome the friction in these parts of the soil. However, the convenience in calculating the discharge outweighs the error thus introduced.

3.4.2.2 Equation of Seepage Line

From Eq. (3.83) the equation of the upper most flow line or seepage line may be obtained in a general form.

$$z^2 = H^2 - \frac{2Qx}{k} \quad (3.84)$$

3.4.2.3 Determination of Outcrop Height

The position of the outcrop height, *h*, is determined so that the discharge *Q* through the vertical face, *b-c*, is maximum. Therefore, substituting *x* by *B + n(H - h)* and *z* by *h* in Eq. (3.83), the following equation is obtained.

$$Q = \frac{k}{2x}(H^2 - z^2) = \frac{k}{2} \left[\frac{H^2 - h^2}{B + n(H - h)} \right] \quad (3.85)$$

The discharge is at its maximum when $\frac{dQ}{dh} = 0$

Hence,

discharge
$$\frac{dQ}{dh} = \frac{k}{2} \frac{[B+n(H-h)] - (2h) - (H^2 - h^2)(-n)}{B+n(H-h)^2} = 0 \quad (3.86)$$

The fraction can be equal to zero in one of the following cases:

- a. if the numerator should be equal to zero, or
- b. if the denominator should be equal to an infinitely large number.

It is obvious that $h/2$ is not zero, and that from practice the denominator is not equal to an infinitely large number. It follows, therefore, that the brackets in the numerator must be zero.

Hence,

$$\{B+n(H-h)\} \{-2h\} - \{(H^2 - h^2)(-n)\} = 0 \quad (3.87)$$

Solving Eq. (3.87) for h one obtains [14]

$$h = \left(H + \frac{B}{n}\right) - \sqrt{\left(H + \frac{B}{n}\right)^2 - H^2} \quad (3.88)$$

The above equation reveals that the outcrop height depends upon the geometry of the dam only.

3.4.2.4 Discharge

Now that h is known, and based on the principle of continuity of flow, the discharge, Q , can be calculated from:

$$Q = \frac{k}{2} \frac{(H^2 - h^2)}{B + n(H - h)} \quad (3.89)$$

When Q is known, then by Eq. (3.84) the ordinates, z , of the seepage line a-b can be calculated and plotted by assuming various x - values for a given coefficient of permeability.

$$z^2 = H^2 - \frac{2Qx}{k} \quad (3.90)$$

3.4.2.5. Graphical Determination of Seepage Line

A typical case in this context is seepage through an earth dam. Seepage water passing through the dam will normally saturate the lower portion while the upper portion remains relatively dry. The problem in this kind of situation is to determine the upper boundary of saturation or the top most flow line. A. Casagrande has given certain empirical rules for estimating the location and shape of the top most flow line in a cross-section of a dam. In general, the top most flow line is parabolic in shape, but deviates from a parabola at the up-stream face of the dam and at the exit face. Fig.3.17 represents a cross section of a dam of homogeneous soil. As can be seen from the figure, the dam rests on an impervious foundation. All seepage water, therefore, flows through the dam. The line of contact with the foundation is one boundary flow line. The up-stream face of the dam represents one equipotential boundary. At down-stream toe of the dam there is a horizontal drainage layer. The line of contact between the dam and this drainage layer is the outlet face and represents the down-stream equipotential boundary of the flow net.

According to A. Casagrande, the construction of basic parabola to represent the top flow line is described as outlined hereunder.

- a) Draw the cross-section of the dam ABCD to scale and establish the reservoir water line KM and drainage layer FEG.
- b) Locate the point K vertically above the point A and lay off the distance $MI = 0.3MK$. I represents a point on the basic parabola.
- c) With I as center and IF as radius describe an arc to cut the extended water line at L.

Fig. 3.18 (a) illustrates the case when the down-stream face of the dam itself serves as discharge face while Fig. 3.18 (b) shows a situation where the up-stream face of a rock-fill toe is used as a discharge face.

When the basic parabola cuts the discharge face at a distance $(b+a)$ from the toe, the corrected seepage line meets the discharge face at a distance a from the toe. For $\alpha < 90^\circ$ the seepage line meets the discharge face tangentially as shown in Fig. 3.18 (a) while for $\alpha > 90^\circ$ as in Fig. 3.18 (b), it drops vertically into the rockfill toe. The ratio of $\frac{b}{a+b}$

for various values of α from 30° to 180° is given in Fig. 3.19

To determine the discharge and outcrop point, for slope angle, α less than 30° , the method of Schaffernack/Casagrande is applied [14]. Referring to Fig. (3.20a), the discharge through any cross-section per unit time will be,

$$Q = kAi = k.zl. \frac{dz}{dx} = k.z. \frac{dz}{dx} \tag{3.91}$$

Noting that at the outcrop of the seepage line

$$z = h = a \sin \alpha \tag{3.92}$$

$$\text{and } \frac{dz}{dx} = \tan \alpha \tag{3.92a}$$

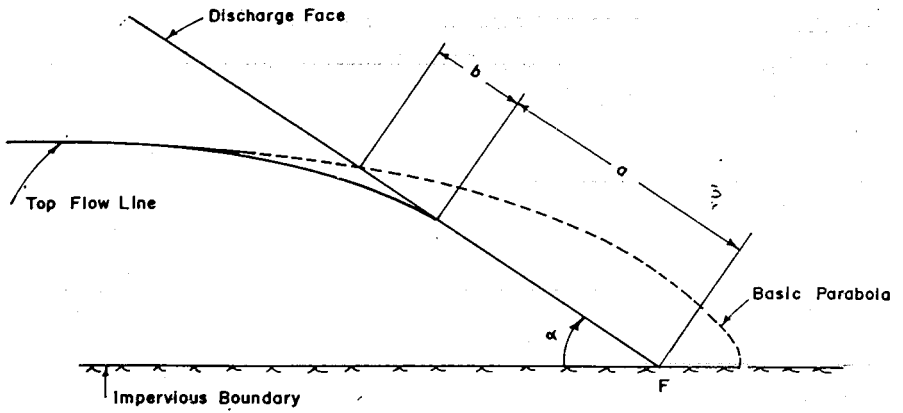
Eq. (3.91) may be expressed as

$$Q = k a \sin \alpha. \tan \alpha \tag{3.93}$$

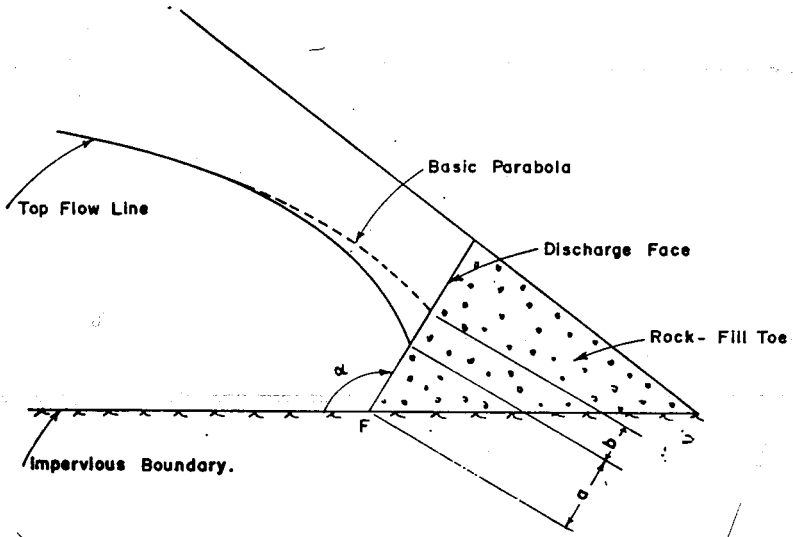
between the limits $x = 0$ and $x = a \cos \alpha$.

The integral of the differential equation (Eq. 3.91) between the the limits $x = a \cos \alpha$ and d (Fig. 3.20a) becomes

$$Q \int_{a \cos \alpha}^d dx = k \int_{a \sin \alpha}^H z dz \tag{3.94}$$



(a)



(b)

Fig. 3.18 Seepage line exit for sloping discharge limits

The solution of Eq.(3.94) after simplification becomes

$$Q = \frac{k(H^2 - a^2 \sin^2 \alpha)}{2(d - a \cos \alpha)} \quad (3.95)$$

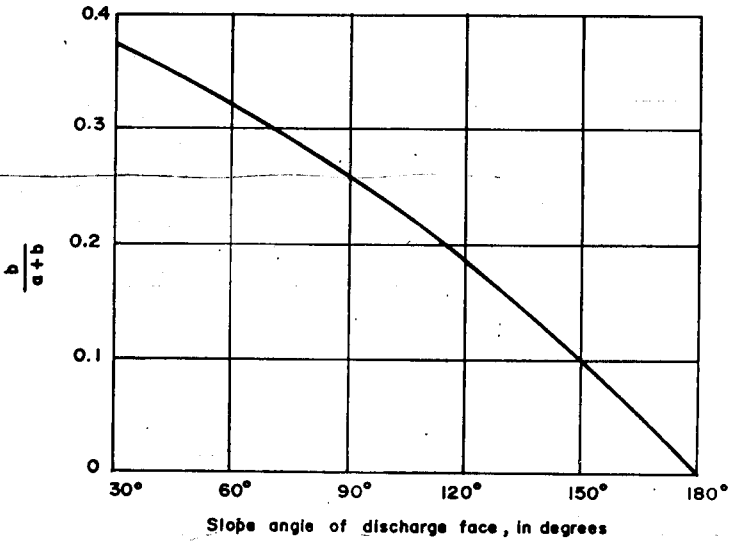


Fig. 3.19 Relation between slope of discharge face and ratio $b/a+b$

By the principle of continuity of flow, the discharge quantities on both sides of the outcrop height, h , must be equal, i.e.

$$Q = k a \sin \alpha \tan \alpha = \frac{k(H^2 - a^2 \sin^2 \alpha)}{2(d - a \cos \alpha)} \quad (3.96)$$

From the above we get,

$$a^2 \sin^2 \alpha - 2ad \sin \alpha \tan \alpha + H^2 = 0 \quad (3.97)$$

The solution of this equation gives the length, a , which determines the outcrop point, S , of the seepage line at the down stream slope of the earth dam. (Fig.3.20a)

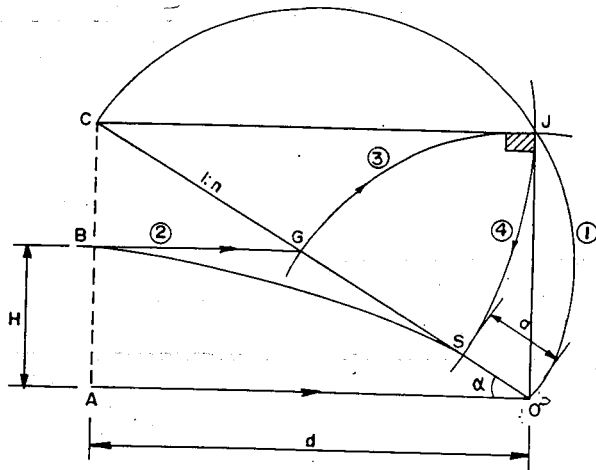
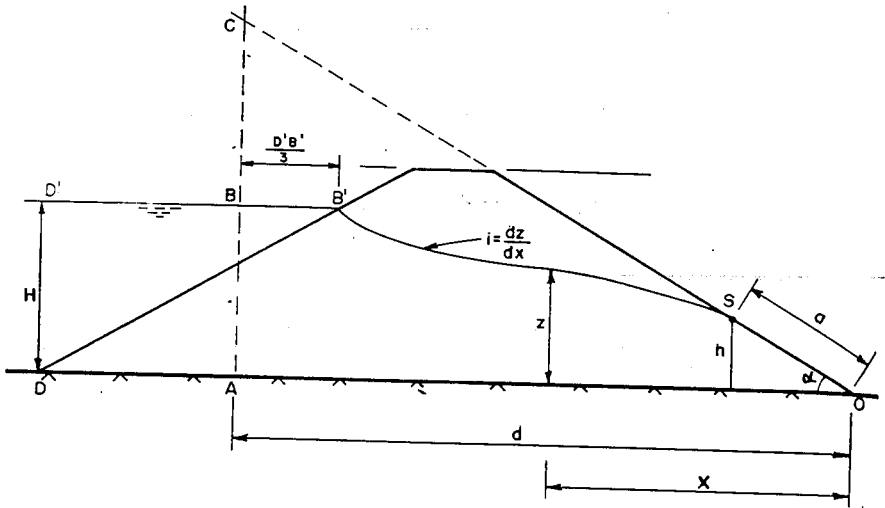


Fig. 3.20 Determination of the outcrop S for α less than 30°

$$a = \frac{d}{\cos \alpha} - \sqrt{\frac{d^2}{\cos^2 \alpha} - \frac{H^2}{\sin^2 \alpha}} \quad (3.98)$$

Based on this analytical approach, the outcrop point S may be determined graphically according to the following procedure (Fig. 3.20b):

- a) Extend AB to intersect line OS extended at C.
- b) Draw a semi-circle with diameter OC.
- c) Locate point G by drawing a line from B parallel to AO.
- d) With center O and radius OG draw an arc cutting the semi-circle at J.
- e) Using point C as center and CJ as radius draw an arc cutting CO at S which is the outcrop point.

The proof of the graphical construction may be shown as follows [14]

Noting that $\angle CJO = 90^\circ$; $OG = OJ$; $CJ = CS$

$$(OJ)^2 + (CJ)^2 = (OC)^2 \quad (3.99)$$

But $OJ = OG = \frac{H}{\sin \alpha}$ (3.100)

$$CS = \frac{d}{\cos \alpha} - a \quad (3.101)$$

$$OC = \frac{d}{\cos \alpha} \quad (3.102)$$

Therefore, $\left[\frac{H}{\sin \alpha} \right]^2 + \left[\frac{d}{\cos \alpha} - a \right]^2 = \left[\frac{d}{\cos \alpha} \right]^2$ (3.103)

Hence, $a = \frac{d}{\cos \alpha} - \sqrt{\frac{d^2}{\cos^2 \alpha} - \frac{H^2}{\sin^2 \alpha}}$ (3.104)

3.5 SEEPAGE THROUGH STRATIFIED SOILS

Natural soil deposits generally show stratification resulting in larger permeability in the horizontal direction than in the vertical direction, or vice versa. When such situation exists, it is necessary to transform the scale of the cross-section of the soil mass before starting to sketch a flow net. When $k_h > k_v$, the transformation is made by dividing the horizontal dimensions of the cross-section by $\sqrt{k_h/k_v}$

where

k_h = the coefficient of permeability in the horizontal direction and

k_v = the coefficient of permeability in the vertical direction.

After the scale transformation has been completed, a flow net is drawn in the normal manner on the transformed section. The final flow net is obtained by retransforming the cross-section including the flow net back to its original scale through multiplication of each horizontal dimension by $\sqrt{k_h/k_v}$. The flow lines and equipotential lines

obtained by so doing will not intersect at right angles, nor will the figures be squares being elongated in the horizontal direction. Fig. 3.21 (a) shows a square in transformed section. Considering the effective permeability as k' the discharge can be written as,

$$\Delta Q = k' \frac{\Delta h}{a_1} (a_1 \cdot 1) = k' \Delta h \quad (3.105)$$

In the transformed or restored section shown in Fig. 3.21(b), Δh is the same, but the horizontal length of the field will be

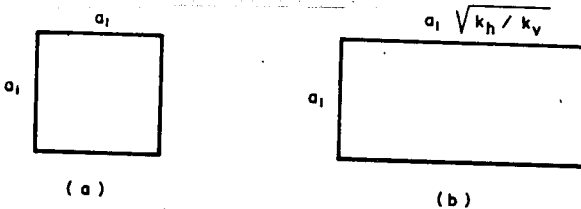


Fig. 3.21 Section transformation

$\sqrt{k_h/k_v} \cdot a_1$ The effective permeability in this section is k_b . The discharge for the restored section can be expressed as,

$$\Delta Q = k_h \frac{\Delta h}{a_1 \sqrt{k_h/k_v}} \cdot (a_1 \cdot 1) = k_h k_v \Delta h \tag{3.106}$$

Equating the discharge from the two sections yields,

$$k' = \sqrt{k_h k_v}$$

Therefore, the effective permeability is $\sqrt{k_h k_v}$. The seepage discharge in stratified section is given by,

$$Q = \sqrt{k_h k_v} \frac{n_f}{n_d} \Delta h \tag{3.107}$$

3.6 EFFECT OF CORE-WALL ON SEEPAGE

Consider seepage through an earth dam (or rock fill dam) shown in Fig. 3.22(a). A section through an earth dam shows that the dam is usually constructed from different materials divided into zones. The core of the dam or the central zone is usually made of impervious material (clay) while the rest is constructed with semi-pervious or pervious materials. In the course of seepage, water passes through sections of the dam with coefficients of permeabilities of k_1 and k_2 as shown in Fig. 3.22(b). Assuming that the soil in each zone is isotropic, the flow lines as well as the equipotential lines deflect as shown in Fig. 3.22(b). The flow lines CDE and FGH cross the interface at angles of approach and departure θ_1 and θ_2 respectively. The flow channel formed by these two flow lines has a width of Δb_1 in zone (1) and Δb_2 in zone (2). From Fig. 3.22(b); it is apparent that

$$DG = \frac{\Delta b_1}{\cos \theta_1} = \frac{\Delta b_2}{\cos \theta_2} \tag{3.108}$$

In addition to the flow lines, three equipotential lines are also indicated whose potentials are h , $h + \Delta h$ and $h + 2\Delta h$. The distances between the potential lines in both zones are ΔS_1 and ΔS_2 . From the figure it is apparent that,

$$KG = \frac{\Delta S_1}{\sin\theta_1} = \frac{\Delta S_2}{\sin\theta_2} \quad (3.109)$$

By dividing Eq. (3.108) by Eq. (3.109) the following relationship is obtained.

$$\frac{\Delta b_1}{\Delta S_1} \tan\theta_1 = \frac{\Delta b_2}{\Delta S_2} \tan\theta_2 \quad (3.110)$$

For the discharge Δq in the flow channel,

$$\Delta q = \Delta b_1 k_1 \frac{\Delta h}{\Delta S_1} = \Delta b_2 k_2 \frac{\Delta h}{\Delta S_2} \quad (3.111)$$

From which it follows that

$$\frac{\Delta b_1}{\Delta S_1} k_1 = \frac{\Delta b_2}{\Delta S_2} k_2 \quad (3.112)$$

If Eq. (3.112) is compared with Eq. (3.110) the following is obtained.

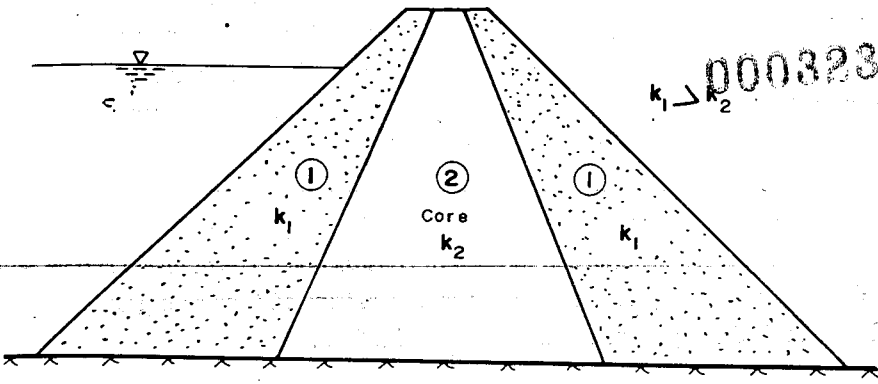
$$\frac{k_1}{k_2} = \frac{\tan\theta_1}{\tan\theta_2} \quad (3.113)$$

From Eq. (3.112) it follows that if a square flow net ($\Delta b_1 = \Delta S_1$)

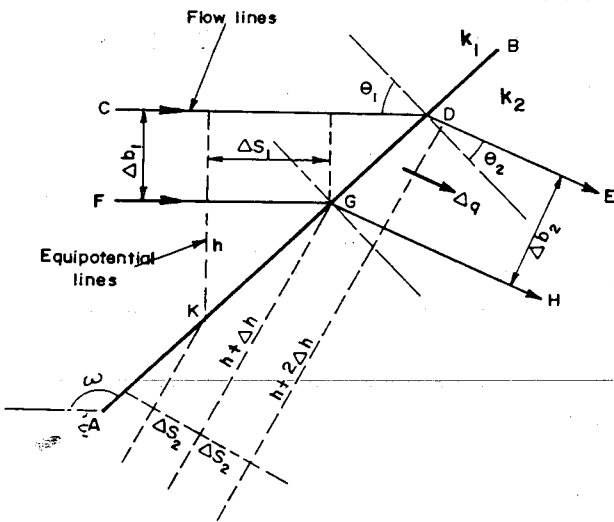
is sketched in zone (1), rectangular flow net with a side ratio k_1/k_2 will emerge on the side of zone (2). If it is desired that all the flow nets in zone (1) and zone (2) be squares, then the relationship required between head drops would be:

$$\frac{\Delta h_2}{\Delta h_1} = \frac{k_1}{k_2} \quad (3.114)$$

The above derived expressions are applicable for cases where the ratio between k_1 and k_2 should not be greater than 10. If the ratio is greater than 10, then the flow in the two zones may be considered to be independent from one another. If there are stratification in the dam and the same stratification ratio holds in both zones, then the same procedure may be used for unzoned sections.



(a) Zoned Section of an Earth Dam



(b) Flow and equipotential lines at the interface AB

Fig. 3.22 Seepage through zoned sections

3.7. FILTERS

Near the downstream toe of an earth dam there is a continuous flow of water which at times develops a high hydraulic gradient. This high hydraulic gradient causes the finer particles of the dam to be washed out and create a condition of failure.

To prevent this *erosion or piping*, internal drainage systems are constructed at the toe of the dam from selected materials known as *filters*.

The drainage system is governed by the height of the dam, permeability of foundation, availability of porous material and the cost of construction. The drainage system must be chosen in such a way that it carries away the anticipated flow with great margin of safety. Simple drainage systems are shown in Fig. 3.23.

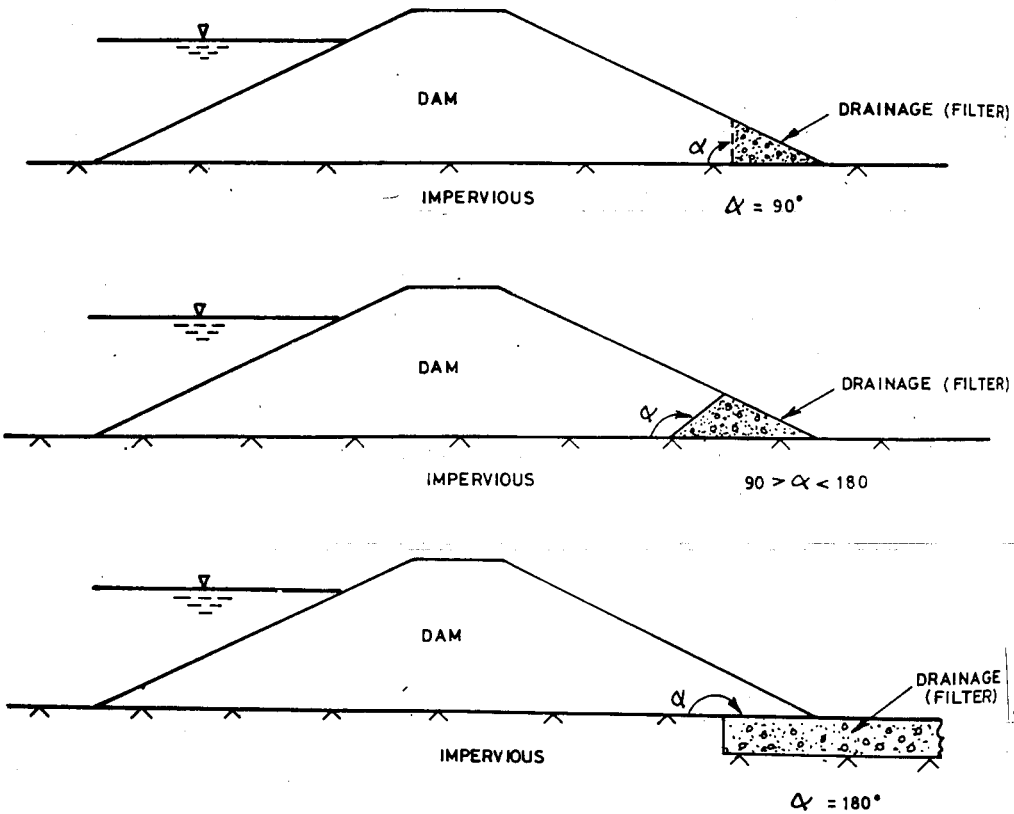


Fig. 3.23 Simple drainage systems

The two principal requirements of the filter material for a satisfactory drainage system are that it must be more pervious than the protected soil so that water may percolate freely through and that it should be fine enough to stop the particles of the protected soil from passing through its voids.

Through experience and experimentation, Terzaghi gave the following design criteria for filter material [31].

$$a) \quad \frac{D_{15} \text{ filter}}{D_{15} \text{ soil}} \geq 5 \quad (3.115)$$

$$b) \quad \frac{D_{15} \text{ filter}}{D_{85} \text{ soil}} \leq 5 \quad (3.116)$$

The geometry of the filters affects the pattern of the flow nets as indicated in Fig. 3.24.

3.8 EFFECTIVE AND TOAL STRESSES IN SOILS

3.8.1 General

If an element inside a loaded soil mass as found in a natural state is considered, the stress imposed on the element will be partly transmitted to the intergranular contact points and partly to the water in the voids. Imagine a small element in a soil mass which is completely saturated (Fig. 3.25 a).

Except for the infinitesimal areas of grain to grain contacts, the water pressure acts over the entire area. The water pressure in the pores is called the *neutral stress*. It has a magnitude of $\gamma_w z$ if static water condition prevails. It is important to note that neutral pressures act on all sides of particles and do not cause particles to press against adjacent particles. They do not have shearing components. The pressure in the intergranular contact points is called the *effective stress* and has normal and shearing components. The sum of intergranular or effective and neutral stress is known as *combined stress* or *total stress*.

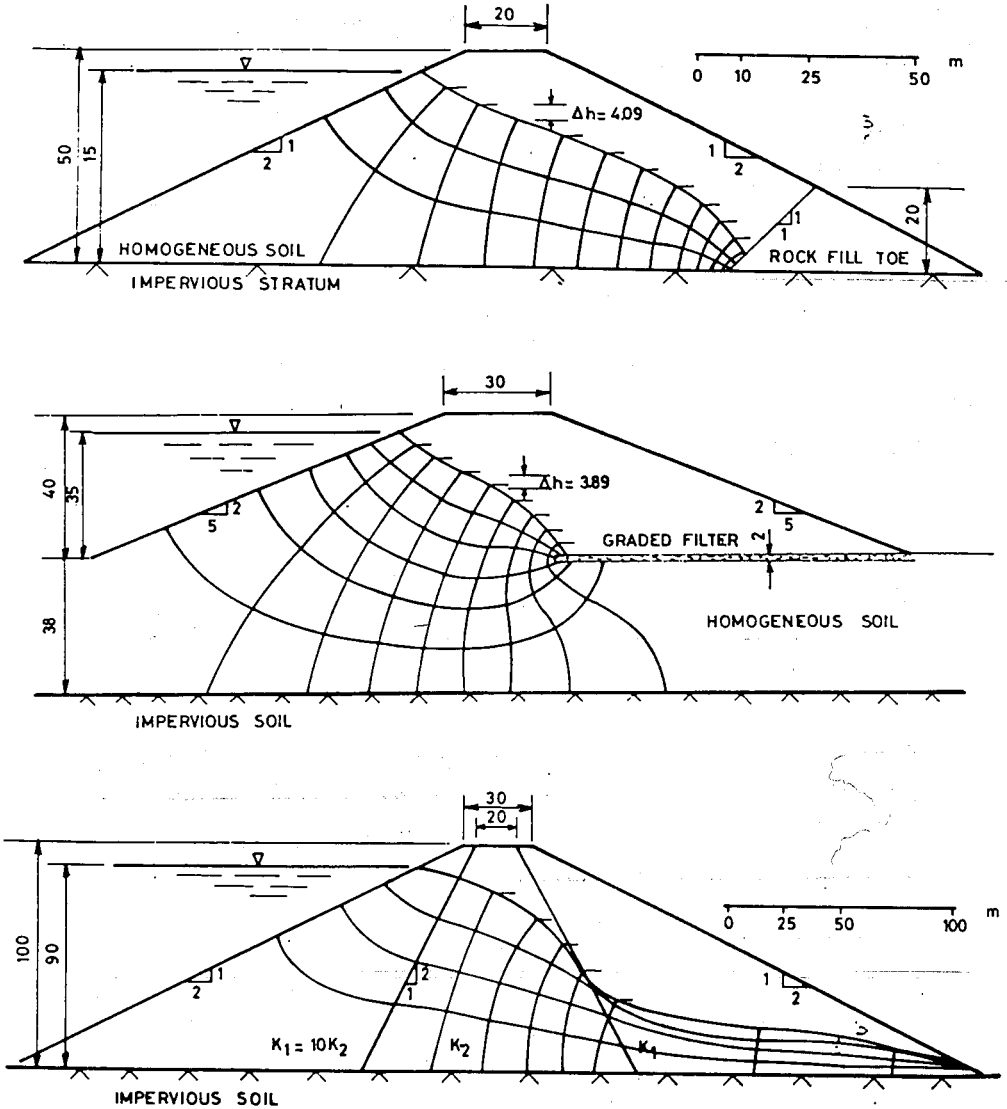


Fig. 3.24 Flow nets for earth dams with different drainage systems

3.8.2 Derivation of Formulas

The stresses developed in the different constituents of a soil may be studied with a help of a figure which represents qualitatively a typical cross section through two soil grains in contact (Fig. 3.25b). The total area of the soil subjected to a load P is A . Contact areas of grain to grain, grain to liquid and grain to air are given as A_s, A_w and A_g respectively.

Let the stresses in solid, liquid and gaseous phases be $\sigma_s, \sigma_w, \sigma_g$ respectively. Now considering the balance of forces in the vertical direction.

$$P = \sigma_s A_s + \sigma_w A_w + \sigma_g A_g \quad (3.117)$$

Dividing both sides by A

$$\frac{P}{A} = \sigma = \alpha \sigma_s + \beta \sigma_w + (1 - \alpha - \beta) \sigma_g \quad (3.118)$$

where σ = total stress over the gross area

$$\alpha = \frac{A_s}{A}, \beta = \frac{A_w}{A} \text{ and } (1 - \alpha - \beta) = \frac{A_g}{A}$$

The parameter β is related to the degree of saturation of the soil. By carrying out certain algebraic simplification the following equation is obtained

$$\sigma = \alpha \sigma_s + (1 - \alpha) \sigma_w + (1 - \alpha - \beta) (\sigma_g - \sigma_w) \quad (3.119)$$

If the soil is completely saturated, then

$$(1 - \alpha - \beta) = 0 \quad (3.120)$$

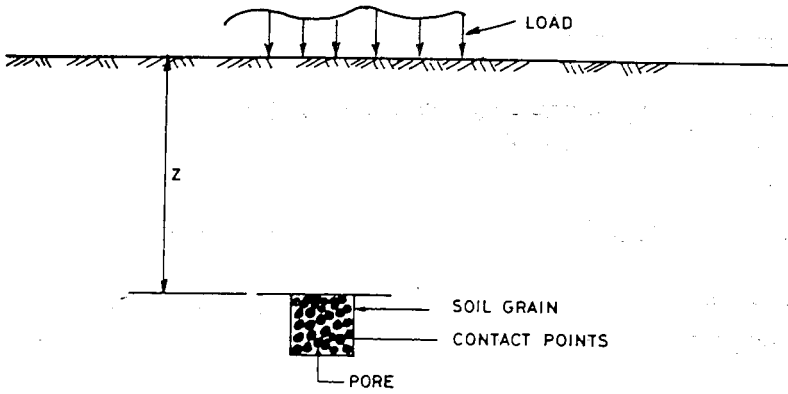
Equation (3.119) becomes

$$\sigma = \alpha \sigma_s + (1 - \alpha) \sigma_w \quad (3.121)$$

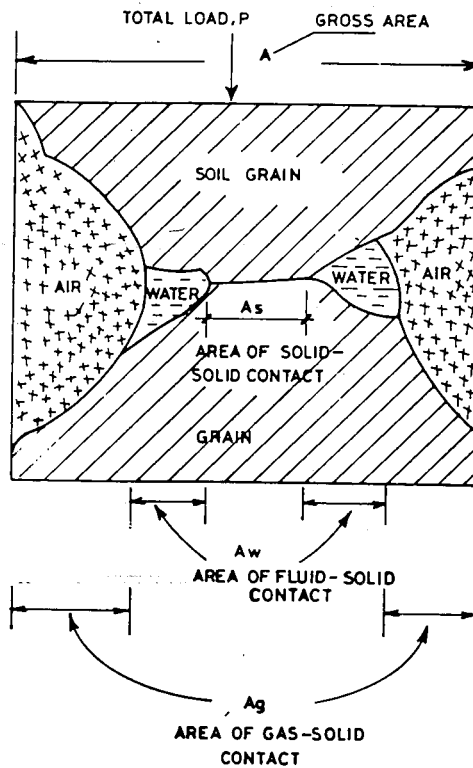
Under the present condition of interest, the ratio α will be very small, so that the term $(1 - \alpha)$ approaches unity. However, σ_s is very high and probably equal to the yield stress of the material at the surface. The product $\alpha \sigma_s$ does not become equal to zero but to a quantity which is called the *effective stress* in the soil skeleton, $\bar{\sigma}$. It can thus

be written:

$$\sigma = \bar{\sigma} + \sigma_w \quad (3.122)$$



(a) SOIL ELEMENT IN THE GROUND



(b) SOIL ELEMENT MAGNIFIED

Fig. 3.25 Study of effective stress

The parameter σ_w may be written as

$$\sigma_w = u + \Delta u \quad (3.123)$$

where u = steady-state pressure in the pore water

Δu = is a transient pore water pressure excess over the steady-state pressure.

3.9 CRITICAL HYDRAULIC GRADIENT

Critical gradient, i_c , is a gradient that is associated with heave or boiling of unrestrained soil surface subjected to seepage. Consider the arrangement shown in Fig. 3.26. Water is percolating upwards through a sand of thickness L and cross-sectional area A . As the water emerges into the atmosphere at the top of the sand, the head loss through the sand is h . At the bottom plane of sand, the total downward force is equal to the saturated weight of the sand. From Eq. 2.19,

$$\gamma_{sat} LA = \frac{(G_s + e)}{1 + e} \gamma_w LA$$

The upward force at the same plane is the pressure of water under a head of $(h+L)$ on an area A and this is equal to $\gamma_w (h+L)A$. If these two forces happen to be equal, the net downward force on the bottom plane will be nil and there will be no force preventing the outflow of sand from the container. For this condition to occur,

$$\frac{(G_s + e)}{1 + e} \gamma_w LA = \gamma_w (h+L)A$$

$$\frac{(G_s + e)}{1 + e} \gamma_w LA - \gamma_w LA = \gamma_w hA$$

$$\frac{h}{L} = i_c = \frac{G_s - 1}{1 + e} = \frac{\gamma_b}{\gamma_w} \quad (3.124)$$

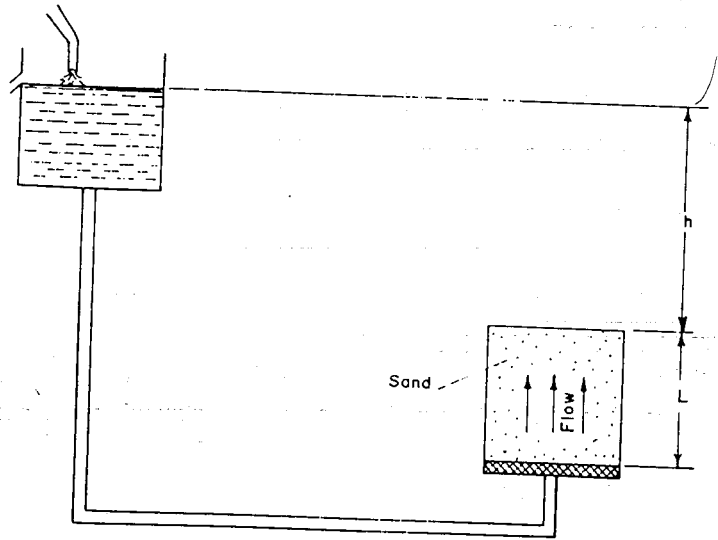


Fig 3.26 Critical hydraulic gradient

i_c is the *critical hydraulic gradient*. It is a gradient through the soil at which the effective pressures on a horizontal plane in the soil are reduced to zero. The sand-water mixture in this condition behaves as a liquid without a shear strength. The soil behaves as though it is weightless and highly unstable. The soil in this condition is described as quick or quick sand. A solid of larger unit weight than the sand-water mixture placed on the surface of sand will sink to the bottom of the container when the critical hydraulic gradient conditions are reached. If the gradient is slightly more than critical, a mixture of sand and water will start flowing out of the container.

3.10 SEEPAGE FORCES

Seepage forces exist in all cases of gravitational flow through soil. Seepage water flowing through soil exerts a force on the soil mass in the direction of flow. This force is proportional to hydraulic gradient. Let h be the head dissipated in moving the water through an element of soil of length d and cross sectional area A (Fig. 3.27a). The seepage force exerts pressure in the direction of flow, which is equal to $h \cdot \gamma_w \cdot A$.

The volume of soil element is $A \cdot d$. Then the seepage force/unit volume will be:

$$\frac{h\gamma_w A}{Ad} = i\gamma_w \quad (3.125)$$

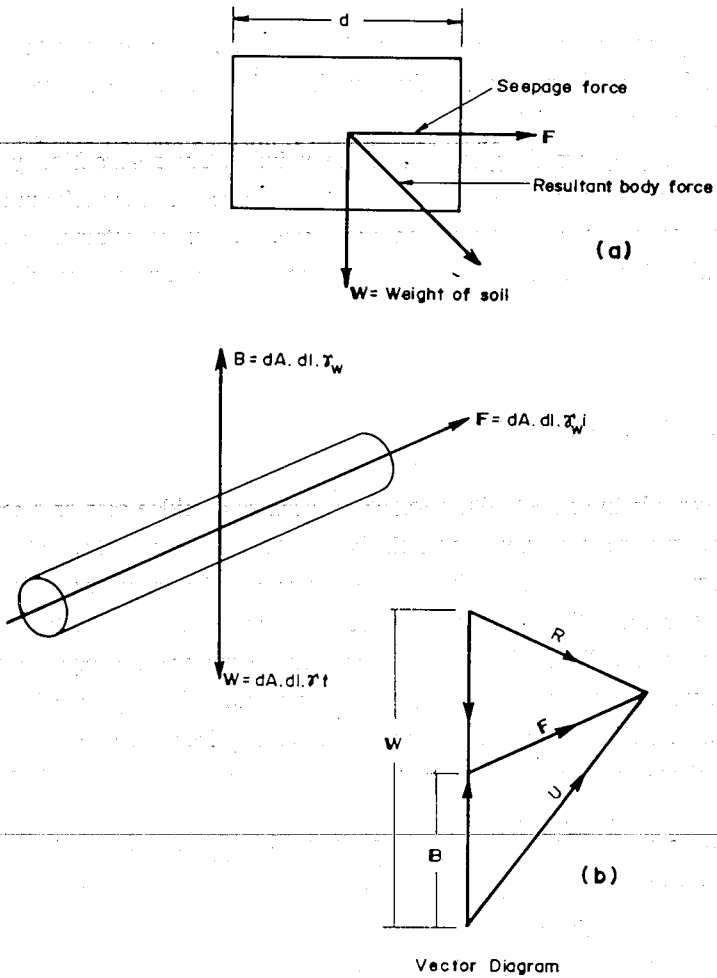


Fig. 3.27 Seepage forces

It will be seen from Eq.(3.125) that the seepage force has the dimension of unit weight. Consider a cylindrical element of length dl and area dA subjected to seepage in axial directions as shown in Fig. 3.27b

The total weight of the cylinder $W = dA \cdot dl \cdot \gamma_t$, where γ_t is the saturated unit weight of the soil. The force of buoyancy, $B = dA \cdot dl \cdot \gamma_w$ and the seepage force $F = i \gamma_w dA \cdot dl$

The vector diagram for these forces is drawn in Fig. 3.27. The weight of the element is W and the buoyant force acts directly opposite to it. Therefore the net effective weight is the submerged weight $= (W-B)$

The seepage force, F , acts along the axis of the cylinder. The resultant body force is obtained as a vector sum of $(W-B)$ and F . Another approach to the problem involves the determination of the total neutral or water force, U . This is obtained as a vector sum of B and F . The combination of W and U again gives the same resultant body force, R .

3.11 UPLIFT PRESSURE

When free water is in contact with a structure, such as a bridge pier or a masonry dam, uplift pressures are exerted against the base of the structure. If the water is static the uplift pressure is equal to the hydrostatic pressure. If seepage water is flowing beneath the structure, the uplift pressure at any point can be estimated from the appropriate flow net. The total head at any point in flowing water is equal to the sum of the velocity head, the pressure head and the elevation head. In practically all cases of flow through soil, velocities are so small that velocity heads are negligible. Total head is, therefore, considered to equal to pressure head plus elevation head. Elevation head is the vertical distance of a point from a datum plane, which is usually chosen as the elevation of the tail water. The total head at any point on the base of a structure can be determined from the equipotential line that intersects the base at the point. Then the difference between the total head and the elevation is the pressure head which may be multiplied by the unit weight of water to obtain the uplift pressure.

3.12 EXAMPLES

E3.1 A cylinder of soil 15 cm in height exhibiting an effective ratio of the area of pores that varies as $\cos \frac{(\pi z)}{3h}$, where z and h are as given in

Fig. 3.1. Determine:

- the volume porosity of the soil sample
- the volume porosity if the cylinder is 30 in height.

SOLUTION

$$a. \quad m = \frac{1}{h} \int_0^h m(z) dz$$

$$= \frac{1}{h} \int_0^h \cos \frac{\pi \cdot z}{3h} dz$$

$$= \frac{1}{h} \left[\frac{3h}{\pi} \cdot \sin \left\{ \frac{\pi z}{3h} \right\} \right]_{z=0}^{z=h}$$

$$= \frac{1}{h} \frac{3h}{\pi} \cdot \sin \frac{\pi}{3} \cdot h$$

$$= \frac{3}{\pi} \sin \frac{\pi}{3}$$

b. The volume porosity is independent of the height.

E. 3.2 A soil sample in a constant head permeameter is 4 cm in diameter and 15 cm long. Under a head of 20cm, the discharge was found to be 60cm³ in 15 minutes. What is the permeability of the soil.

SOLUTION

$$Q = kiA = k \frac{h}{L} A$$

$$L = 15 \text{ cm}$$

$$h = 20 \text{ cm}$$

$$Q = \frac{60}{15} = 4 \text{ cm}^3/\text{min}$$

$$A = \pi r^2 = \frac{\pi d^2}{4} = \frac{3.14(4^2)}{4} = 12.56 \text{ cm}^2$$

$$k = \frac{QL}{hA} = \frac{(4)15}{(20)12.56} = (23.89)10^{-2} \text{ cm/min or } (39.82)10^{-4} \text{ cm/sec}$$

- E3.3 A soil sample in a variable head permeameter is 10 cm in diameter and 12cm high. The permeability of the sample is estimated to be 10×10^{-4} cm/sec. If it is desired that the head in the stand pipe should fall from 20cm to 10 cm in 4 minutes, determine the size of the standpipe which should be used.

SOLUTION

$$K = \frac{2.3aL}{At} \log_{10} h_2/h_1$$

$$a = \frac{KAt}{2.3L \log_{10} h_2/h_1}$$

$$x = \frac{(10)10^{-4} \left(\frac{10^2 \pi}{4} \right) (4 \times 60)}{2.3 \times 12 \log_{10} 20/10} = 2.268 \text{ cm}$$

$$\frac{\pi d^2}{4} = 2.268 \text{ cm}$$

$$d = \sqrt{\frac{2.268(4)}{3.14}} = 1.7 \text{ cm}$$

The required size of the standpipe = 1.70cm

E.3.4 A pumping test was made in a medium of sand and gravel to a depth of 15m where a bed of clay was encountered. The normal water level was at the surface. Observation holes were located at distances of 3m and 7.5m from the pumping well. At a discharge of 200 liters per minute from the pumping well, a steady-state was attained in about 24 hours. The drawdown at 3m was 1.7m. and at 7.5m was 0.4m. Compute the coefficient of permeability of the soil.

$$Q = \frac{k(h_1^2 - h_2^2)}{\log_e \frac{r_1}{r_2}}$$

$$r_1 = 7.5 \text{ m}$$

$$h_1 = 15 - 0.04 = 14.6 \text{ m}$$

$$r_2 = 3 \text{ m}$$

$$h_2 = 15 - 1.7 = 13.3 \text{ m}$$

$$k = \frac{Q \log_e \frac{r_1}{r_2}}{\pi(h_1^2 - h_2^2)}$$

$$k = \frac{(200)(1000) \log_e \frac{7.5}{3}}{3.14(14.6^2 - 13.3^2)} = \frac{58362.464}{213.16 - 176.89}$$

$$= 1609.11 \text{ cm/min} \quad = 26.82 \text{ cm/sec}$$

E.3.5 A sand mass with a void ratio of $e = 0.70$ and $G_s = 2.66$ is given. Determine:

- the critical hydraulic gradient
- the safe hydraulic gradient for the given flow system with a factor of safety = 3.

SOLUTION

$$i) i_c = \frac{G_s - 1}{1 + e} = \frac{2.66 - 1}{1 + 0.07} = 0.976$$

ii) The safe hydraulic gradient:

$$i = \frac{i_c}{3} = \frac{0.976}{3} = 0.325$$

E.3.6 An excavation with a system of sheet piling as indicated in Fig. E 3.1 is given. Evaluate the possibility of quicksand conditions in the excavation.

SOLUTION

From Darcy's Law, $v = ki = k \frac{h}{L}$

$$k_v = \frac{L_1 + L_2}{\frac{L_1}{k_1} + \frac{L_2}{k_2}}$$

$$L = L_1 + L_2; h = h_1 + h_2$$

$$v_{avg} = k_v \frac{h}{L} = \frac{L_1 + L_2}{\frac{L_1}{k_1} + \frac{L_2}{k_2}} \cdot \frac{h_1 + h_2}{(L_1 + L_2)} = \frac{h_1 + h_2}{\frac{L_1}{k_1} + \frac{L_2}{k_2}}$$

$$v_{avg} = \frac{500}{\frac{360}{1} + \frac{500}{0.001}} = (9.9928) 10^{-4} \text{ cm/sec}$$

$$h_1 = v_{avg} \frac{L_1}{k_1} = (9.9928) 10^{-4} \frac{360}{1} = (3.5974) 10^{-1} \text{ cm} = 0.36 \text{ cm}$$

The possibility of quick condition exists for the excavation.

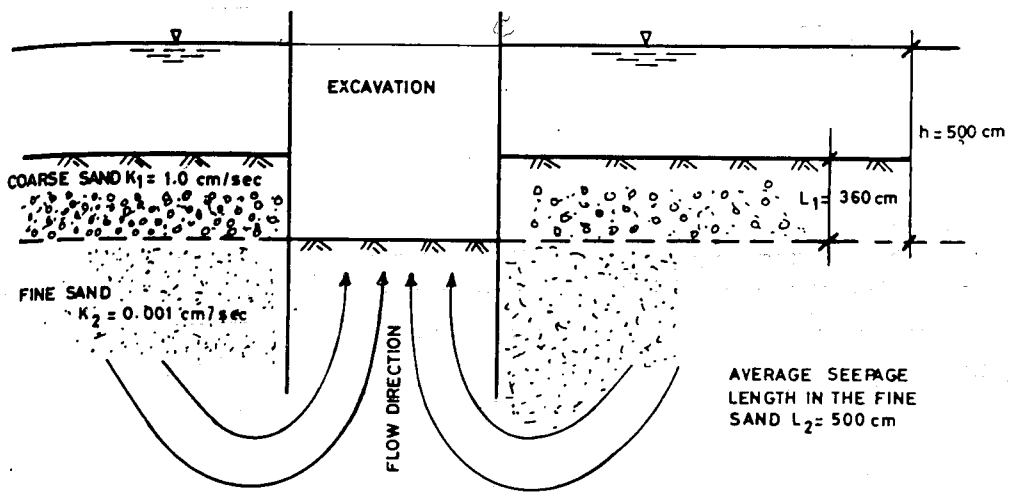
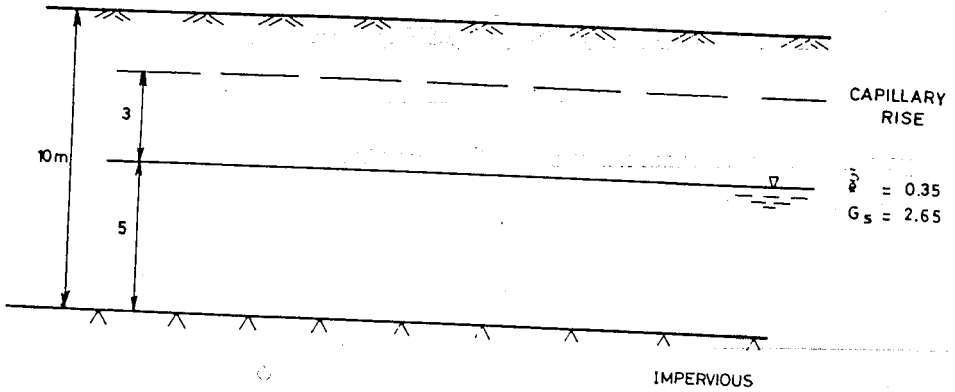
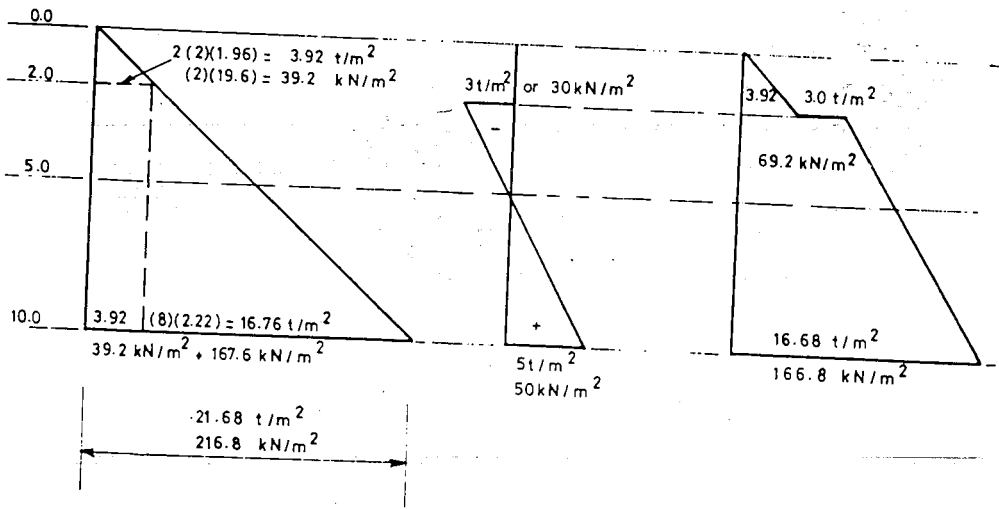


Fig. E.3.1 Excavation problem

E.3.7 For the soil profile given below, sketch the diagram showing the total, neutral and effective vertical stresses in the deposit.



a- SOIL PROFILE



(i) total stress σ

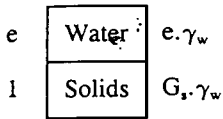
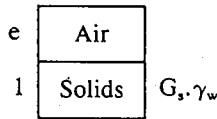
(ii) neutral stress u

(iii) effective stress σ'

b- STRESS DISTRIBUTION

Fig. E.3.2 Soil profile and stress distribution

SOLUTION

Saturated $S=1$ Dry $S=0$

It shall be assumed that above the capillary rise, total dry condition exists. Below the capillary rise total saturation exists.

$$\gamma_t = \gamma_w \left[\frac{G_s + e}{1 + e} \right] = \left[\frac{2.65 + 0.35}{1.35} \right] (1) = 2.22 \text{ t/m}^3 \text{ or } 22.2 \text{ kN/m}^3$$

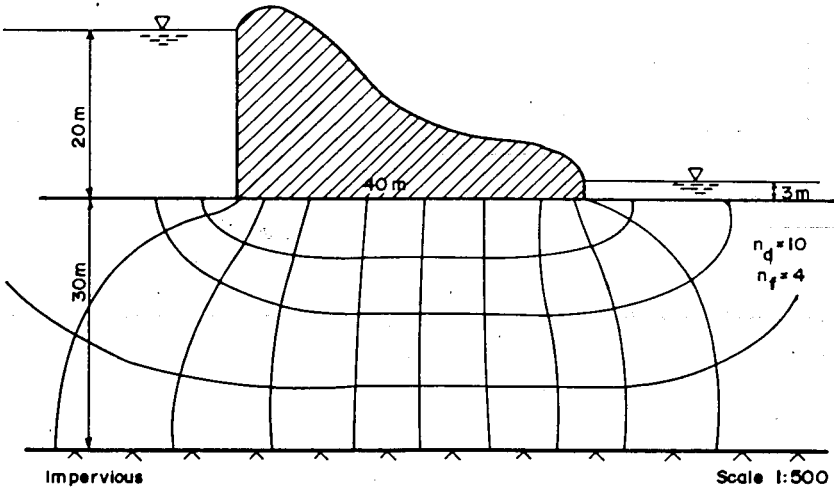
$$\gamma_{dry} = \frac{G_s \cdot \gamma_w}{1 + e} = \frac{2.65}{1.35} (1) = 1.96 \text{ t/m}^3 \text{ or } 19.6 \text{ kN/m}^3$$

The vertical pressure distribution is given in Fig. E.3.2b.

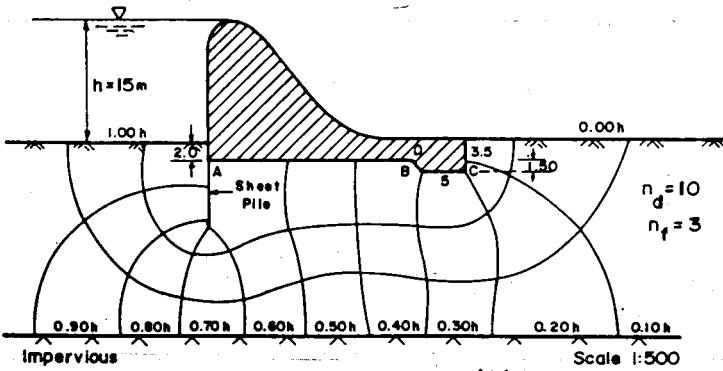
E.3.8 A gravity dam and a wier shown in Fig. E.3.3 is given. Coefficient of permeability $k = 0.0003 \text{ cm/sec}$ and the length of the dam perpendicular to the direction of seepage 200m .

Determine:

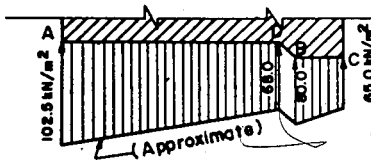
- The total quantity of water that seeps out of the dam (Fig. E. 3.3a).
- The hydraulic uplift pressure distribution under the wier (Fig. E.3.3b)
- The seepage force per unit volume at the toe of the wier and check the danger of piping . Given, $G_s = 2.65$ and $e = 0.72$



(a) Gravity Dam



(b) Wier with sheet pile



(c) Pressure Distribution

Fig. E. 3.3 Seepage analysis

SOLUTION

- a. Using the procedure outlined earlier, the flow net under the dam is constructed. From the sketch $n_d = 10$ and $n_r = 4$

$$c. \text{ Seepage per metre} = k \cdot h_r \frac{n_r}{n_d}$$

$$= \frac{(0.000003)(20)(4)}{10}$$

$$= 0.000024 \text{ m}^3/\text{sec}$$

$$= 0.0864 \text{ m}^3/\text{hr}$$

$$\text{Total Seepage} = 0.0864 (200) = 1.728 \text{ m}^3/\text{hr} \approx 1.73 \text{ m}^3/\text{hr}$$

- b. From the flow nets, $n_d = 10$ and $n_r = 3$

The water pressure, in a still water, follows that $\Delta u = \gamma_w \cdot z$

However, when the water is moving, this law does not apply and the pressure must be computed from flow charts.

The total head h at a point is given by the equipotential line. If the elevation of that point is z then, the pressure head is $h - z$.

The water pressure is $u = \gamma_w (h - z)$. The pressure head at any point at the base of the dam can be calculated from the relation:

Pressure head = total head - elevation head

Point A:

$$\text{Total head} = 0.55h = (0.55)(15) = 8.25\text{m} \quad \text{elevation head} = -2\text{m}$$

$$\text{Pressure head} = 8.25 - (-2) = 10.25\text{m}$$

$$\text{Uplift} = (10.25)(10.0) = 102.5\text{kN/m}^2$$

Point B:

$$\text{Total head} = 0.30h = 0.30(15) = 4.5\text{m}$$

$$\text{Elevation head} = -3.5\text{m}$$

$$\text{Pressure head} = 4.5 - (-3.5) = 8.0\text{m}$$

$$\text{Uplift} = (8.00)(10.0) = 80.0\text{kN/m}$$

Point C:

$$\text{Total head} = 0.20 h = (0.20)(15) = 3.0\text{m}$$

$$\text{Elevation head} = -3.5\text{m}$$

$$\text{Pressure head} = 3.0 - (-3.5) = 6.5\text{m}$$

$$\text{Uplift} = (6.5)(10.0) = 65 \text{ kN/m}^2$$

Point D:

$$\text{Total head} = 0.32h = (0.32)(15) = 4.8\text{m}$$

$$\text{Elevation head} = -2\text{m}$$

$$\text{Pressure head} = 4.80 - (-2) = 6.80\text{m}$$

$$\text{Uplift} = (6.80)(10.0) = 68.0 \text{ kN/m}^2$$

By subdividing the net, the uplift pressure curve for the whole wier could be plotted. (Fig. E.3.3c)

Head drop in the last square = $0.10h = (0.10)(15) = 1.5\text{m}$. Minimum length of seepage path = 3.5m

$$i = \frac{1.5}{3.5} = 0.43$$

$$\frac{G_s - 1}{1 + e} = \frac{2.65 - 1}{1 + 0.72} = \frac{1.65}{1.72} = 0.96$$

Since $i < i_c$, no danger of piping.

3.13 EXERCISES

- 1 A block of soil is 12 cm long and 6cm^2 in cross-section. The water level at one end of the block is 20cm above a fixed plane, and at the other end, it is 3cm above the same plane. The flow rate is 2c.c in 1.5 minutes. Compute the soil permeability.
- 2 A sample of coarse sand, 20cm in height and 5 cm in diameter, is tested in constant head permeater. Water percolated through the soil under a hydrostatic head of 50 cm for a period of 8.0 sec. The discharged water is 450 cm^3 .

- a. What is the coefficient of permeability at test temperature?
b. If the test temperature is 30° , what would be the coefficient of permeability at 20°C ?
- 3 A falling-head permeater test was performed on a clay sample. The diameter of the sample was 5.0 cm and its thickness, L , was 2.5cm. At the start of the test, the water in the 1.5 mm inner diameter glass-tube standpipe was at an elevation $h_1 = 35$ cm. Six minutes later it dropped to 30cm. Compute the coefficient of permeability of the clay at 20°C , if the test was conducted at a temperature of 40°C .
- 4 In order to determine the average permeability of a bed of sand 14 m thick overlying an impermeable stratum, a well was sunk through the sand and a pumping test was carried out. After a certain interval, the discharge was 12.4 liters per second and drawdowns on observation wells at 16m and 33m from the pumping wells were found to be 1.787m and 1.495m respectively. If G.W.L. was originally 2.14m below ground level, find the permeability and an approximate value for the effective grain size.
- 5 A horizontal stratified deposit consists of three layers each uniform in itself. The permeabilities of the layers are 8×10^{-4} cm/sec, 50×10^{-4} cm/sec and 15×10^{-4} cm/sec and their thickness are 6m, 3m and 18m respectively. Find the effective average permeability of the deposit in horizontal and vertical directions.
- 6 A dam to be constructed on a sandy soil which has a coefficient of permeability of 14×10^{-4} cm/sec in horizontal direction and 4×10^{-4} cm/sec in vertical direction. The dam is expected to impound water to a height of 10m. In drawing a flow net it is found that the number of flow channels is 5 and the corresponding number of equipotential drops is 14. Calculate the seepage loss per meter length of the dam, if water on downstream is 1m.
- 7 If the soil layer under the gravity dam shown in Fig.E.3.3 a has $k_v = 0.0005$ cm/sec and $k_h = 0.0020$ cm/sec,

- a. determine the seepage in m^3/day for 100 metre length of dam.
- b. estimate the total uplift under the dam.
- c. check the possibility of "boiling" at the toe of the dam.
- d. suggest an appropriate filter if the soil has the following gradation

D in mm	2	1	0.5	0.25	0.064	0.05	0.02	0.01	0.005	0.001
P in %	100	97	94	90	75	70	50	35	24	8

8 An earth dam similar to the one shown in Fig 3.23 has the following dimension:-
 Slope m = 1:20 water side, 1:25 dry side

- Crest = 6 meters
- Height of impounded water from the base = 10m
- Free board = 2m
- $k = 0.003 \text{ cm/sec}$
- $\alpha = 120^\circ$

1.77

- Height of outcrop from the base = 3m
- a. Construct the basic parabola and determine the phreatic line.
- b. Estimate the seepage in m^3/day if the total length of the dam is 200m.

9 If in Problem 7, $k_v = 0.0001 \text{ cm/sec}$
 and $k_h = 0.0009 \text{ cm/sec}$, estimate the seepage in m^3/day for the total length of dam.

10 A sand deposit with $e = 0.6$, $G_s = 2.65$, is 5 m deep and under it is a 4m deep clay layer with $e = 1.10$ and $G_s = 2.80$. Draw the total, neutral and effective stress distribution in the soil strata, if

- a. ground water is not present.
- b. ground water is at a depth of 4m from the ground surface and the expected capillary rise is two meters.
- c. ground water is at the surface.

11 A foundation trench is to be excavated in a clay stratum 6m thick underlain by sandy stratum. The water table is observed in a bore hole to be 1m below the ground level. Find the depth to which the excavation can proceed without the danger of blow. Take the specific gravity of clay particles to be 2.65 and the water content of the clay soil in a saturated condition equal to 37%.

4. STRESS DISTRIBUTION IN SOILS

4.1 STRESS DUE TO SOIL WEIGHT

The vertical stress at any point in a soil formation with the horizontal surface due to only soil weight is a function of thickness and the unit weights of overlying materials. In a level mass of homogeneous soil having unit weight γ , the vertical stress at any depth, h , due to soil weight is given by $\sigma_v = \gamma h$. If the soil consists of strata, each with different thickness and unit weights, then the vertical stress at any level is expressed by

$$\sigma_v = \gamma_1 h_1 + \gamma_2 h_2 + \dots \quad (4.1)$$

where

- σ_v = vertical stress due to soil weights at depth $h_1 + h_2 + \dots$
- γ_1, γ_2 = unit weights of overlying formation 1, 2, ...
- h_1, h_2 = thickness of overlying formations 1, 2, ...

In making the above calculation, it is the effective (intergranular) stress which is of practical interest. This is especially true when calculations are made for settlement analysis.

4.2 STRESS DUE TO CONCENTRATED SURFACE LOADING

A load applied at the surface of soil mass induces stresses within the entire mass. These stresses decrease with increasing depth and distance from the loaded area. A knowledge of distribution of these stresses is essential for predicting the settlement of structures due to compression of layers buried beneath the surface. For determining the stress distribution in soils, the soil medium is assumed to be an elastic half-space. The bases for determining stresses in the interior of an elastic half space is given by Boussinesq, where he considered the simplest form of loading - an isolated point load acting on the surface (Fig.4.1)

- If
- σ_r = the radial stress
 - σ_z = the vertical stress
 - σ_θ = the tangential stress or horizontal circumferential stress

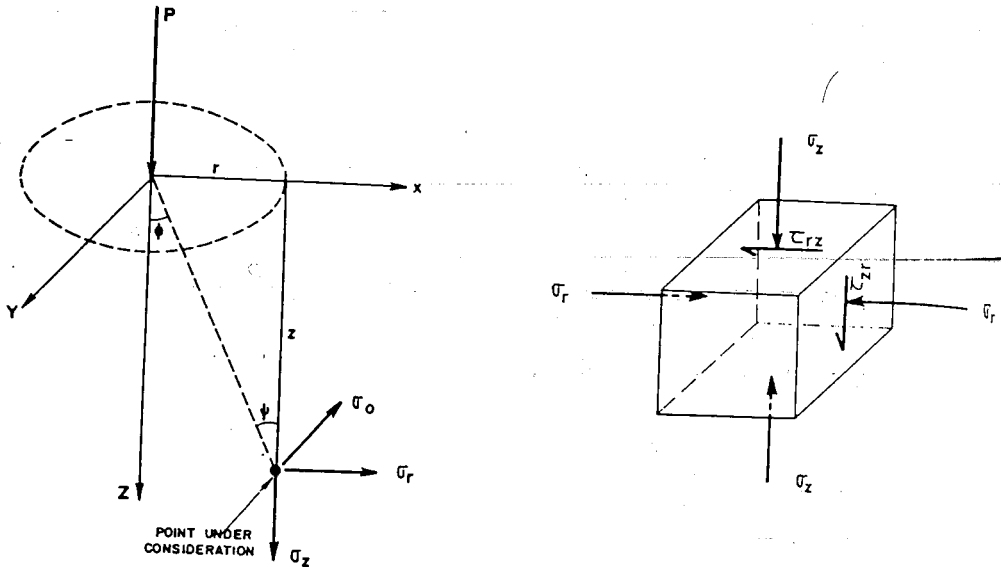


Fig. 4.1 Stress in the interior of an elastic half-space

and τ_{rz} = the shearing stress on the rz plane, their magnitudes are calculated from,

$$\sigma_r = \frac{P}{2\pi z^2} \cdot 3\cos^2\psi \cdot \sin^2\psi \cdot (1 - 2\mu) \cdot \frac{\cos^2\psi}{1 + \cos\psi} \quad (4.2)$$

$$\sigma_z = \frac{3P}{2\pi z^2} \cdot \cos^3\psi \quad (4.3)$$

$$\sigma_\theta = (1 - 2\mu) \frac{P}{2\pi z^2} \cos^2\psi \cdot \frac{\cos^2\psi}{1 + \cos\psi} \quad (4.4)$$

$$\tau_{rz} = \frac{3P}{2\pi z^2} (\cos^4\psi \sin\psi) \quad (4.5)$$

Where μ is the Poisson's ratio and varies between 0 and 0.5. It will be noted that the vertical stress, σ_z , and the shear stress, τ_z , are both independent of μ . The above equations may also be written in terms of r and z .

$$\sigma_r = \frac{P}{z^2} \cdot \frac{1}{2\pi} \left\{ \frac{3 \left(\frac{r^2}{z} \right)^2}{\left[1 + \left(\frac{r}{z} \right)^2 \right]^{5/2}} - \frac{1 - 2\mu}{\left[1 + \left(\frac{r}{z} \right)^2 \right] + \left[1 + \left(\frac{r}{z} \right)^2 \right]^{1/2}} \right\} \quad (4.6)$$

$$\sigma_z = \frac{P}{z^2} \cdot \frac{3}{2\pi \left[1 + \left(\frac{r}{z} \right)^2 \right]^{5/2}} \quad (4.7)$$

$$\sigma_\theta = \frac{P}{z^2} \cdot \frac{1}{2\pi} (1 - 2\mu) \left\{ \frac{1}{\left[1 + \left(\frac{r}{z} \right)^2 \right]^{3/2}} - \frac{1}{\left[1 + \left(\frac{r}{z} \right)^2 \right] + \left[1 + \left(\frac{r}{z} \right)^2 \right]^{1/2}} \right\} \quad (4.8)$$

$$\tau_{rz} = \frac{P}{z^2} \cdot \frac{1}{2\pi} \cdot \frac{r z^3}{\left[1 + \left(\frac{r}{z} \right)^2 \right]^{5/2}} \quad (4.9)$$

Reference to the above equations shows that the stresses are:

- directly proportional to the load, P
- inversely proportional to the square of the depth, z
- proportional to a function of the angle ψ or of the r/z

Therefore, any of the stresses given in the above equations may be written in the form

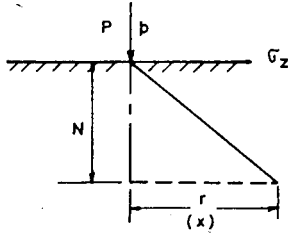
$$\sigma = \frac{P}{z^2} \cdot i \quad (4.10)$$

Since the vertical stress, σ_z , is important in settlement calculation, either Eq. 4.3 or Eq. 4.7 is considered. This may be written as,

$$\sigma_z = \frac{P}{z^2} \cdot i_1 \quad (4.11)$$

The value of i_1 for different $\frac{r}{z}$ ratio are given in Table 4.1

Table 4.1 Coefficients for determining the vertical stress at depth z for point and line loads.



POINT LOAD P			LINE LOAD P	
$\frac{r}{z}$	i_1		$\frac{x}{z}$	i_2
0.00	0.47746	$\sigma_z = \frac{3P}{2\pi} \cdot \frac{z^3}{(r^2 + z^2)^{\frac{5}{2}}} = i_1 \frac{P}{z^2}$ $i_1 = \frac{3}{2\pi} \cdot \frac{1}{\left[\left(\frac{r}{z}\right)^2 + 1\right]^{\frac{5}{2}}}$	0.0	0.63662
0.1	0.46574		0.1	0.62405
0.2	0.43288		0.2	0.58860
0.3	0.38119		0.3	0.53086
0.4	0.32950		0.4	0.47311
0.5	0.27544		0.5	0.40865
0.6	0.22138		0.6	0.34419
0.7	0.18001		0.7	0.29045
0.8	0.13863		0.8	0.23670
0.9	0.11153		0.9	0.19793
1.0	0.08442		1.0	0.15916
1.1	0.06788		1.1	0.13305
1.2	0.05134		1.2	0.10693
1.3	0.04125		1.3	0.08980
1.4	0.03115		1.4	0.07266
1.5	0.02556		1.5	0.06145
1.6	0.01997		1.6	0.05023
1.7	0.01644		1.7	0.04282
1.8	0.01290		1.8	0.03541
1.9	0.01072		1.9	0.03044
2.0	0.00854		2.0	0.02546

$$\sigma_z = \frac{2P}{\pi} \cdot \frac{z^3}{(x^2 + z^2)^2} = i_2 \frac{P}{z^2}$$

$$i_2 = \frac{2}{\pi} \cdot \frac{1}{\left[\left(\frac{x}{z}\right)^2 + 1\right]^2}$$

4.3 STRESS DUE TO UNIFORM LINE LOADING

The stress due to a line load applied at the surface is obtained by replacing P by dp and σ by $d\sigma$ in equations 4.2 to 4.5 and integrating. By so doing the vertical stress due to a line load will have the following form

$$\sigma_z = \frac{2P}{\pi} \frac{z^3}{(r^2 + z^2)^2} \quad (4.12)$$

This equation may be written as

$$\sigma_z = \frac{P}{z} \cdot i_z \quad (4.13)$$

Where i_z is Boussinesq's coefficients given in a tabular form (Table 4.1)

4.4 STRESS DUE TO UNIFORMLY DISTRIBUTED SURFACE LOAD

Loads are never applied at a point in actual structures. They are spread over a certain area. On the basis of Boussinesq's equation for point loads, there are two possible approaches for evaluation of stresses at different depths. The first approach which is relatively approximate involves the division of the loaded area as shown in Fig. 4.2 into smaller areas so that no dimension of such smaller areas is larger than 0.3 times the depth at which the stress intensity is to be evaluated. The total load acting on each small area is then assumed to be concentrated at its center and the effect of all these concentrated loads is determined by Boussinesq's point load equation. The total load on each small area equals to $p \cdot ab$ and acts at the center of the small area.

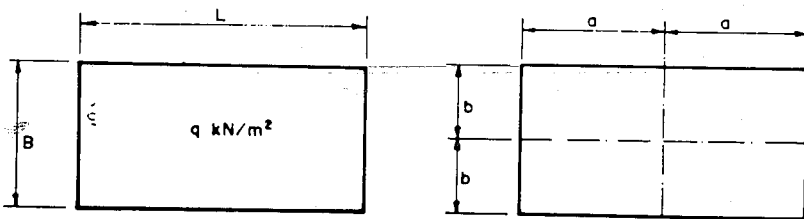


Fig. 4.2 Stress distribution by point load formula

The second approach consists of carrying double integration of Eq. 4.2 to 4.4 both in the x and y directions. This gives the stress at a point which has been given in a tabular form by Steinbrenner (Table 4.2) and in a form of chart by Newmark (Fig 4.3.). While the values given in a tabular form by Steinbrenner are valid for rectangular loaded areas, the influence chart given by Newmark can be used for both regular and irregular geometric shapes.

Procedure for using Steinbrenner's Table

The table of Steinbrenner is used to calculate the vertical stress at any depth z under a corner of a rectangular loaded area. This table could also be used for determining the vertical stress for any other point inside or outside the loaded area. In both cases, the rectangular area will be segmented so that the point under consideration form the corner of each segment (Table 4.2). The coefficient i for each segment is then calculated. The summation of the coefficients for each segment gives the coefficient for the loaded area.

Procedure for using Newmark's Chart

- (a) Draw the foundation on a tracing paper to such a scale that the depth z at which the stress σ_z is to be computed will be equal to distance AB of the chart.
- (b) Lay the tracing of the foundation over the chart in such away that the surface point N beneath which the stress σ_z to be computed coincides with the center of the chart.
- (c) Count the number of blocks covered by the foundation area
- (d) Multiply the number found by counting by the influence value of the chart and the distributed load P .

The product thus obtained gives the value σ_z for that particular point. That is,

$$\sigma_z = I \cdot n \cdot p$$

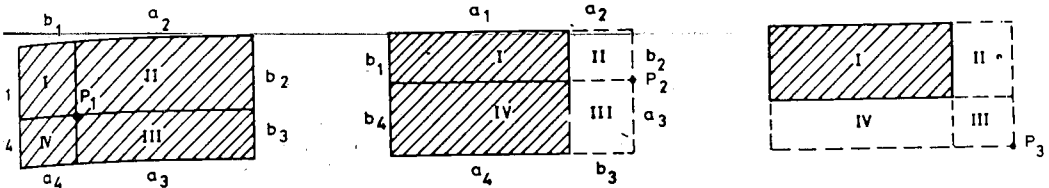
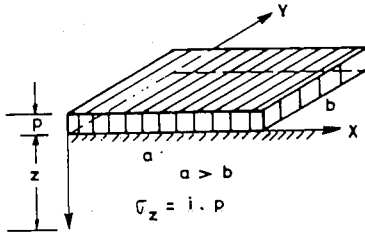
Where

I = influence value of the chart

n = number of blocks

p = distributed surface load.

Table 4.2 Coefficient for determining the vertical stress at a depth z under a corner point for a rectangular loaded area [26]



(a) POINT INSIDE THE LOADED AREA

(b) POINT OUTSIDE THE LOADED AREA

(c) POINT OUTSIDE THE LOADED AREA

$$i = \sum i_1 \cdot i_2 \cdot i_3 \cdot i_4$$

$$i = \sum i_{I, II} \cdot i_{II} \cdot i_{IV, III} \cdot i_{III}$$

$$i = \sum i_{I, II, III, IV} \cdot i_{II, III} \cdot i_{III} \cdot i_{IV, III}$$

DEPTH WIDTH	COEFFICIENT $i = \frac{\sigma_z}{P}$						
	$i = \frac{\sigma_z}{P} = \frac{1}{2\pi} \left[\text{ARC tan } z \sqrt{\frac{ab}{a^2 + b^2 + z^2}} + \frac{abz}{\sqrt{a^2 + b^2 + z^2}} \left(\frac{1}{a^2 + z^2} + \frac{1}{b^2 + z^2} \right) \right]$						
$\frac{z}{b}$	$\frac{a}{b} = 1.0$	$\frac{a}{b} = 1.5$	$\frac{a}{b} = 2.0$	$\frac{a}{b} = 3.0$	$\frac{a}{b} = 5.0$	$\frac{a}{b} = 10.00$	$\frac{a}{b} = \infty$
0.25	0.2473	0.2482	0.2483	0.2484	0.2485	0.2486	0.2485
0.50	0.2325	0.2378	0.2391	0.2397	0.2398	0.2399	0.2399
0.75	0.2060	0.2182	0.2217	0.2234	0.2239	0.2240	0.2240
1.00	0.1752	0.1936	0.1999	0.2034	0.2044	0.2046	0.2046
1.50	0.1210	0.1451	0.1561	0.1638	0.1665	0.1670	0.1670
2.00	0.0840	0.1071	0.1202	0.1316	0.1363	0.1374	0.1374
3.00	0.0447	0.0612	0.0732	0.0860	0.0959	0.0987	0.0990
4.00	0.0270	0.0383	0.0475	0.0604	0.0712	0.0758	0.0764
6.00	0.0127	0.0185	0.0238	0.0323	0.0431	0.0506	0.0521
8.00	0.0073	0.0107	0.0140	0.0195	0.0283	0.0367	0.0394
10.00	0.0043	0.0070	0.0092	0.0129	0.0198	0.0279	0.0316
12.00	0.0033	0.0049	0.0065	0.0094	0.0145	0.0219	0.0264
15.00	0.0021	0.0031	0.0042	0.0061	0.0097	0.0158	0.0211
18.00	0.0015	0.0022	0.0029	0.0043	0.0069	0.0118	0.0177
20.00	0.0012	0.0018	0.0024	0.0035	0.0057	0.0099	0.0159

Circle No	$\bar{\sigma}_z / q_0$	r / z
0	0.0	0.000
1	0.1	0.270
2	0.2	0.400
3	0.3	0.518
4	0.4	0.637
5	0.5	0.766
6	0.6	0.918
7	0.7	1.110
8	0.8	1.387
9	0.9	1.908
	1.0	∞

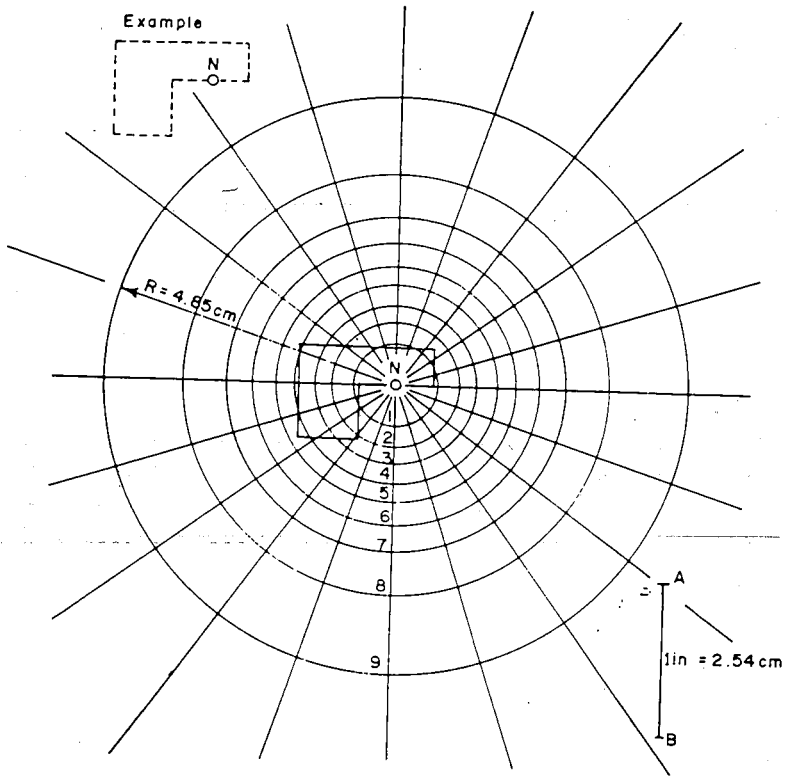


Fig. 4.3 Influence chart for vertical pressure (After Newmark)

4.5 STRESS DUE TO NON-UNIFORMLY DISTRIBUTED SURFACE LOAD

Independent attempts have been made by various authors to determine the stress under a given point, where the variation of the surface loading is not uniform. Such cases are presented in Fig. 4.4 to Fig 4.11 and Table 4.3 to Table 4.5. For detailed treatment of stress in soils refer to Teferra /Schultze [28].

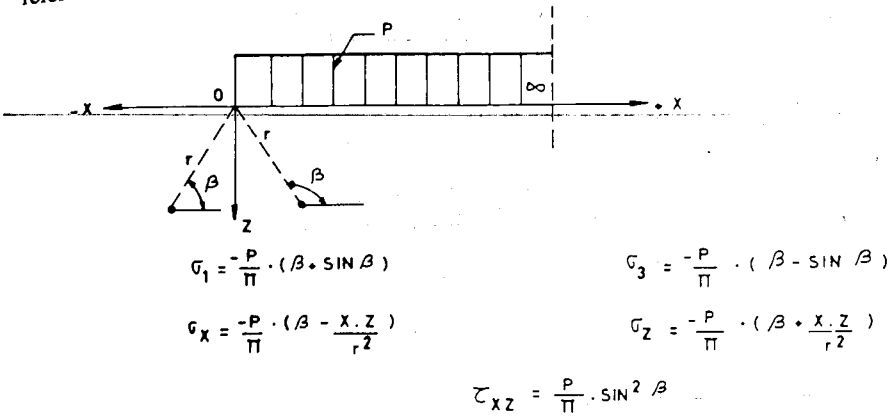
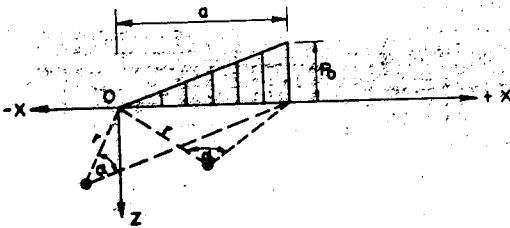


Fig. 4.4 Stresses for uniform surface load [2]



$$\sigma_z = \frac{-P_0}{8\pi} \cdot \left[x \cdot a - \frac{a \cdot z}{(x-a)^2 + z^2} (x-a) \right]$$

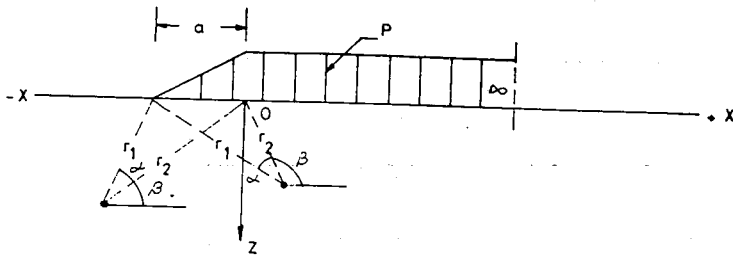
AT $x=0$

$$\sigma_{z_0} = \frac{-P_0}{\pi} \cdot \frac{\sin 2\alpha}{2} = \frac{P_0}{\pi} \cdot \frac{a \cdot z}{a^2 + b^2}$$

AT $x=a$

$$\sigma_{z_a} = \frac{2P_0}{\pi} \cdot a$$

Fig. 4.5 Stresses for a triangular load-right triangle [2]

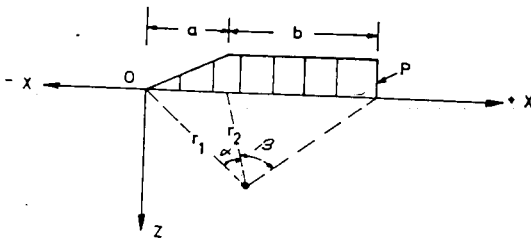


$$\sigma_1 = \sigma_3 = \frac{-P}{\pi \cdot a} \cdot \left[(a \cdot \beta + x \cdot \alpha + z \cdot \ln \frac{r_2}{r_1}) \pm \sqrt{\ln^2 \frac{r_2}{r_1} + \alpha^2} \right]$$

$$\sigma_x = \frac{-P}{\pi \cdot a} \cdot \left[a \cdot \beta + x \cdot \alpha + 2 \cdot z \cdot \ln \frac{r_2}{r_1} \right]$$

$$\sigma_z = \frac{-P}{\pi \cdot a} \cdot [a \cdot \beta + x \cdot \alpha] \quad \tau_{xz} = \frac{+P}{\pi \cdot a} \cdot z \cdot \alpha$$

Fig. 4.6 Stresses for combined uniform and triangular load [?]



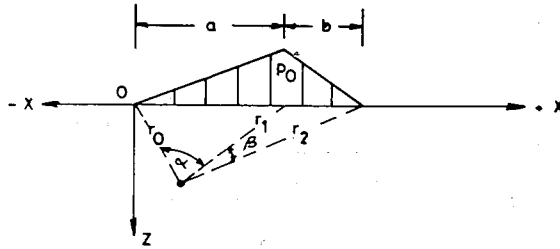
$$\sigma_1 = \sigma_3 = \frac{-P}{\pi \cdot a} \cdot \left\{ a \cdot \beta + x \cdot \alpha + z \cdot \ln \frac{r_1}{r_2} \pm z \cdot \sqrt{\left[\frac{a}{r_2^2} \cdot (x-b) \cdot \ln \frac{r_1}{r_2} \right]^2 + \left[\alpha - \frac{a \cdot z}{r_2^2} \right]^2} \right\}$$

$$\sigma_x = \frac{-P}{\pi \cdot a} \cdot \left[a \cdot \beta + x \cdot \alpha + \frac{a \cdot z}{r_2^2} \cdot (x-b) + 2 \cdot z \cdot \ln \frac{r_1}{r_2} \right]$$

$$\sigma_z = \frac{-P}{\pi \cdot a} \cdot \left[a \cdot \beta + x \cdot \alpha - \frac{a \cdot z}{r_2^2} \cdot (x-b) \right]$$

$$\sigma_{xz} = \frac{+P}{\pi \cdot a} \cdot \left[z \cdot \alpha - \frac{a \cdot z^2}{r_2^2} \right]$$

Fig. 4.7 Stress for trapezoidal load [2]



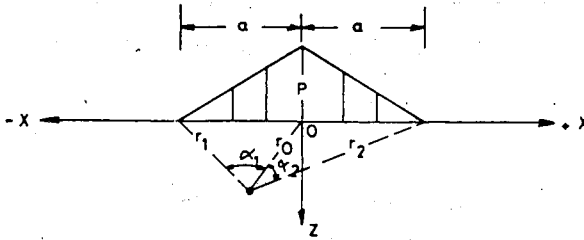
$$\begin{aligned} \sigma_{\bar{1}} = -\sigma_{\bar{3}} &= \frac{P}{\pi} \cdot \left[\frac{x}{a} \cdot \alpha + \left(\frac{a+b-x}{b} \right) \cdot \beta + \left(\frac{z}{a} \cdot \ln \frac{r_1}{r_2} \right) + \left(\frac{z}{b} \cdot \ln \frac{r_1}{r_2} \right) \right] \\ &= \frac{P \cdot z}{\pi} \cdot \sqrt{\left(\frac{1}{a} \cdot \ln \frac{r_1}{r_2} + \frac{1}{b} \cdot \ln \frac{r_1}{r_2} \right)^2 + \left(\frac{\alpha}{a} + \frac{\beta}{b} \right)^2} \end{aligned}$$

$$\sigma_x = \frac{P}{\pi} \cdot \left[\frac{x}{a} \cdot \alpha + \left(\frac{a+b-x}{b} \right) \cdot \beta + \left(\frac{2z}{a} \cdot \ln \frac{r_1}{r_2} \right) + \left(\frac{2z}{b} \cdot \ln \frac{r_1}{r_2} \right) \right]$$

$$\sigma_z = \frac{P}{\pi} \cdot \left[\frac{x}{a} \cdot \alpha + \frac{a+b-x}{b} \cdot \beta \right]$$

$$\tau_{xz} = \frac{P \cdot z}{\pi} \cdot \left[\frac{\alpha}{a} - \frac{\beta}{b} \right]$$

Fig. 4.8 Stresses for triangular load [2]



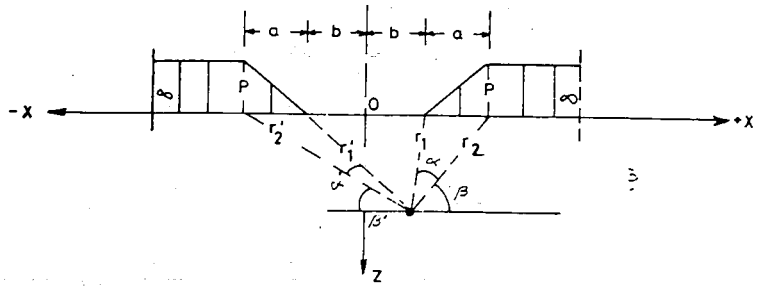
$$\begin{aligned} -\sigma_{\bar{1}} = -\sigma_{\bar{3}} &= \frac{P}{\pi \cdot a} \cdot \left[a \cdot (\alpha_1 + \alpha_2) + (\alpha_1 - \alpha_2) \cdot z - z \cdot \ln \frac{r_1 \cdot r_2}{b^2} \right] = \frac{P \cdot z}{a} \cdot \sqrt{\ln^2 \frac{r_1 \cdot r_2}{b^2} + (\alpha_1 - \alpha_2)^2} \end{aligned}$$

$$\sigma_x = \frac{P}{\pi \cdot a} \cdot \left[a \cdot (\alpha_1 + \alpha_2) + x \cdot (\alpha_1 - \alpha_2) - 2 \cdot z \cdot \ln \frac{r_1 \cdot r_2}{b^2} \right]$$

$$\sigma_z = \frac{P}{\pi \cdot a} \cdot \left[a \cdot (\alpha_1 + \alpha_2) + x \cdot (\alpha_1 - \alpha_2) \right]$$

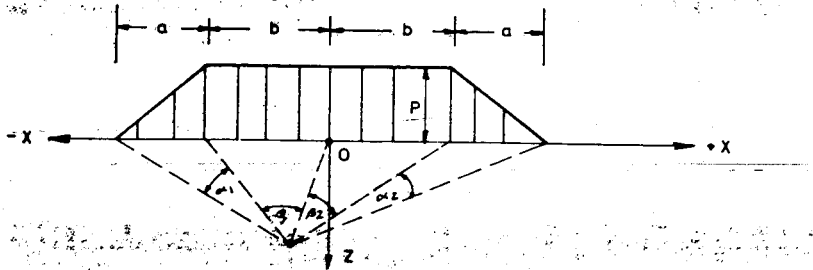
$$\tau_{xz} = \frac{P \cdot z}{\pi \cdot a} \cdot (\alpha_1 - \alpha_2)$$

4.9 Stresses for an isosceles triangular load [2]



$$\begin{aligned}
 -\sigma_1 = -\sigma_3 &= \frac{P}{\pi \cdot a} \left[a \cdot (\beta \cdot \beta') - b(\alpha + \alpha') + x(\alpha + \alpha') \cdot z \cdot \ln \left(\frac{r_2}{r_1} \cdot \frac{r_2'}{r_1'} \right) \right] \\
 &= \frac{P \cdot z}{\pi \cdot a} \cdot \sqrt{\ln^2 \left(\frac{r_2}{r_1} \cdot \frac{r_2'}{r_1'} \right) + (\alpha - \alpha')^2} \\
 \sigma_x &= \frac{-P}{\pi \cdot a} \left[a \cdot (\beta \cdot \beta') + b \cdot (\alpha + \alpha') + x(\alpha - \alpha') + 2z \ln \left(\frac{r_2}{r_1} \cdot \frac{r_2'}{r_1'} \right) \right] \\
 \sigma_z &= \frac{-P}{\pi \cdot a} \left[a(\beta \cdot \beta') - b(\alpha + \alpha') + x(\alpha - \alpha') \right] \\
 \tau_{xz} &= \frac{Pz}{\pi a} (\alpha - \alpha')
 \end{aligned}$$

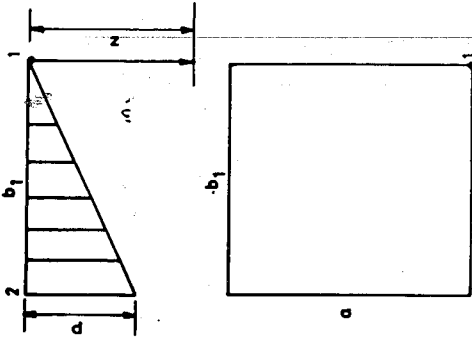
Fig. 4.10 Stresses for combined uniform and triangular symmetrical load [2]



$$\sigma_z = \frac{-P}{\pi a} \left[a(\beta_1 \cdot \beta_2) + (a+b)(\alpha_1 + \alpha_2) + x(\alpha_1 - \alpha_2) \right]$$

Fig. 4.11 Stresses for a trapezoidal load [2]

IN THE RELATION DEPTH TO WIDTH, THE WIDTH SHOULD ALWAYS BE THE SMALLER SIDE.



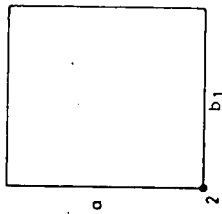
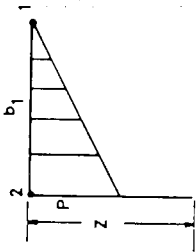
$$C_{z1} = \frac{P}{2\pi} \left[\frac{ab_1z}{R(z^2 + b_1^2)} + \frac{a \cdot z}{b_1 R} \cdot \frac{R - \sqrt{a^2 + z^2}}{\sqrt{a^2 + z^2}} \right] = i_{sd1} \cdot P$$

$$R = \sqrt{a^2 + b_1^2 + z^2}$$

SIDE RATIO	$\frac{z}{a} \cdot \frac{z}{b_1} \cdot \frac{z}{b_1/2} \cdot \frac{z}{a/2}$											
	0.25	0.5	0.75	1.0	1.5	2	3	4	5	6	8	10
1/10	0.0039	0.0071	0.0095	0.0113	0.0132	0.0141	0.0147	0.0146	0.0142	0.0135	0.0119	0.0102
1/5	0.0077	0.0142	0.0190	0.0223	0.0257	0.0269	0.0259	0.0232	0.0201	0.0171	0.0122	0.0090
1/3	0.0128	0.0235	0.0311	0.0357	0.0396	0.0387	0.0318	0.0218	0.0190	0.0146	0.0093	0.0064
1/2	0.0191	0.0348	0.0446	0.0497	0.0502	0.0447	0.0313	0.0216	0.0154	0.0114	0.0068	0.0046
1.0	0.0370	0.0606	0.0687	0.0666	0.0572	0.0384	0.0214	0.0131	0.0089	0.0063	0.0036	0.0024
2.0	0.0374	0.0633	0.0753	0.0773	0.0682	0.0553	0.0352	0.0232	0.0161	0.0118	0.0069	0.0046
5.0	0.0374	0.0637	0.0765	0.0795	0.0732	0.0631	0.0463	0.0349	0.0269	0.0213	0.0139	0.0099

Table 4.3 Influence coefficient i_{sd1} [13]

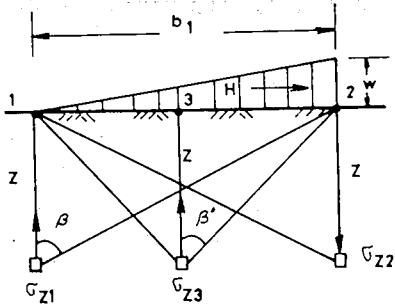
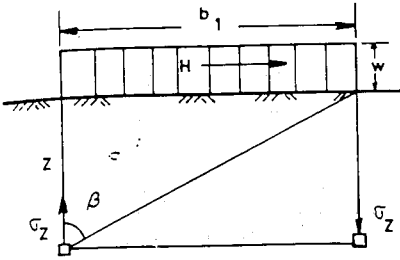
IN THE RELATION DEPTH TO WIDTH, THE WIDTH SHOULD ALWAYS BE THE SMALLER SIDE



$$G_{z2} = \frac{P}{2\pi} \cdot (\text{ARC TAN } \frac{a \cdot b_1}{z \cdot R} + \frac{a \cdot z}{a^2 + z^2} \cdot \frac{R - \sqrt{a^2 + z^2}}{b'}) = i_{sd2} \cdot P$$

SIDE RATIO	$\frac{z}{a} \cdot \frac{z}{b_1} \cdot \frac{z}{b/2}$											
	0.25	0.5	0.75	1.0	1.5	2	3	4	5	6	8	10
1/10	0.2446	0.2328	0.2144	0.1933	0.1538	0.1233	0.0840	0.0612	0.0468	0.0370	0.0248	0.0177
1/5	0.2408	0.2256	0.2049	0.1821	0.1407	0.1094	0.0700	0.0480	0.0331	0.0260	0.0160	0.0108
1/3	0.2356	0.2162	0.1923	0.1675	0.1242	0.9929	0.0550	0.0356	0.0245	0.0177	0.0103	0.0065
1/2	0.2292	0.2043	0.1771	0.1502	0.1059	0.0755	0.0419	0.0259	0.0174	0.0124	0.0072	0.0064
1.0	0.2103	0.1719	0.1373	0.1086	0.0688	0.0456	0.0233	0.0139	0.0091	0.0064	0.0037	0.0024
2.0	0.2110	0.1758	0.1464	0.1226	0.0878	0.0648	0.0380	0.0243	0.0166	0.0120	0.0070	0.0046
5.0	0.2110	0.1762	0.1476	0.1250	0.0933	0.0732	0.0497	0.0364	0.0261	0.0216	0.0141	0.0099

Table 4.4 Influence coefficient i_{sd2} [13]



$$G_z = w \cdot i_{wr}$$

$$w = \frac{H}{b_1}; \quad a/b_1 = \infty$$

$$G_{z1} = w \cdot i_{wd1}$$

$$G_{z2} = w \cdot i_{wd2}$$

$$G_{z3} = w \cdot i_{wd3}$$

$$w = \frac{2H}{b_1}$$

$$a/b_1 = \infty$$

Cot $\beta =$ Z/b_1	$a/b_1 = \infty$			
	TYPE OF LOADING			
	RECTANGULAR i_{wr}	TRINGULAR i_{wd1}	TRINGULAR i_{wd2}	TRINGULAR i_{wd3}
0.00	+0.3183	+0.0000	+0.3183	0.0000
0.25	+0.2936	+0.0868	+0.2128	+0.1125
0.50	+0.2546	+0.1125	+0.1421	+0.0908
0.75	+0.2037	+0.1070	+0.0967	+0.0604
1.00	+0.1592	+0.0908	+0.0683	+0.0405
1.50	+0.0979	+0.0604	+0.0376	+0.0208
2.00	+0.0637	+0.0405	+0.0231	+0.0123
3.00	+0.0318	+0.0208	+0.0110	+0.0057
4.00	+0.0187	+0.0123	+0.0064	+0.0033
6.00	+0.0086	+0.0057	+0.0029	+0.0014
8.00	+0.0049	+0.0033	+0.0016	+0.0008
10.00	+0.0032	+0.0021	+0.0011	+0.0005
12.00	+0.0022	+0.0014	+0.0007	+0.0003
15.00	+0.0014	+0.0011	+0.0003	+0.0003
18.00	+0.0010	+0.0007	+0.0003	+0.0002
20.00	+0.0008	+0.0005	+0.0003	+0.0002

Table 4.5 Influence coefficients i_{wr} and i_{wd} for $u = 0.5$ [7]

4.6 STRESS DUE TO UNIFORMLY DISTRIBUTED LOAD BY APPROXIMATE METHOD

The stress distribution at successive depth beneath a footing due to distributed surface load can be determined by approximate method or by what is known as the Sixty-Degree Approximation. This method assumes that stress increment at successive depths beneath a footing is distributed uniformly over a finite area. The finite area is defined by planes descending at a slope 2:1 (2 vertical and 1 horizontal) from the edges of the footing.

The planes descending from the edges of the footing area, A_1 , at each depth define the area, A_2 , over which the stress is uniformly distributed as shown in Fig. 4.12. Thus the stress increment at any depth is assumed to be equal to the total load P on the footing divided by the area A_2 defined by the planes. The 60° approximation is satisfactory for individual spread

footings of relatively small area. Stress at depth z , $\sigma_z = \frac{P}{A_2}$

• For square footing, $A_2 = (B+Z)^2$

For rectangular footing, $A_2 = (B+Z)(L+Z)$

Fig. 4.13 shows the comparison of vertical stress computed on the basis of 60° - approximation with that determined using Boussinesq's equation.

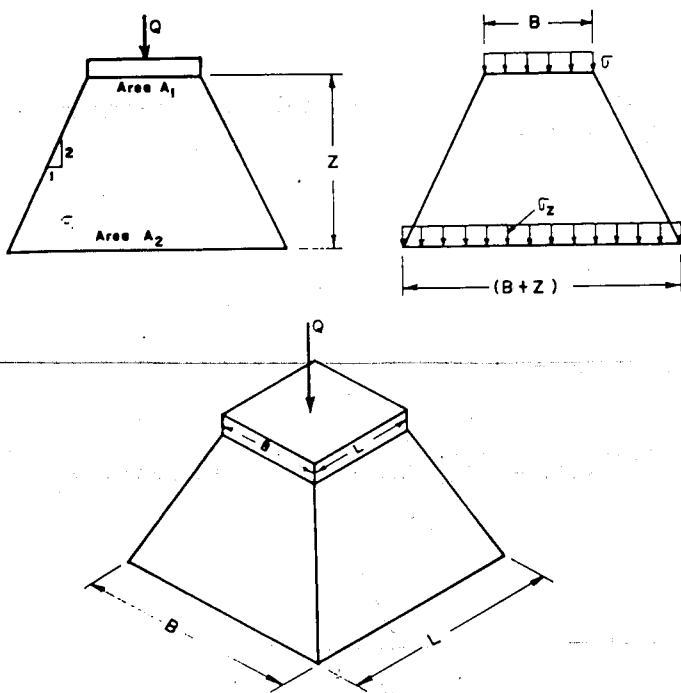


Fig. 4.12 approximate method for computing vertical stress

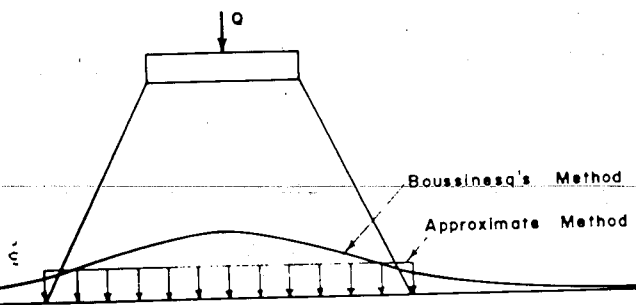


Fig. 4.13 Comparison of vertical stress distribution by Boussinesq and approximate methods.

4.7 EXAMPLES

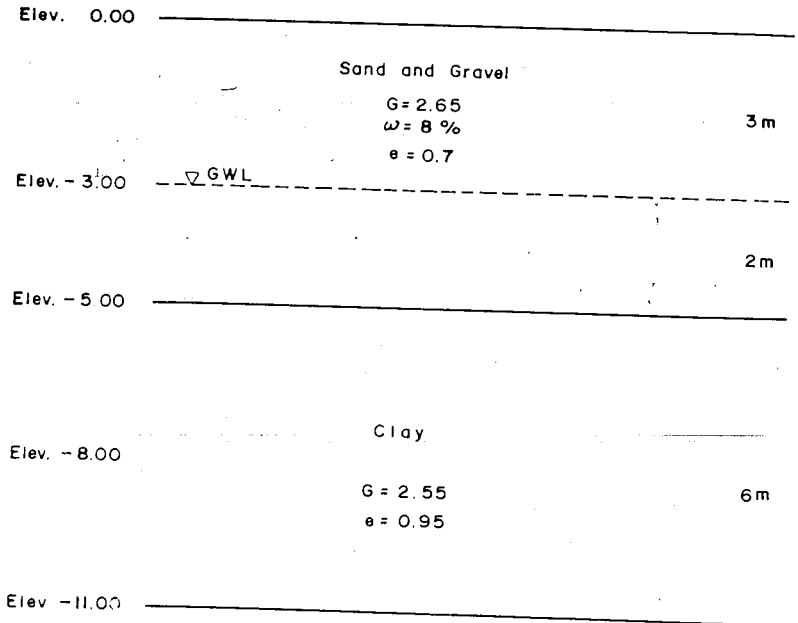
E.4.1 Refer to the soil profile shown below. Find the effective pressure at depth 8m below the ground surface.

SOLUTION

At Elev. -3.00 $\sigma_1 = \gamma_1 h_1$

$$\gamma_1 = \frac{1 + \omega}{1 + e} G_s \gamma_w = \frac{1 + 0.08}{1 + 0.7} (2.65) (10) = 16.84 \text{ kN/m}^3$$

$$\sigma_1 = 16.84 (3) = 50.52 \text{ kN/m}^2$$



At Elev. -5.00 $\sigma_2 = \gamma_2 h_2$

$$\gamma_2 = \frac{G_s - 1}{1 + e} \gamma_w = 1.65 \frac{(10)}{1.7} = 9.71 \text{ kN/m}^3$$

$$\sigma_2 = 9.71 (2) = 19.42 \text{ kN/m}^2$$

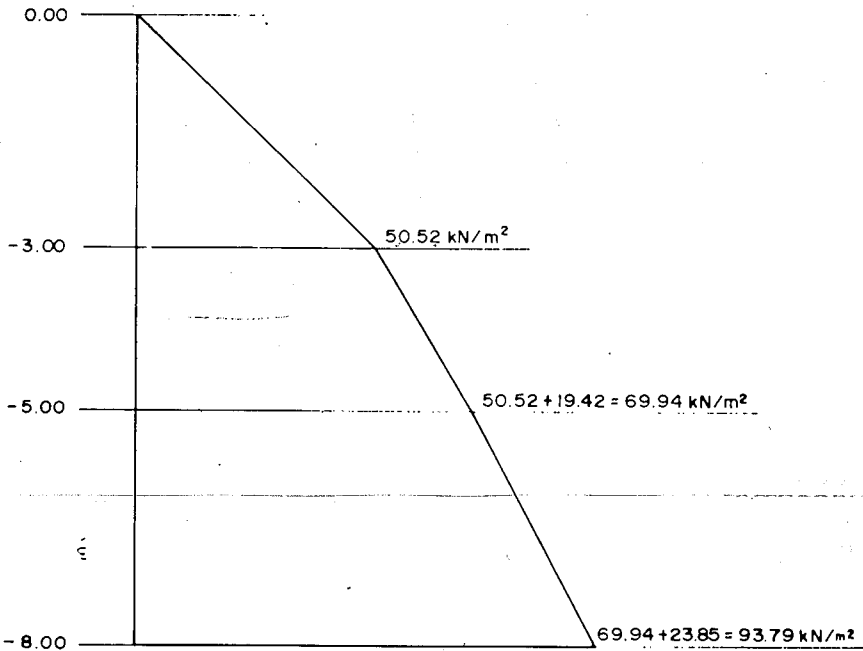
At Elev. -8.00 $\sigma_3 = \gamma_3 h_3$

$$\gamma_3 = \frac{G_s - 1}{1 + e} \gamma_w = \frac{(2.55 - 1) (10)}{1.95} = 7.95 \text{ kN/m}^3$$

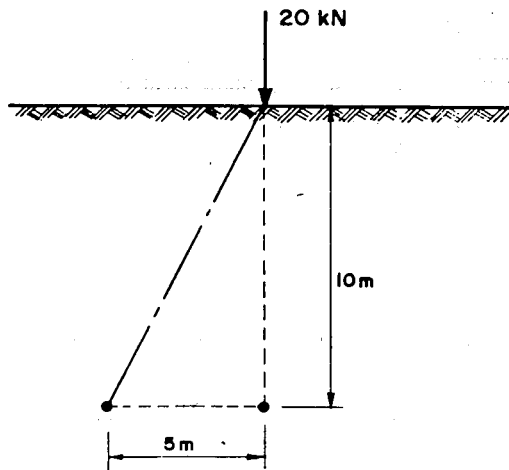
$$\sigma_3 = 7.95 (3) = 23.85 \text{ kN/m}^2$$

Effective pressure at 8m below the ground surface:

$$= 50.52 + 19.42 + 23.85 = 93.79 \text{ kN/m}^2$$



- E.4.2** A concentrated load of 20kN acts on the surface of a homogeneous soil mass of large extent. Find the stress intensity at a depth of 10m
 (a) directly under the load.
 (b) at a horizontal distance of 5m.



SOLUTION

Stress at point A, is given by $\sigma_z = \frac{P}{z^2} i_1$.

$$\text{For } \frac{r}{z} = 0, i_1 = 0.477$$

$$\sigma_z = \frac{20}{10^2} (0.477) = 0.0954 \text{ kN/m}^2$$

$$= 95.4 \text{ N/m}^2$$

Stress at point B, $\sigma_z = \frac{20}{10^2} \cdot i_1$

For $\frac{r}{z} = \frac{5}{10} = 0.5, i_1 = 0.265$

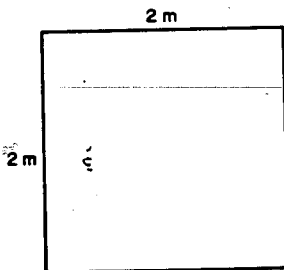
$$\sigma_z = \frac{20}{10^2} (0.265) = 0.053 \text{ kN/m}^2 = 53 \text{ N/m}^2$$

E.4.3

A square footing 2m by 2m carries a uniformly distributed load of ~~3000~~ kN/m^2 . Find the intensity of vertical pressure at a depth of 4m. below the center of footing using

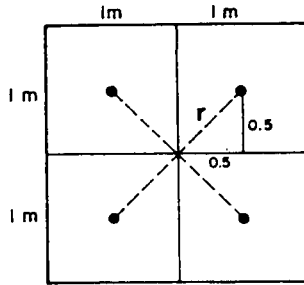
- Boussinesq's solution for distributed load.
- the Approximate method.
- Steinbrenner method.

SOLUTION.

(a) *Boussinesq's Solution*

$$\frac{a}{z} = \frac{2}{4} = 0.5 > 0.3$$

Point load equation is not applicable, hence divide the area into 4 equal parts having sides of 1m each.



$$\frac{a}{z} = \frac{1}{4} = 0.25 < 0.3$$

Point load equation is applicable. Load acting on each square = $1 \times 1 \times 300 = 300 \text{ kN}$.

The load acts at the center of each square. The distance from the point of action of the load to the center of footing is given by

$$r = \sqrt{(0.5)^2 + (0.5)^2} = 0.707$$

$$\frac{r}{z} = \frac{0.707}{4} = 0.177$$

$$\text{For } \frac{r}{z} = 0.177, i_1 = 0.44$$

Stress at 4m depth due to one loaded square,

$$\sigma_z = \frac{P}{z^2} \cdot i_1$$

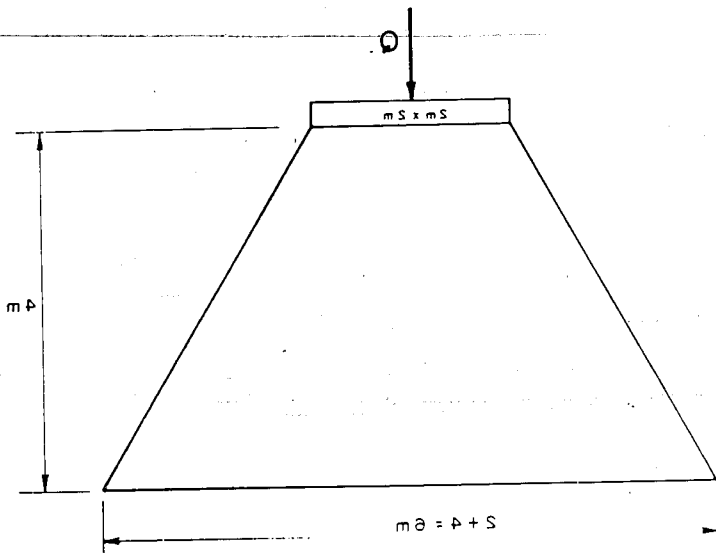
$$= \frac{300}{4^2} (0.44) = 8.25 \text{ kN/m}^2$$

Stress due to loaded square = $8.25 (4) = 33 \text{ kN/m}^2$

(b) Approximate Method

(i) 60° - method

$$P = 2(2)(300) = 1200 \text{ kN}$$



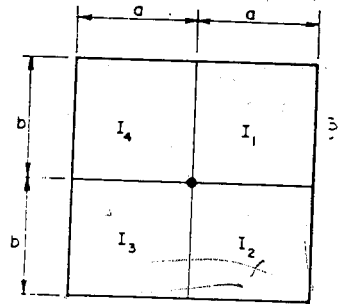
$$\sigma_z = \frac{P_z}{(B + Z)^2} = \frac{1200}{(2 + 4)^2} = 33.33 \text{ kN/m}^2$$

ii) Steinbrenner Method

$$\frac{a}{b} = 1$$

$$\frac{z}{b} = \frac{4}{1} = 4$$

From Table 4.2, $I_1 = 0.0270$



$$I = I_1 + I_2 + I_3 + I_4 \approx 0.270(4) \approx 0.108$$

$$\sigma_z = I \cdot p = 0.108 (300) = 32.4 \text{ kN/m}^2$$

E.4.4 A point {line} load as shown in Fig. E.4.1 is given. Determine:

- a) the variation of the vertical stress along AB
- b) the variation of the vertical stress along CD

SOLUTION

a) Variation of the Vertical Stress along AB

POINT LOAD

The variation of the vertical stress along AB ($r = 0$) for a point load is given by:

$$\sigma_z = 0.47746 \frac{P}{z^2}$$

LINE LOAD

The variation of the vertical stress along AB ($r = 0$) for a line load is given by

$$\sigma_z = 0.63662 \frac{P}{z}$$

The results are given in Table E.4.1

b) *Variation of the Vertical Stress along CD*

POINT LOAD

The vertical stress distribution is given by

$$\sigma_z = i_1 \cdot \frac{P}{z^2} = \frac{1000}{z^2} \cdot i_1$$

LINE LOAD

The vertical stress distribution is given by

$$\sigma_z = i_2 \cdot \frac{P}{z} = \frac{200}{z} \cdot i_2$$

Taking an interval of 1m horizontally, the calculation is compiled in Table E.4.2

Table E.4.1 Vertical stress distribution along AB

z	z ²	Point Load P = 1000 kN	Line Load p = 200 kN/m
		$\sigma_z = 0.4775 \frac{P}{z^2}$	$\sigma_z = 0.6366 \frac{p}{z}$
m	m ²	kN/m ²	kN/m ²
0	0	∞	∞
0.50	0.25	1910	255
1.00	1.00	478	127
1.50	2.25	212	85
2.00	4.00	119	64
2.50	6.25	76	51
3.00	9.00	53	42
3.50	12.25	39	36
4.00	16.00	30	32

Table E.4.2 Vertical stress distribution along CD

$r(x)$	z	$\frac{r}{z}$	$\frac{x}{z}$	i_1	i_2	Point Load $P=1000$ $\sigma_z = i_1 \frac{P}{z^2}$	Line Load $p=200$ $\sigma_z = i_2 \frac{p}{z}$
m	m					kN/m ²	kN/m ²
0.00		0	0	0.47746	0.63662	119	64
1.00		0.50	0.50	0.274544	0.40865	69	61
2.00	2.00	1.00	1.00	0.08442	0.15916	21	16
3.00		1.50	1.50	0.02556	0.06145	6	6
4.00		2.00	2.00	0.00854	0.02546	2	2

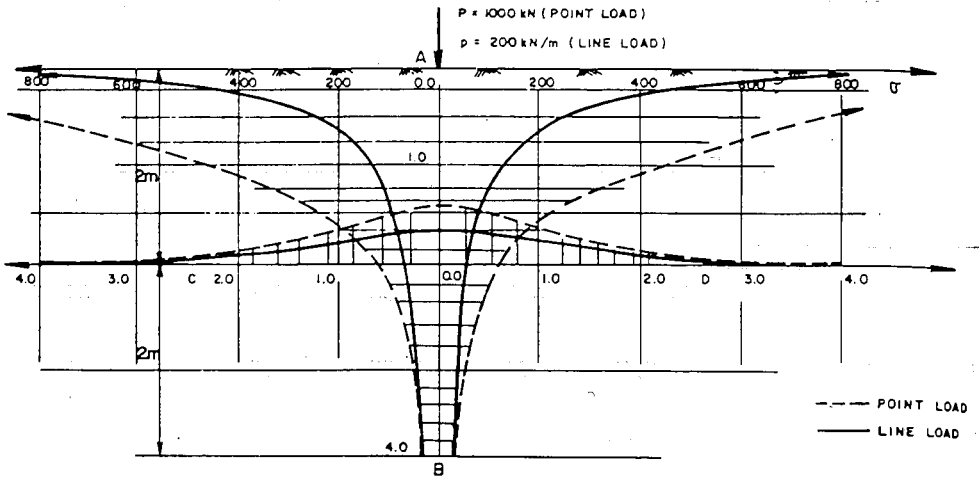


Fig. E.4.1 Vertical pressure distribution along AB and CD for point load and line load

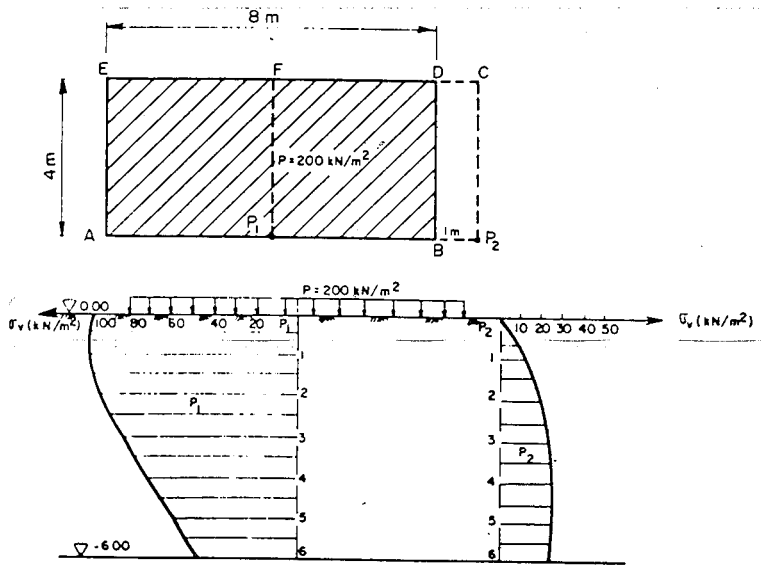


Fig. E.4.2 Vertical pressure distribution under P_1 and P_2

E.4.5 A surface loading of 200 kN/m^2 covering an area of 32m^2 (Fig. E.4.2) is given. Determine the vertical stress distribution under Points P_1 and P_2

SOLUTION

a) *Vertical Stress Distribution under point P_1*

In order to make P_1 form a corner point, one divides the area A B D E in two parts. Namely, A P_1 F E and P_1 B D F.

In order to use Table 4.2, one should first know a/b . In this particular case $a = b = 4\text{m}$, hence, $a/b = 1$. Since the case is symmetrical one needs to calculate only the coefficient for part A P_1 F E. The calculation is tabulated below in Table E.4.3 and plotted in Fig. E.4.2

Table E.4.3 Vertical pressure under point P_1

z	$\frac{z}{b}$	i	$2.i$	$\sigma_z = 2.i.p$
m	-	-	-	kN/m^2
0.0	0.0	0.2500	0.5000	100
1.0	0.25	0.2473	0.4946	99
2.0	0.50	0.2325	0.4650	93
3.0	0.75	0.2060	0.4120	82
4.0	1.00	0.1752	0.3504	70
6.0	1.50	0.1210	0.2420	48

b) *Vertical Stress Distribution under point P_2*

Since P_2 lies outside the loaded area, one determines the coefficient by considering areas $AP_2 CE$ and $BP_2 CD$. The calculation is shown in Table E.4.4 and the result plotted in Fig. E.4.2

Table E.4.4 Vertical pressure under point P_2

Area $AP_2 CE$ $a = 9$ $b = 4$ $a/b = 2.25$		Area $BP_2 CD$ $a = 4$ $b = 1$ $a/b = 4.00$			$i = i_1 - i_2$	$\sigma_z = p \cdot i$
z	$\frac{z}{b}$	i_1	$\frac{z}{b}$	i_2		
m	-	-	-	-	-	kN/m ²
0	0.00	0.2500	0.00	0.2500	0.0000	0
1.0	0.25	0.2483	1.00	0.2039	0.0444	9
2.0	0.50	0.2392	2.00	0.1339	0.1053	21
3.0	0.75	0.2221	3.00	0.0910	0.1311	26
4.0	1.00	0.2008	4.00	0.0658	0.1350	27
6.0	1.50	0.1580	6.00	0.0377	0.1203	24

4.8 EXERCISES

- 1 Find the neutral and effective stresses at a depth of 15m below the ground surface for the following conditions. The water table is 3m below the ground surface. $G_s = 2.65$, $e = 0.7$, average moisture content for soil above the water table = 5%

- 2 A point of 1500 kN acts on the surface of the ground. What is the intensity of vertical stress due to the load, at depths of 2, 4, 8, 10, metres directly below the load?
 What is the intensity of the vertical stresses at the same depths at a horizontal distance of 5 metres from the line of action of the point load?

- 3 Repeat problems 2 with a line load of 500 kN/m.

- 4 A foundation 5x5 m. exerts a pressure of 150 kN/m² at the surface of a sand layer with unit weights of 17.5 kN/m³ and 20.0 kN/m³ when dry and saturated respectively. Below the sand layer, at a depth of 5m, is a clay seam that is 2m thick and has a unit weight of 16.8 kN/m³ when saturated.
 - a. Show the variation of vertical stress under the center of the foundation as a function of depth.
 - b. Show the variation of the effective stress in the soil as a function of depth. The water table is at a depth of 3m.
 - c. Show the variation of the vertical stress at the center of the clay stratum as a function of the horizontal distance from the center line of the footing.

- 5 If the earth dam of problem 3.7 has an average unit of 19.0 kN/m³, show the vertical stress variations along a horizontal plane x-x 1 metre below the dam.

- 6 If structures A and B are erected on clay layer with an average bearing pressure of 100kN/m^2 and 200kN/m^2 respectively as shown below, calculate and plot the variation of the vertical stress distribution under P as a result of structures A and B.

5. COMPRESSIBILITY AND CONSOLIDATION OF SOILS

5.1 COMPRESSIBILITY OF SOILS

5.1.1 General

The compressibility of soil is indicated by its change in volume per unit of load increment. Any structure built on the ground causes increase of pressure on the underlying soil layers. The soil layers being confined by the surrounding soil strata adjust to the new pressure mainly through deformation. As noted in the earlier discussion, soil may be considered to be a skeleton of solid grains enclosing voids which may be filled with gas, liquid, or a combination of gas and liquid. The vertical compression of the soil mass under increased pressure is thus made up of the following components.

- a. A compression of solid matter, which under usual loadings accounts for very small compression.
- b. A compression of the pore fluid, which may be considerable where the pores contain air, but negligible when the pores are completely filled with water.
- c. Reduction of the pore space by expulsion of pore fluid, which forms the major component of the compression.

A honey comb structure, or in general any structure with high porosity, is more compressible than a dense structure. A soil in remolded (disturbed) state may be much more compressible than the same soil in natural state.

Soils show some elastic tendency to a very small degree. That is, when the pressure on a soil is increased in all directions, the volume decreases. However, if the pressure is later decreased to its previous value some expansion will take place, but the expansion (or volume rebound) will not be so great as the preceding compression. A study of compressibility of soil is necessary to be able to forecast the probable settlement of structures on different types of soils.

5.1.2 Measurement of Compressibility

As has been mentioned earlier, the interest of engineers in compression is mainly in relation with settlement. In this regard, the engineer is usually concerned with one-dimensional vertical compression of soil under structure. Although there is generally little lateral displacement, the volume change is assumed to take place through change in thickness.

To simulate field conditions in the laboratory, compression tests are conducted in ring-type compression device called consolidometer using undisturbed samples cut from natural formation.

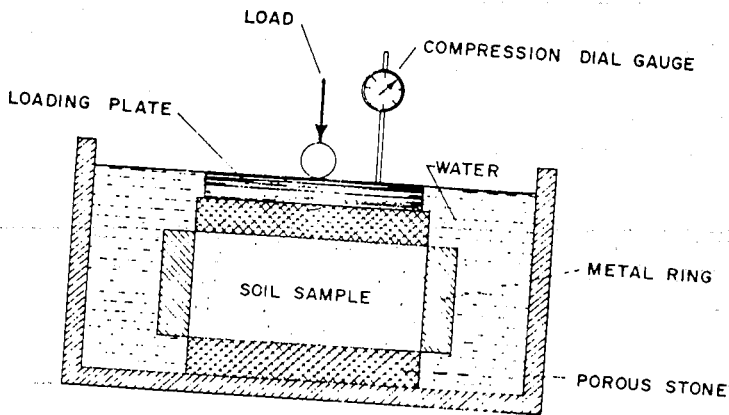


Fig. 5.1 Consolidation apparatus

The metal ring provides lateral confinement. Porous stones are fitted at the top and bottom to allow the escape of air and water without the loss of fines during compression.

To obtain a reasonably correct idea of the in-situ soil properties (soil in its natural state), it is necessary to test undisturbed soil sample. Undisturbed soil samples are cut from natural formation and trimmed to fit exactly the testing device.

After placing the sample in the testing device, it is then subjected to loads in increments. Each increment is applied instantaneously and is maintained at constant value until compression ceases at which time the reading of the dial is noted. Observations of compression dial reading and time are made for each load increment.

Compression of laterally confined specimen is measured in terms of change of thickness. However, the test result is presented graphically in the form of pressure versus void ratio curves. This essentially means that the change in thickness has to be converted to change in void ratio.

The two conventions used in plotting the curves (i.e. e-p curves) are

- (a) the use of natural scale for both co-ordinates
- (b) plotting the void ratio on a natural scale and the applied pressure on a logarithmic scale.

Each point on a pressure versus void ratio curve represents pressure due to applied load and void ratio of the specimen after an equilibrium under the load has been reached.

In an actual experiment a curve of compression versus time is obtained for each increment. To accomplish this, compression dial reading has to be taken at a given time interval until compression ceases. For every load increment, there is one final void ratio, and from the whole series of loads, a curve between pressure and void ratio can be plotted.

Knowing the specific gravity, G_s , of the sample, and its initial height and diameter, the initial void ratio can be determined, if the dry weight of the sample is also known.

Once this is done, the following relationship between change in void ratio and change in thickness is established to determine the final void ratio.

Let V_1 be the total volume at the beginning of the test and V_2 the total volume at the end of the test. Then $\Delta V = V_1 - V_2$

Since change in volume, ΔV , is brought about by change in volume of voids only, the above relationship can be expressed

as, $\Delta V = \Delta V_v = (V_v)_1 - (V_v)_2$ where V_v is the volume of voids. But $V_v = e V_s$

Hence, $\Delta V = (V_s e_1 - V_s e_2) = V_s \Delta e$ (5.1)

But $V_s = \frac{V_1}{1 + e_1}$ (5.2)

Where

V_1 = total volume at the beginning of the test

e_1 = initial void ratio

e_2 = final void ratio

Substituting Eq (5.2) into Eq (5.1), the following is obtained

$$\Delta V = V_1 \frac{\Delta e}{1 + e_1}$$
 (5.3)

Since no lateral strain is assumed, the change in volume is caused by the change in thickness.

$\Delta V = (A) (\Delta H)$ and $V_1 = (A)(H_1)$. Then

$$\Delta H = H_1 \frac{\Delta e}{1 + e_1}$$
 (5.4)

Where

A = cross sectional area

H = initial thickness

ΔH = change in thickness which can be determined from the final compression dial reading.

The final void ratio, e_2 , can be obtained by subtracting Δe from e_1 . For each load increment the above computation is repeated.

5.1.3 Void ratio-pressure Diagram

The sample is first loaded to pressure intensity P_1 and then the load is completely released. This cycle of compression and expansion is shown by curve I (Fig.5.2). The sample is again reloaded. Curve II indicates recompression. A little beyond P_1 , it coincides with the extension of Curve I. *ab* is referred to as virgin compression curve, and *bc* is referred to as expansion or rebound curve. *cd* shows the effect of re-loading. Fig. 5.3 shows void ratio versus pressure on a semi-logarithmic plot. The convex portion of the curve is known as recompression curve. It indicates that the sample has earlier been subjected to compression. In an e-log P curve, convex curvature indicates an earlier compression or precompression.

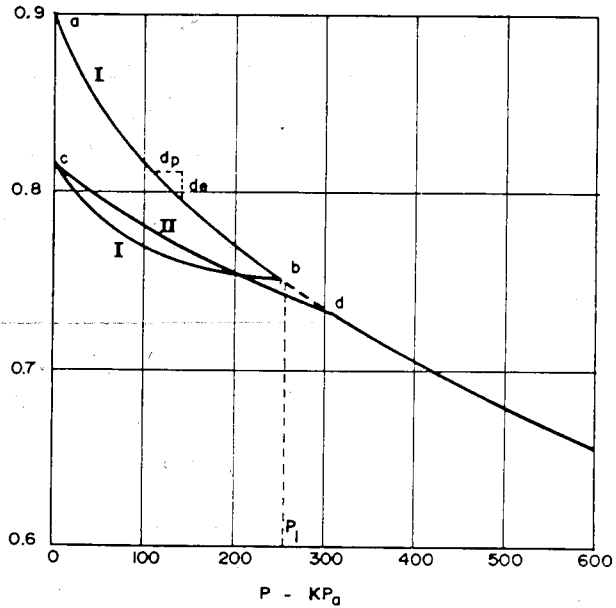


Fig. 5.2 Typical e-p curve

5.1.4 Coefficient of Compressibility

This represents the rate of change of void ratio with pressure. It is numerically equal to the slope of pressure void ratio curve on a natural scale (Fig.5.4a)

$$a_v = \frac{e_1 - e_2}{P_2 - P_1} = \frac{\Delta e}{\Delta P} \text{ OR } \frac{de}{dp} \quad (5.5)$$

a_v has a dimension inverse of pressure. As the e-log p curve is not a straight line, a_v is not constant but decreases with increasing pressure. At any point on the curve, the slope of the tangent with the horizontal gives the value of a_v for that point.

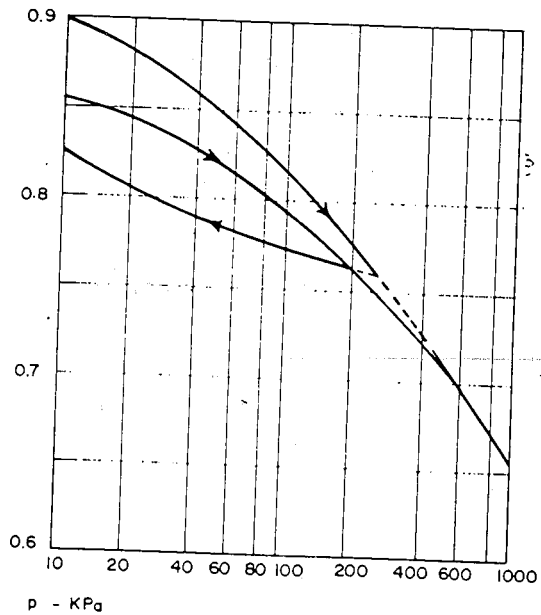


Fig. 5.3 Typical e - $\log p$ curve

5.1.5 Compression Index

Compression index, C_c , is numerically equal to the slope of the straight portion of the e - $\log P$ curve (Fig. 5.4b). Its value is constant beyond the range of the recompression, since beyond this point the plot of e against $\log P$ is a straight line. Noting that,

$$C_c = \frac{e_1 - e_2}{\log P_2 - \log P_1} \quad (5.6a)$$

$$e_2 = e_1 - C_c \log \frac{P_2}{P_1} \quad (5.6b)$$

There appears to be an approximate relationship between the liquid limit of a clay soil and the compression index. Skempton has demonstrated that this relationship can be expressed by the following empirical formula:

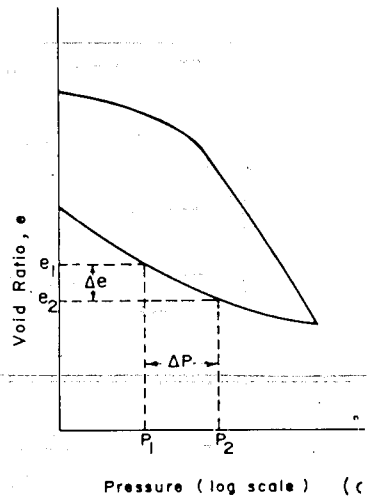
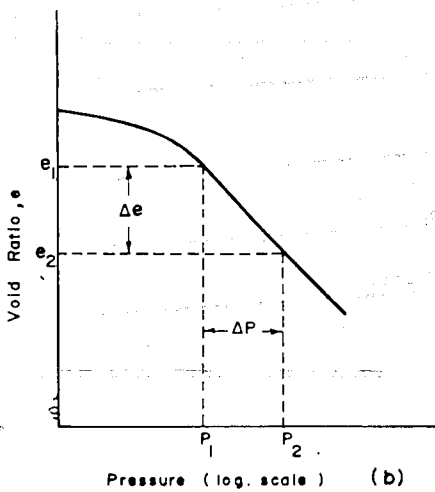
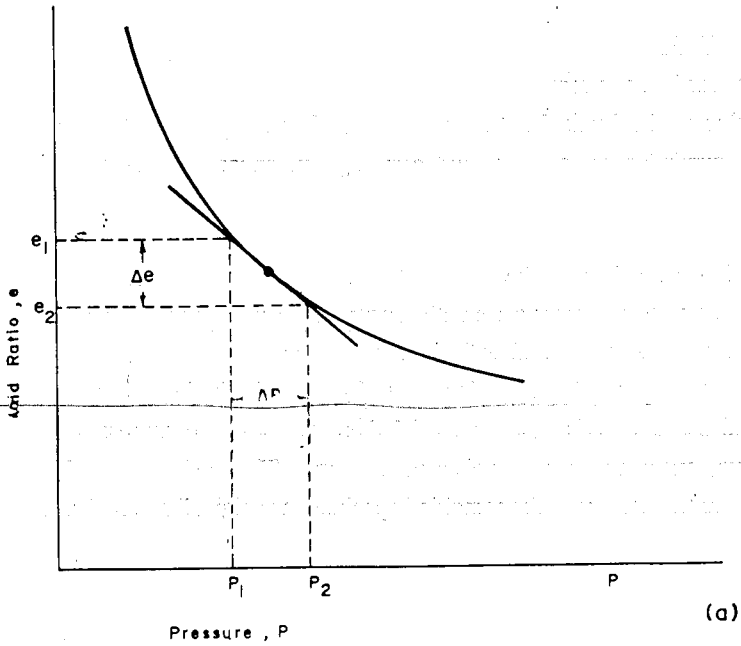


Fig. 5.4 Determination of
 (a) coefficient of compressibility
 (b) compression index
 (c) swelling index

$$C_c = 0.009 (\omega_L - 10\%) \tag{5.7}$$

Where ω_L is expressed in per cent.

Thus, a knowledge of the liquid limit alone may enable an approximate estimate of the settlement of a foundation on clay without carrying out expensive and time consuming consolidation test.

3

The compressibility of soil is indicated by the slope of compression diagram. The compressibility of any one soil type varies with density, history of previous loading, handling prior to and during compression, and with the magnitude of stress increment relative to the existing loading at any point. The more dense a soil is initially the less compressible it will be. For remolded specimen of a given material there is not one compression diagram as represented above, but a numerous number of diagrams. The position and slope of each diagram depends on the density of the remolded specimen as originally placed in the testing device (Fig. 5.5).

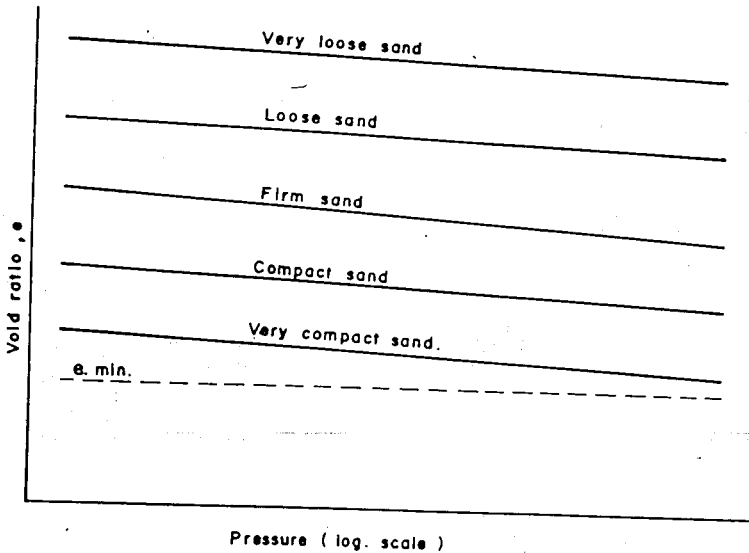


Fig. 5.5 Effect of initial density on the slope of compression diagram for granular soil.

Changes in particle arrangement and soil density due to disturbances or remolding, as distinct from those caused by loading, affect the compression diagram whether they occur initially or during compression. Sand is particularly affected by shock or vibrations.

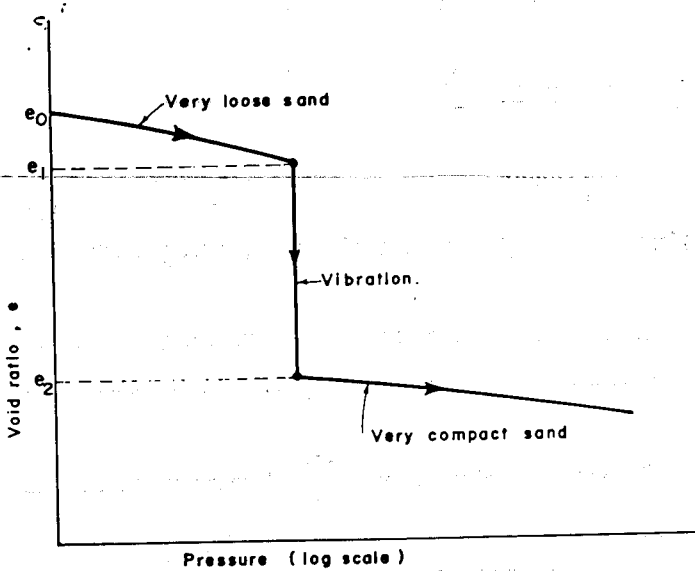


Fig. 5.6 Effect of vibration on compression diagram of sand.

As indicated in Fig. 5.6 an initially loose sand is compressed under static loading from void ratio e_0 to void ratio e_1 . While under load at e_1 , vibrations are applied. Significant decrease in volume then occurs without change in loading (i.e. from e_1 to e_2). Then, if vibrations cease and static loading is increased, compression will occur as shown by the flatter curve from e_2 to e_3 .

If a clay sample is removed from a cycle of loading and unloading and is then completely remolded without change of water content, the diagram obtained for the following recompression will be affected. It is distinctly different from normal recompression diagram.

5.1.6 Swelling Index

C_s denotes the slope of an expansion or rebound curve of e -log P plot (Fig.5.4c). Noting again that,

$$C_s = \frac{e_1 - e_2}{\log P_2 - \log P_1} \quad (5.8)$$

$$e_2 = e_1 - C_s \log \frac{P_2}{P_1} \quad (5.9)$$

5.1.7 Modulus of Compressibility

If the relative settlement, $s' = \frac{\Delta H}{H}$ or the void ratio, e , corresponding to the final dial reading for each initial loading in the consolidation test, is plotted against the effective stress $\bar{\sigma}$, the compressibility curve is obtained. The shape of the curve depends on the soil type, the

geological history and the rate of load increment $\frac{\Delta \bar{\sigma}}{\bar{\sigma}}$. The compressibility curve obtained

from the consolidation test is given in Fig. 5.7a

The curve may be expressed with sufficient accuracy by the following equation:

$$E_s = \frac{d\bar{\sigma}}{ds'} = v(\bar{\sigma})^w \quad (5.10)$$

In order to make the exponent w dimensionless, it is advisable to make $\bar{\sigma}$ also dimensionless

by dividing it by a unit stress σ_0 . Then Eq (5.10) becomes:

$$\frac{d\bar{\sigma}}{ds'} = v(\sigma_0)^w$$

$s' =$ relative settlement

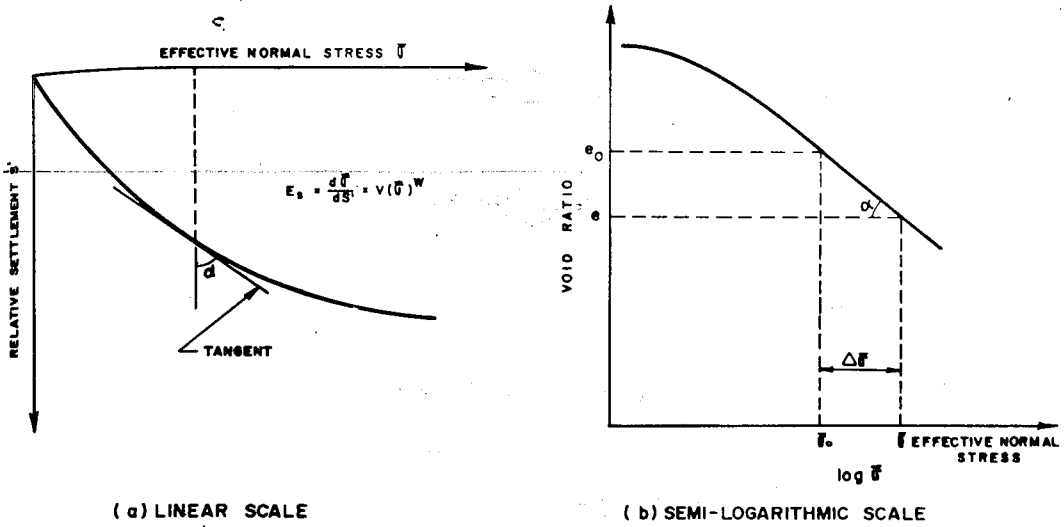


Fig. 5.7 Compressibility curves

where $\bar{\sigma}$ = effective normal stress (kN/m²)

σ_e = unit stress (kN/m²)

$$\bar{\sigma}_e = \frac{\sigma}{\sigma_e}$$

v and w = coefficients

v has a unit of kN/m². It depends on the void ratio, water (moisture) content and consistency of the sample. It could have values ranging from 50 to 30000 kN/m².

w is dimensionless. It depends on the soil type. It could have values ranging from 0 to 1.

The tangent of the compressibility curve, which is a function of $\bar{\sigma}$, gives the modulus of

compressibility E_c (Fig. 5.7a)

From Eq. (5.10)

$$\frac{ds'}{d\bar{\sigma}} = \frac{1}{v(\bar{\sigma})^v} \quad (5.12a)$$

$$ds' = \frac{1}{v} (\bar{\sigma})^{-v} d\bar{\sigma} \quad (5.12b)$$

$$s' = \frac{1}{v} \int (\bar{\sigma})^{-v} d\bar{\sigma} \quad (5.13)$$

For the case $w \neq 1$

$$s' = \frac{1}{v(1-w)} (\bar{\sigma})^{1-v} + C \quad (5.14)$$

Defining $a = \frac{1}{v(1-w)}$ and $k = 1-w$

Eq.(5.13) becomes;

$$s' = a(\bar{\sigma})^k + C \quad (5.15)$$

For the case $w = 1$

$$\frac{ds'}{d\bar{\sigma}} = \frac{1}{v\bar{\sigma}} \quad (5.16)$$

$$s' = \frac{1}{v} \ln \bar{\sigma} + C \quad (5.17)$$

If a plot s' versus $\ln \bar{\sigma}$ is made, one obtains a straight line relationship for some cohesive soils. This would mean that the compressibility of the soil is described by Eq.(5.17).

Other soils give straight line relationship when the results are plotted on a double log scale (Eq. 5.15). The parameters v , a and k give the value of E_c .

Instead of the relative settlement s' , one can use the void ratio e . It can be shown that

$$s' = \frac{\Delta e}{1 + e_0} \quad \text{in which } s' \text{ and } \Delta e = e_0 - e \text{ are related to the corresponding loading and}$$

e_0 is the initial void ratio of the sample.

Similar to Eq (5.10) the following equation may be written.

$$E_0 = -\frac{d\bar{\sigma}}{de} = v(\bar{\sigma}_0)^n \quad (5.18)$$

$$\text{since } s' = \frac{e_0 - e}{1 + e_0} = \frac{e_0}{1 + e_0} - \frac{e}{1 + e_0} \quad (5.19)$$

$$\frac{ds'}{de} = -\frac{1}{1 + e_0} \quad (5.20)$$

$$\frac{d\bar{\sigma}}{ds'} = E_s = -\frac{\frac{d\bar{\sigma}}{de}}{\frac{ds'}{de}} = -\frac{d\bar{\sigma}}{de} (1 + e_0) = E_0 (1 + e_0) \quad (5.21)$$

From Eq.(5.10), Eq.(5.18) and Eq.(5.21) the following expression is obtained.

$$v' = \frac{v}{1 + e_0} \quad (5.22)$$

By definition $a_v = -\frac{de}{d\bar{\sigma}}$ and $m_v = \frac{a_v}{1 + e_0}$, from Eq (5.17) Eq (5.20)

$$E_0 = \frac{1}{a_v} = \frac{E_s}{1 + e_0} \quad (5.23a)$$

$$E_s = \frac{1}{m_v} \quad (5.23b)$$

Where

a_v = coefficient of compressibility

m_v = coefficient of volume compressibility

5.2 INFLUENCE OF TIME ON THE DEVELOPMENT OF STRAIN

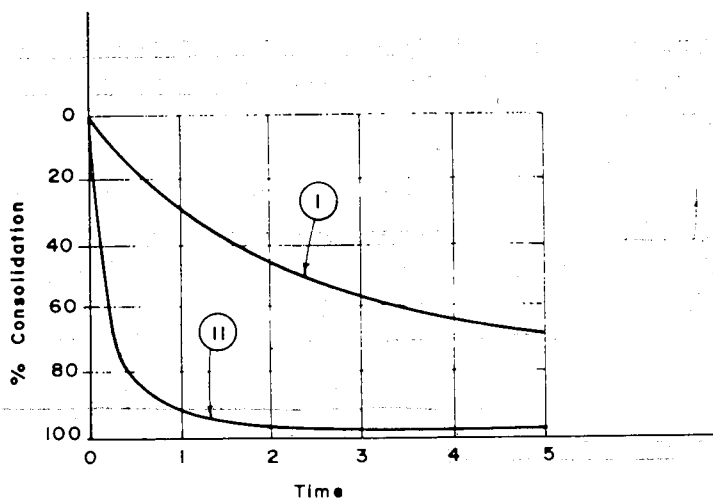
An additional characteristic of the void ratio-pressure relationship of soil, which is of great importance in the study of settlement of structures, is the influence of time upon the development of compressive strain. In steel and concrete, strains develop instantaneously with the application of stress. The strain in soil, however, develops over a period of time after an increment of consolidating pressure is applied. The main reason for this time lag is the fact that some of the water contained in the voids of foundation soil has to be squeezed out before the volume of the voids can decrease. The rate of outflow of the pore water depends on the permeability of the soil.

In relatively coarse-grained soils, the pore water can escape rapidly and the time lag between the application of pressure and the development of strain is relatively small. A structure founded on such soil will usually attain its maximum settlement early, and very little further settlement will occur after the structure is completed. On the other hand, if a structure is founded on a fine-grained clayey soil or if the stratum of such soil is present at some depth beneath, the outflow of water from the voids due to the pressure imposed by the structure will be very slow, due to relatively small coefficient of permeability. Therefore, the settlement of the structure will develop at a very slow rate and may require many years to be completed. The length of time depends on the permeability of the soil, the thickness of the layer, and on the drainage possibility of pore water.

Fig 5.8 shows the influence of time on the development of strain.

As can be seen from the figure the major part of the compression in coarse-grained soil takes place almost instantaneously. This is because of high permeability of coarse-grained soils. These soils hardly ever present a long settlement problem under steady loads.

In contrast to the coarse-grained soil, the fine-grained soil, as shown in Fig. 5.8, takes a considerable time for compression to take place under a given increment of load. As fine-grained soils are relatively impermeable, a long time is required for the expulsion of pore water. It is a well known fact that buildings founded above thick strata of clay undergo settlements that continue for a long period of time at steadily decreasing rates.



- (I) IMPERMEABLE FINE - GRAINED SOIL
 (II) PERMEABLE COARSE - GRAINED SOIL

Fig. 5.8 Time compression curve

5.3 CONSOLIDATION

5.3.1 General

In the discussion of compressibility of soil, only the extent to which the various soils eventually change in volume under a given loading were considered. That is, how much will a given soil sample compress under a given loading. No mention has been made about the rate of volume change or about the factors which influence the rate of volume change. These factors are important and are considered under this topic.

Consolidation is a gradual process involving drainage, compression, and stress transfer. In geology, consolidation refers to the hardening of soil to a rocklike condition. In geotechnical engineering, however, it refers to adjustment of soil to an applied loading. It may require a long time for a soil formation to come to an equilibrium under load. During this time, it is said in engineering that the soil is consolidating under the given load. When an equilibrium condition is reached, it is taken that the soil is fully consolidated. According to the

engineering usage of the term, it simply means completion of adjustment to a particular load at which point the soil may still be relatively loose or soft, and in the geologist estimate still considered as unconsolidated sediment.

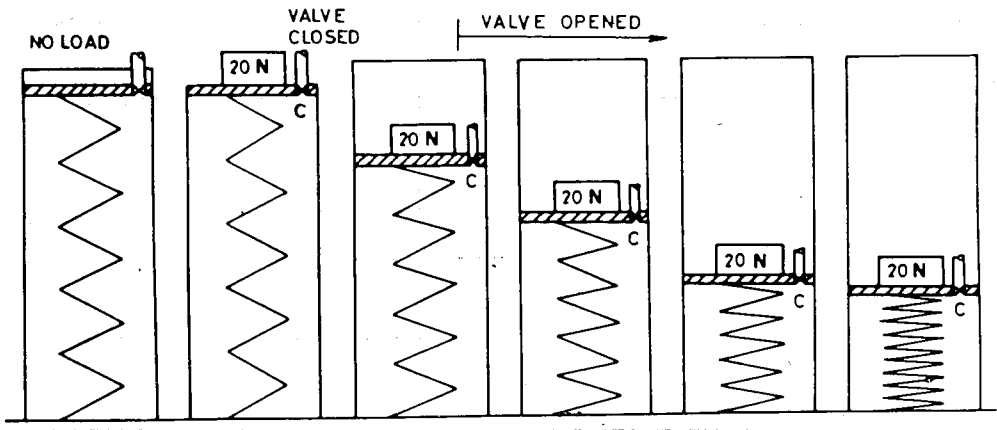
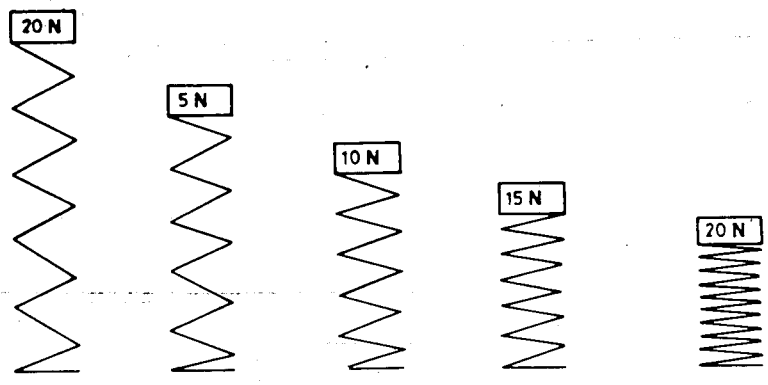
The rate at which the volume change or consolidation occurs is directly related to the permeability of the soil, because the permeability controls the speed at which the pore water can escape. If a saturated soil is quite pervious (e.g. clean sand), its consolidation under newly applied static load will be almost instantaneous, because pore water has no difficulty in escaping from the voids. However, if the saturated soil is clay with low permeability, its consolidation will be quite slow, because the pore water in the voids will take time to be squeezed out.

5.3.2 Mechanics of Consolidation

The process of consolidation may be explained with the help of a piston and spring mechanical analogy as shown in Fig.5.9. The spring is immersed in a cylinder filled with water. Into the cylinder, a frictionless but a tightly fitting piston provided with a vent valve has been fitted. A vertical load (say 20N) is applied on the piston. As long as the vent valve remained closed, the 20N load is carried by the water in the cylinder. When the vent valve is opened, water gushes out of the cylinder and the spring commences to compress.

In this analogy, the spring represents the soil grains and the water represents the moisture in the soil. As observed in the analogy, the spring compresses as the load acting on it increases. This same phenomenon takes place in soils. With the increase of intergranular stress, the void ratio decreases and consequently compression (consolidation) takes place.

Consider a pressure-versus-void ratio plot as shown in (Fig.5.10). Initially, i.e., just before the application of an additional pressure, the sample may be assumed to be under conditions represented by point A, where the effective (intergranular) pressure is designated by $\bar{\sigma}_1$ and the corresponding void ratio by e_1 . The moment $\Delta\bar{\sigma}$ is applied, the total pressure acting on the sample as a whole becomes $\bar{\sigma}_2$. However, like with the spring analogy, the void ratio will still be e_1 since the soil cannot compress instantaneously. $\bar{\sigma}_2$ cannot be effective within the soil



LOAD CARRIED BY WATER	20	20	15	10	5	0
ELAPSED TIME	0	0	t_1	t_2	t_3	t_4
LOAD CARRIED BY SPRING	0	0	5	10	15	20
PERCENT COMPRESSION	0	0	25	50	75	100

Fig. 5.9 Mechanics of consolidation- Piston and spring analogy

until the void ratio becomes e_2 . Hence, the pressure in the soil must still be $\bar{\sigma}_1$. The excess pressure $\Delta\bar{\sigma}$ which would produce a strain represented by $e_1 - e_2$, cannot be effective at once and hence does not act on the soil grains immediately.

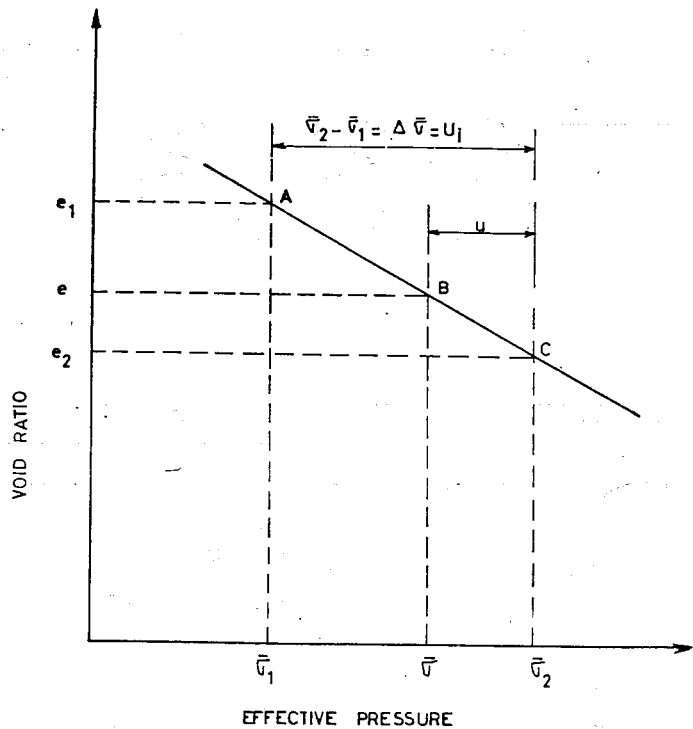


Fig. 5.10 Pressure versus void ratio plot

$\Delta\bar{\sigma}$ is carried by the water in the voids of the soil. The stress existing in the soil water produced by the transient condition is designated as hydrostatic excess pressure and is represented by u . The initial value of u is the maximum value and is equal to $\Delta\bar{\sigma}$ and is designated by u_1 . This excess hydrostatic pressure would be zero when the void ratio becomes e_2 . Theoretically no more water is forced out when the pressure in the soil skeleton is $\bar{\sigma}_2$, and the sample is said to be consolidated under the stress $\bar{\sigma}_2$.

If the entire sample were completely sealed, then $\Delta \bar{\sigma}$ will be carried by the water and no consolidation takes place. If however, drainage is allowed from the top and bottom (say by placing porous stones at top and bottom), the water pressure at the surfaces would be zero, whereas at a short distance inside the sample the water pressure is still $\sigma_2 - \sigma_1$. The high gradient causes a rapid drainage of water from the pores near the surface.

5.3.3. General Outline of Terzaghi-Froehlich's Theory of Consolidation

The general outline of Terzaghi-Froehlich's Theory of Consolidation is explained in reference to Fig. 5.11.

Consider a clay layer $2H$ thick lying between two pervious sand layers and is subjected to a surface unit load equal to σ . Under the influence of this load, the clay layer will begin to compress as the excess water from its pores is squeezed out towards the two pervious boundaries. If the clay is homogeneous, excess pore water from the upper half of the layer will flow towards the upper sand layer, whereas the excess pore water from the lower half of the layer will flow toward the lower sand layer. Such an arrangement is called double drainage.

At the instant the pressure, σ , is applied (i.e. at time $= t_0$) it is entirely carried by the pore water, i.e. $\sigma = u$ and $\bar{\sigma} = 0$. A few instant later, water will start escaping into the sand, so that u at both pervious boundaries will equal to zero. At any time $\sigma = u + \bar{\sigma}$.

As time goes by, the variation of hydrostatic excess pressure, u , over the depth will successively be indicated by the curves t_1, t_2, t_3 as shown in Fig 5.11. After time ($t = \infty$) consolidation will be complete and excess pore pressure will equal zero ($u = 0; \sigma = \bar{\sigma}$).

At any time, the area between the curve pertaining to that time and the initial hydrostatic excess pressure diagram gives the load transferred to the soil grains upto that time. For the time interval t_1 , this area has been shown shaded in the figure. The ratio of this to the area of the initial hydrostatic excess pressure diagram ABCD gives the degree of consolidation at that time and is expressed as a percentage.

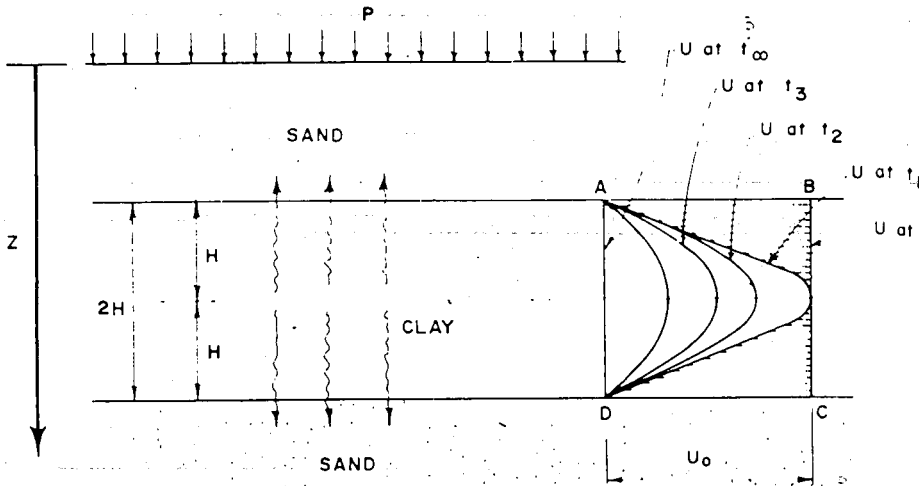


Fig. 5.11 Progress of consolidation

Progress of consolidation process at a given point in the soil is indicated by U_z

$$U_z = \frac{u_i - u}{u_i} = 1 - \frac{u}{u_i} \tag{5.24}$$

where

U_z = per cent consolidation at a point

u_i = initial hydrostatic excess pressure

u = hydrostatic excess pressure at time t .

The average per cent condolidation of the entire layer at any time

is numerically equal to the percentage change in thickness or settlement. Then, to estimate the rate of settlement, it is necessary to establish the variation of U with time. Before delving into the mathematical derivation of Terzaghi-Froehlich Theory of consolidation, the following points need to be understood [29].

a) **Assumption used in Terzaghi Froehlich's Theory**

1. Homogeneous soil
2. Complete saturation
3. Negligible compressibility of soil grains and water
4. One dimensional compression
5. One dimensional flow
6. The validity of Darcy's Law
7. The Coefficient of permeability, k , is the same everywhere within the layer and remains constant during consolidation

b) **Coefficient of Consolidation, c_v**

This is a coefficient containing the physical constant of a soil affecting its rate of volume change. It indicates the combined effects of permeability and compressibility for a given void ratio range.

$$c_v = \frac{k(1+e)}{a_v \gamma_w} \quad (5.25)$$

Where

c_v = coef. of consolidation

k = coef. of permeability

a_v = coef. of compressibility

γ_w = unit weight of water

c) **Longest Drainage Path, H**

It represents the longest distance travelled by drop of pore water in reaching an outlet.

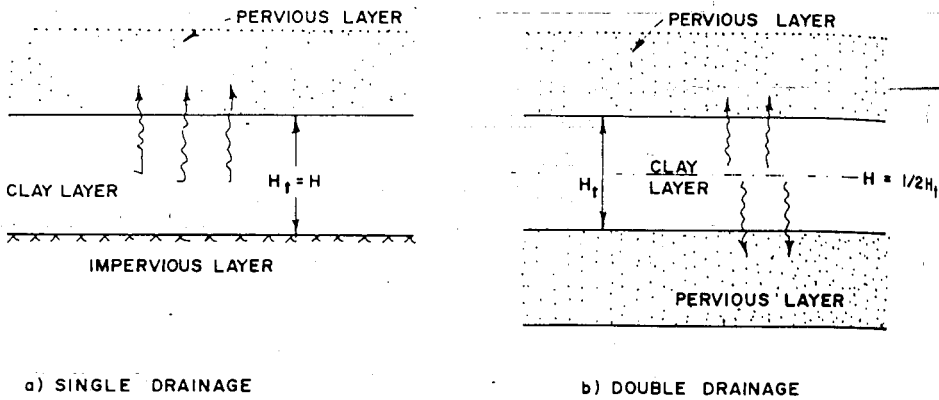


Fig. 5.12 Drainage path

d) Time-rate of settlement

According to Terzaghi's mathematical analysis of consolidation, the time rate of compression of clay stratum depends on the:

- a. thickness of clay layer
- b. number of drainage faces
- c. permeability of the soil
- d. magnitude of the consolidating pressure acting on the layer.

Factors a and b influence the distance through which the water in the soil voids must travel in order to escape and permit the volume of voids to decrease. Factor c controls the rate at which the water can escape. The last factor influences the hydrostatic excess pressure which causes the outflow of water.

5.3.4 Mathematical formulation of Terzaghi-Froehlich Theory of Consolidation

From the fundamental expression of flow in saturated earth masses, the time rate of change of volume is expressed as

$$\left(k_x \frac{\partial^2 h}{\partial x^2} + k_y \frac{\partial^2 h}{\partial y^2} + k_z \frac{\partial^2 h}{\partial z^2}\right) dx dy dz \quad (5.26)$$

From one dimensional flow, and for the case $k_x = k_y = k_z = k$ Eq. (5.26) reduces to

$$k \frac{\partial^2 h}{\partial z^2} dx dy dz \quad (5.27)$$

The volume of the element is $dx dy dz$, the pore volume is $(dx dy dz) \frac{e}{1+e}$ and since all changes in volume must be changes in pore volume, a second expression for the time rate change of volume may be written

$$\frac{\partial}{\partial t} \left(dx dy dz \frac{e}{1+e}\right) \quad (5.28)$$

since in general $V = V_v + V_s$,

$$V_s = V - V_v \text{ or } dx dy dz - \frac{e}{1+e} (dx dy dz)$$

Hence, Eq. (5.28) may be written as

$$\frac{dx dy dz}{1+e} \frac{\partial e}{\partial t} \quad (5.29)$$

Equating Eq. (5.27) and Eq. (5.29) one gets:

$$k \frac{\partial^2 h}{\partial z^2} = \frac{1}{1+e} \frac{\partial e}{\partial t} \quad (5.30)$$

Since only heads due to hydrostatic excess pressures will tend to cause flow in the case under consideration, h in Eq. (5.30) may be replaced by $\frac{u}{\gamma_w}$ giving

$$\frac{k}{\gamma_w} \frac{\partial^2 u}{\partial z^2} = \frac{1}{1+e} \frac{\partial e}{\partial t} \quad (5.31)$$

By definition

$$a_v = \frac{de}{d\bar{\sigma}}, \quad de = -a_v d\bar{\sigma}$$

- In general the effective normal stress $\bar{\sigma}$ is equal to

$$\bar{\sigma} = \sigma - u \quad (5.32)$$

If the neutral stress in the water decreases by Δu_w , the effective stress increases or decreases by the same amount.

$$\begin{aligned} \Delta \bar{\sigma} &= -\Delta u \\ d\bar{\sigma} &= -du \end{aligned}$$

Hence,

$$de = a_v du \quad (5.33)$$

Substituting Eq. (5.33) into Eq. (5.31)

$$\frac{k}{\gamma_w} \frac{\partial^2 u}{\partial z^2} = \frac{1}{1+e} (a_v \frac{\partial u}{\partial t})$$

$$\text{or} \quad \left[\frac{k(1+e)}{a_v \gamma_w} \right] \frac{\partial^2 u}{\partial z^2} = \frac{\partial u}{\partial t} \quad (5.34a)$$

The group of terms in the bracket may be written as:

$$\frac{k(1+e)}{a_v \gamma_w} = c_v \quad (5.34b)$$

The parameter c_v is called the coefficient of consolidation. Its insertion in Eq. (5.34) gives

$$c_v \frac{\partial^2 u}{\partial z^2} = \frac{\partial u}{\partial t} \quad (5.35)$$

In the consolidation theory the z coordinate distance is measured downward from the surface of the clay sample. The thickness of the sample is designated by $2H$, the distance H thus being the length of the longest drainage path (Fig. 5.11).

The boundary conditions are:

- complete drainage at the top and bottom of the sample

b) the initial hydrostatic excess pressure u_i is equal to the pressure increment $\bar{\sigma}_2 - \bar{\sigma}_1$

Hence, for $z = 0$ and $z = 2H$, $u = 0$. For $t = 0$, $u = u_i$.

Using these boundary conditions Eq.(5.35) has been solved and the general solution of which is given as follows.

$$u = \sum_{n=1}^{\infty} \left(\frac{1}{H} \int_0^{2H} u_i \sin \frac{n\pi z}{2H} dz \sin \frac{n\pi z}{2H} \right) e^{-\frac{n^2 \pi^2 c_v t}{4H^2}} \quad (5.36)$$

The above equation enables the hydrostatic excess pressure u to be computed under any initial systems of stress u_i at any depth z and at any time t .

Writing $T = \frac{c_v t}{H^2}$ (5.37)

Where T = time factor. Eq. (5.36) becomes

$$u = \sum_{n=1}^{\infty} \left(\frac{1}{H} \int_0^{2H} u_i \sin \frac{n\pi z}{2H} dz \right) \left(\sin \frac{n\pi z}{2H} \right) e^{-\frac{1}{4} n^2 \pi^2 T} \quad (5.38)$$

In particular if u_i is constant and is designated by u_0 (Fig.5.13), Eq. (5.38) becomes

$$u = \sum_{n=1}^{\infty} \frac{2 u_0}{n\pi} (1 - \cos n\pi) \left(\sin \frac{n\pi z}{2H} \right) e^{-\frac{1}{4} n^2 \pi^2 T} \quad (5.39)$$

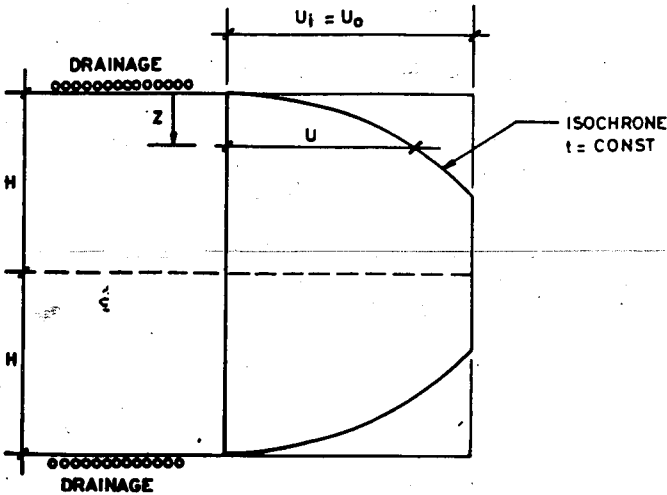


Fig. 5.13 Isochrone for constant hydrostatic excess pressure

In Eq.(5.39), when n is even, $1 - \cos n\pi$ vanishes; when n is odd, this expression becomes

2. Hence, it is convenient to let $n = 2m + 1$ in which m is an integer. $M = \frac{1}{2} \pi (2m + 1)$

Then Eq. (5.39) becomes

$$u = \sum_{m=0}^{m=\infty} \frac{2 u_0}{M} \left(\sin \frac{MZ}{H} \right) e^{-M^2 \tau} \quad (5.40)$$

The consolidation ratio at the depth z (Fig. 5.13) may be calculated from the definition:

$$U_z = 1 - \frac{u}{u_i}$$

$$U_z = 1 - \sum_{m=0}^{m=\infty} \frac{2}{M} \left(\sin \frac{MZ}{H} \right) e^{-m^2 \tau} \quad (5.41)$$

Considering the general equation further, the average degree of consolidation over the depth of the layer at any time during the consolidation process is calculated as follows:

The average initial hydrostatic excess pressure may be expressed as

$$u_{iA} = \frac{1}{2H} \int_0^{2H} u_i dz \quad (5.42)$$

Similarly the average hydrostatic excess pressure at any intermediate time t is

$$u_A = \frac{1}{2H} \int_0^{2H} u dz \quad (5.43)$$

The average consolidation ratio U is the average value of U_z over the depth of the stratum.

It is equal to the average value of $1 - \frac{u}{u_i}$ and may be expressed as

$$U = 1 - \frac{\int_0^{2H} u dz}{\int_0^{2H} u_i dz} \quad (5.44)$$

Substitution of the value of u given in Eq. (5.38) and integration gives

$$U = 1 - \frac{\sum_{m=0}^{\infty} \int_0^{2H} u_i \sin \frac{mz}{H} dz}{M \int_0^{2H} u_i dz} e^{-M^2 T} \tag{5.45}$$

For the special case of constant excess hydrostatic pressure (Fig. 5.13), Eq. (5.45) becomes:

$$U = 1 - \sum_{m=0}^{\infty} \frac{2}{M^2} e^{-M^2 T} \tag{5.46}$$

For the prediction of settlement from one-dimensional consolidation, it is Eq. (5.46) which is used. The variation of U with T is given in the following table.

U	0.10	0.2	0.30	0.40	0.50	0.60	0.70	0.80	0.90
T	0.008	0.031	0.071	0.126	0.196	0.287	0.403	0.567	0.848

When the initial hydrostatic excess pressure u_i is not constant, the consolidation of the layer is expressed by Eq.(5.45). Some of the basic shapes of excess pressure u_i are given in Fig. 5.14.

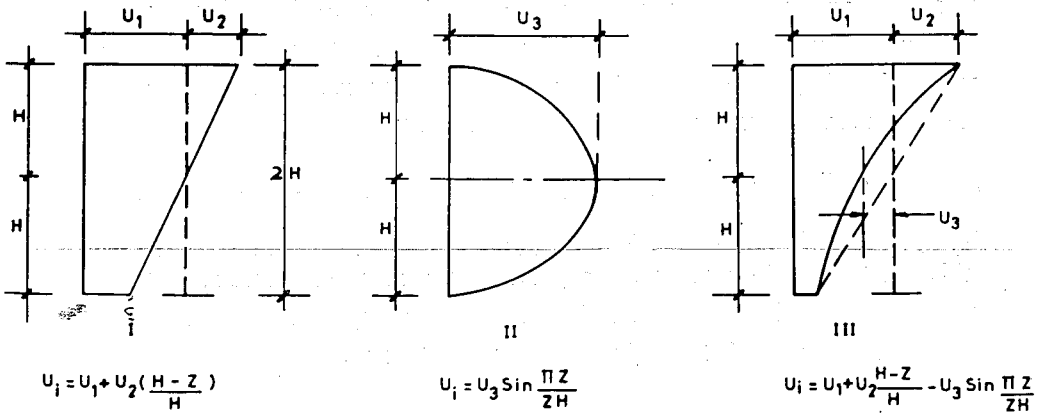


Fig. 5.14 Some basic shapes of hydrostatic excess pressure

With regard to Fig.5.14 the following may be said [30]:

- a) Case I represents the case of linear variation of initial hydrostatic excess pressure. For the consolidation equation one inserts the value of u_i in Eq.(5.45). However, it gives the same result as for constant excess pressure.
- b) Case II shows sinusoidal variation. The insertion of u_i in Eq. (5.45) gives the consolidation curve having the following variation

U	0.10	0.20	0.30	0.40	0.50	0.60	0.70	0.80	0.90
T	0.048	0.090	0.115	0.207	0.281	0.371	0.488	0.652	0.933

- c) Case III is a combination of I and II. The consolidation curve obtained for this case is not different from case I. In conclusion one would say that the case of constant hydrostatic excess pressure $u_i = u_0$ is an adequate representation of typical cases in practice.

5.3.5 Consolidation Test

5.3.5.1 General Description of Test Procedure

As described in 5.12 a small representative sample of undisturbed soil is carefully trimmed and fitted into the rigid metal ring. The soil sample is mounted on a porous stone base, and a similar stone is placed on top to permit water which is squeezed out of the sample to escape freely at the top and bottom. Prior to loading, the height of the sample should be accurately measured. Also, a micrometer dial is mounted in such a manner that the vertical strain in the sample can be measured as loads are applied (Fig. 5.1).

The consolidation-test apparatus is designed to permit the sample to be submerged in water during the test to simulate the position below a water table of the prototype soil sample from which the test sample was taken. Also, the apparatus may be fitted with a vertical glass tube which is connected with the base and serves as a stand-pipe of falling head permeameter.

A petcock is provided between the stand-pipe and the base.

The procedure of conducting a consolidation test is as follows. With no load on the sample and with the petcock to the permeameter stand-pipe closed, record the zero load reading of the compression strain dial. Then apply a suitable increment of load, say 25kPa, to the sample and read the compression dial at various intervals of time.

Readings should be taken frequently at first but may be less frequent as compression under the load increment progresses. When movement of the vertical dial indicates that the sample has virtually reached its maximum compression under the applied load, another increment of load is applied to the sample, and the time-rate of strain under this new increment is observed. This cycle of loading and measuring the time rate of strain is repeated until the total applied load exceeds that to which the prototype soil will be subjected by a proposed structure.

5.3.5.2 Determination of c_v

Two methods are available for evaluating c_v from consolidometer test data. The first called the *square root of time fitting method* is due to Taylor and the second called the *logarithm of time fitting method* is due to Casagrande. The two methods are based on the comparison of laboratory and the theoretical time curves. Since the natural scale does not offer the best representation of time, the square root and the logarithm of time are used.

5.3.5.2.1 The Square Root of Time Fitting Method

It has been observed that up to $U = 60\%$ the relation between T and U can be expressed as,

$$T = \frac{\pi}{4} U^2 \quad (5.47a)$$

Then,

$$U = \frac{2}{\sqrt{\pi}} \sqrt{T} \quad (5.47b)$$

Hence, the plot of U against \sqrt{T} would be straight line up to $U = 60\%$.

This theoretical curve is shown in Fig. 5.15.

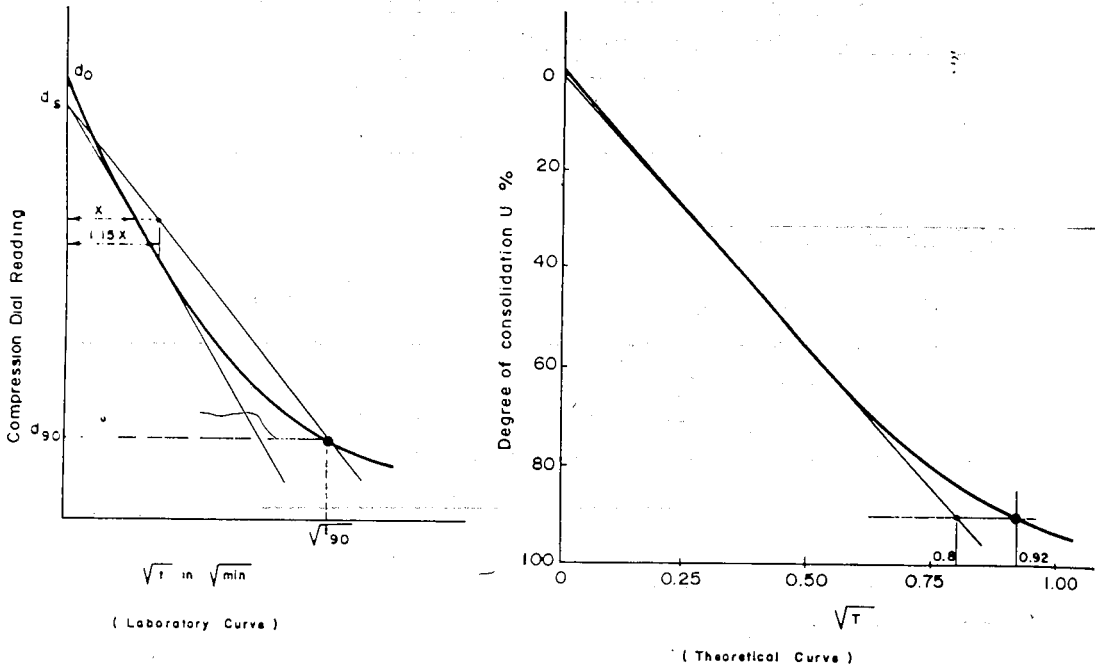


Fig. 5.15 The square root of time fitting method

At $U = 90\%$, $T = 0.848$ (from earlier tabulation)

$$\sqrt{T} = 0.92$$

If the straight portion of the curve is extended, it will meet the 90% U line at

$$\sqrt{T} = \frac{\sqrt{\pi}}{2} U = \frac{\sqrt{\pi}}{2} (0.9) = 0.80$$

The ratio of actual T value to that which is obtained by extension of the straight line is

$$\frac{0.92}{0.8} = 1.15$$

This property of the theoretical curve is utilized to determine a point of 90% consolidation on the laboratory time curve. The straight portion of laboratory curve (compression dial readings against square root of time) is extended backward to cut the $\sqrt{t}=0$ line at d_s . The point where the straight line cuts the $\sqrt{t}=0$ line is called the corrected zero point. A straight line is drawn as shown in Fig. 5.15 from the "corrected zero point" such that its abscissa everywhere is 1.15 times the abscissa of the straight portion of the laboratory curve. The point where this meets the laboratory curve gives the point of 90% consolidation. The time corresponding to this point is designated by t_{90} .

$$T_{90} = \frac{c_v t_{90}}{H^2} \tag{5.48}$$

T = time factor corresponding to 90% consolidation which is equal to 0.848

t_{90} = time elapsed corresponding to 90% consolidation as read from the laboratory curve.

H = (H at beginning of increment + H at end of increment)/2

$$c_v = \frac{0.848 H^2}{t_{90}} \tag{5.49}$$

The total compression in a loading increment is equal to the difference between the initial dial reading d_o and the one-day dial reading d_1 i.e $d_o - d_1$. This consists of three parts, namely:

- a) the initial compression, ($d_o - d_s$), due to the presence of air in the pores.
- b) the primary compression, ($d_s - d_{100}$), which corresponds to the theoretical compression curve, which is due to the expulsion of pore water.
- c) the secondary compression, ($d_{100} - d_1$), which is a slow additional plastic deformation of the soil not related to the escape of pore water.

In general the ratio between primary and total compression is called the primary compression ratio and is designated by r . In relation to the laboratory curve, it would be

$$r = \frac{10 (d_s - d_{90})}{9 (d_o - d_f)} \tag{5.50}$$

5.3.5.2.2 The Logarithm of Time Fitting Method

The intersection of the tangent at point of reversal of curvature and the asymptote to the theoretical consolidation curve is at the ordinate 100% primary consolidation designated by d_{100} .

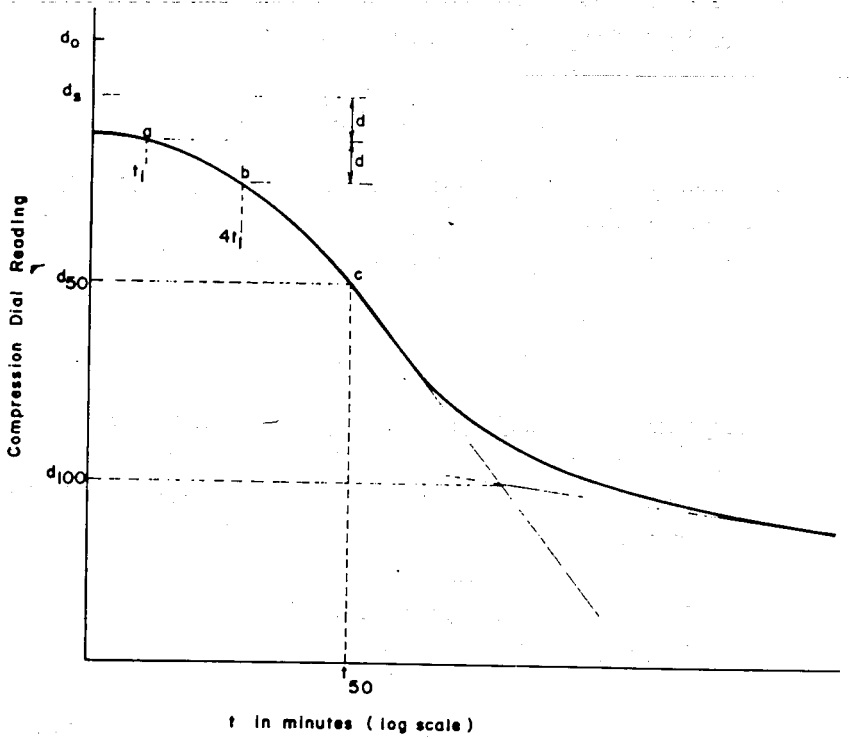


Fig. 5.16 The logarithm of time fitting method.

To find the 100% primary compression point on the laboratory curve, the above fact is utilized. To find the corrected zero point, d_s , use is made of the fact that the first portion of the curve is parabolic. Two time intervals, t_1 and t_2 , are taken such that t_2 is equal to $4t_1$. The difference in ordinates between the two points is marked off as shown in Fig. 5.16. A distance equal to this difference is stepped off above the upper point to obtain the corrected zero point. This corrected point is checked by retrials by using different points on the curve.

Having established the zero and 100% primary compression points, the 50% point and its time can easily be determined. The coefficient of consolidation can be computed from the following:

$$T_{50} = \frac{c_v t_{50}}{H^2} \quad (5.51)$$

$$c_v = \frac{0.196 H^2}{t_{50}} \quad (5.52)$$

$$r = \frac{d_s - d_{100}}{d_0 - d_f} \quad (5.53)$$

5.4 SETTLEMENT OF STRUCTURES

5.4.1 General

Almost all the structures which engineers build rest on soil and as such cause the soil to undergo compressive strains resulting in the settlement of structures. To understand the settlement behaviour of a structure and to predict and make provision for the settlement which may occur during its life, it is necessary to study the stress-strain characteristic of the foundation soil.

Settlement is not necessarily an adverse characteristic of a structure, provided it is uniform and is not excessive. However, if settlements are unequal serious consequences may result.

Unequal settlement may cause the floor and the wall of a building to crack badly, door and window frames to bend. This results in an increase in maintenance cost and rapid deterioration in the value of the building. In extreme case, it may cause the structure to be condemned. If the structure is a tall smokestack, monument etc, unequal settlements of the foundation may cause the structure to lean in unsightly manner. In an extreme case, it may lean far enough to become dangerously unstable.

Settlement of a structure resting on soil may be caused by shear failure of the foundation soil and compressive strain of the foundation soil. Shear failure happens when the load imposed causes shear stresses to develop within the soil mass which are greater than the shearing strength of the foundation soil. When this occurs, the soil fails by sliding downward and laterally, and the structure settles and perhaps tips out of vertical alignment.

Settlement may also result when the load imposed on foundation soil by a structure causes compressive stress accompanied by strain. This strain is a normal phenomenon and should not be regarded as a failure of soil.

5.4.2 Settlement Analysis

In general, the settlement of structures may consist of one or any combination of the following three types of settlements.

- a) Immediate or Elastic Settlement
- b) Consolidation or Primary Settlement
- c) Creep or Secondary Settlement

Immediate or elastic settlement is caused by the elastic behaviour of the soil mass. This settlement may be calculated by using the elastic parameter of the soil (Poisson's ratio, modulus of elasticity) and the rigidity and geometric shape of the foundation structure.

Consolidation settlement is the result of the process of consolidation as already discussed earlier and is calculated using the theory of consolidation. Creep or secondary settlement is a time dependent settlement which is a result of plastic deformation of the soil. While the above two settlements attain finite values for given stress level, the secondary settlement does not.

The secondary settlement for a given time span may be estimated from consolidation test results.

Depending upon the type of soil and duration of loading, the relative magnitude of each component varies. In non-cohesive soils, for example, it is the immediate settlement that prevails. While secondary settlement dominates in highly organic clays, consolidation settlement takes place mainly in inorganic clays. The three different components may be identified in a time-settlement curve of a consolidation test on clays (Fig. 5.17).

Within the frame work of this book, it is intended to limit the discussion on settlements only for the case of consolidation or primary settlement, since it is this settlement that is of primary importance for normally consolidated and pre-compressed inorganic clays.

Since the geological history affects the settlement of the soil, it is legitimate at this stage to discuss this case. Basically, soils in situ may have experienced one of the three conditions in their geological history (Fig. 5.18).

If the soil has been precompressed, the compressibility curves s' versus $\log \bar{\sigma}$ will not be straight line. The curve manifests some kind of curvature. The equations derived from the straight line relationships cannot be used for the whole of the compressibility curve. It is, therefore, necessary to determine the value of the precompression pressure, $\bar{\sigma}_v$, from the consolidation test.

There are various methods for determining $\bar{\sigma}_v$. The two common methods are given in Fig. 5.19.

Soil subjected to stress conditions having values less than the precompression pressure show little settlement.

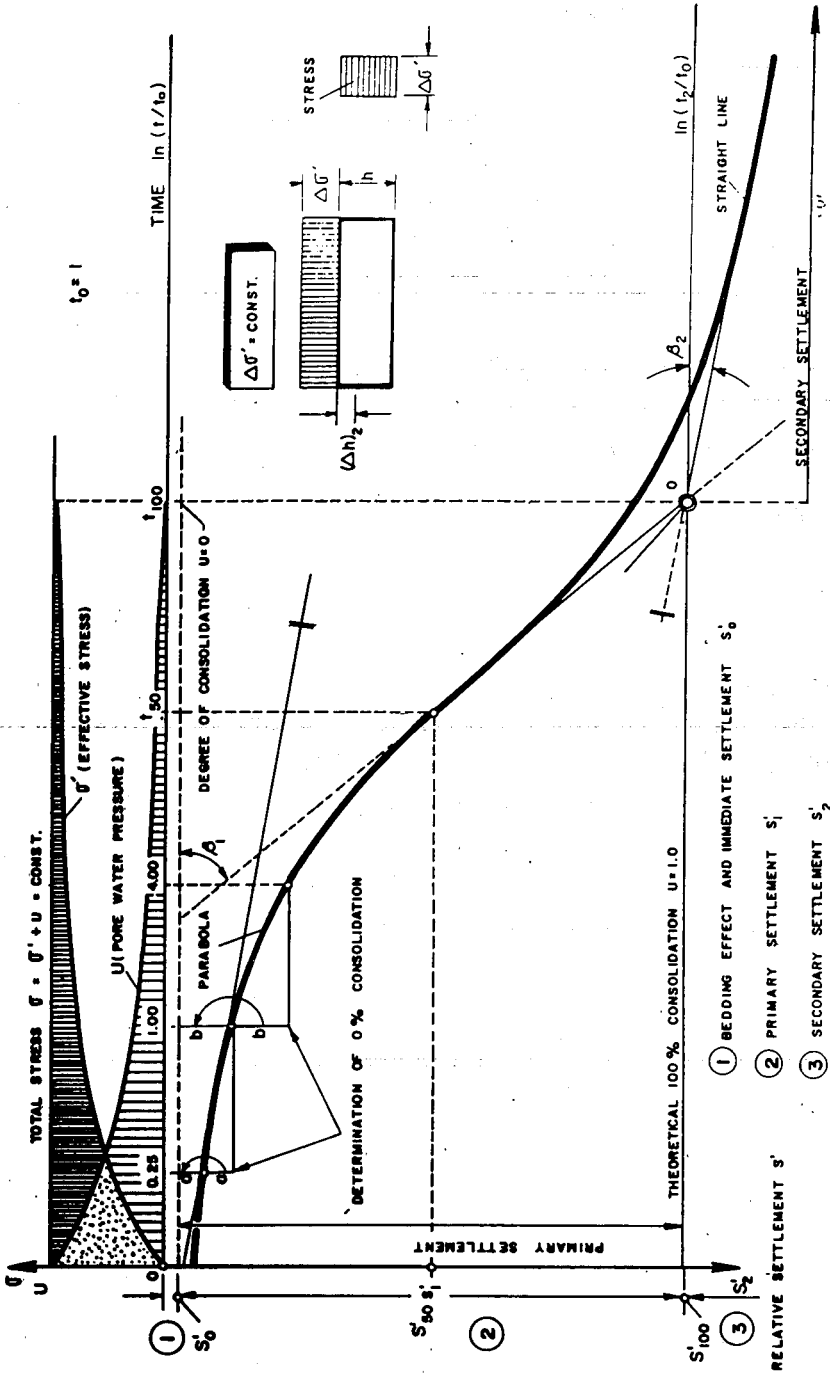


Fig. 5.17 Time settlement curve of a consolidation test.

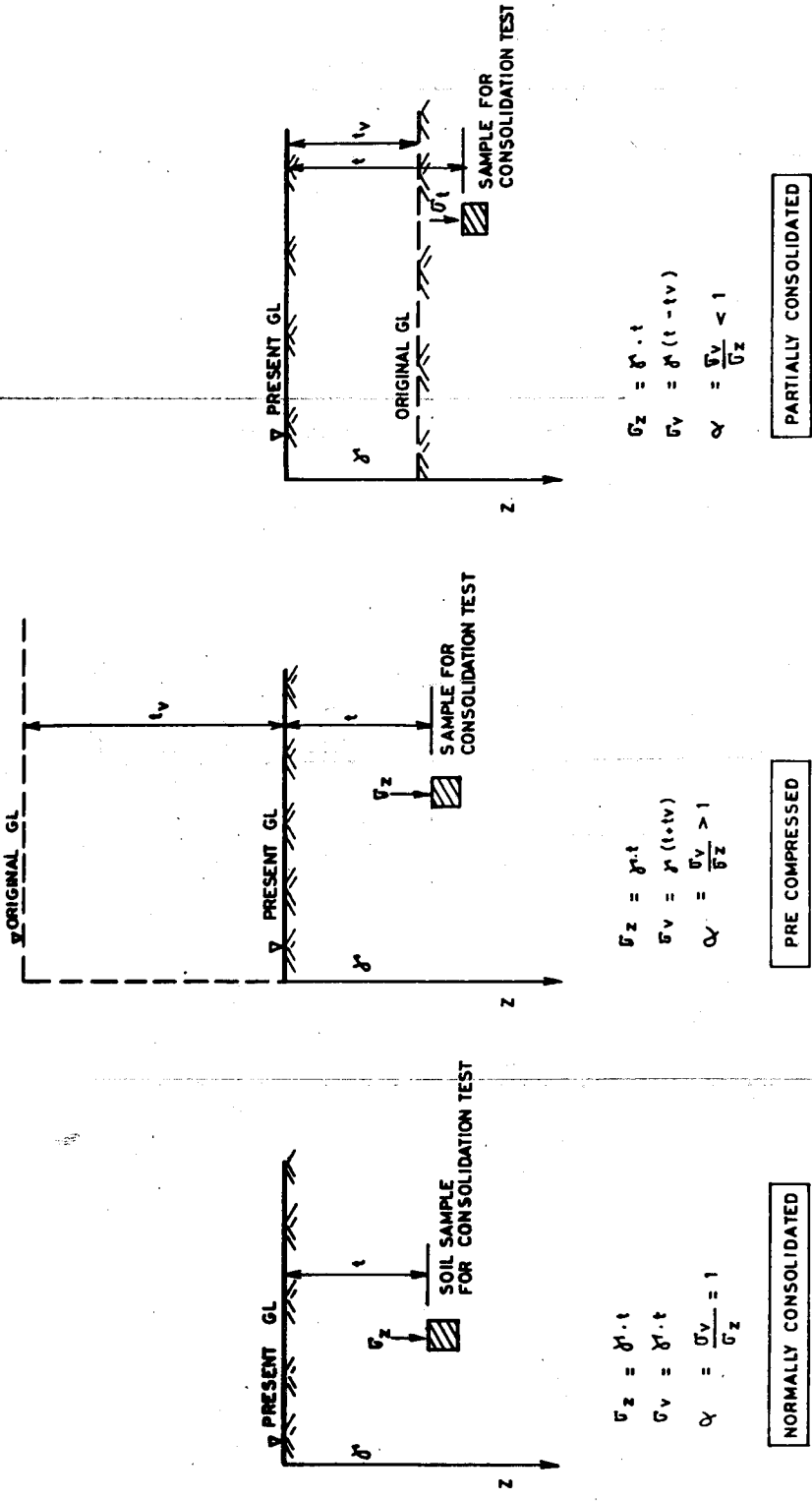
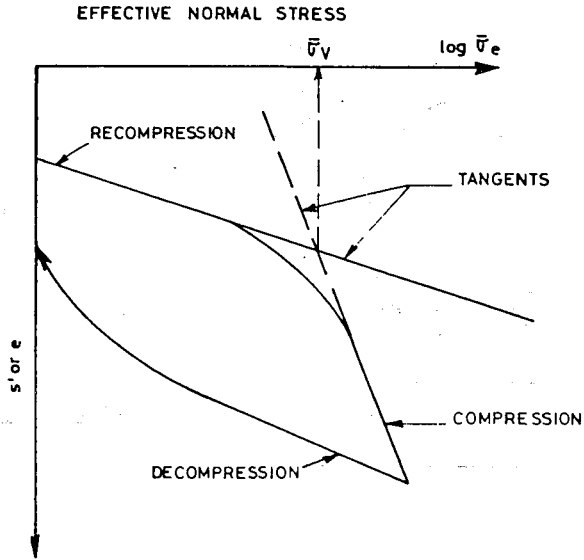
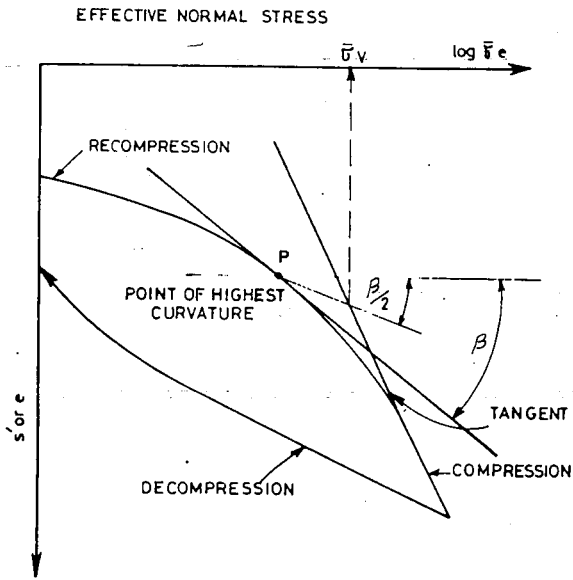


Fig. 5.18 Geological history of a soil sample



(a) SIMPLE METHOD OF TANGENTS



(b) METHOD OF CASAGRANDE

Fig. 5.19 Methods for determining precompression pressure

5.4.2.1 Consolidation Settlement

For computation of consolidation settlements, it is of importance to have the soil profile showing the location and thickness of different soil strata underlying the foundation. Such data as compression index, modulus of compressibility, coefficient of consolidation etc. have to be determined from consolidation test run on undisturbed samples retrieved from the construction site. For determination of preloading pressures (overburden) the index properties of the different layers of soils are essential.

Methods of computations

(A) Compression Index (C_c) - Method

In computing settlements by this method the following steps may be adopted

(a) Determine the pre-loading pressures.

These are vertical pressures exerted by soil weight of practical interest, in this regard, is the intergranular pressure. For thick clay layers, the pressures are usually computed at the top, middle and bottom of clay layer and their average is determined as follows

$$P_{avg} = \frac{1}{6}(P_t + 4P_m + P_b) \quad (5.52)$$

Where t, m, and b indicate top, middle and bottom respectively.

(b) Determine stress induced by column load

These are usually computed on the basis of Boussinesq's equation as explained earlier. If the clay layer is not very thick, the pre-loading as well as the increase in pressure may be computed only for the center of the layer. For thick layers, it is worthwhile determining the pressures at the top, middle and bottom and taking a mean by Simpson's Rule as in (a).

(c) Tabulate final pressure analysis data

(d) Compute the settlement as indicated below

Initial intergranular pressure, $P_{avg} = P_1$

Increased pressure due to column load, $\Delta p_{avg} = \Delta P$

$$P_2 = P_1 + \Delta P$$

Noting from earlier derivations

$$e_1 - e_2 = C_{c \log_{10}} \frac{P_1 + \Delta P}{P_1} = C_{c \log_{10}} \frac{P_2}{P_1}$$

$$\Delta e = C_{c \log_{10}} \frac{P_1 + \Delta P}{P_1} = C_{c \log_{10}} \frac{P_2}{P_1}$$

$$\Delta H = H \frac{\Delta e}{1 + e_1}$$

$$\Delta e = \frac{(1 + e_1) \Delta H}{H}$$

$$\Delta H = H \frac{\Delta e}{1 + e_1} \quad (5.53)$$

$$\Delta H = \frac{C_c H}{1 + e_1} \log_{10} \frac{P_2}{P_1} \quad (5.54)$$

Better results in settlement calculation may be obtained by dividing a given clay layer into n layers and then calculating the pre-loading and incremental pressures at the middle of each layer. Then Δh_i for each layer is calculated by means of (Eq. 5.54). The total settlement for the entire layer can be given by

$$\Delta H = \sum_{i=1}^{i=n} \frac{C_c \Delta H_i}{1 + e_i} \log_{10} \frac{P_2}{P_1} \quad (5.55)$$

B) Average modulus of compressibility (E_c) Method (7)

The average modulus of compressibility, E_c , is obtained first from the results of the consolidation curve. Two points, namely $\bar{\sigma}_{min}$ and $\bar{\sigma}_{max}$ are located on the curve

$$E_s = \tan \alpha = \frac{\Delta \bar{\sigma}}{\Delta s'} \quad (5.56)$$

The total settlement is then calculated by dividing the area of the pressure distribution curve by E_s (Fig. 5.20)

The area may be approximately calculated with the help of Simpson's formulas in (a).

$$A = \frac{z_b - z_t}{6} [\bar{\sigma}_t + 4 \cdot \bar{\sigma}_m + \bar{\sigma}_b] \quad (5.57)$$

For preliminary design the value of E_s given in Table 5.1 may be used.

C) Variable Modulus of Compressibility (Graphical Method) [7]

As could be seen in Fig. 5.20 the slope of the consolidation curve varies from point to point. The average modulus of compressibility, E_s , approximates the curve between $\bar{\sigma}_{min}$ and $\bar{\sigma}_{max}$ with a straight line. The variable modulus of compressibility method

takes into account the variation of the compressibility curve. In this respect, this graphical method is more accurate than the constant E_s method. However, the accuracy depends like in all graphical methods on the accuracy of the drawing.

From the consolidation curve (Fig. 5.20) the relative settlement s'_r for the total effective stress $\bar{\sigma}_r = \bar{\sigma}_o + \Delta \bar{\sigma}$ and the relative settlement s'_o for the effective stress due to the overburden pressure $\bar{\sigma}_o$ are determined.

The relative settlement due to the net pressure would be

$$\Delta s' = s'_r - s'_o \quad (5.58)$$

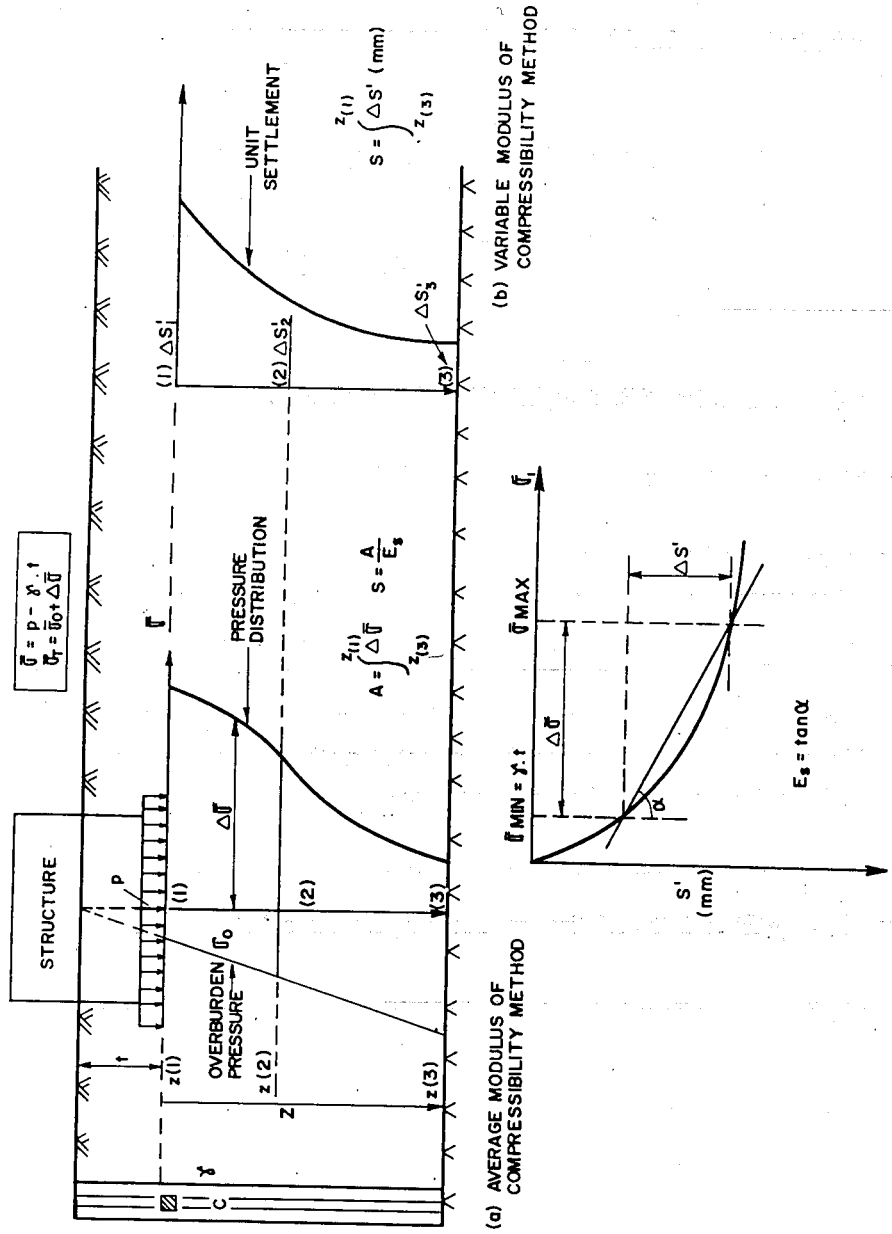


Fig. 5.20 Methods of settlement calculation

Table 5.1 Mean Soil Properties for Preliminary Designs [10]

Types of soil	Bulk Density		Final Strength		Initial Strength	Modulus of compressibility
	Above water γ kN/m ³	submerged γ' kN/m ³	Angle of Internal friction (degrees) ϕ or ϕ'	Cohesion c' kN/m ²	Undrained shear strength c_u kN/m ²	E_s kN/m ²
Non cohesive soil sand, loose, round	18	10	30	-	-	20000 - 50000
Sand, loose, angular	18	10	32.5	-	-	40000 - 80000
Sand, medium dense, round	19	11	32.5	-	-	50000 - 100000
Sand, medium dense, angular	19	11	35	-	-	80000 - 150000
Gravel without sand	16	10	37.5	-	-	100000 - 200000
Coarse gravel, sharp edged	18	11	40	-	-	150000 - 300000
Cohesive soils	(Empirical Values for Undisturbed Samples from the North German Area)					
Clay, semi-firm	19	9	25	25	500 - 100	500 - 10000
Clay, difficult to knead, stiff	18	8	20	20	25 - 100	2500 - 5000
Clay, easy to knead, soft	17	7	17.5	10	10 - 25	1000 - 2500
Boulder clay, solid	22	12	30	25	200 - 700	30000 - 100000
Loam, semi-firm	21	11	27.5	10	50 - 100	5000 - 20000
Loam, soft	19	9	27.5	-	10 - 25	4000 - 80000
Silt	18	8	27.5	-	10 - 50	3000 - 10000
Soft, org. slightly clayey sea silt	17	7	20	10	10 - 25	2000 - 5000
Soft, very org. strongly clayey sea silt	14	4	15	15	10 - 20	500 - 3000
Peat	11	1	15	5	-	400 - 1000
Peat under moderate initial loading	13	3	15	10	-	800 - 2000

- ϕ = Angle of internal friction in non-cohesive soils
 ϕ' = Effective angle of internal friction in cohesive soils
 c' = Effective cohesive corresponding to ϕ'
 c_u = Undrained shear strength in water saturated cohesive soils

The settlement for a thin layer of soil with a thickness of Δd_s would be

$$\Delta S = \Delta S'_m \cdot \Delta d_s \tag{5.59}$$

where $\Delta S'_m$ = the relative settlement $\Delta S'$ at the middle of the layer Δd_s .

If the whole soil layer is divided into n strips with widths Δd_s , then the total settlement would be:

$$S = \sum_{z=0}^{z=n} \Delta S' \tag{5.60}$$

If the unit settlement distribution curve with depth is continuous (Fig 5.20) Simpson's formula may be applied. Then,

$$S' = \frac{z_b - z_t}{6} [\Delta S'_t + 4 \cdot S'_m + \Delta S'_b] \tag{5.61}$$

5.4.2.2 Immediate Settlement (Elastic Settlement)

The settlement computation method discussed above is based on consolidation test. To compute settlements in such soils as granular soils, non-saturated clays and silts, the theory of elasticity can be used. It is to be noted that the theory of consolidation does not apply to these soils.

$$\Delta H = qB \frac{1 - \mu^2}{E} I_w \tag{5.62}$$

Where

- ΔH = immediate settlement
- q = intensity of contact pressure
- μ = Poisson's ratio (Table 5.2)
- E = modulus of elasticity of soils (Table 5.3)
- B = least lateral dimension of footing
- I_w = influence factor (Table 5.4)

Table 5.2 Typical range of values for Poisson's ratio [9]

Types of Soil	μ
Clay, saturated	0.4 - 0.5
Clay, unsaturated	0.1 - 0.3
Sandy clay	0.2 - 0.3
Silt	0.3 - 0.35
Sand (dense)	0.2 - 0.4
Sand (Coarse)	0.15
Sand (fine-grained)	0.25

Table 5.3 Range of values for modulus of elasticity [9]

Type of soil	E_s (kPa)
Very soft	$0.35 \times 10^3 - 2.8 \times 10^3$
Soft clay	$1.75 \times 10^3 - 4.2 \times 10^3$
medium clay	$4.2 \times 10^3 - 8.4 \times 10^3$
Hard clay	$7 \times 10^3 - 17.5 \times 10^3$
Sand clay	$28 \times 10^3 - 42 \times 10^3$
Silty sand	$7 \times 10^3 - 21 \times 10^3$
Loose sand	$10.5 \times 10^3 - 24.5 \times 10^3$
Dense sand	$49 \times 10^3 - 84 \times 10^3$
Dense sand and Gravels	$98 \times 10^3 - 196 \times 10^3$

Table 5.4 Influence factors for various shaped foundation elements [9]

Shape	Flexible (I_w)				Rigid
	Center	Corner	Average	I_w	I_m^*
Circle	1.00	0.64	0.85	0.88	
Square	1.12	0.56	0.95	0.82	3.7
Rectangle					
L/B = 1.5	1.36	0.68	1.20	1.06	4.12
2	1.53	0.77	1.31	1.20	4.38
5	2.10	1.05	1.83	1.70	4.82
10	2.52	1.26	2.25	2.10	4.93

* Influence value of rigid footing subjected to eccentric loading or moment. Rotation of the rigid footing is considered.

5.4.3 Correction of Settlement

5.4.3.1 Construction Period Correction

The load due to a building or other structures is not applied instantaneously, but is spread over a certain period of time. First there is excavation for foundation which results in relief of pressure. This is followed by the construction of structure leading to gradual loading till the original pressure is reached and then exceeded as shown in Fig. 5.21.

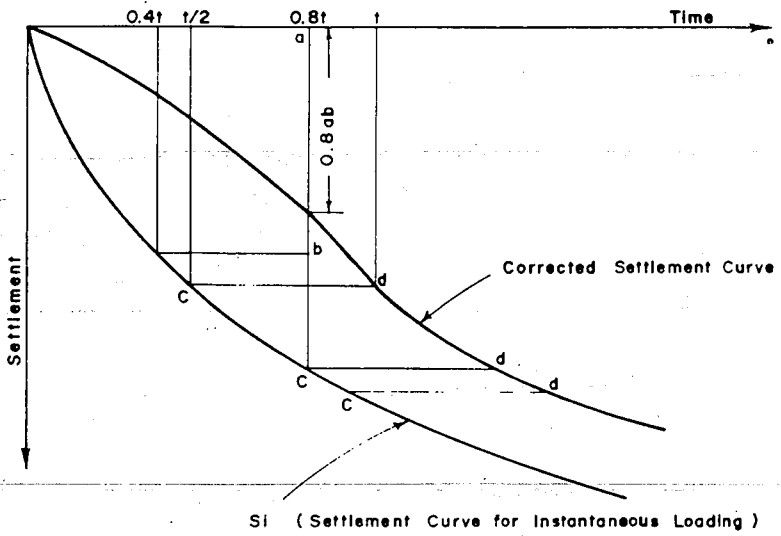
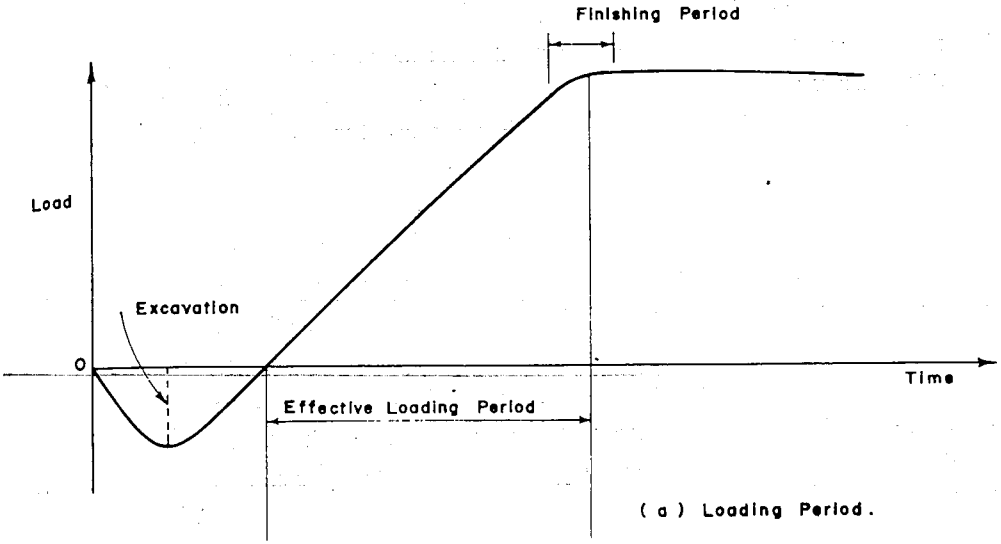


Fig. 5.21 Construction period correction

The correction to be applied is as follows:

Referring to Fig 5.21 b, S_1 is the settlement curve for instantaneous application of the load W_c . The correct settlement at time t is assumed to be the same as if the load is applied at time $t/2$. This is found by drawing a vertical line from $t/2$ to S_1 and moving horizontally to the time t .

The same procedure may be applied for points between 0 and t . For example, take point $0.8t$. At point $0.8t$, the corrected settlement is found by drawing a vertical line from $0.4t$ to curve S_1 and then horizontally to the line $0.8t$ to give ab . Since the load added at this time is $0.8W_c$, the settlement is multiplied by a factor 0.8. This follows the same reasoning as noted above in that load applied gradually over the time $0.8t$ will have the same effect as the same load applied instantaneously at time $0.4t$. Points beyond the time t are determined by displacing the curve S_1 a horizontal distance equal to $t/2$ or cd as shown in Fig. 5.21

5.4.3.2. Rigidity Correction [7]

In many cases a uniform distribution of contact pressure under a footing, irrespective of the nature of the rigidity of the structure, is considered. The contact pressure under a rigid foundation is parabolically distributed and that under a yielding (very flexible) foundation is uniformly distributed (Fig. 5.22). The settlements vary according to the stiffness of the foundation. A comparison of the settlement trough shows that

- a) the settlement of a rigid foundation is .75 that of an elastic foundation at the middle of the footing (Fig. 5.22).
- b) the settlement of a rigid and elastic foundation at a distance of $0.74b/2$ - called the *characteristic point* is the same (Fig. 5.22).

Since the tables and formulas used for calculating stress distribution assume elastic foundations, the calculation for actual foundations should be made either at the middle or at the characteristic points (Fig. 5.22).

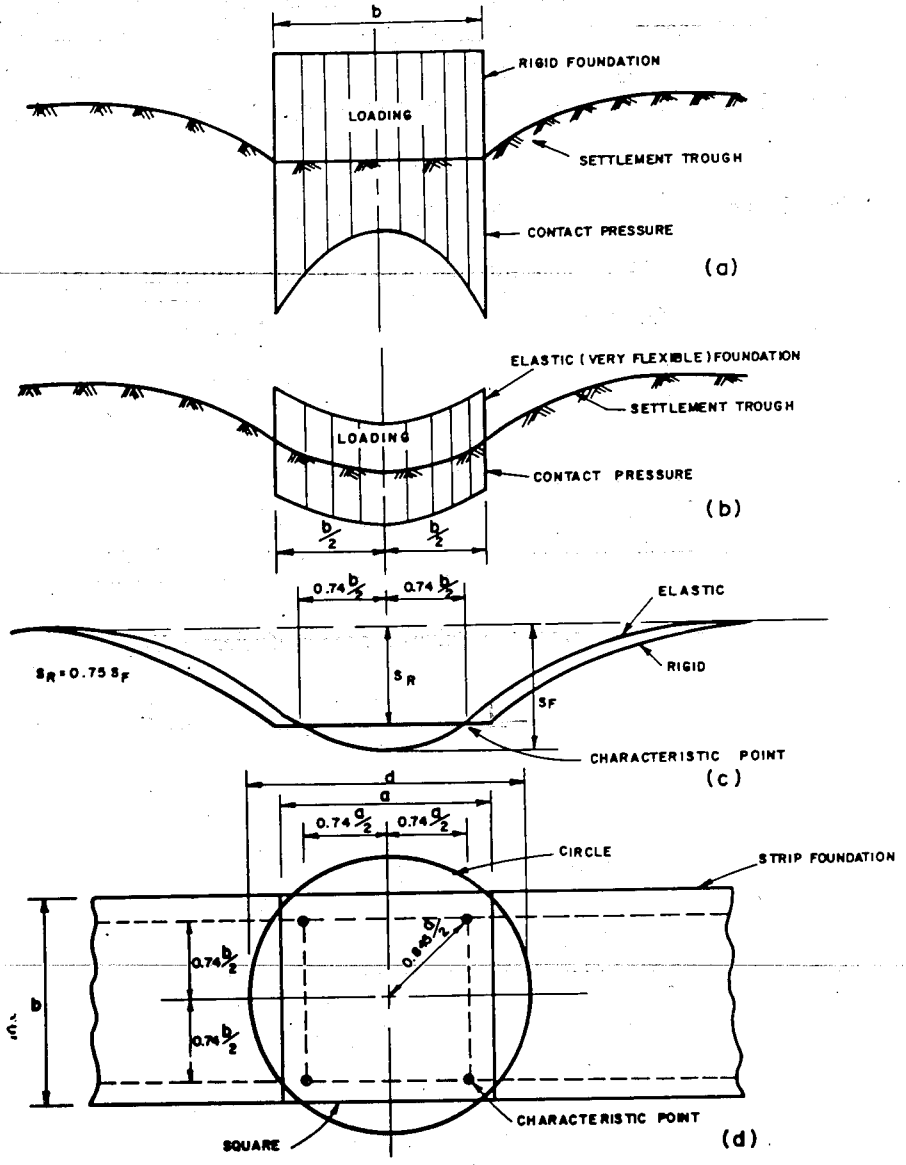


Fig. 5.22 Settlement trough

5.4.3.3 Correction due to Method of Calculation

The calculated settlements normally give higher values when compared with actual measured settlements. In order to remedy this discrepancy empirical formulas have been suggested. Skempton and Bjerrum [24] suggest the following relationships from which the calculated settlements should be multiplied by the coefficient β .

$$\beta = A + \alpha (1 - A) \tag{5.63}$$

The values of A and α are given in Tables 5.5 and 5.6

Table 5.5 Values for pore water pressure coefficient A [24]

Soil type	Coefficient A
Sand	0.30 ——— + 0.50
Silt	+0.50 ——— + 1.00
Soft clay (very sensitive)	+1.00 ——— > + 1.00
Normally consolidated clay	+0.50 ——— + 1.00
Precompressed clay	+0.25 ——— + 0.50
Highly precompressed clay	-0.60 ——— +0.25

Table 5.6 Values for the coefficient α [24]

$\frac{ds}{b}$	Circle, Square	Strip
0.00	1.00	1.00
0.25	0.67	0.80
0.50	0.50	0.63
1.00	0.38	0.53
2.00	0.30	0.45
4.00	0.28	0.40
10.00	0.26	0.36
∞	0.25	0.25

ds = thickness of consolidating layer
 b = foundation width

5.5 EXAMPLES

E.5.1 Refer to the sketch shown below. Two column footings A and B are 1.5m by 1.5m each and are located 6.5 center to center. Each foundation transmits a load of 250kN. Treating the loads as point loads, calculate the total expected settlement and the time for 60% settlement.

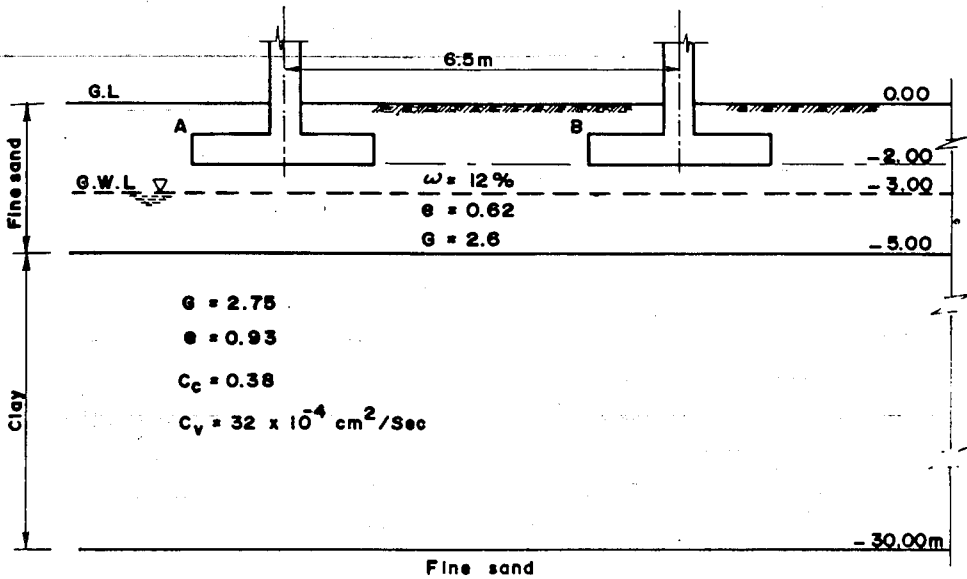


Fig. E.5.1 Loading and Soil Soil Condition

SOLUTION

Table E.5.1 Pre-loading Pressure

Datum	Depth	Calculation	Inter-granular pressure	Formula
-	m		kN/m ²	
-3.0	3.0	$P'_{1} = (3)2.6(1+.012)10/(1+0.62)$	53.93	$P'_{1} = h_{1}\gamma_{1}$ $= h_{1}G_{1}(1+\omega)\gamma_{w}/(1+e)$
-3 to -5	2.0	$P'_{2} = 2(2.6-1)10/1.62$	19.75	$P'_{2} = h_{2}\gamma_{2}$ $= h_{2}(G_{2}-1)\gamma_{w}/(1+e)$
-5	5.0	73.63	
-5 to -17.5	12.5	$P'_{3} = 12.5(2.75-1)10/(1+0.93)$	113.34	$P'_{3} = h_{3}\gamma_{3}$ $= h_{3}(G_{3}-1)\gamma_{w}/(1+e)$
-17.5	17.5	187.02	
-17.5 to -30.0	12.5	$P'_{4} = 12.5(2.75-1)10/1.93$	113.34	$P'_{4} = h_{4}\gamma_{4}$ $= h_{4}(G_{4}-1)\gamma_{w}/(1+e)$
-30	30.0	300.36	

Table E.5.2 Stress due to column loads

Below column	Stress due to column	r	At elev. -5.0 z=3			At elev.-17.5 z = 15.5m			At elev.-30.0 z = 28.0m		
			r/z	i ₁	Q.i ₁	r/z	i ₁	Q.i ₁	r/z	i ₁	Q.i ₁
			B	6.5	2.17	0.006	1.5	0.42	0.35	87.5	0.23
A	0.0	0.0	0.477	119.3	0.0	0.477	119.3	0.0	0.47	119.3	
A	$\sigma_z = \frac{\sum Q i_1}{z^2}$		ΣQi_1		120.8	ΣQi_1		206.8	ΣQN_1		224.3
			13.37kN/m ²			0.86kN/m ²			0.29kN/m ²		

Table E.5.3 Tabulation of average pressure

Elevation (pressure)	-5.0 (p ₁)	-17.5 (p _m)	-30 (P ₂)	$p_{avg} = 1/6(p_1 + 4p_m + p_2)$
Initial Pressure, p ₁ (kN/m ²)	73.68	187.02	300.36	187.02
Increased Pressure, Δp (kN/m ²)	13.37	0.86	0.29	2.85

$p_1 = 187.02 \text{ kN/2}$

$\Delta p = 2.85 \text{ kN/m}^2$

$p_2 = 189.87 \text{ kN/m}^2$

$$\Delta H = \frac{C_c H}{1 + e} \log_{10} \frac{P_2}{P_1} = \frac{0.38 (25)}{1.93} \log_{10} \frac{189.87}{187.02} = 0.0323 \text{ m}$$

Total expected settlement = 3.23cm

$$T = \frac{c_v t}{H^2}$$

$$H = 25/2 = 12.5\text{m}$$

$$U = 60\%, T_{60} = 0.287$$

$$t = \frac{TH^2}{c_v} = \frac{0.287 (12.5 \times 100)^2}{32 \times 10^{-4}} = 14013.67 \times 10^4 \text{secs}$$

$$= 1622 \text{days}$$

E. 5.2 A structure having a raft foundation 4m x 4m erected on a site as shown in the figure (Fig. E.5.2) is given.

Determine

- a) the expected settlement
- b) the time required for 50 percent consolidation

SOLUTION

The settlement shall be calculated at the center of the foundation.

i) Calculation of stress distribution

Unit weight above ground water level = 19 kN/m³

Unit weight below ground water level = 9 kN/m³

Net pressure acting on the ground: 250 - (19) = 250 - 19 = 231.0 kN/m²

The vertical pressure distribution due to the overburden pressure and superimposed load will be calculated under the center of the foundation at an interval of 1m and the result tabulated (Table E.5.4).

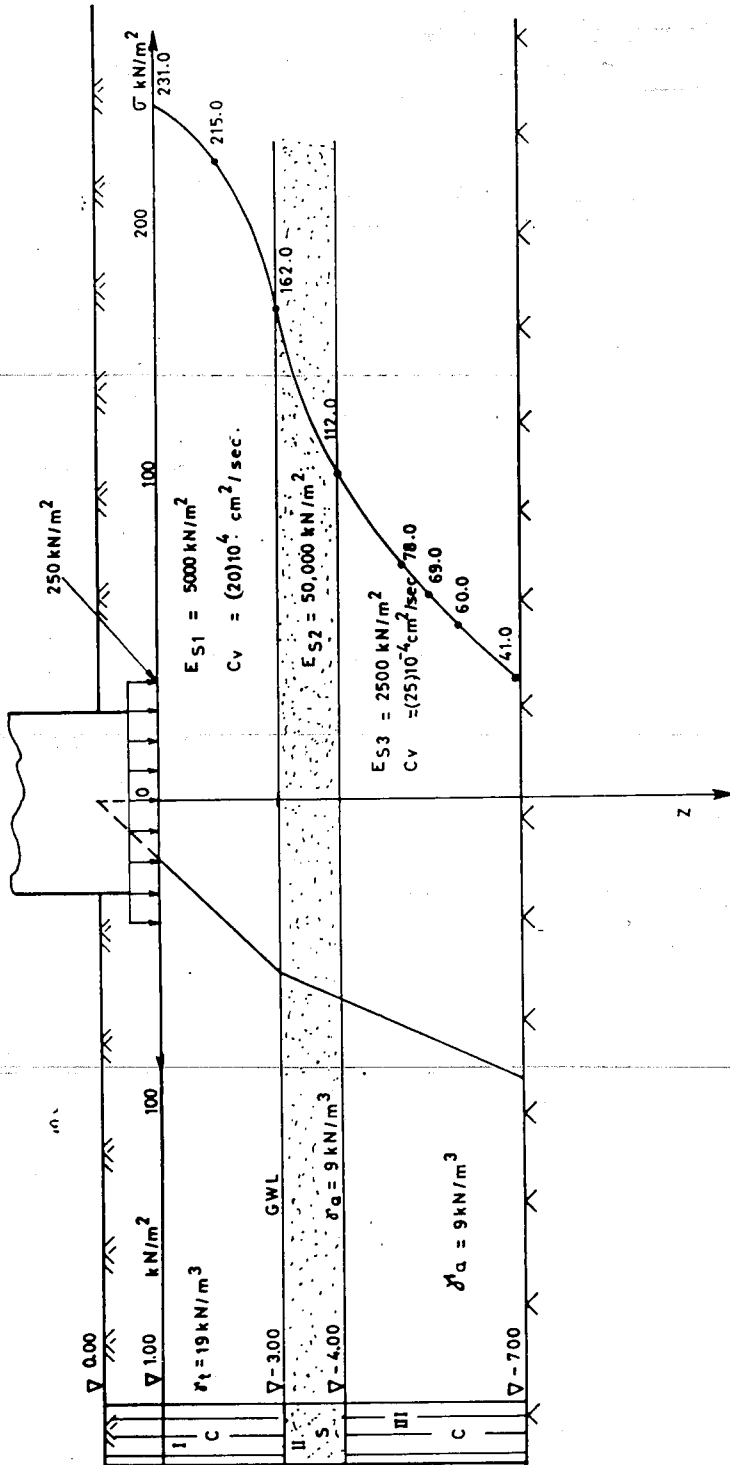


Fig. E.5.2 Loading and soil condition

Table E.5.4 Calculation of pressure distribution

Ordinate	Depth under the foundation	Unit wt.	Overburden prcs.	Pres. due to $P=231\text{kN/m}^2$ $a=b=2\text{m}$ $a/b=1$			
	z	γ	$\bar{\sigma}_o$	z/b	i	$4i$	$\sigma_z = 4i p$
	m	kN/m^3	kN/m^2	-	-	-	kN/m^2
-1	0	19	19	0	0.2500	1.0000	
-2	1	19	38	0.5	0.2325	0.9300	231.00
-3	2	19	57	1.00	0.1752	0.7000	215.0
-4	3	9	66	1.50	0.1210	0.4840	162.0
-5	4	9	75	2.00	0.0840	0.3360	112.0
-6	5	9	84	2.50	0.0644	0.2576	78.0
-7	6	9	93	3.00	0.0447	0.1788	60.0
							41.0

The variation of the stress with depth is given in Fig. E.5.2

ii) Settlement calculation

The total stress area in the different layers is calculated using Simpson's formula.

Clay layer I

$$\sum \bar{\sigma}_I = \frac{2-0}{6} [231.0 + 4(215.0) + 162] = 417.7 \text{ kN/m}^2$$

Sand layer II

$$\sum \bar{\sigma}_{II} = \frac{1}{2} (162.0 + 112.0) = 137.0 \text{ kN/m}$$

Clay layer III

$$\sum \bar{\sigma}_{III} = \frac{6-3}{6} [112 + 4(69.0) + 41] = 214.5 \text{ kN/m}$$

$$S_I = \frac{\sum \bar{\sigma}_I}{E_{s1}} = \frac{417.7}{5000} = 0.084 \text{ m}$$

$$S_{II} = \frac{\sum \bar{\sigma}_{II}}{E_{s2}} = \frac{137.0}{50000} = 0.003 \text{ m}$$

$$S_{III} = \frac{\sum \bar{\sigma}_{III}}{E_{s3}} = \frac{214.5}{2500} = 0.086 \text{ m}$$

Settlement corrections only due to rigidity are introduced in this example giving the final anticipated settlement.

$$S_{IF} = (0.75) (0.084) = 0.60 \text{ m} = 6 \text{ cm}$$

$$S_{IIF} = (0.75) (0.003) = 0.00 \text{ m} = 0 \text{ cm}$$

$$S_{IIIF} = (0.75) (0.086) = 0.06 \text{ m} = 6 \text{ cm}$$

iii) Time - settlement calculations

$$\text{In general, } T = c_v \cdot t / H^2$$

Clay layer I

For this case it will be assumed that drainage facilities will be introduced at the bottom of the foundation and therefore, double drainage is assumed.

$$H = 100 \text{ cm}$$

$$t = \frac{100^2 \cdot T}{c_v} = \frac{100^2 (T)}{(20) 10^{-4} (60) (60)} = 1388.89 T \text{ hrs}$$

Clay layer III

Here the drainage is in one direction only

H = 300 cm

$$t = \frac{300^2 \cdot T}{C_v} = \frac{300^2 \cdot T}{(25)(10^{-4})(60)(60)} = 10000T \text{ hrs}$$

The time taken by each layer for a given degree of consolidation is calculated for the two layers and the result tabulated (Table E.5.5)

Table E.5.5 Time - settlement calculation

U	T	U{S _{IF} }	t _{SIF}	U {S _{INF} }	t _{SINF}
-	-	cm	hrs	cm	hrs
0.10	0.008	0.6	11.11	0.6	80
0.20	0.031	1.2	43.06	1.2	310
0.30	0.071	1.8	98.61	1.8	710
0.40	0.126	2.4	175.00	2.4	1260
0.50	0.197	3.0	273.61	3.0	1970
0.60	0.287	3.6	398.61	3.6	2870
0.70	0.403	4.2	559.72	4.2	4030
0.80	0.567	4.8	787.50	4.8	5670
0.90	0.848	5.4	1177.78	5.4	8480
1.00	∞	6.0	∞	6.8	∞

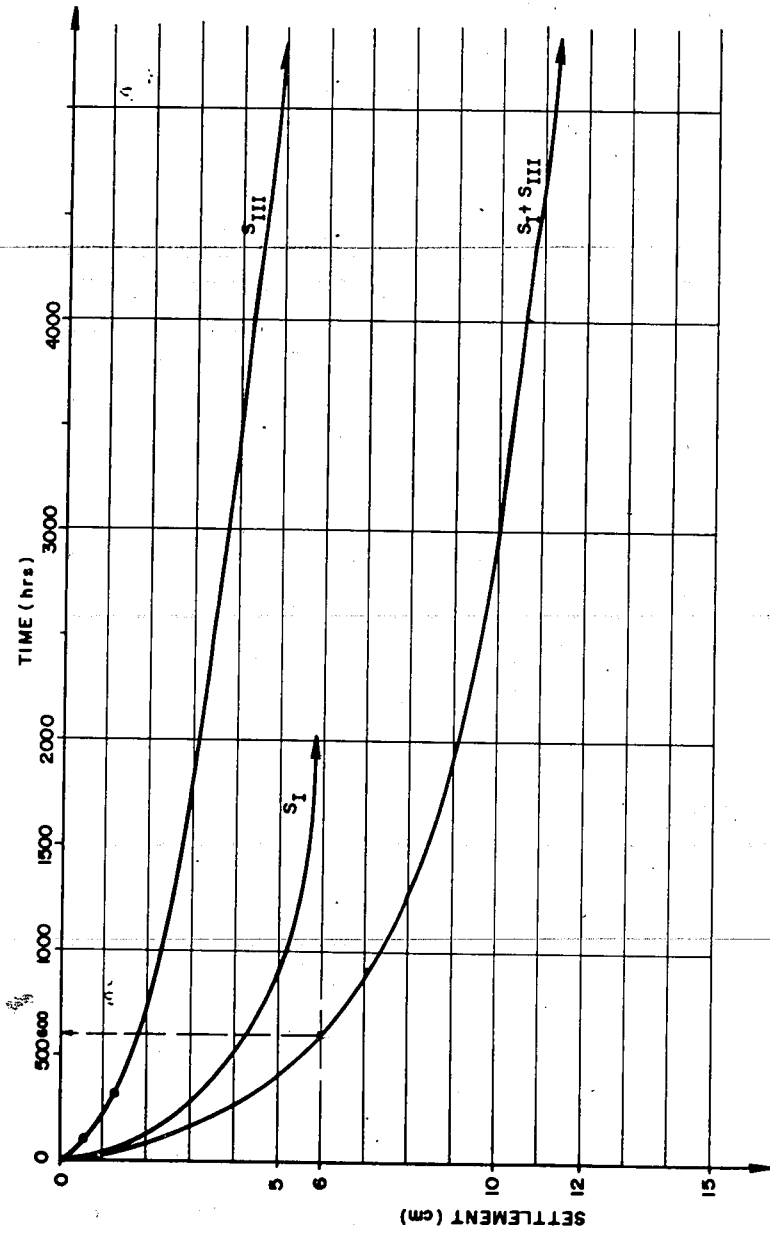


Fig. E.5.3 Time settlement curves

Since the two layers have different rates of consolidation, in order to obtain the rate of consolidation for the whole layers, the curves must be added (Fig. E. 5.3).

From the graph (Fig. E. 5.3) the time required for 50% consolidation i.e. $1/2(6+6)$ is 600 hrs.

5.6 EXERCISES

- 1 The soil profile at a building construction site is as shown below. If the water table is lowered by pumping from elevation -2.00m to elevation -9.00m and is permanently held there, determine the resulting settlement. The soil above water table (for each position) may be assumed to have water content of 28%. Assume $C_c=0.38$ and $c_v=40 \times 10^{-4}$ cm²/sec. Calculate the time required in days for 50% of the ultimate settlement to occur.

	0.00
Initial Water Table	-2.00
Silty sand $G_s=2.64, e=0.72$	
	-6.00
Final Water Table	-9.00
Sand $G_s=2.68, e=0.63$	
	-12.00
Clay $G_s=2.72, e=0.92$	
	-26.00
Impervious layer	

- 2 A load of 3000kN is being taken by a square footing 3m x 3m. The footing rests on silty soil which has a value of Poisson's ratio of 0.3. To find the modulus of elasticity of the soil, a soil sample was stressed to 300kN/m² at strain of 0.06%. Compute the settlement at the center and the edge of the footing.
- 3 A water tower carrying 8000kN terminates in a square footing 4m x 4m. The base of the footing is located 2m below the ground surface and rests on a dense sand which extends up to a depth of 10m. below the ground surface. A 3m. thick compressible clay soil exists below the dense sand. The effective overburden pressure at the middle of the clay layer is 140kN/m². Estimate the amount of settlement that will take place as a result of compression of the compressible soil.
Liquid limit of the compressible soil = 52% and average void ratio = 1.13.
- 4 The construction of a super-structure of a building lasted from March 1962 to August 1963. In August 1966, the average settlement of the building was found to be 6cm. Estimate the settlement in December 1967, given that the ultimate settlement is 15cm.
- 5 A very thick deposit of sand has a 2 m clay seam which is located at a depth of 5m. The ground water level is located at a depth of 4 m. The total unit weight of the sand is 17.7 kN/m³ above the ground water level and 20.4 kN/m³ below the ground water level. The clay has a moisture content of 45 per cent and a particle specific gravity of 2.78. The clay is normally consolidated and has a compression index of 0.6. A structure built on the sand stratum increased the pressure in the clay by an average value of 18kN/m².
- a. (i) Find the settlement of the structure.
(ii) Find the time required for 80 per cent consolidation if $c_v = 23 \times 10^{-4} \text{ cm}^2/\text{sec}$.
- b) If there is a thin layer of sand at a depth of 6 m, at what time will 80 per cent consolidation occur?

- 6 If in problem 6 of exercises 4.8, the clay has an average modulus of compressibility of 5000 kN/m^2 , what per cent of the total settlement under point P shall be contributed by structure B?
- 7 A raft foundation $10 \times 10\text{m}$ with an average bearing pressure of 200 kN m^2 is erected on a 10m , silt layer with consolidation test results as indicated below. The base of the foundation is located at a depth of 1.5m . The ground water level is also located at this depth. Specific gravity of the solids is 2.65 and the initial void ratio is 0.625 . Estimate the settlement of the foundation below the the *characteristic point*: using
- the Average Modulus of Compressibility, E_v , method.
 - the variable Modulus of Compressibility method.
 - compression index C_c method.

Consolidation test data

Stress Ncm^2	Strain $s' = h/h_0$	Void Ratio, e
0.00	0	0.652
1.62	0.0036	0.645
3.25	0.0051	0.643
6.50	0.0102	0.634
13.00	0.0167	0.624
26.00	0.0306	0.600
52.00	0.0553	0.560
104.00	0.0860	0.508
26.00	0.0800	0.520
6.50	0.0750	0.527
1.62	0.0705	0.535
0.00	0.0655	0.544

- 8 If in problem 5.6 the ground water level sinks by 3 m from its original position which is located at the level of the foundation, determine the settlement caused due to the sinking of the ground water level. Use the Average Modulus of Compressibility method for your calculation.

6. SHEARING STRENGTH OF SOILS.

6.1 GENERAL

Shearing strength is one of the most important properties of soils. It is a property which enables soil to resist sliding along internal surfaces within a mass. Because of the existence of this property it is possible to form all kinds of sloping surfaces in soil, such as man-made cuts and fills, river banks, earth dams etc.

The shearing strength of soil is used for:

- (a) the determination of ultimate bearing capacity of soils.
- (b) the evaluation of lateral pressure of soil masses against earth retaining structures.
- (c) the determination of stability of natural slopes, earthen embankments and cuts.

6.2. GENERAL CONSIDERATION OF FRICTION BETWEEN SOLID BODIES

In order to explain shearing strength, it will be of advantage to review some of the basic principles of friction between solid bodies.

Consider a body resting on a horizontal surface, Fig. 6.1. The body is in equilibrium under a total vertical force, P_n , and a reaction, P_r , which is equal and opposite to P_n . Suppose that a horizontal force, P'_h , as indicated in the figure is applied to the body. To resist P'_h , a frictional force, P'_f , developed as a result of a vertical force, P'_n , and roughness characteristics of the bottom of the body and supporting medium comes into play. P' is the resultant of P'_n and P'_f , and α is the angle of obliquity of the resultant. If now the applied horizontal force is gradually increased, the resisting force will likewise increase, being always equal in magnitude but opposite in direction to the applied force. The obliquity angle also increases at the same time. Finally, when the horizontal applied force $P'_h = P'_f$ and $\alpha = \phi$, slip becomes incipient.

Further increase in magnitude of the horizontal force, P_h , even though very small, will initiate slip. This movement or slippage is a shear failure. The applied horizontal force is a shearing force and the developed force is friction or shearing resistance. The maximum

shearing resistance which the materials are capable of developing is called the shearing strength.

The maximum value the resisting force can attain is given by

$$P_r = P_n \tan \phi = P_n f \tag{6.1}$$

Where

ϕ = angle of friction

f = coefficient of friction

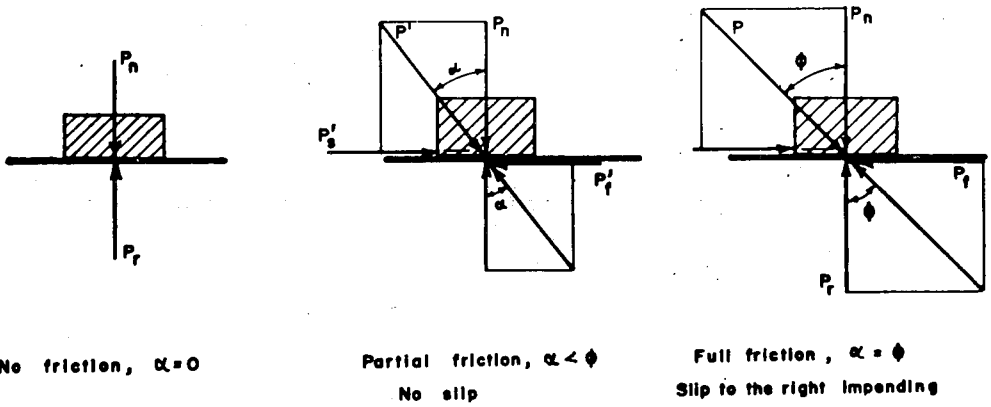


Fig. 6.1 Friction between solid bodies

6.3 SHEARING STRENGTH OF GRANULAR SOILS

The shearing strength of granular soils, such as clean sand, sand-gravel mixture etc, is closely similar to frictional resistance of solids in contact. In sands and in other cohesionless granular materials, however, the resistance to sliding on any plane through the material is made up of:

- (a) sliding friction, similar to the one discussed above.
- (b) rolling friction, resulting from changes of position by rolling
- (c) interlocking. (applies only to dense sand).

In geotechnical engineering, the expression for the force required to overcome frictional resistance and cause slip on a plane through a mass of granular soil is given by the following relationship.

$$P_s = P_n \tan \phi$$

$$s = P_s/A = (P_n/A) \tan \phi = \sigma \tan \phi \quad (6.2)$$

Where

- s = shearing strength
- σ = normal stress
- A = failure plane area
- ϕ = angle of internal friction

The angle of internal friction, ϕ , for granular soil depends very much upon density. The angle of internal friction for clean dry loose granular soil is sometimes taken as identical with the angle of repose of soil. The angle of repose is defined as the angle between the horizontal and the maximum slope at which a soil may remain stable (Fig. 6.2)

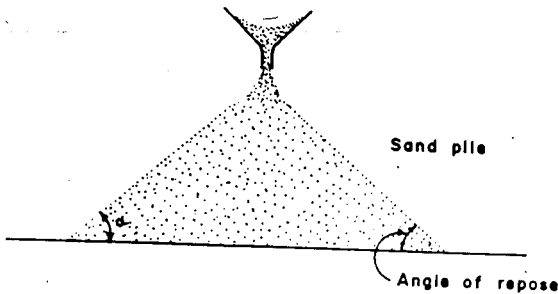


Fig. 6.2 Determination of angle of repose

6.4 SHEARING STRENGTH OF COHESIVE SOILS

A characteristic of true clays is the property of *cohesion*, sometimes referred to as no load shearing strength. Unconfined specimens of clay derive their strength and firmness from cohesion. Cohesionless soils are dependent for their strength upon normal loading.

The shearing strength of saturated cohesive clay soil in undrained shear test (i.e. test in which change in volume is prevented) is derived entirely from cohesion. In such a case, the shearing strength is independent of the magnitude of normal stress. However, in slow shear test, in which consolidation takes place, the shearing strength of clay increases with normal stress as indicated in Fig. 6.3.

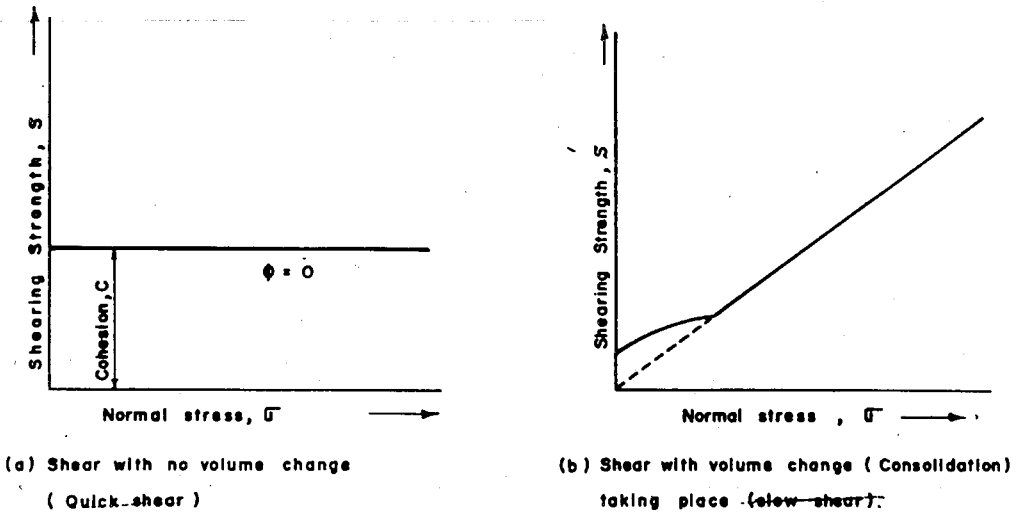


Fig. 6.3 Shearing strength versus normal stress

It is well known that the shearing strength of cohesive clay varies with its consistency. A clay which is at liquid limit has very little shearing strength, whereas the same clay at lower moisture content may have considerable shearing strength (Fig. 6.4.)

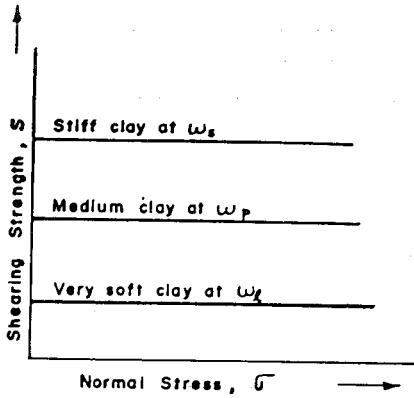


Fig. 6.4 Variation of cohesion with consistency

6.5 SHEARING STRENGTH OF SOILS WITH BOTH COHESION AND FRICTION

The shearing strength of soils with both cohesion and friction owe their strength both to cohesion and friction. Coulomb, many years ago, recognized that soils in general derive their strength from cohesion and friction. According to him the shearing strength may be expressed as follows:

$$s = c + \sigma \tan \phi \quad (6.3)$$

Where

s = unit shearing strength

c = unit cohesion

σ = normal stress

ϕ = angle of internal friction

The graphical representation of Eq.6.3 is given in Fig 6.5

6.6 SHEAR TESTS

The most common laboratory methods for conducting shear test are direct shear test, triaxial compression test and unconfined compression test.

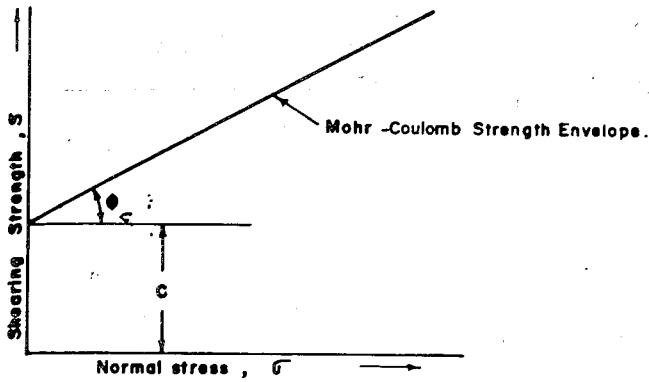


Fig. 6.5 Graphical representation of Coulomb's formula

6.6.1 Direct Shear Test

In the direct shear test there are two main procedures in the application of shear force. Viz: a) *Strain controlled* (strain increased at constant rate) and b) *Stress controlled* (stress increased at a constant rate) Basically, the direct shear machine has a shear box consisting of upper and lower frames (Fig.6.6.). One of the frame is movable while the other is fixed in place.

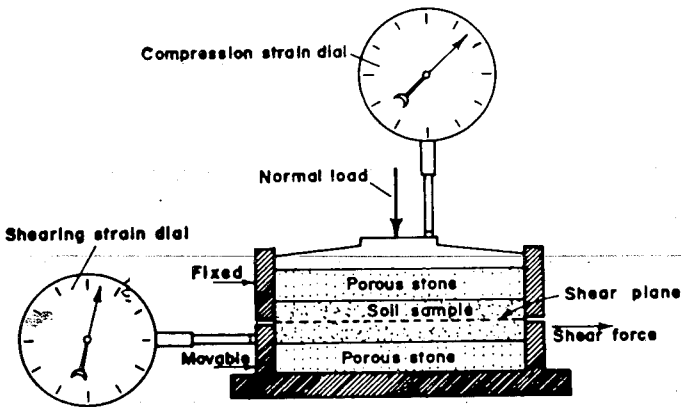


Fig. 6.6 Direct shear apparatus

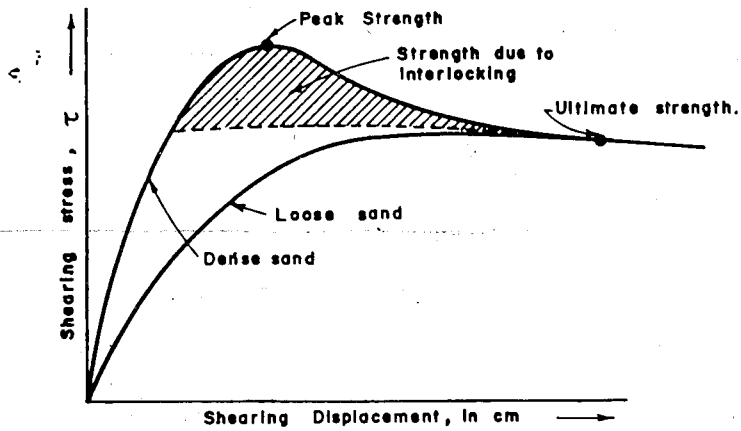
During testing, a soil sample is placed in a shear box and a known load is applied in the direction normal to the shear plane. Then a shearing force is applied parallel to the shear plane. The normal load is held constant while the shearing force is increased gradually. The first increments of shearing forces cause only slight movements or shearing strains but as the test progresses a point is reached where continuous displacements at virtually constant shearing force takes place. This is an indication of failure of the sample along the shear plane. The shearing force required to produce continuous movement is a measure of shearing strength of the specimen. Dividing the normal load and the maximum applied shear force by the cross-sectional area of the specimen at the shear plane gives the unit normal pressure and shear stress at failure respectively. The results of direct shear test is presented in a stress-strain diagram as shown in Fig. 6.7a. From a series of direct shear tests under different normal loads, a relation between normal stress and shear stress at failure as illustrated in Fig. 6.7b can be established.

6.6.2 Triaxial compression test

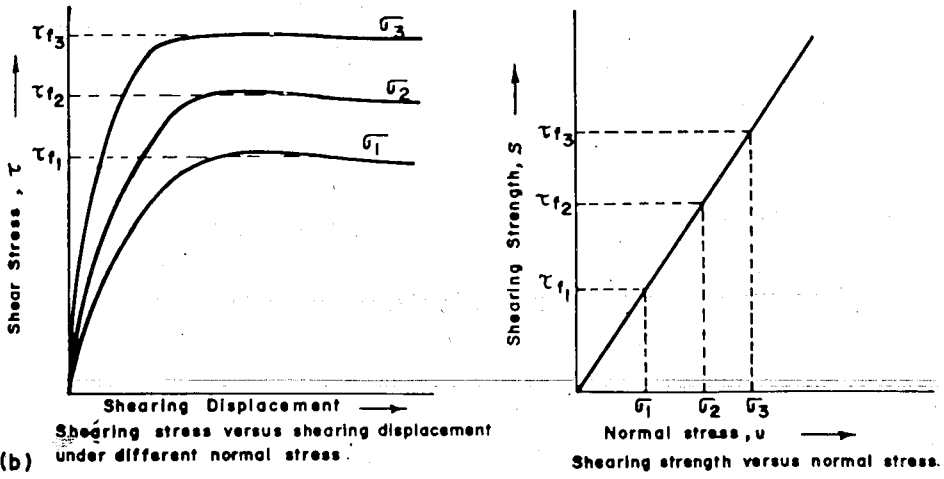
In contrast to direct shear test apparatus, the triaxial apparatus allows the testing of undisturbed soils and the measurement of pore water pressure. All the limitations of the direct shear apparatus are avoided with the triaxial testing. Drainage during shearing of saturated samples can easily be controlled with triaxial apparatus.

In this apparatus, a cylindrical soil sample is enclosed in a water tight cover and placed in a chamber which will later be filled with water under pressure (Fig. 6.8). The chamber pressure acts uniformly all around the specimen. An additional axial pressure is introduced till the sample fails. By means of valves, the pore water in the sample may be allowed to leave during deformation through the porous stones via the valves.

In the performance of a *slow* or a *consolidated-quick test*, the sample is allowed to consolidate completely under the all round chamber pressure $\sigma_2 = \sigma_3$. For the *slow test*, the valves remain open and the axial stress is applied slowly so that the pore water will have adequate time to dissipate. In the *consolidated-quick test*, after the sample has consolidated completely, the valves are closed so as to prevent the change of moisture content while the axial load is applied.



(a)



(b)

Fig. 6.7 Typical direct shear test results for cohesionless material

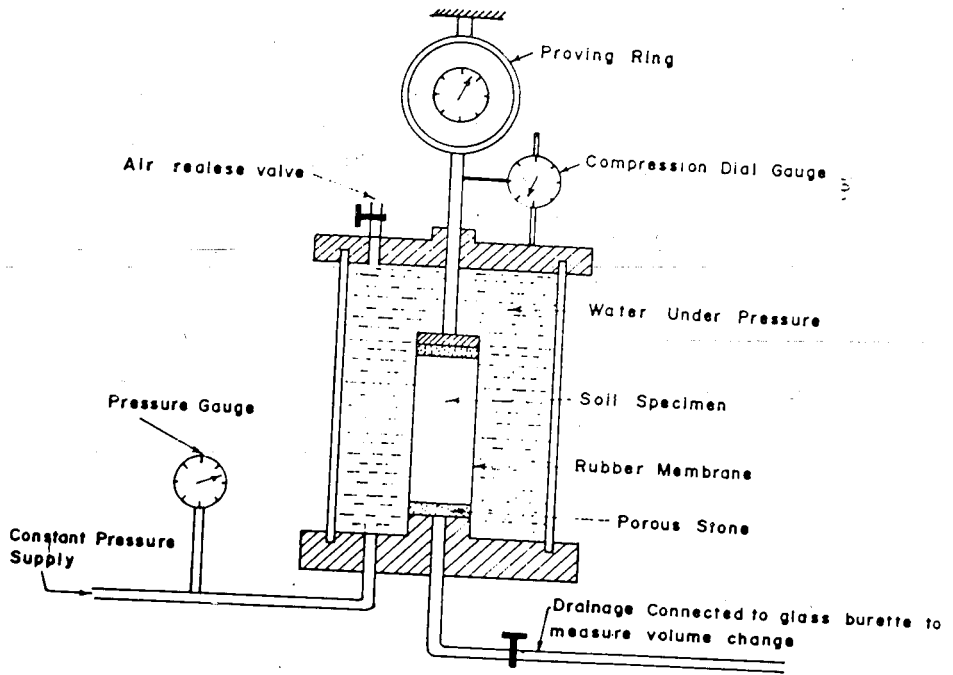


Fig. 6.8 Triaxial apparatus

On examining the stress conditions of the soil sample, we find that the chamber pressure stands for minor principal stress designated by σ_3 . The intensity of incremental axial stress plus chamber pressure represent the major principal stress indicated by σ_1 . (For stress analysis read discussions on Mohr stress circle).

For proper graphical presentation of the laboratory data, the following procedure for calculating the necessary parameter for each test is followed (Fig 6.9)

$$\sigma_1 = \Delta\sigma + \sigma_3 = \frac{P}{A} + \sigma_3 \quad (6.4)$$

P is increased continuously until failure occurs. But σ_3 is always kept constant for a given test. As P is increased there will be a change in volume and this is reflected by a change in length. The cross-sectional area of the sample also changes.

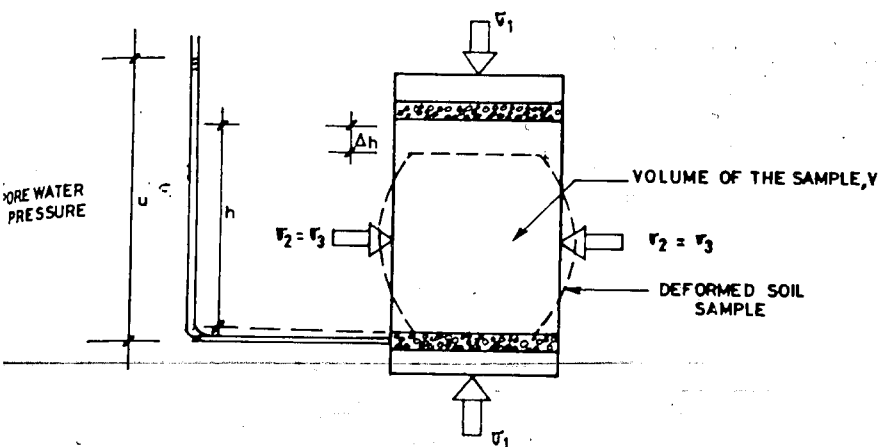


Fig. 6.9 Stresses in triaxial testing

Average cross-sectional area,

$$A = \frac{A_o}{1 - \frac{\Delta L}{L_o}} \tag{6.5}$$

Where

L_o = original length

A_o = cross-sectional area of the specimen before the start of the experiment.

The results of triaxial compression tests are given graphically as shown in Fig 6.10

6.6.3 Unconfined compression test

In unconfined compression test, the sides of the soil sample are not acted on by the lateral pressure σ_3 . The axial load is gradually increased until the sample fails (Fig. 6.11). The value of σ_1 which causes failure is called the *unconfined compressive strength* and is designated by q_u (Fig 6.11).

The stress-strain curve also provides the elasticity modulus, E . The test result of unconfined compression may be represented using Mohr diagram (Fig.6.11).

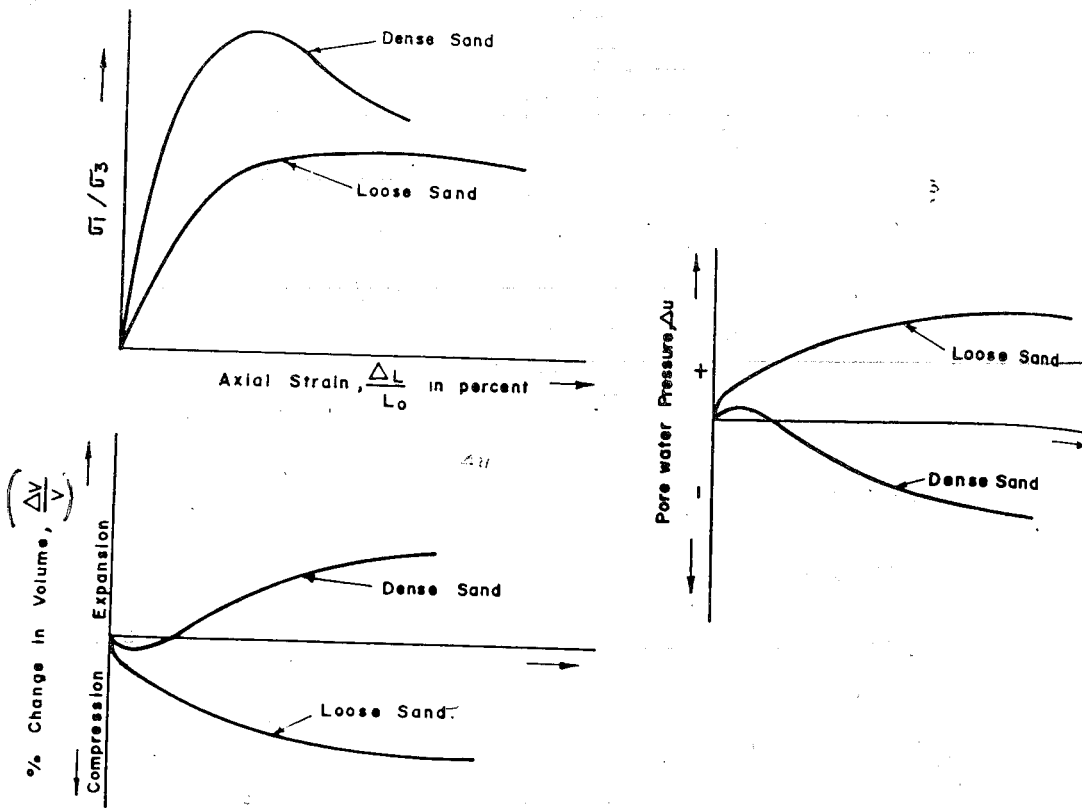


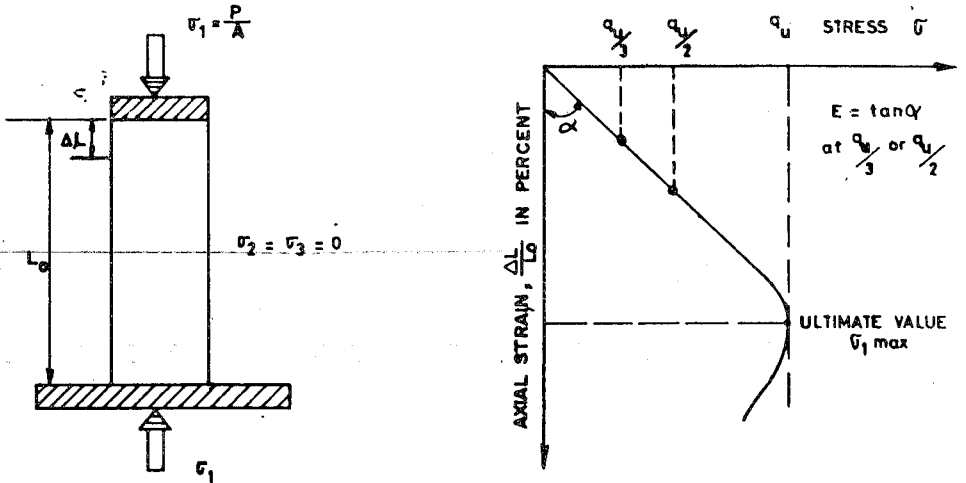
Fig. 6.10 Stress versus strain and volume change versus strain

6.7 SHEAR CHARACTERISTICS OF GRANULAR SOILS

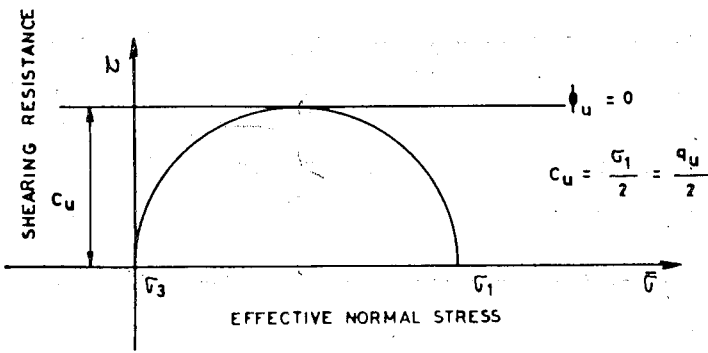
In sands, all shear strength is due either to friction and/or interlocking. The latter phenomenon contributes strength only in dense sands.

6.7.1 Angle of Internal Friction

As noted earlier, an approximate estimate of the angle of internal friction of loose sands is obtained by measuring the angle of repose. The proper method of determining the angle of internal friction of sands is by conducting direct shear test or by triaxial shear test.



(a)



(b)

Fig. 6.11 Unconfined compression test results

The angle of internal friction of sands depends on shape, gradation and mineralogical characteristics of the grains.

6.7.2 Saturated Granular Soil

The shearing strength of sand in saturated condition is generally less than the shearing strength of the same sand in dry condition. This is because the normal pressure is affected by pore pressure (i.e. the effective pressure, or the intergranular pressure is reduced).

$$s = (\sigma - u) \tan \phi = \bar{\sigma} \tan \phi \quad (6.6)$$

Where

σ = applied normal pressure

$\bar{\sigma}$ = effective normal pressure

u = pore pressure

* Loose sands tend to undergo decrease in volume during shearing but this is prevented by water in the pores, resulting in reduced effective normal pressure between grains and corresponding reduction in shear strength. The reduction in strength may sometimes be of such magnitude as to cause partial *liquefaction* (or cause the sand to behave almost as a liquid). Fine loose deposit of sand below a water table may display such a liquefaction when subjected to sudden shear force as for example by an earthquake shock, or a blasting shock.

In the case of dense sands the reverse is true. Dense sands when subjected to shear stress usually tend to expand. This expansion of soil under shear is called *dilatancy*. If this expansion is prevented by preventing drainage in a laboratory specimen or by sudden application of stress in the field, tensile stresses are thrown into the pore water. This results in increased effective normal stress and consequently in greater shearing strength.

As noted above, dense sands attain greater strength when volume changes are prevented during shear and loose sands lose strength. In between the dense and loose state, there is a density at which prevention of volume change results in no change in strength. The void ratio corresponding to this density is called *critical void ratio*, defined as void ratio at which prevention of volume change leads to no strength change.

6.8 SHEAR CHARACTERISTICS OF CLAYS

Clays are divided into two types, namely, the *normally loaded clays* and the *pre-compressed clays*.

6.8.1 Normally Loaded Clays

The strength of normally loaded clays are affected by remoulding. The shear strength of normally loaded clays in natural state exhibit higher strength than clays in remoulded state. If a saturated remoulded clay is allowed to stand for any length of time at a constant moisture content, it regains a considerable portion of its strength. The phenomenon responsible for gain of strength is called *thixotropy*.

The effect of remoulding is more pronounced in some clays than in others. This effect is measured in terms of sensitivity of the clay, designated by S_t .

Sensitivity for most clays ranges between 2 and 4 and for sensitive clays between 4 and 8

$$S_t = \frac{\text{cohesion of an undisturbed sample}}{\text{cohesion of a remoulded sample}}$$

$$= \frac{\text{unconfined compressive strength of undisturbed sample}}{\text{unconfined compressive strength of remoulded sample}}$$

6.8.2 Pre-Compressed Clays

Pre-compressed clays exhibit greater strength than normally loaded clays because of over-consolidation pressure. Because of pre-consolidation pressure, it has lower void ratio, a lower water content and hence, a higher shearing strength.

6.9 STRESS AT A POINT

6.9.1 General

Through every point in a stressed body there are three planes at right angles to each other which are acted upon by normal stresses with no accompanying shearing stress. These three planes are called *principal planes* and the normal stresses acting on them are called *principal stresses*.

Depending upon the magnitude of principal stresses acting on them, the three planes are known as *major*, *intermediate* and *minor principal planes*.

The three principal stresses acting at a point in a stressed medium differ in magnitude. They are designated as major principal stress σ_1 (acting on major principal plane) intermediate principal stress σ_2 (acting on intermediate plane) and minor principal stress σ_3 (acting on minor principal plane). The major and minor principal stresses represent the maximum and minimum normal stresses at a point respectively. They are important because once they are determined the stresses on any other plane through the point can be evaluated.

6.9.2 Derivation

Consider point A in a body acted upon by a system of forces (Fig. 6.12a). Take a small element ABCD located within a body oriented in such a way that AB is the major principal plane, and BC is the minor principal plane. The stresses acting on this body are shown in Fig 6.12b.

Let plane BE pass through the element such that it makes angle θ with the major principal plane. Consider the free body diagram shown in Fig 6.12c. The stresses acting on plane BE are normal stress σ , and shearing stress, τ .

$$\begin{aligned} \text{Let} \quad AB &= 1 \\ AE &= 1 \tan \theta = \tan \theta \end{aligned}$$

$$\text{Total stress on AB} = \sigma_1$$

$$\text{Total stress on AE} = \sigma_3 \tan \theta$$

$$BE \cos \theta = 1$$

$$BE = \frac{1}{\cos \theta} = \sec \theta$$

Summing up

$$\sigma \sec \theta = \sigma_1 \cos \theta + \sigma_3 \tan \theta \sin \theta$$

$$\sigma = \sigma_1 \cos^2 \theta + \sigma_3 \sin^2 \theta$$

(6.7)

$$\tau \sec \theta = \sigma_1 \sin \theta - \sigma_3 \sin \theta$$

$$\tau = \sigma_1 \sin \theta \cos \theta - \sigma_3 \sin \theta \cos \theta$$

$$= (\sigma_1 - \sigma_3) \sin \theta \cos \theta$$

(6.8)

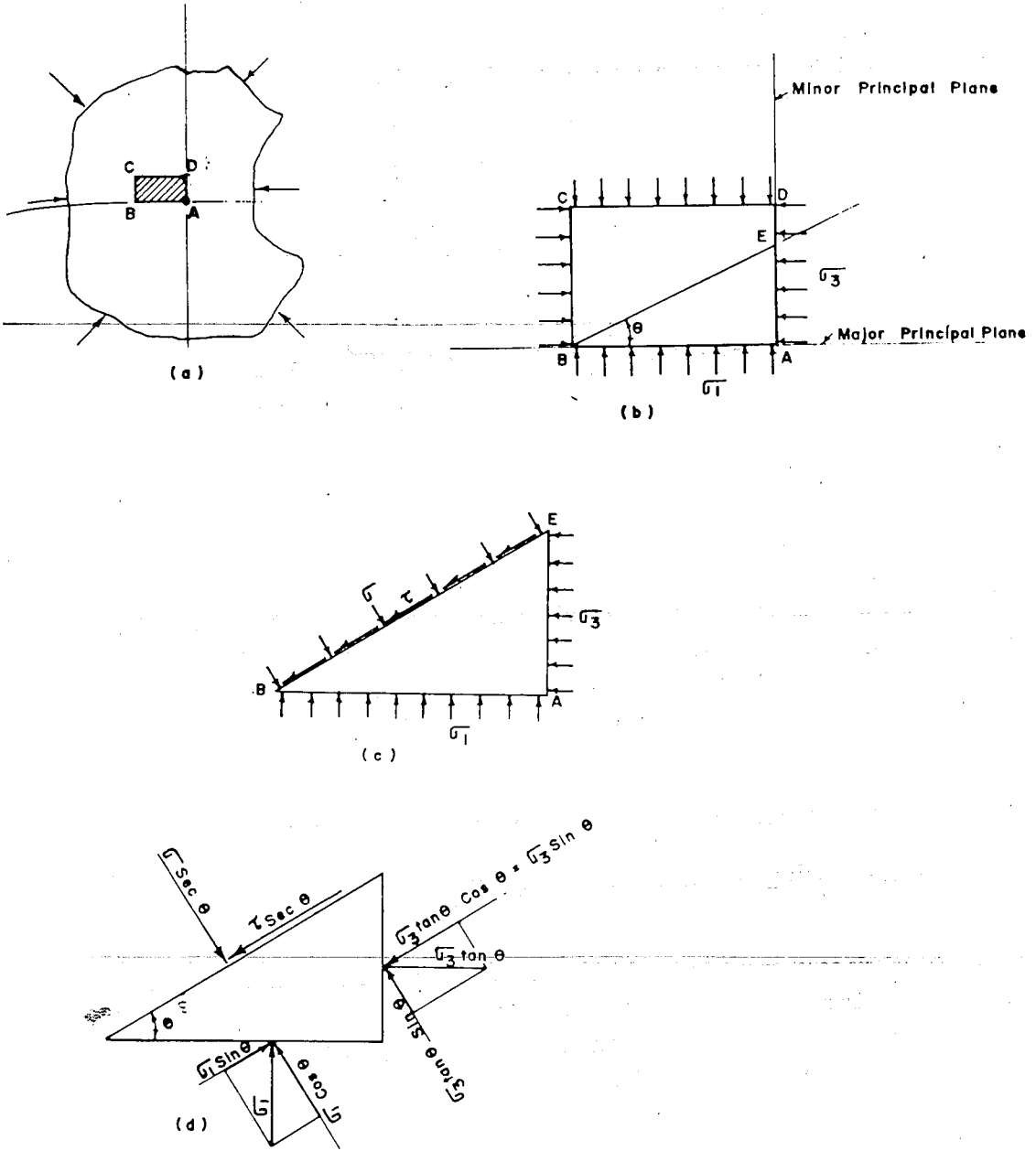


Fig. 6.12 Stress at a point

$$\cos^2\theta = \frac{1 + \cos 2\theta}{2}$$

Eq (6.7) and (6.8) may also be expressed as indicated below:

$$\begin{aligned}\sigma &= \sigma_1 \left(\frac{1 + \cos 2\theta}{2} \right) + \sigma_3 \left(1 - \frac{1 + \cos 2\theta}{2} \right) \\ &= \sigma_1 \left(\frac{1 + \cos 2\theta}{2} \right) + \sigma_3 - \sigma_3 \left(\frac{1 + \cos 2\theta}{2} \right) \\ &= (\sigma_1 - \sigma_3) \left(\frac{1 + \cos 2\theta}{2} \right) + \sigma_3 = (\sigma_1 - \sigma_3) \cos^2\theta + \sigma_3\end{aligned}\quad (6.9)$$

$$\tau = (\sigma_1 - \sigma_3) \sin\theta \cos\theta \quad (6.10)$$

6.9.3 Mohr Circle

Elimination of the angle θ from the two equations shown above leads to the following relationship.

$$\tau^2 + \left[\sigma - \left(\frac{\sigma_1 + \sigma_3}{2} \right) \right]^2 = \left(\frac{\sigma_1 - \sigma_3}{2} \right)^2 \quad (6.11)$$

This equation is the equation of a circle whose center has the co-ordinates

$$\tau = 0 \text{ and } \sigma = \left(\frac{\sigma_1 + \sigma_3}{2} \right) \text{ and whose radius is } \left(\frac{\sigma_1 - \sigma_3}{2} \right)$$

A plot of this equation is known as Mohr circle. Stress at any given point may be represented in a Mohr diagram according to the following procedures.

- (a) Two co-ordinate axes are first drawn. The origin for these co-ordinate axes is the origin of stress O_s .
- (b) Stresses are represented on these co-ordinates by vectors drawn to scale.

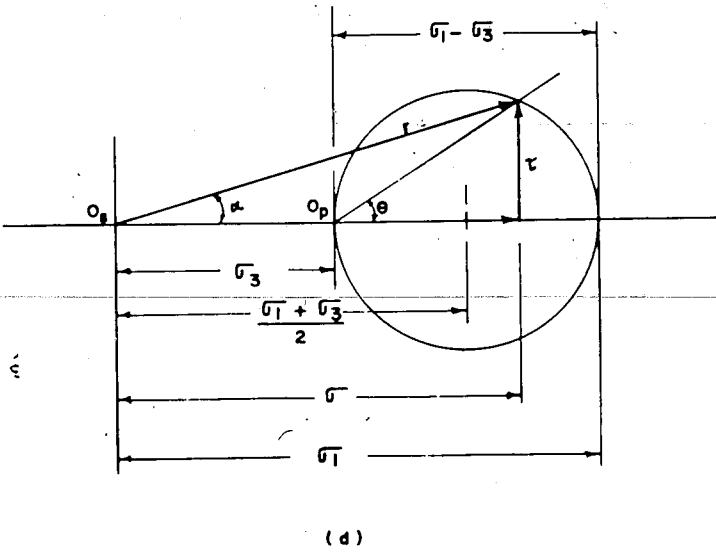
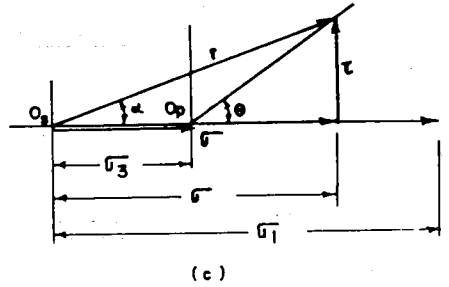
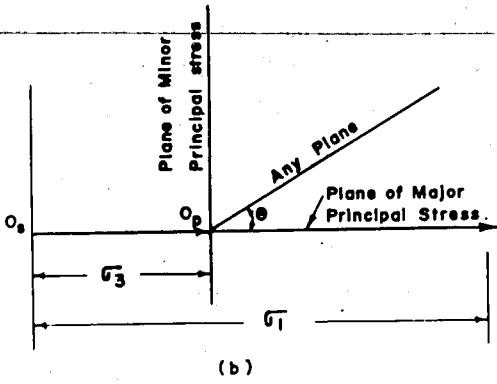
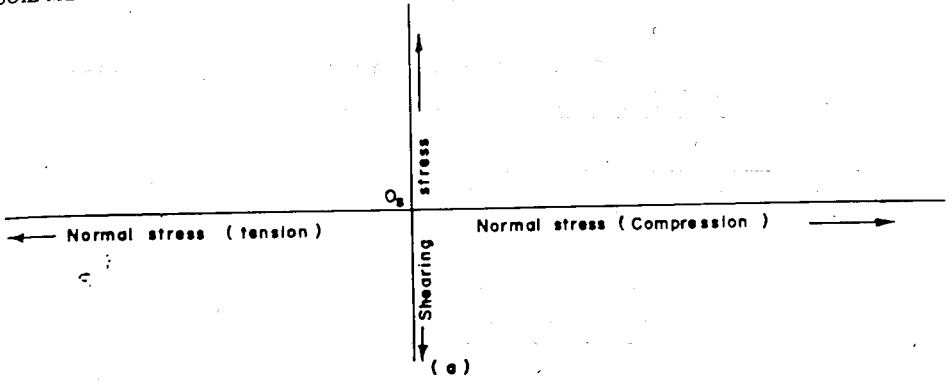


Fig. 6.13 Steps in drawing Mohr stress circle.

- (c) Normal stresses are represented by vector drawn in horizontal direction from O_s (Fig. 6.13a).
- (d) Shearing stresses (tangential stresses) are represented by vectors drawn in vertical direction from the end of normal stress vectors.
- (e) A second origin of co-ordinates known as origin of plane is introduced. This is designated by O_p (Fig.6.13b).
- (f) Values of the normal and shearing stress on a plane inclined at θ degree with the horizontal are plotted as indicated in (Fig. 6.13c). The shearing stress as noted earlier is drawn not from the origin of stress but vertically from the end of the normal stress.
- (g) A line drawn from the origin of stress to the tip of the shearing stress will indicate the resultant stress, r , on the plane inclined at angle θ . The resultant stress is inclined at angle α with the normal stress. This angle is known as angle of obliquity of the resultant.
- (h) If the same construction is done for all planes inclined at all possible values of θ , it will be seen that, for given values of σ_3 and σ_1 , the ends of vectors representing shearing stresses on inclined planes will lie in a circle as shown in Fig.6.13d. This is what is called the Mohr stress circle. The diameter of the circle as already indicated on the sketch equals $(\sigma_1 - \sigma_3)$ and this is sometimes termed *deviator stress*.

For the case when the major principal plane is in the horizontal direction and minor principal plane is in the vertical direction, O_p lies on the σ -axis.

6.9.4 Mohr Strength Theory

On any plane the shearing stress may be expressed as $\tau = \sigma \tan \alpha$. The shearing strength s , for cohesionless soil for condition $\alpha_m = \phi$ is given by $s = \sigma \tan \phi$. It is assumed that the value of friction angle is constant and the effect of intermediate stress on the strength of soil is negligible. In the study of strength of soils, it must be noted that while Mohr strength

envelopes depend on the property of the soil being considered, the Mohr circle is independent of the nature of the medium, but depends on the state of stress at a point.

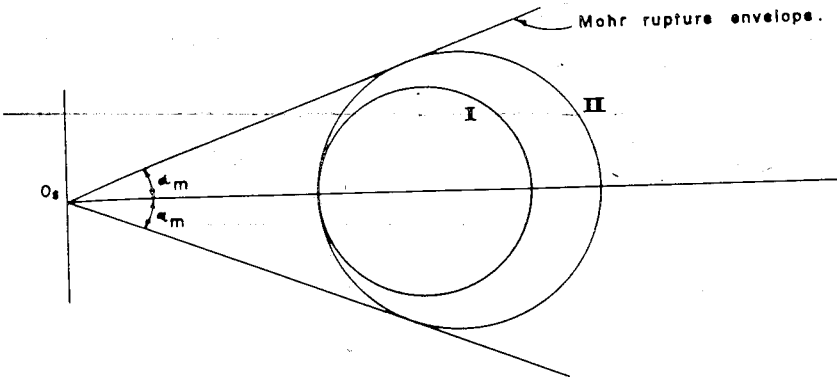


Fig. 6.14 Mohr circle representing stable and unstable conditions

Circle I shown in Fig. 6.14 represents the state of stress when obliquity on any plane is smaller than maximum obliquity a soil mass can have (i.e. $\alpha < \phi$). The soil mass in such a condition is in elastic state.

When the stress condition is such that the Mohr stress circle touches the Mohr strength envelope as circle II does, the soil is in a plastic state indicating that the soil is on the verge of failure ($\alpha_m = \phi$).

6.9.5 Relationships Derived From Mohr Strength Theory

The following relationships may be derived from Mohr strength theory (Fig 6.15).

- a. Maximum shearing stress also called principal shearing stress = $\frac{1}{2}(\sigma_1 - \sigma_3)$ = radius of Mohr circle. It occurs on a plane inclined at 45° as shown in Fig. 6.15a.

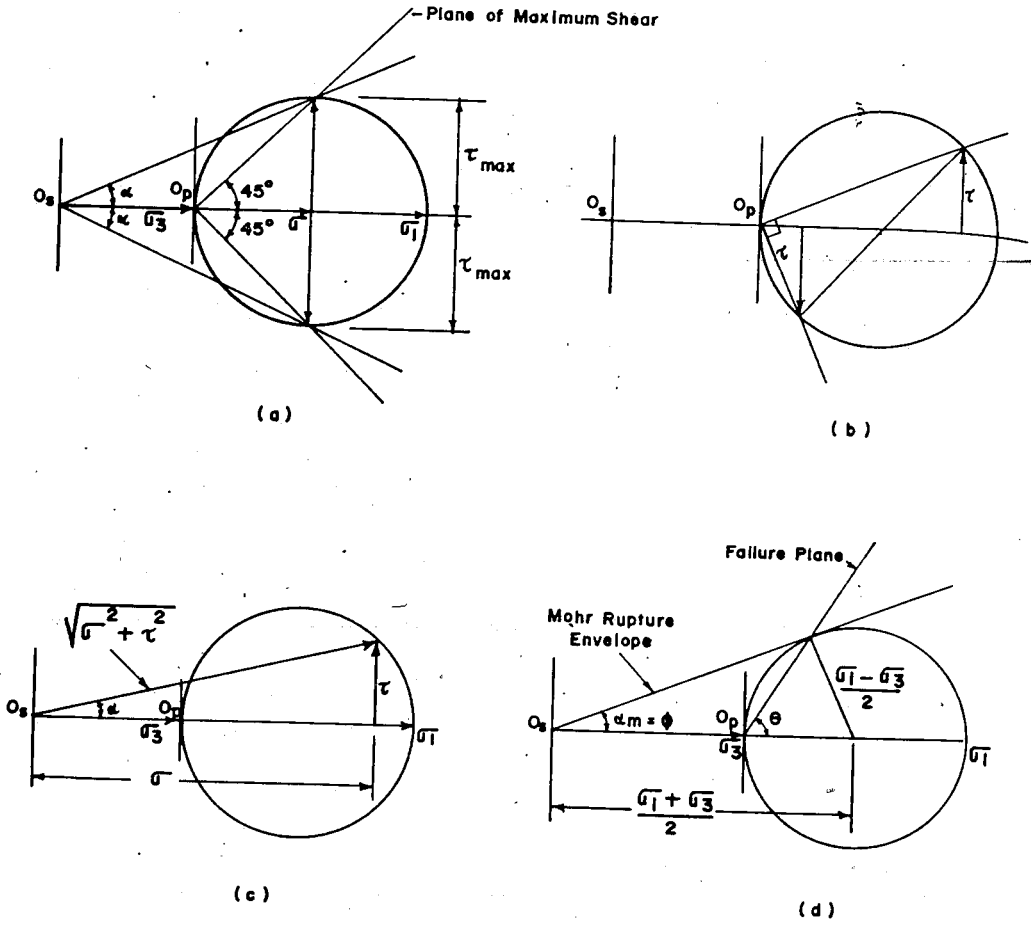


Fig. 6.15 Relationships evident from Mohr stress circle

- b. Shearing stress on planes inclined at 90° to each other are numerically equal but opposite in sign. These are called conjugate shearing stresses (Fig. 6.25b)

- c. The magnitude of the resultant stress on any plane = $(\sigma^2 + \tau^2)^{1/2}$ and its obliquity $\alpha = \text{arc tan } \tau/\sigma$ as indicated in Fig. 6.15 c
- d. The maximum value of obliquity angle is α_m . This can be determined by drawing a tangent to the circle as shown in Fig. 6.15d. This is done when failure is likely to occur, i.e. when $\alpha_m = \phi$. The coordinates of the point of tangency are the stresses on the plane of maximum obliquity.

As seen above, the shearing stress on the plane of maximum obliquity is less than the maximum shearing stress. The obliquity in the case of maximum shearing stress is less than that of maximum obliquity. Since the condition of failure is maximum obliquity, it is on the plane of maximum obliquity and not on the plane of maximum shear which the soil is most liable to fail.

Important relationships can be derived from Mohr diagram representing failure (Fig. 6.15d)

$$(a) \quad \sin \alpha_m = \sin \phi = \frac{\sigma_1 - \sigma_3}{\sigma_1 + \sigma_3}$$

$$\frac{\sigma_1}{\sigma_3} = \frac{1 + \sin \phi}{1 - \sin \phi} \quad (6.12)$$

$$(b) \quad \text{Failure plane, } \theta = 45 + 1/2 \alpha_m = 45 + 1/2 \phi \quad (6.13)$$

6.10 APPLICATION OF MOHR DIAGRAM TO CONVENTIONAL SHEAR TESTS

6.10.1 Triaxial Compression Test

A Mohr circle may be drawn to show the stress conditions at any time during a cylindrical compression test. During a conventional test at constant σ_3 , the value of σ_1 increases.

Thus the radius of the Mohr circle increases until it attains a maximum value as indicated in Fig 6.16.

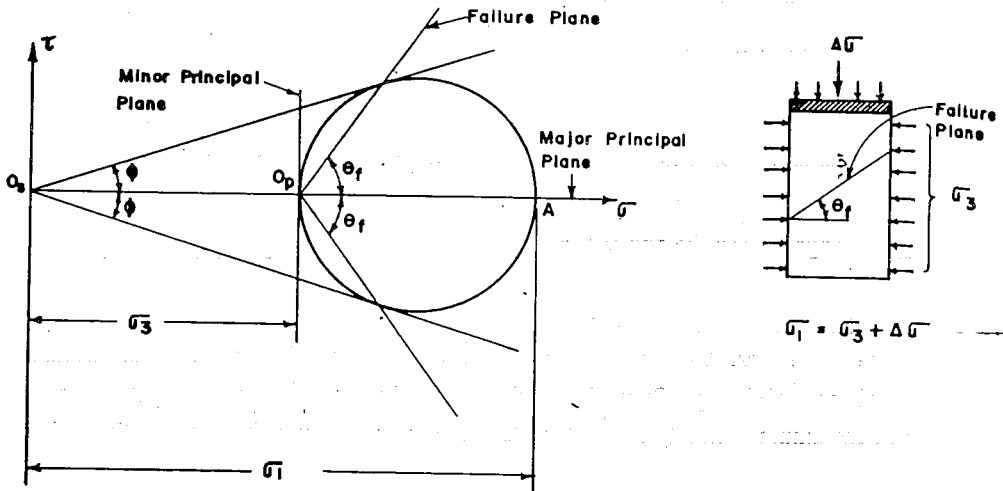


Fig. 6.16 Mohr diagram for cylindrical compression test at failure

In a triaxial test, the major principal plane is horizontal and the minor principal plane is vertical as shown above. By definition the shear stress on these planes is zero. Thus point A represents state of stress on the major principal plane. A line drawn perpendicular to the major principal plane cuts the circle at O_p which is the origin of the planes. The failure plane is at angle θ_f to the horizontal. It may be noted that this angle at times is approximately the same as the angle of slip on the sample.

6.10.2 Direct Shear Test

The values of the stress τ and σ , which act at the time of failure on the failure plane in a direct shear test, may be plotted on a Mohr diagram to give point A as indicated in Fig. 6.17. Assuming that the Mohr envelope is a straight line through the origin of stress, it can be said that the maximum obliquity occurs on the failure plane. Thus the line from the origin to A must be tangent to the Mohr circle and the circle may be constructed on this basis. Since failure is on the horizontal plane, the origin of the planes is obtained by drawing a horizontal line through A giving O_p .

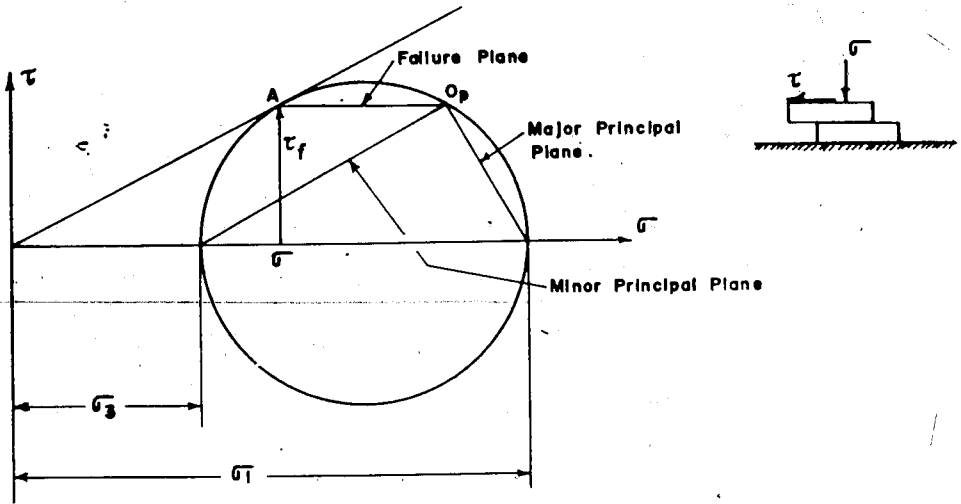


Fig. 6.17 Mohr diagram for direct shear test at failure

6.10.3 Unconfined Compression Test

The Mohr diagram representing unconfined compression test is shown in Fig 6.18.

6.10.4 Drainage During Shear

The shear strength of saturated soils is influenced by drainage conditions before and during shear. Hence, shear tests have been devised to measure strength of soils under three different drainage conditions.

6.10.4.1 Consolidated-Undrained or Consolidated Quick Test (CU-Tests)

In this case the soil is first consolidated under the applied lateral loads. After consolidation is complete, the soil is subjected to shear with no drainage allowed to take place.

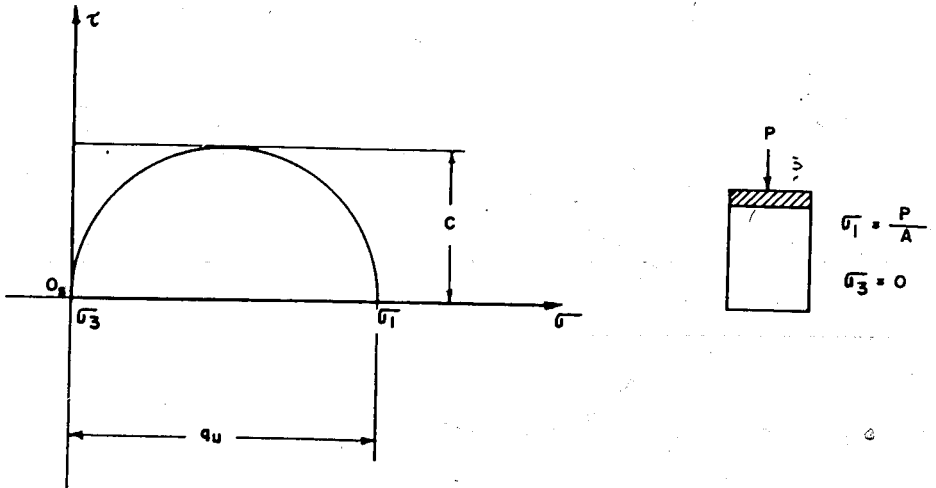


Fig. 6.18 Mohr diagram for unconfined compression test at failure

Thus volume change during shear is not possible and this may lead to development of pore pressure during shear. The test result may be expressed in terms of total or effective stress as indicated below:

Consolidating pressure (lateral pressure) = σ_3

Incremental axial pressure = $\Delta\sigma$

Total axial pressure, $\sigma_1 = \sigma_3 + \Delta\sigma$

Since no drainage is allowed, $\Delta\sigma = \Delta u$

As water acts in all directions, Δu acts in the direction of both σ_3 and σ_1 .

Hence, the effective stress at failure is given by

$$\sigma_1' = \sigma_1 - \Delta u = \sigma_3 + \Delta\sigma - \Delta\sigma = \sigma_3$$

$$\sigma_3' = \sigma_3 - \Delta u = \sigma_3 - \Delta\sigma$$

A Mohr diagram is plotted with these data as shown in Fig. 6.19



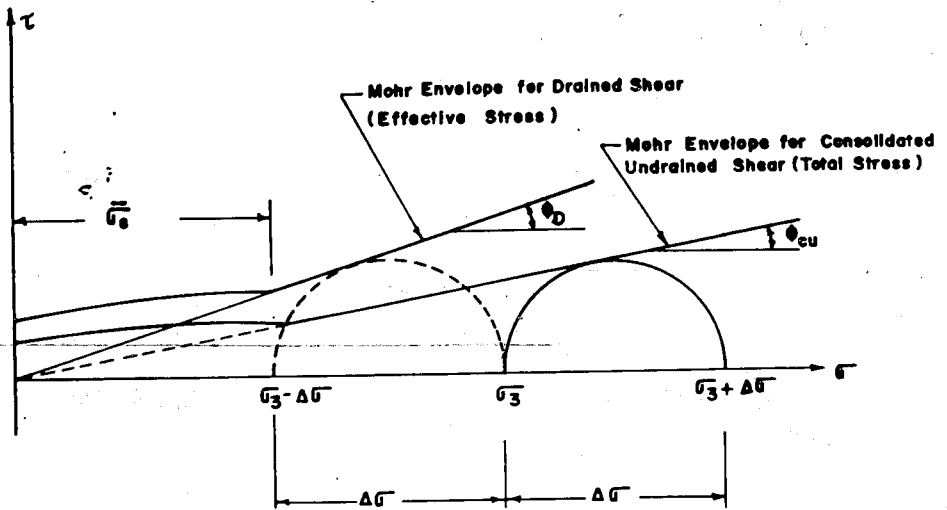


Fig. 6.19 Mohr diagram for consolidated drained and undrained shear test on precompressed clay

The test results of consolidated quick test can also be presented by stress-path method as shown in Fig. 6.20.

6.10.4.2 Unconsolidated-Undrained Test or Quick Test (UU-Test)

In this test no drainage is permitted during the application of lateral loads to the soil sample and during shearing operation. Since no pore water can escape, a pore water pressure is set up which may be measured during the test. The shear strength may be expressed in terms of total stress, or effective stress as indicated below. Let the initial overburden pressure under which the soil was consolidated = $\bar{\sigma}_c$.

Initially, $\sigma_1 = \bar{\sigma}_c$ and $\sigma_3 = \bar{\sigma}_c$

In terms of effective stress $\sigma_1' = \bar{\sigma}_c$ and $\sigma_3' = \bar{\sigma}_c$

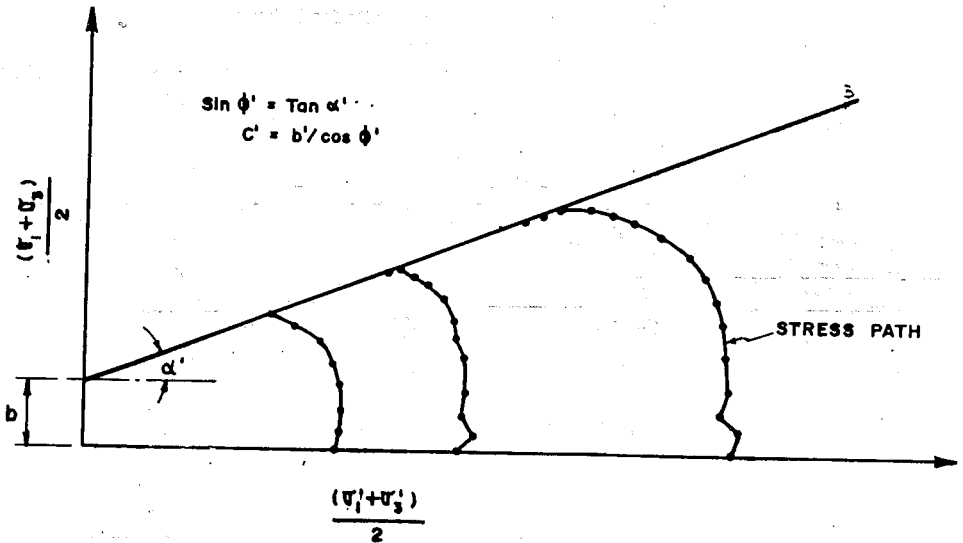


Fig. 6.20 Consolidated quick test with pore pressure measurement (CU-Test)

As no drainage is allowed, an increment of lateral pressure, $\Delta \sigma_3$, will be supported by water, that is $\Delta \sigma_3 = \Delta u_1$. Hence, total stress, $\sigma_1 = \bar{\sigma}_c + \Delta \sigma_3 = \bar{\sigma}_c + \Delta u_1$ and $\sigma_3 = \bar{\sigma}_c + \Delta \sigma_3 = \bar{\sigma}_c + \Delta u_1$

When an increment axial stress, $\Delta \sigma$, is added, the additional neutral stress would be Δu_2 . The total neutral stress now becomes $u = \Delta u_1 + \Delta u_2 = \Delta \sigma_3 + \Delta \sigma$. The total stress becomes

$$\sigma_1 = \bar{\sigma}_c + u = \bar{\sigma}_c + \Delta \sigma_3 + \Delta \sigma \text{ and } \sigma_3 = \bar{\sigma}_c + \Delta \sigma_3$$

The effective stress,

$$\sigma_1' = \sigma_1 - u = \bar{\sigma}_c + \Delta \sigma_3 + \Delta \sigma - (\Delta \sigma_3 + \Delta \sigma) = \bar{\sigma}_c \text{ and } \sigma_3' = \sigma_3 - u = \bar{\sigma}_c + \Delta \sigma_3 - (\Delta \sigma_3 + \Delta \sigma) = \bar{\sigma}_c - \Delta \sigma$$

A Mohr diagram using the above data is plotted as shown in Fig.6.21.

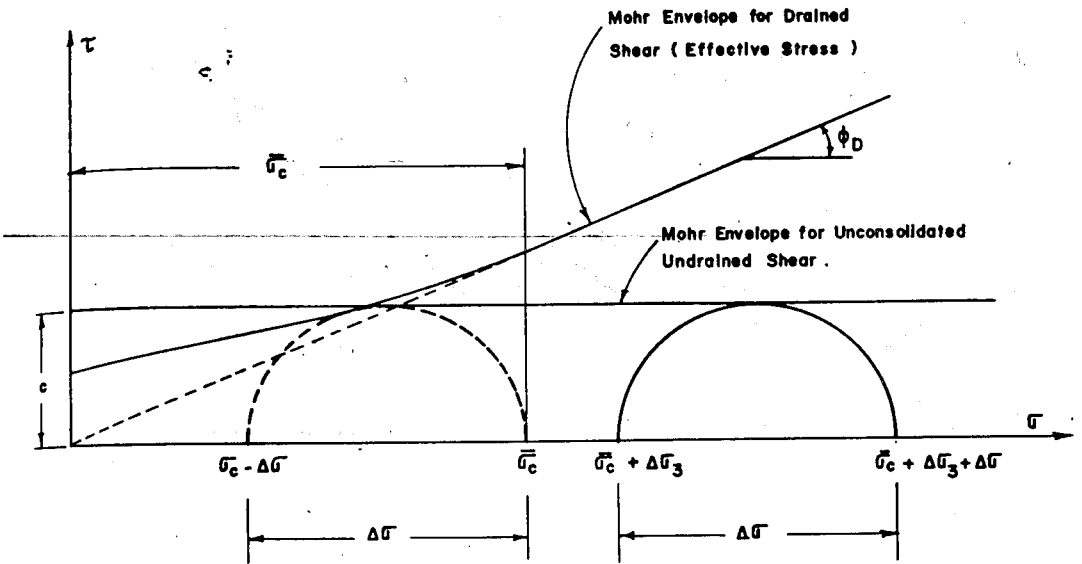


Fig. 6.21 Mohr diagram for undrained unconsolidated test

6.10.4.3 Drained or Slow Test (D-Test)

Full consolidation is allowed under lateral loads. During shear also free drainage is allowed. Under this condition there is no pore pressure build-up. All stresses are intergranular (See Fig. 6.19).

The test results of slow test can also be presented by means of stress path as shown in Fig. 6.22.

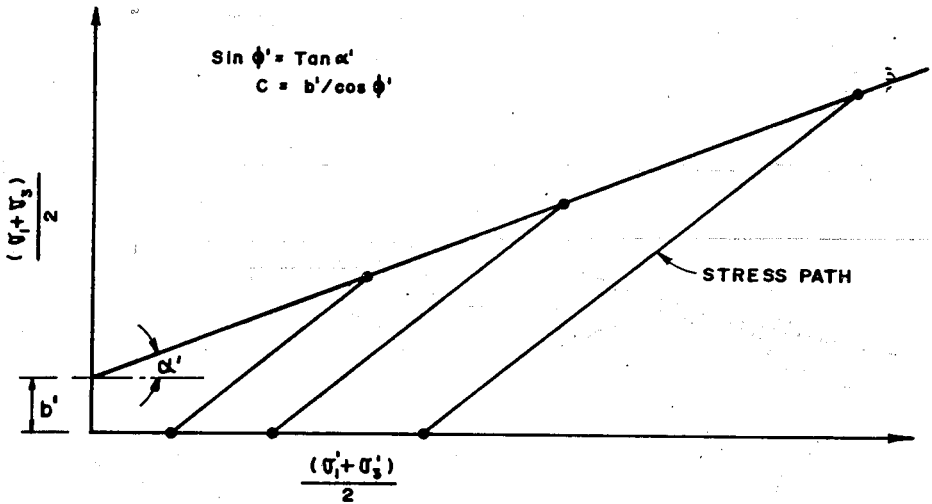


Fig. 6.22 Slow test (D-Test)

6.11 EXAMPLES

E.6.1 In a triaxial test the following data were recorded.

$\Delta L = 0.04 \text{ cm}$

$\sigma = 200 \text{ kPa}$

$P = \text{incremental load} = 0.8 \text{ kN}$

If the original length of the sample is 16 cm and its initial area = 40 sq. cm., determine the vertical stress (axial stress) and axial strain.

SOLUTION

$$A_o = \frac{40}{(100)^2}$$

$$A = \frac{A_o}{1 - \frac{\Delta L}{L_o}} = \frac{40}{1 - \frac{.04}{16}} = \left[\frac{40}{(100)^2} \right] \left[\frac{1}{0.0075} \right]$$

$$A = \frac{40}{9975}$$

$$\Delta \sigma = \frac{P}{A} = \frac{0.8}{\frac{40}{9975}} = \frac{(0.8)(9975)}{40} = 199.5 \text{ kN/m}^2$$

$$\sigma_1 = \Delta \sigma + \sigma_3 = 199.5 + 200 = 399.5 \text{ kN/m}^2$$

$$\epsilon = \frac{\Delta L}{L_o} (100) = \frac{.04}{16} (100) = \frac{4}{16} = 0.25 \%$$

E.6.2 In unconfined compression test on soft clay the following data was observed.

Length of the sample	= 10 cm
Initial area	= 10cm ²
Load at failure	= 0.20kN
Compression of the sample at failure	= 2cm.

Determine the unconfined compressive strength and shear strength.

SOLUTION

$$A = \frac{A_o}{1 - \epsilon} = \frac{10}{1 - \frac{2}{10}} = 0.00125 \text{ m}^2$$

$$q_u = \frac{12.5}{(100)^2} \frac{2000}{12.5} = 160 \text{ kN/m}^2$$

$$s = c = \frac{q_u}{2} = \frac{160}{2} = 80 \text{ kN/m}^2$$

- E.6.3 The major and minor principal stresses at a point are 450 kN/m^2 and 20 kN/m^2 respectively.
- What is the value of the maximum shearing stress?
 - What is the value of the normal stress on the plane of the maximum shearing stress?
 - What is the value of the maximum resultant stress on a plane at angle of 27° with plane of minor principal stress?

SOLUTION

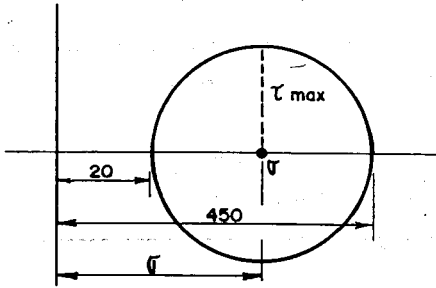


Fig.E.6.1 Mohr diagram

$$(a) \tau_{\max} = \frac{450 - 20}{2} = \frac{430}{2} = 215 \text{ kN/m}^2$$

Maximum shearing stress = 215 kN/m^2

$$(b) \sigma = 20 + \frac{450 - 20}{2} = 215 + 20 = 235 \text{ kN/m}^2$$

Normal stress on the plane of maximum shearing stress = 235 kN/m^2

$$BCA = 90 - 27 = 63^\circ$$

$$\therefore BAD = 63 \times 2 = 126^\circ ; BAC = 180 - 126 = 54^\circ$$

$$BE = \tau = AB \sin 54^\circ = 215 \sin 54^\circ = 174 \text{ kN/m}^2$$

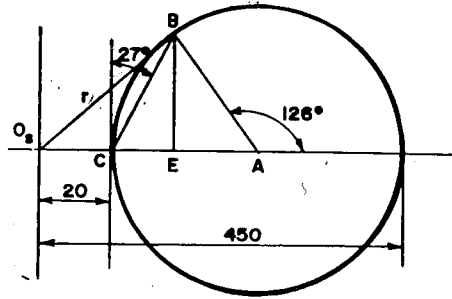
$$AE = AB \cos 54^\circ = 215 \cos 54^\circ = 126 \text{ kN/m}^2$$

$$O_s E = \sigma = 20 + (215 - 126) = 109 \text{ kN/m}^2$$

$$r = \sqrt{\tau^2 + \sigma^2} = \sqrt{174^2 + 109^2}$$

$$= \sqrt{30276 + 11881} = 205.3 \text{ kN/m}^2$$

Maximum resultant stress = 205.3 kN/m²



E.6.4

A certain sand sample is just at the point of failure in triaxial shear test. The major and minor principal stress are 400 kN/m² and 100 kN/m² respectively. Draw the Mohr diagram and determine the normal and shearing stresses and obliquity angles on the plane of maximum shear and on the plane of maximum obliquity.

SOLUTION

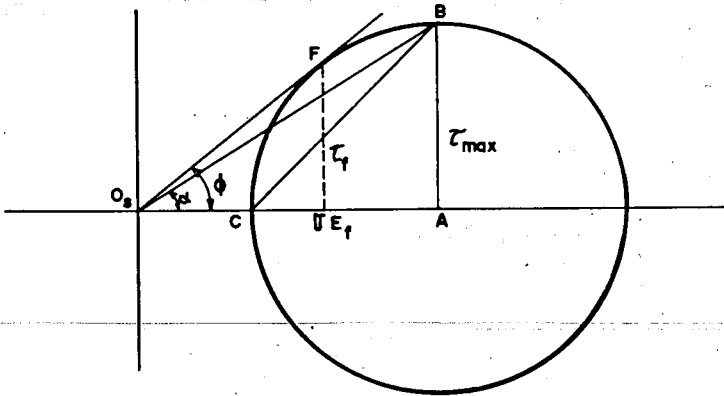


Fig. E.6.2 Mohr diagram

$$\begin{aligned}
 CD &= 3\text{cm} \\
 \tau_{\max} &= 3/2 \times 100 = 150\text{kN/m}^2 \\
 O_1A &= 5\text{cm} \\
 \sigma &= 5/2 \times 100 = 250\text{kN/m}^2 \\
 \phi &= 31.0^\circ \\
 \phi &= 36.3^\circ \\
 FE_r &= 2.5\text{cm}
 \end{aligned}$$

$$\tau_f = \frac{2.5}{2} \times 100 = 125\text{kN/m}^2$$

$$O_1E_r = 3.4\text{cm}$$

$$\sigma_f = \frac{3.4}{2} \times 100 = 170\text{kN/m}^2$$

E.6.5

$$\text{Given } \sigma_1 = 1000\text{kN/m}^2$$

$$\sigma_3 = 200\text{ kN/m}^2$$

Required

τ and σ on a plane making $\theta = 30^\circ$ with the major principal plane.

SOLUTION

a) Analytical

Using Eq. (6.9) and Eq. (6.10) respectively,

$$\begin{aligned}
 \tau &= \frac{1}{2} (\sigma_1 - \sigma_3) \sin 2\theta \\
 &= \frac{1}{2} (1000 - 200) \sin 60 \\
 &= 400 \cdot \sin 60 = 346\text{ kN/m}^2
 \end{aligned}$$

$$\begin{aligned}
 \sigma &= \sigma_3 + (\sigma_1 - \sigma_3) \cos^2 \theta \\
 &= 200 + (1000 - 200) \cos^2 30 \\
 &= 200 + 800 (0.75) \\
 &= 800\text{ kN/m}^2
 \end{aligned}$$

(b) GRAPHICAL

i) Choose a convenient scale and plot σ_1 and σ_3 on the σ - axis.

ii) Draw a circle with a radius of $\frac{\sigma_1 - \sigma_3}{2}$

$$= \frac{100 - 200}{2} = \frac{800}{2} = 400 \text{ kN/m}^2$$

Center of circle is at $\frac{\sigma_1 + \sigma_3}{2} = \frac{1000 + 200}{2} = 600 \text{ kN/m}^2$

iii) Measure angle of $2\theta = 60^\circ$ from the center to cut the circle at σ and τ .

iv) Scale off σ and τ . One should get $\sigma = 800 \text{ kN/m}^2$ and $\tau = 346 \text{ kN/m}^2$

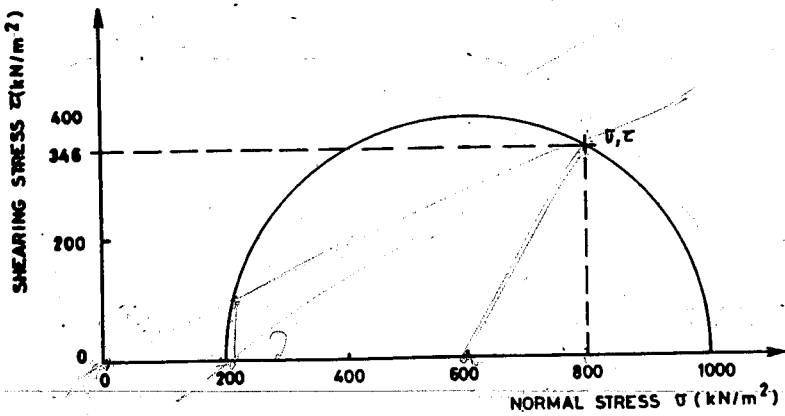


Fig. E.6.3 Mohr diagram

E. 6.6

Given

Two planes with normal and shearing stresses of 1600 kN/m^2 , 400 kN/m^2 and 100 kN/m^2 , 300 kN/m^2 respectively.

Required

The major and minor principal stresses and the angle between the two planes.

SOLUTION

The simplest way of solving this problem is using the Mohr's diagram.

- i) Using a convenient scale, plot the stress coordinates.
- ii) Locate the center of the circle. The center is located at the intersection of the perpendicular bisectors of the line joining two given points.
- iii) measure σ_1 and σ_3 . Accordingly, one obtains
 $\sigma_1 = 1700 \text{ kN/m}^2$
- iv) The angle between the planes is obtained from the figure. It is
 $\frac{1}{2}(2\theta_2 - 2\theta_1) = \frac{1}{2}(160 - 30) = \frac{1}{2}(130) = 65^\circ$

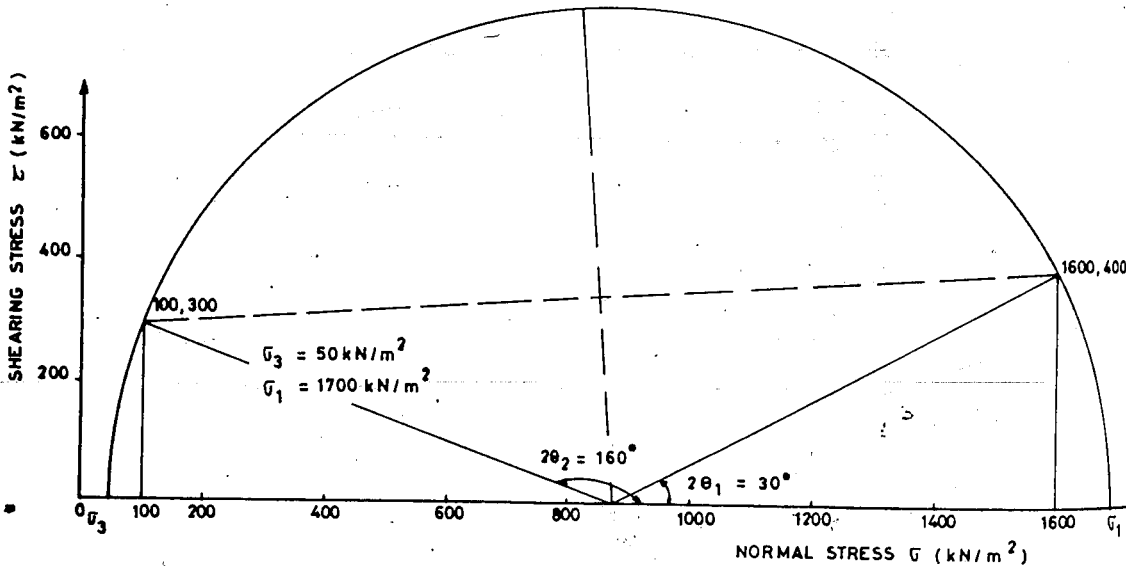


Fig. E.6.4 Mohr diagram

E.6.7 Given

Triaxial compression test results of two sets of tests, the shearing resistance of which is governed by Coulomb's equation $\tau = c' + \bar{\sigma} \tan \phi'$

test no.1 $\bar{\sigma}_1 = 800 \text{ kN/m}^2$, $\bar{\sigma}_3 = 200 \text{ kN/m}^2$

test no.2 $\bar{\sigma}_1 = 1050 \text{ kN/m}^2$, $\bar{\sigma}_3 = 350 \text{ kN/m}^2$

Required

The values of c' and ϕ'

SOLUTION

- i) Draw the Mohr circles corresponding to the given major and minor principal stresses (Fig. E.6.2)

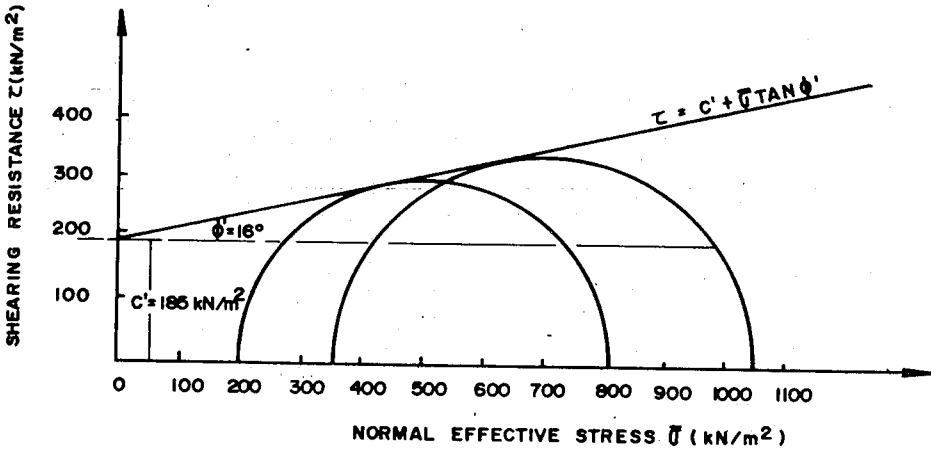


Fig. E.6.5 Mohr diagram

- ii) Since the shearing resistance of the soil is governed by the equation of Coulomb, draw the tangent of the two circles.

The intercept of the tangent with the τ - axis gives the value of c' and the inclination of the tangent gives the value of ϕ'

- iii) From the figure $c' = 185 \text{ kN/m}^2$, $\phi' = 16^\circ$

6.12 EXERCISES

- 1 Develop the following expression:-

$$\sigma_t = \sigma_3 (1 + \sin \phi)$$

where

$$\sigma_t = \text{normal stress on the failure plane}$$

- 2 The major and minor principal stresses at a point are 300 kN/m^2 and 125 kN/m^2 respectively. What is the value of the angle between the plane of major principal stress and the plane on which the angle of obliquity of the resultant stress has its maximum value?
- 3 The normal stresses on two perpendicular planes are 1800 and 300 kPa , and shear stresses are 600 kPa . Find the major and minor principal stresses graphically. Check your answer analytically.
- 4 A sample of sandy soil in a direct shear test fails when the normal stress is 600 kPa and shear stress is 400 kPa . Find the angle of internal friction and the principal stresses, if the Mohr rupture envelop passes through the origin of stress. Show the orientation of the principal planes.
- 5 Two triaxial tests were done on soil samples. In the first test the all-round pressure was 240 kPa and failure occurred at an added axial stress of 750 kPa . In another test the all-round pressure was 400 kPa and failure occurred at a total axial stress of 1600 kPa . Calculate the values of cohesion and angle of internal friction at failure.
- 6 An embankment will be constructed of soil having effective cohesion, $c' = 400 \text{ kPa}$ and effective friction angle, $\phi' = 26^\circ$. Evaluate the shear strength of the material on a horizontal plane at a point 10 m below the surface of the embankment, if bulk unit weight of the soil is 23 kN/m^3 and the pore pressure at that point is 180 kPa .
- 7 A triaxial compression test was carried out on a sandy soil. Calculate the major principal stress at the time of failure, if the chamber pressure was 400 kPa and the angle of internal friction was 35° .

- 8 In a triaxial compression test done on $c-\phi$ soil, the cell pressure was 250kN/m^2 and failure occurred at an added axial pressure of 350kN/m^2 . If the failure plane made an angle of 52° with horizontal, find out c and ϕ for the soil and normal and shear stress on failure plane.
- 9 In a triaxial compression test on a sample of remoulded clay the following results were obtained.

Lateral Pressure kN/m^2	0.0	150	300
Max. deviator stress kN/m^2	140	310	490

Plot the Mohr circle corresponding to these results and determine the apparent cohesion of the soil and the angle of shearing resistance.

- 10 Consolidated undrained triaxial test was carried out on a soil sample giving the following results.

Cell pressure (kPa)	1000	1800
Deviator stress at failure (kPa)	1600	2200
Pore pressure (kPa)	400	800

Determine the values c and ϕ based on

- total stress
 - effective stress
- 11 A triaxial compression test on a cohesive soil, cylindrical in shape, yielded the following.
- $\sigma_1 = 70\text{ N/cm}^2$, $\sigma_3 = 15\text{ N/cm}^2$
and the angle of inclination of the rupture plane with the horizontal is 60° .
- Determine analytically the normal stress, the shear stress and resultant stress on the rupture plane, through a point.
 - What are the magnitudes of c and ϕ ?
 - Write the Coulomb's shear strength equation pertaining to this problem.

(d) Present all the information in the form of Mohr's stress diagram.

- 12 Given the following data from unconfined compression test of a saturated clay sample,

Stress in N/cm ²	0	9.8	19.6	29.4	34.3	39.2
Strain	0	0.0035	0.0080	0.0170	0.0270	0.0650

- (a) plot the stress-strain curve.
- (b) find the shear strength.
- (c) find the modulus of elasticity of the soil.
- 13 A cylindrical soil sample was subjected to unconfined compression test in a triaxial machine. At failure the axial stress was 12.2 N/cm² and the pore water pressure (u) at failure was -5.0 N/cm². The failure plane was found to be inclined at 50° to the horizontal.
- (a) Construct the Mohr circle at failure in terms of effective stress.
- (b) Construct the probable failure envelope and find the cohesion intercept and angle of internal friction in terms of effective stress.
- (c) Draw the stress vector acting on the failure plane.
- 14 Given the normal stresses on two perpendicular planes as 11.2 N/cm² and 5.9 N/cm², the shear stress on each 11.2 N/cm², draw Mohr's circle.
- (a) Can tension occur on any plane with stress condition?
- (b) Find the principal stresses.
- (c) What are the shear and normal stresses on a plane making an angle of 74° with the direction of the major principal stress?
- 15 A thin seam of sand lies inclined at an angle of 25° and intersects the base of a cliff. The drainage of the sand is stopped by talus. The sand is overlaid by clay 15m thick and 1.5m of top soil. The ground surface slopes at 25° and there is a deep vertical crack extending through the clay 20m from the face of the cliff. The clay and top soil have a unit weight of 17.6 kN/m² and the angle of internal friction of the sand is 32.5°. How high must the water rise in the sand before the block of clay slides upon the sand layer?

7 EARTH PRESSURES

7.1 GENERAL

The pressure exerted by a soil mass on structures providing lateral support to the soil is called lateral earth pressure. Soil has special characteristics of exerting lateral pressure against an object with which it comes in contact. Such a property of soil is highly important in engineering practices, since it influences the design of retaining walls, bulkheads, abutments, sheeting and bracing in cuts. The common types of structures used for retaining earth is shown in Fig.7.1

There are two distinct types of lateral soil pressures, namely, active lateral pressure and passive lateral pressure (Fig.7.2).

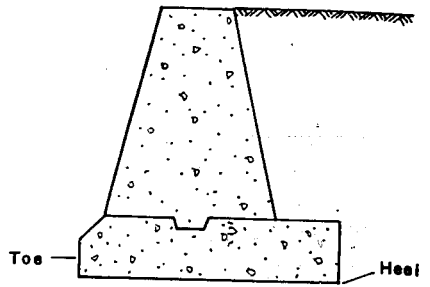
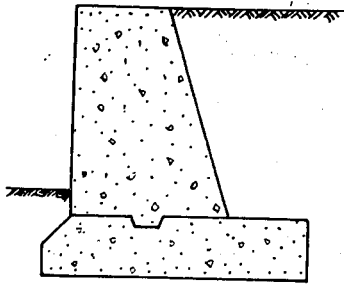
Active Earth Pressure, P_a , is a pressure caused by soil moving forward because of yielding of the support. It is a minimum value of earth pressure.

Passive Earth Pressure, P_p , is a pressure developed as a result of the soil being pushed backwards by the support. It is a maximum value of earth pressure.

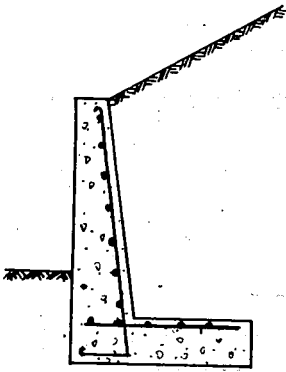
Earth Pressure at Rest, P_o , is intermediate between active and passive state and exists when there is no motion in either direction. It is, therefore, a pressure which develops at zero movement. Its value is somewhat larger than the active pressure.

The effect of wall movement on lateral pressure developed in granular material as investigated by Terzaghi is illustrated in Fig. 7.3.

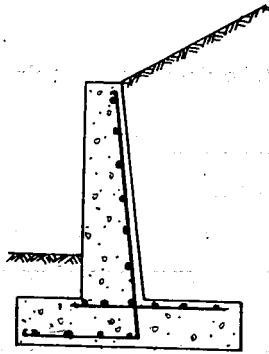
The ordinate of point A represents the lateral pressure at rest. As the wall moves away from the backfill, the pressure decreases from A to active value at B. The amount of movement required for the active pressure to develop is quite small, and it can practically always be expected to occur when a backfill is placed behind the wall. Minimum tilt of retaining wall necessary to develop active and passive states is indicated in Table 7.1.



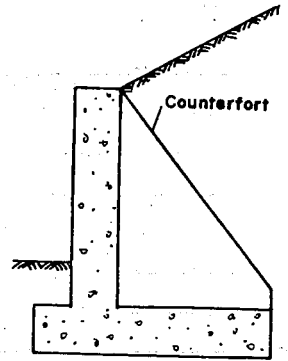
(a) Mass Concrete Gravity Walls.



L - Shaped

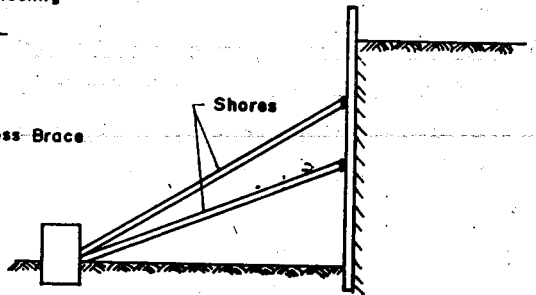
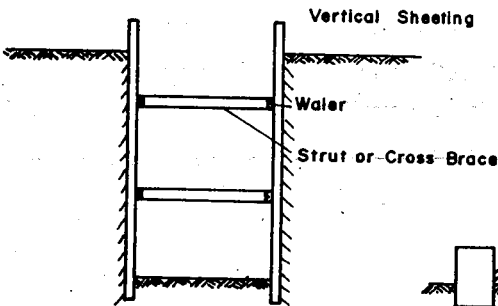


T - Shaped



Counterfort Wall

(b) Reinforced Concrete Cantilever Walls.



(c) Braced Walls and Sheetings

Fig. 7.1 Common types of retaining walls

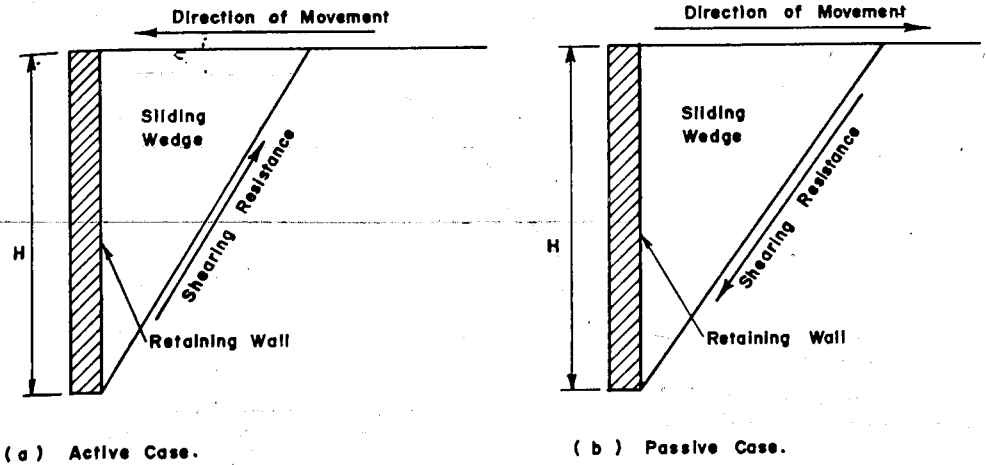


Fig. 7.2 Lateral earth pressure on a retaining wall.

In essence what happens is that the movement of the wall causes the development of strains within the soil mass. These strains mobilize shearing stresses which are directed in such a way that they help to support the mass and reduce the amount of pressure exerted by the soil against the structure. In the passive case, when the wall is pushed against the backfill, the pressure is increased from A to passive value at C. Here again internal shearing stresses also develop, but they act in the opposite direction from those in the active case and must be overcome by the movement of the structure. This difference in the direction of internal shearing stresses accounts for the difference in magnitude between active pressure and passive pressure.

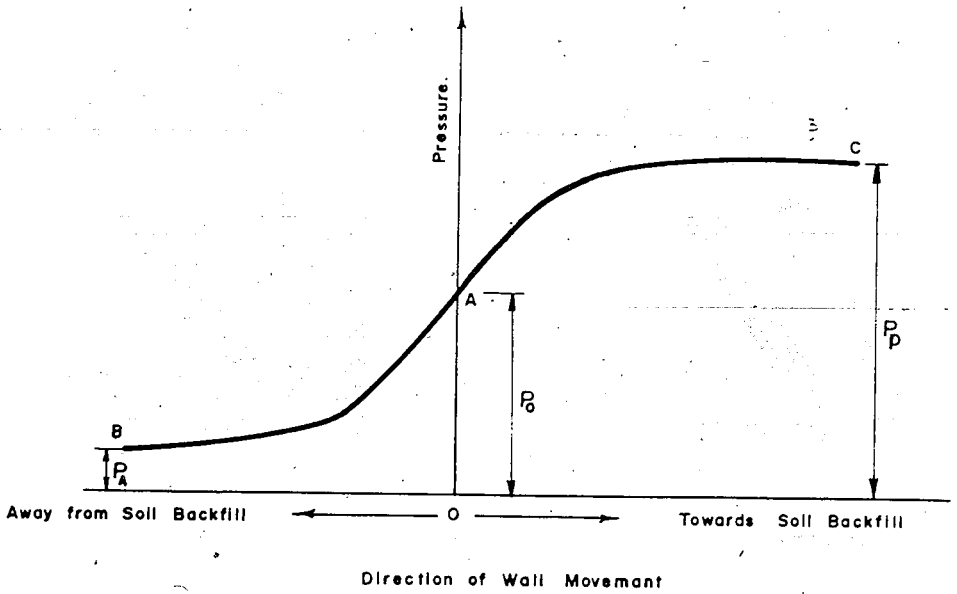


Fig. 7.3 Relation between direction of wall movement and soil pressure.

Table 7.1 Minimum tilt of a retaining wall necessary to mobilize the active and passive states [29].

Soil	Active State	Passive State
Dense Cohesionless	0.0005 H	0.005 H
Loose Cohesionless	0.002 H	0.01 H
Stiff Cohesive	0.01 H	0.02 H
Soft Cohesive	0.02 H	0.04 H

7.2 EARTH PRESSURE THEORIES

The two well-known classical earth pressure theories adopted for the determination of earth pressure are Rankine's theory (named after the British Engineer W.J. Rankine (1857)) and Coulomb's theory (named after the French Scientist C.A. Coulomb (1776)).

7.2.1 Rankine's Earth Pressure Theory:

The assumptions used in Rankine's theory are the following;

- (a) the backwall face is smooth and vertical
- (b) deformation condition for plastic equilibrium is satisfied

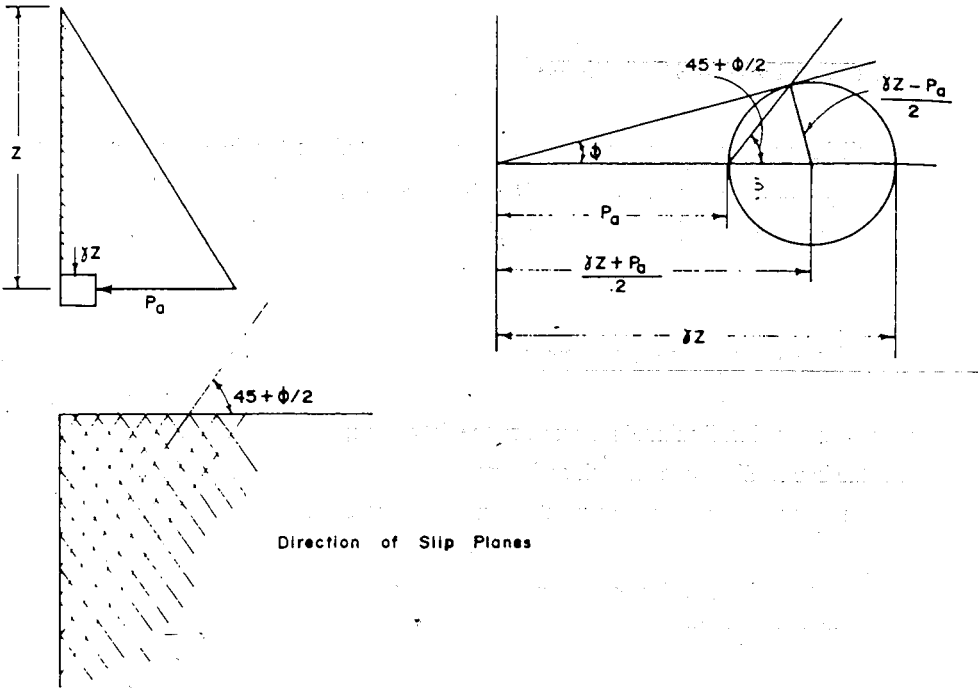
In this analysis, one should differentiate between the general state of plastic equilibrium and local state of plastic equilibrium.

7.2.1.1 General State of Plastic Equilibrium

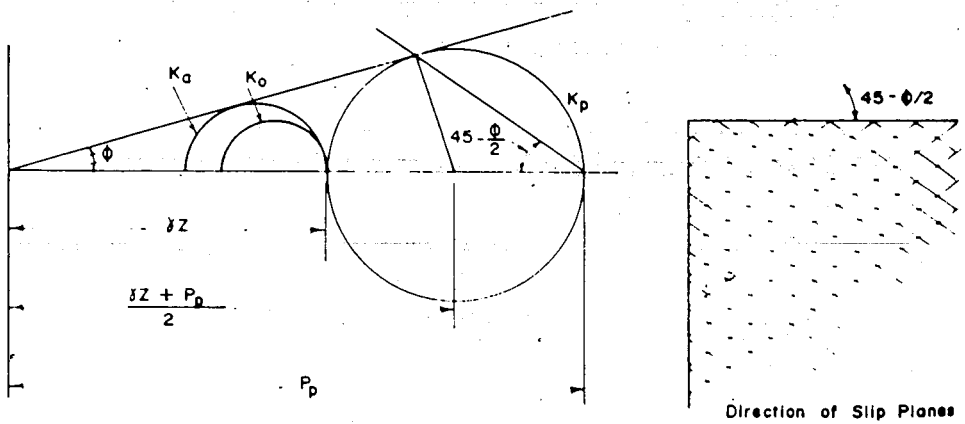
A general state of plastic equilibrium occurs if every part of semi-infinite mass is on the verge of failure due to horizontal tension or compression.

Consider an element of soil in a semi-infinite mass of cohesionless soil located at a depth z as shown in Fig. 7.4(a). If the unit weight of soil is taken as γ , the vertical overburden pressure acting on the element is γz .

The vertical pressure and active lateral earth pressure, P'_a , acting on a prism at the moment of failure are the principal stresses $\sigma_1 = \gamma \cdot z$ and $\sigma_3 = P'_a$ (Fig. 7.4 a)



(a) Active Case .



(b) Passive Case

Fig. 7.4 Relation of vertical stress to horizontal stress.

$$\text{From Fig. 7.4a, } \sin \phi = \frac{\gamma z - P_a}{\gamma z + P_a}$$

$$\text{Then, } P_a = (\gamma \cdot z) \frac{1 - \sin \phi}{1 + \sin \phi} \quad (7.1)$$

$$\frac{1 - \sin \phi}{1 + \sin \phi} = \tan^2 (45 - \phi/2) = K_a = \text{coefficient of active earth pressure}$$

The derivation for the passive case follows from Fig. 7.4b

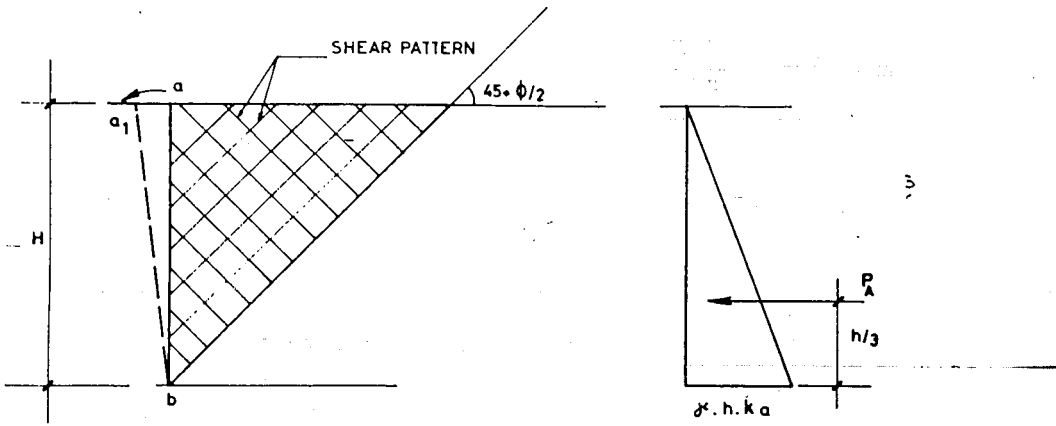
$$\sigma_3 = \gamma \cdot z \text{ and } \sigma_1 = P_p \text{ and from the figure, } \sin \phi = \frac{P_p - \gamma \cdot z}{P_p + \gamma z}$$

$$\text{Then, } P_p = (\gamma \cdot z) \frac{(1 + \sin \phi)}{(1 - \sin \phi)}$$

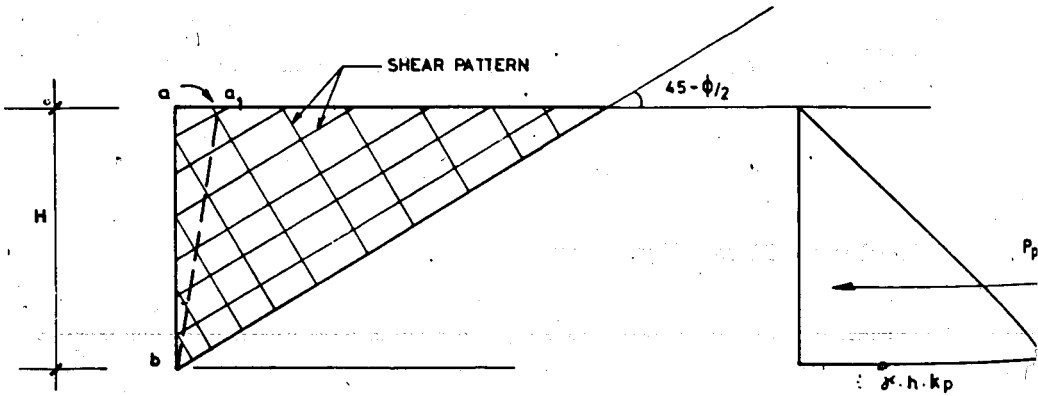
$$\frac{(1 + \sin \phi)}{(1 - \sin \phi)} = \tan^2 (45 + \phi/2) = K_p = \text{coefficient of passive earth pressure}$$

7.2.1.2. Local State of Plastic Equilibrium

General state of plastic equilibrium occurs only by geological process where horizontal tension or compression takes place. In a local state of plastic equilibrium, the failure occurs in a limited zone as shown in Fig. 7.5. It is this local state of plastic equilibrium that is frequently met in practice (retaining walls, sheet piles, etc.)



(a) WALL ab IS ROTATED TO a_1b
(BOUNDARY CONDITION : SMOOTH WALL)



(b) WALL ab IS ROTATED TO a_1b
(BOUNDARY CONDITION : SMOOTH WALL)

Fig. 7.5 Local state of plastic equilibrium.

7.2.1.3 Earth pressure against smooth vertical walls

For a vertical smooth wall with horizontal surface, the active and passive pressure distribution is governed by local state of plastic equilibrium.

7.2.1.3.1 Cohesionless Soils

The active earth pressure at a depth H against a retaining wall with a cohesionless backfill which is horizontal is, $P_a = K_a \gamma H$. The pressure for the totally active case acts parallel to the face of the backfill and varies linearly with depth as shown in Fig. 7.6. The resultant thrust on the wall acts at $\frac{1}{3}H$ from the base. It is equal to,

$$P_A = 1/2 K_a \gamma H^2 \tag{7.3}$$

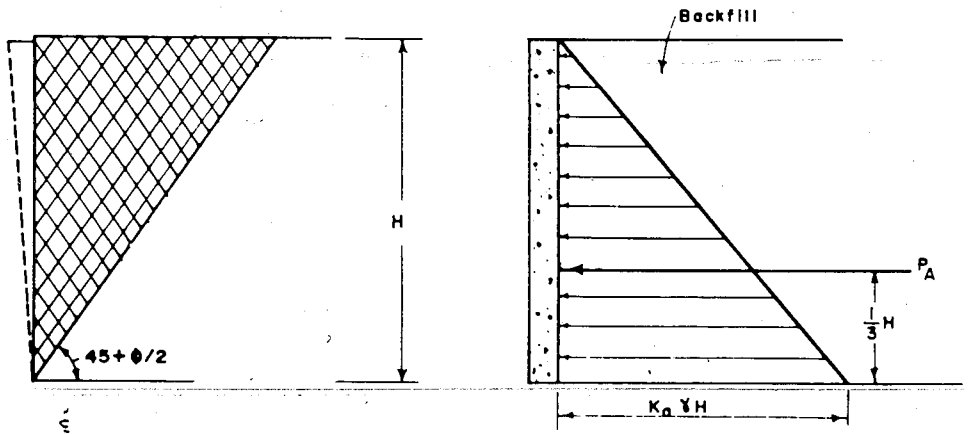


Fig. 7.6 Lateral active earth pressure (cohesionless backfill)

The passive pressure varies linearly with depth as shown in Fig. 7.7. Here again, the resultant thrust on the wall acts at $\frac{1}{3}H$

$$P_p = \frac{1}{2} K_p \gamma H^2 \quad (7.4)$$

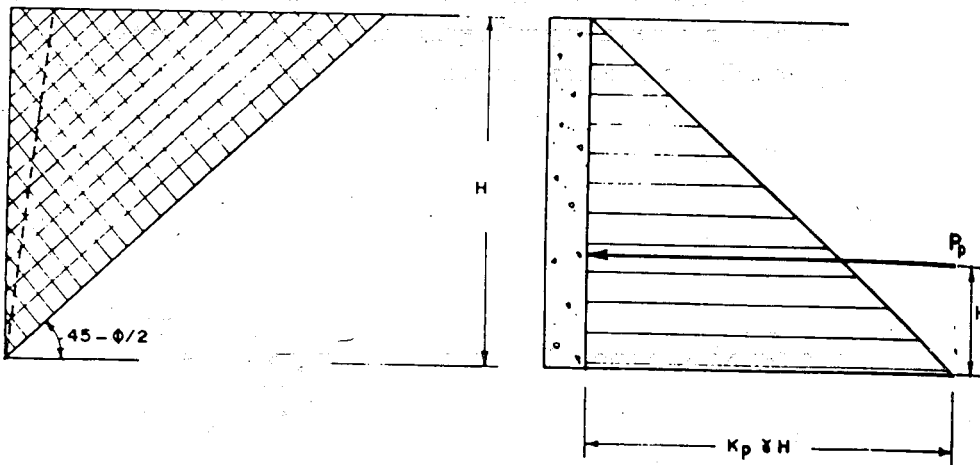


Fig. 7.7 Lateral passive earth pressure (cohesionless backfill)

The Rankine theory may be applied for the following different situations.

- a) *Partially Submerged Backfill*
For partially submerged backfill (Fig 7.8a),

$$P_a = K_a \gamma H_1 + K_a \gamma_b H_2 + \gamma_w H_2 \quad (7.5)$$

b) *Inclined Backfill*

In spite of the Rankine's basic assumptions of smooth vertical wall and horizontal backfill, the theory is being modified to apply for inclined backfill and sloping backwall case as shown in Fig. 7.8 (b) and 7.8 (c) to yield an approximate result [27]

$$\text{Active force, } P_A = \frac{\gamma H^2}{2} \cos i \cdot \frac{\cos i - \sqrt{\cos^2 i - \cos^2 \phi}}{\cos i + \sqrt{\cos^2 i - \cos^2 \phi}} \quad (7.6)$$

$$\text{Passive force, } P_P = \frac{\gamma H^2}{2} \cos i \cdot \frac{\cos i + \sqrt{\cos^2 i - \cos^2 \phi}}{\cos i - \sqrt{\cos^2 i - \cos^2 \phi}} \quad (7.7)$$

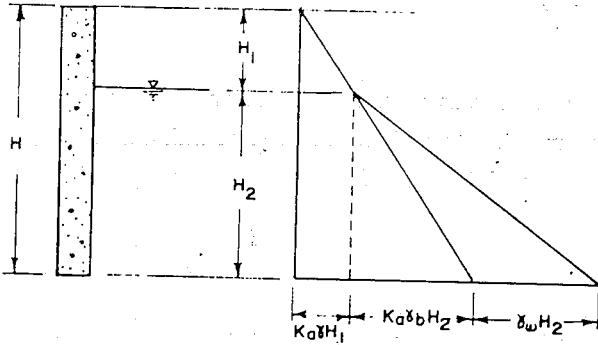
c) *Sloping back Wall Case*

If the back of the wall slopes as in Fig. 7.8(c), it is assumed that the lateral pressure acts horizontally on a vertical plane in the backfill and the wedge of earth with weight W_1 acts as part of the wall.

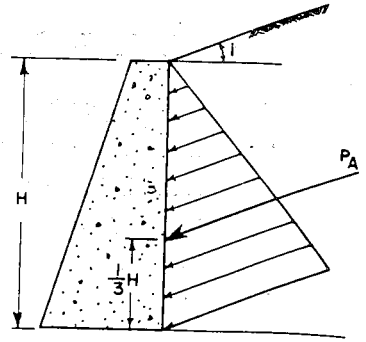
d) *Backfill with Surcharge Loading*

Loading imposed on the backfill is commonly referred to as surcharge. It may be either live or dead loading and may be distributed or concentrated. When a uniformly distributed surcharge is applied to the backfill, the vertical pressures at all depths in the backfill are increased equally. The lateral pressure distribution is shown in Fig. 7.8(d). The resultant active force would be:

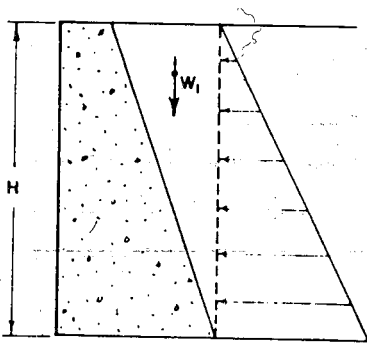
$$P_A = \frac{R \Delta PK}{2} + \frac{\gamma H^2}{2} K_a \quad (7.8)$$



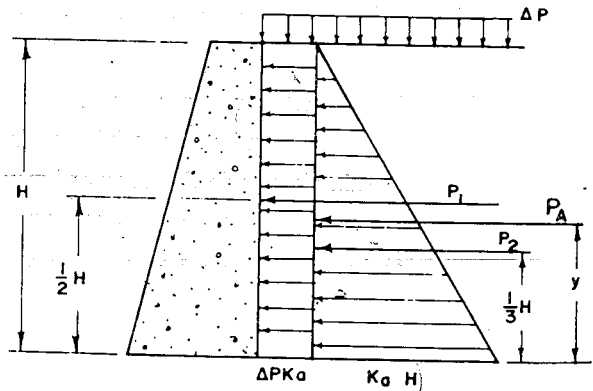
(a) Partially Submerged Backfill Soil



(b) Inclined Backfill Soil



(c) Wall with Sloping Back



(d) Wall with a Uniform Surcharge on Backfill

Fig. 7.8 Rankine active earth pressure diagram for different cases.

The line of action of the resultant force is located at

$$y = \frac{H}{3} \frac{3\Delta P + \gamma H}{2\Delta P + \gamma H} \quad (7.9)$$

The pressure distribution for both active and passive case in cohesionless backfill subjected to surcharge loading and partial submergence is shown in Fig. 7.9.

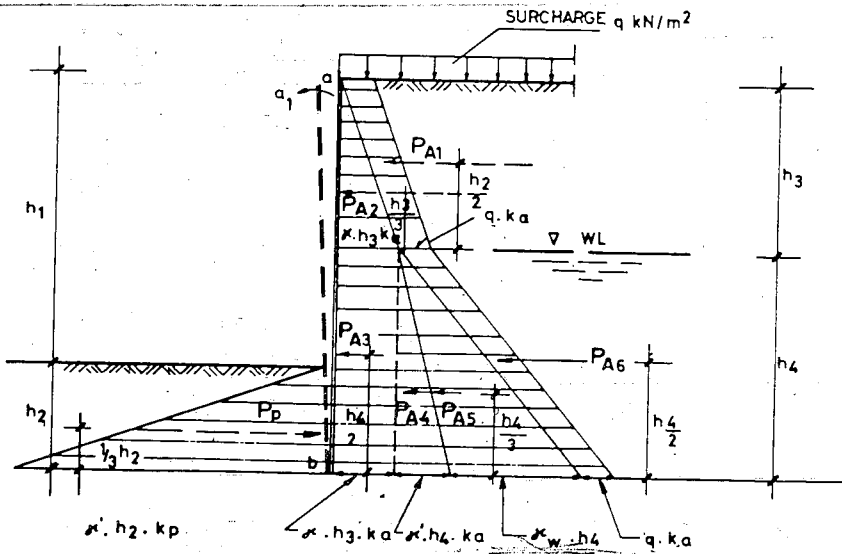


Fig. 7.9 Active and passive earth pressure distribution for cohesionless soils

7.2.1.3.2 Cohesive Soils

7.2.1.3.2.1 Backfill containing clay with $c = c_u$ and $\phi = 0$ conditions

Vertical and lateral stress relations may be developed with reference to Mohr stress diagram shown in Fig. 7.10. In this case, the stress relations are established in terms of unit cohesion rather than the friction angle assuming that clay in undrained condition has shearing strength due only to cohesion.

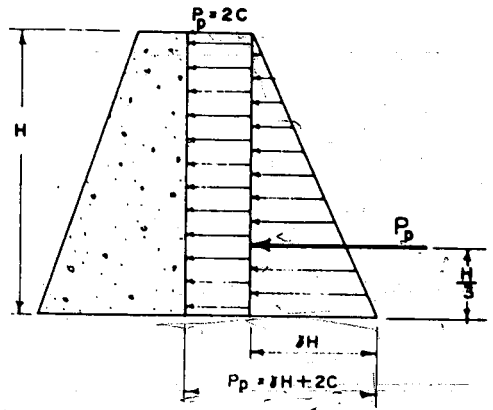
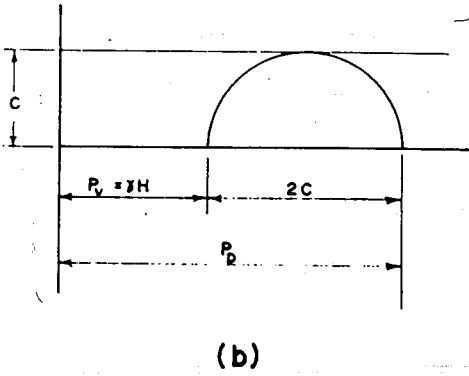
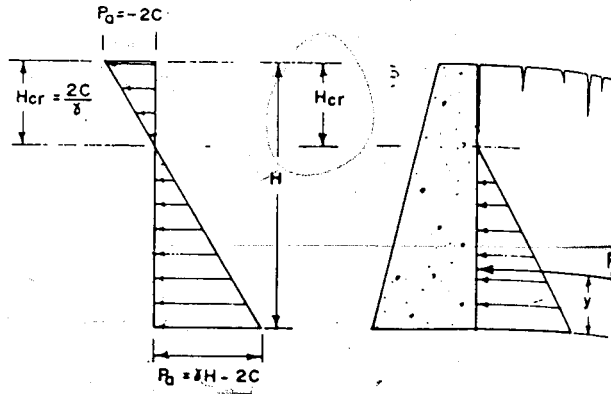
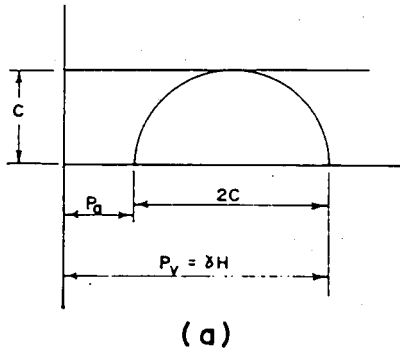


Fig. 7.10 Lateral pressure for cohesive soil in undrained condition.

The active lateral earth pressure due to clay backfill is determined as illustrated in Fig. 7.10a. At the bottom of the backfill $P_a = P_v - 2c = k_a \gamma H - 2c$ and at the ground surface $\gamma H = 0, P_a = 0$. Hence, $P_a = -2c$.

It is found that to a certain height a bank of clay with an approximate vertical face may stand without a lateral support. The height referred to the above is termed the *critical height*, which is designated by H_{cr} equalling to $2c/\gamma$ (Fig. 7.10a).

The clay is in tension between $H=0$ and H_{cr} . The tension decreases from $2c$ at the surface to 0 at H_{cr} . Active earth pressure will develop on $(H - 2c/\gamma)$ portion of the wall.

Resultant thrust on the wall, $P_A = \frac{\gamma}{2} \left(H - \frac{2c}{\gamma} \right)^2$ and is located at

$$y = \frac{1}{3} \left(H - \frac{2c}{\gamma} \right) = H/3 - \frac{2c}{3\gamma}$$

The passive lateral pressure due to clay backfill is determined as shown in Fig. 7.10b. At the bottom of the backfill $P_p = \gamma H + 2c$ and at the ground surface $P_p = 2c$

7.2.1.3.2.2 Backfill containing clay with both cohesion and friction (c - ϕ soil)

Like in the previous case, vertical and lateral stresses may be developed with reference to Mohr stress diagram as indicated in Fig. 7.11 for the active and passive cases.

The active lateral earth pressure is determined using Fig. 7.11.a. From this figure it follows:

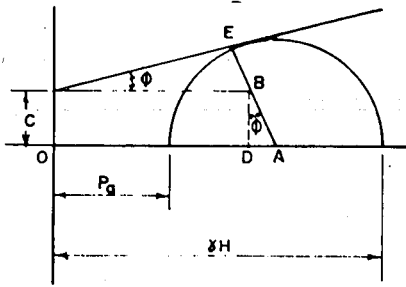
$$OA = \frac{P_a + \gamma H}{2}$$

$$BE = CB \sin \phi$$

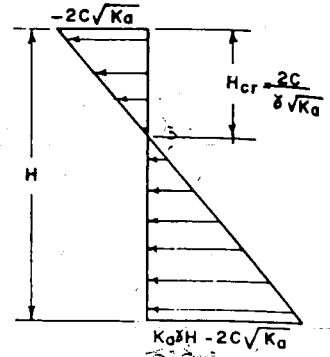
$$BA \cos \phi = c$$

$$AD = c \tan \phi$$

$$CB = OA - AD$$

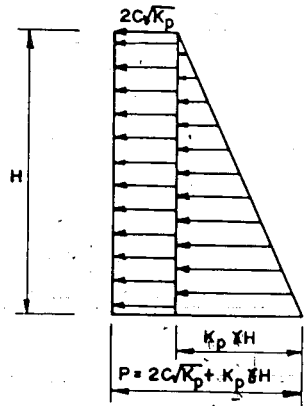
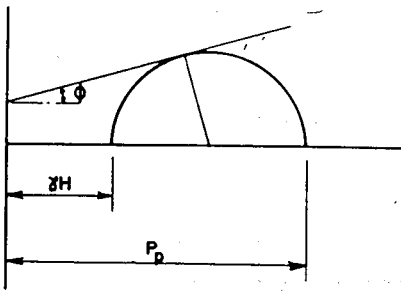


Mohr circle



Pressure distribution on the wall

(a) ACTIVE PRESSURE



(b) PASSIVE PRESSURE

Fig. 7.11 Lateral pressure for cohesive soil containing both cohesion and friction

$$CB = \frac{P_a + \gamma H}{2} - c \tan \phi$$

$$\text{Hence, } BE = \left[\frac{P_a + \gamma H}{2} - c \tan \phi \right] \sin \phi$$

$$\text{But, } BE + BA = \frac{\gamma H - P_a}{2}$$

$$\text{That is, } \left[\frac{P_a + \gamma H}{2} - c \tan \phi \right] \sin \phi + \frac{c}{\cos \phi} = \frac{\gamma H - P_a}{2}$$

After simplification and rearrangement of terms,

$$P_a = \gamma H k_a - 2c \sqrt{k_a} \quad (7.10)$$

The variation of this pressure with depth is as shown in Fig.7.11(a)

At the top of the backfill $P_a = -2c \sqrt{k_a}$ and at the bottom

$$P_a = K_a \gamma H - 2c \sqrt{K_a}$$

From the equation, it is seen that the cohesion reduces the active earth pressure by an amount equal to $2c \sqrt{K_a}$. This indicates that the soil is more self-supporting.

When $P_a = 0$, the critical depth, H_{cr} would be,

$$H_{cr} = \frac{2c \sqrt{k_a}}{\gamma k_a} = \frac{2c}{\gamma \sqrt{k_a}} \quad (7.11)$$

The critical depth indicates the depth of tension cracks. The magnitude of tension decreases from $-2c \sqrt{k_a}$ at the ground surface to 0 at H_{cr} .

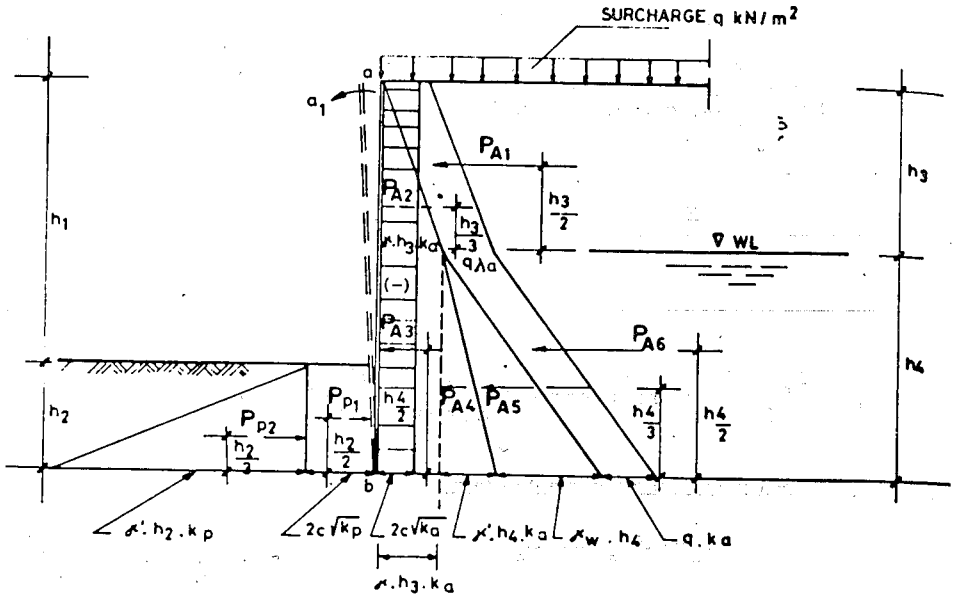


Fig. 7.12. Active and passive earth pressure distribution for cohesive soils

The resultant thrust, $P_A = \frac{1}{2} K_a \gamma H^2 - 2cH \sqrt{K_a}$ (7.12)

From Fig. 7.11b, it can easily be seen that the passive pressure at top, $P_p = 2c \sqrt{K_p}$ and at

the bottom, $P_p = 2c \sqrt{K_p} + K_p \gamma H$.

Fig. 7.12 shows active and passive distribution for soils containing both cohesion and friction with surcharge loading and partial submergence.

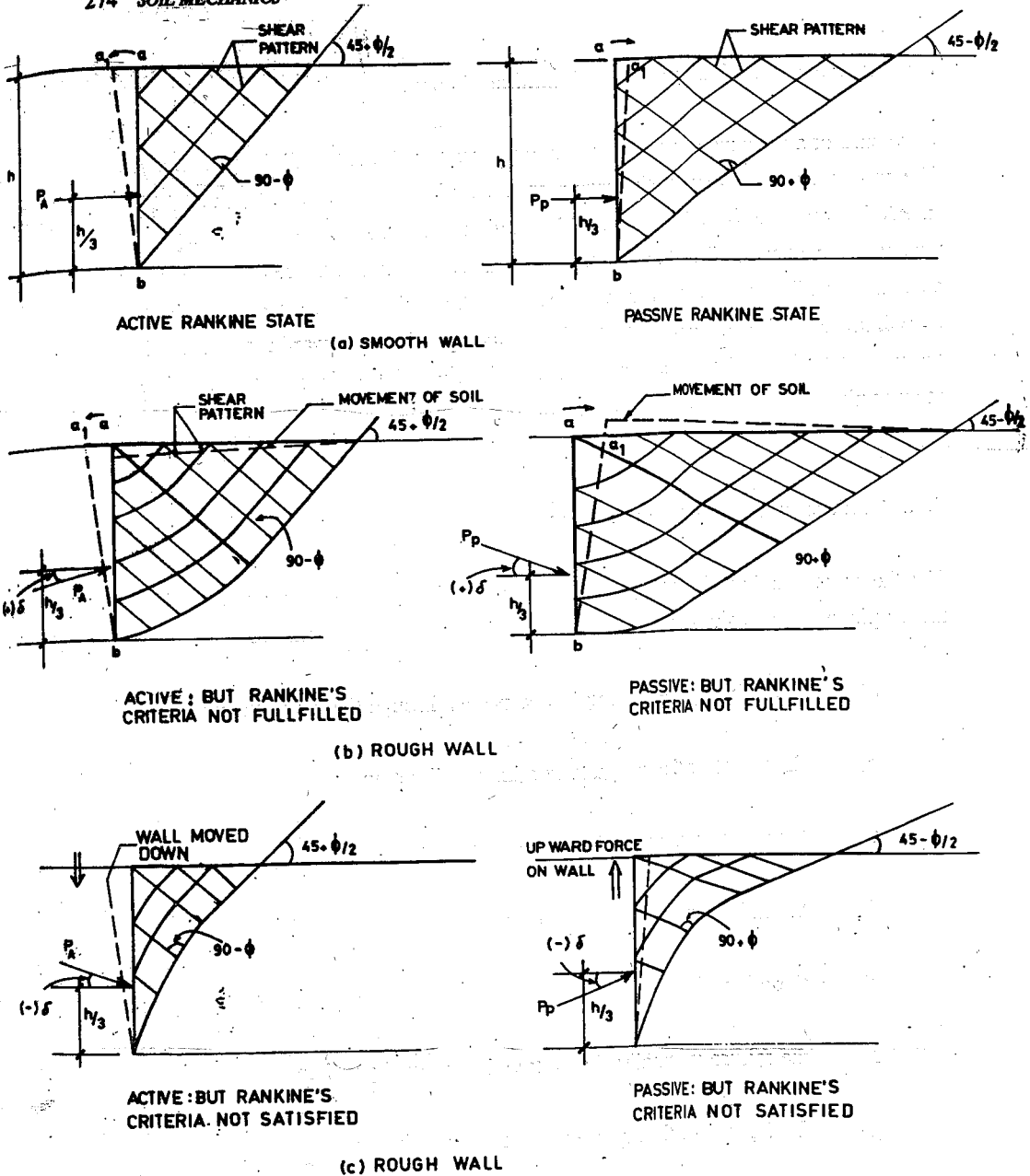


Fig. 7.13 Influence of wall friction.

7.2.2 Influence of Wall Friction on Rankine Theory

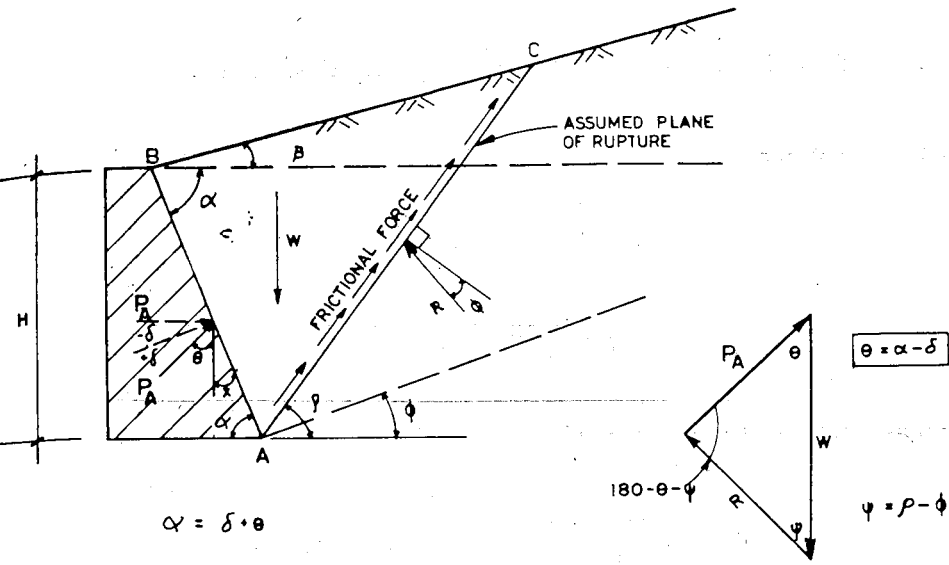
If the back of a retaining structure is not smooth, frictional forces will develop along the wall. The movement of the soil with respect to the wall causes the resultant active force to be inclined at an angle δ to the normal. This angle is known as the *angle of wall friction*. The algebraic sign of the wall friction will be determined according to the relative movement of the soil. If the wall moves downward with respect to the soil for the active case, the direction of P_A will be inclined at angle δ . If the wall is acted upon by an upward force which is equal to the weight of the wall plus the frictional force between the wall and soil, P_p will be inclined at an angle $-\delta$ (Fig. 7.13).

7.2.3 Coulomb's Earth Pressure Theory

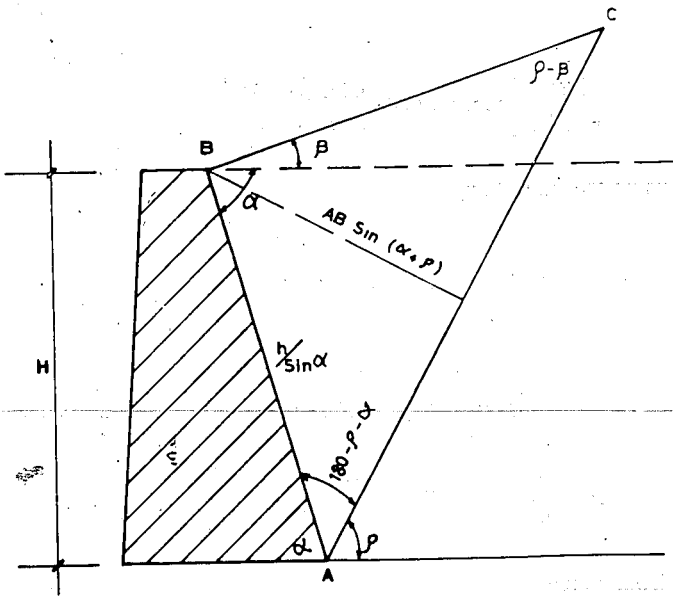
This theory is based on the concept of the sliding wedge bounded by the face of the wall and failure plane. The basic assumptions made in the Coulomb analysis are:

- a) the failure plane is straight and passes through the toe of the wall.
- b) the thrust on the wall acts in a known direction
- c) the soil is isotropic and homogeneous
- d) the failure wedge is a rigid body
- e) there is wall friction
- f) the failure is considered as a two dimensional problem
- g) the friction on the rupture plane is evenly distributed

To derive Coulomb's theory, an arbitrary rupture plane making an angle ρ with the horizontal is considered (Fig. 7.14)



(a) FORCES REPRESENTATION



(b) GEOMETRICAL REPRESENTATION

Fig. 7.14 Coulomb's earth pressure theory for the active case.

$$\text{The area of the wedge } ABC = \frac{1}{2} AC \cdot BD = \frac{1}{2} AC \cdot AB \sin(\alpha + \rho)$$

From the rule of sine

$$\frac{AC}{\sin(\rho - \beta)} = \frac{AB}{\sin(\alpha + \beta)}$$

$$AC = \frac{AB \sin(\alpha + \beta)}{\sin(\rho - \beta)}$$

The weight of the wedge per unit length,

$$W = A \cdot l \cdot \gamma$$

$$= \frac{1}{2} \cdot \frac{AB \sin(\alpha + \beta)}{\sin(\rho - \beta)} \cdot AB \sin(\alpha + \beta) \cdot \gamma$$

$$= \frac{1}{2} \cdot \frac{H}{\sin \alpha} \cdot \frac{\sin(\alpha + \beta)}{(\rho - \beta)} \cdot \frac{H}{\sin \alpha} \cdot \sin(\alpha + \beta) \cdot \gamma$$

$$= \frac{\gamma \cdot H^2}{2 \sin^2 \alpha} \left[\sin(\alpha + \rho) \frac{\sin(\alpha + \beta)}{\sin(\rho - \beta)} \right]$$

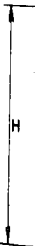
From the force triangle, using the rule of sine

$$\frac{P_A}{\sin(\rho - \phi)} = \frac{W}{\sin(180^\circ - \alpha - \psi)}$$

$$= \frac{W \sin(\rho - \phi)}{\sin(180^\circ - \alpha - \rho + \phi)}$$

$$P_A = \frac{W \sin(\rho - \phi)}{\sin(180^\circ - \alpha - \rho + \phi)}$$

Inserting the value of W from above,



From the geometry of the figure,

$$W = \frac{\gamma H^2}{2} \sin(\alpha + \rho) \frac{\sin(\alpha + \beta)}{\sin(\alpha - \beta)}$$

From the force triangle,

$$P_p = \frac{W \sin(\rho - \phi)}{\sin(180 - \rho - \phi - \delta - \alpha)}$$

Setting $\frac{dP_p}{d\rho} = 0$, one would get the minimum value of P_p .

$$P_p = \frac{\gamma H^2}{2} \left\{ \frac{\sin^2(\alpha - \phi)}{\sin^2 \alpha \sin(\alpha + \delta) \left[1 - \sqrt{\frac{\sin(\phi + \delta) \sin(\phi + \beta)}{\sin(\alpha + \delta) \sin(\alpha + \beta)}} \right]} \right\} \quad (7.16)$$

If $\beta = \delta = 0$ and $\alpha = 90$, Eq. (7.16) simplifies to the equation of Rankine for the passive case.

Eq. (7.16) may also be written in a general form,

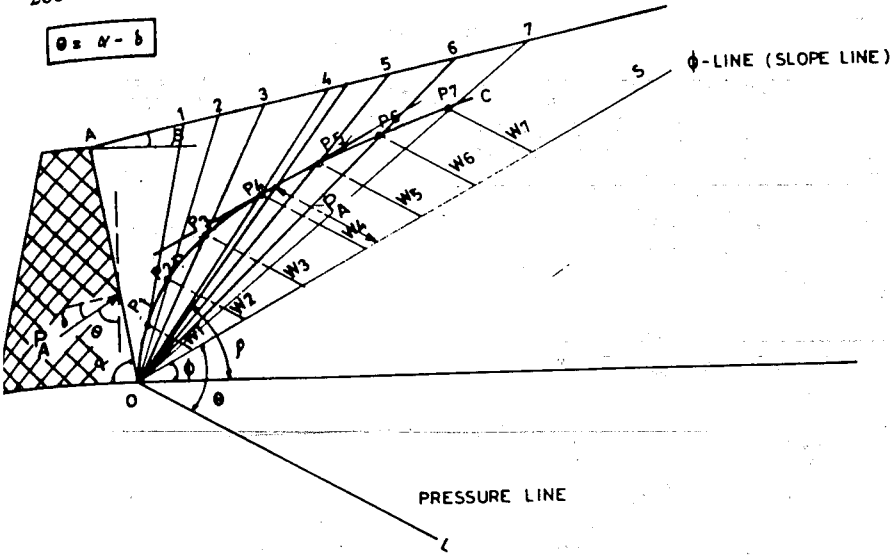
$$P_p = \frac{\gamma H^2}{2} \cdot K_p \quad (7.17)$$

where $K_p = f(\alpha, \beta, \delta, \phi)$

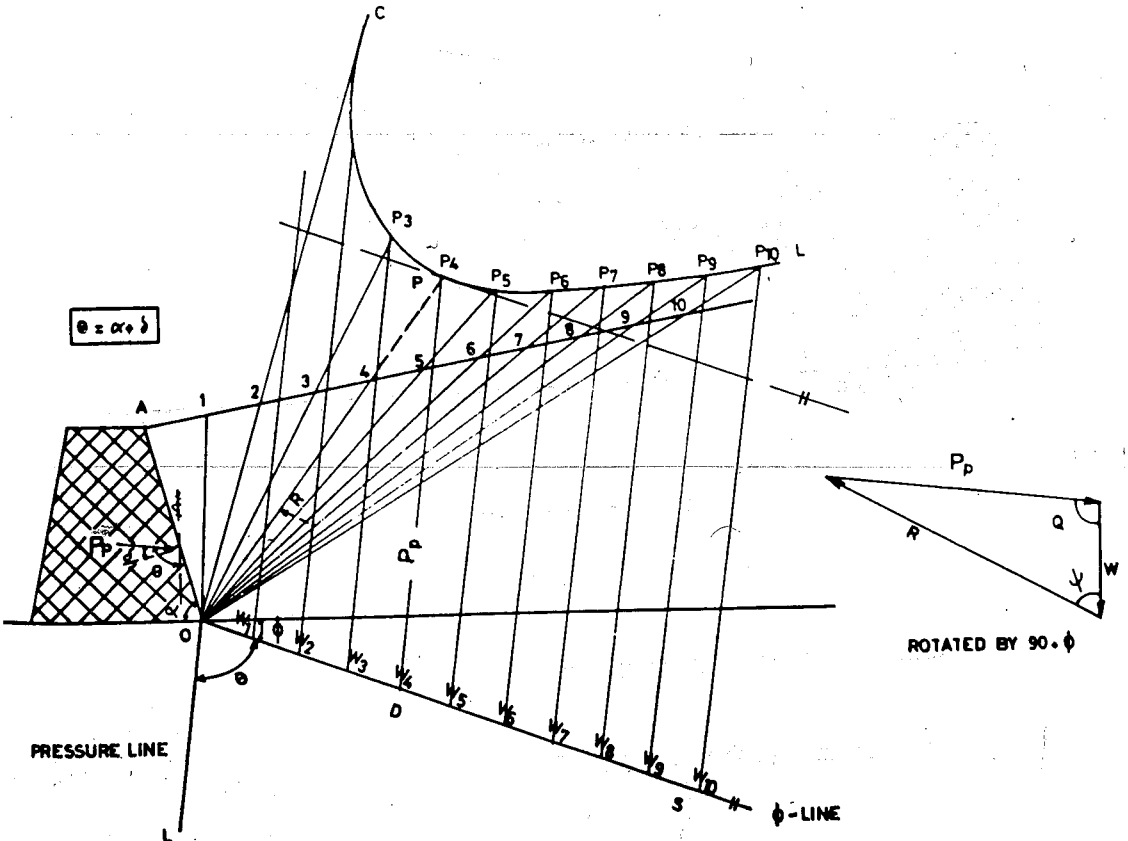
7.2.4 Culmann's Graphical Construction

Culmann suggested an expedient graphical method for determining the active and passive forces using the Coulomb's theory.

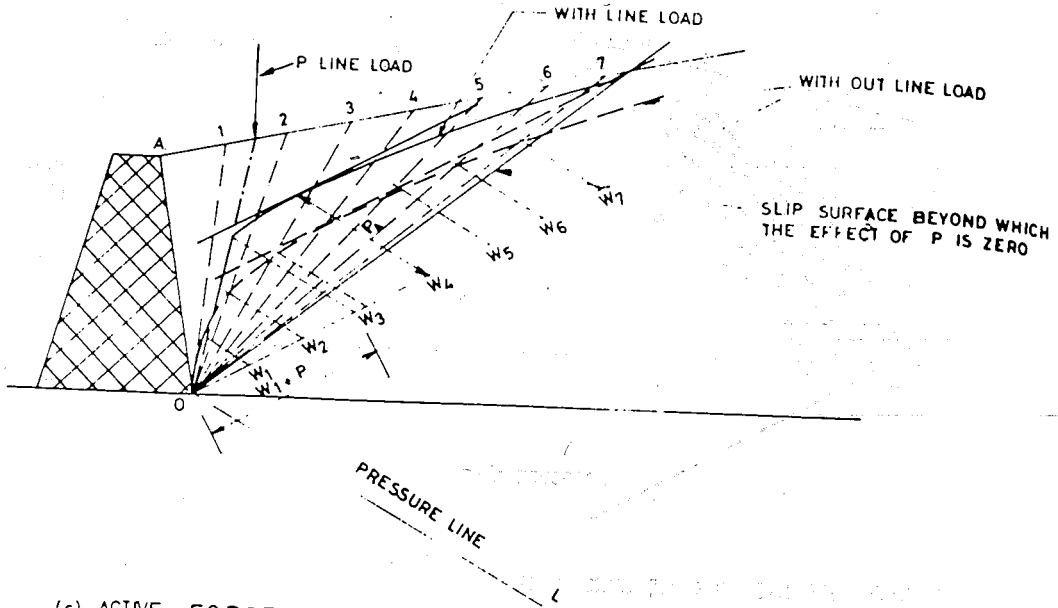
Given a retaining wall with δ , β , α , ϕ and γ (Fig. 7.16), one draws the ϕ -line (slope-line) making an angle ϕ from the horizontal reference line. Then the pressure line OI makes an angle θ with OS. The backfill is then subdivided into arbitrary wedges AO1, 102, 203, etc..



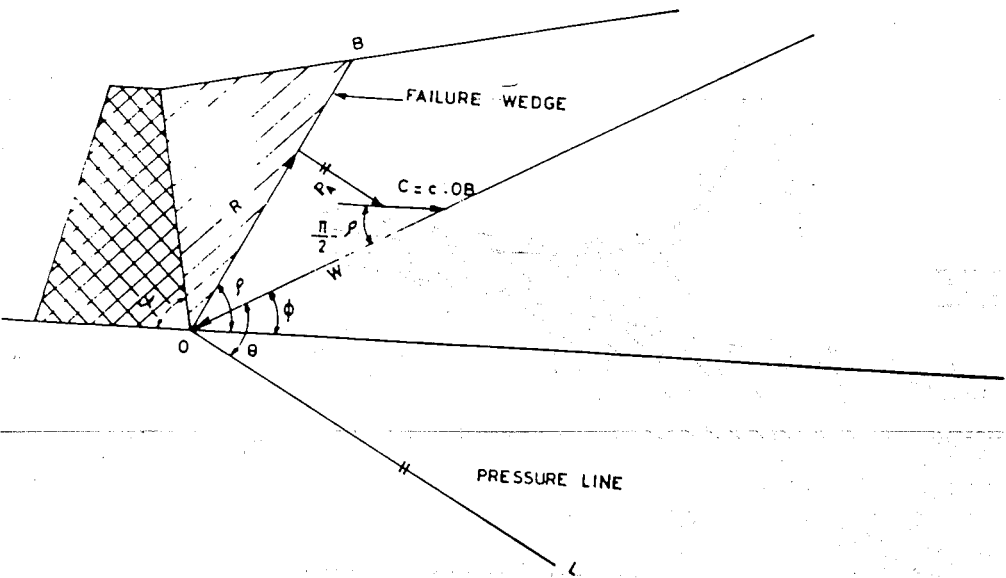
(a) ACTIVE EARTH THRUST WITH OUT SURCHARGE



(b) PASSIVE EARTH THRUST WITH OUT SURCHARGE



(c) ACTIVE FORCE WITH SURCHARGE



(d) ACTIVE FORCE WITH COHESION

Fig. 7.16 Culmann's graphical construction

Weights of each wedge are calculated to get W_1, W_2, W_3 , etc.. Selecting a convenient scale, W_1, W_2, W_3 etc are marked off along the ϕ - line. From W_1, W_2, W_3 , etc., lines parallel to the pressure line are drawn to cut the line O_1, O_2, O_3 , etc., at P_1, P_2, P_3 , etc.. The points are then joined with smooth curve to get the Culmann curve OC for the active case or CM for the passive case. A tangent parallel to the ϕ - line is then drawn so that it touches the Culmann curve at point \bar{P} . The distance PD then represents the active earth thrust P_A or the passive earth force P_p . The real surface of sliding is OP (Fig. 7.16 a,b). In this method, the effect of a surcharge is considered by adding it with the weights of the appropriate wedges (Fig.7.16c). The method of Culmann may be extended for determining the active pressure of cohesive soils (Fig. 7.16d).

The main limitation of the Coulomb's theory lies enter alia, on the assumption of a plane surface of rupture. This method entails an error of about 5% for the active case and about 30% for the passive case. While this method is acceptable for active thrust, one has to look for other methods for determining the passive thrust. The most common methods are the semi-graphical methods which are discussed below.

7.2.5 Semi-Graphical Methods for Determining the Passive Resistance in Soils

The actual surface of rupture may be approximated by combining either an arc of a circle or logarithmic spiral with straight line. Two semi-graphical methods for determining the passive resistance will be discussed below. In both cases the upper part of the composite slip surface is a straight line inclined at an angle $45 - \phi/2$ with the horizontal (Fig. 7.17).

7.2.5.1 The ϕ - circle Method

In this method the curved part of the slip surface is taken to be an arc of a circle. For the sake of calculation, cohesive and non-cohesive soils are treated separately.

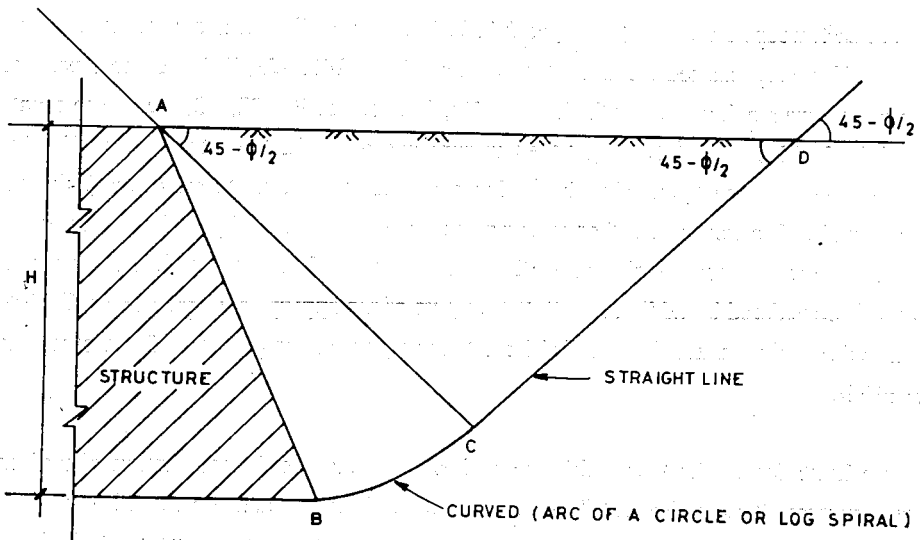


Fig. 7.17 Slip surface

7.2.5.1.1. Cohesionless Soils

Considering Fig. 7.18, if a line FC is drawn vertical from C, then the effect of FCD can be represented by Rankine's passive force,

$$P'_p = \frac{1}{2} \gamma (FC)^2 K_p$$

The problem at hand thus resolves itself into a study of the equilibrium of the portion of the wedge ABCF. According to the method in question, the curved portion BC is considered as an arc of a circle. At point C, the line CD must be tangent to the circular arc BC. From geometry, the center of the arc lies on the line CL and it must be so located that it passes through B.

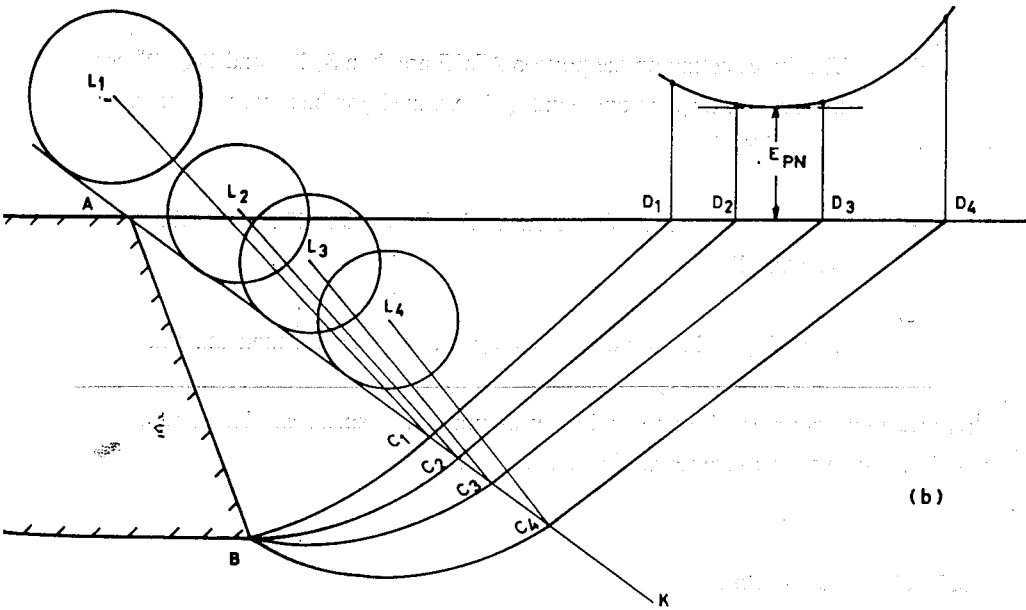
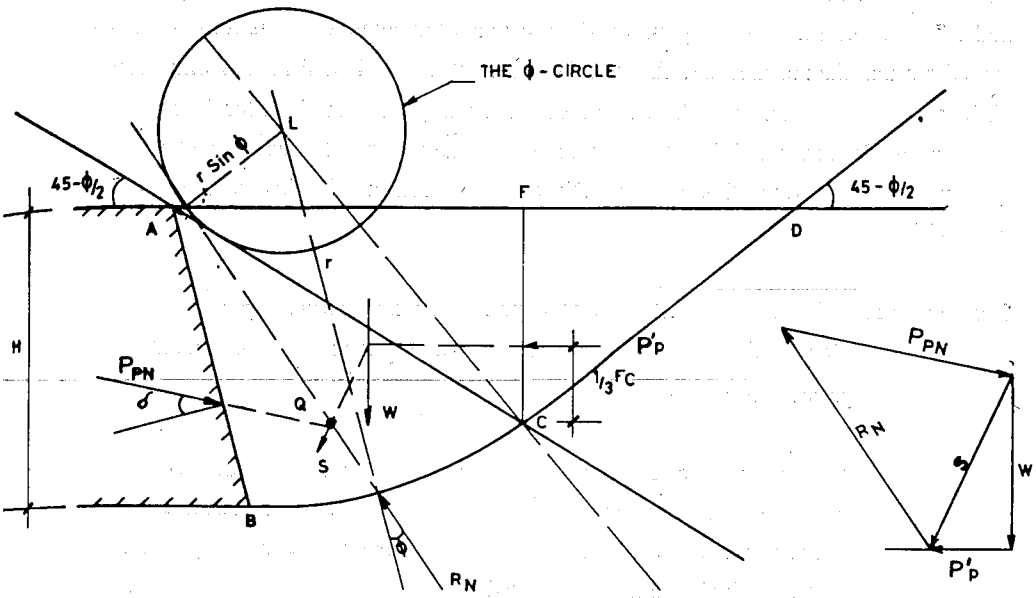


Fig. 7.18 the ϕ -circle method for cohesionless soil.

At the point of failure the full frictional resistance of the cohesionless soil will be mobilized and the resisting force at any point on BC must act at an angle ϕ to the normal. Along the curved portion, the normals pass through the center of the circle and the resisting forces must all be tangent to a smaller circle whose radius is $r \sin \phi$. The circle is the *friction circle* or ϕ - circle. It is assumed that the resultant of all the resisting forces is also tangent to the ϕ - circle. Eventhough this is not strictly true, it is sufficiently close to the reality and is acceptable.

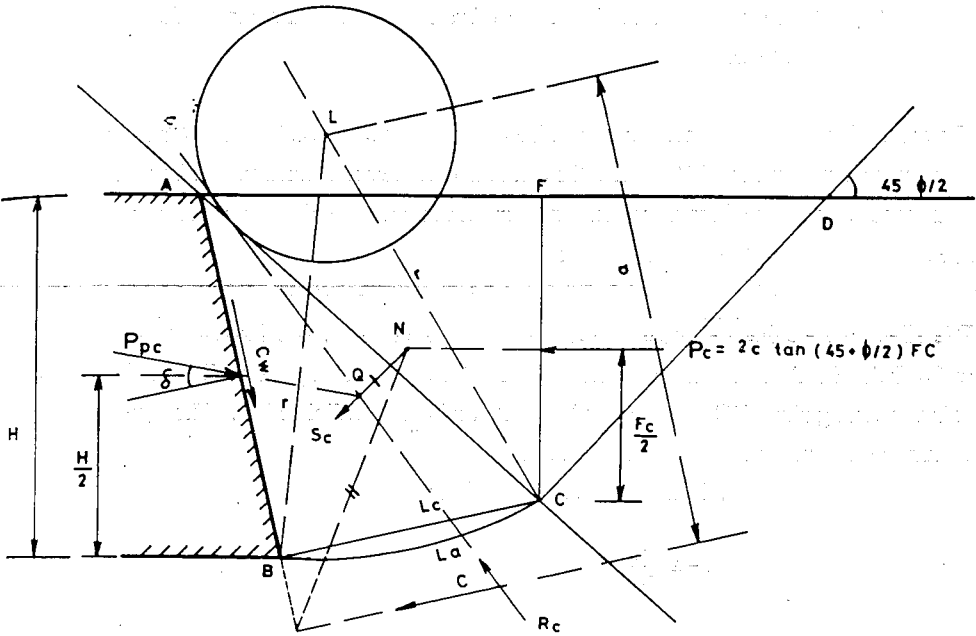
For determining the passive resistance one should follow the following procedure [3]

- a) Measure the vertical line FC and calculate P_p from Rankine's equation for the passive case.
- b) Measure the area ABCF and calculate the weight W. The centroid of the area may be obtained by cutting out a cardboard template and suspending it freely from several points in turn. Vertical lines through these points pass through the centroid which can thus be located.
- c) Combine these graphically to give the resultant S.
- d) The forces acting on the portion ABCF are then S, R_N and P_{PN} . These forces must all act through one point Q determined graphically by the intersection of P_{PN} and S.
- e) Draw a line through Q tangent to the ϕ - circle. This is the direction of the resultant R_N .
- f) Draw P_{PN} and R_N on the force diagram and scale off their magnitudes.

This procedure is repeated for several other assumed slip surfaces. The least value of P_{PN} would then give the passive resistance (Fig.7.18b).

7.2.5.1.2. Cohesive Soils

Soils possessing both cohesion and friction show less active pressure and more passive resistance than cohesionless soils other factors remaining the same.



$$P_c = 2c \tan(45^\circ + \phi/2) FC$$

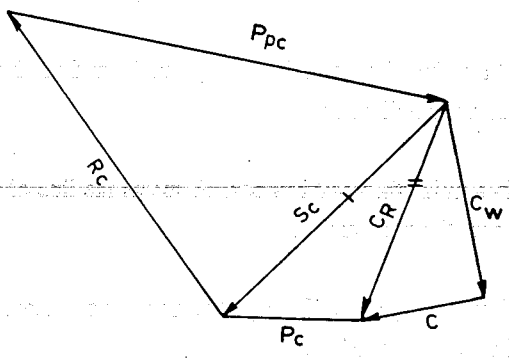


Fig. 7.19 The ϕ -circle method for cohesive soils

For convenience, the passive resistance of cohesive soils is considered to be made up of

- a) the resistance due to the weight of the wedge and/or any surcharge
- b) the resistance offered by the cohesive forces along the slip surface and the back of the wall.

The evaluation of (a) is the same as for cohesionless soils discussed above. The evaluation of (b) is as indicated in Fig. 7.19. Since the soil is in compression, tension cracks do not develop at the surface and hence, the cohesive forces are assumed to be distributed uniformly over the back of the wall and the curved portion BC.

The effect of the cohesive forces on CF can be replaced by P_c . The force P_c acts at a distance of $1/2 FC$. Similarly P_{pc} acts at a distance of $H/2$. C_w acts along the wall AB. The resultant cohesion acting along BC is given by $C = L_c \cdot c$ and acts parallel to BC. The line of action of C may be determined by taking moment at L .

$$c \cdot L_a \cdot r = c \cdot L_c \cdot a, \text{ thus giving}$$

$$a = r \frac{L_a}{L_c}$$

The steps necessary to determine the passive resistance due to cohesion are outlined as follows [3]:

- a) Obtain the value of C_w , C , and P_c by calculation.
- b) Draw the triangle of forces C , and C_w and mark resultant C_r in its position on the wedge diagram.
- c) Determine the point N where P_c meets the line of action of the resultant C_r and draw the resultant S_c .
- d) S_c meets P_{pc} at Q . Through Q draw a line tangent to the ϕ - circle. This is the line of action of R_c .
- e) Complete the force polygon and determine the value of P_{pc} .

The total passive resistance $P_{PT} = P_{PC} + P_{PN}$. The point of action of P_{PT} is found by taking moments.

7.2.5.2 The Logarithmic Spiral Method [30]

Instead of an arc of a circle, the slip surface BC is substituted by a logarithmic spiral (Fig. 7.20) whose equation is $r = r_0 e^{\theta \tan \phi}$. Since point C is the point of tangency, the center of the spiral will be located on the line ACK. From the equation of a logarithmic spiral the radius of the spiral makes angle of ϕ with the normal where it intersects the curve. The resultant force R_N also makes an angle of ϕ with normal and it passes through the center of the Spiral O.

Like in the previous cases, the problem in question will be divided into two segments namely,

- the passive resistance for cohesionless soil and
- the passive resistance for cohesive soil

(a) Cohesionless Soils

One selects arbitrarily the surface of sliding BCD, where BC is a part of logarithmic spiral with its center at O (Fig. 7.20a). The forces acting on the element ABCF are the weight, W, the passive resistance, P'_p , the reaction R_N and the passive force P_{PN} .

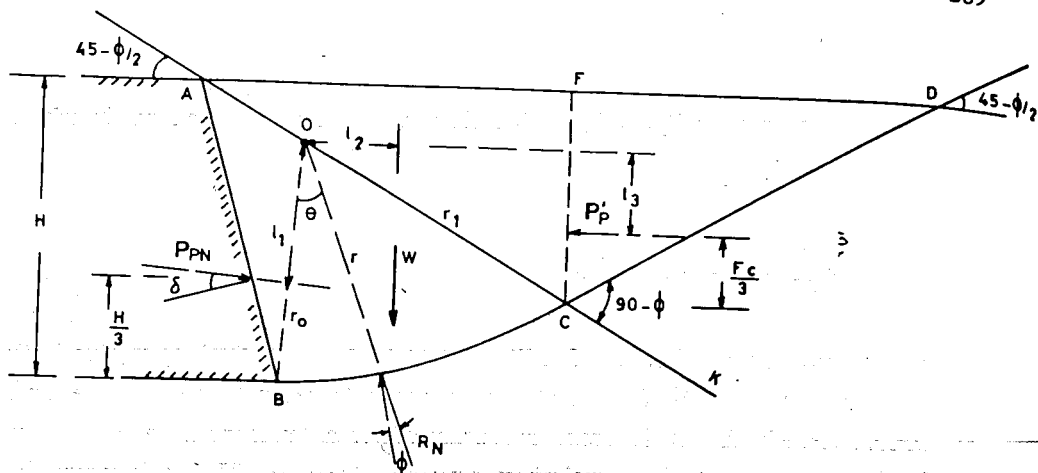
$$P'_p = \frac{1}{2} \cdot (CF)^2 \cdot K_p$$

R_N is unknown in magnitude, however, it passes through O. The weight of the element, W, is determined from the area and its unit weight, P_{PN} , is known in direction only.

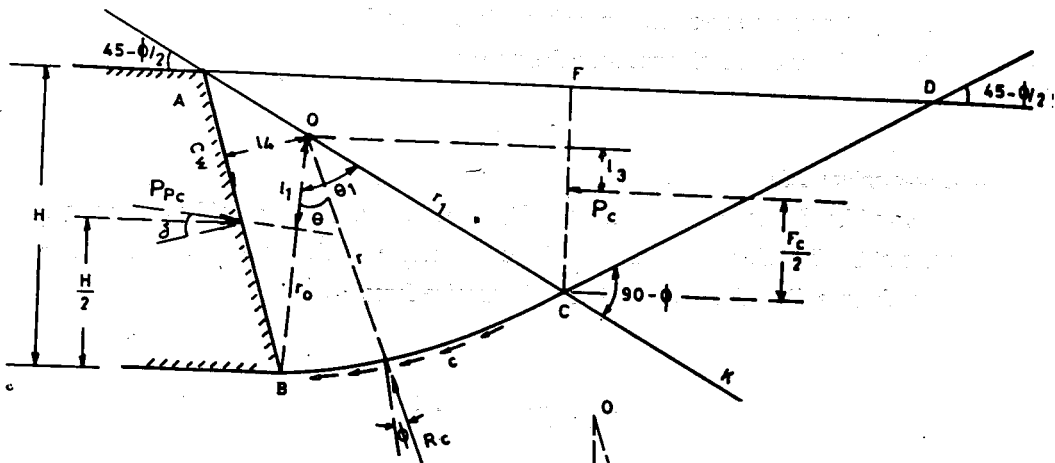
Taking moments about O, $P_{PN} \ell_1 - W \cdot \ell_2 - P'_p \ell_3 = 0$

$$P_{PN} = \frac{W \ell_2 + P'_p \ell_3}{\ell_1} \quad (7.18)$$

The value of P_{PN} is plotted above F. Other surfaces of sliding are tried.



(a) COHESIONLESS SOIL



(b) COHESIVE SOIL

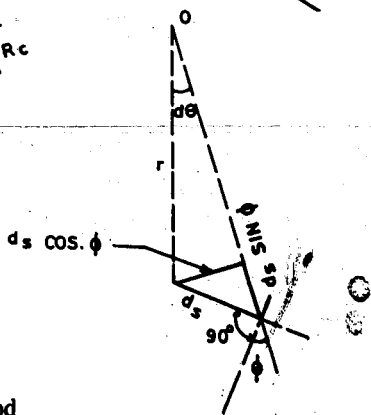


Fig. 7.20 The logarithmic spiral method

(b) Cohesive Soils

The cohesion along BC can be calculated using Fig. 7.20b. The cohesion on ds is given by $c \cdot ds$. The moment of the cohesion about O may be written as $dM_c = r c ds \cos \phi$.

One may approximately state that $r d\theta = ds \cos \phi$. Hence, $ds = \frac{rd\theta}{\cos \phi}$

Therefore,

$$dM_c = rc \cdot \frac{rd\theta}{\cos \phi} \cdot \cos \phi = r^2 c d\theta \quad (7.19)$$

Integration of Eq. (7.19) gives the following

$$M_c = \int_0^{\theta_1} r^2 c d\theta = \frac{c}{2 \tan \phi} (r_1^2 - r_0^2) \quad (7.20)$$

Taking moments about O,

$$P_{FC} \cdot \ell_1 - M_c - P_c \cdot \ell_3 + C_w \ell_4 = 0 \quad (7.21)$$

$$P_{FC} = \frac{M_c + P_c \cdot \ell_3 - C_w \cdot \ell_4}{\ell_1} \quad (7.22)$$

For soils possessing both friction and cohesion, the values of P_{FN} and P_{FC} are added and the results plotted above F. This should be repeated for many slip surfaces till the minimum $P_{FT} = P_{FN} + P_{FC}$ is obtained.

7.2.6. Tables for Active and Passive Pressures

There are various tables and curves available for determining the active and passive pressures, Jumikis [14], Kezdi [15], (Krey [16]. etc..) each with a certain degree of limitations. For preliminary design, values presented in Table 7.2 and Table 7.3 may be used.

Table 7.2 Active earth pressure coefficient K_{ah} (horizontal component) for vertical wall, horizontal fill and $\delta = +2/3 \phi$ and a plane slip surface [21]

ϕ	K_{ah}	ϕ	K_{ah}
deg	-	deg	-
2.5	0.89	20.0	0.43
5.0	0.80	22.5	0.38
7.5	0.72	25.0	0.35
10.0	0.65	27.5	0.31
12.5	0.58	30.0	0.28
15.0	0.52	32.5	0.25
17.5	0.47	35.0	0.22
		37.5	0.20

Table 7.3 Passive earth pressure coefficient K_{ph} (horizontal component) for vertical wall, horizontal fill and $\delta = -\phi$ and a circular slip surface [21]

ϕ	K_{ph}	ϕ	K_{ph}
deg	-	deg	-
2.5	1.12	20.0	3.01
5.0	1.28	22.5	3.53
7.5	1.46	25.0	4.15
10.0	1.67	27.5	4.75
12.5	1.92	30.0	5.88
15.0	2.22	32.5	7.10
17.5	2.58	35.0	8.40
		37.5	10.5

7.2.7 Earth Pressure at Rest

As defined earlier the earth pressure at rest exists when there is no lateral yielding. In this condition, the soil is in elastic equilibrium. The lateral pressure is given by,

$$\sigma_h = \frac{\mu}{1-\mu} \sigma_v$$

where $\sigma_v = \gamma z$

(7.23a)

$$P_o = \sigma_h = \frac{\mu}{1-\mu} \gamma z = K_o \gamma z$$
(7.23b)

Where

- K_o = coefficient of earth pressure at rest
- μ = Poisson's ratio. For sand and normally consolidated clays K_o can be represented by the empirical relation $K_o = 1 - \sin \phi$.

Table 7.4 Typical values of K_o [9]

Soil type	K_o
Loose sand, gravel	0.6
Dense sand, gravel	0.4
Sand, tamped in layers	0.8
Soft clay	0.6
Hard clay	0.5

The value of K_o depends on the relative density of sands and the process by which the deposit was formed.

7.3. SHEET PILES

7.3.1 General

Sheet piles are types of retaining walls which are frequently used where the construction of concrete, masonry, etc. retaining walls are not feasible. They are often used as water front

structures in harbours to support deep trenches. etc.. The materials for sheet piling may either be wood or steel depending on the purpose for which they are intended to be used.

7.3.2 Types of Sheet Piles

With regard to their structural functions, sheet piles can be categorized into two types. Namely, cantilever sheet piles and anchored sheet piles (anchored bulkheads).

7.3.2.1 Cantilever Sheet Piles

Cantilever sheet piles are normally used when the height of the earth to be retained is small. The piles that are driven into the ground have cantilever action. Here the active earth pressure is fully mobilized (Fig. 7.21) and it must be resisted by the development of passive resistance that constitutes the necessary fixing moment for the cantilever. If the wall undergoes small angular rotation about point C at a distance x from D, passive resistance will be mobilized along BC and CD. The theoretical pressure distribution would be as shown in Fig. 7.21 (b).

The minimum driving depth d for equilibrium can be determined by solving simultaneously two equations in which x and d are the unknowns, $\Sigma H=0$ and $\Sigma M_D=0$. The solution can be simplified, by assuming the passive reaction P_{p2} as a concentrated force at the foot of the pile. The simplified arrangement is shown in Fig. 7.21c.

For equilibrium, the moments of the active pressure on the right and the passive resistance on the left about the point of action of P_{p2} must balance

$$P_{p1} \cdot \frac{d}{3} - P_A \frac{(h+d)}{3} = 0$$

Noting that,

$$P_{p1} = \frac{1}{2} K_p \gamma d^2$$

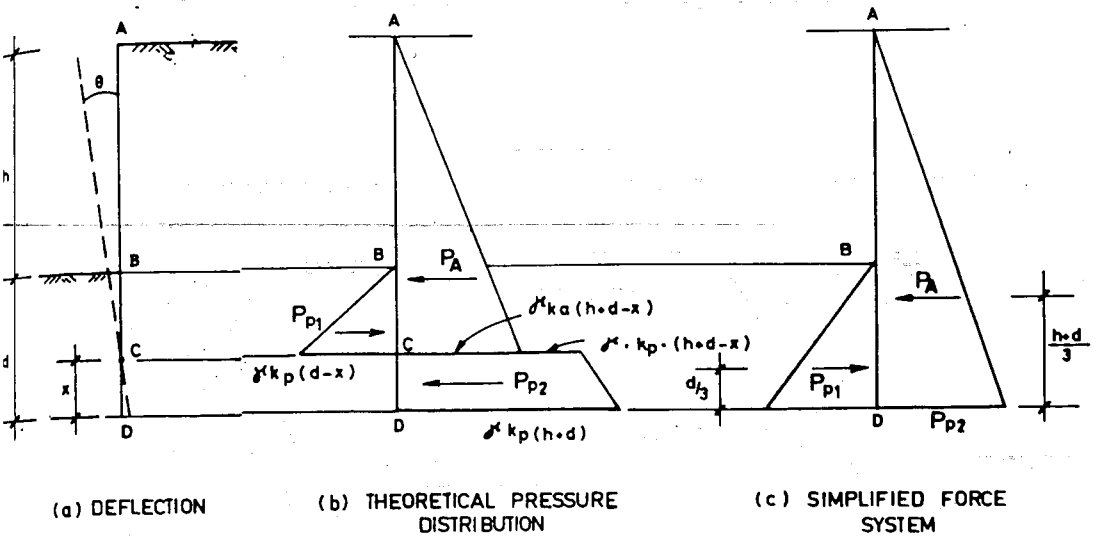


Fig. 7.21 Cantilever sheet pile

$$P_A = \frac{1}{2} K_a \gamma (h+d)^2 \quad (7.24a)$$

$$K_p d^3 - K_a (h+d)^3 = 0 \quad (7.24b)$$

The solution of Eq. (7.24) gives a guide to the driving depth required. The depth thus calculated is normally increased by 20% to provide a margin of safety and to allow extra length for the development of the passive force P_{p2} .

7.3.2.2 Anchored Sheet Piles

7.3.2.2.1 General

These are a system of sheet pile walls held in tact by tie-rods anchored into the soil (Fig. 7.22).

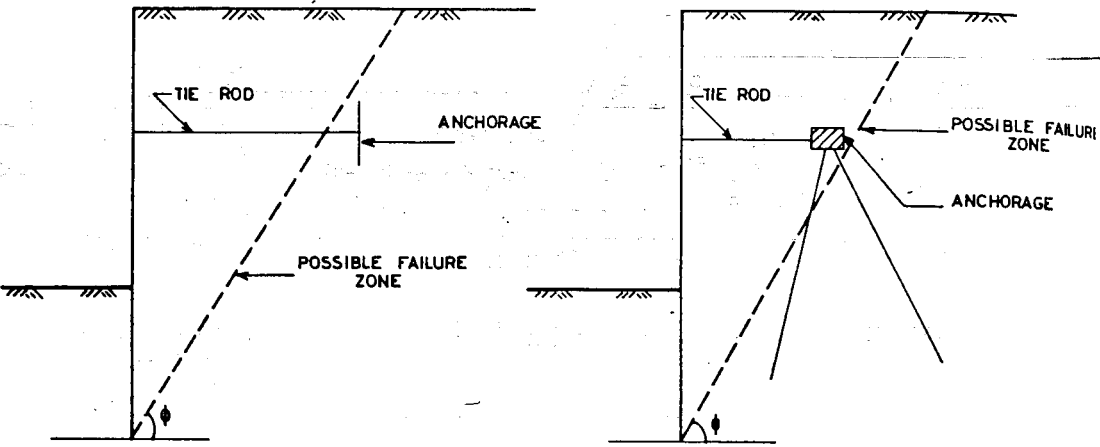


Fig. 7.22. Anchorage systems for sheet pile walls.

The stability of these piles does not depend so much on the development of large passive pressure as it is the case in cantilever sheet piles. Here the driving depth is generally smaller in proportion to the depth of retained soil.

The principal methods of analysing the equilibrium of anchored piling are based on one of two assumptions related to the method of support of the driven end. These are known as the *free earth support* and the *fixed earth support* methods respectively.

7.3.2.2.2 Free Earth Support Method

Here the wall is assumed to rotate freely about its base and freely supported near the top by the anchorage force and below the ground level by the passive resistance (Fig. 7.23).

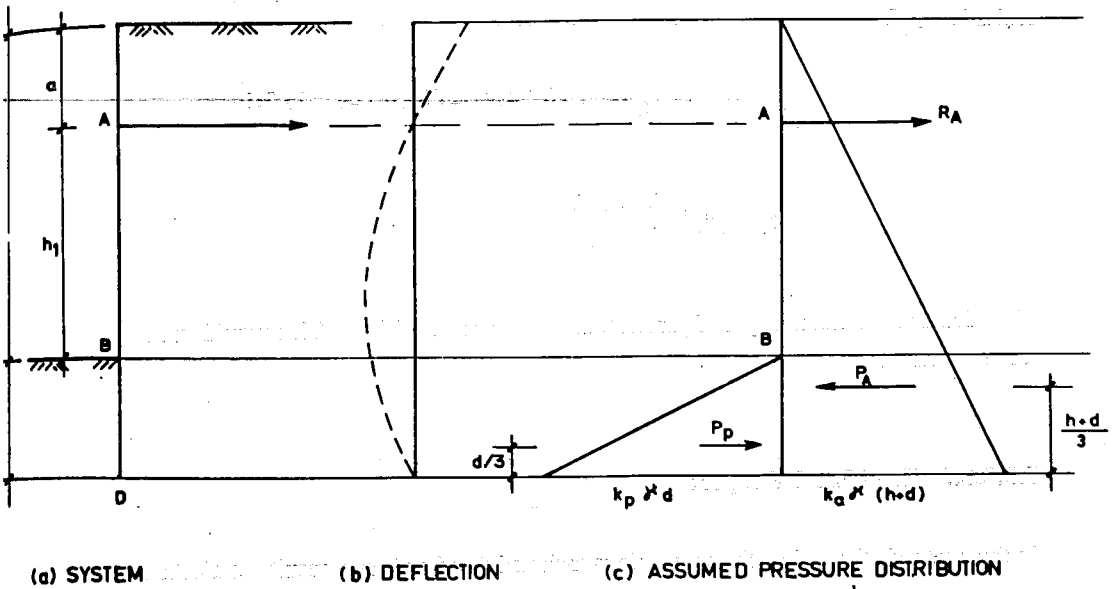


Fig. 7.23 The free-earth support method.

Let d be the minimum depth required for stability. Since

$$P_p = \frac{1}{2} K_p \gamma d^2 \text{ and } P_a = \frac{1}{2} K_a \gamma (h+d)^2, \text{ taking moments about A, gives}$$

$$\begin{aligned} \frac{1}{2} K_p d^2 (h_1 + 2/3d) &= \frac{1}{2} K_a \gamma (h+d)^2 \left[\frac{2}{3} (h+d) - (h-h_1) \right] \\ &= \frac{1}{2} K_a \gamma (h+d)^2 (2/3d - 1/3h + h_1) \end{aligned} \quad (7.25)$$

The above cubic equation is normally solved by trial by assigning values to d . The force in the anchor ties can be found by taking moments about the line of action of the passive resistance P_p .

$$\begin{aligned} R_A (h_1 + 2/3d) &= \frac{1}{2} K_a \gamma (h+d)^2 \left[\frac{1}{3} (h+d) - 1/3d \right] \\ R_A &= \frac{K_a \gamma (h+d)^2 h}{6 (h_1 + 2/3d)} \end{aligned} \quad (7.26)$$

The calculated minimum depth of penetration is increased by 20%. This would influence the force on the ties.

7.3.2.2.3 Fixed Earth Support

In this method, the end of the sheet pile is assumed fixed and as a result the elastic line will be as indicated in Fig.(7.24).

If point C is considered as a hinge transmitting shear only, the bending moment at this point is zero. Hence, the structure may be regarded as two separate beams, AC and DC. The force R_c is the reaction at the hinge. This method is called the equivalent beam method.

The procedure of analysis is as follows:

- a) The position of C is estimated from the relationship that exists between the angle of internal friction ϕ the distance y [3] as indicated in Table 7.5

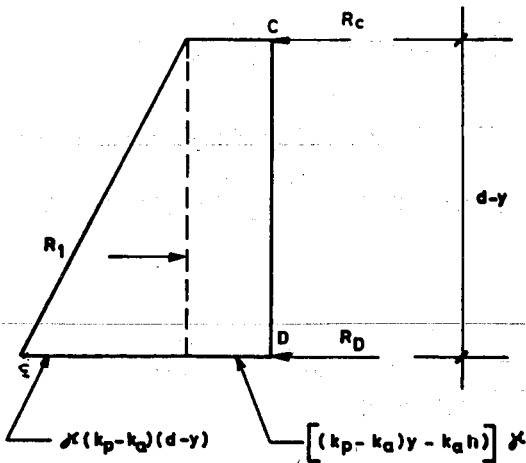
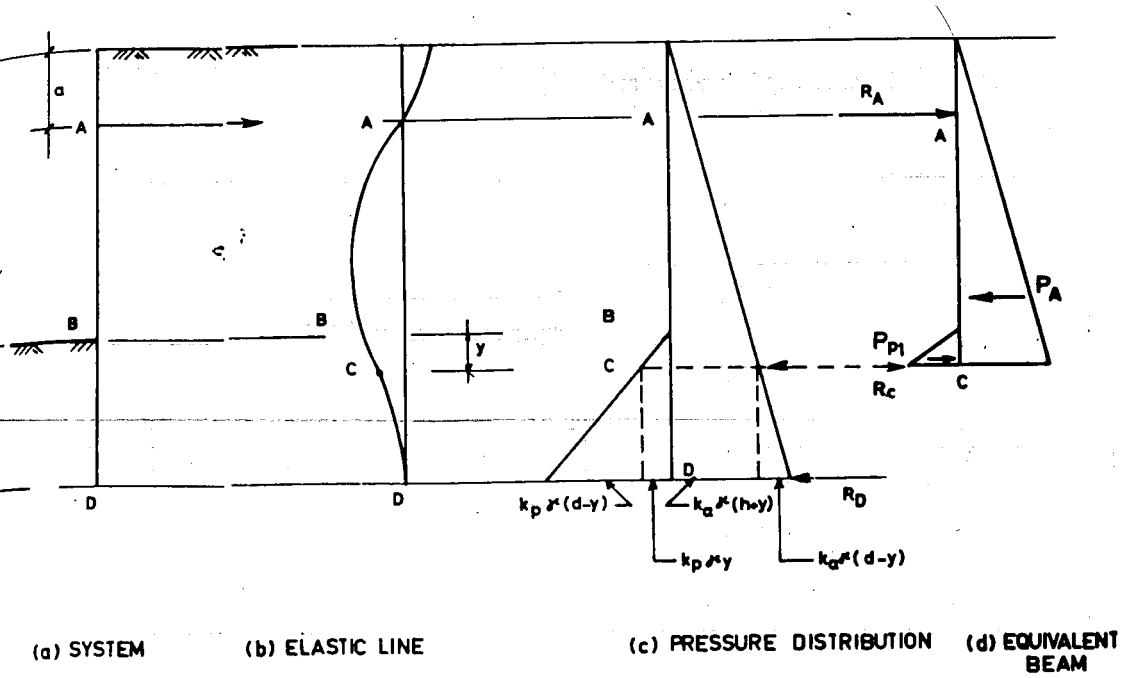


Fig. 7.24 Fixed-earth support method.

Table 7.5 Relationship between ϕ and y [3]

ϕ	y	
20°	0.25h	For normal frictional soils it is sufficient to use $y = 0.1h$
25°	0.15h	
30°	0.08h	
35°	0.035h	
40°	-0.006h	

b) The forces on the upper beam AC are calculated from the active and passive pressures.

$$P_A = \frac{1}{2} K_a \gamma (h+y) \text{ and } P_P = \frac{1}{2} K_p \gamma y^2$$

c) The reaction R_c at the "hinge" C is found by taking moments of forces about A.

$$R_c (h+y-a) + \frac{1}{2} K_p \gamma^2 y (h-a+2/3y) - \frac{1}{2} K_a \gamma (h+y)^2 [2/3 (h+y) - a] = 0$$

$$R_c = \frac{\frac{1}{2} K_a \gamma (h+y)^2 \left[\frac{2}{3} (h+y) - a \right] - \frac{1}{2} K_p \gamma^2 (h-a + \frac{2}{3} y) y}{(h+y-a)} \quad (7.27a)$$

The anchor force R_A is found either by taking moments about C or from

$$\sum R_A + P_A + P_P + R_c = 0 \quad (7.27b)$$

d) The loads on the beam CD are represented by trapezoidal pressure areas, which can be divided into rectangles and triangles, giving the net distribution indicated in Fig. 7.24c. Taking moments about D,

$$R_c (d-y) = \frac{1}{2} (K_p - K_a) \gamma \frac{(d-y)^3}{3} + [(K_p - K_a) \gamma - K_a h] \gamma \frac{(d-y)^2}{2} \quad (7.28a)$$

Re-arranging terms, one obtains

$$\frac{6R_c}{(K_p - K_a) \gamma} = (d-y)^2 + \left(3y - \frac{3K_a h}{K_p - K_a} \right) (d-y) \quad (7.28b)$$

Solving Eq. (7.28b) as a quadratic in (d-y) one obtains,

$$d-y = \frac{3}{2} \left(\frac{K_a}{K_p - K_a} h - y \right) + \sqrt{\frac{9}{4} \left(y - \frac{K_a h}{K_p - K_a} \right)^2 + \frac{6R_c}{\gamma (K_p - K_a)}} \quad (7.28c)$$

$$\text{or } d = \frac{3}{2} \left(\frac{K_a}{K_p - K_a} \right) h - \frac{y}{2} + \sqrt{\frac{9}{4} \left(y - \frac{K_a h}{K_p - K_a} \right)^2 + \frac{6R_c}{\gamma (K_p - K_a)}} \quad (7.28d)$$

The first term under the root in Eq. (7.28d) is very small compared with the second and may be neglected. Hence,

$$d = \frac{3}{2} \left(\frac{K_a}{K_p - K_a} \right) h - \frac{y}{2} + \sqrt{\frac{6R_c}{\gamma (K_p - K_a)}} \quad (7.28e)$$

Substituting the appropriate values of y and R_c in Eq. (7.28e), one determines the minimum driving depth d.

As in the case of cantilever sheet piling the calculated driving depth should be increased by 20% to allow for the fact that the lower passive resisting force R_D is not a knife-edge reaction as assumed in the simplified calculation.

7.3.3 Graphical Methods of Analysis

The penetration depth and the forces in the tie rods may also be determined graphically according to Blum's method [1] as outlined below (Fig. 7.25).

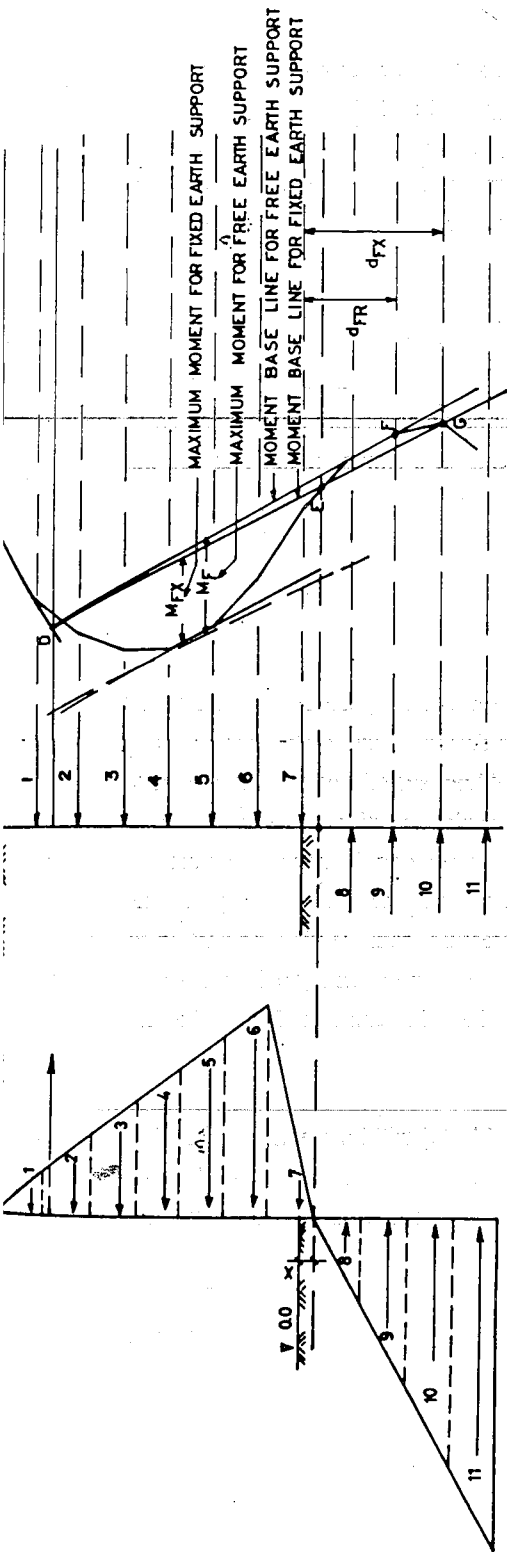
- a) Draw the active and passive forces acting on the sheet pile wall for some assumed penetration depth. Divide the loaded area into horizontal strips and determine the total force on each strip. The respective force acts at the center of gravity of each strip (Fig. 7.25a). The point of zero loading which is at a distance x from the ground level is determined from:

$$x = \frac{P_a}{\gamma (K_a - K_p)} . \text{ The value of } P_a \text{ is at elevation 0.0 (Fig. 7.25a).}$$

- b) Construct a vector diagram for each of the forces acting on the wall along a base line (Fig. 7.25b).
- c) Select a pole point O about the base line having a pole distance of about $\frac{1}{4} (\sum F_1 + F_2 + \dots + F_7)$ and draw the rays (Fig. 7.25b).
- d) Project horizontal lines through the center of gravity of each strip and then construct the bending moment polygon. Draw a line parallel to ray $O-0$ to cut the tensile line at D (Fig. 7.25c).

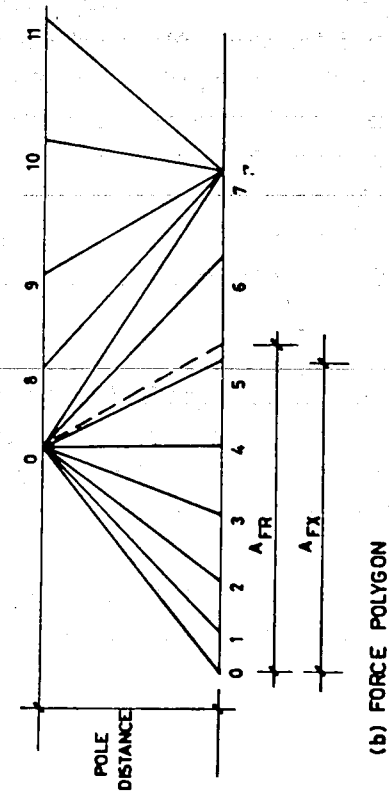
7.3.4 Comparison Between Free Earth and Fixed Earth Support Methods

The difference between the two methods is clearly illustrated by the respective magnitudes of the depth of penetration and the span moments. The depth of penetration in the free earth support method is smaller than in the fixed earth support method. The span moment, however, is substantially bigger in the free earth support.



(a) PRESSURE DISTRIBUTION

(c) MOMENT DISTRIBUTION



(b) FORCE POLYGON

Fig. 7.25 Blum's graphical method.

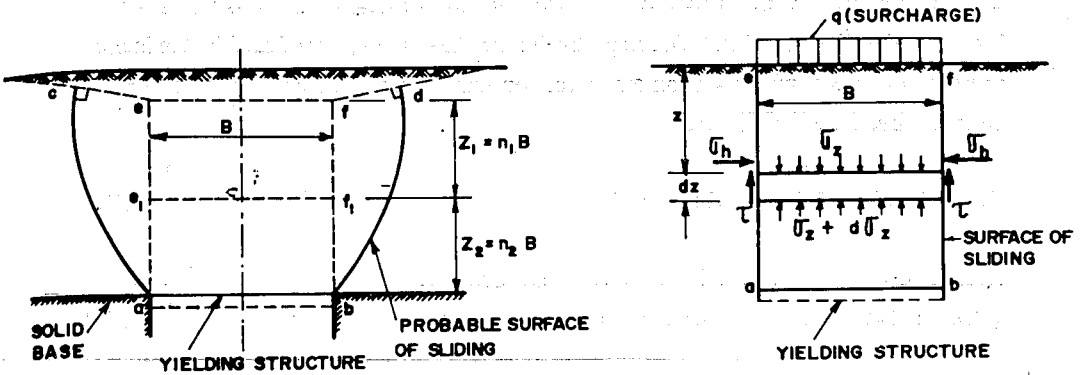
- e) From D draw a base line tangential to the moment diagram and establish point F. The distance from F to the ground surface gives the penetration depth according to the Free-Earth support method. The tie force in the rod is determined by drawing a line from O parallel to the base line of the moment diagram to cut the base line of the vector diagram. Measure the distance (Fig. 7.25b).
- f) Through the point of zero-loading, draw a horizontal line to cut the moment diagram at E. From D, draw a line DEG. The distance from the ground level to point G gives the depth of penetration according to the fixed earth support method. The tie force is determined in a similar manner as for the case of Free-Earth support method (Fig. 7.25b).

7.4 ARCHING EFFECT

Before concluding the discussion on earth pressure, it is appropriate to introduce arching phenomenon that plays a considerable role in the design of buried structures. If a portion of a buried structure yields, the soil resting on the yielding part of the structure moves out of line from the adjoining soil mass which stays in its original position. The relative movement of the soil would cause the development of shear resistance along the zone of contact between the yielding and the non-yielding masses. This shearing resistance tends to keep the yielding soil in its original position and as a result transfers pressure from the yielding part on to the stationary part of the soil mass. This transfer of pressure from a yielding mass of soil onto adjoining stationary parts is called *arching effect*. The soil is said to arch over the yielding part of the support.

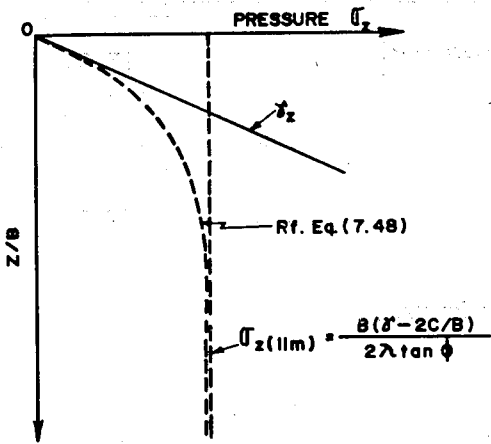
In the following pages the simple theory of Terzaghi [29] will be presented. The fundamental assumption in his theory is the existence of vertical sliding surface ae and bf rather than the probable surface of sliding ac and bd (Fig. 7.26a). It should also be noted that the soil mass is considered to be incompressible.

Consider the equilibrium of a slice dz per unit length perpendicular to the plane of the figure at a distance z from the top (Fig. 7.26b).

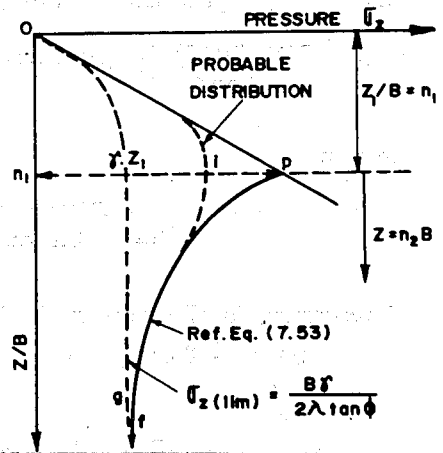


a) FAILURE CAUSED BY YIELDING OF STRUCTURE IN SAND ACCORDING TO TERZAGHI

b) SIMPLIFIED THEORY OF ARCHING ASSUMING VERTICAL SURFACES OF SLIDING ca AND bf



c) VERTICAL PRESSURE DISTRIBUTION DUE TO ARCHING-YIELDING STRUCTURE AT SHALLOW DEPTH.



d) VERTICAL PRESSURE DISTRIBUTION DUE TO ARCHING IN SAND-YIELDING STRUCTURE AT GREAT DEPTH

Fig.7.26 Terzaghi's theory of arching.

The force acting are the weight of the slice, dw ; the vertical earth pressure at the top and bottom of the slice σ_z and $\sigma_z + d\sigma_z$ respectively; the shear strength produced by the lateral earth pressure $\sigma_h = \lambda\sigma_z$ where λ is an empirical constant. Taking the summation of force in the vertical direction equal to zero,

$$dw + B\sigma_z = B(\sigma_z + d\sigma_z) + 2\tau dz \quad (7.29a)$$

Since $dw = \gamma B dz$ and $\tau = c + \sigma_h \tan \phi$,

$$\gamma B dz + B\sigma_z = B\sigma_z + B d\sigma_z + 2cdz + 2\lambda\sigma_z \tan \phi dz. \quad (7.29b)$$

After simplification and arrangement of terms, one obtains

$$\frac{d\sigma_z}{dz} = \gamma - \frac{2c}{B} - \frac{\lambda\sigma_z \tan \phi}{B} \quad (7.29c)$$

From the boundary conditions,

at $z = 0$, $\sigma_z = q$ and solving the differential equation one obtains the following expression:

$$\sigma_z = \frac{B(\gamma - 2c/B)}{2\lambda \tan \phi} \left[1 - e^{-2\lambda(z/B) \tan \phi} + q e^{-2\lambda(z/B) \tan \phi} \right] \quad (7.30)$$

For $z = \infty$

$$\sigma_{z_{lim}} = \frac{B(\gamma - 2c/B)}{2\lambda \tan \phi} \quad (7.31)$$

Investigating Eq. (7.30) one would observe the following

(i) for $c = 0$ and $q = 0$

$$\sigma_z = \frac{B\gamma}{2\lambda \tan \phi} \left(1 - e^{-2\lambda(z/B) \tan \phi} \right) \quad (7.32)$$

(ii) For $c = 0$ and $q \neq 0$

$$\sigma_z = \frac{B\gamma}{2\lambda \tan \phi} \left(1 - e^{-2\lambda(z/B) \tan \phi} + q e^{-2\lambda(z/B) \tan \phi} \right) \quad (7.33)$$

(iii) For $c \neq 0$ and $q = 0$

$$\sigma_z = \frac{B(\gamma - 2c/B)}{2\lambda \tan \phi} \left[1 - e^{-2\lambda(z/B) \tan \phi} \right] \quad (7.34)$$

(iv) $\phi = 0$

$$\sigma_z = (\gamma - 2c/B) z + q \quad (7.35)$$

Terzaghi reports that experimental investigations in sand have indicated that at elevations of more than about $5B$ above the level of the structure, the yielding of the structure seems not to have any effect on the stress distribution. This would imply that above this height, the shearing resistance is not mobilized and no arching effect is felt. One may then consider the weight of the column of soil as a surcharge q and the stress may be calculated from Eq. (7.33). If $z_1 = n_1 B$ is the depth in which there is no shear strength mobilization, the vertical pressure acting on $e_1 f_1$ is $q = \gamma z_1 = \gamma n_1 B$ (Fig. 7.26a).

Introducing the new value of q and assigning $z = z_2 = n_2 B$ to Eq. (7.33), one obtains

$$\sigma_v = \frac{B\gamma}{2\lambda \tan \phi} \left[1 - e^{-2\lambda n_2 \tan \phi} + \gamma n_1 B e^{-2\lambda n_2 \tan \phi} \right] \quad (7.36)$$

A plot z/B versus σ_z for depths within n and $z = n_1 B$ is shown in Fig. (7.26d). The line op represents the linear distribution of the vertical stress and curve pf is the distribution according to Eq. (7.36). Og is for the condition $n_1 = 0$ which is similar to the curve in Fig. 7.26c. Curve oif represents the probable distribution of the vertical pressure for the condition under consideration.

For the case of a tunnel in sand, the state of the stress is similar to the above derived equations. In this particular case, the sides of the tunnel yield causing a failure zone corresponding to the active Rankine state and form a sliding surface inclined at an angle of $45 + \phi/2$ from the horizontal or $45 - \phi/2$ from the vertical. At the level of the roof of the tunnel, the width of the yielding strip is,

$$B_1 = B_o + 2 \left[H_o \tan (45 - \phi/2) \right] \quad (7.37)$$

It is assumed that the yielding lines are vertical as indicated by $e_1 b_1$ in Fig. 7.27a.

By replacing B by B_1 , z/b by H/B_1 , the vertical pressure on level $b_1 - b_1$ would then be determined from Eq.(7.32).

$$\sigma_v' = \frac{B_1 \gamma}{2\lambda \tan \phi} \left(1 - e^{-2\lambda H/B_1 \tan \phi} \right) \quad (7.38)$$

If the tunnel is located at great depths, then up to H_2 , there will be no arching effect and the vertical pressure at this level would be $q = H_2$ (Fig.7.27c). Beyond this depth, arching is effective and the vertical pressure on the wall of the tunnel would be determined from Eq. (7.33). Replacing B by B_1 ; q by H_2 γ and z by H_1

$$\sigma_v'' = \frac{B_1 \gamma}{2\lambda \tan \phi} \left[1 - e^{-2\lambda H_1/B_1 \tan \phi} \right] + \gamma H_2 e^{2\lambda H_1/B_1 \tan \phi} \quad (7.39)$$

If H_1 increases and reaches the value of $1/5$ of $(H_1 + H_2)$, then beyond this depth the second expression of the above equation becomes negligible and the expression within the bracket approaches the value of 1. Hence, at great depth the limiting value of the vertical pressure would be

$$\sigma_{z_{11a}} = \frac{b_1 \gamma}{2\lambda \tan \phi} \quad (7.40)$$

7.5 EXAMPLES

- E.7.1 Compute the active earth pressure at the base of a retaining wall 5m in height. Take the backfill material as sand whose angle of internal friction is 37° and unit weight in dry state is 15.6 kN/m^3 . Assuming that the water table is located at a depth of 1.5m below the ground surface, compute the active earth pressure at the base of the wall and the resultant thrust per linear meter of wall and its location. Take the saturated unit weight of sand as 19.85 kN/m^3 .

SOLUTION

- (a) For the dry condition,

$$P_a = K_a \gamma H$$

$$K_a = \frac{1 - \sin \phi}{1 + \sin \phi} = \frac{1 - \sin 37}{1 + \sin 37} = 0.24$$

$$P_a = 0.248 (15.6 (5)) = 19.38 \text{ kN/m}^2$$

(b) For the case of partial submergence

Depth of sand below the water table = $5 - 1.5\text{m} = 3.5\text{m}$

$$\gamma_b = \gamma_{\text{sat}} - \gamma_w = 19.85 - 10 = 9.85\text{kN/m}^3$$

$$P_{a1} \text{ due to dry sand} = K_a \gamma H_1 = (0.248)(9.85)(3.5) = 8.55\text{ kN/m}^2$$

$$P_a \text{ due to water} = \gamma_w H_2 = 10(3.5) = 35\text{kN/m}^2$$

$$P_a \text{ due to dry sand} = K_a \gamma H_1 = 0.248(15.6)(1.5) = 5.80\text{kN/m}^2$$

Resultant thrust per linear meter (kN/m)	Moment Arm from the base (m)	Moment (kN-m)
$P_{A1} = \frac{P_{a1}}{2} (H_1) \cdot 1 = \frac{5.8}{2} (1.5) = 4.35$	$\frac{1.5}{3} + 3.5$	17.4
$P_{A2} = P_{a2} (H_2) \cdot 1 = 5.8 (3.5) = 20.30$	$\frac{3.5}{2}$	35.53
$P_{A3} = \frac{P_{a3}}{2} (H_2) \cdot 1 = \frac{8.55}{2} (3.5) = 14.96$	$\frac{3.5}{3}$	17.46
$P_{A4} = \frac{P_{a4}}{2} (H_2) \cdot 1 = \frac{35}{2} (3.5) = 61.25$	$\frac{3.5}{2}$	71.46
$\sum P_A = 100.86\text{kN/m}$	$\sum M = 141.85\text{kN-m}$	

$$x \sum P_A = \sum M$$

$$100.86 (x) = 141.85$$

$$x = \frac{141.85}{100.86} = 1.41\text{m}$$

Location of the resultant from the base of the wall = 1.41m

E.7.2 A masonry retaining wall with vertical back face is 4m high. It has a sandy backfill up to its top. The top of the fill is horizontal and carries a uniform surcharge of 85kN/m². Determine the lateral thrust per meter length of the wall, considering the backface of the wall as smooth

SOLUTION

Porosity, $n=30\%$

$$e = \frac{n}{1-n} = \frac{0.3}{1-0.3} = \frac{3}{7} = 0.4$$

$$\gamma_{\text{sat}} = \gamma_d(1+\omega) = 18.5(1.12) = 20.72 \text{ kN/m}^3$$

$$\gamma_b = \left(\frac{G-1}{1+e} \right) \gamma_w = \frac{2.65-1}{1.43} \gamma_w = \frac{2.65-1}{1.43} (10) = 11.54 \text{ kN/m}$$

$$K_a = \frac{1 - \sin 30^\circ}{1 + \sin 30^\circ} = \frac{1 - 0.5}{1 + 0.5} = \frac{1}{3} = 0.3$$

Computation of Active Earth Pressure

(a) Due to soil above water table

$$P_{a1} = K_a \gamma H_1 = 0.33 (20.72)(1) = 6.84 \text{ kN/m}^2$$

(b) Due to submerged soil

$$P_{a2} = K_a \gamma_b H_2 = 0.33(11.54)(3) = 11.43 \text{ kN/m}^2$$

c) Due to water

$$P_{a3} = \gamma_w H_2 = 10(3) = 30 \text{ kN/m}^2$$

(d) Due to surcharge pressure

$$P_{a4} = K_a \Delta P = 0.33(85) = 28.05 \text{ kN/m}^2$$

Computation of Resultant Thrust

$$P_{A1} = \frac{6.84}{2}(1) = 3.42 \text{ kN/m}$$

$$P_{A2} = \frac{11.43}{2}(3) = 17.15 \text{ kN/m}$$

$$P_{A3} = \frac{30}{2}(3) = 45.00 \text{ kN/m}$$

$$P_{A4} = 28.05(4) = 112.20 \text{ kN/m}$$

$$P_{A5} = 6.84(3) = 20.52 \text{ kN/m}$$

$$\sum P_A = 198.29 \text{ kN/m}$$

Resultant thrust = 198.29 kN/m

E.7.3 A retaining wall with smooth vertical backface has a purely cohesive backfill soil. The wall is 12m high and the backfill material has a unit weight of 20.4 kN/m^3 and a unit cohesion of 11 kN/m^2 . Compute the lateral thrust per linear meter of the wall. Determine also the depth of the tension crack and the location of the resultant from the ground surface.

SOLUTION

$$P_a = \gamma H K_a - 2c\sqrt{K_a}$$

For purely cohesive soil, $\phi = 0$

$$K_a = \frac{1 - \sin\phi}{1 + \sin\phi} = \frac{1 - 0}{1 + 0} = 1$$

$$P_a = \gamma H - 2c$$

At the ground surface, $h = 0$

$$P_a = -2c = -2(11) = -22 \text{ kN/m}^2$$

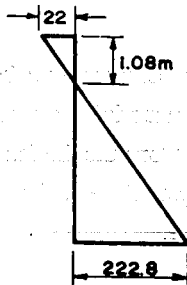
$$H_{cr} = \frac{2c}{\gamma}$$

$$= \frac{2(11)}{20.4} = 1.08$$

Depth of tension crack from the ground surface = 1.08m

At the bottom of the ground,

$$P_a = \gamma H - 2c = 20.4(12) - 2(11) = 222.8 \text{ kN/m}^2$$



Total thrust on the wall

$$= \frac{222.8}{2} \times (12 - 1.08)$$

$$= \underline{\underline{1216.49 \text{ kN/m}}}$$

Location of the resultant from the ground surface

$$= 1.08 + \frac{2}{3}(12 - 1.08)$$

$$= 1.08 + 7.28 = 8.36 \text{ m}$$

E.7.4 A retaining wall with vertical back is 8m high. The unit weight for the top 3m of fill is 18kN/m^3 and the angle of internal friction is 30° . For the lower 5m of fill the unit weight is 20kN/m^3 and the angle of internal friction is 35° . Find the magnitude and point of application of the resultant on the wall per linear meter (Fig. E.7.1).

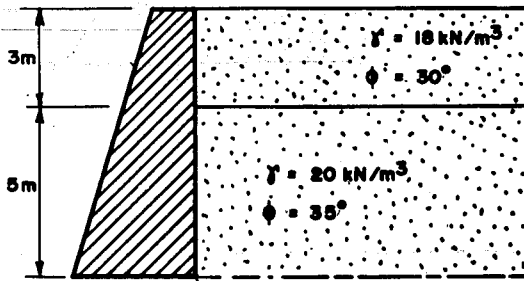


Fig. E.7.1 Retaining wall with soil data

SOLUTION

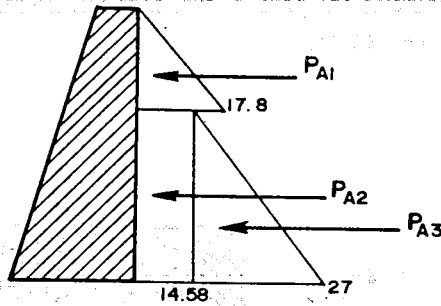
$$K_{a1} = \frac{1 - \sin 30}{1 + \sin 30} = 0.33$$

$$K_{a2} = \frac{1 - \sin 35}{1 + \sin 35} = 0.27$$

$$P_{a1} = K_{a1} \gamma_1 h_1 = 0.33 (18) (3) = 17.82 \text{ kN/m}^2$$

$$P'_{a1} = \gamma_1 h_1 k_{a2} = 18 (3) (0.27) = 14.58 \text{ kN/m}^2$$

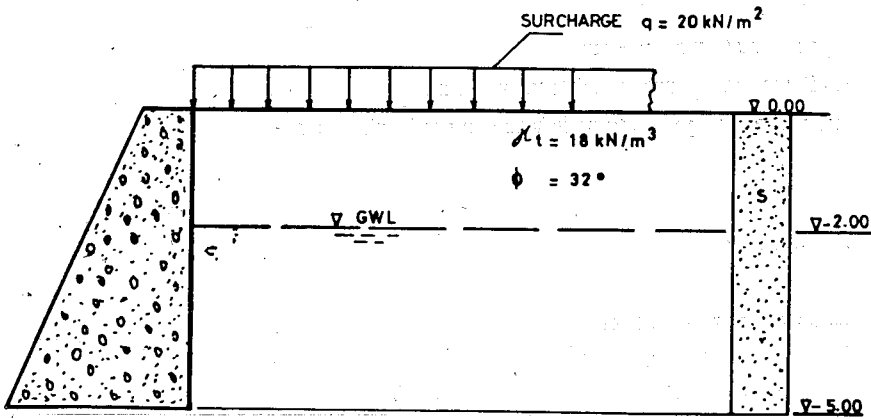
$$P_{a2} = \gamma_2 h_2 k_{a2} = 20 (5) (0.27) = 27 \text{ kN/m}^2$$



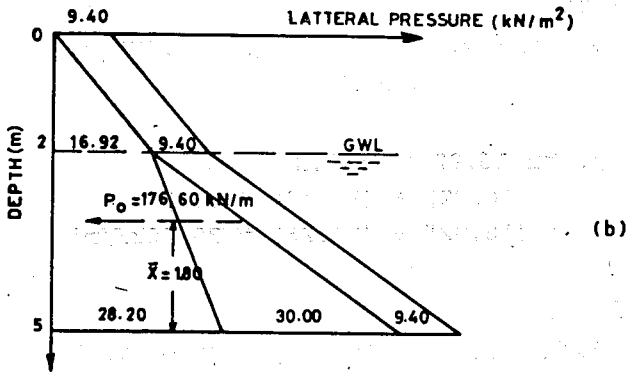
Resultant thrust kN/m	Moment Arm from base (m)	Moment kN-m
$P_{A1} = \frac{17.82}{2} (3) = 26.73$	$\frac{3}{3} + 5$	160.38
$P_{A2} = 14.58 (5) = 72.9$	$\frac{5}{2}$	182.25
$P_{A3} = \frac{27}{2} (5) = 67.5$	$\frac{5}{3}$	112.50
$\Sigma P_A = 167.13 \text{ kN/m}$	$\Sigma M = 455.13 \text{ kN-m}$	

E.7.5 Given

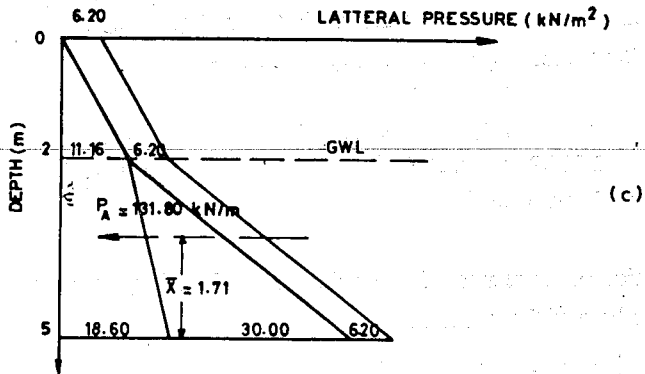
A smooth vertical wall with the loading condition shown in Fig. E.7.2.



(a)



(b)



(c)

Fig. E.7.2 Retaining wall with soil and ground water data.

Required

Approximate wall pressure

(i) if the wall is prevented from yielding

(ii) if the wall yields to satisfy the active Rankine state.

SOLUTION

(i) For at rest condition

$$k_o = 1 - \sin \phi$$

$$= 1 - \sin 32 = 1 - 0.53 = 0.47$$

The pressure distribution will be calculated using this coefficient.

From surcharge $q \cdot K_o = 20 \cdot (0.47) = 9.4 \text{ kN/m}^2$

From overburden

At depth - 2.00m : $\gamma \cdot 2 \cdot k_o = (18) (2) (0.47)$
 $= 16.92 \text{ kN/m}^2$

At depth - 5.00m: $16.92 + \gamma' \cdot 3 \cdot K_o$

$$= (16.92) + (8) (3) (0.47)$$

$$= (16.92) + (11.28) = 28.20 \text{ kN/m}^2$$

From hydrostatic

At depth - 5.00m: $\gamma_w \cdot 3 = (10) (3) = 30.0 \text{ kN/m}^2$

The calculated pressure distribution is plotted in Fig. E.7.2b.

The resultant force $P_A = P_{A1} + P_{A2} + \dots + P_{An}$

$$= \frac{1}{2} (16.92) (2) + 16.92 (3)$$

$$+ \frac{1}{2} (11.28) (3) + 5 (9.40) + \frac{1}{2} (30) (3)$$

$$= 16.92 + 50.76 + 16.92 + 47.00 + 45.00$$

$$= 176.6 \text{ kN/m}$$

The location of the resultant force is determined by taking moments of forces about the base of the wall:

$$P_A \bar{x} = \sum P_{A1} x_1 + P_{A2} x_2 + \dots + P_{An} x_n$$

$$= 176.6 \bar{x} = 16.92 \left(3 + \frac{2}{3} \right) 3 + 50.76 \left(\frac{3}{2} \right) + 16.92 \left(\frac{3}{3} \right)$$

$$c = 9.40 (2) (3+1) + 9.4 (3) \left(\frac{3}{2} \right) + \left(\frac{3}{3} \right) (45)$$

$$= 62.10 + 76.14 + 16.92 + 75.20 + 42.30 + 45$$

$$= 317.66$$

$$\bar{x} = \frac{317.66}{176.6} = 1.80 \text{ m}$$

(ii) For the active Rankine state, one uses the coefficient

$$K_a = \tan^2 (45 - \phi)$$

$$= \tan^2 \left(45 - \frac{32}{2} \right) = 0.31$$

The corresponding pressure distribution should be calculated using this coefficient.

From surcharge : $q \cdot K_a = (20) (0.31) = 6.20 \text{ kN/m}^2$

From overburden:

At depth - 2.00 $\gamma \cdot 2 \cdot K_a = (18) (2) (0.31)$
 $= 11.16 \text{ kN/m}^2$

At depth - 5.00: $11.16 + \gamma (3) (K_a)$

$$= 11.16 + 8 (3) (0.31)$$

$$= 11.16 + 7.44 = 18.60 \text{ KN/m}^2$$

From hydrostatic

At depth - 5.00 : $\gamma_w \cdot 3 = (10) (3) = 30.00 \text{ kN/m}^2$

The pressure distribution is plotted in Fig. E.7.2c.

The resultant force $P_A = \Sigma P_{A1} + P_{A2} + \dots + P_{An}$
 $= \frac{1}{2} (11.16) (2) + (11.16) (3)$

$$+ \frac{1}{2} (3) (7.44) + 5 (6.20) + \frac{3}{2} (30)$$

$$= 11.16 + 33.48 + 11.16 + 31.00 + 45.00$$

$$= 131.80 \text{ kN/m}$$

The location of the resultant force P_A :

$$P_A \cdot \bar{x} = \sum P_{A1} \cdot x_1 + P_{A2} \cdot x_2 + \dots + P_{An} \cdot x_n$$

$$131.80 \cdot \bar{x} = 11.16 (3 + 2/3) + 33.84 (1.5) + 11.16 (3/3)$$

$$+ 6.20 (2) (3 + 1) + 6.20 (3) (1.5) + 45 (3/3)$$

$$= 40.96 + 50.76 + 11.16 + 49.60 + 27.90 + 45.00$$

$$= 225.38 \text{ kN/m}$$

$$\bar{x} = \frac{225.38}{131.80} = 1.71 \text{ m}$$

E.7.6 Given

A retaining wall shown in Fig. E.7.3(a).

Required

Active and Passive earth pressure,

- (i) analytically using the method of Coulomb,
- (ii) graphically using the method of Culmann,

SOLUTION

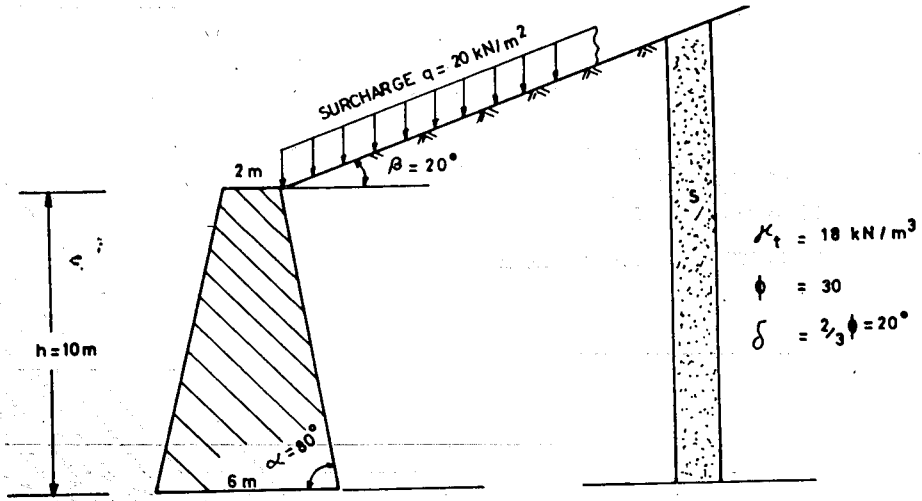
(i) Analytical Solution

Active Force

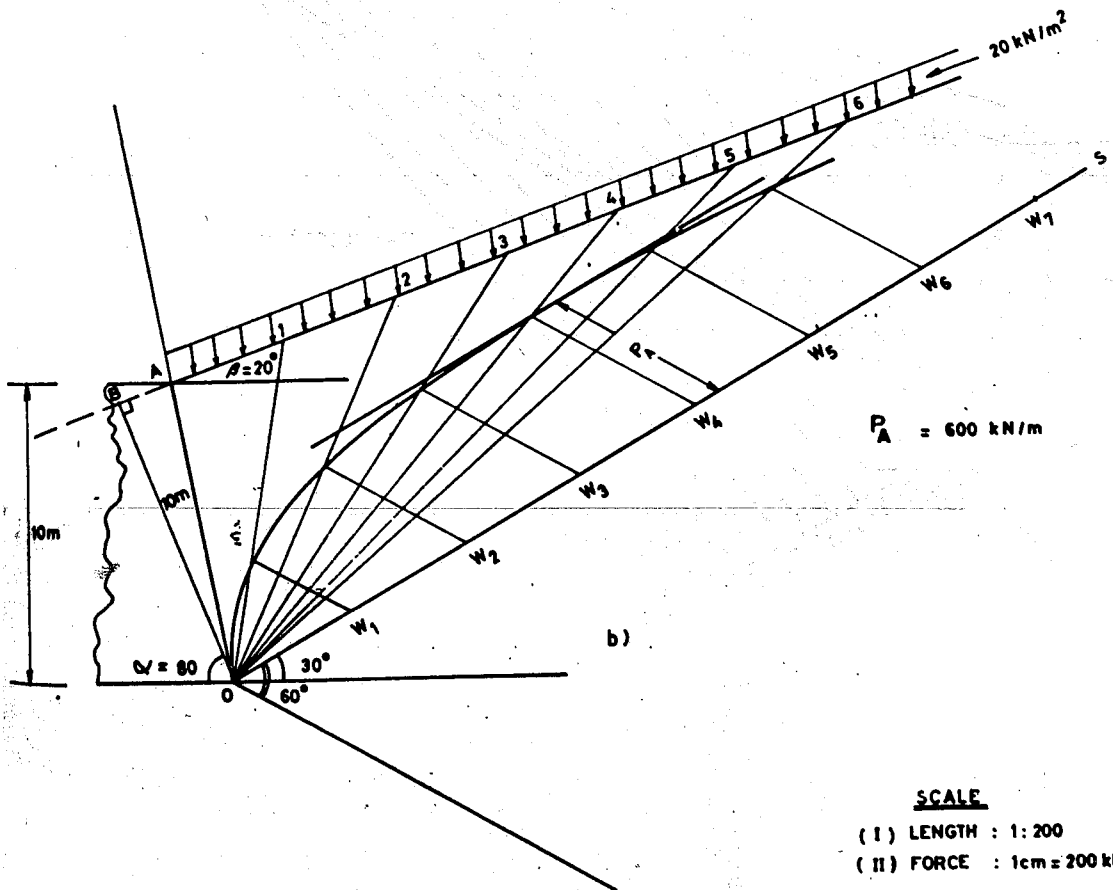
The effect of the surcharge will be taken care of by converting it into an equivalent ideal height.

$$h_1 = \frac{q}{\gamma} = \frac{20}{18} = 1.11 \text{ m}$$

$$h = h_0 + h_1 = 10 + 1.11 = 11.11 \text{ m}$$



a)



b)

SCALE

- (I) LENGTH : 1 : 200
- (II) FORCE : 1cm = 200 kN/m

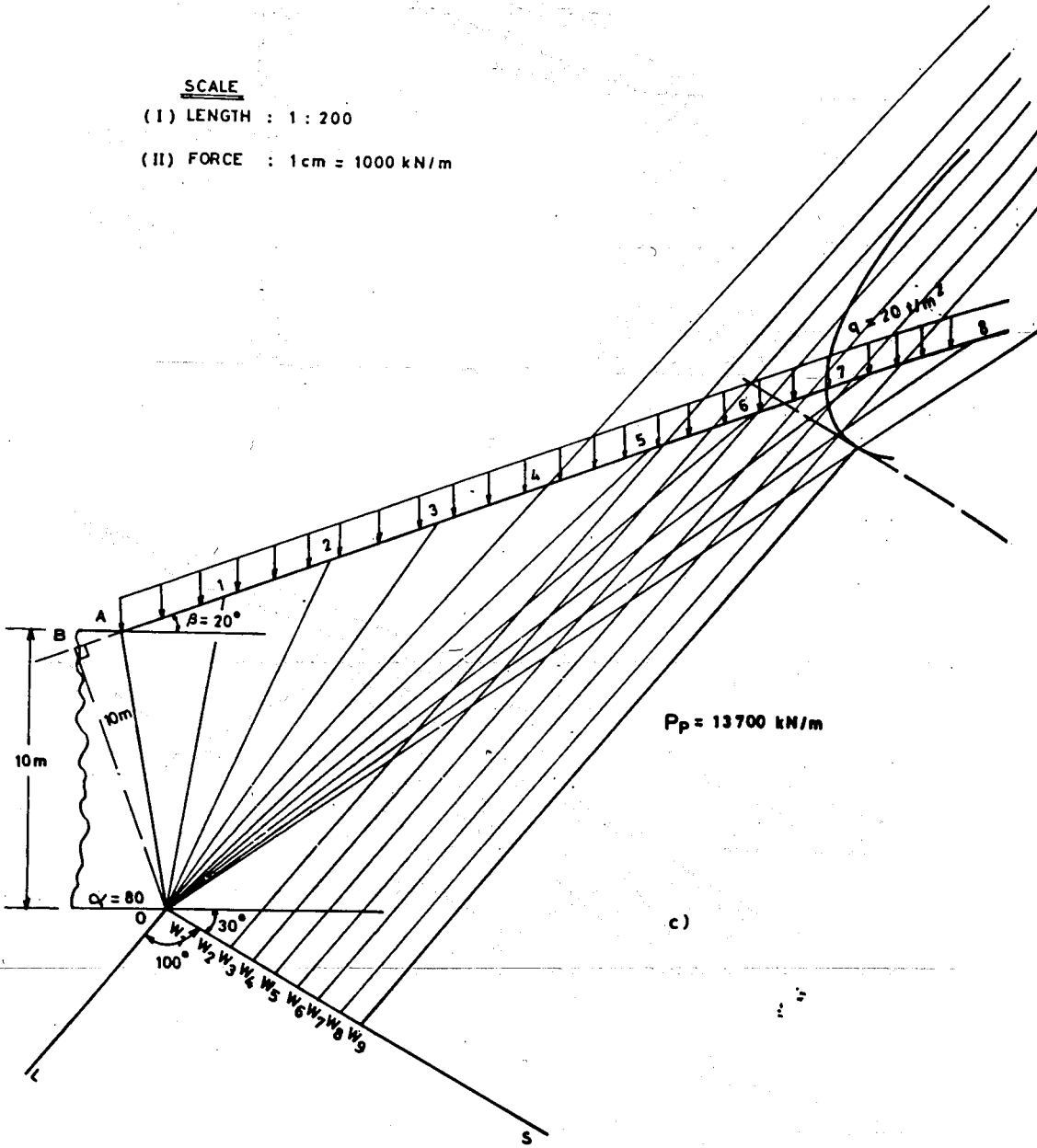


Fig. E.7.3 Retaining wall with an inclined ground surface.

$$P_A = \frac{\gamma h^2}{2} \left\{ \frac{\sin^2(\alpha + \phi)}{\sin^2 \alpha \sin(\alpha - \delta) \left[1 + \sqrt{\frac{\sin(\phi + \delta) \sin(\phi - \beta)}{\sin(\alpha - \delta) \sin(\alpha + \beta)}} \right]^2} \right\}$$

$$= \frac{18 (11.11)^2}{2} \left\{ \frac{\sin^2(80 + 30)}{\sin^2 80 \sin(80 - 20) \left[1 + \sqrt{\frac{\sin(30 + 20) \sin(30 - 20)}{\sin(80 - 20) \sin(80 + 20)}} \right]^2} \right\}$$

$$= 1110.89 \left\{ \frac{0.88}{(0.97)(0.87) \left[1 + \sqrt{\frac{(0.77)(0.17)}{(0.87)(0.98)}} \right]^2} \right\}$$

$$= 1110.89 \left\{ \frac{0.88}{(0.97)(0.87)(1.94)} \right\} = 597 \text{ kN/m}$$

PASSIVE FORCE

$$P_P = \frac{\gamma h^2}{2} \left\{ \frac{\sin^2(\alpha - \phi)}{\sin^2 \alpha \sin(\alpha + \delta) \left[1 - \sqrt{\frac{\sin(\phi + \delta) \sin(\phi + \beta)}{\sin(\alpha + \delta) \sin(\alpha + \beta)}} \right]^2} \right\}$$

$$P_P = 110.89 \left\{ \frac{\sin^2(80 - 30)}{\sin^2 80 \sin(80 + 20) \left[1 - \sqrt{\frac{\sin(30 + 20) \sin(30 + 20)}{\sin(80 + 20) \sin(80 + 20)}} \right]^2} \right\}$$

$$= 1110.89 \left\{ \frac{0.59}{(0.97)(0.98) \left[1 - \sqrt{\frac{(0.77)(0.77)}{(0.98)(0.98)}} \right]^2} \right\}$$

$$= 1110.89 \left\{ \frac{0.59}{(0.97)(0.98)(0.05)} \right\} = 13790 \text{ kN/m}$$

(ii) GRAPHICAL ANALYSIS

ACTIVE FORCE

Base of the wedges { A-1, 1-2, 2-3 ...etc } = 4m

Height of the wedges, OB = 10m

Weight of the wedges, $w_1 = w_2 = \dots w_n = (2)(10)(18)$

$$+ (20)(4)$$

$$= 360 + 80 = 440 \text{ kN/m}$$

E.7.7 Given

Anchored bulkhead shown in Fig. E.7.4a.

Required

The minimum penetration depth, d , and the tie rod force, R_A , according to

- the Free-Earth-Support Method
 - the Fixed-Earth-Support Method
- Analytically and Graphically.

SOLUTION

ANALYTICAL METHOD

a) FREE - EARTH SUPPORT METHOD

The lateral pressure distribution is shown in the figure. The effect of the hydrostatic distribution is shown separately. From equilibrium conditions: $\sum M_A = 0$

Letting d to be the minimum penetration depth, then the moment about A

$$P_p (8 + 2/3d) = P_{A1} \left[\frac{d+7}{2} + 1 \right] + P_{A2} [2/3(d+7) + 1], >$$

$$+ W_1 (1.67) + W_2 \left[\frac{(6+d)}{2} + 2 \right]$$

Noting that,

$$P_{A1} = (3\gamma K_a) (d+7)$$

$$P_{A2} = \frac{(7+d)}{2} \cdot K_a \gamma' (d+7)$$

$$W_1 = \frac{1}{2} (1) (10) = 5 \text{ kN/m}$$

$$W_2 = 10 (d+6)$$

$$P_p = \frac{1}{2} (K_p \cdot \gamma' \cdot d) \cdot d$$

After re-arranging terms one gets the following general expression in terms of d

$$(2 K_p \gamma' - 2 K_a \gamma') d^3 + (24 K_p \gamma' - 9 K_a \gamma - 45 K_a \gamma - 10) d^2 - (144 \gamma K_a + 336 K_a \gamma' + 160) d = 567 \gamma K_a + 833 K_a \gamma' + 650.10$$

Inserting in the above expression, the following known quantities

$$K_p = 5.88 \text{ (Table 7.3)}$$

$$K_a = 0.28 \text{ (Table 7.2)}$$

$$\gamma = 18 \text{ kN/m}^3$$

$$\gamma' = 8 \text{ kN/m}^3$$

$$\begin{aligned} & [(2)(5.88)(8) - (2)(0.28)(8)]d^3 + [(24)(5.88)(8) \\ & - (9)(0.28)(18) - (45)(0.28)(8) - 10]d^2 \\ & - [(144)(18)(0.28) + (366)(0.28)(8) + 160]d \\ & = (567)(18)(0.28) + (833)(0.28)(8) + 650.10 \\ & (94.08 - 4.48)d^3 + (1128.96 - 45.36 - 100.80 - 10)d^2 \\ & - (725.76 + 752.64 + 160)d = 2857.68 + 1865.92 + 650.10 \\ & 89.6d^3 + 972.80d^2 - 1638.40d = 5373.70 \\ & d^3 + 10.86d^2 - 18.29d = 59.97 \end{aligned}$$

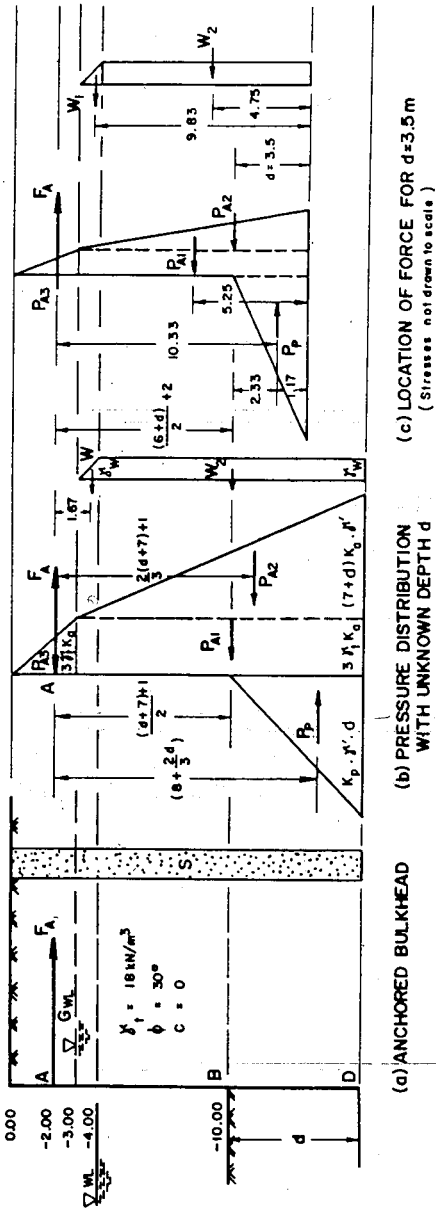


Fig. E.7.4 Anchored bulkhead (Free-Earth-Support method)

By trial the value of $d = 2.9$ m.

In order to find the tie rod force R_A , one takes the moment of forces about the line of action of P_p .

Since the value of d is known, one may determine the following forces.

$$P_{A1} = (3 \cdot \gamma K_a) (7 + D) = (3) (18) (0.28) (9.9) = 149.69 \text{ kN/m}$$

$$P_{A2} = \frac{(7+d)^2}{2} K_a \gamma' = \frac{(7+2.9)^2}{2} (0.28) (8) = 109.77 \text{ kN/m}$$

$$P_{A3} = \frac{3}{2} \gamma K_a \cdot 3 = \frac{9}{2} (18) (0.28) = 22.68 \text{ kN/m}$$

$$W_1 = 5 \text{ kN/m}$$

$$W_2 = 10(d + 6) = (10) (8.9) = 89 \text{ kN/m}$$

$$P_p = \frac{1}{2} (K_p \gamma' d) d = (0.5) (5.88) (8) (2.9)^2 = 197.80 \text{ kN/m}$$

Taking moments about line of action P_p

$$10.33R_A = (10.33) P_{A3} + (5.25 - 1.17) P_{A1} + (3.5 - 1.17) P_{A2}$$

$$+ (9.83 - 1.17) W_1 + (4.75 - 1.17) W_2$$

$$10.33 R_A = (10.33) (22.68) + (4.08) (149.69) + (2.33) (109.77)$$

$$+ (8.66) 5 + (3.58) (89) = 1462.70$$

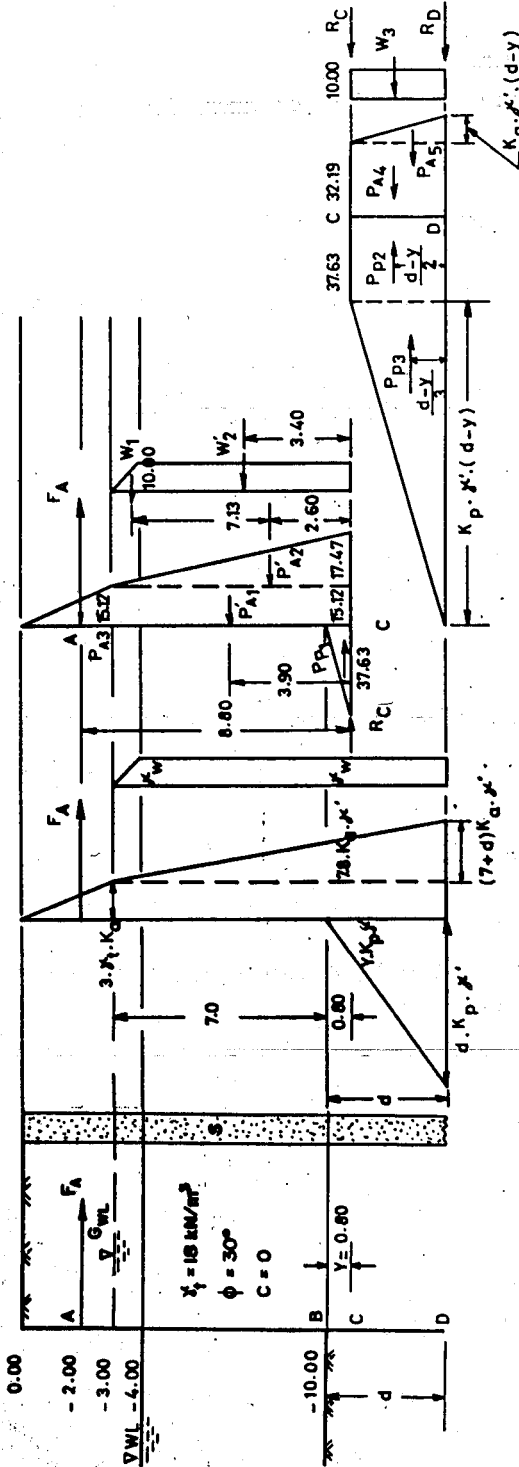
$$R_A = 141.60 \text{ kN/m}$$

The calculated depth of penetration will be increased by 20% and one would finally get $d = 3.5$ m.

b) FIXED - EARTH SUPPORT METHOD

From Table 7.5 the location of $C = 0.08h = 0.80$ m

The reaction R_c at the "hinge C" is found by taking moments of the forces about A.



(a) ANCHORED BULKHEAD (b) PRESSURE DISTRIBUTION WITH UNKNOWN d (c) EQUIVALENT BEAM METHOD

Fig. E.7.5 Anchored bulkhead (Fixed-Earth-Support-Method)

$$R_c(8.80) + P_{p1} \left(8.80 - \frac{0.80}{3}\right) = P_{A3}(0) + P_{A1}(8.80 - 3.90) \\ + P'_{A2}(8.80 - 2.60) + W_1(2.00 - 0.33) + W'_2(8.80 - 3.40)$$

Inserting the following quantities in the above equation

$$\begin{aligned} P_{A3} &= 22.68 \text{ kN/m} \\ P'_{A1} &= 117.94 \text{ kN/m} \\ P'_{A2} &= 68.13 \text{ kN/m} \\ W_1 &= 5 \text{ kN/m} \\ W'_2 &= 68.00 \text{ kN/m} \\ P_{p1} &= 15.05 \text{ kN/m} \end{aligned}$$

One obtains

$$R_c = 141.76 \text{ kN/m}$$

The tie rod force R_A may be found by taking moment about C.

$$R_A(8.80) + P_{p1} \frac{(0.80)}{3} = P_{A3}(8.80) + P_{A1}(3.90) + P'_{A2}(8.80) + P_{A1}'(3.90) \\ + P'_{A2}(2.60) + W_1(7.13) + W'_2(3.40)$$

From the above expression

$$R_A = 124.94 \text{ kN/m}$$

In order to determine the depth of penetration one takes moment of the forces about D

$$P_{p3} \frac{(d-y)}{3} + P_{p2} \frac{(d-y)}{2} = P_{A4} \frac{(d-y)}{2} + P_{A5} \frac{(d-y)}{3} + W_3 \frac{(d-y)}{2} + R_c(d-y)$$

Inserting the following quantities in the above equation,

$$P_{p3} = K_p \cdot \gamma' \frac{(d-y)^2}{2} = \frac{(5.88)(8)(d-y)^2}{2} = 23.52(d-y)^2$$

$$P_{p2} = 37.63 (d-y)$$

$$P_{A4} = 32.59 (d-y)$$

$$P_{A5} = \frac{K_a \gamma'}{2} (d-y)^2 = \frac{(0.28)(8)(d-y)^2}{2} = 1.12 (d-y)^2$$

$$W_3 = 10 (d-y)$$

$$R_c = 141.76 \text{ kN/m}$$

One obtains

$$(d-y) = 4.19\text{m}$$

$$d = 4.19 + 0.80 = 4.99\text{m}$$

An increase by 20% would finally give $d = 6\text{m}$

GRAPHICAL SOLUTION

The passive and active forces acting on the wall are drawn. The effect of the hydrostatic pressure is added together with the other forces.

The point of zero loading is determined from

$$x = \frac{P_a}{\gamma (K_p - K_a)}$$

Where P_a = active pressure at elevation 0.00

$$x = \frac{40.80}{8(5.88 - 0.28)} = 0.91\text{m}$$

Below this point, the ordinate of the passive pressure,

$P'_p(x)$, at any depth x will be calculated from,

$$P'_p(x) = \gamma \cdot x (K_p - K_a) - P_a$$

$$P'_p(x) = 44.80x - 40.80$$

The active and passive force distribution is divided into strips having width of 2m. The force within each strip is calculated.

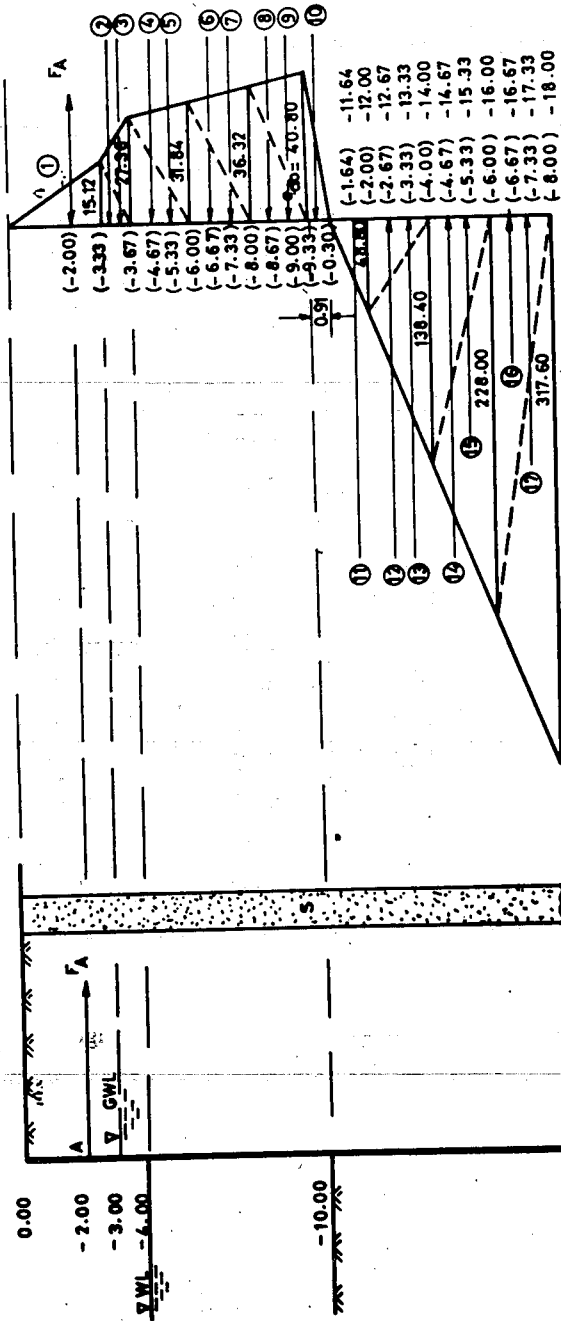
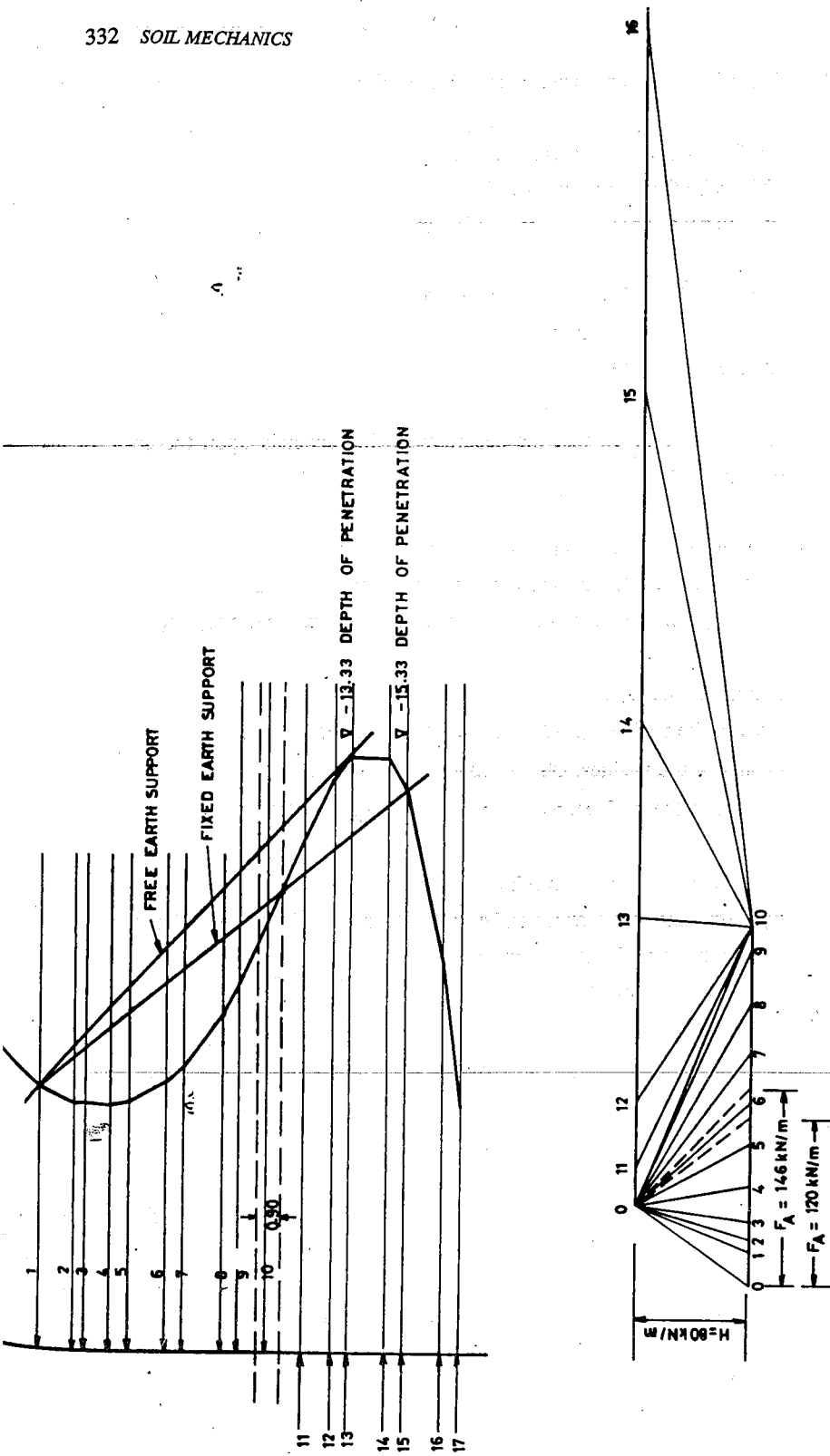


Fig.E.7.6 Anchored bulthead (lateral pressure distribution)

The results are tabulated as follows

Identification	Magnitude	Location	Remark
-	kN/m	m	-
1	22.68	- 2.0	Active Force
2	7.60	- 3.33	" "
3	13.68	- 3.67	" "
4	27.36	- 4.67	" "
5	31.84	- 5.33	" "
6	31.84	- 6.67	" "
7	36.32	- 7.33	" "
8	36.32	- 8.67	" "
9	40.80	- 9.33	" "
10	18.56	-10.33	" "
11	26.60	-11.64	Passive Force
12	48.40	-12.67	" "
13	138.40	-13.33	" "
14	138.40	-14.67	" "
15	228.00	-15.33	" "
16	228.00	-16.67	" "
17	317.60	-17.33	" "

The forces are plotted in Fig. E.7.6. and Fig. E.7.7. The pole height will be taken about $\frac{1}{4}(F_1+F_2 \dots F_{10})=80$ KN. Using the method of Blum the bending moment Polygon is constructed.



SCALE : 1cm = 40 kN/m

Fig. E.7.7 Anchored bulkhead (graphical method)

According to the graphical method, the following results are obtained:-

FREE-EARTH SUPPORT METHOD

- (i) Depth of penetration = 3.3m
- (ii) Tie rod force = 146 kN/m

FIXED - EARTH SUPPORT METHOD

- (i) Depth of penetration = 5.3m
- (ii) Tie rod force = 120 kN/m

It should be noted that the accuracy of this depends upon the scale of the drawing.

The respective weights are laid to scale on OS.

From w_1, w_2, \dots etc. lines are drawn parallel to OL to cut

0-1, 0-2, etc. thus tracing the Culmann curve. From the figure, $P_A = 600$ kN/m

PASSIVE FORCE

Base of the wedges (A-1, 1-2, 2-3, etc) = 4m

Height of the wedges, OB = 10m

Weight of the wedges, $w_1 = w_2 = \dots w_n = 440$ kN/m

The respective weights are laid to scale on OS. From w_1

w_2, \dots etc. lines are drawn parallel to OL to cut 0-1, 0-2, etc. thus tracing the

Culmann curve. From the figure,

$P_p = 13700$ kN/m

7.6 EXERCISES

- 1 A concrete wall with smooth vertical back 10m high retains a silty soil with $\phi = 20^\circ$ and $c' = 50$ kN/m² and has a horizontal surface. The soil supports a uniformly distributed load of 100 kN/m². The water level behind the wall is located 4m below the surface. The total unit weight of the soil is 18.5 kN/m³.

- (a) What is the pressure against the wall, if the wall is prevented from yielding ?
- (b) If the wall yields to satisfy the active Rankine state, what is the pressure on the wall?
2. A vertical retaining wall, 10m high, is observed to fail when a total horizontal load of 100 kN per meter is measured as acting on it. The backfill is horizontal and composed of unsaturated sand with a unit weight of 17.6 kN/m^3 . The failure plane of the soil behind the wall comes out on the soil surface at a distance of 5m from the top of the wall. Assuming that the wall has yielded according to the theoretical Rankine conditions.
- (a) What is the total shearing force in kN acting on the failure plane per linear meter of wall?
- (b) If the wall is completely submerged with water on both sides, what would then be the force acting on the wall?
Use $\gamma = 20.0 \text{ kN/m}^3$.
3. A retaining wall is 10m high and supports a cohesionless backfill whose angle of internal friction is 30° . The surface of the backfill is level with the top of the wall and carries a uniformly distributed surcharge of 200 kN/m^2 . The unit weight of the top 3m of the fill is 21 kN/m^3 and the rest is 23 kN/m^3 . Neglect friction on the back of the wall,
- (a) compute the active earth pressure on the wall and draw the pressure diagram.
- (b) determine the resultant active thrust per linear meter of wall and locate its point of application.
4. A vertical wall 9m high moves outward enough to establish the active state in a dry sand backfill.
- (a) Draw the pressure diagram and compute the resultant thrust P_A , if the sand has $\phi = 37^\circ$ and unit weight of 17 kN/m^3 .

- (b) Compute the pressure and the resultant on the assumption that the wall does not move at all.
- 5 A vertical wall 7.5 high has a soft clay backfill whose unit weight is 18kN/m^3 and its shearing strength c is 36kN/m^2 .
- (a) Compute the active pressure and draw the pressure diagram.
 (b) Determine the lateral thrust and its location from the top of the wall.
- 6 A soil has the following properties:
 $c' = 9\text{ kN/m}^2$, $\phi' = 20^\circ$ and $\gamma = 18.0\text{ kN/m}^3$.
 Calculate the critical depth of a vertical excavation that can be made in the soil without any lateral support. The ground carries a surcharge load of 30 kN/m^2 .
- 7 Determine the active and passive pressure using the graphical method of Culmann for a wall similar to that given in Fig. 7.10a, if
- $h = 10\text{ m}$
 $\beta = 20$
 $\alpha = 85^\circ$
 $\phi = 30^\circ$
 $\delta = \frac{2}{3}\phi = 20^\circ$
 $\gamma = 19.0\text{ kN/m}^3$
- Check your results analytically. Locate the resultant active and passive forces.
- 8 Compute the total passive resistance against a vertical face of a foundation in contact with a frictional soil mass having a height of 3m,
- (a) according to the ϕ - Circle method.
 (b) according to the Logarithmic - Spiral method.
 The soil has $\phi' = 25^\circ$, $c = 20\text{ kN/m}^2$, $c_w = 15\text{ kN/m}^2$
 $\delta = 15^\circ$, $\gamma = 19.0\text{ kN/m}^3$

- 9 It is intended to drive a cantilever sheet pile wall into a soil whose profile is indicated below. If a surcharge of 20kN/m^2 acts on the surface of the backfill and the net height of the backfill is 10m, what is the minimum driving depth of the sheet pile?
- 10 An anchored bulkhead is to be designed to retain a granular backfill of 9m height above the dredge line. The anchor rod is to be provided at a depth of 1m below the top level of the fill. Assuming that the water table is 2m below the top of the fill and that the back fill soil as well as the soil below the dredge line have the same soil properties ($\phi = 32^\circ$, $\gamma = 20.0\text{ kN/m}^3$), compute the penetration depth of the bulkhead and the tensile force in the anchor rod. Use the "Free - Earth Support" method.
- 11 If, in problem 1, an anchored sheet pile is used and the anchor rod is placed 2m below the surface of the fill, determine the minimum depth of penetration and the anchor force
- according to the "Free - Earth Support Method".
 - according to the "Fixed - Earth Support Method".
- Check your results graphically.

8. STABILITY OF SLOPES

8.1 GENERAL

Any exposed ground surface standing at an inclination is referred to as *unretained* earth slope. This term is applicable whether this surface is nearly vertical or has only a moderate slope. Man made slopes may be created by either excavation or filling, whereas slopes formed by nature are due to crustal movement, erosion etc.

Every slope is constantly subjected to natural forces tending to cause movement of soil from high to low points. The most important of such forces is the component of gravity that acts in the direction of probable motion. Also important is the force of seeping water. Earthquakes may also contribute large forces.

These forces cause shearing stress throughout the soil. If the shearing strength of the soil is greater than the stress on the most severely stressed internal surfaces, the slope will remain stable. If on the other hand the strength is less than the stress, the soil will slide down.

Any analysis of the stability of a slope involves,

- (a) the determination of the most severely stressed internal surface and the magnitude of shearing stress to which it is subjected.
- (b) the determination of the shearing strength along the same surface followed by computation of safety factor.

8.2 SLOPE MOVEMENTS

8.2.1 Soil-Creep

This refers to the tendency of soil to move down hill gradually and almost imperceptibly. One of the causes of creep is the alternate expansion and contraction of soil near the surface resulting from variation of temperature, alternate wetting and drying and freezing and thawing. The factors involved in creep are numerous and difficult to evaluate.

8.2.2. Mass Slides

Mass slides refer to sudden outward movement of large earth mass which breaks away from the main slope as relatively intact mass. The sliding mass usually moves on a failure surface which in cross-section approximates a segment of circular arc.

8.2.3 Flow Slides

Flow slides occur when the soil in the slide area first changes from a reasonably firm to an almost liquid condition and then flows outward and downward from its original position. Flow slides occurring in clays are known as *mud flows*. In granular soils flow slides occur by process known as *liquefaction*.

8.3 FACTOR OF SAFETY

This is an index of stability with respect to failure. In general terms this is expressed as,

$$F_s = \frac{\text{Resisting Forces}}{\text{Forces Causing Sliding}}$$

A slope on the verge of failure has a factor of safety of 1.0. The value of the factor of safety of ordinary slopes may be in the range of 1.5 or 2. Generally, the factor of safety may be expressed as,

$$F_s = \frac{s}{\tau} \quad (8.1)$$

where s = shear strength

τ = shear stress developed along the failure surface

$$\begin{aligned}
 s &= c + \bar{\sigma} \tan \phi \\
 \tau &= c_d + \bar{\sigma} \tan \phi_d \\
 F_s &= \frac{c + \bar{\sigma} \tan \phi}{c_d + \bar{\sigma} \tan \phi_d}
 \end{aligned}
 \tag{8.2}$$

Where

c = actual cohesion

ϕ = actual friction

c_d = developed cohesion

ϕ_d = developed friction

If $\phi = 0$ (soft clay) the general equation becomes

$$F_H = \frac{c}{c_d} \tag{8.3}$$

F_H = the factor of safety with respect to cohesion or height

F_s = the factor of safety with respect to shear strength

8.4 METHODS OF ANALYSIS

In the analysis of the stability of slopes, distinction between infinite slope and simple slopes should be made.

An infinite slope is an ideal case where the inclination is constant and stretches to unlimited extent (Fig. 8.1a). The soil strata may be varied, but for the purpose of analysis a homogeneous soil is assumed.

A simple slope on the other hand has limited boundaries (Fig. 8.1b). Since the analysis of the two types of slopes varies to a certain extent, each will be treated separately.

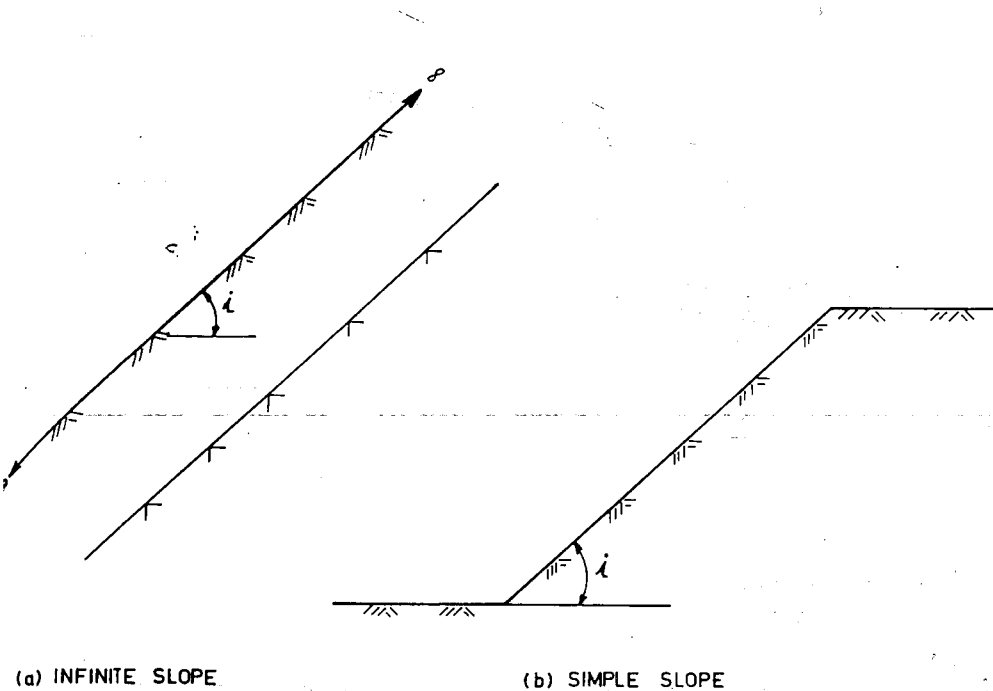


Fig. 8.1 Types of slopes

8.4.1. Infinite Slope

The stability of slopes in general is influenced by the presence of seepage force. Analysis for both non-seepage and seepage case will be made hereunder.

Analysis with no Seepage Condition

Consider the equilibrium of the wedge of homogeneous soil of unit thickness shown in Fig. 8.2. The thickness of soil down to the assumed failure plane is H . The forces on the two sides of vertical section are considered equal and opposite and therefore are ignored in the analysis.

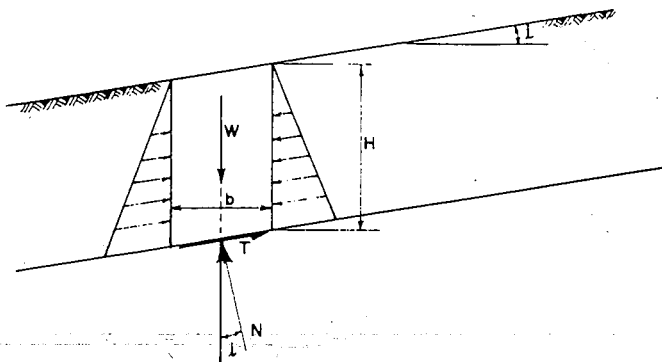


Fig. 8.2 Infinite slope

Weight of the wedge, $W = \gamma bH.l$. On the bottom of the wedge, the weight, W , is balanced by normal force, N , and shearing force, T . $N = W \cos i$ and $T = W \sin i$. Dividing these forces by the base of the wedge gives the normal stress, σ , and shear stress, τ .

$$\begin{aligned} \bar{\sigma} &= \frac{N}{A} \\ A &= \frac{b}{\cos i} \cdot l = \frac{b}{\cos i} \\ \frac{N}{b/\cos i} &= \frac{W \cos i}{b/\cos i} = \frac{W \cos^2 i}{b} = \frac{\gamma b H \cos^2 i}{b} = \gamma H \cos^2 i \end{aligned} \quad (8.4)$$

$$\begin{aligned} \tau &= \frac{T}{b/\cos i} = \frac{W \sin i}{b/\cos i} = \frac{W \sin i \cos i}{b} \\ &= \frac{\gamma H b \sin i \cos i}{b} \end{aligned}$$

$$\tau = \gamma H \sin i \cos i \quad (8.5)$$

The unit shearing stress may also be expressed in terms of resistance required for equilibrium.

$$\begin{aligned}\tau &= c_d + \sigma \tan \phi_d \\ &= c_d + \gamma H \cos^2 i \tan \phi_d\end{aligned}\quad (8.6)$$

Equating the two values of τ

$$c_d + \gamma H \cos^2 i \tan \phi_d = \gamma H \sin i \cos i$$

$$c_d = \gamma H \sin i \cos i - \gamma H \cos^2 i \tan \phi_d$$

$$= \gamma H \cos^2 i (\tan i - \tan \phi_d)$$

$$\frac{c_d}{\gamma H} = \cos^2 i (\tan i - \tan \phi_d) \quad (8.7)$$

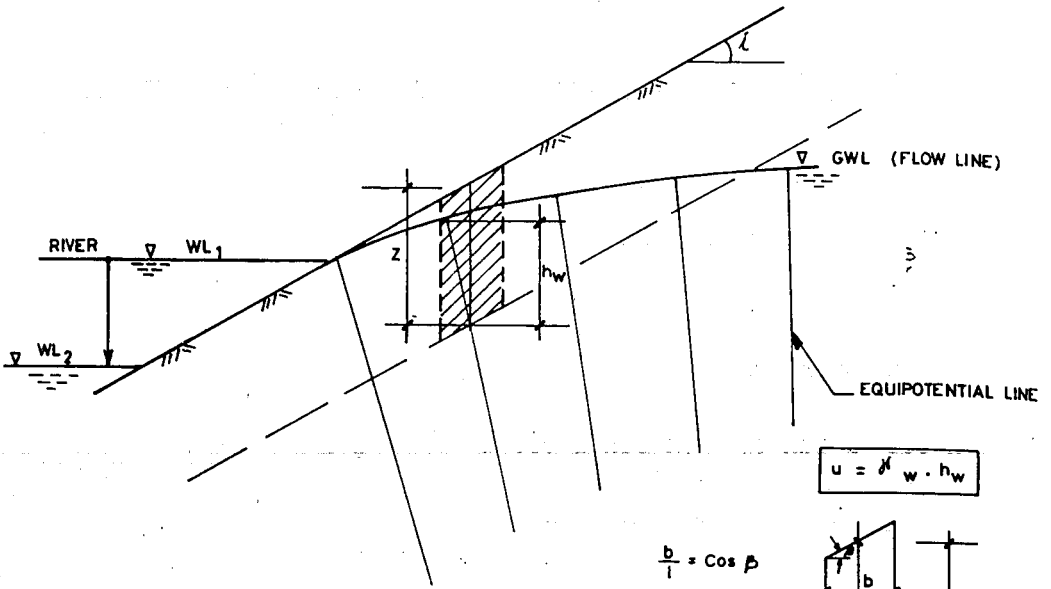
$\left(\frac{c_d}{\gamma H}\right)$ is a dimensionless ratio which Taylor (1937) called the stability number. ✓

For any value of ϕ_d , a relationship between the stability number and the slope angle i may be plotted. Such plots provide a convenient means for finding c_d at any depth H when i and ϕ_d are given or assumed.

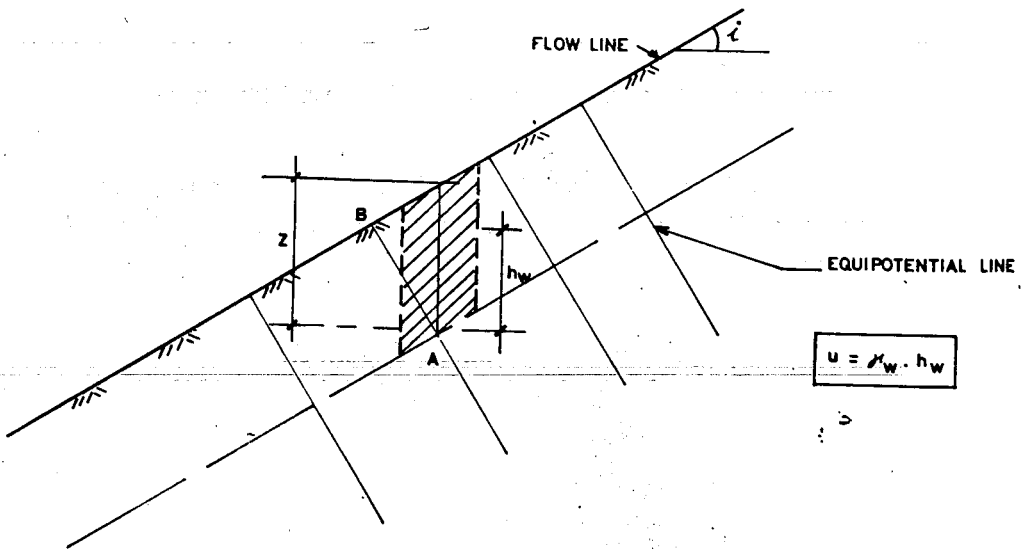
$$F_s = \frac{\text{shear strength}}{\text{shear stress developed for equilibrium}}$$

$$F_s = \frac{s}{\tau} = \frac{c + \bar{\sigma} \tan \phi}{\tau}$$

$$F_s = \frac{c + \gamma H \cos^2 i \tan \phi}{\gamma H \sin i \cos i} \quad (8.8)$$



(a) RAPID DRAW DOWN



(b) FLOW PARALLEL TO THE SURFACE

Fig. 8.3 Infinite slope with seepage

Noting that $\sin i \cos i = \cos^2 i \tan i$

$$F_s = \frac{c + \gamma H \cos^2 i \tan \phi}{\gamma H \cos^2 i \tan i}$$

$$F_s = \frac{c}{\gamma H \cos^2 i \tan i} + \frac{\tan \phi}{\tan i} \quad (8.9)$$

From Eq 8.4 it can be noticed that for cohesionless soil ($c=0$), the factor of safety of a slope is independent of its height and the slope is stable as long as $i < \phi$. If on the other hand $\phi=0$, the factor of safety varies inversely as the height of the slope.

Analysis with Seepage

a) Rapid-draw down condition

From Fig. 8.3a, let the pore water pressure induced by seepage at the base of the element be designated by u .

The normal total stress $\sigma = \frac{N}{A} = \frac{W \cos i}{A} = \frac{W \cos^2 i}{b}$

The normal effective stress $\bar{\sigma} = \sigma - u$. This may be written as, $\bar{\sigma} = \frac{W \cos^2 i}{b} - u$

Inserting the known parameter in the above equation,

$$\bar{\sigma} = \frac{\gamma \cdot H \cdot b \cos^2 i}{b} - u, \quad \text{which when simplified gives,}$$

$$\bar{\sigma} = \gamma \cdot H \cdot \cos^2 i - u \quad (8.10)$$

The shear stress, $\tau = \frac{T}{l} = \frac{W \sin i}{l}$

$$\tau = \frac{\gamma \cdot H \cdot \sin i \cdot b}{b} \cos i$$

Which when simplified gives,

$$\tau = \gamma \cdot H \cdot \sin i \cos i \quad (8.11)$$

Neglecting the effect of cohesion,

$$F_s = \frac{\bar{\sigma} \tan \phi}{\tau} = \frac{(\gamma H \cdot \cos^2 i - u) \tan \phi}{\gamma \cdot H \cdot \sin i \cos i} \quad (8.12a)$$

Further simplification gives,

$$F_s = 1 - \frac{u}{\gamma \cdot H \cdot \cos^2 i} \frac{\tan \phi}{\tan i} \quad (8.12b)$$

• b) Flow Parallel to the Surface

Referring to Fig. 8.3b. and from geometry

$$\frac{h_w}{AB} = \cos i \text{ and } AB = H \cos i$$

Hence, $h_w = H \cdot \cos^2 i$

Since $u = h_w \cdot \gamma_w$, then

$$u = H \cdot \cos^2 i \gamma_w \quad (8.13)$$

In principle the structure of Eq. (8.12b) remains unchanged. Inserting

Eq. (8.13) into Eq. (8.12b)

$$F_s = \frac{1 - H \cos^2 i \gamma_w}{\gamma \cdot H \cdot \cos^2 i} \frac{\tan \phi}{\tan i} \quad (8.14a)$$

Which when simplified gives,

$$F_s = 1 - \frac{\gamma_w}{\gamma} \frac{\tan \phi}{\tan i} \quad (8.14b)$$

$$F_s = \frac{\gamma - \gamma_w}{\gamma} \frac{\tan \phi}{\tan i} = \frac{\gamma_b}{\gamma} \frac{\tan \phi}{\tan i} \quad (8.14c)$$

8.4.2 Simple Slope

Before going into the analysis of simple slopes, it is essential to know the type of simple slope failures.

8.4.2.1 Types of Failure Surfaces

Generally failure surface are classified as shown in Fig. 8.4.

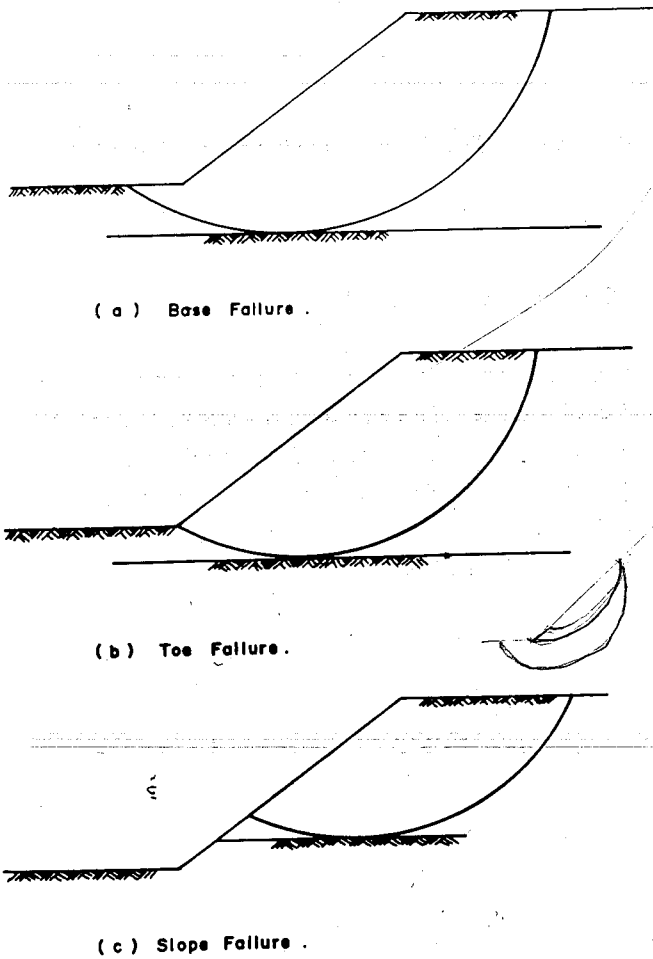


Fig. 8.4 Types of simple slope failures

Base Failure

This type of failure occurs in relatively flat slopes. The critical circle as shown in Fig. 8.4(a) has an appreciable curvature and dips into the base of the slope, and may pass outside the toe of the slope. The base failure develops in soft clays and in soils with numerous soft seams.

Toe Failure

This kind of failure takes place in moderate slope (Fig. 8.4b). The circle has less curvature and usually passes through the toe. Such failures occur in soils having appreciable internal friction.

Slope Failure

Slope failure occurs in appreciably steep slopes. This kind of failure is also called *face failure* (Fig. 8.4 c).

8.4.2.2 Location of Critical Slip Circle for Homogeneous Soils

There is not a fixed rule for locating the critical circle (failure surface) in the analysis of slope stability. There may be infinite number of possible failure circles. In cases where the critical circle is likely to pass through the toe of the slope, the construction developed by Fellenius is used for moderate slopes in a homogeneous material. The first approximation of worst circle is done by locating the center of rotation with the help of the table given in Fig. 8.5, which leads to the location of the center of rotation of the critical circle.

8.4.2.3 Methods of Calculations for Homogeneous Soils

8.4.2.3.1. General

An analysis of the stability of simple slopes consists of first determining the most severely stressed internal surface known as the critical surface. The resultant of all forces acting on the mass above the critical surface is determined. This resultant force is called the *actuating force*.

Slope	i	α	β
1 on 0.5	63°26'	38°	40°
1 on 1	45°	35°	37°
1 on 1½	33°47'	32°	35°
1 on 2	26°34'	30°	35°
1 on 3	18°26'	30°	35°
1 on 5	11°19'	30°	37°

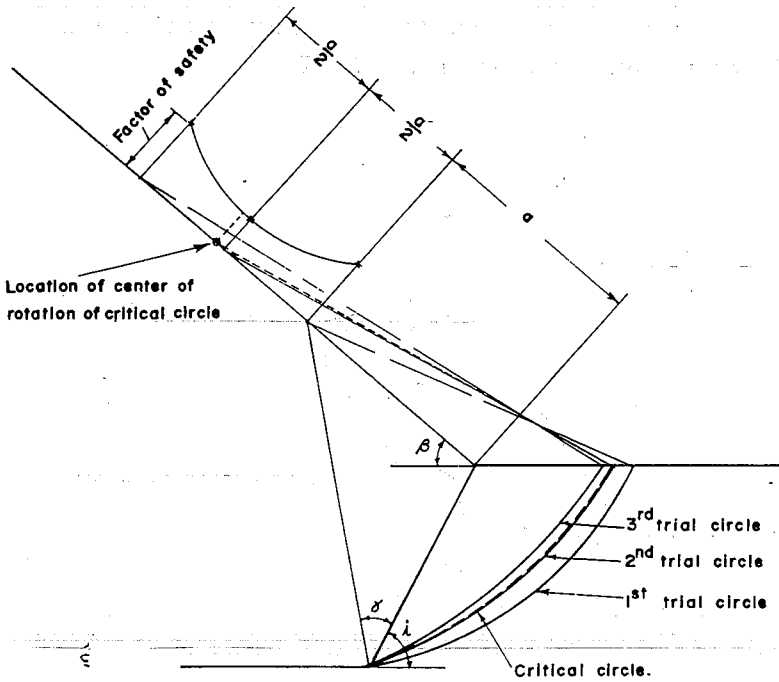


Fig. 8.5 Location of critical circle

The available resisting force which is made up of total cohesion on the critical surface; the resultant of all normal pressure acting across the surface on to the mass above; and all friction that the normal pressure is capable of developing is computed. The sum of cohesion and friction according to Coulomb's empirical law constitute the shearing strength of soil, which finally is used to determine the safety factor as previously indicated.

8.4.2.3.2 The Swedish Circle Method of Analysis

This is sometimes called the circular arc method or $\phi = 0$ method of analysis. In this method, failure surfaces are assumed to be of cylindrical shape and they appear on cross-sections as circular arcs. Several slip circles are drawn from different centers of rotation and by a process of trial and error the slip circle giving the lowest factor of safety is found. The disturbing moment about the center of rotation as shown in Fig. 8.6 = Wd .

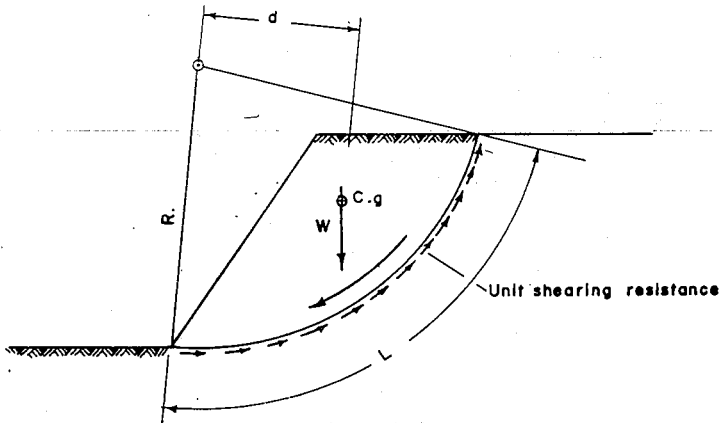


Fig. 8.6 The Swedish circle method

The resisting moment = $R \cdot s \cdot \hat{L} \cdot b$

The disturbing moment = $W \cdot d$

where

s = average unit shearing strength

W = weight of sliding mass with depth b

b = depth perpendicular to surface (commonly taken as unity)

\hat{L} = arc length

d = moment arm of sliding mass about the center of rotation

As slippage is about to take place, the resisting moment equals to the disturbing moment. In order to have a margin of safety, the resisting moment must be greater than the disturbing moment.

$$F_s = \frac{\text{Resisting Moment}}{\text{Disturbing Moment}} = \frac{Rs\hat{L}}{Wd} \quad (8.15)$$

8.4.2.3.3 The Friction Circle Method

A circular rupture arc with radius R is assumed. A concentric circle having a radius $R \sin \phi$ is constructed as shown in Fig. 8.7.a. At any point on the arc the direction of soil reaction is inclined at angle ϕ to the radial direction at that point and is tangent to the inner circle. This inner circle is called the *friction circle*.

Forces considered in this method of analysis, neglecting the neutral forces for the present are:

- (a) the force which acts vertically downward through the center of gravity of the soil mass above the slip circle.
- (b) the cohesion which acts along the arc, opposite to the direction of probable motion (Fig. 8.7b).
- (c) the soil reaction which acts at maximum obliquity and is tangent to the inner circle (Fig. 8.7c)

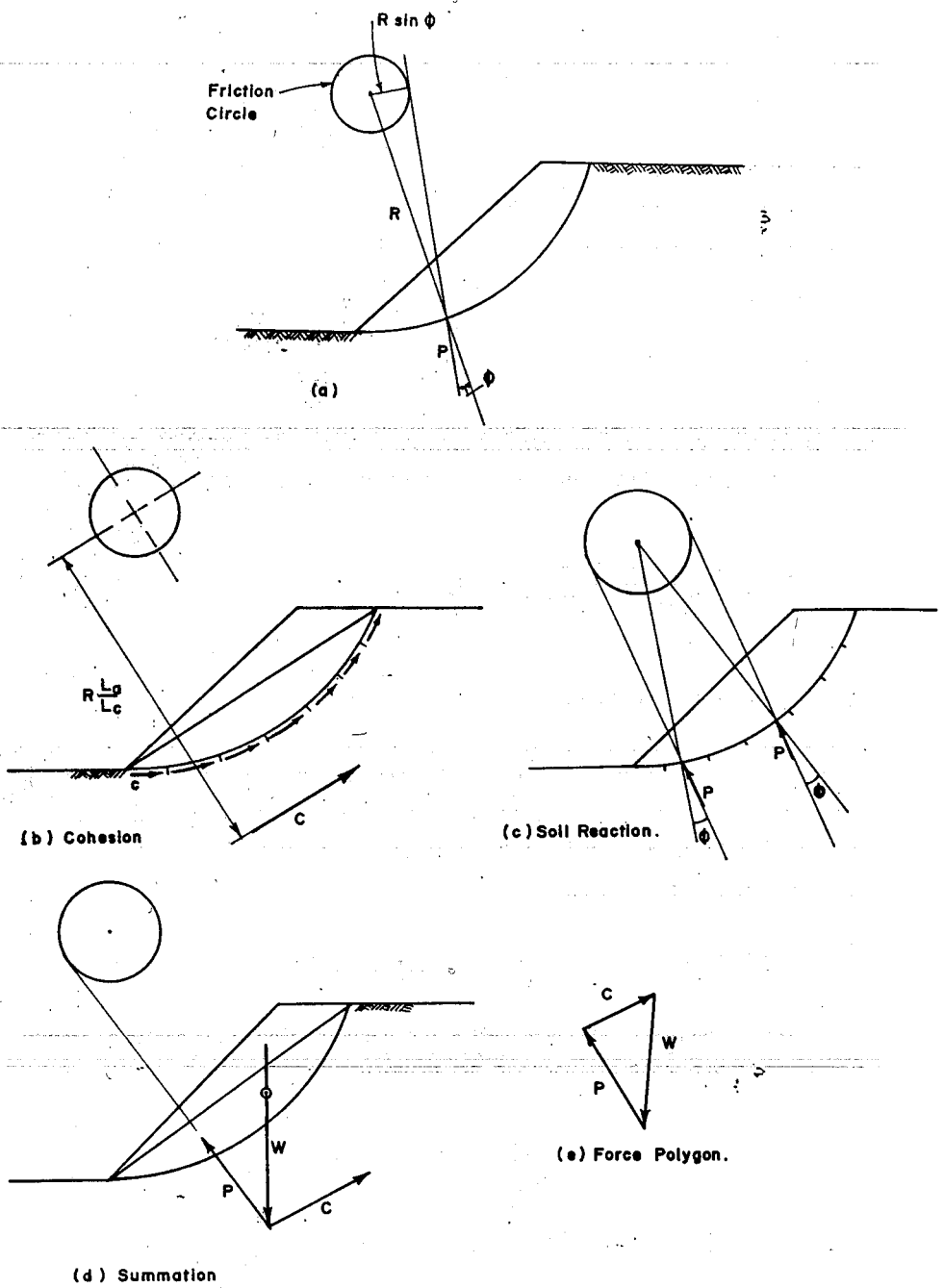


Fig. 8.7 Friction circle method

Consider L_a to be the length of the trial arc and L_c the length of the chord. The algebraic sum of all cohesive forces along the arc is $c_d L_a$. If the small cohesion forces on small segments of the arc are resolved into components normal and parallel to the chord, the parallel components will be additive. The normal components, however, will cancel. Therefore, the vector sum of all cohesive forces is $c_d L_c$.

To determine the line of action of $c_d L_c = C$, the sum of the moments of all the elementary cohesion forces acting along the arc must be equated to the moment of the resultant

$$c_d L_a R = c_d L_c \cdot a$$

$$\text{and } a = \frac{RL}{L_c}$$

This equation determines the line of action of the cohesion force. It acts parallel to the chord.

The ϕ - circle method applies to slopes which are just at equilibrium. The stability analysis by this method can be performed in two-ways.

- (1) Using a known cohesion of soil, c , the necessary angle of friction required, ϕ_d , for maintaining equilibrium, is determined.
- (2) Using a known angle of friction of soil, ϕ , the necessary amount of cohesion, c_d , for keeping equilibrium is determined.

The effective weight of the soil mass, W , is completely known. The cohesive force, C , is known in direction and line of action. The resultant soil reaction, P , must pass through the intersection of the first two and is tangent to the friction circle. Hence, the line of action of P is determined as shown in Fig. 8.7d.

A force triangle may now be drawn by first drawing the weight vector, W , and then drawing lines parallel to known direction of C and P . From the force triangle, the value of cohesive force needed to maintain stability is obtained as shown in Fig. 8.7e.

The total cohesive force divided by the length of the chord gives the unit cohesion, c_d , required to maintain equilibrium. The factor of safety with respect to cohesion = c/c_d , where c is the actual cohesive strength of the soil.

8.4.2.3.4 Wedge Method (Culmann's Method)

Plane failure surface is assumed in this method of analysis. This approach, sometimes referred to as classical approach, is attributed to Culmann.

Consider the equilibrium of the triangular wedge formed by the assumed failure surface OB inclined at angle θ shown in Fig. 8.8. The forces acting on the wedge AOB are its weight, W , a cohesive force, C , and the resultant, R , of the normal and frictional forces.

Cohesive force, $C = c_d L$, where c_d = required unit cohesion.

$W = \gamma (A.1)$ From Fig 8.8

$$A = \frac{H \sin(i-\theta)}{\sin i} \cdot \frac{L}{2} = \frac{1}{2} HL \frac{\sin(i-\theta)}{\sin i} \quad \text{and}$$

$$W = \frac{1}{2} \gamma HL \frac{\sin(i-\theta)}{\sin i}$$

Applying the law of sines to the equilibrium force polygon,

$$\frac{C}{\sin(\theta - \phi_d)} = \frac{W}{\sin(90 + \phi_d)}$$

$$\frac{c_d L}{\sin(\theta - \phi_d)} = \frac{\frac{1}{2} \gamma HL \frac{\sin(i-\theta)}{\sin i}}{\sin(90 + \phi_d)}$$

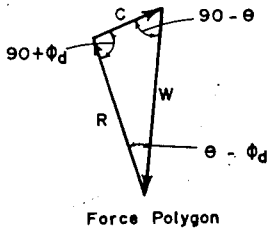
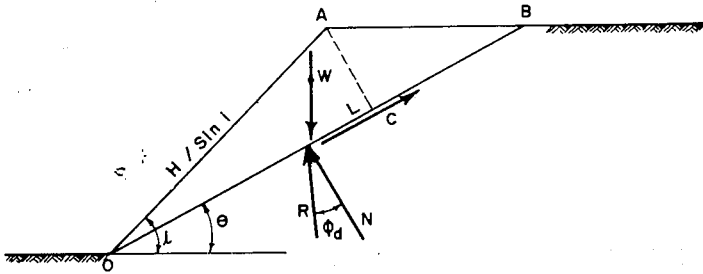


Fig. 8.8 The wedge method

$$\frac{c_d}{\gamma H} = \frac{\sin(\theta - \phi_d) \sin(i - \theta) L}{2 \sin i \cos \phi_d} \quad (8.16)$$

To find the critical plane which gives the lowest factor of safety, the above expression is differentiated with respect to θ and set equal to zero.

$$\frac{dc_d}{d\theta} = \frac{\gamma HL}{2 \sin i \cos \phi_d} [\cos(\theta - \phi_d) \sin(i - \theta) - \sin(\theta - \phi_d) \cos(i - \theta)] = 0$$

$$\cos(\theta - \phi_d) \sin(i - \theta) = \sin(\theta - \phi_d) \cos(i - \theta)$$

$$\frac{\sin(i-\theta)}{\cos(i-\theta)} = \frac{\sin(\theta-\phi_d)}{\cos(\theta-\phi_d)}, \text{ i.e. } \tan(i-\theta) = \tan(\theta-\phi_d)$$

It follows,
$$\theta = \frac{1}{2} (i + \phi_d) \quad (8.17)$$

The critical value of θ representing failure surface is given by $\frac{1}{2} (i + \phi_d)$.
Substituting the critical value of θ in Eq. (8.16) yields the maximum stability number.

$$\left(\frac{c_d}{\gamma H} \right)_{\max} = \frac{\left(\sin \frac{(i + \phi_d)}{2} - \phi_d \right) \sin \left(i - \frac{i + \phi_d}{2} \right)}{2 \sin i \cos \phi_d} \quad (8.18)$$

After simplification and rearrangement of terms

$$\left(\frac{c_d}{\gamma H} \right)_{\max} = \frac{1 - \cos(i - \phi_d)}{4 \sin i \cos \phi_d} \quad (8.19)$$

Equation 8.19 is stability number of plain failure surface for c - ϕ soil. If $\phi = 0$, the equation reduces to

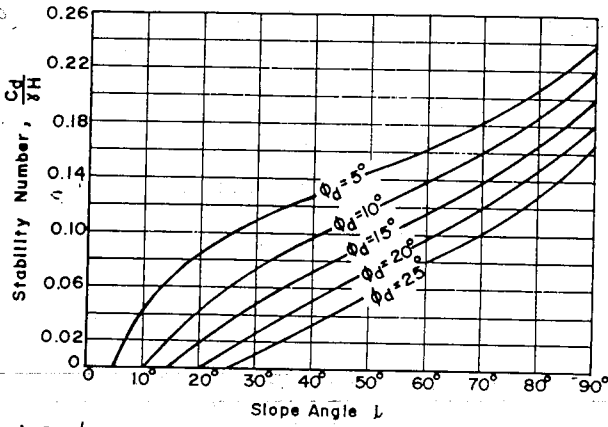
$$\left(\frac{c_d}{\gamma H} \right)_{\max} = \frac{1 - \cos i}{4 \sin i} \quad (8.20)$$

When full cohesion is developed $c_d = c$ and the critical height corresponding to this condition is obtained from Equation 8.19.

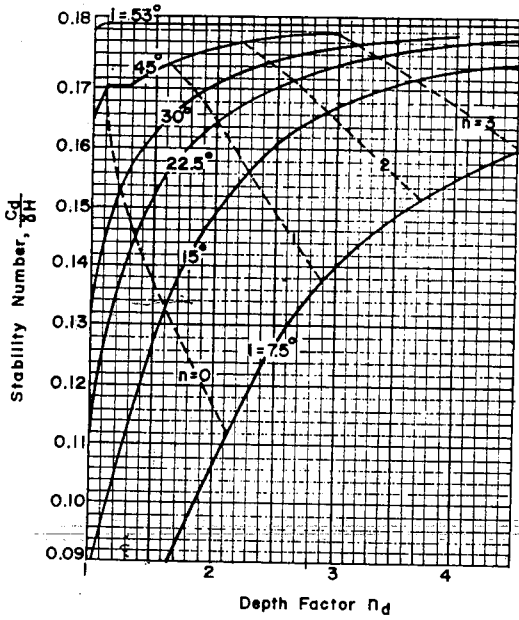
$$H_{(crit)} = \frac{4c}{\gamma} \left[\frac{\sin i \cos \phi_d}{1 - \cos(i - \phi_d)} \right] \quad (8.21)$$

For purely cohesive soil where $\phi = 0$,

$$H_{(crit)} = \frac{4c}{\gamma} \left[\frac{\sin i}{1 - \cos i} \right] \quad (8.22)$$



(a) C- ϕ Soil



(b) Purely Cohesive Soil ($\phi = 0$)

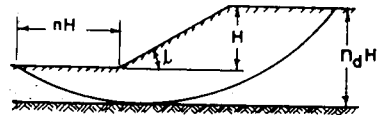


Fig. 8.9 Stability chart according to Taylor (27)

8.4.2.3.5 Stability Chart Method

A simple slope in homogeneous soil may be analyzed by slope stability charts devised by D. Taylor (27) and presented in Fig. 8.9a. The special case of uniform slope in homogeneous soft clay having undrained shear resistance equal to c can be solved analytically and the results are presented by a dimensionless number, m , called stability number. The stability number depends on the angle of slope i and the depth factor n_d as shown in Fig. 8.9b.

8.4.2.4 Calculation Method for Non-Homogeneous Soils

Several methods exist for analyzing the stability of slopes. Basically all the methods are based on one of the following methods:

- (i) The method of slices: Here the equilibrium of an elemental slice is considered.
- (ii) The wedge method: Instead of slice element, the equilibrium of a sliding wedge is considered.
- (iii) The block method: In this method, the equilibrium of a block, whose sliding surface may consist of two or more plain surfaces, is considered.

In this book only the method of slices will be considered.

8.4.2.4.1 Simplified Method of Slice

The approach of this method may be explained in reference to Fig. 8.10. A circular failure arc is assumed. A sector of unit thickness is divided into a number of vertical slices. The forces considered to act along the slip plane of an individual slice of unit thickness are shown in Fig 8.10. For simplicity, pore water pressure is assumed to be zero.

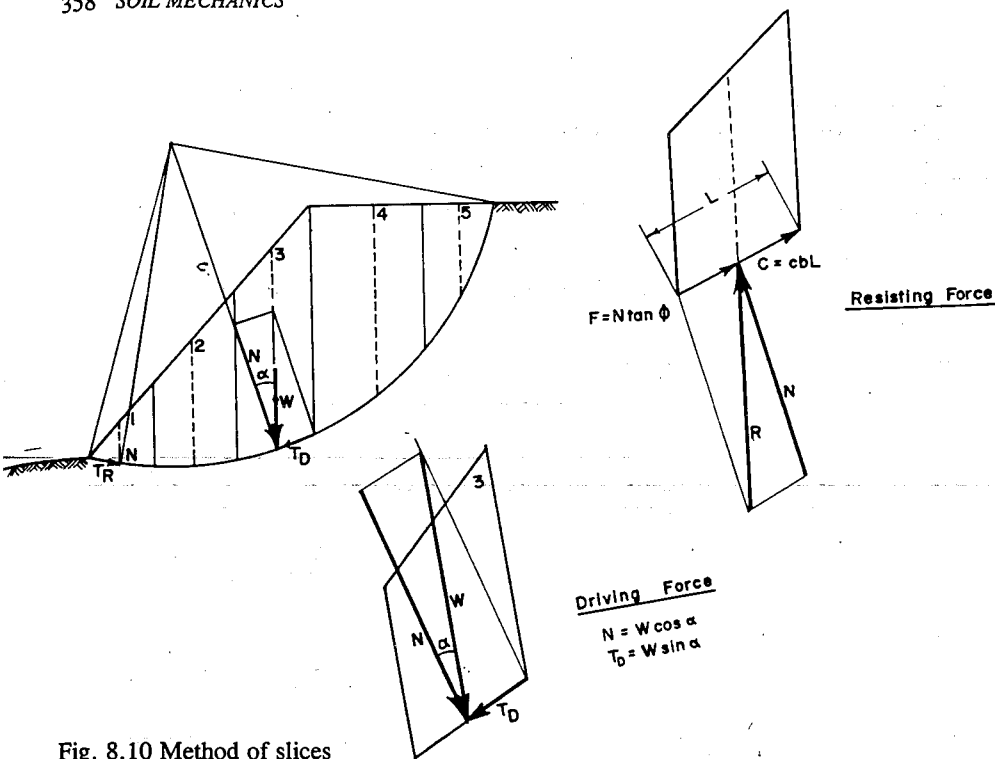


Fig. 8.10 Method of slices

The weight of each slice is represented by a vector drawn vertically through the center of gravity of the area. This vector is then resolved into components normal and tangential to the sliding surface. The normal component passes through the assumed center of rotation of sliding mass and hence does not contribute to the tendency of the slice to move. It has, however, great importance in regard to the development of frictional resistance.

On the other hand, the tangential component of the weight does affect stability as it tends to cause movement along the sliding surface. Tangential components of the weight of slice to the right of center of rotation constitute driving forces, but those to the left provide resistance.

In the slices method, it is considered that both the resisting and driving forces act along the failure surface. The factor of safety is, therefore, computed as the ratio of those forces rather than of their moments.

$$F_s = \frac{\sum cL + \sum N \tan \phi}{\sum T_D - \sum T_r} \quad (8.23)$$

where

- F_s = factor of safety
- ΣcL = summation of resistance due to cohesion
- $\Sigma N \tan \phi$ = summation of resistance due to soil friction
- ΣT_R = summation of resistance due to tangential components of weight tending to resist rotation.
- ΣT_D = summation of tangential components tending to cause rotation.

For convenience, the slope shown in Fig. 8.10 is for homogeneous soil.

The general procedure of stability analysis for layered soils is shown in Fig. 8.11.

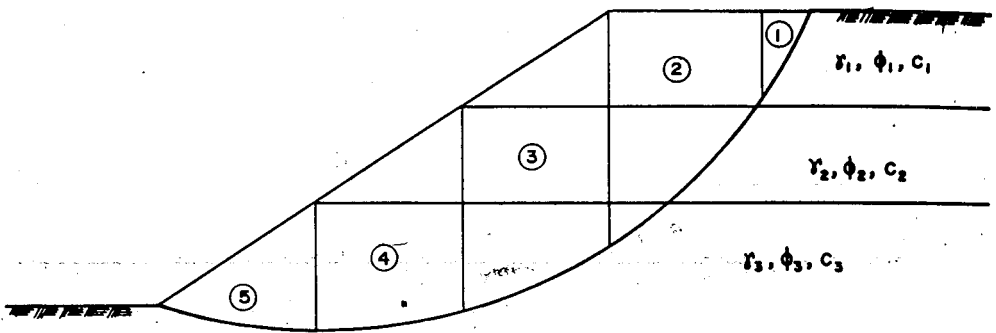


Fig. 8.11 Method of slices for layered soils

The values of ϕ and c will not be the same for all slices. For example, in Fig. 8.11 for slice 1, $\phi = \phi_1$ and $c = c_1$; for slice 2, $\phi = \phi_2$ and $c = c_2$; similarly for slices 3 up to 8, $\phi = \phi_3$ and $c = c_3$.

Fig. 8.12 shows a slope through which there is a steady-state seepage. The trial failure surface is AB and the soil above it is divided into a number of slices. For the n^{th} slice, the average pore water pressure, u , acting at the bottom of the slice can be evaluated from the average pressure head h (which is a vertical distance from E to F.) as $u = \gamma_w h$.

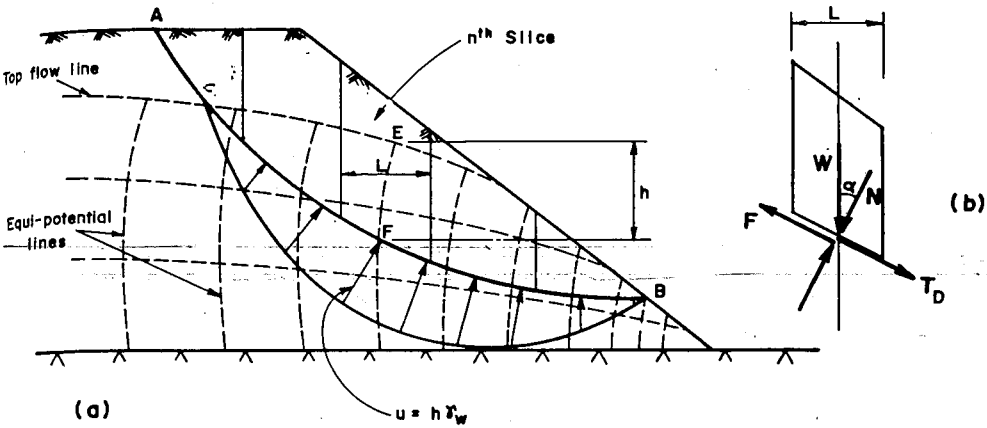


Fig. 8.12 Method of slices for steady - seepage state

The total force due to the pore water pressure at the bottom of the n^{th} slice is uL . From Fig.

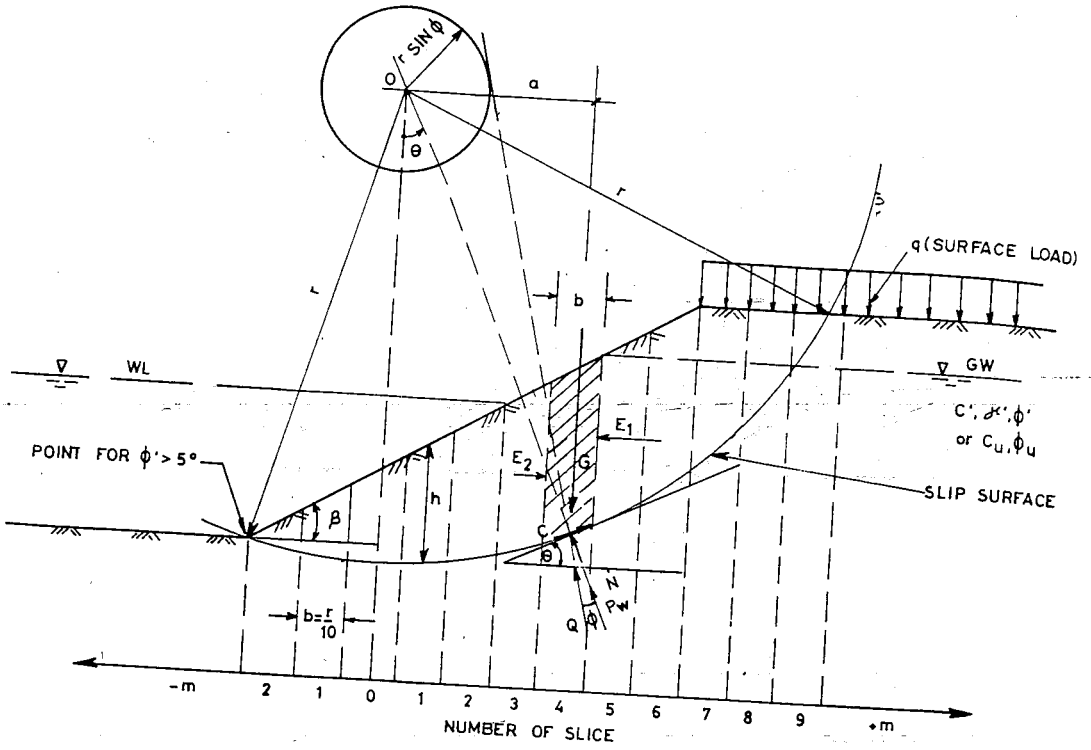
$$8.12b, N = W \cos \alpha, T_D = W \sin \alpha, F = N \sin \phi$$

Since $\bar{N} = N - uL, F = \bar{N} \tan \phi = (W \cos \alpha - h \gamma_w L) \tan \phi$

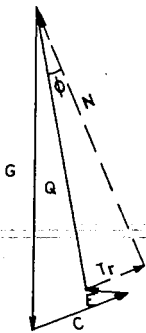
$$F_s = \frac{cL + \bar{N} \tan \phi}{\sum T_D - \sum T_R} = \frac{\sum cL + \sum (W \cos \alpha - h \gamma_w L) \tan \phi}{\sum W \sin \alpha} \tag{8.24}$$

8.4.2.4.2 German Code DIN 4048 [8]

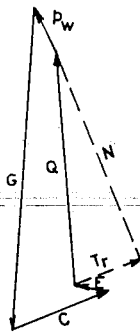
In this method, arbitrary trial arcs of circle are drawn (Fig. 8.13). From the relationships of the moments of the resisting to overturning forces acting along the slip surface, the factor of safety for the selected arc is determined. This procedure is repeated for arcs of circles until a minimum factor of safety for the given slope is obtained. While investigating stability of a given slope, the following forces are to be considered.



(a) NUMBER OF SLICES



(i) OWN WEIGHT



(ii) OWN WEIGHT and PORE WATER PRESSURE

(b) FORCE POLYGON

Fig. 8.13 Method of slices according to DIN 4048 [8]

- a. Forces acting inside or on the sliding element.
- b. Weight of the sliding element.
- c. Pore water pressure.

This is illustrated by considering an element as indicated in Fig.8.13. The specific forces acting on the elements are:

- G = weight of the element
 C = cohesion
 b. = width of the element
 Q = reaction force with the following components:
 N = normal force acting on the slip surface
 $T_r = N \cdot \tan \phi$ = frictional force
 $E = E_1 - E_2$ = earth pressure difference between the right and left side of the element.
 P_w = resultant of the pore water pressure acting on the sliding surface (Fig.8.14).

Moment equations for different trial circles are determined. The slip surface in which the ratio of the resisting moment to the overturning moment is the minimum is taken. For the slope to be safe, the factor of safety should not be less than 1.4.

In this method, the width of the scale will be $\frac{r}{10}$

The safety factor is then calculated using the general formula.

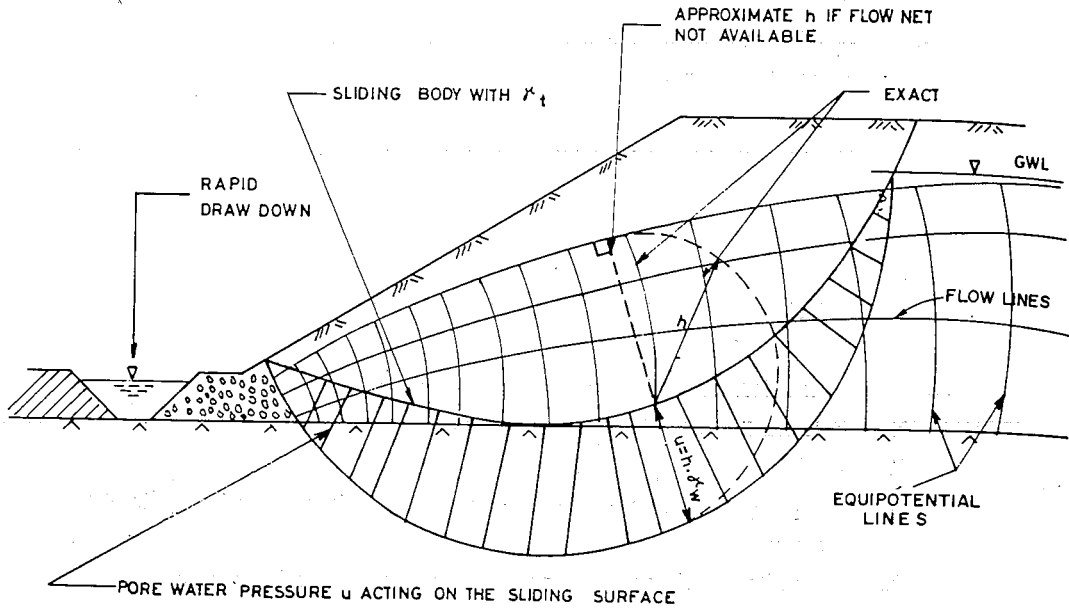
$$F_s = \frac{\sum (C + T_r) r}{\sum G \cdot a} \quad (8.25)$$

Or using the expression of Kery

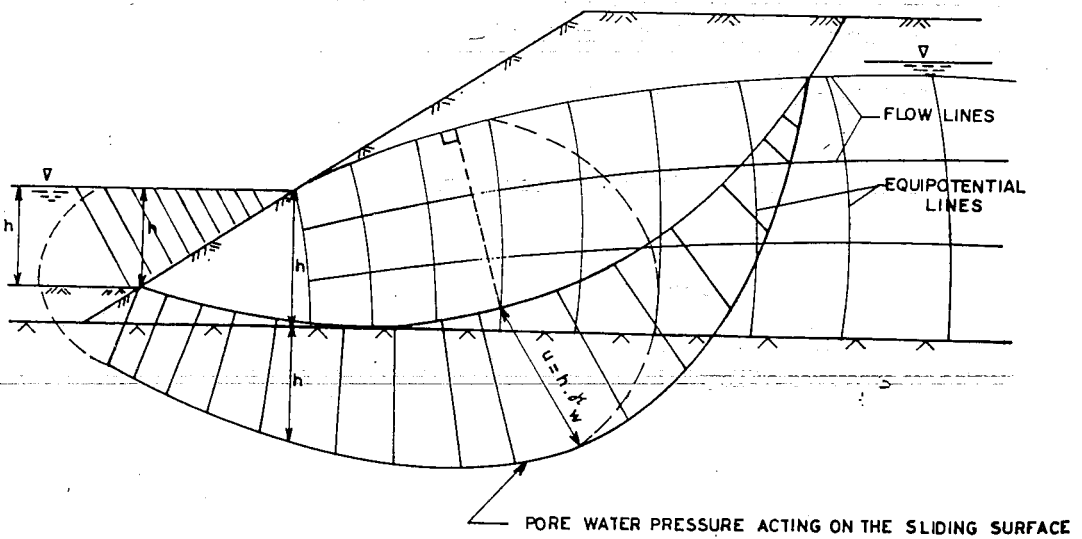
$$F_s = \frac{\sum T_w \cdot r}{\sum G \cdot r \cdot \sin \theta + \sum M} \quad (8.26)$$

Where

- G = weight of the individual slice
 M = moment of force about O not included in G
 T_w = existing resisting tangential force acting on the slip surface.



(a) RAPID DRAW DOWN



(b) CONTINUOUS FLOW

Fig. 8.14 Determination of pore water pressure distribution on the sliding surface.

$$\sin\theta = \frac{m}{n}$$

m = number of the slice

n = r/b , normally $n = 10$

$$T_w = \frac{G + c \cdot b \cot\phi - (u + \Delta u) b}{\cos\theta - \cot\phi + \sin\theta}$$

where

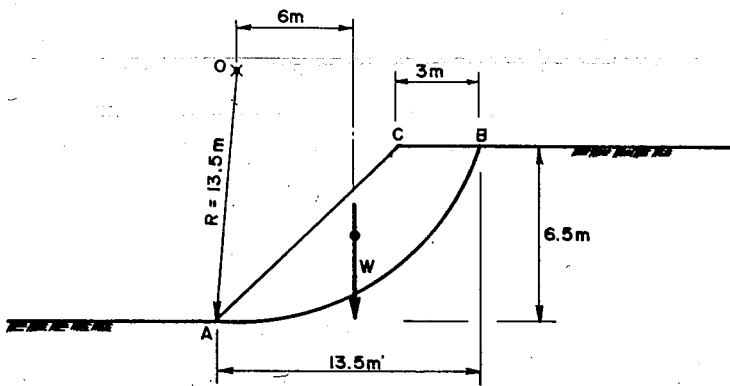
G = weight of the individual slice.

u = pore water pressure determined from flow net.

Δu = excess pore water pressure as a result of consolidation.

8.5 EXAMPLES

- E.8.1 The figure shown below indicates a cutting in a purely cohesive soil (i.e. $\phi=0$). The unit weight of the soil is 20kN/m^3 and the average cohesive strength is 30kPa . Calculate the factor of safety for the slip circle shown.



SOLUTION

Construction of the critical circle to scale

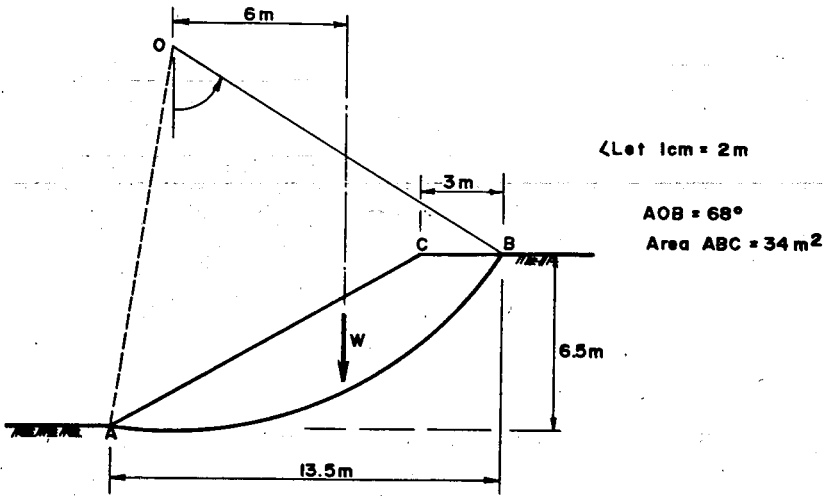
$$\text{Arc length } AB = \frac{68}{180} (\pi \cdot R) = \frac{68}{180} (3.14) (13.5) = 16.01\text{ m}$$

Moment about O

$$\text{Disturbing moment} = W(6) = 34 (20) (6) = 4080 \text{ kN.m}$$

$$\text{Resisting moment} = c\bar{AB} = 30 (16.01) (13.5) = 6484.05 \text{ kNm}$$

$$F_s = \frac{6484.05}{4080} = 1.59$$

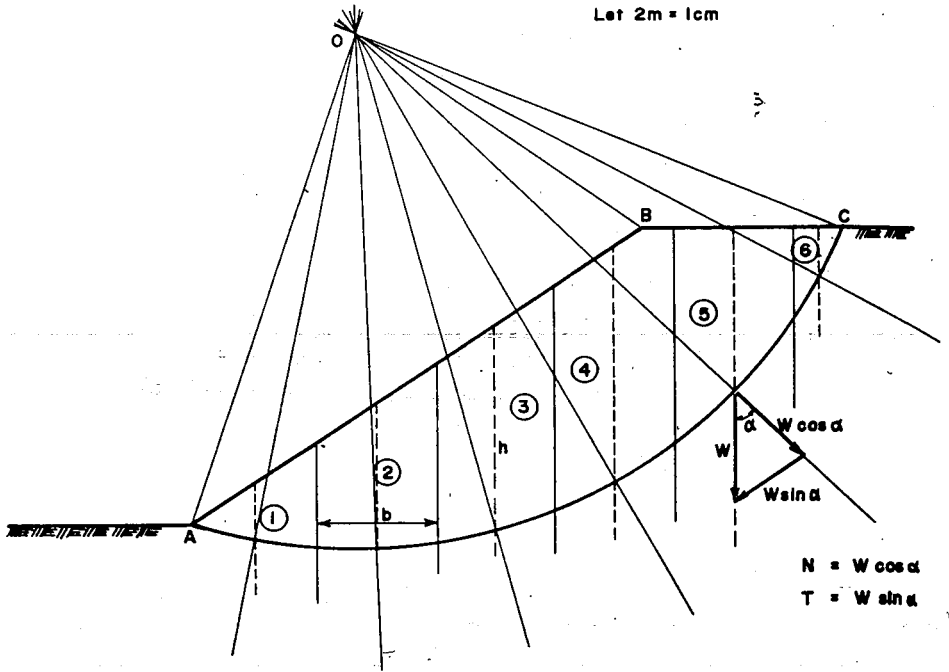


E.8.2 A 10m deep cutting has a slope of $1:1\frac{1}{2}$, (that is 1 vertical and $1\frac{1}{2}$ horizontal). The soil has a unit weight of 19 kN/m^3 , $c=25 \text{ kPa}$, and $\phi=8^\circ$. Calculate the factor of safety of the slip of circle. The center of rotation can be found by means of the Table in Fig.8.5 which gives the following data:-

For slope $1:1\frac{1}{2}$, $\alpha = 32^\circ$
 $\beta = 35^\circ$
 $I = 33.8^\circ$

Using the data, construct a slip circle to scale and divide it into 6 sections.

SOLUTION



$$\sum T = 755.2 \text{ kN}$$

$$\sum N = 1855.9 \text{ kN}$$

$$AOC = 85^\circ$$

$$R = 8.8 (2) = 17.6 \text{ m}$$

$$\text{Length of Arc AC, } \hat{L} = \frac{85}{180} \pi R = \frac{85}{180} (3.14) (17.6) = 26.10 \text{ m}$$

From table:

$$\text{Driving Force, } \sum T = 755.2 \text{ kN}$$

$$\begin{aligned} \text{Resisting Force} &= cL + \sum N \tan \phi = 25 \times 26.10 + 1855.9 \tan 8^\circ \\ &= 652.6 + 260.8 = 913.4 \text{ kN} \end{aligned}$$

$$F_s = \frac{\text{Resisting force}}{\text{Driving force}} = \frac{913.4}{755.2} = 1.21$$

Silce No.	h	b	α	$W=b.h.\gamma_w$	$T=W \sin \alpha$	$N=W \cos \alpha$
	(m)	(m)	deg	kN	kN	kN
1	1.8	4	12	136.8	-28.4	133.8
2	4.7	4	2	357.2	12.5	357
3	6.8	4	16	516.8	142.4	496.8
4	7.8	4	30	592.8	296.4	569.8
5	5.4	4	47	410.4	300.1	279.9
6	1.4	1.4	60	37.2	32.2	18.6

E.8.3 A cutting of depth 11m is to be made in soil of which the unit weight is 18.4kN/m^3 and the cohesion $=40\text{kN/m}^2$. There is a hard stratum under the clay at 13m below the ground surface. Assuming $\phi=0$ and allowing for a factor of safety of 1.5, find the slope of the cutting.

SOLUTION

Depth factor, $n_d = \frac{\text{Depth to hard stratum}}{\text{Depth of cutting}}$

$$= \frac{13}{11} = 1.2$$

$$m = \frac{c_d}{\sqrt{H}} = \frac{c}{F_c \gamma H} = \frac{40}{1.5 (18.4) 11} = 0.134$$

From Fig 8.9, for $n_d = 1.2$ and $m = 0.134$,

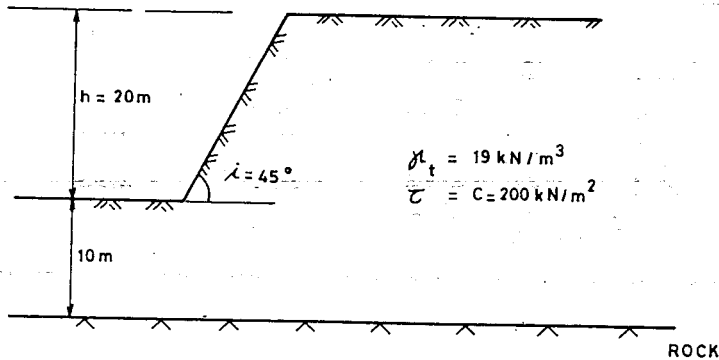
The slope of cutting $= 22^\circ$

E.8.4 Given

A slope with $i = 45^\circ$, height 20m as shown below

Required

The factor of safety, F_s , of the proposed slope.



SOLUTION

$$n_d = \frac{20 + 10}{20} = \frac{30}{20} = 1.5$$

With $n_d = 1.5$ and $i = 45^\circ$ one obtains from Fig. 8.9b

$$m = 0.174$$

$$F_s = \frac{c}{m \cdot \gamma \cdot h} = \frac{200}{0.174 (19) (20)} = 3.0$$

E.8.5 Given

Same as E8.4 but $c' = 4\text{ t/m}^2$, $\phi' = 20^\circ$

Required

The factor of safety, F_s , of the proposed slope.

SOLUTION

Using the values of i and ϕ' ($i = 45^\circ$, $\phi' = 20^\circ$) one obtains $m = 0.06$ from Fig. 8.9a

$$F_s = \frac{c}{m \cdot \gamma \cdot h} = \frac{40}{(0.06)(19)(20)} = 1.75$$

E.8.6 Given

Soil parameters same as example E.8.5

Required

The safe slope of the embankment

SOLUTION

In this particular case the given soil parameters should be reduced by certain safety coefficients. The reduction may be done according to prevailing codes.

In this example DIN 19700 [21] is used.

$$F_\phi = 1.3 \text{ (safety factor for friction)} = \frac{\tan \phi_{\text{existing}}}{\tan \phi_{\text{required}}} = \frac{\tan \phi}{\tan \phi_d}$$

$$F_c = 1.5 \text{ (safety factor for cohesion)} = \frac{c_{\text{existing}}}{c_{\text{required}}} = \frac{c}{c_d}$$

For soils possessing *friction* and *cohesion*, the reduction factor for cohesion is

$$\text{given by } \frac{F_c}{F_\phi}$$

Hence, in this example,

$$\tan \phi'' = \frac{\tan \phi'}{F_\phi} = \frac{\tan 20^\circ}{1.3} = 0.28$$

$$\phi'' = 15.64^\circ$$

$$c'' = \frac{\frac{c'}{F_c}}{F_\phi} = \frac{\frac{40}{1.5}}{1.3} = 34.8 \text{ kN/m}^2$$

$$m = \frac{c''}{\gamma h} = \frac{34.8}{(19)(20)} = 0.092$$

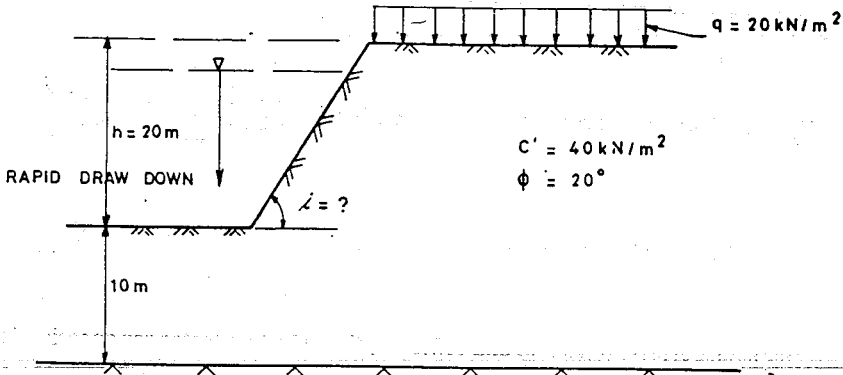
Using the value of $\phi'' = 15.64^\circ$ and $m = 0.092$ one reads from Fig. 8.9a, $i = 48^\circ$

E.8.7 Given

An embankment shown in the figure below is subjected to a rapid draw down.

Required

The safe slope of the embankment



SOLUTION

From E 8.6, $\phi'' = 15.64^\circ$, $c'' = 34.8 \text{ kN/m}^2$

Eventhough the charts prepared by Taylor and Fellenius do not consider the effect of seepage and surcharge, one may use them provided the following corrections are made.

- i) The effect of seepage may be considered by reducing the angle of internal friction by $\frac{Y_b}{Y}$
- ii) The acting distributed live load, q , may be converted into equivalent height (ideal height) so that the overall height of the dam will be $h_o = h + h_i = h + \frac{q}{Y}$.

Hence,

$$h_o = 20 + \frac{20}{19} = 20 + 1.05 = 21.05 \text{ m}$$

$$\phi'' = \phi' \frac{Y_b}{Y} = (15.64) \left(\frac{9}{19} \right) = 7.45^\circ$$

$$m = \frac{c''}{Y \cdot h_o} = \frac{34.8}{(19)(21.05)} = 0.08$$

Hence, with $m = 0.087$ and $\phi'' = 7.45^\circ$ one obtains $i = 27^\circ$

E.8.8 Given

An embankment as shwon in Fig. E.8.4 below

Required

Factor of safety of the embankment using DIN 4084

SOLUTION

$$\text{From Eq.(8.21)} \quad F_s = \frac{\sum T_w \cdot r}{\sum G \cdot r \sin \theta + \sum M}$$

$$\text{In this particular case} \quad T_w = \frac{G + c \cdot b \cdot \cot \phi}{\cos \theta \cdot \cot \phi + \sin \theta}$$

The results of the calculation are tabulated below

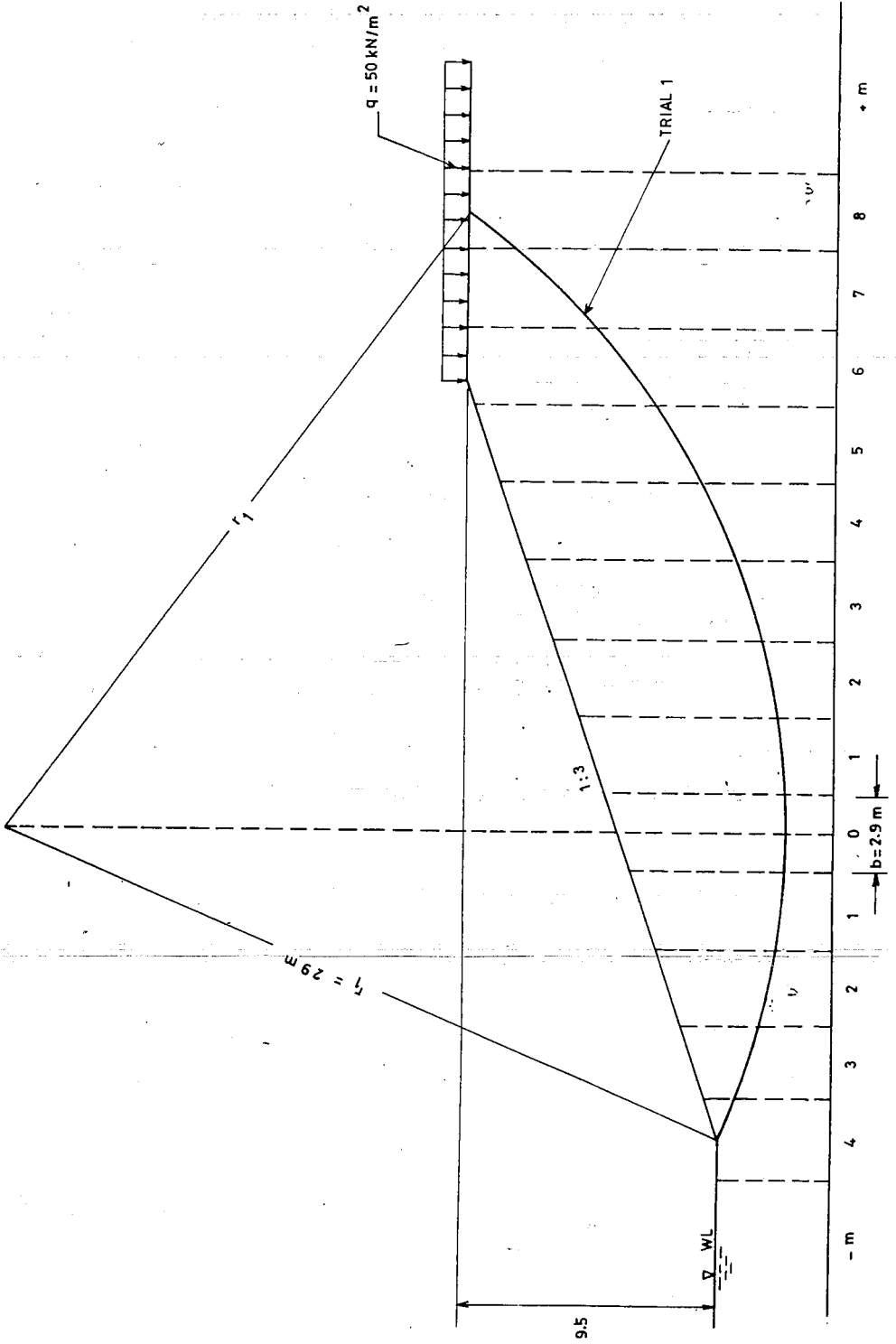


Fig. E.8.4 Safety of an embankment according to DIN 4084

Calculation of weights of individual slice

slice no.	h	γ	γh	$G = (\gamma \cdot h + q) \cdot b$	$\sin \theta = \frac{m}{n}$	θ	$\cos \theta$	$G + c \cdot b \cdot \cot \phi'$	$\cos \theta \cot \phi'$	$\cos \theta \cot \phi' + \sin \theta$	T_w	$T_w \cdot r$	$G \cdot r \cdot \sin \theta$
-	m	kN/m ³	kN/m ²	kN/m	-	deg.	-	kN/m	-	-	kN/m	kN	kN
-4	0	19	0	0	-0.4	-23.38	0.92	35.9	2.28	1.88	19.1	553.9	0.00
-3	1.8		34.2	99.2	-0.3	-17.46	0.95	135.1	2.35	2.05	65.9	1911.1	-863.0
-2	3.6		68.4	198.4	-0.2	-11.54	0.98	235.3	2.43	2.23	105.1	3041.9	-1150.7
-1	4.8		91.2	264.5	-0.1	-5.74	0.99	300.4	2.45	2.35	127.8	3706.2	-761.1
0	6.0		114.0	330.6	0	0.00	1.00	366.5	2.48	2.48	147.8	4286.2	0.00
+1	6.8		129.2	374.7	0.1	5.74	0.99	410.6	2.45	2.56	160.4	4651.6	+1086.6
+2	7.4		140.6	407.7	0.2	11.54	0.98	443.6	2.43	2.63	168.7	4892.3	+2364.7
+3	7.4		140.6	407.7	0.3	17.46	0.95	443.6	2.35	2.65	167.4	4854.6	+3547.0
+4	7.3		138.7	402.2	0.4	23.58	0.92	438.1	2.28	2.68	163.5	4741.5	+4565.5
+5	6.8		129.2	374.7	0.5	30.00	0.87	410.6	2.15	2.65	154.9	4492.1	+5433.2
+6	5.8		110.2	424.6	0.6	36.87	0.80	459.5	1.98	2.58	178.1	5164.9	+7388.0
+7	3.2		60.8	521.3	0.7	44.43	0.71	357.2	1.76	2.46	145.2	4210.8	+6522.4
+8	0		0	72.5	0.8	53.13	0.60	108.4	1.49	2.29	47.3	1371.7	1682.0
											47878.8	29908.6	

$$F_s = \frac{47878.8}{29908.6} = 1.6$$

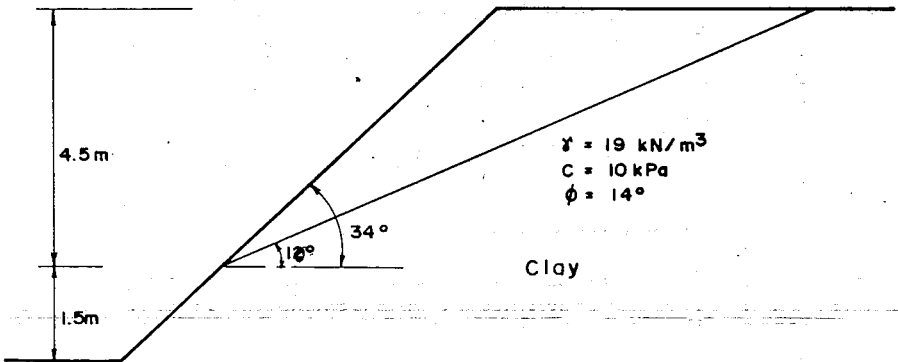
$$T_w = \frac{G + cb \cot \phi'}{\cos \theta \cot \phi' + \sin \theta}$$

$$\phi = 22^\circ$$

- $c' = 50 \text{ kN/m}^2$
- $b = 2.90 \text{ m}$
- $\cot \phi' = 2.48$
- $cb \cot \phi' = 359.6 \text{ kN/m}$

8.6 EXERCISES

- 1 A cut is to be made at angle of 65° in a partially saturated clay with $c=24\text{kN/m}^2$, $\phi = 15^\circ$ and $\gamma=18\text{kN/m}^3$. How deep can this cut be made before the safety factor of 1.2 is reached?
- 2 The soil at a given site has the following properties:
 $c=24\text{kN/m}^2$, $\phi=15^\circ$, $\gamma=20\text{kN/m}^3$. A cutting is to be made in this soil with a slope of 30° to the horizontal and a depth of 16m. Find the factor of safety of the slope against slip. Assume that friction and cohesion are mobilized to the same proportion.
- 3 Refer to the figure shown below. A deep railway cut intersects the plane of contact of two soil strata, the lower one of which is highly impervious and is cohesive clay. The plane of contact makes an angle of 10° with the horizontal. Given that the shearing strength between the two strata is $c = 10\text{kPa}$ and $\phi=14^\circ$, determine the factor of safety against sliding.



- 4 An embankment 23m high 12m wide at the top is constructed with a slope of 50° . The soil is partially saturated clay. The upper 15m. of soil has $c=96\text{kN/m}^2$, $\phi = 15^\circ$, and $\gamma = 18\text{kN/m}^3$. The remaining 8m. has $c=43\text{kN/m}^2$, $\phi=12^\circ$ and $\gamma=17\text{kN/m}^3$. Compute the safety factor. Use the method of slices.
- 5 A vertical cut to be made in clay soil having $\gamma=17\text{kN/m}^3$, $c=36\text{kN/m}^2$ and $\phi=0$. Find the maximum height for which the cut may temporarily be unsupported.
- 6 Using the data of E 8.4, plot a curve showing factor F_s versus the embankment slope, i , for values of i ranging from 20° to 90° .
- 7 An embankment 10m high and carrying a surcharge of 50kN/m^2 is proposed for a certain project. For determining the shear parameters of the soil, a triaxial test was carried out and the Mohr envelope gave shearing resistance of 273 kN/m^2 and 506 kN/m^2 for effective normal stresses of 500^2 kN/m^2 and 1000kN/m^2 respectively. If $\gamma = 19\text{ kN/m}^3$, determine the safe slope of embankment,
- for 'no - seepage' condition
 - for a 'rapid drawdown' condition
- 8 Determine the safety factor of slope of the earth dam given below, if $c' = 20\text{ kN/m}^2$ and $\phi' = 28^\circ$ using the method of slices considering
- rapid drawdown
 - steady flow

9. BEARING CAPACITY OF SOILS

9.1 General

The load of all structures has finally to be transmitted to the underlying soil by means of some type of foundations which are designed in such a way that the stresses induced in the soil are within the bearing capacity of soil. If the soil is overstressed, a shear failure may result causing the soil to slide from underneath.

In general, foundation can be grouped as shallow foundations or deep foundations. The common types of shallow foundations are spread and continuous footings, raft etc. (Fig. 9.1). Deep foundations include pile and pier foundations (Fig. 9.2). The main distinction between the two major foundation systems is based on the relationship between the width, B , and depth, D_f , of the foundation.

If $D_f \leq B$, the foundation system is referred to as shallow foundation. If on the other hand $D_f > B$, the foundation is referred to as deep foundation.

9.1.1 Ultimate Bearing Capacity

This is the ultimate resistance offered by a foundation material when subjected to loading. When this ultimate resistance is fully mobilized the foundation material fails and the structure sinks. The resulting pressure is known as *ultimate bearing capacity* designated by q_{ult} .

9.1.2 Allowable Bearing Capacity

The allowable bearing capacity (sometimes referred as safe bearing capacity), q_a , of a soil is a loading intensity which provides an adequate safety factor *against soil rupture* and also insures that settlement due static loading will not exceed the tolerable value.

When determining safe bearing capacity, one should make certain that the loading intensity is low enough not to cause excessive settlement of the structure. The amount of settlement that can be tolerated varies greatly depending on the type of structure, its rigidity, flexibility and its function.

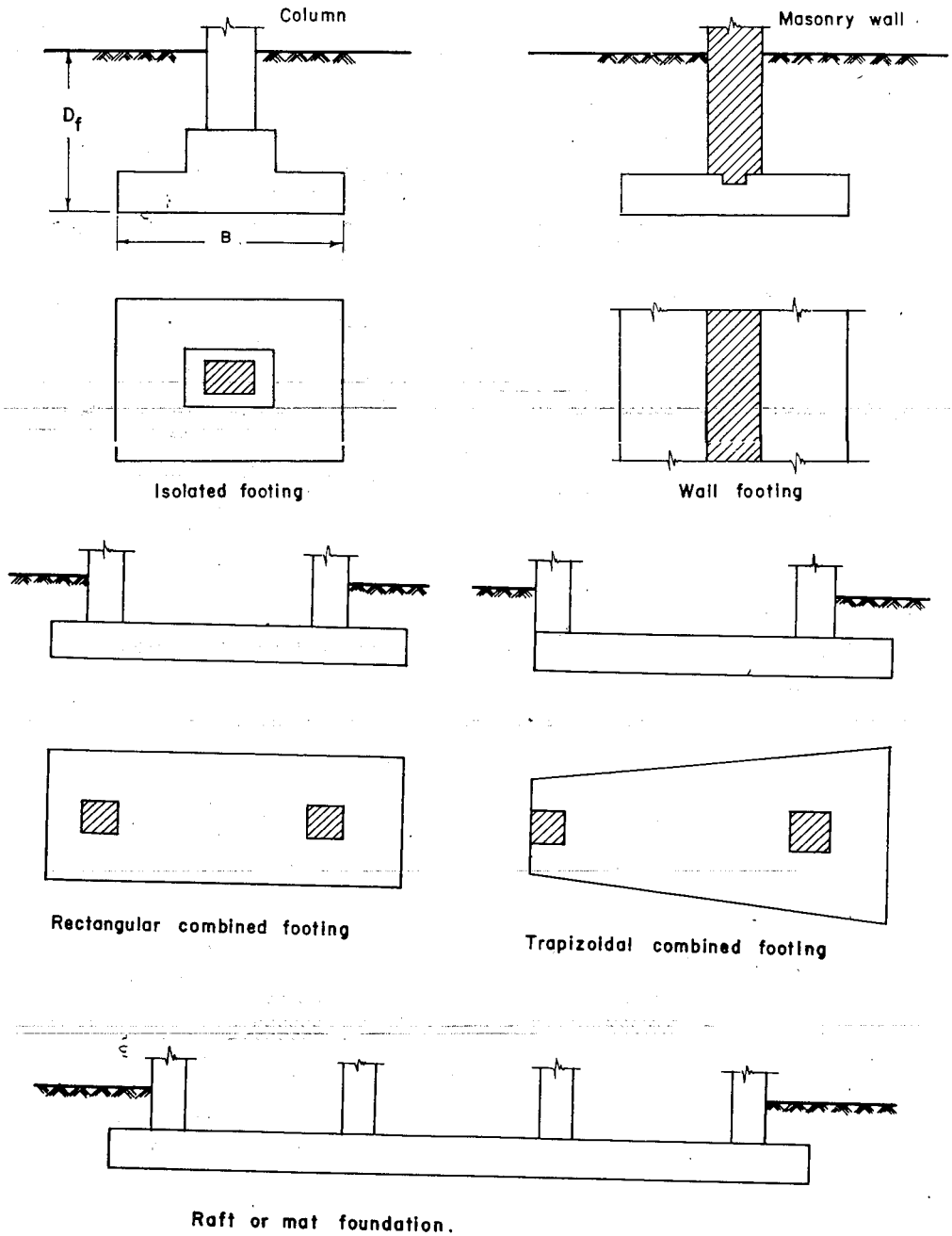
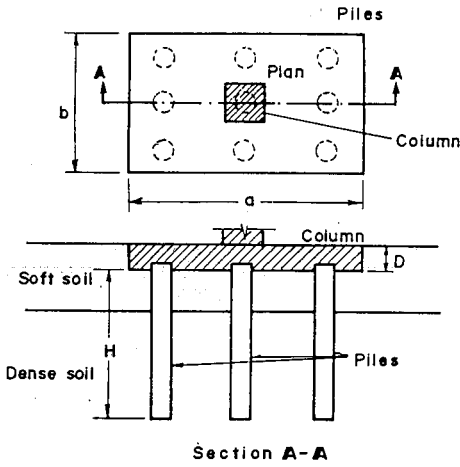
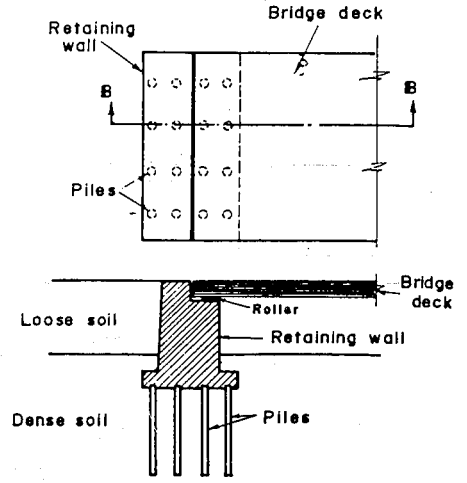


Fig. 9.1 Types of shallow foundations



Piles under columns



Piles under retaining walls

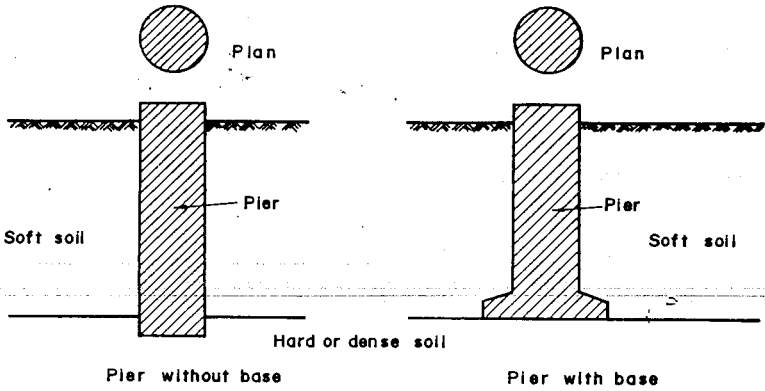
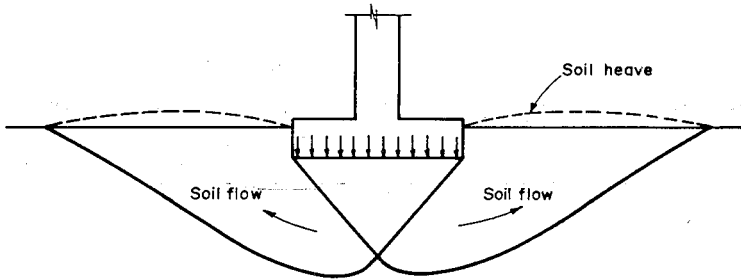


Fig. 9.2 Types of deep foundations

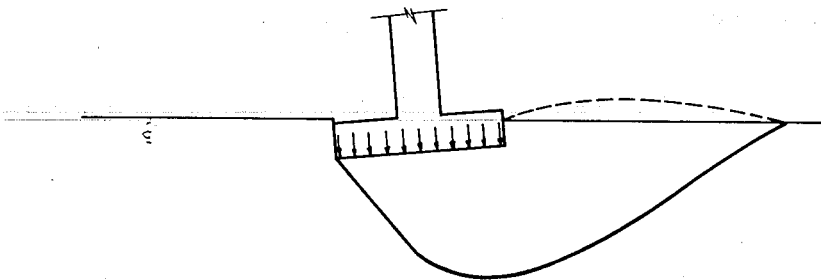
9.2 BEARING CAPACITY OF SHALLOW FOUNDATION

9.2.1 General

Under sufficiently heavy loads, the footing may sink into the ground as a result of shear failure. When this occurs, a footing resting in predominately dense granular material, experience shows that an inverted triangular prism soil having a base width equal to the width of the footing is forced downward. As this prism moves, the soil at its sides is forced laterally outward, and this lateral movement in turn causes the soil adjacent to the footing to buldge upward. If the soil foundation bed is reasonably homogeneous and the foundation is is symmetrically-loaded, the lateral movement and the tendency to buldge upward may occur symmetrically on both sides as shown in Fig. 9.3a. If on the other hand the soil is somewhat non- homogeneous or the load somewhat eccentric, shear failure will occur on one side only causing the foundation to tip as it settles (Fig. 9.3b)



(a) Symmetrical shear failure.



(b) Unsymmetrical shear failure.

Fig. 9.3 Foundation settlement due to shear failure

9.2.2 Failure Zones Below Smooth Base: Footing Loaded at Ground Level

Consider a surface footing shown in Fig. 9.4. When the soil is overloaded, the material in zone I is forced downward, displacing materials in zones II and III. The material in zone III develops passive resistance. Zone I is referred to as active Rankine zone and zone III as passive Rankine zone. Zone II is called zone of radial shear.

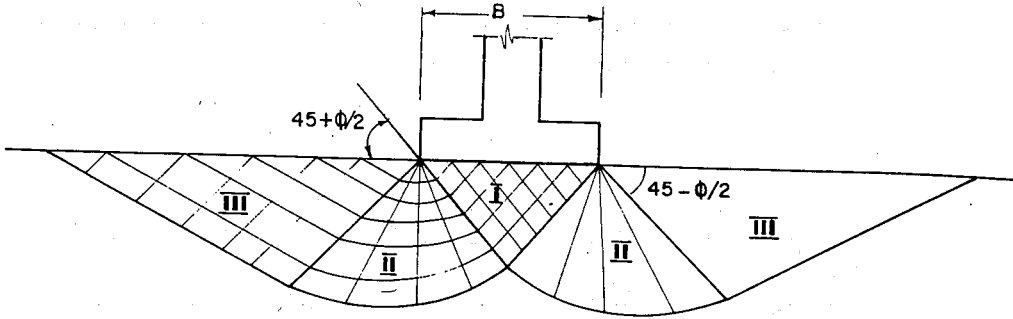


Fig. 9.4 Failure zones below smooth base footing loaded at ground level.

9.2.3 Failure Zones Below Rough Base: Footing Loaded at Ground Level

In the case of rough footing base, the soil in zone I cannot expand laterally because of friction and adhesion between the base of the footing and the soil. The soil essentially remains in elastic state and acts as part of the footing. Zones III and II are the same as the previous one (Fig. 9.5).

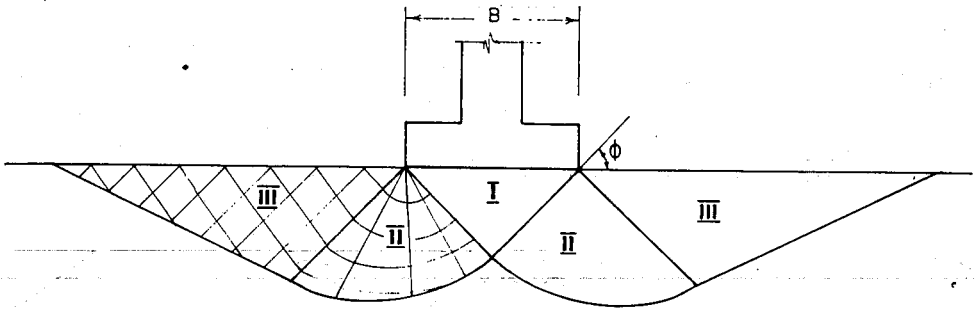


Fig. 9.5 Failure zones below rough base footing.

9.2.4 Ultimate Bearing Capacity of Shallow Foundation

9.2.4.1 Analytical Methods

Most methods of analysis are based on the assumption of zones of plastic equilibrium in the soil supporting the footing.

9.2.4.1.1 Prandtl's Method

Prandtl's method [20] presents the ultimate bearing capacity of loaded area with width B . Prandtl assumes the existence of three zones after failure is reached (Fig. 9.6). Zone I is the active Rankine zone, with the failure plane making an angle of $45 + \phi/2$ with the horizontal. It moves downward as a unit. All radial planes through points A and B are failure planes. The curved boundary is a logarithmic spiral. In zone III (which is the passive Rankine zone) the failure planes make an angle of $45 - \phi/2$ with the horizontal. They move upward and outward as a unit.

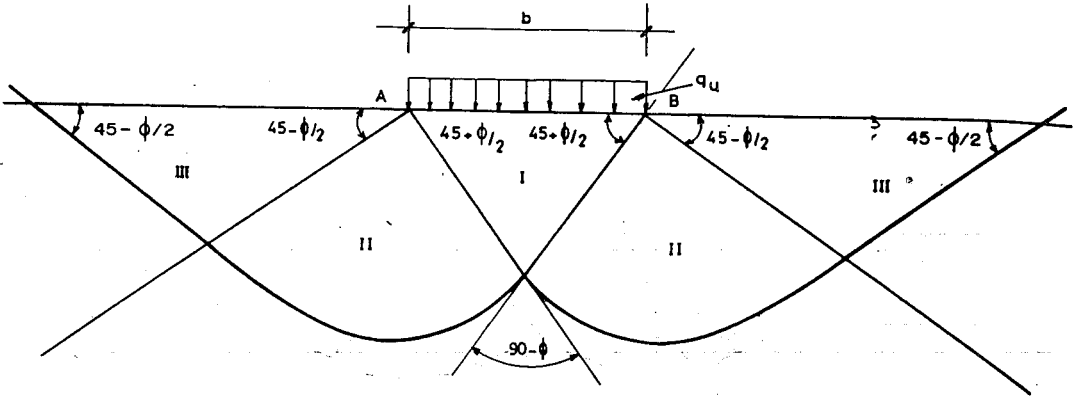


Fig. 9.6 Prandtl's method

The section is symmetrical up to point of failure, with an equal chance of failure occurring on both sides. On the basis of the assumption that the shearing strength of any soil may be generally be expressed by the well known Coulomb's equation $\tau = c + \sigma \tan \phi$, Prandtl's expression for the ultimate bearing capacity of any soil is given by

$$q_{ult} = \frac{c}{\tan \phi} [K_p e^{n \tan \phi} - 1] \quad (9.1)$$

In the above expression, for $c = 0$, the value of $q_{ult} = 0$. In order to avoid this discrepancy and taking into account the strength caused by the overburden pressure the following corrected relation is given.

$$q_{ult} = \left(\frac{c}{\tan \phi} + \frac{1}{2} \gamma B \sqrt{K_p} \right) (K_p e^{n \tan \phi} - 1) \quad (9.2)$$

Because of their compressibility, soils do not show close agreement with Prandtl's hypothesis which was originally set up for metals.

9.2.4.1.2 Terzaghi's Method

Terzaghi [29] considers two states of failure as shown in Fig.9.7

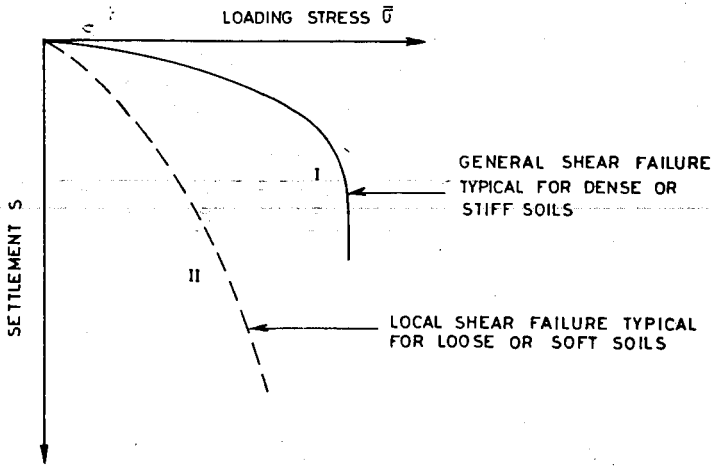


Fig. 9.7 State of failure

Accordingly he gave equations for general shear failure which are valid for curve I, and equations for local shear failure which are valid for curve II.

Theoretical methods for predicting the ultimate bearing capacity of soils are generally based on the general shear failure case. Factors that determine the ultimate bearing capacity are size and shape of the foundation element, the depth of the foundation element beneath the ground surface and the nature of the soil in which it rests.

The general form of bearing capacity equation for $c - \phi$ soil can be developed as follows.

Consider the ultimate load, Q_{ult} , on a rough continuous footing of width B shown in Fig. 9.8.

Equilibrium of the footing requires

$$Q_{ult} = 2P_p + 2C_a \sin \phi \tag{9.3}$$

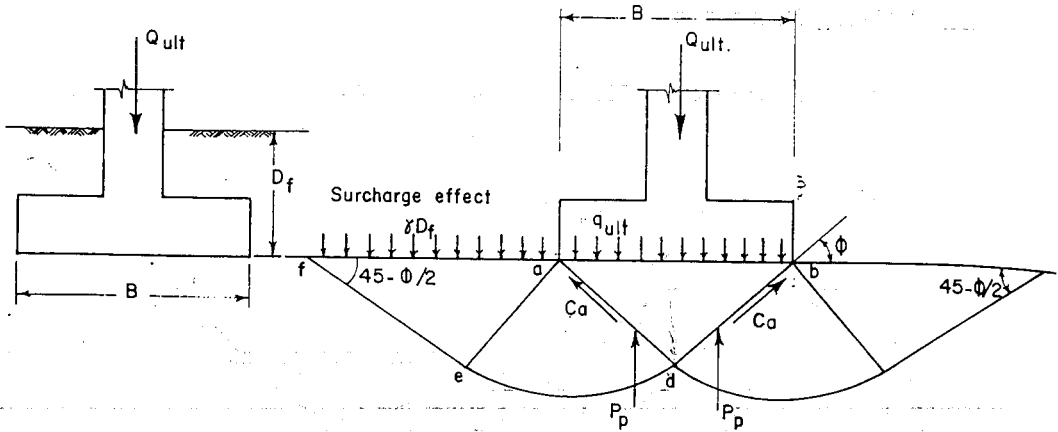


Fig. 9.8 Terzaghi's bearing capacity theory

From Fig 9.8, $a d = \frac{B}{2 \cos \phi}$ and $C_a = \frac{c}{2} \frac{B}{\cos \phi}$

Where

C_a = cohesive force

c = unit cohesion

$$Q_{ult} = 2P_p + 2 \left(\frac{c}{2} \frac{B}{\cos \phi} \right) \sin \phi = 2P_p + B \cdot c \tan \phi \quad (9.4a)$$

P_p is made up of:

- (a) P'_p passive earth force due to weight of wedge a-d-e-f. This is computed by considering the stability of the wedge and assuming $c = 0$, $D_f = 0$. It acts at $1/3$ distance from d.
- (b) P_c , passive earth force due to cohesive force only. This is computed on the assumption that $\gamma = 0$, $D_f = 0$. It acts at the middle of ad and bd
- (c) P_q , passive earth force due to surcharge. It is computed by considering $\gamma = 0$, $c = 0$. It acts at the middle of ad and bd. Therefore, Eq.(9.4) becomes,

$$Q_{ult} = 2 \left(P'_p + P_c + P_q + \frac{1}{2} Bc \tan \phi \right)$$

$$Q_{ult} = B \left(\frac{2P'_p}{B} + \frac{2P_q}{B} + \frac{2P_c}{B} + c \tan \phi \right) \quad (9.4b)$$

Let $\frac{2P_c}{B} + c \tan \phi = N_c c$

$$\frac{2P'_p}{B} = N_\gamma \frac{\gamma B}{2}$$

$$\frac{2P_q}{B} = N_q \gamma_1 D_f$$

Hence, $Q_{ult} = B(cN_c + \frac{1}{2} \gamma B N_\gamma + \gamma_1 D_f N_q)$ (9.5)

since, $q_{ult} = \frac{Q_{ult}}{A}$ and (for strip footing) $A = B \cdot 1$

$$q_{ult} = cN_c + \frac{1}{2} \gamma B N_\gamma + \gamma_1 D_f N_q \quad (9.6)$$

Terzaghi's equations establish ultimate bearing value as a function of resistance due to three factors, namely, cohesion, internal friction and surcharge effect.

The general expression for ultimate bearing capacity for *general shear failure condition* is given by, $q_{ult} = K_1 N_c + K_2 \gamma_2 N_\gamma + N_q \gamma_1 D_f$ (9.7)

Where

c = Unit cohesion

γ_2 = Effective unit weight of soil below footing grade

γ_1 = Effective unit weight of soil above footing grade

B = Width of footing

D_f = Depth of footing

K_1, K_2 = Coefficients dependent on the type of footing

For continuous footing, $K_1 = 1.0$ and $K_2 = 0.5$

For square footing, $K_1 = 1.3$ and $K_2 = 0.4$

For round footing, $K_1 = 1.3$ and $K_2 = 0.3$

N_c, N_γ, N_q = bearing capacity factors (Fig 9.9)

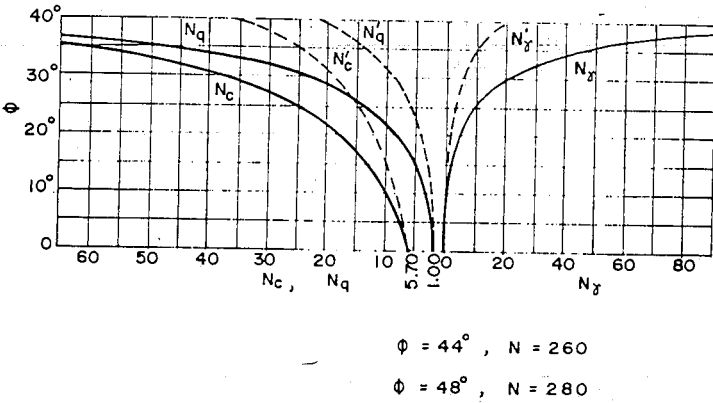


Fig. 9.9 Bearing capacity factors according to Terzaghi

The equation for the *local shear failure condition* assumes the same form as the Eq.(9.7.) However, the values of c and ϕ should be reduced as follows:

$c' = 2/3 \cdot c$ and $\tan \phi' = 2/3 \tan \phi$. The corresponding bearing capacity factors are designated by N'_c, N'_γ and N'_q (Fig 9.9). For cohesive clay soils where $\phi = 0$, from Fig. 9.9, $N_c = 5.7$ and $N_q = 1.0$

$$q_{ult} = 5.7K_1c + \gamma_1 D_f \tag{9.8}$$

If on the other hand $D_f = 0$,

$$q_{ult} = 5.7 K_1c = 5.7c \tag{9.9}$$

Eq. (9.9) indicates that the ultimate bearing capacity of clay soil varies directly with cohesion and is independent of footing width and soil weight.

For cohesionless sand where $c = 0$ the ultimate bearing capacity is expressed as,

$$q_{ult} = K_2 \gamma_2 N_\gamma B + N_q \gamma_1 D_f \quad (9.10)$$

For a footing on the surface of cohesionless soil, the ultimate bearing capacity will be,

$$q_{ult} = K_2 \gamma_2 N_\gamma B \quad (9.11)$$

Equation (9.7) represents that the ultimate bearing capacity of $c-\phi$ soil is a function of cohesion, soil density or unit weight, friction angle as reflected by bearing capacity factors and also the width of the footing. It should be noted that the presence of water table around a footing reduces its bearing capacity. For a fully submerged footing buoyant unit weights must be used for γ_1 and γ_2 . If the water table is at a distance B below the base of the footing, it is considered as having no effect. When the water table is at the base of the footing, only γ_2 will be replaced by with buoyant unit weight, γ_b . For intermediate position of the water table, the unit weight must be adjusted by interpolation.

The allowable bearing capacity is determined from the ultimate bearing capacity using the following relationship:

$$q_a = \frac{q_{ult}}{F_s} \quad (9.12)$$

F_s = Safety factor (usually taken as 2 or 3.)

The formulae for continuous, square and circular footings derived by Terzaghi are applicable for axially loaded conditions. One may however use the formulae for estimating the bearing capacity for eccentric loads. The formulae are not applicable for inclined loads. One should also observe that Terzaghi does not give bearing capacity formula for rectangular footings.

9.2.4.1.3 German code - DIN 4017 [5]

The German code is based on the failure surface of Prandtl, with some modifications. The analytical method given by the DIN 4017 is strictly valid for uniform soils. If the soil consists of different layers, a graphical method should be used.

9.2.4.1.3.1 Bearing Capacity of Footings Subjected to Centric Vertical Loads (Fig. 9.10)

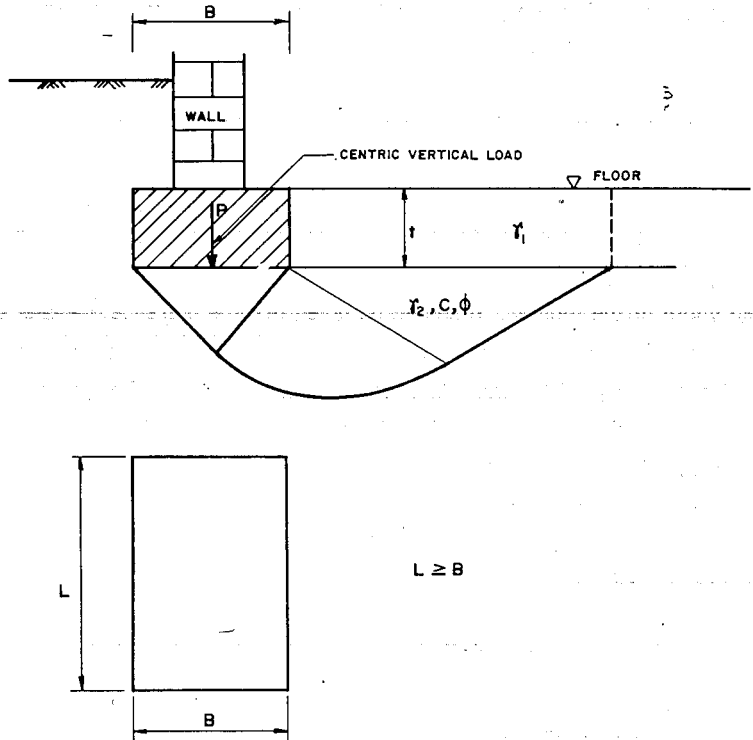


Fig. 9.10 Bearing capacity calculation for centric vertical loads according to DIN 4017

Equation for the bearing capacity is given as follows

$$Q_{ult} = B \cdot L \cdot q_{ult} = B \cdot L (c \cdot N_c \cdot s_c + \gamma_1 \cdot D_f \cdot N_q \cdot s_q + \gamma_2 \cdot B \cdot N_\gamma \cdot s_\gamma) \quad (9.13)$$

Where

- Q_{ult} = failure load (kN)
- q_{ult} = ultimate bearing capacity (kN/m²)
- B = width of foundation $B < L$ or diameter of circular foundation (m)
- L = length of foundation (m)
- D_f = minimum depth either below the original ground or below the basement floor (m)

c = cohesion (kN/m^2),

N_c, N_q, N_γ = bearing capacity coefficients, that depend on the friction angle ϕ , to account for cohesion, depth and width of foundation respectively. (Table 9.1)

s_c, s_q, s_γ = shape factors to account for cohesion, depth and width, respectively (Table 9.2),

γ_1 = unit weight above the foundations level (kN/m^3)

γ_2 = unit weight below the foundations level (kN/m^3)

$$Q_a = \frac{Q_{ult}}{F_s}$$

$$F_s = 2$$

Table 9.1 Values of bearing capacity coefficients

ϕ	N_c	N_q	N_γ
deg	-	-	-
0	5.0	1.0	0
5	6.5	1.5	0
10	8.5	2.5	0.5
15	11.0	4.0	1.0
20	15.0	6.5	2.0
22.5	17.5	8.0	3.0
25	20.5	10.5	4.5
27.5	25.0	14.0	7.0
30	30.0	18.0	10.0
32.5	37.0	25.0	15.0
35	46.0	33.0	23.0
37.5	58.0	46.0	34.0
40	75.0	64.0	53.0
42.5	99.0	92.0	83.0

Table 9.2 Values of shape factors

Type of footing	Shape factors			
	s_c		s_q	s_γ
	$\phi \neq 0$	$\phi = 0$		
Continuous Footing (strip)	1.0	1.0	1.0	1.0
Rectangular Footing	$\frac{s_q \cdot N_q - 1}{N_q - 1}$	$1 + \frac{0.2B}{L}$	$1 + \frac{B \sin \phi}{L}$	$1 - 0.3 \frac{B}{L}$
Square/Circular Footing	$\frac{s_q \cdot N_q - 1}{N_q - 1}$	1.2	$1 + \sin \phi$	0.7

9.2.4.1.3 Bearing Capacity of footing Subjected to Eccentric Loads

This code is valid for eccentric and inclined loadings with rectangular dimensions which are often used in retaining walls, quays, bridge abutments and towers.

The bearing capacity is calculated as eccentrically loaded foundation with the dimension L' and B' .

where

$$L' = L - 2e_L \text{ and}$$

$$B' = B - 2e_B$$

Noting that e_L and e_B are the distances of the resultant force from the central axis of the foundation in the direction of L and B respectively, the equation of the bearing capacity is expressed as,

$$V_f = L' \cdot B' \cdot q_{ult} \quad (9.14)$$

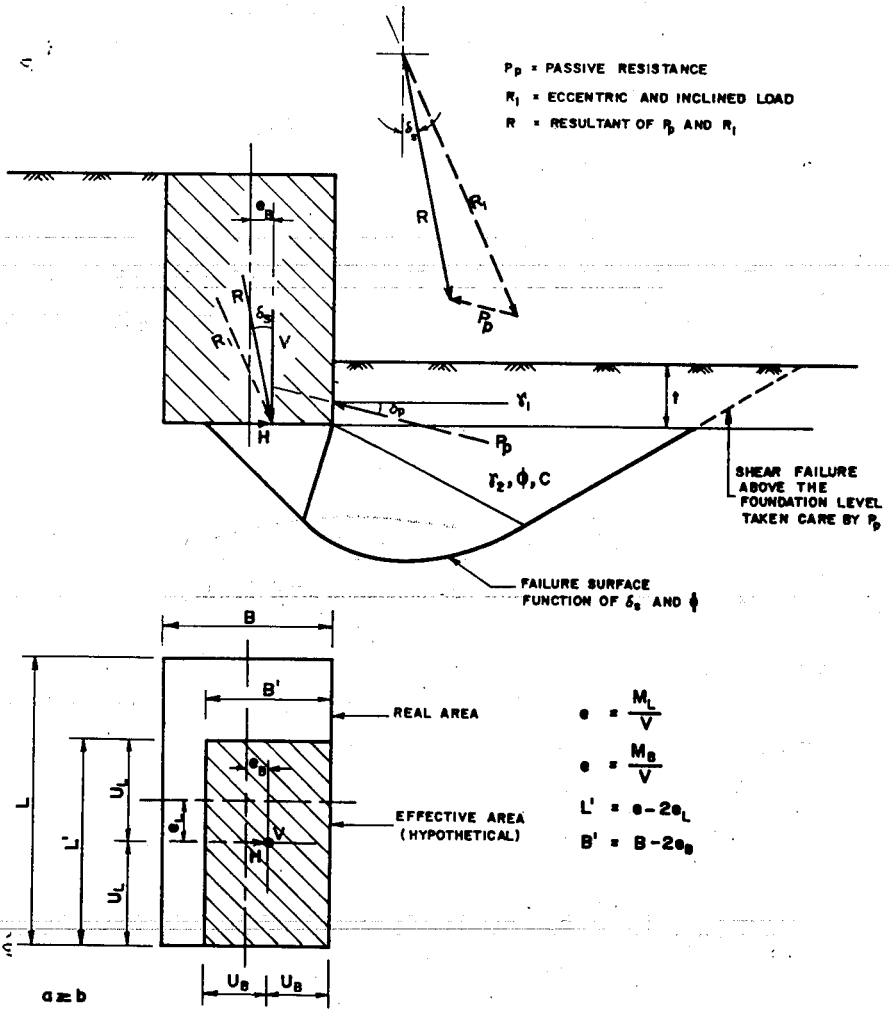


Fig. 9.11 Bearing capacity calculation for eccentric and inclined loads according to DIN 4017 [6]

B' represents always the smaller side of the hypothetical dimension and by inclined loading the horizontal component H should always be parallel to B' .

$$q_{ult} = c \cdot N_c \cdot i_c \cdot s'_c + \gamma_1 \cdot D_f \cdot N_q \cdot i_q \cdot s'_q + \gamma_2 \cdot B' \cdot N_\gamma \cdot i_\gamma \cdot s'_\gamma \quad (9.15)$$

where

V_f = vertical component of the critical load (kN)

q_{ult} = average ultimate bearing capacity acting under the hypothetical dimension (kN/m²)

A' = $L' \cdot B'$ = hypothetical (effective) area (m²)

L' = hypothetical length (m)

B' = hypothetical width (m)

c = cohesion (kN/m²)

D_f = foundation depth (m). If the base of the foundation is inclined to increase sliding resistance, the depth D_f taken will be from the deepest point.

N_c, N_q, N_γ = bearing capacity coefficients

i_c, i_q, i_γ = inclination coefficients

s'_c, s'_q, s'_γ = shape factors depending B'/L' corresponding to the factors according to Table 9.2

γ_1 = unit weight above the foundation level (kN/m³)

γ_2 = unit weight below the foundation level (kN/m³)

Inclination Coefficients

Generally the inclination coefficients depend on $\tan \delta_s$ and the direction of horizontal force (Fig 9.11)

Horizontal Force Parallel to B'

i) For the case $\phi_u = 0, c_u \neq 0$

$$i_q = 1$$

$$i_c = 0.5 + 0.5 \sqrt{1 - \frac{H_f}{A' \cdot c_u}}$$

During the dimensioning of the foundation, for a given load, the parameter A' must be selected so that the following condition is satisfied.

$$\frac{H_f}{A' \cdot c_u} \leq 1 \quad (9.16)$$

ii) For the case $\phi \neq 0; c \neq 0$

$$i_q = \left[1 - \frac{0.7 H_f}{V_f + A' \cdot c \cdot \cot \phi} \right]^3 \quad (9.17)$$

where

$H_f = F_s, H$ (horizontal critical load)

$V_f = F_s, V$ (Vertical critical load)

$$i_v = \left[1 - \frac{H_f}{V_f + A' \cdot c \cdot \cot \phi} \right]^3 \quad (9.18)$$

$$i_c = i_q - \frac{1 - i_q}{N_q - 1} \quad (9.19)$$

iii) For the case $\phi \neq 0; c = 0$

$$i_q = (1 - 0.7 \tan \delta_s)^3 \quad (9.20)$$

$$i_v = (1 - \tan \delta_s)^3 \quad (9.21)$$

B Horizontal Force Parallel to L

i) For the case $\phi_u = 0; c_u \neq 0$

$$i_q = 1$$

$$i_c = 0.5 + 0.5 \sqrt{1 - \frac{H_f}{A' \cdot c_u}} \quad (9.22)$$

ii) For the case $\phi \neq 0; c_u \neq 0$

$$i_q = i_v = 1 - \frac{H_f}{V_f + A' \cdot c \cdot \cot \phi} \quad (9.23)$$

$$i_c = i_q - \frac{1 - i_q}{N_q - 1} \quad \text{for } L/B > 2 \quad (9.24)$$

(iii) For the case $\phi \neq 0; c = 0$

$$i_q = i_v = 1 - \tan \delta_s \tag{9.25}$$

9.2.4.1.4 Approximate Methods for Determining Bearing Capacity of Purely Cohesive Soils ($\phi = 0$)

In reality soil without frictional resistance does not exist. However, a case $\phi = 0$ may arise when loading is applied suddenly.

Ultimate Bearing Capacity by the Method of Slip Circle

The expression of ultimate bearing capacity by this method is derived in reference to Fig. 9.12.

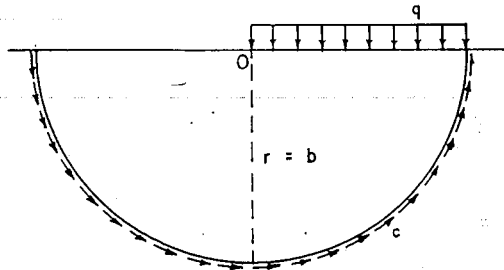


Fig. 9.12 Method of slip circle

Taking moment about O

Driving moment, $M_o = (b) (q) \left(\frac{b}{2}\right) = \frac{qb^2}{2}$

Resisting moment, $M_r = (b \pi c) b = \pi c b^2$

For equilibrium condition,

$$\frac{qb^2}{2} = \pi c b^2, \text{ it follows that } q = 2\pi c$$

$$q_{ult} = (2)(3.14) c = 6.28c \quad (9.26)$$

Ultimate bearing capacity of long footings on cohesive soil by Fellenius method

Fellenius method of circular failure surfaces shown in Fig. 9.13 may be used to determine the ultimate bearing capacity of highly cohesive soils. The expression for long (continuous) footing on highly cohesive soil is derived in reference to Fig.9.13.

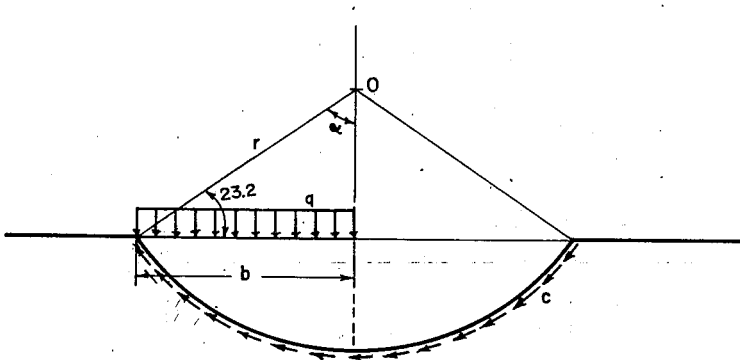


Fig. 9.13 Fellenius method

$$L_c = 2\alpha r$$

Where

L_c = length of the arc

The cohesive force = $2\alpha r c$

Taking moment about O

Resisting moment, $M_r = 2\alpha c r^2$, noting that $b = r \sin \alpha$ and $r = \frac{b}{\sin \alpha}$

Driving moment, $M_o = q \cdot b \left(\frac{b}{2} \right)$

For equilibrium condition, resisting moment = driving moment.

Nothing that $b = r \sin \alpha$ and $r = b/\sin \alpha$

$$\frac{qb^2}{2} = 2 \cdot c\alpha \left(\frac{b}{\sin \alpha} \right)^2 = \frac{2\alpha cb^2}{\sin^2 \alpha}$$

$$q = \frac{4\alpha c}{\sin^2 \alpha} \quad (9.27)$$

$$\frac{q}{4c} = \frac{\alpha}{\sin^2 \alpha}$$

For minimum value of α ,

$$\frac{d}{d\alpha} \left[\frac{\alpha}{\sin^2 \alpha} \right] = 0$$

$$\frac{\sin^2 \alpha \cdot 1 - 2 \sin \alpha \cdot \cos \alpha \cdot \alpha}{\sin^4 \alpha} = 0$$

Simplifying the above, one obtains

$$\sin^2 \alpha = 2 \sin \alpha \cdot \cos \alpha \cdot \alpha$$

Dividing by $\sin \alpha$

$$\sin \alpha = 2 \cos \alpha \cdot \alpha$$

Further simplification gives

$$\tan \alpha = 2 \alpha \quad (9.28)$$

Solving Eq. (9.27) with tangent series yields the value of $\alpha = 0.37 \pi = 66.8^\circ$

Inserting the value of α in Eq. (9.27) yields.

$$q_{ult} = \frac{(4)(c)(0.37\pi)}{\sin^2 66.8} = 5.5c \quad (9.29)$$

Fellenius method is extended to footings founded below the ground (Fig.9.14). Wilson found that for depth 1.5 times the breadth, the expression of ultimate bearing capacity for long footing below the surface of highly cohesive soil is expressed as

$$q_{ult} = 5.5c \left(1 + 0.38 \frac{d}{b} \right) \quad (9.30)$$

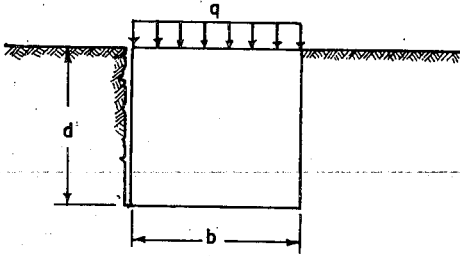


Fig. 9.14 Fellenius method for footing below ground surface

Skempton's Work

Skempton developed an equation for ultimate bearing capacity of cohesive soil for $\phi = 0$ condition. His equation for a footing of width B and depth D_f may be written as follows:

$$q_{ult} = c N_c + \gamma \cdot D_f$$

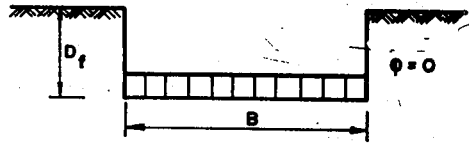
The value of N_c can be obtained from Table 9.3.

Table 9.3 Bearing capacity coefficients according to Skempton [23]

$\frac{D_f}{B}$	N_c	
	Circle or Square N_{cr}	Strip N_{cs}
0	6.2	5.14
0.25	6.7	5.6
0.5	7.1	5.9
0.75	7.4	6.2
1.0	7.7	6.4
1.5	8.1	6.8
2.0	8.4	7.0
2.5	8.6	7.2
3.0	8.8	7.4
4.0	9.0	7.5
> 4.0	9.0	7.5

For intermediate shapes, the values of N_{cr} for a rectangle, length L , breadth B , may be obtained from that for a strip, N_{cs} by the relation

$$N_{cr} = \left\{ 1 + 0.2 \frac{B}{L} \right\} N_{cs}$$



For intermediate shapes, the values of N_{cr} for a rectangle, length L , breadth B may be obtained from that for a strip, N_{cs} by the relation

$$N_{cr} = \left(1 + 0.2 \frac{B}{L} \right) N_{cs}$$

9.2.4.2 Graphical Method for Determining Ultimate Bearing Capacity of Homogeneous Soils

The bearing capacity of a homogeneous soil may also be determined graphically. In general, the equilibrium of a rigid element bounded by active and passive wedges using Prandtl's failure criterion is considered. From the equilibrium equation the component of the ultimate load is determined. Then through vectorial addition, the magnitude of the ultimate load is finally obtained. The above general procedure may be illustrated by considering the case shown in Fig. 9.15. The rigid wedge BGC - which is in a state of equilibrium - is bounded by the active wedge ABG and the passive wedge BCD. The forces acting on this wedge are:

- (i) Cohesion forces C_1 , C_2 and C_3 which are known in magnitude and direction.
- (ii) Q_1 - which is the component of G_1 - inclined at angle of ϕ from the normal and acting on the plane GB.
- (iii) Q_p - which is the component of the ultimate load P - having a line of action shown in the figure. The magnitude of this force is unknown.
- (iv) Reaction force Q_2 with a line of action that passes through B. This force is inclined at an angle ϕ with the normal. Its magnitude is also unknown.
- (v) G_2 - the weight of the wedge - acting at the centroid of the wedge.
- (vi) Q_3 and Q_4 - which are the components of the known forces G_3 and G_4 respectively - acting as indicated in the figure.

From equilibrium, the summation of the moments of the above forces about point B should be zero. Hence,

$$\sum M_B = Q_p \cdot a + Q_1 \cdot a_1 - G_2 \cdot a_2 - Q_3 \cdot a_3 - Q_4 \cdot a_4 - C_2 \cdot a_c = 0 \quad (9.31)$$

From Eq. (9.31) the magnitude of Q_p is determined. Since Q_p is a component of the ultimate load P , its magnitude should easily be determined from the force triangle indicated in the figure. Using the procedure outlined above, the ultimate load may be determined for the different loading conditions shown in Fig 9.16 and 9.17. For the case of Fig. 9.17, the magnitude of θ should first be determined from Fig. 9.18.

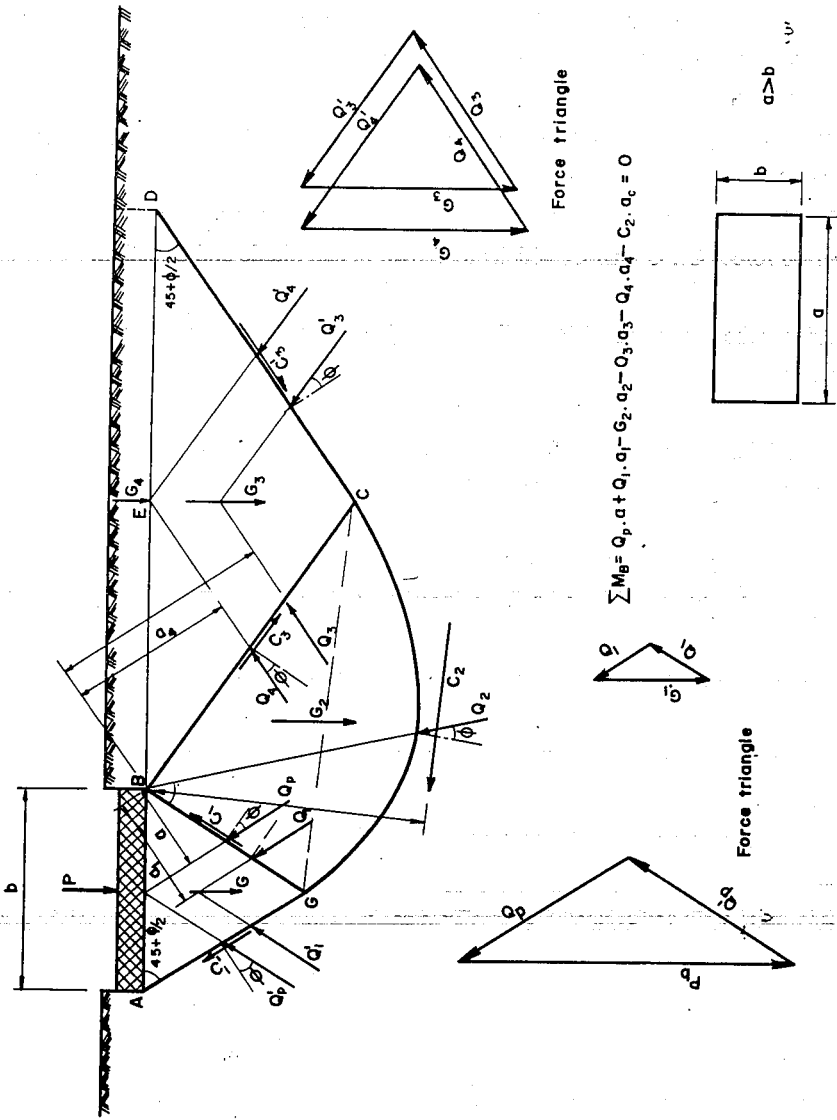


Fig. 9.15 Bearing failure under centrally loaded foundation for long term loading condition ($c \neq 0, \phi \neq 0$)

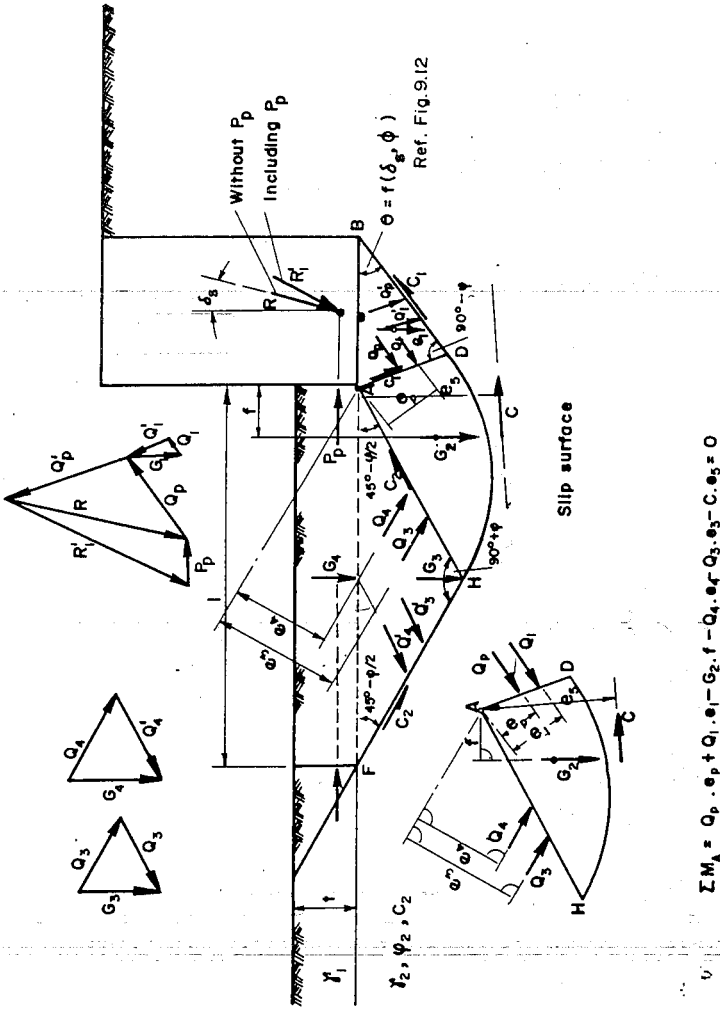
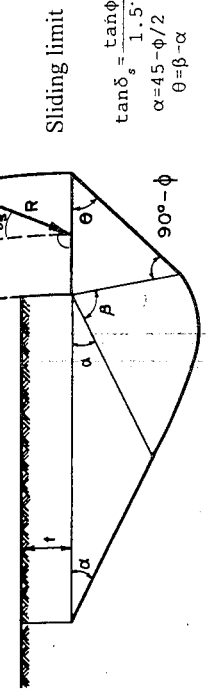


Fig. 9.17 Bearing failure under inclined loaded foundation for long term loading condition ($c \neq 0, \phi \neq 0$)



Sliding limit
 $\tan \delta_s = \frac{\tan \phi}{1.5}$
 $\alpha = 45 - \phi/2$
 $\theta = \beta - \alpha$

$$\tan \theta = \frac{\cos \delta_s \sqrt{\cos^2 \delta_s - \cos^2 \phi} + \cos^2 \phi + \cos^2 \delta_s - \cos^2 \phi}{(\sin \phi) (\cos \phi) + (\sin \delta_s) (\cos \delta_s) + \sin \delta_s \sqrt{\cos^2 \delta_s - \cos^2 \phi}}$$

φ [Degree]	δs Degree																			
	2.5	5.0	7.5	10.0	12.5	15.0	17.5	20.0	22.5	25.0	27.5	30.0	32.6	35.0	37.5	40.0	42.5	45.0	47.5	50.0
10.0	41.48	32.11	21.89	0.00																
12.5	44.19	36.88	28.96	19.58	0.00															
15.0	46.41	40.17	33.61	26.46	17.88	0.00														
17.5	48.34	42.83	37.11	31.12	24.42	16.55	0.00													
20.0	50.0	45.13	40.01	34.75	29.15	22.91	15.48	0.00												
22.5	51.47	47.17	42.54	37.76	32.78	27.48	21.61	14.58	0.00											
25.0	53.30	49.06	44.76	40.38	35.85	31.12	26.07	20.49	13.81	0.00										
27.5	54.80	50.82	46.80	42.71	38.53	34.21	29.69	24.86	19.52	13.13	0.00									
30.0	56.26	52.49	48.69	44.85	40.93	36.92	32.77	28.42	23.78	18.65	12.53	0.00								
32.5	57.68	54.09	50.48	46.83	43.13	39.36	35.49	31.49	27.39	22.82	17.88	11.99	0.00							
35.0	59.08	55.64	52.18	48.70	45.17	41.59	37.95	34.28	30.33	26.27	21.95	17.17	11.50	0.00						
37.5	60.45	57.14	53.82	50.47	47.09	46.68	40.21	36.66	33.03	29.27	25.31	21.14	16.52	11.04	0.00					
40.0	61.81	58.61	55.40	52.17	48.92	48.92	42.31	38.93	35.49	31.95	28.30	24.47	20.40	15.92	10.61	0.00				
42.5	63.16	60.05	56.94	53.81	50.66	47.49	44.29	41.05	37.75	34.39	30.95	27.38	23.66	19.70	15.35	10.22	0.00			
45.0	64.49	61.47	58.44	55.40	52.35	49.27	46.17	43.84	39.87	36.65	33.37	30.00	26.53	22.90	19.04	14.82	9.84	0.00		
47.5	65.81	62.86	59.91	56.95	53.97	50.98	47.97	44.94	41.87	38.77	35.62	32.40	29.11	25.72	22.17	18.42	14.30	9.48	0.00	
50.0	67.13	64.24	61.35	58.46	55.55	52.63	49.70	46.75	43.77	40.76	37.72	34.63	31.49	28.26	24.94	21.48	17.82	13.81	9.13	0.00
52.5	68.43	65.60	62.77	59.94	57.09	54.24	51.37	48.49	45.59	42.66	39.71	36.72	33.69	30.60	27.45	24.20	20.81	17.24	13.34	8.79
55.0	69.73	66.95	64.17	61.39	58.60	55.80	52.99	50.17	47.33	44.48	41.61	38.70	35.76	32.78	29.75	26.66	23.47	20.16	16.67	12.87
57.5	71.03	68.29	65.56	62.82	60.07	57.32	54.56	51.79	49.01	46.22	43.41	40.58	37.72	34.83	31.90	28.93	25.89	22.77	19.53	16.12

Fig. 9.18 Values of θ

9.2.4.3 Ultimate Bearing Capacity of Stratified Soils

The bearing capacity formulae given above are strictly valid for homogeneous soils or for a two-layered soil system in which the first layer is located at or above the foundation level and the second layer covering the whole of the rupture line.

If the ground consists of numerous layers, the bearing capacity of the ground could only be determined approximately. Here again, a rupture line consisting of logarithmic spiral and straight lines is assumed. Two methods are available for the analysis depending upon the difference between the mean value of the angle of internal friction ϕ_a of the whole layer and that of the angle of internal friction ϕ of each layer.

These methods are

(i) Method of DIN 4017 [5]

(ii) Method of Schultze [21]

9.2.4.3.1 Method of DIN 4017

In this method one assumes an initial angle of internal friction, ϕ_1 , or take the value of the angle of internal friction, ϕ_1 , of the first layer under the foundation. One then establishes the rupture line. From the rupture line one calculates the weighted average values of the angle of internal friction, ϕ_m , and that of the cohesion, c_m . If the difference between the initial ϕ_1 and that of ϕ_m is bigger than 3%, one alters the magnitude of the angle of internal friction, which would consequently give a different rupture line and repeats the calculation until the difference between the altered ϕ and calculated ϕ_m is less than 3%. An illustrative example to elucidate this method has been worked out (E9.6 and E9.7). It should be noted that this method is permissible only if the difference between the mean value of the angle of internal friction of the whole layer ϕ_a and the respective value of the angle of internal friction of each layer is not greater than 5° . If the deviation is greater than 5° , one may use a semi-graphical method as proposed by Schultze.

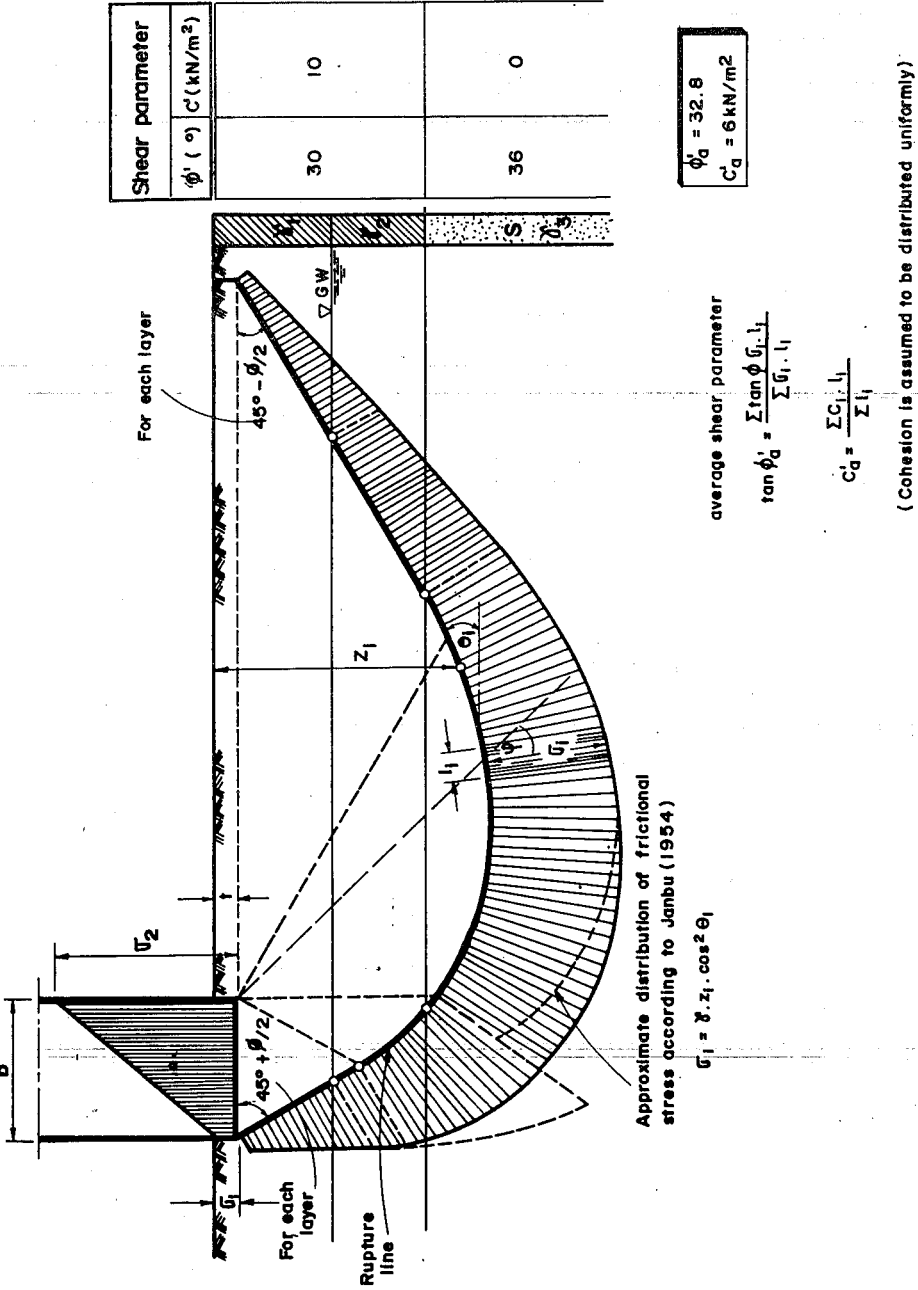


Fig. 9.19 Estimation of bearing capacity for layered soils according to Schultz

9.2.4.3.2 Method of Schultze

Here also the Prandtl's failure criterion is used. However, the actual value of the friction angle of each layer is considered. This results in a broken rupture line, which is then approximated by continuous line (Fig. 9.19). One then considers the variation of the vertical stress along the rupture line. This is determined using the equation of Jambu [21]

$$\sigma_i = \gamma z_i \cos^2 \theta_i \quad (9.32)$$

where

γ = unit weight of soil (for convenience assumed to be = 1) z_i = depth of the rupture line at point i

θ_i = tangent angle at point i

As is evident from Fig. 9.19, the loads from the superstructure are converted to an equivalent ideal heights, $h_1 = \sigma_1/\gamma$ and $h_2 = \sigma_2/\gamma$. This would give a jump in the vertical stress distribution. However, for practical purposes, the distribution is approximated to give a smooth curve as indicated in the figure. The weighted average shear parameter are then calculated from the following.

$$\tan \phi'_a = \frac{\sum \sigma_i l_i \tan \phi_i}{\sum \sigma_i l_i} \quad (9.33)$$

$$c'_a = \frac{\sum c_i l_i}{\sum l_i} \quad (9.34)$$

Hence, by inserting the values of ϕ'_a and c'_a into the available bearing capacity formulae for homogeneous soils, one is in a position to determine approximately the bearing capacity of a layered system.

9.2.4.4 Allowable Bearing Capacity From Settlement Consideration

9.2.4.4.1 General

Besides satisfying shear failure requirement, the design of foundation must ensure that the footing must not settle more than a specified amount. As a general rule, every footing settles under an applied load. Settlement would be inconsequential if all footings settle the same amount. However, due to the variation in the nature of the strata, sizes of the footings, and unit pressure below the base of the footings, differential settlements of footings result.

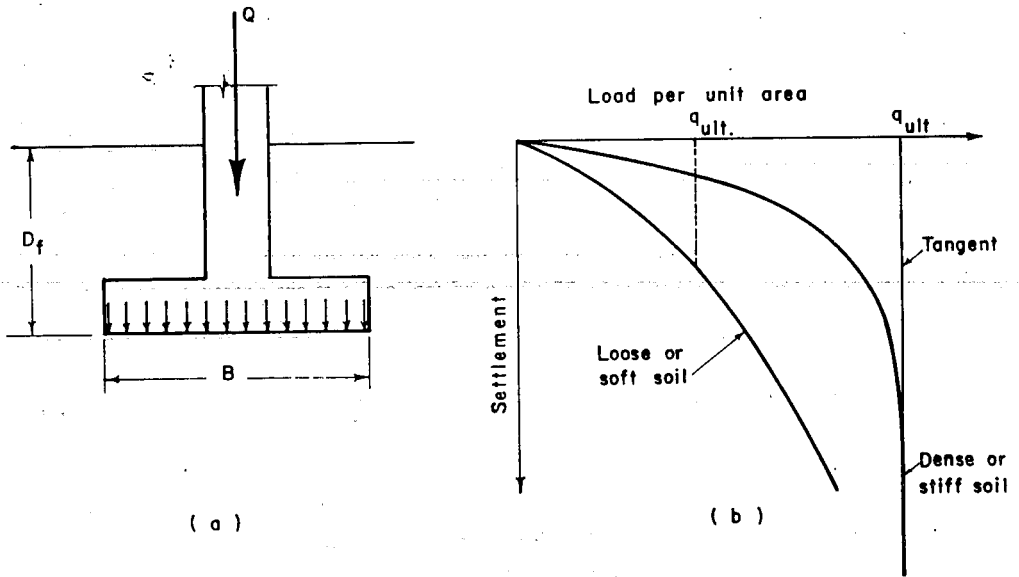


Fig. 9.20 Generalized load settlement curve

To determine the allowable bearing pressure corresponding to the permissible settlement, loading tests must sometimes be carried out. This is especially necessary for footing on sand and fissured clays.

When a load is applied to a shallow footing of depth D_f and width B , the footing settles. The relation between the average load per unit area and settlement is as shown in Fig. 9.20.

As can be seen from Fig 9.20b, an increase in the load causes an increase in the settlement almost proportional upto a certain point. On further loading, the rate of settlement increases suddenly. The abscissa, q_{ult} , of the tangent to the lower steep portion of the curve is the ultimate load which the soil can carry before failure. This load divided by the area of the footing gives the ultimate bearing capacity of the soil. Fig. 9.20b shows also the load settlement curve for a loose or fairly soft soil.

The point of failure or ultimate bearing capacity is not well defined. In such cases, the ultimate bearing capacity may be taken to correspond to a point where the settlement curve becomes fairly steep and approaches a straight line.

9.2.4.4.2 Plate-Loading Test

This is a semi-direct method is appropriately used for estimating the bearing capacity of homogeneous non-cohesive soils in the field. It consists essentially of applying load increments to a model footing (plates of standard size) shown in Fig. 9.21a and measuring the amount of settlement caused by the applied load. The load test is carried out to the point of failure or up to a load 1½ times the design load. The data of the load test are presented as a curve of settlement versus bearing pressure for the test plate as shown in Fig. 9.21. From the plate-loading test, the bearing capacity of non-cohesive soils is determined from settlement consideration [30]. The maximum permissible settlement, S_f , of a footing of width B_f under the same intensity of loading is given by

$$S_f = S_p \left(\frac{2B_f}{B_f + B_p} \right) \quad (9.35)$$

where

S_p = settlement of a plate in cm.

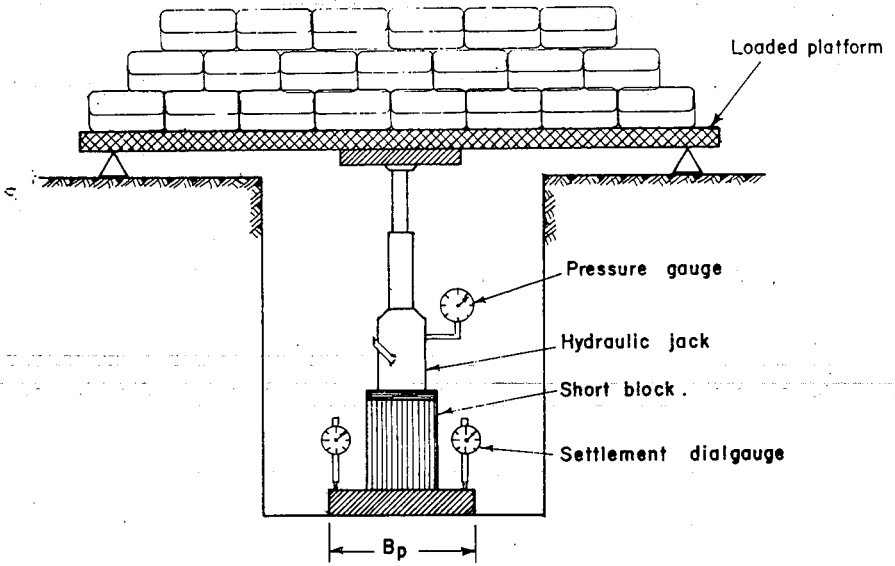
S_f = settlement of a footing in cm.

B_p = width of a plate in cm.

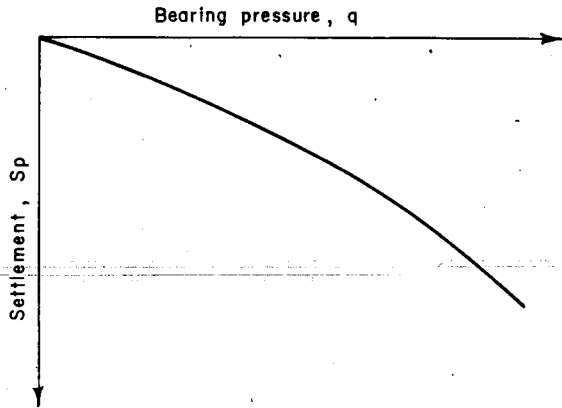
B_f = width of a footing in cm.

Using the value, S_p , computed from Eq.(9.35), the loading intensity under the footing can be read from load-settlement curve. The settlement of footing in clay is normally determined from principles of consolidation. However, for relatively dry condition one may use a plate-load test. The approximate settlement of footing of width B can be determined using the following expression.

$$S_f = S_p \frac{B_f}{B_p} \quad (9.36)$$



(a .) Plate loading set up



(b) Settlement versus bearing pressure .

Fig. 9.21 Plate loading test

In using the results of plate-loading test care must be exercised lest serious errors might be committed. Consider the situation shown in Fig 9.22.

From Fig. 9.22 it can be observed that the significant stress transmitted by the test plate wholly lies in the firmer material. Under the full size footing, however, the stress would be transmitted to the softer material. Hence, the test plate reveals the strength character of the firmer material and thus indicates a high bearing capacity. The stress influence of the actual footing of the same stress intensity penetrates to a softer material causing deformation which consequently leads to excessive settlement.

From the above example the danger that may result can be seen, if one relies wholly on the result of the plate - loading test, which shows no significant settlement for the situation considered. It can in short be said that plate-loading test data must be carefully examined and interpreted before their application in the design of foundations.

9.3 ULTIMATE BEARING CAPACITY OF DEEP FOUNDATIONS

9.3.1 General

The most common types of deep foundations are piles and drilled piers. Both systems of foundation are used to transfer loads to firmer soils located at a greater depth when the surface soils are not capable of supporting the applied loads. Piles can be of reinforced concrete or steel section. The most common in this country is reinforced concrete piles which are cast-in-place.

Depending on the kind of support they obtain, piles can be classified as end bearing and friction piles. End bearing piles obtain support from bearing on the bottom end of the pile, while friction piles get the necessary resistance from friction along the surface of the piles (Fig. 9.23).

Loads are generally transmitted to piles through reinforced concrete pile caps. For the evaluation of the capacity of the foundation system, both individual and group action of piles are considered. The capacity of the individual piles can be estimated by

- (a) static formulae (b) dynamic formulae
- (c) sounding tests (d) pile loading tests, and (e) building codes.

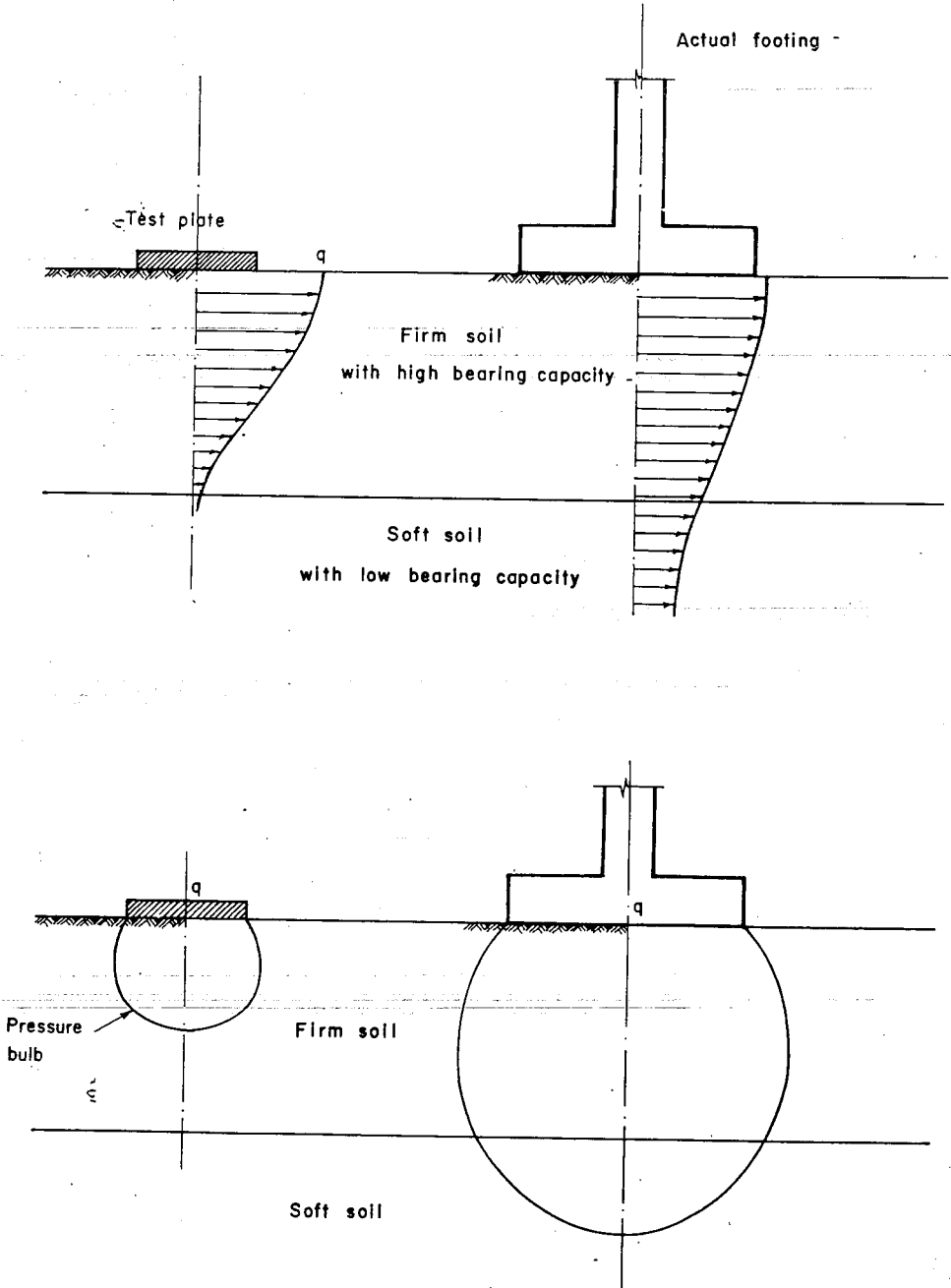


Fig. 9.22 Stress influence of test plate and footing

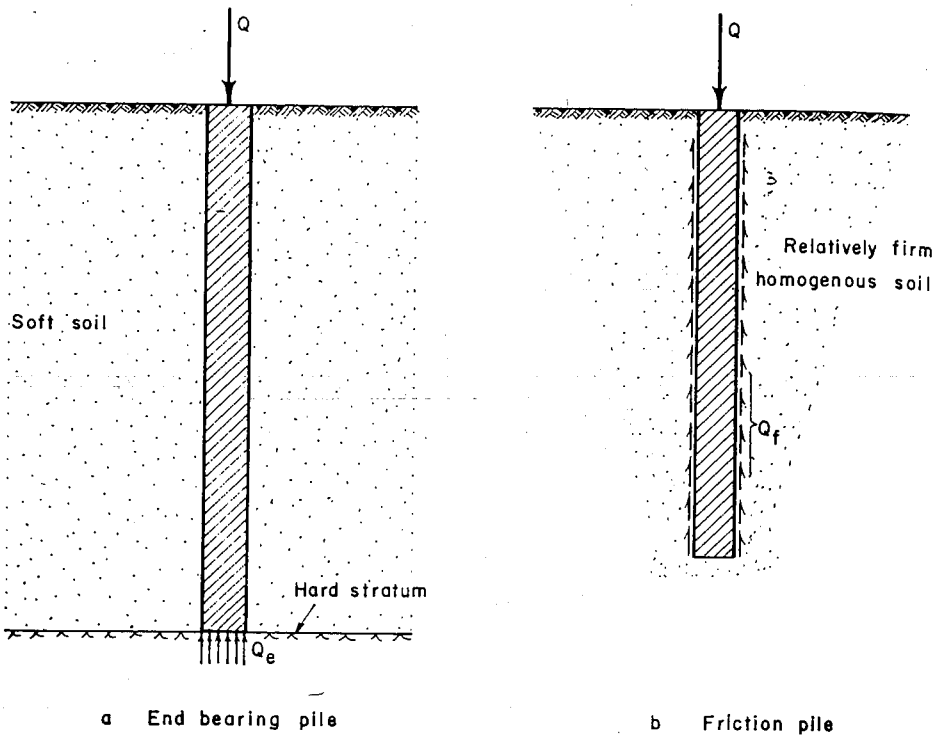


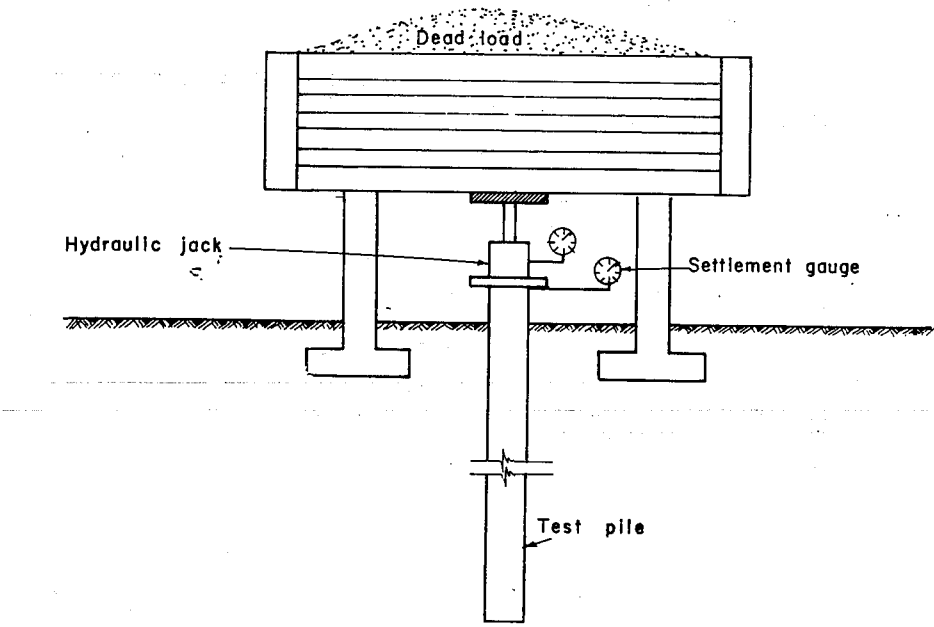
Fig. 9.23 Classification of piles

In this text only the pile loading test is discussed briefly. This is because the pile loading test has proved to be the most reliable method of estimating the capacity of individual piles. The reader is referred to other texts for the different methods of determining pile capacity.

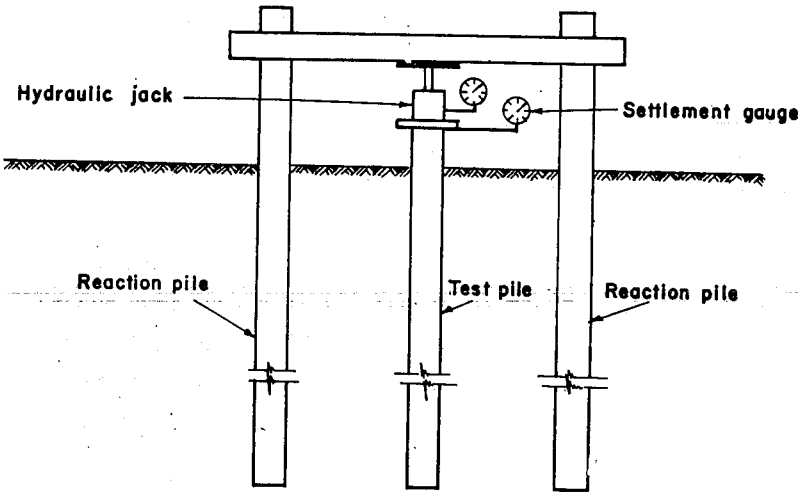
9.3.2 Pile load test

The arrangement of pile load test is shown in Fig. 9.24a. Loads are applied in increments to a test pile and the resulting settlement under each increment is noted. The loading is continued until failure or up to $1\frac{1}{2}$ times the design load.

Instead of the dead load, reaction piles can sometimes be used (Fig 9.24b). The results of the pile load test is presented as load versus settlement curve shown in Fig. 9.24c.



(a) Dead load setup



(b) Reaction pile setup

Fig. 9.24 Pile load test

9.3 EXAMPLES

- E. 9.1 Determine the safe bearing capacity of sand having $\phi = 36^\circ$ and effective unit weight 18kN/m^3 for the following cases:
- 1m wide strip footing
 - 1m x 1m square footing
 - circular footing of 1m diameter

SOLUTION

consider $D'_f = 1\text{m}$ and no problem of water table rising.

Take $F_s = 3$

Use Terzaghi's theory

For $\phi = 36^\circ$, $N_q = 47$, $N_\gamma = 43$

(a) Strip footing

$$q_{ult} = k_2 \gamma_2 B N_\gamma + \gamma_1 D_f N_q$$

$$q_a = \frac{1}{F_s} (k_2 \gamma_2 B N_\gamma + \gamma_1 D_f N_q) = \frac{1}{3} [0.5 (18) (1) (43) + 18 (1) (47)]$$

$$= 4111 \text{ kN/m}^2$$

(b) Square footing

$$q_a = \frac{1}{3} [0.4 (18) (1) (43) + 18 (1) (47)] = 385.2 \text{ kN/m}^2$$

(c) Circular footing

$$q_a = \frac{1}{3} (0.3) (18) (1) (43) + 18 (1) (4) = 359.4 \text{ kN/m}^2$$

- E.9.2 A square column footing rests 1.5m. below the ground surface. The total load transmitted by the footing is 2000kN. The water table is located at the base of the footing. Assuming a saturated unit weight of sand as 24kN/m^3 and angle of internal friction of 33° , find a suitable size footing for the above condition. Take $F_s = 3$.

SOLUTION

$$q_{ult} = K_1 c N_c + K_2 \gamma_2 N_\gamma B + \gamma_1 D_f N_q$$

$$K_1 = 1.3, K_2 = 0.4$$

For sand, $c = 0$

$$\gamma_2 = \gamma_{sat} - \gamma_w = 24 - 10 = 14 \text{ kN/m}^3$$

$$\gamma_1 = 24 \text{ kN/m}^3$$

For $\phi = 33^\circ$, $N_\gamma = 32$, $N_q = 32$

Since B is not known, the problem is solved by trial and error.

Assume $B = 1.5 \text{ m}$.

$$\begin{aligned} q_{ult} &= (0.4)(14)(32)(1.5) + 24(1.5)(32) \\ &= 268.8 + 1152 = 1420.8 \text{ kN/m}^2 \end{aligned}$$

$$q_a = \frac{q_{ult}}{3} = \frac{1420.8}{3} = 473.6 \text{ kN/m}^2$$

$$\text{Allowable Load} = q_a \cdot A = 473.6(1.5)^2 = 1065.6 \text{ kN} < 2000 \text{ kN}$$

The assumed size is not good

Assume $B = 2 \text{ m}$.

$$\begin{aligned} q_{ult} &= (0.4)(14)(32)(2) + (24)(1.5)(32) \\ &= 358.4 + 1152 = 1510.4 \text{ kN/m}^2 \end{aligned}$$

$$q_a = \frac{1510.4}{3} = 503.47 \text{ kN/m}^2$$

$$\text{Allowable load} = 503.47(2^2) = 2013.87 \text{ kN} > 2000 \text{ kN}$$

Hence, use footing $2 \text{ m} \times 2 \text{ m}$

- E. 9.3 Given a foundation shown below. It is required to determine the allowable bearing capacity for a vertical load with eccentricity in both directions.

SOLUTION

The bearing capacity will be determined according to Eq. (9.15)

$$L' = L - 2e_L = 8 - 2(1) = 8 - 2 = 6.0 \text{ m}$$

$$B' = B - 2e_B = 3 - 2(0.5) = 3 - 1 = 2.0 \text{ m}$$

$$V_f = L' \cdot B' \cdot \sigma_f$$

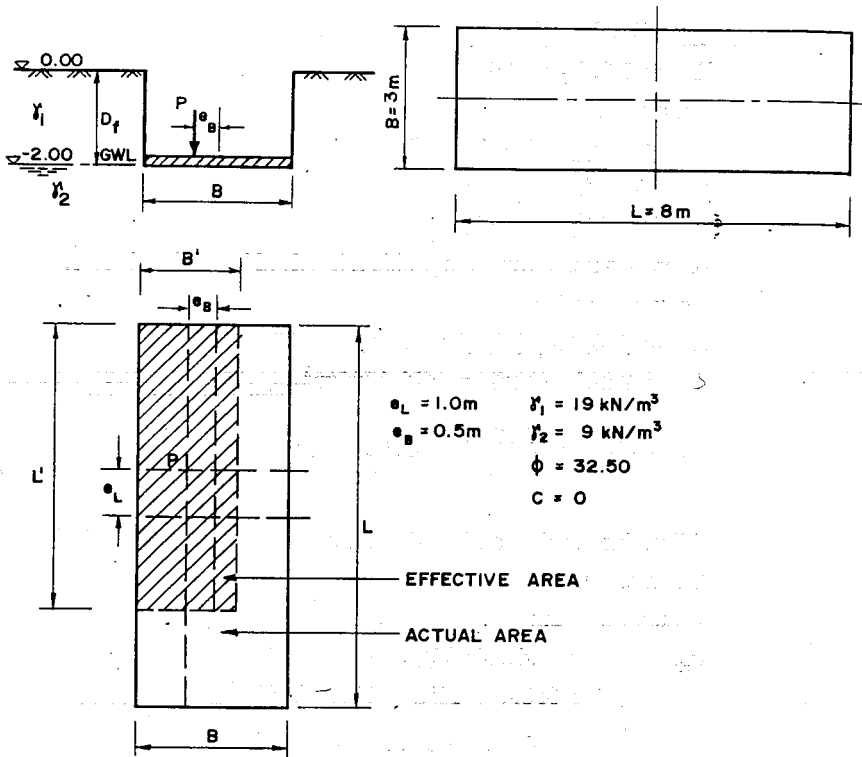


Fig. E.9.1

$$q_{ult} = c \cdot N_c \cdot i_c \cdot s'_c + \gamma_1 \cdot D_f \cdot N_q \cdot i_q \cdot s'_q + \gamma_2 \cdot B' \cdot N_\gamma \cdot i_\gamma \cdot s'_\gamma$$

For $c = 0$, $\phi = 32.5^\circ$ and $\delta_s = H_f = 0$, the values of the coefficients should be calculated. The results are tabulated below.

N_c	N_q	N_γ	i_c	i_q	i_γ	s'_c	s'_q	s'_γ
0	25	15	-	1	1	-	1.18	0.9

Inserting the above values into the equation

$$q_{ult} = 19(2)(25)(1)(1.18) + (9)(2)(15)(1)(0.9) = 1364 \text{ kN/m}^2$$

$$V_f = L' \cdot B' \cdot q_{ult}$$

$$= (6)(2)(1364) = 16368.0 \text{ kN}$$

The allowable bearing capacity will be found by dividing the ultimate value by a factor of safety. Taking a factor of safety, $F_s = 2$

$$Q_a = \frac{V_f}{F_s} = \frac{16368}{2} = 8184 \text{ k}$$

- E.9.4 A foundation similar to E.9.3 is given. However, the load, whose magnitude is given, acts at the center of the foundation with an inclination of 7.5° as shown below. It is required to determine the available factor of safety of the foundation.

SOLUTION

The procedure is similar to E.9.3

Since $e_L = e_B = 0$.

$L' = L = 8.0 \text{ m}$

$B' = B = 3.0 \text{ m}$

Resolving the given force into horizontal and vertical components,

$$H = P \sin \delta_s = 8000 \sin 7.5^\circ = 1044.2 \text{ kN}$$

$$V = P \cos \delta_s = 8000 \cos 7.5^\circ = 7931.6 \text{ kN}$$

The inclination coefficients should be calculated using Eq(9.20) and Eq(9.21).

$$i_q = (1 - 0.7 \tan \delta_s)^3 \\ = (1 - 0.7 \tan 7.5^\circ)^3 = 0.75$$

$$i_v = (1 - 1.0 \tan \delta_s)^3 \\ = (1 - 1.0 \tan 7.5^\circ)^3 = 0.65$$

Calculation of shape coefficients gives

$$s_q = 1.20, s_v = 0.89$$

Inserting the coefficients into the bearing capacity equation,

$$Q_{ult} = \gamma_1 \cdot D_f \cdot N_q \cdot i_q \cdot s'_q + \gamma_2 \cdot B' N_\gamma \cdot i_\gamma \cdot s'_\gamma \\ = (19) (2) (25.0) (0.75) (1.20) + (9) (3) (15.0) (0.65) (0.89) \\ = 1089.3 \text{ kN/m}_2$$

$$V_f = L \cdot B \cdot Q_{ult} = (8) (3) (1089.3) = 26143.2 \text{ kN}$$

$$F_s = \frac{V_f}{V} = \frac{26143.2}{7931.6} = 3.3$$

- E.9.5 The loading of E9.4 with eccentricities as in E9.3 is given. It is required to determine the factor of safety of the foundation.

SOLUTION

$$L' = 6.0 \text{ m}, i_q = 0.75, s'_q = 1.18$$

$$B' = 2.0 \text{ m}, i_v = 0.65, s'_v = 0.9$$

$$\begin{aligned} q_{ult} &= \gamma_1 \cdot D_f \cdot N_q \cdot i_q \cdot s'_q + \gamma_2 \cdot B' \cdot N_v \cdot i_v \cdot s'_v \\ &= (19)(2)(25)(0.75)(1.18) + (9)(2)(15.0)(0.65)(0.90) \\ &= 998.8 \text{ kN/m}^2 \end{aligned}$$

$$V_f = L' \cdot B' \cdot q_{ult} = (6)(2)(998.8) = 11985.6 \text{ kN}$$

$$F_s = \frac{V_f}{V} = \frac{11985.6}{7931.6} = 1.5$$

- E.9.6 The loading and soil profile as in the Fig. E.9.2 below are given. (This example is taken from Din 4017 [5].

It is required to determine the bearing capacity of the foundation.

SOLUTION

(i) Existing loads

Given vertical load, $P_a = 6575.00 \text{ kN}$

The weight of foundation = $(4)(5)(1.00)(24) = 480.0 \text{ kN}$

Bouyant force = $-(4)(5)(10)(2-1.60) = -80.0 \text{ kN}$

Total load, $P = 6975.0 \text{ kN}$

(ii) Iterative calculation of the soil parameters

$$\text{Mean value of } \phi_a = \frac{30 + 25 + 22.5}{3} = 25.8^\circ$$

The difference between the mean value ϕ_a and the respective values for each layer is less than 5° . Hence calculation using this method is permissible.

a) First iteration

Start with $\phi_0 = 30^\circ$ and determine the rupture line (Fig. E9.2b)

$$\beta = 45 - \frac{\phi_0}{2} = 45 - \frac{30}{2} = 30$$

$$\alpha = 45 + \frac{\phi_0}{2} = 60^\circ$$

Hence, $\omega = 90^\circ$

$$r_0 = \frac{b}{\sin(90 - 30)} \sin \alpha$$

$$= \frac{4}{\sin(90 - 30)} \sin 60 = 4.00 \text{ m}$$

$$\begin{aligned} r_1 &= r_0 e^{(\text{arc } \omega \tan \phi)} \\ &= 4. e^{(90. \pi / 180 \tan 30)} = 9.91 \text{ m} \end{aligned}$$

$$\begin{aligned} \text{The distance of the EP}_6 \text{ (Fig E9.2b)} &= 2. r_1 \cos \beta \\ &= (2) 9.91 (\cos 30) \\ &= 17.16 \text{ m} \end{aligned}$$

$$\begin{aligned} \text{The depth of the rupture line; max } d_s &= r_0 \cos \phi_0 e^{(\text{arc. } \theta. \tan \phi)} \\ &= 4 (\cos 30) e^{(60. \pi / 180. \tan 30)} \\ &= 6.34 \text{ m} \end{aligned}$$

Hence, the location of the deepest point of the rupture line is $\text{max } d_s + d = 6.34 + 2.00 = 8.34 \text{ m}$ below the ground surface.

For simplifying the calculation, part of the rupture line, which is a logarithmic spiral, is approximated by sets of straight lines as shown in the figure. The angle ω of the logarithmic spiral is subdivided into three equal parts. The whole of the rupture line now consists of series of straight lines from P_1 to P_6 .

Finally, the points at which the rupture line cuts the horizontal soil layers, S_{3r} , S_{4r} and S_{4r} , are determined. It should be noted that these points may also be determined graphically.

Taking P_1 as reference point for a coordinate system in x and z , the coordinate of the point at which the rupture line cuts the horizontal soil layers are as follows:

$$S_{3t} (0.87, 1.50)$$

$$S_{3r} (18.56, 1.50)$$

$$S_{4t} (1.73, 3.00)$$

$$S_{4r} (15.96, 3.00)$$

From these data, one may determine the following lengths

$$l_3 = l_{3t} + l_{3r} = 1.73 + 3.00 = 4.73 \text{ m}$$

$$l_4 = l_{4t} + l_{4r} = 1.73 + 3.00 = 4.73 \text{ m}$$

$$l_5 = 16.12 \text{ m}$$

$$\text{Total length } l_{\text{tot}} = 25.58 \text{ m}$$

With these lengths, the first iteration for the weighted average angle of internal friction will be obtained.

$$\begin{aligned} \tan \phi_{mi} &= \frac{l_3 \cdot \tan \phi_3 + l_4 \tan \phi_4 + l_5 \cdot \tan \phi_5}{l_3 + l_4 + l_5} \\ &= \frac{(4.73) (\tan 30) + (4.73) (\tan 25) + (16.12) (\tan 22.5)}{25.58} \end{aligned}$$

This gives $\phi_{mi} = 24.42^\circ$

The deviation from the initial value of $\phi_o = 30^\circ$

$$\Delta_1 = \frac{30 - 24.42}{30} = 18.6\%$$

Since this deviation is greater than 3%, it would be necessary to carry another iteration with the following angle of internal friction.

$$\phi_1 = \frac{24.42 + 30}{2} = 27.21^\circ$$

b) *Second iteration*

One repeats basically the same calculations, except that the angle of internal friction will be 27.21° . The length of the rupture line will be found to be

$$l_3 = 4.64 \text{ m}$$

$$l_4 = 4.64 \text{ m}$$

$$l_5 = 13.49 \text{ m}$$

The weighted average angle of internal friction would be

$$\tan \phi_{m2} = \frac{(4.64)(\tan 30) + (4.64)(\tan 25) + (13.49)(\tan 22.5)}{22.7}$$

From this it follows that $\phi_{m2} = 24.61^\circ$

$$\Delta_2 = \frac{27.21 - 24.61}{27.21} (100) = 9.55\%$$

Since the deviation is greater than 3%, another iteration is necessary.

$$\phi_2 = \frac{27.21 + 24.61}{2} = 25.91^\circ$$

c) *Third iteration*

The calculation of the third iteration gives the weighted average angle of internal friction as $\phi_{m3} = 24.70$

$$\Delta_3 = \frac{25.91 - 24.70}{25.91} = 4.67\%$$

Here again, since Δ_3 is greater than 3% it is necessary to perform another iteration.

$$\phi_3 = \frac{25.91 + 24.70}{2} = 25.31^\circ$$

d) *Fourth iteration*

The calculations of the fourth iteration gave $\phi_{m4} = 24.74^\circ$ with a deviation of 2.22% which is smaller than 3%. Hence, further iteration is not necessary.

For calculating the bearing capacity one may use

$$\phi_4 = \frac{25.31 + 24.74}{2} = 25.0^\circ$$

(iii) *Bearing capacity calculation*

Analogous to the first iteration, the lengths of the rupture line are calculated with the angle of internal friction of ϕ_4 .

$$l_3 = 4.57\text{m}$$

$$l_4 = 4.57\text{m}$$

$$l_5 = 15.62\text{m}$$

a) *Weighted mean cohesion*

The weighted mean cohesion c would be

$$c = \frac{(l_3 c_3 + l_4 c_4 + l_5 c_5) / l_{\text{tot}}}{24.76}$$

$$= \frac{(4.57)(0.00) + (4.57)(5.00) + (15.62)(2.00)}{24.76}$$

$$= 2.19 \text{ kN/m}^2$$

b) *Weighted unit weights*(i) *Under the foundation level*

The weighted unit weight will be determined from the areas A_3 , A_4 , and A_5 as indicated in Figure E.9 3b.

$$A_3 = 23.13 \text{ m}^2$$

$$A_5 = 15.62 \text{ m}^2$$

$$A_4 = 18.17 \text{ m}^2$$

$$A_{\text{tot}} = A_3 + A_4 + A_5 = 56.92 \text{ m}^2$$

$$\text{Weighted unit weight } \gamma = \frac{(A_3 \cdot \gamma_3 + A_4 \cdot \gamma_4 + A_5 \cdot \gamma_5)}{A_{\text{tot}}}$$

$$= \frac{(23.13)(11.00) + (18.17)(12.00) + (15.62)(10.02)}{56.92}$$

$$= 11.05 \text{ kN/m}^3$$

(ii) Above the foundation level

$$\gamma_1 = \frac{(0.50)(18.00) + (1.10)(18.50) + (0.40)(11.00)}{2.00}$$

$$16.88 \text{ kN/m}^3$$

(c) Bearing capacity

With the calculated values of ϕ , c , γ , and γ the bearing capacity may now be calculated using the bearing capacity formula of DIN 4017.

For $\phi = 25^\circ$,

$$N_q = 10.7$$

$$N_c = 20.8$$

$$N_\gamma = 4.5$$

The shape factors are

$$S_q = 1.34$$

$$S_c = 1.37$$

$$S_\gamma = 0.76$$

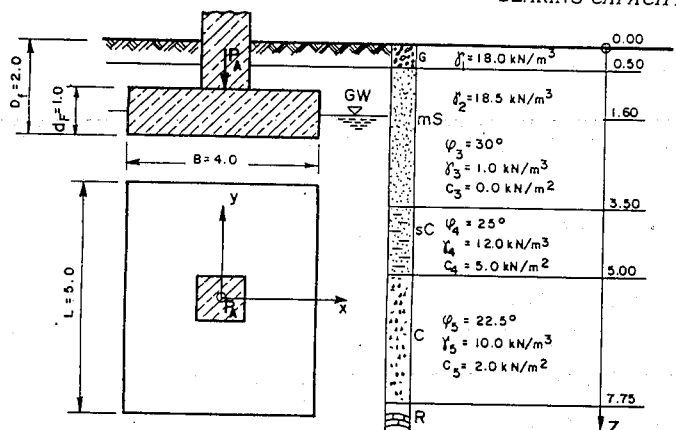
Hence, introducing these values into the general equation

$$Q_{ult} = B.L(c \cdot N_c \cdot S_c + \gamma_1 D_f N_q S_q + \gamma_2 \cdot B \cdot N_\gamma S_\gamma)$$

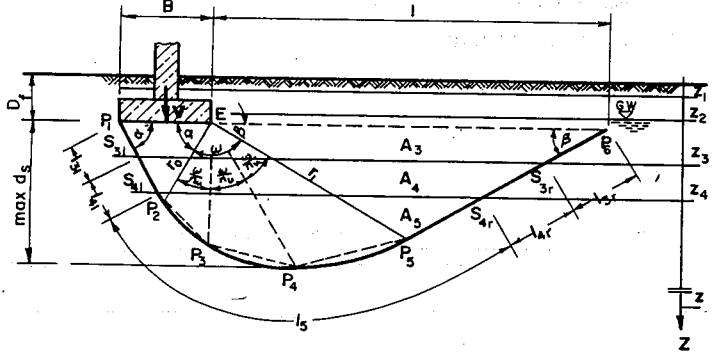
$$Q_{ult} = (5.00)(4.00)[(2.22)(20.8)(1.37) + (16.88)(2.00)(10.69)(1.34) + (11.05)(4.00)(4.52)(0.76)] = 13967 \text{ kN}$$

$$F_s = \frac{Q_{ult}}{P} = \frac{13697}{6975} = 2.$$

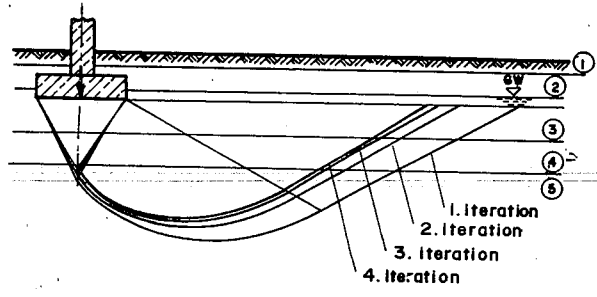
The changes of the rupture line in accordance with the various iterations are shown in Fig. E.9.2.



(a) Loading and soil profile



(b) Rupture line



(c) Changes of the rupture lines corresponding to the iteration

Fig. E.9.2 Bearing capacity calculation according to DIN 4017

E 9.7 The loading and soil profile as indicated in Fig. E.9.3 are given (This example is taken from DIN 4017 [6]).

It is required to determine the bearing capacity of the foundation.

SOLUTION:

(i) *Existing loads*

a) *Vertical loads*

Given vertical load, $P_a = 4230.00 \text{ kN}$

Weight of foundation = $(4)(5)(1)(24) = 480.00 \text{ kN}$

Bouyant force = $-(4)(5)(10)(2-1.6) = -80.00 \text{ kN}$

Total vertical load, $P_T = 4630.00 \text{ kN}$

b) *Horizontal loads*

$H_x = 450.00 \text{ kN}$

$H_y = 300.00 \text{ kN}$

c) *Moment loads*

α) *Existing*

$M_y = 1865.00 \text{ kN.m}$

$M_x = -857.50 \text{ kN.m}$

β) *From horizontal loading*

$M_y = 450.00 \text{ kN.m}$

$M_x = -300.00 \text{ kN.m}$

Total moment, $M_{y \text{ tot}} = 2315.00 \text{ kN.m}$

$M_{x \text{ tot}} = -1157.50 \text{ kN.m}$

d) *Eccentricities*

$$e_x = \frac{M_{y \text{ tot}}}{P} = \frac{2315.00}{4630.00} = 0.50$$

$$e_y = \frac{M_{x \text{ tot}}}{P} = -\frac{1157.50}{4630.00} = -0.25 \text{ m}$$

$$b' = b - 2e_x = 4.00 - (2)(0.50) = 3.00 \text{ m}$$

$$a' = a - 2e_y = 5.00 - (2)(0.25) = 4.50 \text{ m}$$

(ii) *Iterative calculation of the soil parameters*

$$\text{Mean value of } \phi_a = \frac{30.0 + 25.0 + 22.5}{3} = 25.8^\circ$$

The difference between the mean value ϕ_a and the respective ϕ - values for each layer is less than 5° . Hence, calculation is permissible. Within the framework of this example, calculations are carried out for a slip surface in the x- direction. It is in this direction that the moment and horizontal load have maximum values.

The calculation in the y - direction may be carried out analogous to the x - direction.

$$\tan \delta_s = \frac{H_x}{P} = \frac{450.00}{4630.00} = 0.09$$

$$\delta_s = 5.55^\circ$$

a) *First iteration*

As in the previous example, start with $\phi_0 = 30^\circ$ and determine the rupture line (Fig. E.9.4b).

$$\beta = 45 - \frac{\phi_0}{2} = 45 - \frac{30}{2} = 30$$

One may determine the magnitude of the angle θ from a formula as given in DIN 4017 or from Fig. 9.18.

Accordingly,

$$\tan \theta = \frac{\cos \delta'_s \sqrt{\cos^2 \delta'_s - \cos^2 \phi} + \cos^2 \delta'_s - \cos^2 \phi}{(\sin \phi)(\cos \phi) + (\sin \delta'_s)(\cos \delta'_s) + \sin \delta'_s \sqrt{\cos^2 \delta'_s - \cos^2 \phi}}$$

for $0 \leq \delta'_s \leq \phi$

where

$$\delta'_s = \frac{H_f}{V_f + c \cdot \cot \phi}; \quad \text{and } \phi = \text{angle of internal friction.}$$

In this particular example, $c = 0$, hence $\delta = 9.55^\circ$

Inserting the values of $\phi = 30^\circ$ and $\delta_s = 5.55^\circ$ into the above equation.

$$\tan\phi = \frac{(\cos 5.55) \sqrt{\cos^2 5.55 - \cos^2 30} + \cos^2 5.55 - \cos^2 30}{(\sin 30)(\cos 30) + (\sin 5.55)(\cos 5.55) + \sin 5.55(\cos^2 5.55 - \cos^2 30)^{1/2}}$$

$$= 1.264$$

From Fig. 9.18 for $\phi = 30^\circ$ and $\delta_s = 5.55^\circ$ one also obtains $\theta = 51.65^\circ$

Since $\theta = \omega - \beta$

$$\omega = \theta + \beta = 51.65 + 30 = 81.65^\circ$$

From the rule of sines

$$\frac{b'}{\sin(90 - \phi)} = \frac{r_0}{\sin\theta}$$

$$r_0 = \frac{b'}{\sin(90 - \phi)} = \sin\theta$$

$$= \frac{(3.00)(\sin 51.65)}{(\sin(90 - 30))} = 2.71 \text{ m}$$

$$r_1 = r_0 \cdot [e^{\text{arc } \omega (\tan 30)}]$$

$$= 6.18 \text{ m}$$

$$\text{Distance of } EP_6 \text{ (Fig. E.9.3)} = 2 \cdot r_1 \cos \beta$$

$$= 2(6.18)(\cos 30) = 10.71 \text{ m}$$

$$\text{The depth of the rupture line, max } d_s = r_0 \cos \phi_0 e^{(\text{arc } \theta \tan \phi_0)}$$

$$= 2.71 \cos 30 e^{[(51.64)(\pi/180)(\tan 30)]} = 3.95 \text{ m}$$

Hence, the location of the deepest point of the rupture line is

$\text{max } d_s + d = 3.95 + 2 = 5.95 \text{ m}$ below the ground surface. For simplifying the calculation, part of the rupture line, which is a logarithmic spirale, is approximated by sets of straight lines as shown in the figure.

§ The angle ω of the logarithmic spirale is subdivided into three equal parts. The whole of the rupture line now consists of series of straight lines from p_1 to p_6 . Finally the points at which the rupture line cuts the horizontal soil layers s_{31} , s_{3r} , s_{41} and s_{4r} are determined. It should be noted that these points may be also determined graphically.

Taking P_1 as a reference point for a coordinate system in x and z , the coordinate of the points at which the rupture line cuts the horizontal soil layers are as follows:

$$S_{3l} (1.18, 1.50)$$

$$S_{3r} (11.11, 1.50)$$

$$S_{4l} (2.61, 3.00)$$

$$S_{4r} (8.51, 3.00)$$

From these data one may determine the following lengths:

$$l_3 = l_{3l} + l_{3r} = 1.91 + 3.00 = 4.91\text{m}$$

$$l_4 = l_{4l} + l_{4r} = 2.08 + 3.00 = 5.08\text{m}$$

$$l_5 = 6.27\text{m}$$

Total length, $l_{\text{tot}} = 16.27\text{m}$

With these lengths, the first iteration for the weighted average angle of internal friction will be obtained

$$\begin{aligned} \tan \phi_{m1} &= \frac{l_3 \tan \phi_3 + l_4 \tan \phi_4 + l_5 \tan \phi_5}{l_3 + l_4 + l_5} \\ &= \frac{(4.91) (\tan 30) + (5.08) (\tan 25) + (6.27) (\tan 22.5)}{16.27} \end{aligned}$$

This gives $\phi_{m1} = 25.62^\circ$

The deviation from the initial value of $\phi_0 = 30^\circ$

$$\Delta_1 = \frac{30 - 25.62}{30} (100) = 14.57\%$$

Since this deviation is greater than 3%, it would be necessary to carry another iteration with the following angle of internal friction:

$$\phi_1 = \frac{25.62 + 30.00}{2} = 27.81^\circ$$

b) Second iteration

One repeats basically the same calculations, except that the angle of internal friction will be 27.81° . The length of the rupture line will be found to be:

$$l_3 = 4.85\text{m}$$

$$l_4 = 5.29\text{m}$$

$$l_5 = 4.63\text{m}$$

$$\text{Total length } l_{\text{tot}} = 14.77$$

The weighted average angle of internal friction would be:

$$\tan \phi_{m2} = \frac{(4.85)(\tan 30) + (5.29)(\tan 25) + (4.63)(\tan 22.5)}{14.77}$$

This gives $\phi_{m2} = 25.94^\circ$

$$\Delta_2 = \frac{27.81 - 25.94}{27.81} (100) = 6.73\%$$

Here again, since Δ_2 is greater than 3% it is necessary to perform another iteration.

$$\phi_2 = \frac{27.81 + 25.94}{2} = 26.87^\circ$$

c) *Third iteration*

The result of the third iteration is $\phi_{m3} = 26.08$. In this case the deviation from the preceding values is 2.9% which is less than 3%. Hence further iteration is not necessary.

For calculating the bearing capacity one may use

$$\phi_3 = \frac{26.87 + 26.08}{2} = 26.48^\circ$$

(iii) *Bearing capacity calculation*

Analogous to the first iteration, the lengths of the rupture line are calculated for

$$\phi = 26.48^\circ$$

$$l_3 = 4.83\text{m}$$

$$l_4 = 5.46\text{m}$$

$$l_5 = 3.68\text{m}$$

$$l_{\text{tot}} = 13.97\text{m}$$

a) *Weighted mean cohesion*

The weighted mean cohesion c would be:

$$\begin{aligned} c &= (l_3 \cdot c_3 + l_4 \cdot c_4 + l_5 \cdot c_5) / l_{\text{tot}} \\ &= \frac{4.83(0.00) + (5.46)(5.00) + (3.68)(2.00)}{13.91} = 2.48 \text{ kN/m}^2 \end{aligned}$$

b) Weighted unit weights

Under the foundation level

The weighted unit weight will be determined from the areas A_3 , A_4 , and A_5 as indicated in Fig. E.9.3b.

$$A_3 = 14.79\text{m}^2 \quad A_4 = 9.03\text{m}^2$$

$$A_5 = 0.97\text{m}^2 \quad A_{\text{tot}} = 24.80\text{m}^2$$

$$\text{Weighted unit weight } \gamma = (A_3 \cdot \gamma_3 + A_4 \cdot \gamma_4 + A_5 \cdot \gamma_5) / A_{\text{tot}}$$

$$= \frac{(14.79)(11.00) + (9.03)(12) + (0.97)(10)}{24.80}$$

$$= 11.32 \text{ kN/m}^3$$

Above the foundation level

$$\gamma_1 = \frac{(0.50)(18.00) + (1.10)(18.50) + (0.40)(11.00)}{2.00} = 16.87 \text{ kN/m}^3$$

With the calculated value of ϕ , c , γ , and γ_1 the bearing capacity may now be calculated using the bearing capacity formula of DIN 4017.

$$\text{For } \phi = 26.48^\circ \quad N_q = 12.48$$

$$N_c = 23.04 \quad N_\gamma = 5.72$$

The shape factors are

$$S'_q = 1.29 \quad S'_c = 1.32$$

$$S'_\gamma = 0.80$$

The inclination coefficients are

$$i_q = 0.81 \quad i_c = 0.79$$

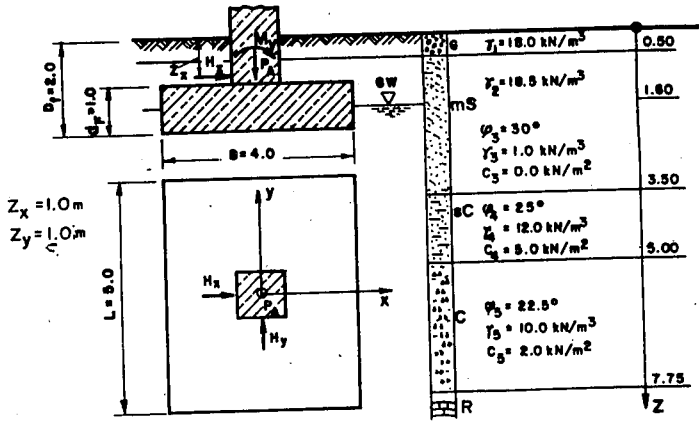
$$i_\gamma = 0.73$$

Hence introducing these values into the general equation

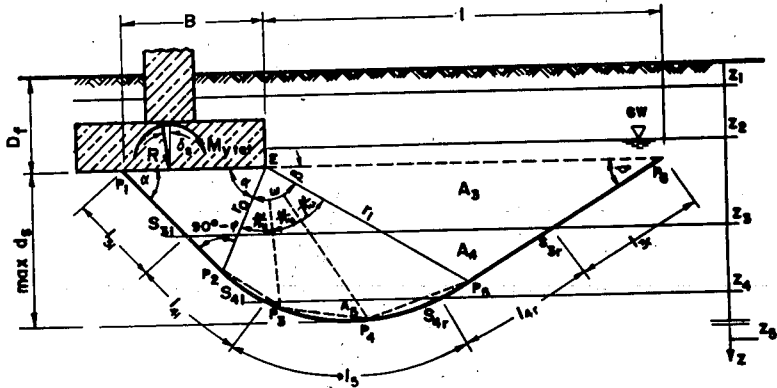
$$\begin{aligned} Q_{ult} &= L' B' (c N_c i_c S'_c + \gamma_1 D_f N_q i_q S'_q \\ &+ \gamma_2 B' N_\gamma i_\gamma S'_\gamma V'_b) \\ &= (4.50)(3.00) [(2.48)(23.05)(1.32)(0.79) \\ &+ (16.87)(2.00)(12.48)(1.30) + 81 \\ &+ (11.33)(3.00)(5.72)(0.80)(0.74)] \\ &= 8341.0 \text{ kN} \end{aligned}$$

$$F_s = \frac{Q_{ult}}{P} = \frac{8341.0}{4630.0} = 1.8$$

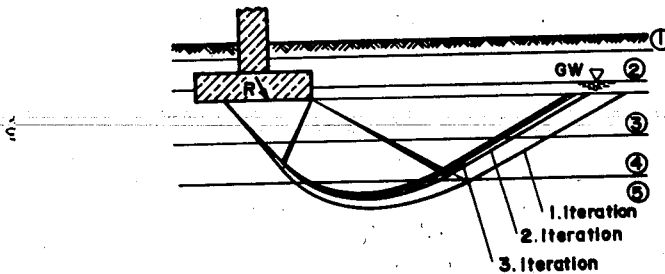
The changes of the rupture line in accordance with the various iteration are shown in the Fig. E.9.3.



(a) Loading and soil profile



(b) Rupture line



(c) Changes of the rupture lines corresponding to the iterations

Fig. E.9.3 Bearing capacity calculation according to DIN 4017

9.5 EXERCISES

- 1 A strip foundation is 4m wide and rests in a sand at a depth of 1.5m below the ground surface. Using a factor of safety of 2.5, determine the allowable bearing capacity, if the unit weight of sand is 19kN/m^3 and angle of internal friction is 30° .
- 2 A strip footing 1.5m. wide is to be constructed at a depth of 4m in a purely cohesive soil having $c=138\text{kN/m}^2$ and $\gamma = 17.6\text{kN/m}^3$. Estimate the ultimate bearing capacity from theories of Terzaghi and Skempton.
- 3 The size of an isolated footing is to be 1.5 by 1.5m. Calculate the depth at which the footing should be placed to take a load of 2000kN. The soil is sandy having $\phi = 30^\circ$. Use $F_s = 3$.
- 4 A strip footing is to be laid at a depth of 2m below the ground surface in a saturated clay. Unconfined compression test run on the soil samples taken from the construction site gave an average compressive strength of 108kN/m^2 . The unit weight of the soil is 17.6kN/m^3 . What is the ultimate bearing capacity?
- 5 A column has a footing 2.5m by 2.5m and 0.75m. thick. The footing is founded at a depth of 3m in a clay having a shear strength of 50kN/m^2 and a unit weight of 21kN/m^3 .

Determine the safe load that the footing can take.

Use $F_s = 3$ and unit weight of concrete = 24kN/m^3 .

- 6 Compute the bearing capacity of a square footing $2\text{m} \times 2\text{m}$ on a dense sand with $\phi' = 35^\circ$, $\gamma_t = 20.0 \text{ kN/m}^3$, if the depth of foundation 0, 1, 1.5, 2, and 3m is, respectively.

a. According to Terzaghi's Formula

b. According to DIN 4017

Discuss the result.

- 7 A footing is to be placed at a depth of 1.5m on a homogeneous clay layer with
 $\gamma = 19.0 \text{ kN/m}^3$
 $c' = 20 \text{ kN/m}^2$
 $\phi' = 15^\circ$.

The water level is located at a depth of 1.00m below the ground surface.

- a) Determine the maximum centric load if a strip footing with $B=3.0\text{m}$ is used. Check your results graphically.
- b) Determine the maximum centric load that the footing can sustain if it is $3\text{m} \times 3\text{m}$.
- c) If the dimension of the footing is changed to $1.5 \times 6\text{m}$, would there be a change on the magnitude of the maximum load?

- 8 A footing $3\text{m} \times 4\text{m}$ supporting an inclined load of 1200kN with $\delta_s = 15^\circ$, is to be placed at a depth of 2.0m below the ground surface. The ground consists of normally consolidated clay with $e = 1.08$, $\omega = 40\%$, $G_s = 2.70$, $\phi' = 25$ and $c' = 40\text{kN/m}^2$. The ground water is at the level of the footing. Determine the available safety factor.

- 9 A rectangular footing with a side ratio $L/B = 1.5$ is to sustain an axial load of 800 kN and moments $M_L = 800\text{kN.m}$, $M_B = 600 \text{ kN.m}$ in the direction of L and B respectively about both axes. The footing is to be placed 2.0m below the ground surface. If the foundation soil is silty clay with $\phi' = 20^\circ$, $c' = 20 \text{ kN/m}^2$ and $\gamma_t = 18 \text{ kN/m}^3$, determine the appropriate dimension of the footing using a factor of safety of 2.

- 10 If in E 9.6, $P = 5000\text{kN}$, $H_x = 500\text{kN}$ and $H_y = 300\text{kN}$, determine the bearing capacity of the foundation.
- 11 Compare the result of problem 9.10 with that of the method of Schultze.

10 EXPANSIVE SOILS

10.1 GENERAL

Expansive soils are clay soils with high plasticity. As the name of the soils suggests, these soils are known for their peculiar nature of expanding or shrinking when exposed to moisture changes. Commonly, they are known as black clays or in some regions as "black cotton" soils. The name *black cotton* came from the fact that the soils are found favourable in some regions for growing cotton.

In dry state, the soils exhibit a high bearing capacity which is gradually lost with increase in moisture content. If prevented from swelling following exposure to moisture, the soils exert high swelling pressure. The pressure build-up is usually responsible for cracking of buildings, distortion of pavement surfaces and damage to other structures.

On drying the soils crack very badly. In some cases the cracks are seen to extend to as deep as 1.5m. Excavated vertical banks in these soils stand so long as the moisture content does not change. Excessive drying makes the soils to crumble along crack lines and fall into excavated area.

10.2 ORIGIN OF EXPANSIVE SOILS

The parent materials associated with expansive soils are either basic igneous rocks or sedimentary rocks. In basic igneous rocks, they are formed by decomposition of feldspar and pyroxene and in sedimentary rocks, they are constituents of the rock itself.

Parent materials of expansive soils

Basic igneous rocks	Sedimentary rocks
Basalts Dolerite sills and dykes Gabros and Norites	Marls and limestones Shales

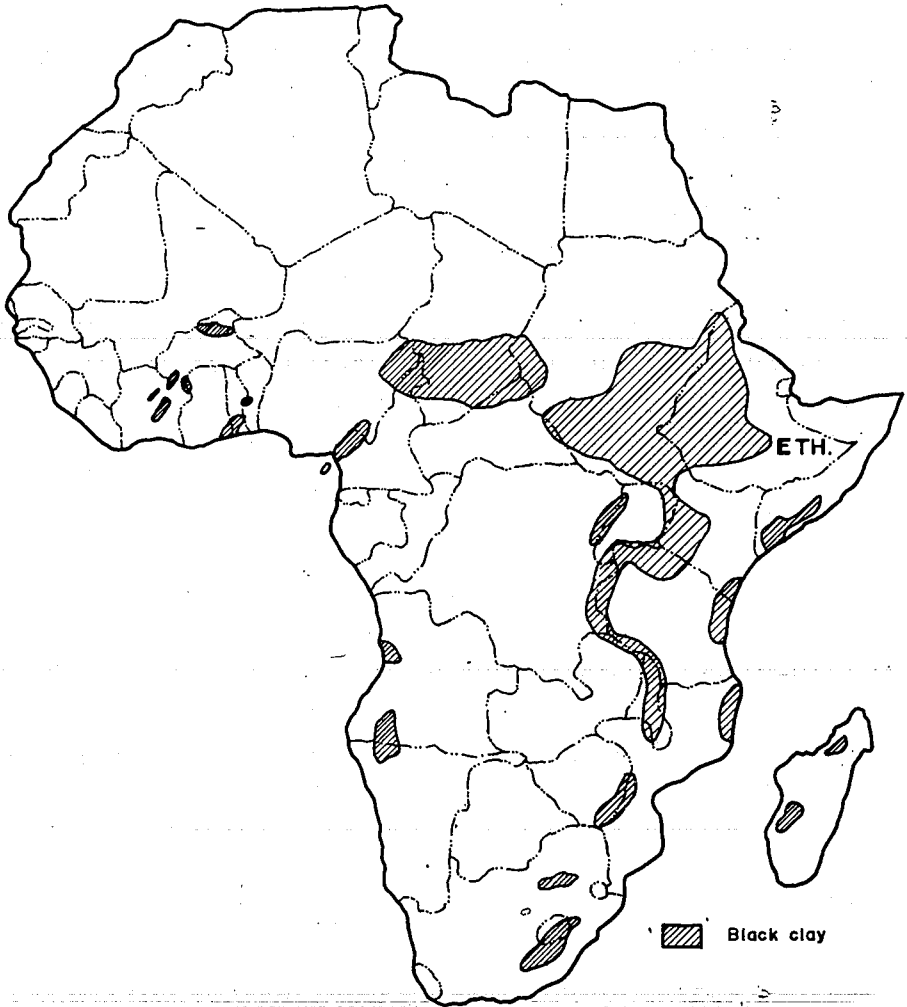


Fig. 10.1 Distribution of expansive soils in Africa

10.3 DISTRIBUTION OF EXPANSIVE SOILS

Expansive soils are widespread in the African continent (Fig.10.1), occurring in South Africa, Ethiopia, Kenya, Mozambique, Morocco, Ghana, Negeria etc. In other parts of the world cases of expansive soils have been widely reported in U.S.A, Australia, Canada, India, Spain, Israel, Turkey, Argentina, Venezuala etc.

10.4 MINERALOGY OF EXPANSIVE CLAY SOILS

Expansive soils have a very high clay content. There are three common types of clay minerals. They are in increasing order of their expansiveness.

Kaolinite	- low degree of expansiveness
Illite	- moderate degree of expansiveness
Montmorillonite	- very high of expansiveness

10.4.1 Kaolinite

Kaolinite has a structural unit made up of alumina sheets joined to silica sheet and is symbolized as indicated in Fig. (10.2a). Kaolinite consists of many such layers stacked one on top of the other as shown in Fig. 10.2(b)

The bond that exists between layers is tight and hence it is difficult to separate the layers. As a result Kaolinite is relatively stable and water is unable to penetrate between the layers. Consequently Kaolinite shows little swelling on wetting.

10.4.2 Illite

Illite has a basic structure similar to that of montmorillonite (Fig.10.2a). However, the basic illite units are bonded together by potassium ions which are non-exchangeable (Fig. 10.2b). because of this, the illite units are reasonably stable and so that mineral swells much less than montmorrillonite.

From the above it follows that montmorillonite is the most active clay mineral that imparts swelling characteristic to clays.

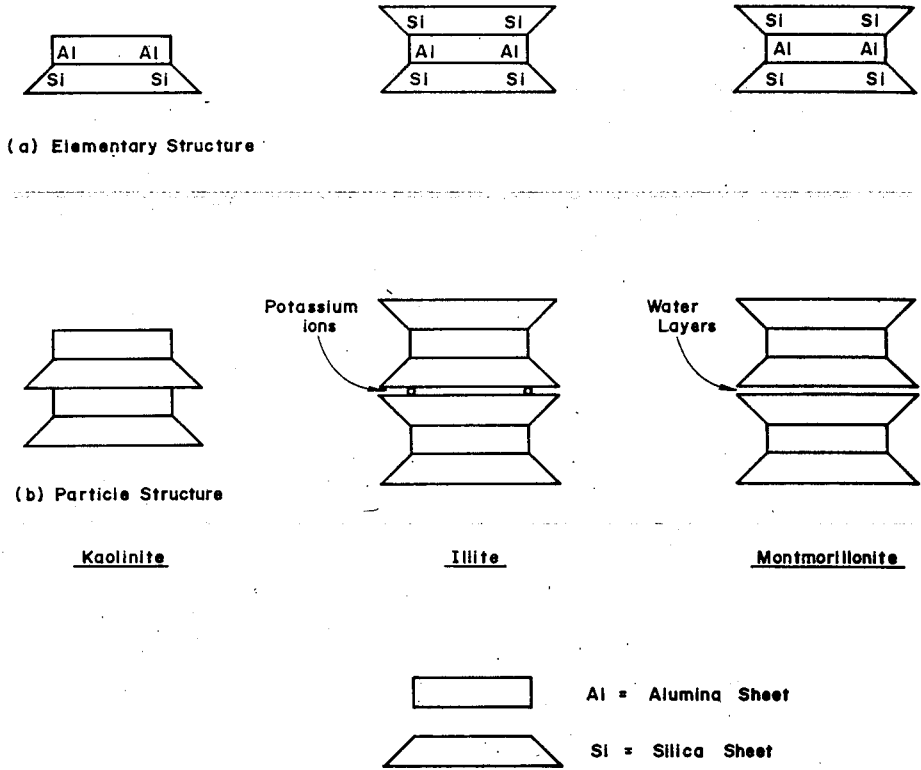


Fig. 10.2 Symbolic structure of clay minerals

10.4.3 Montmorillonite

Montmorillonite is the most common of all the clay minerals and is well known for its swelling properties. Its basic structure consists of an alumina sheet sandwiched between two silica sheets and is symbolically represented as shown in Fig.10.2a.

The basic montmorillonite units are stacked one on top of the other, but the bond between the individual units is relatively weak so that water is easily able to penetrate between the sheets and cause their separation and hence swelling (Fig.10.2b).

Montmorillonite is extremely active and its activity decreases as the adsorbed cation exchanges in the following order:

Sodium (most active), lithium, potassium, calcium, magnesium and hydroxyl (most stable). As the result of exchange of adsorbed cation of montmorillonite by those listed above, its activity is reduced. Making use of this fact, lime, cement and gypsum are used to stabilize montmorillonitic soils (expansive soils) in the process of which the active sodium ions are replaced by less active calcium ions.

10.5 IDENTIFICATION AND CLASSIFICATION OF EXPANSIVE SOILS

10.5.1 Identification of Expansive Soils

The common methods of identification of expansive soils consist of the following.

10.5.1.1. X-ray Diffraction, Differential Thermal Analysis and Electronmicroscope Resolution.

These methods are usually employed for mineralogical examination. As they involve a high investment cost in equipment, they are used for important research projects.

10.5.1.2. Index Property Tests

These are the most commonly applied methods in all soil testing laboratories and consists of:

- a) Grain size analysis
- b) Consistency tests
- c) Free swell
- d) Vertical swell under a small load (1 psi) in a consolidometer ring.

Results of these tests which are crucial in identifying the expansive soils are percentage of clay fraction smaller than 2 microns, liquid limit, plastic limit, shrinkage limit and free swell (Table 10.1).

10.5.1.2.1. Activity (Colloidal Activity)

$$A = \frac{I_p}{C} \quad [25] \quad (10.1)$$

C = per cent of clay fraction finer than 2 micron

A = activity

10.5.1.2.2. Free swell of Clay Particles

This test is carried out by first pouring 10 c.c of air dried soil passing sieve No. 40(0.42mm) into a 100 c.c. graduated cylinder. Then distilled water is added into the graduated cylinder up to 100 c.c. calibration mark. The cylinder with its contents is set aside until the soil particles settle. Periodic readings of the change in soil volume is taken until the specimen attains maximum swelling. This usually takes 2 to 3 days. The swelled volume is then computed using the following relationship.

$$\text{Free swell (in per cent)} = \frac{V_f - V_i}{V_i} \quad (10.2)$$

where

V_i = initial volume

V_f = final volume

Table 10.1 Indicative properties of Ethiopian expansive soils

Clay content smaller than (2 microns) or 0.002 mm	50 - 80%
Liquid limit	80 - 120%
Plasticity limit	55 - 90%
Shrinkage limit	10 - 16%
Free swell	90 - 23%

10.5.1.2.3 Swell Potential

Swell potential is expressed as the percentage of swell of laterally confined sample which has been soaked under a surcharge of 1 psi. Seed, Woodward and Lundgreen [22] established the following relationship for sample compacted following AASHTO compaction test to maximum density and optimum moisture content and allowed to swell in consolidometer under a surcharge of 1 psi.

$$S = 60K(I_p)^{2.44} \quad (10.3)$$

where

S = swell potential

K = 3.6×10^{-5} (and is constant).

Relation between swelling potential of clays and plasticity index is indicated in Table 10.2.

Table 10.2 Swelling potential

Swelling Potential	Plasticity index
Low	0 - 15
Medium	10 - 35
High	20 - 55
Very high	55 and above

10.5.2 Classification Methods of Expansive Clays

There are a number of classification systems. The following are some of the common methods.

10.5.2.1 Skempton's Method [25]

Skempton classifies clays according to their activities. Following his classification, three degrees of colloidal activity have been established as indicated in Table 10.3.

Table 10.3 Degrees of colloidal activity

Degree of activity	Activity
Inactive clay	< 0.75
Normal clay	0.75 - 1.25
Active clay	> 1.25

Following this classification, montmorillonitic clay (expansive clay) is defined as active, illitic clay as normal and kaolinitic clay as inactive. The above classification method is also presented in a form of chart called activity chart Fig. 10.3. Based on this classification, the expansive soils found in and around Addis Ababa fall way above activity 1.

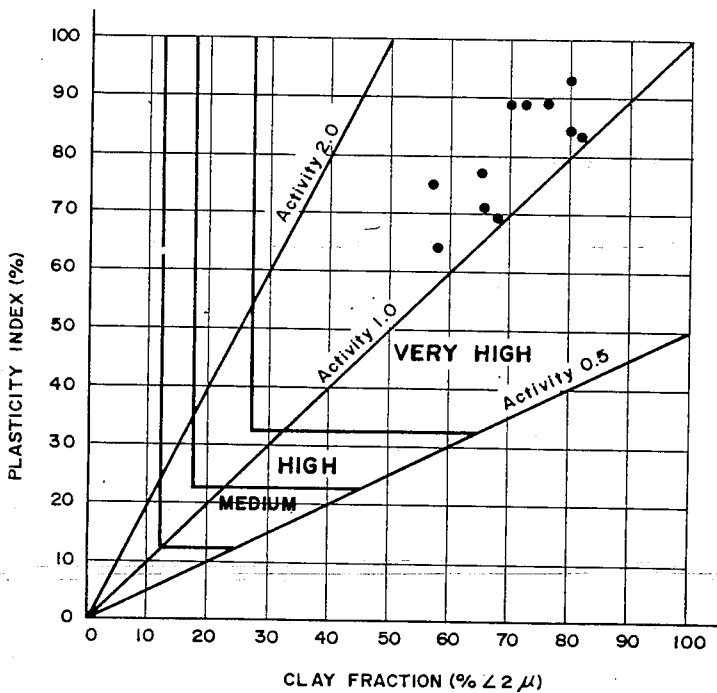


Fig. 10.3 Activity chart (After A.A.B. Williams, 1957-58)

10.5.2.2. U.S.B.R. Classification Method

This method was developed by Holtz and Gibbs [12] to establish degree of expansion based on simultaneous consideration of shrinkage limit (ω_s), plasticity index (I_p), percent smaller than 0.001mm (1μ), free swell (FS) and percent swell under a pressure of 1 psi. The relationship between degree of swell and indicative clay properties as established by Holtz and Gibbs are presented in Table 10.4.

Table 10.4 Relationships between degree of swell and clay properties [12]

Degree of expansion or swell	Swell in oedometer under a pressure of 1.0psi.(%)	ω_s %	I_p %	Per cent smaller than 1μ	FS %
Very high	> 30	< 10	> 32	> 27	> 100
High	20-30	6-12	23-45	18-37	> 100
Medium	10-20	8-18	12-34	12-27	50-100
Low	< 10	> 13	< 20	< 17	< 50

10.5.2.3 Activity Method (Seed's Classification Method) [22]

Seed et al [22] classify clayey soil according to its swelling potential defined as the per cent vertical swell under a pressure of 1 psi of a laterally confined sample compacted following AASHTO compaction method to maximum density and optimum moisture content. Seed et al established the following expression.

$$S = Kc^X \quad (10.4)$$

where

S = Swelling potential in percent

C = percentage of colloids smaller than 2μ

X = a constant depending on the clay type and equal to 3.44 for clays tested.

K = a factor depending on the type of clay minerals, calculated from the intercept of straight line relating log S to log C

From the relationship between K and activity, A , it was possible to develop for the clays tested the following relationships.

$$K = (3.6 \times 10^{-5}) A^{2.44} \quad (10.5)$$

$$S = (3.6 \times 10^{-5}) A^{2.44} C^{3.44} \quad (10.6)$$

The major disadvantage of Seed's work is that it was done on clays prepared in the laboratory by mixing percentages of different clay minerals. The general expression for

$$A = \frac{I_p}{C}$$

For natural soils, $A = \frac{I_p}{C-n}$ where $n=5$

$$\text{Hence, } S = \frac{(3.6 \times 10^{-5}) (I_p)^{2.44} C^{3.44}}{(C-n)^{2.44}} \quad (10.7)$$

From the above equation a classification chart shown in Fig. 10.4 was developed.

Seed et al [22] give the relationship between the degree of swell and swelling potential as indicated in Table 10.5

Table 10.5 Relationship between degree of swell and swelling potential [22]

Degree of swell	Swelling potential %
Low	0 - 1.5
Medium	1.5 - 50
High	5 - 25
Very high	> 25

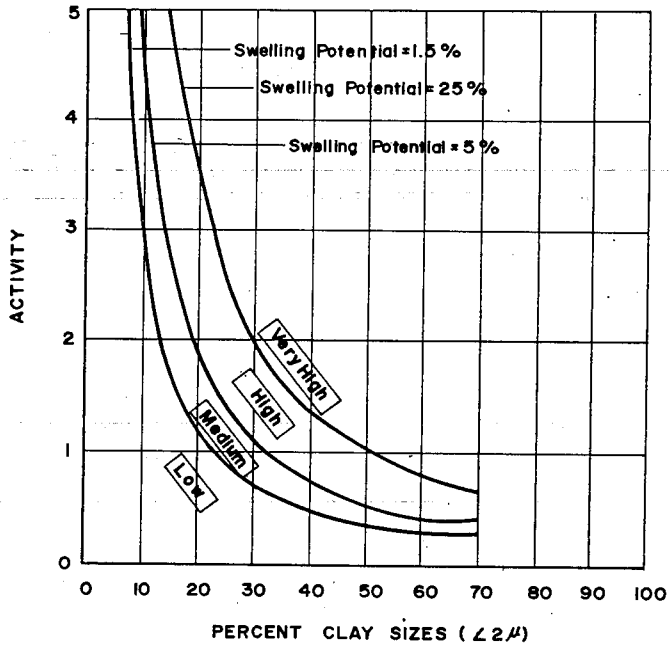


Fig. 10.4 Classification chart for swelling potential [22]

10.5.2.4 Unified Soil Classification Method

This classification method is based on the plasticity chart. Normally, expansive soils found in and around Addis Ababa are located above the A-line in the region of high plasticity as shown in Fig. 10.5.

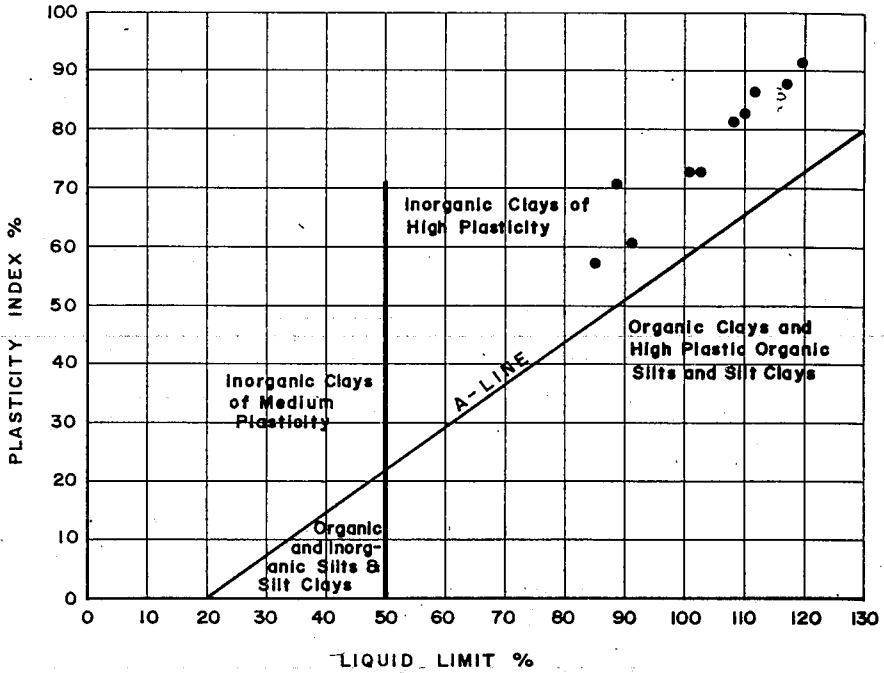


Fig. 10.5 Plasticity chart

10.6 SWELLING POTENTIAL AND SWELLING PRESSURE

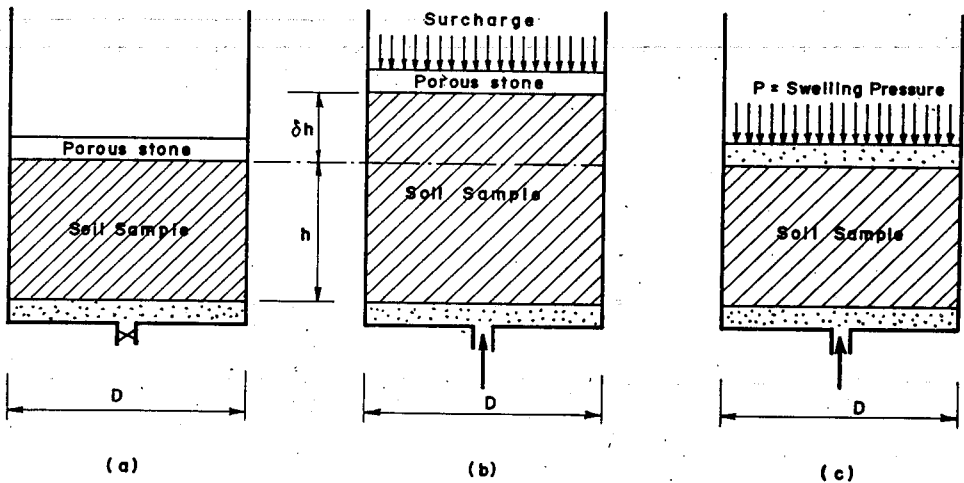
10.6.1 General

The term swelling potential is generally used to indicate the amount of vertical swell (expressed as per cent of initial sample thickness) obtained under a particular surcharge (usually 1psi). In short it can be referred to as vertical strain under a surcharge that the sample undergoes following exposure to water as shown in Fig. 10.6b.

$$S_p = \frac{\delta_h}{h} (100) \quad (10.8)$$

where

- S_p = swelling potential in per cent
- δ_h = amount of vertical swell
- h = initial height



a) Initial condition

b) Maximum swelling

c) Final condition

Fig. 10.6 Diagrammatic description of swelling pressure and swelling potential

The swelling pressure is defined as the vertical pressure required to prevent volume change of laterally confined sample when it is allowed to take in water as indicated in Fig. 10.6.

The relationship between percent - swell and pressure can be expressed by a curve shown in Fig. 10.7. Such a curve is very useful in the prediction of stress-deformation behaviour of expansive soils.

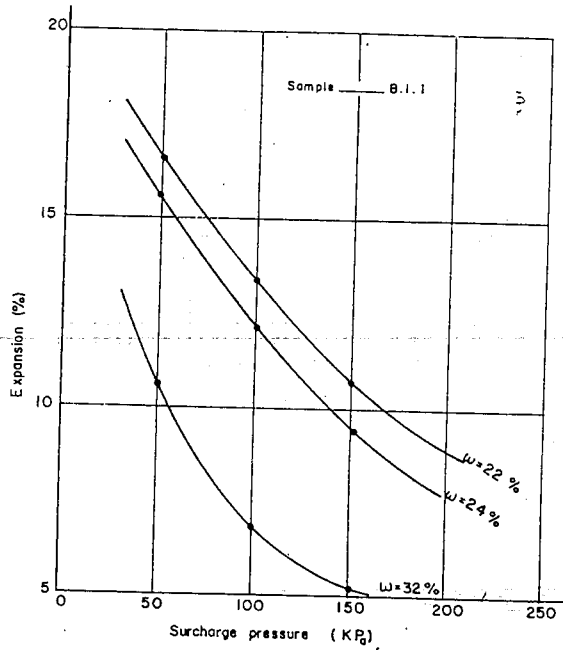


Fig 10.7 Load expansion curve of a clay sample with given initial moisture content. [18]

10.6.2 Factors Affecting Swelling Potential

Plastic clays are capable of large volume changes. The volume changes that take place can be either expansion or shrinkage. This is primarily governed by initial moisture content and change in moisture conditions. Swelling is usually accompanied by wetting of soil which initially was dry. Shrinkage, on the other hand, is associated with drying of soil which initially was quite wet.

The magnitude of swelling and/or swelling pressure is governed by the following factors:

- a) Amount and type of clay in the soil

- b) Placement conditions which involve initial water content, initial density and confining pressure
- c) Time allowed for swelling

The influences of the placement conditions on the magnitudes of swell and swelling pressures are as illustrated in Fig.10.8 and that of time allowed for swelling in Fig. 10.9.

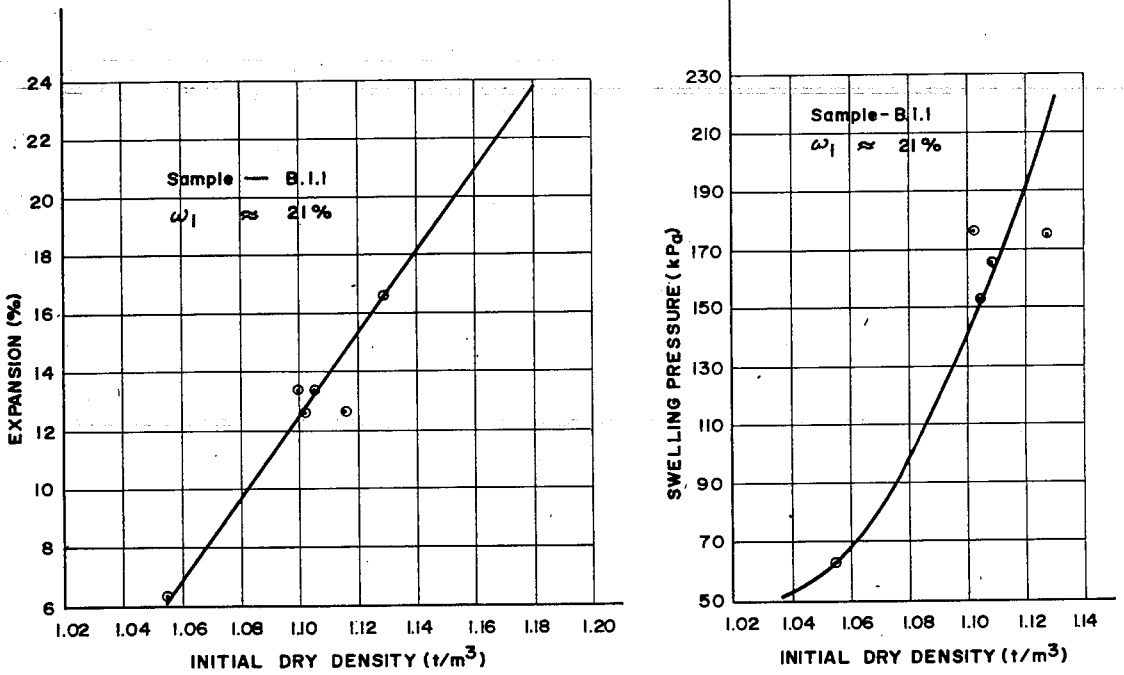


Fig. 10.8 Influence of density on percent swell and swelling pressure [18].

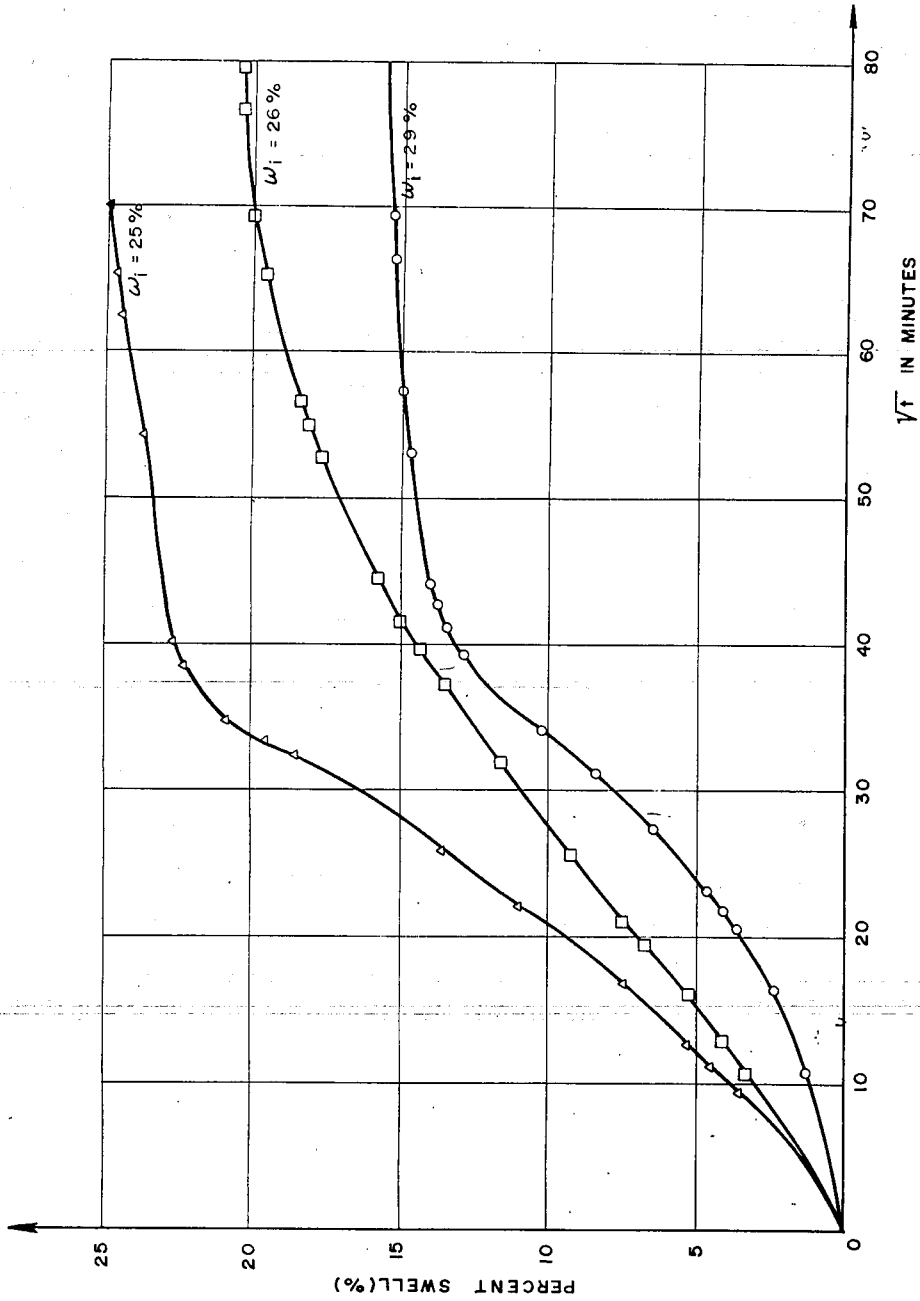


Fig. 10.9 Influence of time on the magnitude of % swell [18]

From the above figures it may be noticed that

- (a) for a given dry density percent expansion decreases with increase in initial moisture content (Fig. 10.7)
- (b) for a given initial moisture content the swelling pressure increases with increase in dry density (Fig. 10.8). Percent expansion also increases with increase in dry density for a given initial moisture content (Fig. 10.8).
- (c) percent expansion decreases with increase in confining pressure for a given initial moisture content and density (Fig. 10.7).
- (d) for full expansion time is necessary (fig. 10.9). The same thing is true for swelling pressure.

10.6.3. Laboratory Testing Methods for Determining Swelling Potential

10.6.3.1 General

The available techniques for quantitative measurement of expansive soils can be categorized into three groups. Namely, oedometer tests, soil suction tests and empirical methodology. Among these techniques the oedometer tests are capable of simulating some of the factors which affect the swelling characteristics of expansive soils. It should be noted, however, that the oedometer tests have limitation. The oedometer tests consider moisture as well as volume change in one dimension only. In the in-situ, the above changes take place in three directions. For simplicity, however, the oedometer testing techniques have become popular and are extensively used. Therefore, this method is discussed. In the section to follow some of the methods which use the oedometer will be reviewed.

10.6.3.2 Different Pressure Method

In this method several identical samples (three or more) are loaded with different loads close to expected swelling pressure. The samples are set aside to consolidate in the dry state. When equilibrium is reached, then they are submerged in water and the subsequent swell is recorded. The samples are again left until they reach equilibrium and the swelling practically ceases. The vertical movement are plotted against applied pressure as shown in Fig. 10.10. The pressure corresponding to zero volume change is taken as the swelling pressure.

The different pressure method has the same sequence with regard to loading wetting events as in the field. That is, the loads are firstly applied to unsaturated soil and the soil undergoes compression under these loads. Then, after a period of time, the soil comes in contact with the source of water and an upward movement starts.

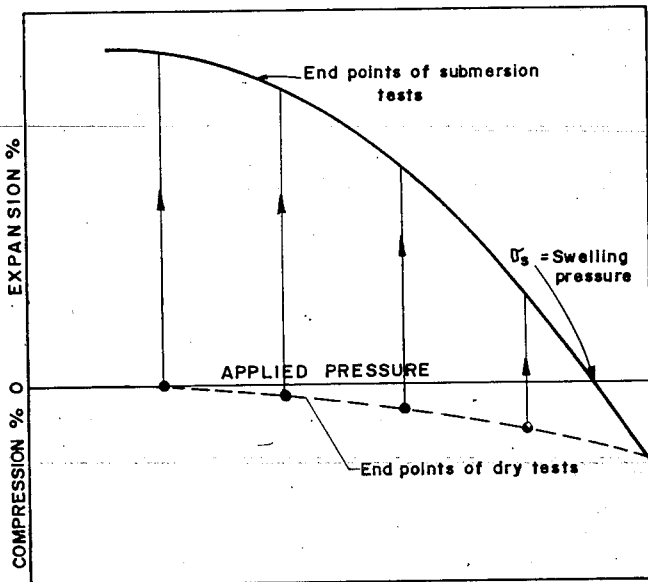


Fig. 10.10 Determination of swelling potential by different pressure method

The data obtained by this method can provide much information useful for design such as swelling pressure corresponding to zero volume change, the vertical movement that is to be expected under the loads imposed by the structure and the loads that could be applied to develop a certain swelling within a tolerable limit.

10.6.3.3 Swell-Consolidation Method (Free Swell Method)

In this method an undisturbed sample is allowed to absorb water under a load of 1 psi (7kN/m^2) and is put aside to fully expand and reach equilibrium. Then it is consolidated by increasing the applied pressure in intervals following the conventional consolidation test procedure. The load increment is continued until the sample reaches its initial volume (zero volume change). The load corresponding to zero volume change is taken as swelling pressure. Fig.10.11 shows the stress-strain relationship for this test.

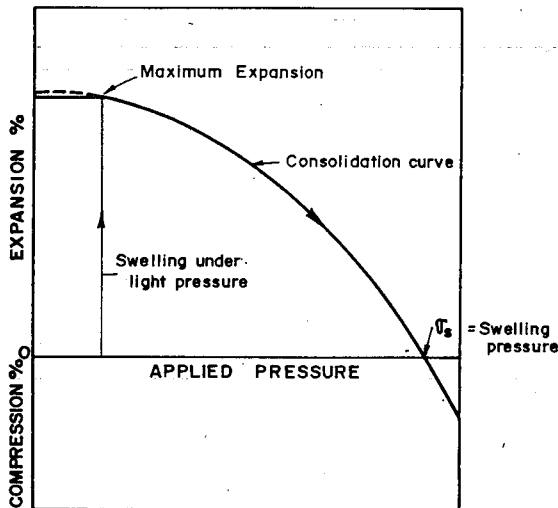


Fig. 10.11 Determination of swelling potential by swelling consolidation method

This method is quite popular and many investigators have used this method to establish a relationship between swell and applied pressure and to evaluate swelling pressure. The most serious draw back of this method is that it does not represent the normal sequence of *load-submersion*. In the field the soil is first subjected to the structural load and then swell later following exposure to moisture but not vice versa. This method also yields a higher swelling pressure than other method. The higher swelling pressure is attributed to the great energy required to expel the absorbed water.

10.6.3.4 Double Oedometer Method

This method was proposed by Jennings and Knight and has been used by many investigators to study the swell-pressure relationship of an expansive soil.

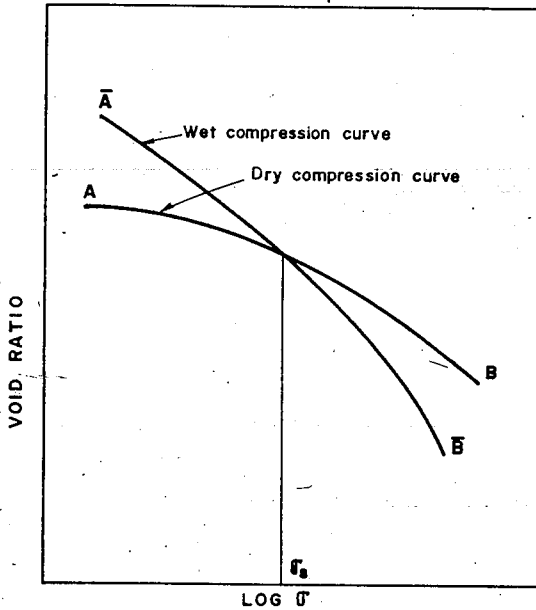


Fig. 10.12 Determination of swelling pressure by double oedometer method

This method is based on subjecting two identical samples to consolidation test. The first sample is consolidated at its natural moisture content while the second sample is first-allowed to absorb water and swell under light load followed by consolidation. For the two samples the applied pressures are plotted against vertical strain (or void ratio) on the same diagram. The pressure corresponding to the intersection point of the two curves is taken as the swelling pressure as shown in Fig. 10.12.

This method usually gives a relatively high swelling pressure. This is due to the fact that the pressure taken as the swelling pressure is not that required to bring the sample to its initial volume, but to its volume after being compressed in the dry state to a pressure equal to the swelling pressure.

10.6.3.5 Constant Volume Method

The specimen in the constant volume method is allowed to absorb water without any increase in volume by increasing the applied pressure as the test proceeds until the sample reaches equilibrium (Fig. 10.13). The test can be carried out using oedometer, where more load is added to keep the volume of the sample constant while the sample absorbs water. The same test can also be run using a rigid proving ring. The swelling pressure can be determined by plotting the applied pressure against change in volume as shown in Fig 10.13. This method does not represent the in-situ condition where the applied load, after the structure is in service, does not change with time. When the swelling process occurs, a constant pressure acts rather than different pressure which increase with time to counter act the swelling process. Information such as the amount of heave which could be expected under application of a certain load or the load which could be applied to limit the heave within tolerable limit cannot be furnished by this method. The method needs uninterrupted monitoring for a long period.

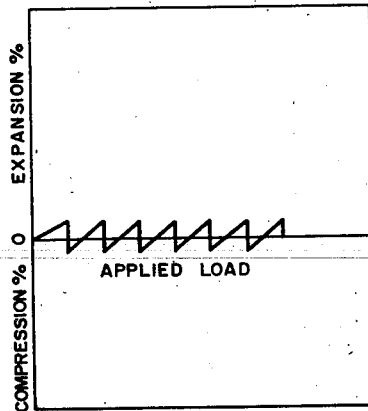


Fig. 10.13 Determination of swelling pressure by the constant volume method

10.6.3.6 Comparison of the Different Testing Methods

The swelling pressure value of identical specimens determined by various testing method are presented by Rabba 1975 as indicated below.

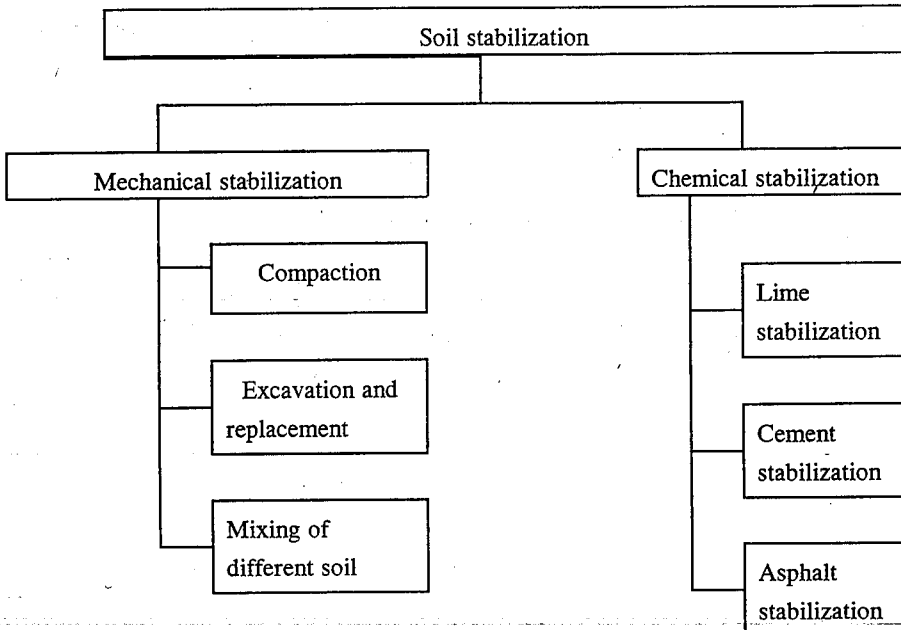
Method	Swelling Pressure
	KN/m ₂
Different Pressure	1800
Swell-consolidation	2200
Double Oedometer	3400
Constant volume	1900

11 IMPROVING SOIL CONDITIONS AND PROPERTIES

1.1 SOIL STABILIZATION

11.1.1 General

The soils available for construction often do not meet the requirements for construction. The process by which the properties of the soil are improved so as to meet the construction requirement is called stabilization. In its broadest sense, soil stabilization may also be defined as the method used to change one or more properties of soil so as to improve the desired performance of the soil. Soil stabilization may be broadly classified as follows



11.1.2 Compaction

Compaction is the process whereby soil is mechanically compressed through a reduction in the air voids. In other words, it is a process of increasing soil unit weight (density) by forcing the solid matter of the soil into a tighter state and reducing the air voids.

The purpose of compaction is to produce soil having physical properties appropriate for a particular project. For example, good compaction is needed in road construction for building of embankments, improvement of subgrades and building of sub-bases. Compaction reduces settlements of the fill in embankment; reduces percolation of water through the fill and also increases shearing resistances.

Compaction is measured quantitatively in terms of dry density. The increase in dry density of soil is a function of the moisture content of the soil and the amount of compaction (compactive effort).

11.1.2.1 Role of Moisture in Compaction

For a given compactive effort the dry density (dry unit weight) will vary with the water content as shown in Fig. 11.1. The water content at which the dry density is a maximum is termed as optimum water content. The behavior of soil at different water content is explained as follows.

When the water content is low, the soil is stiff and difficult to compress, thus low dry density and high air contents are obtained. As the moisture content is increased, the water acts as lubricant causing the soil to soften and become more workable. This results in the closer packing (higher dry density) of the soil grains and lower air contents. If more water is added to the soil, however, a stage is reached when water tends to keep the particles apart (pore pressure is set up) and prevent any appreciable increase in air content. The total voids continue to increase with the moisture content and hence the dry density of the soil falls.

To the right of the peak of the dry density versus water content curve shown in Fig. 11.1 is curve relating dry density with moisture content for soil containing no air voids.

This curve represents an upper bound for dry density (dry unit weight) and is drawn using the following equation which is derived from Eq. (2.15) and Eq. (2.20).

$$Y_d = \frac{G_s}{1+e} Y_w = \frac{G_s}{1 + \frac{(\omega G_s)}{s}} Y_w \quad (11.1)$$

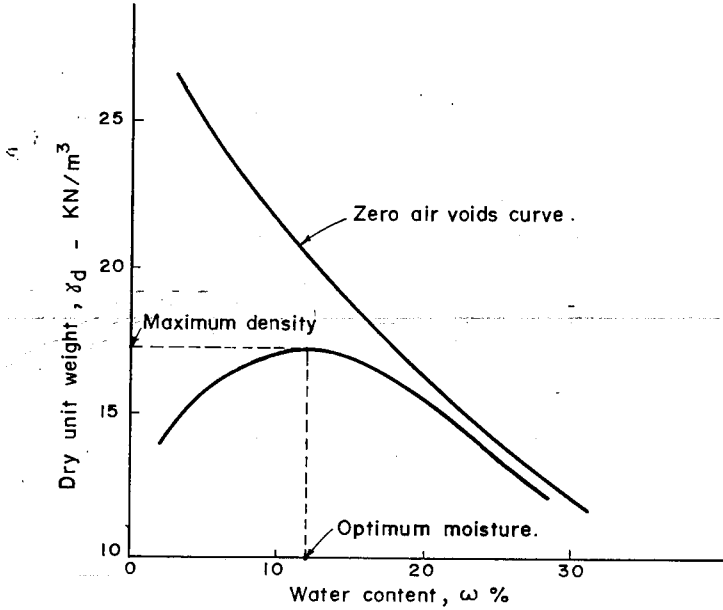


Fig. 11.1 Compaction curve

11.1.2.2 Compaction Effort

Increasing amounts of compaction, that is the energy applied per unit weight of soil, results in an increase in the maximum dry density and a decrease in the optimum moisture content as shown in Fig. 11.2. If light compaction is used, more water will be needed to overcome the resistance of the soil grains to packing. In using heavy compaction, however, the soil grains can be forced over each other with less water and the amount of water occupying the pore spaces can be kept at minimum. This latter case results in a denser packing. It can, therefore, be concluded that the greater the compactive effort, the higher the maximum dry density and the lower the optimum moisture content.

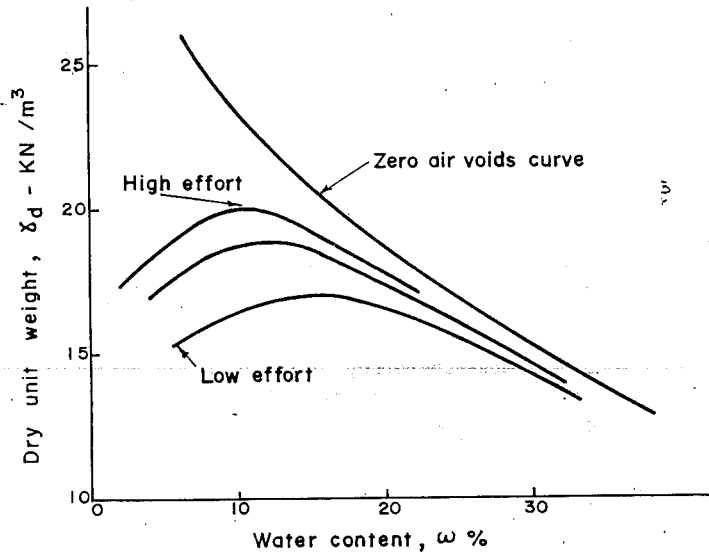


Fig. 11.2 Compaction curve for different compactive effort

11.1.2.3 Laboratory Compaction Tests

11.1.2.3.1 General

Standard compaction tests were developed by Proctor in 1933 and is widely used to determine the optimum moisture content and the maximum dry density under normal compactions. Two types of compaction tests are in use today. They are the standard Proctor compaction test and the modified Proctor (modified AASHO compaction test).

The apparatus used in both tests consists of cylindrical mold having a capacity of $1/30$ cubic feet ($945 \times 10^{-6} \text{ m}^3$) with an internal diameter of 4 inches (10 cm) and a height of 4.6 inches (11.5cm). A detachable collar is attached to the mold on top. The mold itself is bolted to a base plate at the bottom as shown in Fig. 11.3.

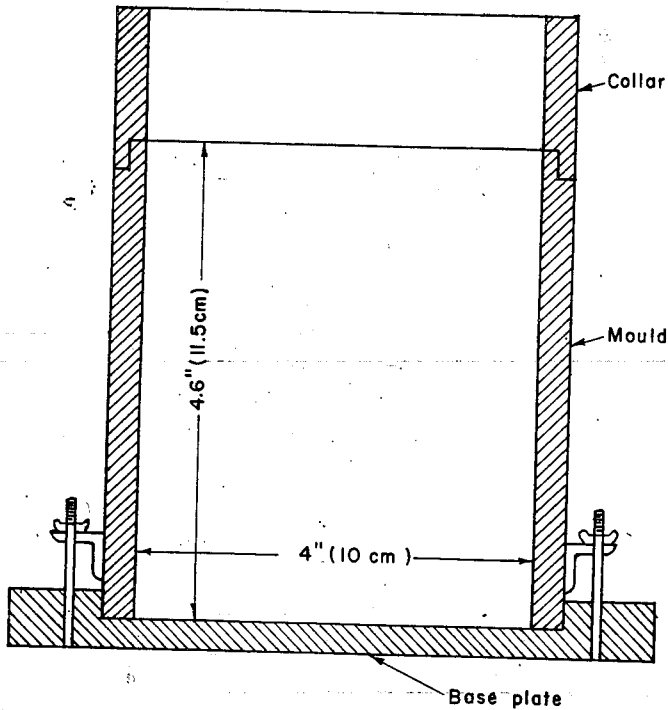


Fig. 11.3 Standard Proctor mold

The compaction tests are designed to simulate the density of soils compacted by field methods. For most applications such as retaining wall backfill, highway fills and earth dams the standard Proctor test is adequate compaction. For heavier load applications such as airport and highway base courses, the modified Proctor test is used.

11.1.2.3.2 Standard Proctor Test

The soil to be tested is thoroughly mixed with measured quantity of water and is then filled in the mold in three layers of approximately equal thickness. Each layer is compacted by 25 blows of a standard rammer weighing 5.5 pounds (25N) which is allowed to drop freely from a height of 12 inches (0.3m) at each blow. After compaction of three layers, the soil is trimmed to the top of the mold. The mold with its content is removed from the base plate

and weighed. Moisture content determination is made on a sample of soil and the dry density is then calculated as follows:

Weight of empty mold	= W_1
Weight of the mold and the compacted soil	= W_2
Moisture content of the compacted soil determined by drying a sample in the oven	= ω
Volume of the mold	= V
Moist unit weight, γ_{wet}	= $\frac{W_2 - W_1}{V}$
Dry unit weight (dry density), γ_d	= $\frac{\gamma_{wet}}{1 + \omega}$

The above procedure is repeated at several increasing moisture contents and a compaction curve as shown in Fig. 11.4 is obtained. The co-ordinates of the peak give the maximum dry density and the optimum moisture content. At a given moisture content, the maximum possible compaction would be obtained when the air is completely expelled and the soil is fully saturated. In practice this is not possible to attain. A certain amount of air will remain entrapped within the water as minute bubbles and will not be expelled by any amount of compaction. It is only then possible to express the dry density of a soil with a given moisture content at a particular saturation ratio as expressed by Eq.(11.1). As may be noticed from Fig. 11.4 for a constant ω , γ_d increases as S increases attaining a maximum at full saturation, i.e. $S = 100\%$.

11.1.2.3. Modified Proctor Test

In this test the same procedure as described in section 11.1.2.3.2 is followed, but the compaction is carried out by blows of 10 pounds (45N) rammer dropped from a height of 18 inches (0.46m) on each 5 layers. The number of blows per layer is the same as standard Proctor test.

11.1.2.4 Field Compaction

Compaction in the field is carried out by different methods using such machines as tampers, smooth drum roller, pneumatic-tired roller, sheepfoot roller, vibratory roller etc. The compacted dry density to be attained is specified depending on the type of equipment to

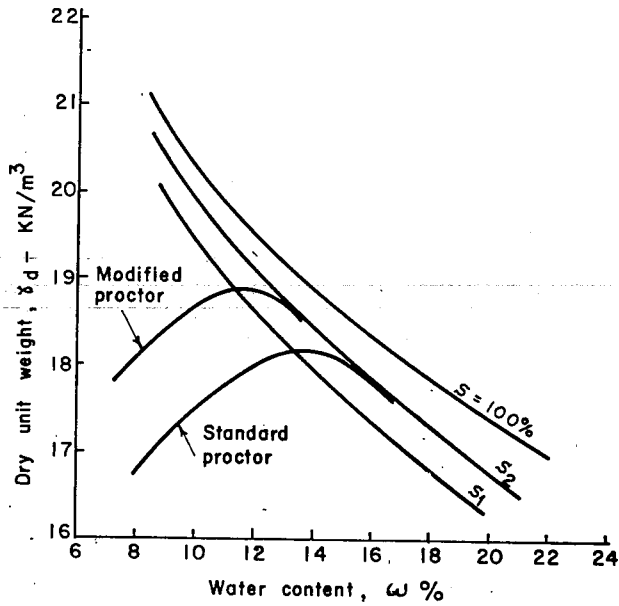


Fig. 11.4 Compaction curves resulting from standard Proctor and modified Proctor tests

be used on the basis of laboratory standard Proctor or modified AASHO tests. As it is difficult to maintain strict control of compaction in the field, the specifications usually require attainment of 90% to 95% of the dry density obtained in the laboratory.

The type of compaction methods to be adopted in the field depends on the kind of soil to be compacted. Cohesionless soils are effectively compacted by imparting vibrations. Rolling for such type of soils is least effective. For silty soils of low plasticity, pneumatic tyred rollers are preferred. Plastic soils of moderate cohesion and cohesive clay soils are best compacted by sheepfoot rollers.

11.1.2.5 Field Control of Compaction

11.1.2.5.1 Density Control

Undisturbed soil sample is obtained by pushing a thin walled cutter 10cm in diameter and 12.5 cm high into the compacted soil layer. The cutter is weighed with its contents and the moisture content of the soil is found by the usual procedure. Using the moisture content thus obtained, the dry density is determined and compared with the dry density obtained in the laboratory standard test.

For gravelly soil, the sand cone method is used. The method consists of digging a hole 10 to 15 cm in diameter and 15cm deep. The soil obtained from the hole is weighed and tested for moisture content. The volume of the hole is measured by filling it with loose dry sand that falls from a fixed height through a cone-shaped stand. An alternate method of measuring the hole volume is to line it with a thin rubber (rubber balloon method) and fill it with water (For detailed procedure consult ASTM)

11.1.2.5.2 Penetration Control

This is done by means of a penetrometer. During the laboratory compaction testing a penetrometer reading can be obtained for the material in the Proctor mold after each test. A correlation between penetration resistance, dry density and moisture content can be established (Fig. 11.5) to serve as calibration curve.

The penetrometer can later be used to test the material as it is compacted in the field. The penetration resistance values as obtained in the field are compared with those obtained in the laboratory to determine the acceptance of the compaction work. Penetrometer is used in most soil compaction control cases excepting in stony soils.

11.1.3 Excavation and Replacement

Excavation and replacement is sometimes used where a problematic soil layer is of small thickness and is located close to the ground surface. In such cases, it would be economical to remove the soil and replace it with well graded soil that can be compacted to a dense state.

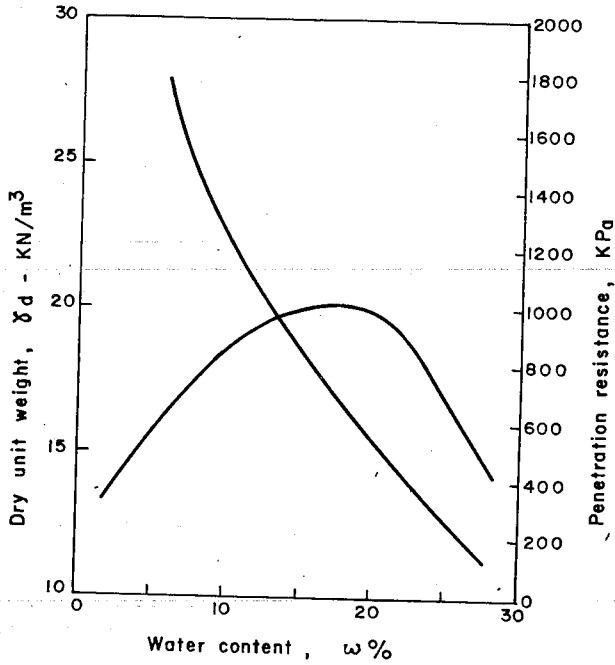


Fig. 11.5 Correlation between penetration resistance, dry density and water content

11.1.4 Mixing of Different Soils

Mixing of different soils is usually undertaken when the natural soil at the construction site is either too coarse or too fine to be compacted to a dense structure to serve as subbase in highway construction or floor foundation for building construction. In such a case the natural soil is excavated to sufficient depth and then blended with selected soils brought from elsewhere. The mixed soil is laid in layers and compacted following the given specification.

11.1.5. Lime Stabilization

In general, lime stabilization improve the strength, stiffness and durability of fine grained soils. Adding lime to soil produces lower maximum density and a higher optimum moisture content. It has a pronounced stabilizing effect on expansive soil. It lowers the plasticity index and greatly reduces shrink-swell characteristic of expansive soil. Such an action of lime takes places quite rapidly and requires 2 to 3 per cent lime. The slow action of lime which is due to pozzolanic activity requires sufficient time (weeks) and quantity of lime and results in increase in strength. It has been found that there is an optimum lime content up to which strength increases and beyond which strength decreases. This calls for special care in the design of lime treated soil.

11.1.6 Cement Stabilization

Portland cement and soil mixed at the proper moisture content is used to stabilize soils in special situation. The main use has been to stabilize soil bases under concrete pavement for highways and airfields. Soil cement mixtures are also used to protect dams against erosion by waves and as cores for some small earth dams.

There are a number of factors which affect the strength and durability of soil-cement. Some of these are soil type, cement content, aging, curing condition, compaction condition etc. Almost any inorganic soil that can be pulverized effectively can be stabilized with cement. A well graded soil is most suitable for cement stabilization. Stabilization of low plasticity and sandy soils usually require 5 to 14% cement by volume.

The strength of soil cement increases with curing period. During the initial stage of curing, the soil-cement must be kept moist, otherwise fine cracks may develop in soil cement. The time elapsed between mixing and compaction or in other words aging has negative effect on density, strength and durability of soil cement. The detrimental effect of aging on strength and durability can be minimized, if compaction moisture content is kept above the optimum moisture content as obtained from Proctor compaction test. In this regard it has been recommended (for expected delay of 2 to 6 hours between mixing and compaction) to use 2 to 4% moisture content above the optimum for such soils as silty loams, silty clays and sandy loams. The compaction moisture content for fine-grained soils is suggested to be 3 to 4% above the optimum moisture content even if delay is not expected.

11.1.7 Asphalt Stabilization

Bituminous materials are employed in various consistencies to improve the geotechnical properties of soils. When mixed with cohesive soils, bituminous materials improve the bearing capacity and soil strength by water-proofing the soil and preventing high moisture content. Bituminous materials act as a cementing agent when added to sand and produce a strong coherent mass. The amount of bitumen added range from 4 to 7% for cohesive material and from 4 to 10% for sandy material. Bitumen stabilized soils are used as base course in road construction.

11.2 INJECTION AND GROUTING

Grouting is widely used to control ground water flow. It is also used to increase soil strength and prevent settlement. Grouting consists of injecting under pressure cement slurry or chemicals or bentonite into a soil to improve its properties or control ground water flows. It is effectively applied into a soil only if the soil is sufficiently pervious to permit the easy passage of solution or if it contains cracks which require filling. Grout may therefore be designed to penetrate through the void system of the soil mass or to displace soil and improve the properties by densifying a loose soil. Methods of applying grouts into the soil vary. In one method a casing is driven and injection is made under pressure as the casing is withdrawn. In another method a grout hole is drilled to a depth at which grout is required and the grout is forced into the soil as soon as the drill is withdrawn. Another method requires the casing to be perforated and left permanently there. Displacement grouting (consisting of Portland cement and sand slurry) is used to displace soil and compact the surrounding material about a central core of grout. Injection of lime sometime used to produce lenses in the soil that will block the flow of water and reduce compressibility and expansion properties of the soil. Injection and grouting techniques of stabilizing soils are generally found to be expensive when compared to other methods and hence are used only in special situations.

11.3 DYNAMIC STABILIZATION

Dynamic stabilization techniques are often used to stabilize cohesionless soils. The most common methods of dynamic stabilization are vibroflotation, blasting and compaction piles. Each of these techniques is briefly described.

11.3.1 Vibroflotation

The vibroflot is cylindrical tube provided with water jets at top and bottom. It is equipped with eccentric weight which develops horizontal vibratory motion. The vibroflot is sunk into the ground with the help of the lower jets and then raised in small stages, in the course of which the surrounding soil is compacted by the vibration process. The enlarged hole made by the vibroflot is filled with suitable granular material and is compacted by the jet action. This method is very effective for increasing the density of a loose sand deposit for depth up to 30m.

The spacing of compaction probes should be on grid of about 2m. In soft cohesive soils and organic soils the vibroflotation method has been used with a gravel as a backfill material. The resulting densified granular material column called stone column effectively reinforces softer soils and acts as a bearing pile for foundations. The stone columns furnish drainage channels for moisture in the soil and accelerate consolidations.

11.3.2. Blasting

Explosive charges buried at a greater depth are very effective in producing deep densification of granular materials when detonated at intervals. The holes of explosive charges can be patterned in grids of suitable size. This technique is used in areas where surrounding structures are located at far enough distance to prevent damage.

11.3.3 Compaction Piles

Compaction piles are commonly used to densify a loose deposit of sand. In this method pipe piles provided with caps are driven to the desired depth. As they are extracted the holes are backfilled with granular materials. Both the process of driving the pile and the displacement of soil due to the pile produce densification of surrounding sandy material.

11.4 PRECOMPRESSION

Precompression involves preloading the soil to produce settlement before the start of construction work. The preload is usually in the form of an earth fill which is kept in place long enough to produce the required settlement. In order to check when sufficient settlement

has taken place, a settlement monitoring system such as settlement plates are installed. After the required settlement has taken place, part or all of the preload may be removed prior to construction of buildings or other structures at the site.

Precompression is used on large-scale construction site composed of weak silts and clay or organic materials and other compressible soils. To decrease the time of primary consolidation, a pattern of vertical sand drains are used in conjunction with preloads. The sand drains decrease the length of the consolidation drainage path and hence decrease the time required for settlement.

Careful consideration must be given to the stability of the foundation soil under preload prior to the use of this technique in improving the foundation soil.

11.5 DRAINAGE

Drainage can improve the engineering properties of soil by reducing the water content. This is especially true in the construction of foundations in granular soils with high permeability. Drainage may be accomplished to shallow depth by using ditches and sumps or to a deeper depth using well points and deep wells.

Example 11-1

The following data were obtained from Proctor compaction test on a soil

$\omega(\%)$	9.6	11	12.5	14	16	18	19.5
$\gamma_{wet} (KN/m^3)$	18	19	19.6	20.45	21	20.5	20.1

specific gravity of soil grains is 2.6 Determine the maximum dry density and optimum moisture content for the soil. Plot the zero air curve and 85% saturation curve.

$$\gamma_d = \frac{\gamma_{wet}}{1 + \omega} = \frac{18}{1 + 0.096} = 16.42 \text{ KN/m}^3$$

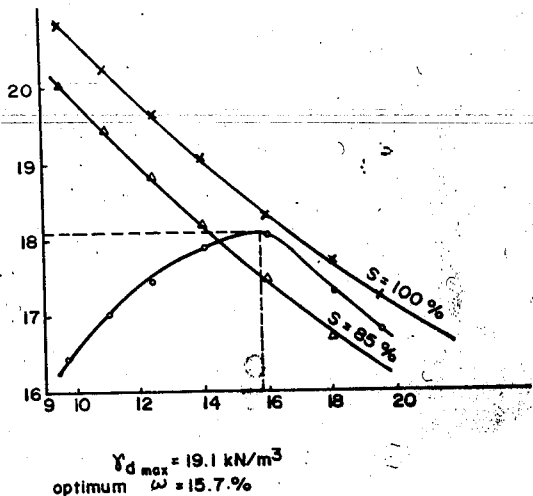
The same calculation is carried out for each moisture content.

$$\gamma_d = \frac{G \gamma_w}{1 + \frac{\omega G}{S}} = \frac{(2.6)(10)}{1 + \frac{(0.096)2.6}{1}} = \frac{26}{1.2496} = 20.81 \text{ KN/m}^3$$

Keeping $S = 1$, for each moisture content γ_d is determined.

With $S = 0.85$, γ_d is computed for each moisture content.

$\omega(\%)$	9.6	11	12.5	14	16	18	19.5
$\gamma_d (KN/m^3)$	16.42	17.12	17.42	17.94	18.10	17.37	16.82
γ_d for $S=100\% (KN/m^3)$	20.81	20.22	19.62	19.06	18.36	17.71	17.25
γ_d for $S=85\% (KN/m^3)$	20.09	19.46	18.81	18.20	17.46	16.76	16.29



11.6 EXERCISES

- 1 The Following are the results of Proctor compaction test on a given soil sample

Wt. of mold + wet soil in N	33.2	34.38	37.78	37.76	36.88
Moisture Content (%)	5.18	8.45	14.95	16.83	19.70

If the weight of the mold is 17.86N and volume 940 c.c., determine the maximum dry density and optimum moisture content.

- 2 In a Proctor compaction test the maximum dry density was found to be 18KN/m^3 and optimum moisture content 15.2%. If the specific gravity of soil grains is 2.65, calculate the degree of saturation and void ratio at maximum dry density.
- 3 From Proctor compaction test the dry maximum density of soil was found to be 17.5KN/m^3 and optimum moisture content 14.5%. The specific gravity of soil grains was 2.6. Find the degree of saturation and percentage of air voids at the optimum condition.

REFERENCES

- AASHTO - Standard Specifications for Transportation Materials and Methods of Sampling and Testing, Part II, July 1978
- Atterberg, A. - Über die physikalische Bodenuntersuchung und Über die Plastizität der Tone.
Int. Mitt für Bodenkunde, 1, 1911.
- Bishop, A.W. - The Use of Slip Circle in the Stability Analysis of Slopes.
Geotechnique, 1955.
- Blum, H. [1] - Einspannungs verhältnisse bei Bohlwerken Wilhelm Ernst und Sohn, Berlin, 1931.
- Bölling, W.H. [2] - Sickerströmungen und Spannungen in Böden.
- Boussinesq, J. - Application des Potentiels a L'etude de L'equilibre et duo mouvement des Solids Elastiques.
Gauthier-Villars, Paris, 1885.
- Bowels, J.E. - Foundation Analysis and Design. McGraw-Hill, New York 1968.
Engineering Properties of Soils and Their Measurement,
2nd Ed., McGraw-Hill, N.Y. 1978.
- Capper, P.L. / Cassie, W.F [3] - The Mechanics of Engineering Soils
E.& F.N. Spon, London, 1961.
- Casagrande, A./Fadum, - Notes on Soil Testing for Engineering Purposes.

- R.E. [4] Cambridge Mass., Harvard University
Publication No. 268, 1939/40.
- Coulomb, C.A. - "Essai sur une Application des Règles des Maximis et Minims à quelques Problèmes de Statique Relatifs à l'Architecture", Mém. Acad. R. Sci, 1776.
- Culmann, K. - Die Graphische Statik Zurich, 1866.
- DIN 4017 Blatt 1 [5] - Baugrund: Grundbruchberechnungen von lotrecht mittig belasteten Flachgrundungen. Richtlinien, 1965
- DIN 4017 Blatt 2 [6] - Baugrund: Grundbruchberechnungen von aussermittig und schräg belaster Flachgrundungen. Empfehlungen, 1970.
- DIN 4019 Blatt 2 [7] - Baugrund: Setzungsberechnungen bei schräg und bei aussermitig wirkender Belastung - Richtlinien, 1961.
- DIN 4048 Blatt 2 [8] - Baugrund: Standsicherheitsberechnung bei Böschungen zur Verhinderung von Böschungsbruch, 1974.
- Dunn, I.S./Anderson, L.R. and Keifer, F.W. [9] - Fundamentals of Geotechnical Analysis. John Wiley & Sons, New York, 1980.
- EAU (Empfehlungen des Arbeitsausschusses Ufereinfassung) [10] - Mittlere Bodenwerte für Vorentwürfe (E9) Wilhelm Ernst und Sohn Berlin /Munchen/ Düsseldorf, 1970.

- Fellenius, W. - Erdstatische Berechnungen, Berlin, 1939.
- Hansen, J.B. - "A General Formula for Bearing Capacity", Bulletin 1961.
- Harr, M.E. [20] - Groundwater and Seepage. McGraw-Hill Book Co., Inc. New York / London / Toronto, 1962
- Holtz, W.G. Gibbs, H.J. [12] - Engineering Properties of Expansive Clays. Translation ASCE, Vol. 121, 1956.
- Hough, B.K. - Basic Soils Engineering, 2nd Ed., Ronald Press, New York, 1969.
- Jelinek, R. [13] - Setzungsberechnung ausmittig belasteter Fundamente. Bauplanung und Bautechnik 3, 1949.
- Jumikis, A.R. [14] - Soil Mechanics. D. Van Nostrand Co. Inc. Princeton, 1962.
- Kezdi, A. [15] - Erddrucktheorien. Springer - Verlag, Berlin, 1962.
- Krey, H.D [16] - Erddruck, Erdwiderstand und Tragfähigkeit des Baugrundes. Wilhelm Ernst und Sohn., 1963.
- Lambe, T.W. [17] - Soil Testing for Engineers
- Lambe, T.W./Witman, R.V. - Soil Mechanics, John Wiley & Sons, New York, 1969.

- Leikun, M [18] - Foundation Problems on Expansive Soils found in and around Addis Ababa, 1983.
- Meyerhof, G.G. - "The Bearing Capacity of Foundations under Eccentric and Inclined Loads", Proceedings, 3rd International Conference Soil Mechanics and Foundation Engineering, Zurich, 1953.
- Mitchell, J.K. - Fundamentals of Soil Behaviour Wiley, New York, 1976.
- Newmark, N.M. [19] - Influence charts for Computation of Stresses in Elastic Foundations. Engineering Experiment Station Bulletin Series No.338, University of Illinois, 1942.
- Prandtl, L. [20] - Über die Härte Plastischer Körper
Nachrichten von der Königlichen Gessellschaft der Wissenschaften zu Gottingen, 1920.
- Rankine, W.M.J. - "On Stability of Loose Earth". Phil. Trans., Royal Soc., London, 1857.
- Schultze, E. [21] - Zahlenbeispiele für die Bearbeitung der Übungsaufgaben.
Lehrstuhl für Verkerkehreswasserbau, Grundbau und Bodenmechanik TH-Aachen, 1970.
- Seed, H.B/ Woodward, R.J. and Lundgren, R [22] - Prediction of Swelling Potential for Compacted Clays.
Proceedings ASCE, Vol 88, No. SM3, June 1962.
- Skempton, A.W. [23] - The Bearing Capacity of Clays
Building Research Congress, Division I, 1951.

- Skempton, A.W./Bjerrum, L. [24] - A Contribution to the Settlement Analysis of Foundations on Clays. *Geotechnique*, Vol. VII., 1957.
- Skempton, A.W. [25] - The Colloidal Activity of Clays. *Proceedings Third International Conference - Soil Mechanics and Foundation Engineering*, 1953.
- Sowers, G.B./Sowers, G.F. - *Introductory Soil Mechanics and Foundations*, 3rd Ed., MacMillan Publishing Company, New York, 1976.
- Spangler, M.G./Handy, R.L. - *Soil Engineering*. 3rd Ed., Intext, New York, 1973.
- Steinbrenner, W. [26] - *Tafeln zur Setzungsberechnung* Strasse 1, 1934 und *Schriftenreihe Strasse 3*, 1937.
- Taylor, D.W. [27] - *Fundamentals of Soil Mechanics* John Wiley & Sons, Inc., New York, 1960.
- Teferra, A - *Foundation Engineering*, Addis Ababa University Press, 1990.
- Teferra, A /Schultze, E. [28] - *Formulae, Charts and Tables in the Area of Soil Mechanics and Foundation Engineering. Stress in Soils.* A.A. Balkema, Retterdam, Brookfield, 1988.
- Terzaghi, K. [29] - *Theoretical Soil Mechanics* John Wiley & Sons, Inc., New York, 1956.
- Terzaghi, K./Peck, R.B. [30] - *Soil Mechanics in Engineering Practice* John Wiley & Sons, Inc., New York, 1960.
- U.S. Waterways Experiment Station [31] - *Investigation of Filter Requirements for Underdrains.* Tech. Memo. No. 183-1, 1941.

SUBJECT INDEX

- Atterberg limits 24
 - determination of, 27
- Activity, 441, 443
- Adsorbed Water, 30,51
- A.A.S.H.O. classification, 33
- Arching effect, 303
- Angle
 - of internal friction, 219,221,227
 - of friction, 218
 - of Wall friction, 275
- Average degree of Consolidation, 184,185
- Bearing Capacity, 377
 - of shallow foundation, 380,381
 - of deep foundation, 411
 - Terzaghi's theory of , 384
 - Prandtl's theory of, 382
 - allowable, 377,407,411
 - ultimate ,377,395,396,398,400,405
 - factors for general shear, 384,386
 - factors for local shear, 384, 387
- Block diagram,5
- Boussineq's equation, 122
- Capillary
 - Water,52
 - forces,52
 - rise, 56
 - movement, 56
 - factors affecting, 58
- Clay
 - minerals,32
 - normally consolidated, 230
 - over consolidated, 230,242
- Classification of Soils, 33
 - grain-size, 33
 - M.I.T,33
 - International Society of Soil Science, 33
 - AASHO, 33
 - Textural, 34
 - Casagrande, 35
- Coefficient
 - of active earth pressure (Coulomb), 291
 - of active earth pressure (Rankine),262
 - of passive earth pressure(Rankine), 262
 - of passive pressure (Coulomb), 291
 - of earth pressure at rest, 292
 - of permeability, 61, 69
- Cohesion, 219
- Colloids, 31
- Compressibility
 - of soil, 154
 - measurement of , 155
- Compression index, 159
- Compaction, 459
 - role of moisture in, 459
 - Proctor, 462
 - modified Proctor, 463
 - field, 463, 465
- Compactive effort, 460
- Concavity coefficient, 19
- Consolidation, 168
 - mechanics of, 169
 - Terzaghi-Frohlich's theory of 172, 176
 - Progress of,173
 - test, 181
 - settlement, 192
- Consolidameter, 155
- Consolidated-Undrained test,240
- Coulomb's theory, 275
 - of active case,276
 - of passive case, 278
- Culmann's
 - graphical method of earth pressure determination, 279
 - method of slope stability analysis, 353
- Critical
 - hydraulic gradient, 106
 - void ratio, 229
- Darcy's law, 61
 - range of validity of, 61
- Degree
 - of consolidation, 179,180
 - of saturation, 8
- Direct shear test, 222
- Discharge Velocity, 62
- Drained test, 244
- Dry unit Weight, 12
- Earth pressure, 256
 - active, 256,259,261,264,269,271,290
 - passive, 256,259,261,265,269,271,282,285, 290
 - at-rest,256,292
 - theories, 260
- Effective stress, 102,104
- Elevation head, 109
- Equipotential line, 81,82
- Expansive Soils, 436